

Synthesis of Hyper-branched Oligosaccharide Epitopes from Glycoprotein GP72 of *T. cruzi* and  
Evaluation of their Binding to the WIC26.29 Monoclonal Antibody

by

Mikel Jason Allas

A thesis submitted in partial fulfillment of the requirements for the degree of  
Doctor of Philosophy

Department of Chemistry  
University of Alberta

© Mikel Jason Allas, 2024

## Abstract

Chagas disease is caused by the parasitic protozoan *Trypanosoma cruzi*, which is transmitted to humans mostly by contact with insects called ‘kissing bugs’. The presence of an immunogenic glycoprotein, GP72, on the cell surface of *T. cruzi* has a key role in the parasite’s life cycle. A monoclonal antibody (WIC29.26) that recognizes the unusual glycan portion of GP72 prevents the transformation of *T. cruzi* to its human infectious form suggesting that antibodies against this glycan may be an effective vaccine against the disease. This 13-residue glycan has a highly unusual structure of six different monosaccharides in seven different linkages, as well as two highly-branched residues, a fucose and a xylose. This research is focused on the synthesis of this glycan structure and fragments, which were to be used to probe the binding specificity of WIC29.26 mAb. The presence of the two ‘hyper-branched’ sugar residues is anticipated to pose a significant challenge in synthesizing the glycan structure.

In Chapter 2, I describe my work on the synthesis of these fragments and the strategies employed. The hexasaccharide and heptasaccharide fragments each contain the ‘hyper-branched’ fucose and xylose residues, respectively. The synthesis of the hexasaccharide fragment was accomplished using a ‘pendulum’ glycosylation sequence while the heptasaccharide was accomplished using a ‘clockwise’ glycosylation sequence.

In Chapter 3, I present my work describing the attempted synthesis of the whole tridecasaccharide glycan epitope of GP72. Unfortunately, multiple attempts to synthesize the whole glycan fragment were unsuccessful. The most significant progress achieved was the successful synthesis of an undecasaccharide intermediate which was synthesized from a linear synthesis starting from an octasaccharide acceptor. Further efforts, using a range of different approaches, to synthesize the tridecasaccharide by an [11+2] glycosylation was futile. Due to the limited and depleted amount of intermediates and the number of steps required to synthesize them, I have decided to finish my work at this point, but have proposed other synthetic routes to be investigated in the future.

In Chapter 4, I report my work on the binding analysis performed between the smaller GP72 glycan fragments synthesized in Chapter 2 and the monoclonal antibody WIC29.26. These analyses were done using Bio-layer Interferometry (BLI) on an OctetRed96 machine. A dot blot assay was also performed to qualitatively analyze binding between the glycans and the mAb. However, the binding analyses performed did not show any significant binding between the glycans and the mAb. There is a possibility that these fragments adopt conformations that are not the same as in the whole glycan epitope found in the glycoprotein. Another possible reason could be the absence of the phosphate moieties in the synthetic glycans tested that are present in the native glycan.

## **Preface**

Chapter 2, 3 and 4 – The work described in these chapters were completed solely by me and have not been published.

## Acknowledgments

First of all, I would like to express my utmost gratitude and appreciation to my PhD supervisor, Dr. Todd Lowary, for all his help and guidance both for my research and personal life. Todd had taught me countless lessons that helped me to be a better chemist but much more importantly, be a better person. My successes in the past years during my stay in this program would not be possible without him and my success in the future would be in no doubt because of all the opportunities he has given me. I would be forever grateful, and words are not enough to thank him.

I am also thankful for my Supervisory Committee and Ph.D. Examination Committee members: Professor Dennis Hall, Matthew Macauley, Frederick West, and Spencer Williams – for their guidance and help in this thesis. In addition, I would like to acknowledge Professor Michael Ferguson for his help in my research.

I would like to thank the administrative services at the University of Alberta, specifically, for the help provided by Anita Weiler and Connor Part. I would also like to thank all the Scientific Services Staff of the Department of Chemistry, including Dr. Randy Whittal, Bela Reiz, Jing Zheng, Dr. Angelina Morales-Izquierdo, Wayne Moffat, Dr. Ryan McKay, Mark Miskolzie for helping me to obtain the compound characterizations required for my project. I also would like to thank the Services Staff in Academia Sinica especially to Dr. Chris Jao of the Biophysical Core Facility in the Institute of Biological Chemistry for helping me perform the BLI experiments. In addition, I would also like to thank my TA Supervisors Dr. Hayley Wan and Dr. Yoram Apelblat. One of the highlights of my graduate school life is being a TA, and these two are nothing but wonderful inspirations for me.

I would also like to thank past and present members of the Lowary Lab. I was lucky to meet and work with these incredible people that I could honestly call as my friends. My PhD journey would be incredibly dull without your presence, and I might not even have survived it without your help. I would like to give my sincere gratitude to Dr. Maju Joe, Dr. Junfeng Zhang and Dr. Sicheng Lin for all their helpful expertise, suggestions, and knowledge about carbohydrate chemistry, without them and their help, I do not think my success would be possible. I would like to thank Dr. Tzu-Ting Gao, Dr. Anthony Chu, and Ms. Pei-ru Liao for all their help when I relocate to Taiwan. Thank you for helping me feel welcome in your home country and make my transfer as smooth as possible. Special thanks to Mr. Yel Macale, Ms. Karen Wang, and Ms. Lian Tsai for helping me perform experiments related to biology, without them, I would be lost. I would also like to thank Dr. Vitor Cunha, Ms. Wei-ting Chang, Mr. Po-sen Tseng, Dr. Pei-Jhen Li, Dr. Tracy Lin, Dr. Jenny Lin, Mr. Richard Brunton, Dr. Joe Narsico, Mr. David Hsu, Ms. Kerwin Chen, Mr. Ha Nam Duong, and Ms. Wendy Wu for the wonderful friendships and memories. Your friendship means the world to me, and I would always be grateful for it. Many thanks also go to Dr. Winston Lim, Dr. Bo-shun Huang, Dr. Narasimha Thota, Dr. Ryan Sweeney, Mr. Fazheng Han, Mr. Jeremy Nothof, Dr. Mike Bell, Ms. Rebecca Kim, Mr. Brock Byers, Dr. Teddy Ehianeta, Dr. Larry Lico, Dr. Tarique Anwar, Mr. Sony Chang, Mr. Victor Liao, Ms. Yi-chia Su, and Ms. Vicky Tsuo for the kindness they have shown me throughout these years.

Lastly, I would like to thank my family and friends for their unconditional support, love, and encouragement throughout these years. I dedicate this work to my parents Nestor and Cely, siblings Mark, Mae and Marvin, and my partner, Che-Li. Without them, I would not be here today.

## Table of Contents

<b>Chapter 1 Introduction</b> .....	1
1.1 Chagas Disease.....	2
1.1.1 <i>Trypanosoma cruzi</i> .....	2
1.1.1.1 Life cycle of <i>T. cruzi</i> .....	3
1.1.2 Transmission of Chagas Disease.....	5
1.1.2.1 Vector-borne transmission.....	5
1.1.2.2 Other non-vector mode of transmission.....	5
1.1.3 Clinical manifestations of Chagas disease.....	6
1.1.4 Diagnosis of Chagas disease.....	7
1.1.5 Treatment and Prevention of Chagas disease.....	7
1.2 <i>T. cruzi</i> cell surface.....	8
1.2.1 Glycoprotein GP72.....	9
1.2.1.1 Recognition of GP72 by WIC29.26 mAb.....	10
1.2.1.2 Role of GP72 in <i>T. cruzi</i> morphology.....	10
1.2.1.3 GP72 can induce protective immune response.....	12
1.2.1.4 GP72 and its role in <i>T. cruzi</i> infectivity.....	12
1.3 Structure of antigenic epitope of GP72.....	14
1.4. Synthesis of highly congested oligosaccharides.....	15
1.5 Research objective – Synthesis of glycan fragments of the hyperbranched WIC29.26 mAb glycan epitope from <i>T. cruzi</i> GP72.....	24
1.6 References.....	27

<b>Chapter 2 Synthesis of Fragments Derived from the Immunogenic Glycan Epitope of Glycoprotein GP72 of <i>T. cruzi</i></b> .....	36
2.1 Background.....	37
2.2 Results and discussion.....	39
2.2.1 Synthesis of hexasaccharide <b>2.2</b> .....	40
2.2.1.1 Synthesis of building blocks <b>2.8–2.13</b> .....	41
2.2.1.2 Attempted synthesis of hexasaccharide <b>2.2</b> using a ‘counterclockwise’ approach.....	45
2.2.1.3 Synthesis of hexasaccharide <b>2.2</b> using a ‘clockwise’ and ‘pendulum’ approach...50	
2.2.1.3.1 Synthesis using ‘clockwise’ approach.....	50
2.2.1.3.2 Synthesis using ‘pendulum’ approach.....	52
2.2.1.4 Summary .....	57
2.2.2 Synthesis of heptasaccharide <b>2.3</b> .....	58
2.2.2.1 Synthesis of trisaccharide <b>2.4</b> .....	60
2.2.2.2 Synthesis of tetrasaccharide <b>2.5</b> .....	63
2.2.2.3 Synthesis of heptasaccharide <b>2.3</b> using a [4+3] glycosylation.....	70
2.2.2.4 Summary.....	72
2.3 <sup>1</sup> H NMR comparison between native GP72 and synthetic glycans.....	73
2.4 Conclusions.....	75
2.5 Experimental section.....	77
2.6 References.....	158
<b>Chapter 3 Synthesis of a Highly Branched Immunogenic Glycan Epitope of Glycoprotein GP72 of <i>T. cruzi</i></b> .....	164

3.1 Background.....	165
3.2 Results and discussion.....	165
3.2.1 Attempted glycosylations with heptasaccharide donor <b>2.78</b> .....	166
3.2.2 Synthesis of octasaccharide <b>3.11</b> .....	171
3.2.3 Attempted [8+5] glycosylations.....	173
3.2.3.1 Synthesis of pentasaccharide <b>3.12</b> .....	175
3.2.3.2 Synthesis of tetrasaccharide <b>3.24</b> and attempted [8+4] glycosylation.....	178
3.2.3.3 Synthesis of tetrasaccharide <b>3.25</b> and attempted [8+4] glycosylation.....	183
3.2.4 Attempted linear synthesis towards the whole glycan structure.....	185
3.2.4.1 Synthesis of undecasaccharide <b>3.38</b> .....	187
3.2.4.2 Attempted [11+2] glycosylation with undecasaccharide acceptor <b>3.38</b> .....	191
3.2.5 Proposed synthetic routes towards synthesis of the whole glycan structure.....	194
3.3 Summary and conclusions.....	196
3.4 Experimental methods.....	198
3.5 References.....	245
<b>Chapter 4 Study on the Binding of Synthetic Glycan Fragments of GP72 and WIC29.26</b>	
<b>mAb</b> .....	249
4.1 Protein–Glycan interactions.....	250
4.1.1 Bio-layer Interferometry (BLI) .....	252
4.2 Results and Discussion.....	255
4.2.2 Bio-layer Interferometry (BLI) binding analysis between synthetic glycans and	
WIC29.26 mAb.....	255
4.2.2.1 Immobilization of glycans onto biosensors.....	255

4.2.2.1.1 Choice of the BLI biosensor and immobilization method.....	256
4.2.2.1.1.1 Synthesis of biotin-tagged glycans.....	256
4.2.2.1.1.2 Immobilization of biotin-tagged glycans on biosensors.....	258
4.2.2.2 Binding analysis with WIC29.26 using BLI.....	261
4.2.2.3 Binding analysis with purified WIC29.26 mAb using BLI.....	267
4.2.3 Binding analysis with WIC29.26 mAb using a dot blot assay.....	272
4.3 Summary, conclusions and recommendations.....	275
4.4 Experimental methods.....	277
4.4.1 Synthesis of biotinylated glycans <b>4.2–4.5</b> .....	277
4.4.2 Bio-layer interferometry experiments.....	282
4.4.2.1 Immobilization of biotinylated glycans on SAX biosensors.....	282
4.4.2.2 Binding assay with WIC29.26 mAb.....	283
4.4.2.3 Binding assay with purified WIC29.26 mAb.....	284
4.4.3 Sodium dodecyl sulfate polyacrylamide gel electrophoresis.....	285
4.4.4 Dot Blot Assay Protocol.....	285
4.5 References.....	287
<b>Chapter 5 Summary and Future Work</b> .....	<b>292</b>
5.1 Summary and future work.....	293
5.1.1 Synthesis of glycan epitope of GP72.....	293
5.1.2 Binding analysis between synthetic glycan fragments and WIC29.26 mAb.....	299
5.2 References.....	302
<b>Bibliography</b> .....	<b>303</b>

<b>Appendix</b> .....	322
BLI sensograms for immobilization of biotinylated glycans on SAX sensors.....	305
BLI sensograms for binding analysis of glycan fragments with WIC29.26 mAb using 1x PBS containing 0.1% BSA and 0.05% Tween 20 as the buffer assay.....	308
BLI sensograms for binding analysis of glycan fragments with WIC29.26 mAb using 50 mM Tris buffer (pH = 7.4, 0.15 M NaCl, 0.25% BSA and 0.05% Tween 20, 0.05% NaN <sub>3</sub> ) as the buffer assay.....	311
BLI sensograms for binding analysis of glycan fragments with purified WIC29.26 mAb using 1x PBS containing 0.1% BSA and 0.05% Tween 20 as the buffer assay.....	314

## List of Figures

<b>Figure 1-1:</b> Life cycle of <i>Trypanosoma cruzi</i> .....	4
<b>Figure 1-2:</b> Structures of the two approved clinical treatments for Chagas disease.....	8
<b>Figure 1-3:</b> Scanning electron micrographs of wild type (A) and GP72 null mutant (B) <i>T. cruzi</i> epimastigotes showing difference in the protozoan's flagellum morphology.....	11
<b>Figure 1-4:</b> Structure of the WIC29.26 mAb glycan epitope found in <i>T. cruzi</i> GP72 glycoprotein in both pictorial and line-bond form.....	15
<b>Figure 1-5:</b> Structures of highly branched carbohydrate residues <b>1.1–1.4</b> , which have been previously synthesized.....	16
<b>Figure 1-6:</b> Structures of target fragments derived from the immunogenic glycan epitope from GP72.....	25
<b>Figure 1-7:</b> Structure of the target immunogenic glycan epitope from GP72.....	26
<b>Figure 2-1:</b> Structure of the immunogenic glycan epitope of GP72.....	37
<b>Figure 2-2:</b> Structures of the synthetic targets derived from the immunogenic glycan epitope from GP72.....	38
<b>Figure 2-3:</b> Structure of GP72 native glycan and synthetic fragments <b>2.2</b> and <b>2.3</b> .....	74
<b>Figure 3-1:</b> Structure of the immunogenic glycan epitope of GP72.....	165
<b>Figure 4-1:</b> Schematic diagram illustrating BLI spectroscopy.....	252
<b>Figure 4-2:</b> BLI sensogram showing the immobilization, association, dissociation, and regeneration phases.....	254
<b>Figure 4-3:</b> Structure of the biotinylated glycans to be used for binding experiments.....	258
<b>Figure 4-4:</b> Immobilization of biotinylated glycans on SAX biosensors followed by blocking with biocytin.....	259

<b>Figure 4-5:</b> A) Biosensor and sample plate layout for glycan <b>4.4</b> immobilization and blocking with biocytin; B) Sensograms during the immobilization and blocking steps.....	260
<b>Figure 4-6:</b> Sensogram during the biocytin loading on two reference SAX sensors.....	261
<b>Figure 4-7:</b> Process used for binding analysis between immobilized glycans and WIC29.26 mAb.....	262
<b>Figure 4-8:</b> Biosensor and sample plate layouts during the binding analysis for glycan <b>4.4</b> .....	263
<b>Figure 4-9:</b> A) Sensogram for the binding analysis using ligand sensors immobilized with glycan <b>4.4</b> . B) Sensogram for the binding analysis using reference sensors.....	265
<b>Figure 4-10:</b> Subtracted and stacked sensograms for binding analysis with glycan <b>4.4</b> .....	266
<b>Figure 4-11:</b> A) SDS PAGE of the WIC29.26 mAb sample. B) SDS PAGE profiles of each eluted fractions during Protein A agarose affinity gel chromatography.....	268
<b>Figure 4-12:</b> A) Sensogram for the binding analysis of sensors with glycan <b>4.4</b> immobilized using purified WIC29.26 mAb. B) Sensogram for the binding analysis using reference sensors with purified WIC29.26 mAb.....	270
<b>Figure 4-13:</b> A) Subtracted sensogram for the binding analysis using sensors with glycan <b>4.4</b> immobilized with purified WIC29.26 mAb. B) Stacked sensogram for the binding analysis using reference sensors with purified WIC29.26 mAb at multiple concentrations.....	271
<b>Figure 4-14:</b> Schematic diagram for dot blot assay to analyze WIC29.26 mAb–glycan interaction.....	272
<b>Figure 4-15:</b> Fluorescence imaging of nitrocellulose membrane blotted with WIC29.26 mAb after incubation with biotinylated glycans then with Neutravidin Dylight488.....	274
<b>Figure 5-1:</b> Structures of synthesized fragments derived from the immunogenic glycan epitope from GP72.....	294

**Figure 5-2:** Schematic diagram of the BLI binding analysis between immobilized glycans and WIC29.26 mAb.....300

**Figure 5-3:** Schematic diagram for dot blot assay to analyze WIC29.26 mAb–glycan interaction.....301

## List of Schemes

<b>Scheme 1-1:</b> Synthesis of side chain A rhamnogalacturonan (RGII) tetrasaccharide <b>1.9</b> by sequential addition of monosaccharide donors.....	17
<b>Scheme 1-2:</b> Synthesis of a RGII side chain B fragment.....	18
<b>Scheme 1-3:</b> Synthesis of a highly congested mannose residue in <i>C. neoformans</i> .....	19
<b>Scheme 1-4:</b> Synthesis of ACTV-1 hexasaccharide fragment <b>1.30</b> by Lin and Lowary.....	21
<b>Scheme 1-5:</b> Synthesis of ACTV-1 congested glycans by Wang et.al.....	23
<b>Scheme 2-1:</b> Retrosynthetic analysis of hexasaccharide <b>2.2</b> .....	41
<b>Scheme 2-2:</b> Synthesis of linker <b>2.16</b> .....	42
<b>Scheme 2-3:</b> Synthesis of building block <b>2.8</b> .....	43
<b>Scheme 2-4:</b> Synthesis of building block <b>2.9</b> .....	44
<b>Scheme 2-5:</b> Synthesis of disaccharide acceptor <b>2.26</b> .....	45
<b>Scheme 2-6:</b> Synthesis of disaccharide acceptor <b>2.7</b> .....	46
<b>Scheme 2-7:</b> Synthesis of tetrasaccharide <b>2.30</b> .....	48
<b>Scheme 2-8:</b> Failed O-3 glycosylation attempts on acceptor <b>2.31</b> .....	49
<b>Scheme 2-9:</b> Failed O-3 glycosylation attempts on acceptor <b>2.33</b> .....	50
<b>Scheme 2-10:</b> Synthesis of tetrasaccharide <b>2.38</b> .....	52
<b>Scheme 2-11:</b> Synthesis of tetrasaccharides <b>2.38</b> and <b>2.43</b> .....	53
<b>Scheme 2-12:</b> Synthesis of hexasaccharide <b>2.45</b> .....	55
<b>Scheme 2-13:</b> Synthesis of target hexasaccharide fragment <b>2.2</b> .....	56
<b>Scheme 2-14:</b> Retrosynthetic analysis of heptasaccharide <b>2.3</b> and smaller fragments <b>2.4</b> and <b>2.5</b> .....	59
<b>Scheme 2-15:</b> Synthesis of building block <b>2.50</b> .....	60

<b>Scheme 2-16:</b> Synthesis of trisaccharide <b>2.47</b> .....	61
<b>Scheme 2-17:</b> Synthesis of trisaccharide <b>2.4</b> .....	62
<b>Scheme 2-18:</b> Synthesis of building block <b>2.52</b> .....	64
<b>Scheme 2-19:</b> Synthesis of building block <b>2.53</b> .....	65
<b>Scheme 2-20:</b> Synthesis of tetrasaccharide <b>2.72</b> .....	66
<b>Scheme 2-21:</b> Synthesis of tetrasaccharide <b>2.5</b> .....	69
<b>Scheme 2-22:</b> Synthesis of heptasaccharide <b>2.77</b> .....	70
<b>Scheme 2-23:</b> Synthesis of heptasaccharide <b>2.3</b> .....	72
<b>Scheme 3-1:</b> Retrosynthetic analysis of tridecasaccharide <b>2.1</b> through a [6+7] glycosylation....	167
<b>Scheme 3-2:</b> Synthesis of target hexasaccharide fragment <b>3.2</b> .....	168
<b>Scheme 3-3:</b> Unsuccessful attempt on [6+7] glycosylation.....	169
<b>Scheme 3-4:</b> Synthesis of acceptors <b>3.5</b> and <b>3.6</b> .....	170
<b>Scheme 3-5:</b> Unsuccessful attempt on [3+7] and [4+7] glycosylation.....	171
<b>Scheme 3-6:</b> Model reaction between acceptor <b>3.6</b> and donor <b>3.7</b> .....	172
<b>Scheme 3-7:</b> Synthesis of acceptor <b>3.9</b> .....	172
<b>Scheme 3-8:</b> Successful [1+7] glycosylation between <b>2.78</b> and <b>3.9</b> and synthesis of acceptor <b>3.11</b> .....	173
<b>Scheme 3-9:</b> Retrosynthetic analysis of tridecasaccharide <b>2.1</b> through a [8+5] glycosylation....	174
<b>Scheme 3-10:</b> Synthesis of pentasaccharide <b>3.19</b> using the ‘reversed pendulum’ approach.....	176
<b>Scheme 3-11:</b> Failed attempt to synthesize <b>3.20</b> from <b>3.19</b> .....	178
<b>Scheme 3-12:</b> Retrosynthetic analysis of tridecasaccharide <b>3.1</b> through a [8+4] glycosylation...	179
<b>Scheme 3-13:</b> Formation of unwanted product <b>3.21</b> and proposed mechanism for its formation.....	181

<b>Scheme 3-14:</b> Synthesis of <b>3.24</b> from <b>3.17</b> .....	182
<b>Scheme 3-15:</b> An [8+4] glycosylation attempt between <b>3.11</b> and <b>3.24</b> .....	183
<b>Scheme 3-16:</b> Retrosynthetic analysis of trisaccharide donor <b>3.25</b> .....	183
<b>Scheme 3-17:</b> Synthesis of donor <b>3.25</b> .....	184
<b>Scheme 3-18:</b> An [8+4] glycosylation attempt between <b>3.11</b> and <b>3.25</b> .....	185
<b>Scheme 3-19:</b> Unsuccessful synthesis of disaccharide <b>3.30</b> .....	185
<b>Scheme 3-20:</b> Retrosynthetic analysis of tridecasaccharide <b>2.1</b> via a linear synthesis from <b>3.11</b> .....	186
<b>Scheme 3-21:</b> Synthesis of <b>3.33</b> using acceptor <b>3.11</b> and donors <b>2.9</b> and <b>3.32</b> .....	188
<b>Scheme 3-22:</b> Synthesis of undecasaccharide <b>3.38</b> .....	190
<b>Scheme 3-23:</b> Attempted [11+2] glycosylation with acceptor <b>3.38</b> and donor <b>2.7</b> .....	191
<b>Scheme 3-24:</b> Attempted [11+2] glycosylation with acceptor <b>3.38</b> and donor <b>2.29</b> .....	192
<b>Scheme 3-25:</b> Attempted [11+2] glycosylation with acceptor <b>3.38</b> and donor <b>2.7</b> under neutral conditions.....	193
<b>Scheme 3-26:</b> Attempted [11+2] glycosylation with acceptor <b>3.38</b> and donors <b>2.27</b> and <b>3.43</b> .....	194
<b>Scheme 3-27:</b> Proposed synthesis of tridecasaccharide using linear addition of monosaccharide donors.....	195
<b>Scheme 3-28:</b> Proposed synthesis of tridecasaccharide by glycosylation on O-4 then O-2 at the fucose residue.....	196
<b>Scheme 5-1:</b> Successful synthesis of hexasaccharide <b>2.2</b> by ‘pendulum’ addition of sugar building blocks.....	295
<b>Scheme 5-2:</b> Successful synthesis of heptasaccharide <b>2.3</b> by ‘clockwise’ addition of sugar building blocks.....	296

**Scheme 5-3:** Attempted [8+4] glycosylations resulted to intramolecular reaction of the donor...297

**Scheme 5-4:** Synthesis of **3.38** through linear addition but failed final [11+2] O-4 glycosylation.....298

## List of Tables

<b>Table 2-1.</b> $^1\text{H}$ NMR data for the GP72 native glycan and synthetic hexasaccharide <b>2.2</b> .....	74
<b>Table 2-2.</b> $^1\text{H}$ NMR data for the GP72 native glycan and synthetic heptasaccharide <b>2.3</b> .....	75

## List of Abbreviations

[ $\alpha$ ] <sub>D</sub>	specific rotation (sodium D Line)
Å	4 Angstrom molecular sieve
Ac	acetyl
Ac <sub>2</sub> O	acetic anhydride
AcOH	acetic acid
AgOTf	silver trifluoromethanesulfonate
AIDS	Acquired immunodeficiency syndrome
All	allyl
APS	ammonium persulfate
app	apparent (NMR spectra)
Ar	aromatic
ATCV-1	<i>Acanthocystis turfacea</i> chlorella virus 1
BLI	bio-layer interferometry
Bn	benzyl
br s	broad singlet (NMR spectra)
BSA	bovine serum albumin
Bz	benzoyl
Cbz	benzyloxycarbonyl
CD	Chagas disease
CH <sub>3</sub> OTf	methyl trifluoromethanesulfonate
COSY	correlation spectroscopy
CSA	camphorsulfonic acid

d	doublet (NMR spectra)
<i>D. discoidium</i>	<i>Dictyostelium discoideum</i>
1,2-DCE	1,2-dichloroethane
DCM	dichloromethane
dd	doublet of doublet (NMR spectra)
ddd	doublet of doublet of doublet (NMR spectra)
DDQ	2,3-Dichloro-5,6-dicyano-1,4-benzoquinone
DHB	2,5-dihydroxybenzoic acid
dHex	deoxyhexose
DMAP	4-(dimethylamino)pyridine
DMF	<i>N,N</i> -dimethylformamide
DMP	2,6-dimethylphenyl
2,2-DMP	2,2-dimethoxypropane
DNA	Deoxyribonucleic acid
dq	doublet of quartet (NMR spectra)
dt	doublet of triplet (NMR spectra)
dTBMP	2,6-di-tert-butylmethylpyridine
DTBS	di-tert-butylsilyl
DTBS(OTf) <sub>2</sub>	di-tert-butylsilyl bis(trifluoromethanesulfonate)
ECG	electrocardiogram
EDC·HCl	<i>N</i> -(3-dimethylaminopropyl)- <i>N'</i> -ethylcarbodiimide hydrochloride
ESI	electrospray ionization

Et <sub>2</sub> O	diethyl ether
Et <sub>3</sub> SiH	triethylsilane
EtOAc	ethyl acetate
Fuc	fructose
Gal	galactose
GC-MS	gas chromatography-mass spectrometry
Glc	glucose
GlcNAc	<i>N</i> -acetylglucosamine
GlcN <sub>3</sub>	2-deoxy-2-azidoglucose
GP	glycoprotein
HMBC	heteronuclear multiple bond correlation
HRMS	high-resolution mass spectrometry
HSQC	heteronuclear single quantum coherence
Hz	hertz
ITC	isothermal titration calorimetry
[Ir(COD)(CH <sub>3</sub> Ph <sub>2</sub> P) <sub>2</sub> ]PF <sub>6</sub>	(1,5-cyclooctadiene)bis (methylphenylphosphine)iridium (I) hexafluorophosphate
LCMS	liquid chromatography mass spectrometry
Lev	levulinoyl
LevOH	levulinic acid
LRMS	low-resolution mass spectrometry
m	multiplet (NMR spectra)

<i>m/z</i>	mass per charge
mAb	monoclonal antibody
MALDI	matrix-assisted laser desorption/ionization
Me	methyl
Me <sub>3</sub> SnOH	trimethyltin hydroxide
MS	mass spectrometry
MW	molecular weight
NAP	2-methylnaphthyl
NBS	<i>N</i> -bromosuccinimide
<i>n</i> -Bu <sub>2</sub> SnO	di- <i>n</i> -butyltin oxide
NIS	<i>N</i> -iodosuccinimide
NMR	nuclear magnetic resonance
Nu	nucleophile
PBCV-1	<i>Paramecium bursaria</i> chlorella virus 1
PBS	phosphate buffered saline
PCR	polymerase chain reaction
PEG	polyethylene glycol
Ph	phenyl
PMB	<i>p</i> -methoxybenzyl
<i>p</i> -TsOH	<i>p</i> -toluenesulfonic acid
pyr	pyridine
q	quartet (NMR spectra)
quant	quantitative

<i>R. prolixus</i>	<i>Rhodnius prolixus</i>
R <sub>f</sub>	retention factor
RG II	rhamnogalacturonan II
Rha	rhamnose
ROESY	rotating-frame nuclear Overhauser effect spectroscopy
s	singlet (NMR spectra)
SAX	High Precision Streptavidin Biosensor
SDS PAGE	sodium dodecyl sulfate–polyacrylamide gel electrophoresis
SE	2-trimethylsilylethyl
Ser	serine
SPR	surface plasmon resonance
<i>T. cruzi</i>	<i>Trypanosoma cruzi</i>
<i>T. dimidiata</i>	<i>Triatoma dimidiata</i>
<i>T. infestans</i>	<i>Triatoma infestans</i>
TBAB	tetra- <i>n</i> -butylammonium bromide
TBAF	tetra- <i>n</i> -butylammonium fluoride
TBST	tris-buffered saline with Tween 20
t-Bu	tert-butyl
TFA	trifluoroacetic acid
TFAA	trifluoroacetic anhydride
TfOH	trifluoromethanesulfonic acid

THF	tetrahydrofuran
Thr	threonine
TLC	thin layer chromatography
TMS	trimethylsilyl
TMSOTf	trimethylsilyl trifluoromethanesulfonate
TOF	time-of-flight
Tol	<i>p</i> -tolyl
TOCSY	total correlation spectroscopy
Troc	2,2,2-trichloroethoxycarbonyl
UV	ultraviolet
VT-NMR	Variable-temperature nuclear magnetic resonance spectroscopy
WHO	World Health Organization
Xyl	xylose

# **Chapter 1**

## **Introduction**

## 1.1 Chagas Disease

Chagas disease (CD), also known as American trypanosomiasis, is a life-long infectious disease caused by the parasitic protozoan *Trypanosoma cruzi*, which is transmitted to humans mostly by contact with the urine or feces of the vector (or host) insect: triatomine or 'kissing bugs'.<sup>1</sup> The disease is a significant health, social and economic problem in several Latin American countries where it is estimated that around eight million people are afflicted with the disease.<sup>2,3</sup> Most of the infected people are not aware of the infection while in their asymptomatic phase, but it is estimated that three out of ten will progress to fatal cardiac and digestive complications.<sup>4</sup> The disease was first described in 1909 by the Brazilian physician Carlos Ribeiro Justiniano Chagas, hence the name of the disease. The report published by Chagas is unique because this is one of the few times that a single scientist was able to describe in extreme detail the mode of transmission, which includes the parasite, insect vector and human host, and the early clinical symptoms of the disease.<sup>5</sup> While CD is considered endemic to the Latin American region, the disease was recently been reported in non-endemic regions like North America and Europe due to mass human migration from endemic regions.<sup>6</sup> In United States alone, it is estimated that around 450,000 people have the disease, and most are unaware of the infection that could lead to life threatening complications in the future.<sup>7</sup> As an emerging global health concern, the World Health Organization (WHO) has classified Chagas disease as one of the most neglected tropical diseases of the world.<sup>8</sup>

### 1.1.1 *Trypanosoma cruzi*

Chagas Disease is caused by *Trypanosoma cruzi*, a parasite that requires being inside its hosts to replicate.<sup>9</sup> The species' name *cruzi* was given by Chagas' disease discoverer Carlos Chagas to honor his mentor, Oswaldo Cruz.<sup>10</sup> The parasite has multiple forms in its life cycle with

infectious forms usually having flagella to help for movement and infectivity.<sup>11</sup> It can infect multiple types of cells like epithelial cells, macrophages and fibroblasts. There are currently six main genetic strain types for the parasite.<sup>12</sup>

#### **1.1.1.1 Life cycle of *T. cruzi***

*Trypanosoma cruzi* undergoes an elaborate and complex life cycle between its insect and mammalian hosts. Several developmental forms have been identified during the life cycle of the protozoan in its hosts. The parasite forms identified in the insect hosts are the replicative epimastigotes and the infective metacyclic trypomastigotes while those in the mammalian hosts are the non-replicative bloodstream trypomastigotes and replicative intracellular amastigotes.<sup>13</sup> Both trypomastigote forms in the insect and human can be differentiated compared to other forms by the presence of a long flagellum. This flagellum is important in its continuous and fast movement, which is essential to its capability to infect.<sup>11</sup>

The life cycle of *T. cruzi* starts when an infected triatomine takes a blood meal on the mammalian host and releases infective metacyclic trypomastigotes. The trypomastigotes penetrate through the insect bite wound and, once inside host, infect and invade a wide range of cells where they differentiate into intracellular amastigotes, which can replicate. Inside the cells of infected tissues, the amastigotes multiply and differentiate into flagellated non-replicative trypomastigotes before they are released to the bloodstream. These bloodstream trypomastigotes, while incapable of replication, can infect other tissues, and transform again into replicative amastigotes inside the cells. This infective cycle results in the acute clinical phase of the disease. The cycle returns into the insect host once a new triatomine bug takes a bloodmeal from an infected mammalian host ingesting trypomastigotes. These trypomastigotes travel to the midgut transforming into

replicative epimastigotes that proliferate. The epimastigotes then descend into the triatomine bug's hindgut where they grow flagella and differentiate into metacyclic trypomastigotes. The cycle comes to a close when the insect infects a new mammalian host.<sup>13-15</sup>

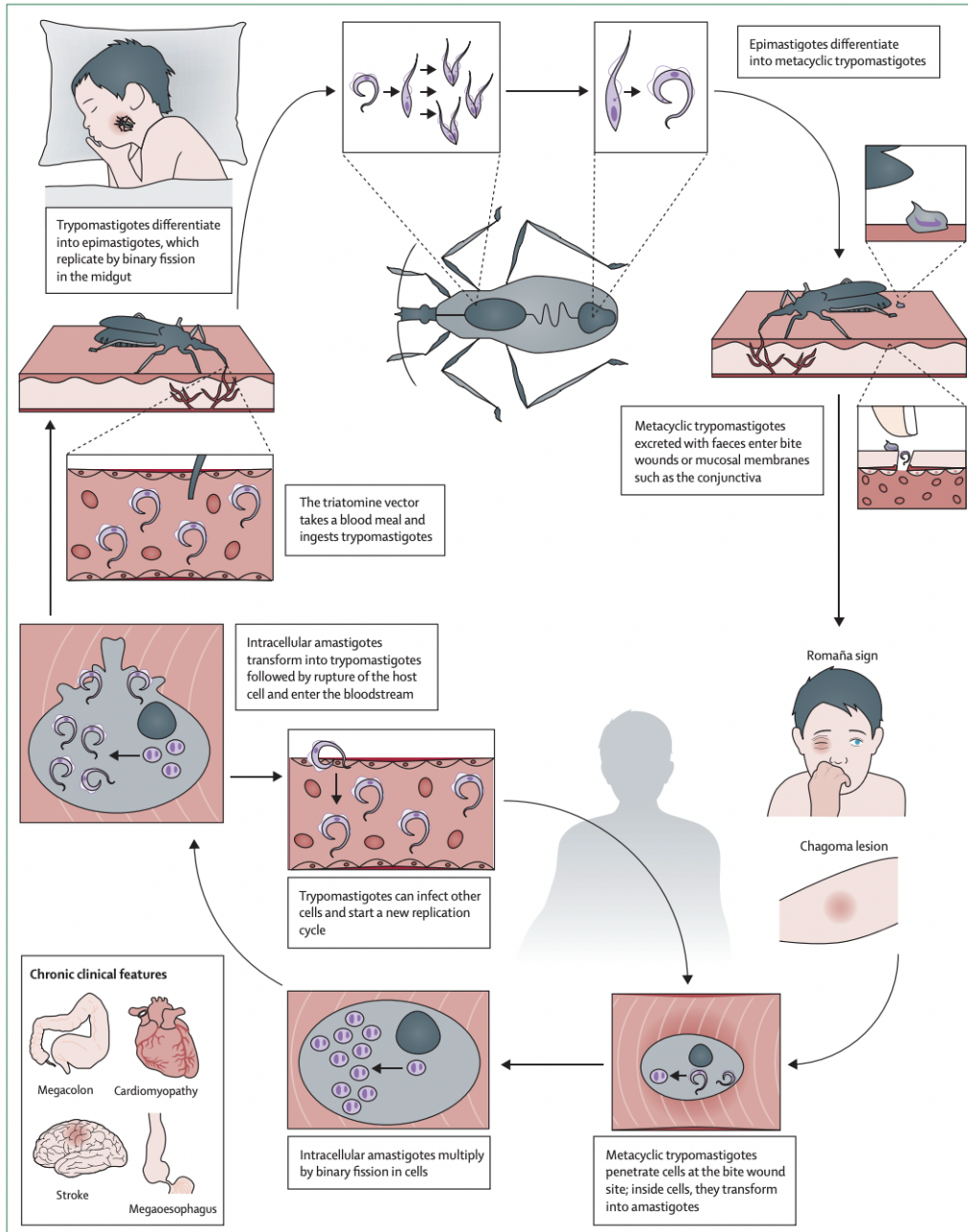


**Figure 1-1:** Life cycle of *Trypanosoma cruzi*. Reprinted with permission from the Elsevier:

*Lancet* 2018, 391: 82–94.

## **1.1.2 Transmission of Chagas Disease**

### **1.1.2.1 Vector-borne transmission**

Aside from humans, Chagas disease can be transmitted to a variety of mammals both wild (rodents, and marsupials) and domesticated (dogs, cats, and guinea pigs) when they get in contact with parasite-carrying triatomine bugs.<sup>16</sup> While over a hundred species of triatomine bugs exist, only few can act as vectors of *T. cruzi*.<sup>17</sup> Three of the main triatomine vector species responsible for transmission of Chagas disease to humans are *Triatoma infestans*, *Rhodnius prolixus*, and *Triatoma dimidiata*. Among the three, *T. infestans* has been the most significant carrier in history and it is mostly reported to be the major vector in the southern South America (sub-Amazonian). *R. prolixus* and *T. dimidiata* are primarily reported in northern South America and Central America with the latter extending its infection area reaching all the way into Mexico. Triatomine bugs can carry and transmit *T. cruzi* in any of its multiple nymphal stages, although adult bugs have a higher probability to be infected as they have taken more bloodmeals throughout their existence.<sup>4,18</sup>

### **1.1.2.2 Other non-vector mode of transmission**

While most people infected with CD are infected being bitten by an insect carrying the parasites, other mechanisms can also infect humans. In fact, non-vectorial modes of transmission are the dominant cause of infection in urbanized and non-endemic regions. Blood transfusion from an infected donor to a healthy patient can transmit Chagas disease. It is estimated that there is a 10–20% chance that a person can be infected with Chagas disease after receiving one unit of blood from an infected donor though the chances are affected by factors like parasite concentration, blood component transfused and the parasite's strain. Congenital transmission can also possibly occur, but the chances greatly depend on multiple reasons which includes but are not limited to the

parasite strain and the mother's immunological status. Transmission can also happen after a solid organ or a bone marrow donation from an infected donor, which has been documented multiple times in the endemic Latin region but also in non-endemic regions like USA, Canada and Europe. While rare, ingestion of food and beverages with *T. cruzi* or accidental ingestion of live parasite samples in the lab can be the causes of contracting the disease. A high volume of the parasite in contaminated foods has resulted in more severe acute symptoms and high fatality rates.<sup>6,18</sup>

### **1.1.3 Clinical manifestations of Chagas disease**

The early acute stage of Chagas infection is typically asymptomatic or a mild influenza-like illness that is usually ignored and will not be recognized as Chagas disease. A red, hardened bulging nodule at the site of entry of infection called a chagoma can be seen in people. Other symptoms that may be observed are fever, malaise, and enlargement of liver, spleen, and lymph nodes. Few rare and more serious complications during the acute phase include heart-related complications.<sup>19</sup>

After about four to eight weeks of the acute phase of the infection, the infection enters the chronic phase and, if no treatment is received, the disease will stay for life. Up to 80% of the people with chronic infection never show symptoms of Chagas disease and the disease is said to be in an indeterminate form. Individuals with an indeterminate form of the disease have a normal physical examination and a normal electrocardiogram (ECG).<sup>20</sup> However, an indeterminate form of chronic infection can be reactivated to a determinate form in some cases due to a weakening of the immune system. The determinate form disease can be fatal, and symptoms typically include complications involving the heart, gastrointestinal tract, or both. Infected individuals with AIDS or in

immunosuppression treatments usually experience an intensification of chronic infection due to the increase of parasite count and replication.<sup>21</sup>

#### **1.1.4 Diagnosis of Chagas disease**

During the acute phase of the infection, the main method of diagnosis is by microscopic detection of bloodstream trypomastigotes. On the other hand, diagnosis of the disease during the chronic phase is usually through the detection of the presence of IgG antibodies against *T. cruzi*. To confirm diagnosis, serological methods, usually enzyme-linked immunological assay, indirect immunofluorescence or indirect hemagglutination are performed. Polymerase chain reaction (PCR)-based diagnosis is also a powerful tool due to its high sensitivity compared to other methods but is rarely used in routine diagnosis due to poor standardization, lack of laboratory facilities, potential sample cross-contamination, and varying results from one laboratory to another.<sup>22</sup>

#### **1.1.5 Treatment and Prevention of Chagas disease**

Due to the complexity of the biology and pathology of the infection, finding treatment for Chagas disease has always been a difficult challenge. Currently, there are only two drugs, benznidazole and nifurtimox, proven to be effective in eradicating *T. cruzi* infection and are used for the treatment of Chagas infection. Benznidazole, a nitroimidazole derivative, works by inhibiting the protein and ribonucleic acid synthesis in *T. cruzi*.<sup>23</sup> On the other hand, nifurtimox's mode of action, as with other nitrofurans, is to generate oxidative stress that is fatal to the trypanosomes. Nifurtimox also inhibits typanothione reductase, an important enzyme for the parasite's redox homeostasis.<sup>24</sup> Benznidazole is usually administered as a first-line treatment over nifurtimox due to better safety and adverse effects.<sup>14</sup> Moreover, it is also administered in fewer

doses and a shorter total course of treatment which are both favorable. The drugs tend to be more effective and have less adverse effect on children compared to adults. The most common side effects for benznidazole are allergic dermatitis, peripheral neuropathy, headache, and weight loss.<sup>25</sup> For nifurtimox, most patients complain about gastrointestinal side effects that are usually mild.<sup>26</sup>

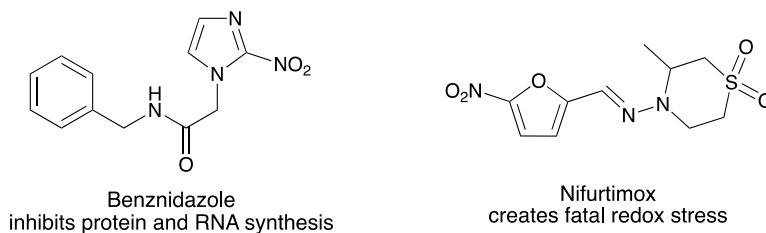


**Figure 1-2:** Structures of the two approved clinical treatments for Chagas disease.

Unfortunately, there is no currently available vaccine or drug to prevent the transmission of the disease to humans. There have been several recombinant DNA and protein vaccines, as well as live attenuated parasite vaccines, that provide some protection; however, there is none of these are in the clinical phase.<sup>27,28</sup> The main approach to prevent the spread of the disease is still vector control, which includes improvement of houses, application of insecticides and increase of disease awareness.<sup>29,30</sup> Non-endemic countries, where the main mode of transmission is through blood transfusion, have increase blood screening process in blood banks.<sup>31</sup>

## 1.2 *T. cruzi* cell surface

*Trypanosoma cruzi* interacts with its mammalian and insect hosts mostly through its cell surface.<sup>32</sup> *T. cruzi* undergoes multiple transformations during its life cycle between hosts and each stage has differences in the composition and function of their surface, especially surface membrane proteins. Due to growing interest in the importance of cell surface proteins of *T. cruzi*, multiple

proteins have been discovered and studied by immunological methods, lectin binding, and electrophoresis. The parasite surface has mucin-like molecules that contain sugar residues like glycosylphosphatidylinositol-anchored molecules and free glycosylphosphatidylinositol glycolipids.<sup>33</sup> These molecules perform key roles in the parasite's infectivity and survivability by modulation of immune response from the host. Another group of cell surface proteins are enzymes with trans-sialidase and/or neuraminidase functions.<sup>34,35</sup> These enzymes can cleave terminal sialic acid residues from host donor glycans followed by their transfer onto parasite surface proteins. This is important because trypanosomes cannot biosynthesize sialic acid. The newly sialylated surface of the parasite provides a blanket of protection from the mammalian immune system and helps for its survivability inside the hosts. It is also suggested that neuraminidases cleave off sialic acids from molecules in the host-cell or the parasite, which are vital for the internalization of the parasite.

Multiple stage-specific glycoproteins on the *T. cruzi* cell surface have been discovered. Examples include GP85 from tissue culture trypomastigotes,<sup>36</sup> GP82 from metacyclic trypomastigotes<sup>37</sup> and amastin from amastigotes.<sup>38</sup> Another stage specific glycoprotein that has been relatively more widely studied is the epimastigote specific glycoprotein GP72.<sup>39</sup> GP72 is essential to the parasite's morphology and infectivity.<sup>40-45</sup> In addition, this glycoprotein is recognized by monoclonal antibody, WIC29.26, which prevents the transformation of non-infectious epimastigotes to human infectious metacyclic trypomastigotes.<sup>39</sup>

### **1.2.1 Glycoprotein GP72**

Glycoprotein GP72 is a 72 kDa molecular weight *T. cruzi* cell surface glycoprotein.<sup>46</sup> It was initially thought to be only found in the epimastigote stage of the parasite but was later shown

to be present in all stages, but lacking the glycan epitope recognized by WIC29.26 mAb.<sup>47</sup> It is not widely abundant, only accounting to about 4% of the cell surface's glycoproteins, but it is distributed broadly on the cell surface of the parasite as well as the flagellum adhesion zone.<sup>43,47</sup>

### **1.2.1.1 Recognition of GP72 by WIC29.26 mAb**

The glycoprotein was first described and isolated after immunoprecipitation with WIC29.26, a carbohydrate recognizing monoclonal antibody produced by immunization with *T. cruzi* epimastigotes. The binding of WIC29.26 mAb with GP72 prevents the conversion of the epimastigote form to the metacyclic trypomastigotes, the human infectious form.<sup>39</sup> It was hypothesized that this interaction was analogous to the interaction between GP72 and a lectin in the midgut of the insect host. This interaction could similarly prevent the transformation of the epimastigotes to metacyclic trypomastigotes. Consequently, the loss of this interaction when the epimastigotes moved to the hindgut of the insect permits the differentiation to metacyclic trypomastigote form.<sup>48–50</sup>

### **1.2.1.2 Role of GP72 in *T. cruzi* morphology**

About a decade after the first description of GP72, the GP72 gene knockout *T. cruzi* cell line was produced by targeted gene replacement.<sup>40</sup> This *T. cruzi* GP72 null mutant is shown not able to produce GP72 peptide but not the glycan epitope that WIC29.26 mAb recognizes, as the said epitope was found in other glycoproteins. Remarkably, the null mutant epimastigotes were found to have its flagellum detached from its body and its shape altered when examined under a scanning and transmission electron microscope. It was also seen that the anterior end of the GP72 null mutant parasite is shorter and broader than that of the wild type. The unusual morphology of

the flagella of the epimastigotes also affected the parasites' mobility as the null mutants were observed to descend faster than the wild type mutants in a liquid culture.<sup>40</sup>

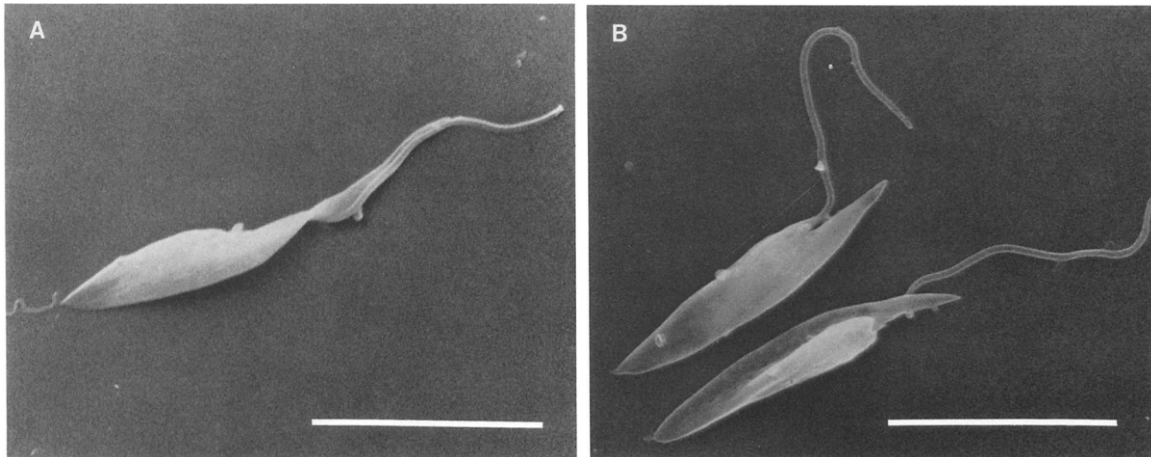


**Figure 1-3:** Scanning electron micrographs of wild type (A) and GP72 null mutant (B) *T. cruzi* epimastigotes showing difference in the protozoan's flagellum morphology. Reprinted with permission from the Rockefeller University Press: *J Cell Biol* **1993**, *122*: 149–156.

To ensure that the observed change in morphology is due to the absence of GP72 and not to possible changes in other protein expression after targeted gene replacement, a functional complementation of the GP72 null mutant was performed by reinserting a GP72 gene. The mutant with the restored GP72 gene was found to have a restored morphology suggesting that the loss of GP72 is responsible for the change in parasite's morphology in the previous null mutant. The restoration of the morphology greatly correlated with the amount of WIC29.26 mAb glycan epitope but not the GP72 glycopeptide implying that only a properly glycosylated GP72 is able to function properly.<sup>47,51</sup>

### **1.2.1.3 GP72 can induce a protective immune response.**

In a study done by Snary, two *T. cruzi* cell surface glycoproteins, GP90 and GP72, were tested using a mice model to examine whether immunization with these glycoproteins provides protection against a lethal dose of the parasite. The mice immunized with the glycoproteins produced high antibody levels against the glycoproteins compared to the control. The immunized mice were then given a lethal dose of metacyclic or blood trypomastigotes. All normal mice died after 20 days when injected with metacyclic trypomastigotes while those mice immunized with the glycoproteins survived the threat and had reduced blood parasite levels. GP90 immunization was more effective than GP72 as mice immunized with GP90 had lower blood parasite counts and cleared the parasite in shorter period. On the other hand, only the mice immunized with GP90 survived with lowered blood parasite level when challenged with blood trypomastigotes. All the other mice, including those immunized with GP72, died with the blood trypomastigote challenge. This difference can be attributed to the glycoproteins' stage specificity. GP72 is found on insect-derived stages of *T. cruzi* and thus only gave protection against the insect-derived metacyclic trypomastigote. On the other hand, GP90 is found in all stages of the parasite and can protect against metacyclic and blood trypomastigote challenges. The authors also found that antibodies recognizing GP72 and GP90 are present in the sera of Chagas patients. Antibodies against GP72 are more abundant in the sera of patients in the acute phase of the disease while antibodies against GP90 are more abundant in the sera of patients in the chronic phase of the disease.<sup>46</sup>

### **1.2.1.4 GP72 and its role in *T. cruzi* infectivity**

Glycoprotein GP72 is also important for the infectivity of *T. cruzi* on insect and mammalian hosts. Using a GP72 null mutant<sup>40</sup>, the group of Cross showed that the absence of the GP72 gene

and glycoprotein decreases the infectivity of *T. cruzi* to its hosts. In the insect host, a significant decrease of parasite level was found in the feces or urine of *T. infestans* when the insects were fed with the mutant compared to those fed with the wild type. The parasite level of the wild-type was found to increase 360-fold vs two-fold in the GP72 mutant. Mice models were used to determine the effect of the absence of GP72 on the infectivity level of *T. cruzi* on mammalian hosts. Mice infected with null mutant complement-resistant forms show no circulating trypomastigotes after a microscopic detection unlike those mice infected with the wild type. PCR and hemocultures were also consistently negative for the presence of the parasite in the mice infected with the null mutant. When immunocompromised mice were used instead, all animals showed high parasite levels and died within 35 days after challenge with the wild-type strain. On the other hand, only four out of 16 mice inoculated with the null mutant gave a positive hemoculture results. Interestingly, the parasite recovered from the mice conserved their mutant flagellar morphology and was found to still not be able to infect immunocompetent mice. Overall, it was shown that the GP72 null mutants have decreased infectivity in both the insect and mice hosts.<sup>45</sup>

The protective capability of the mutant strain was also tested by immunizing adult mice with one dose of  $10^6$  of wild-type or mutant epimastigotes followed by a low  $10^3$  dose of a blood trypomastigote after ten days. Both animal groups, vaccinated with wild-type and mutant, showed a significant decline of the parasite count compared to non-immunized mice. Despite the low infectivity of the mutant compared to that of the wild-type, there is practically no difference in the protection they provide against a low level challenge of a virulent strain.<sup>45</sup> This result shows a possibility of using *T. cruzi* genetically attenuated parasites as a vaccine against the disease.<sup>27</sup>

### 1.3 Structure of antigenic epitope of GP72

GP72 has a very high carbohydrate content composing around 50% of the glycoprotein by weight.<sup>52,53</sup> The epitope WIC29.26 mAb recognizes is a glycan structure anchored to the protein via threonine (Thr) and serine (Ser) residues.<sup>52</sup> Further studies have shown that the glycan components are connected to the Thr and Ser residues via phosphodiester linkages. An initial and partial structure of the epitope was suggested by Ferguson and coworkers in 1996 to contain a Gal $\beta$ -dHex-dHex-(Gal $\beta$ )-(P-Gal $\beta$ )Xyl-Xyl-OH substructure with phosphorylation in one or two of the Gal $\beta$  residues.<sup>55</sup> This structure was revised by the same group two decades later.

The antigenic glycan epitope was first purified from pronase-digested glycoprotein GP72 by affinity chromatography using a WIC29.26–Sepharose column. The antigenic glycan epitope was released from the peptides by treatment with aqueous HF. The monosaccharide composition and their absolute configuration was determined using GCMS analysis of derivatized monosaccharides from the glycans. The connectivity of the sugars was determined by methylation linkage analysis, several 2D NMR experiments such as COSY, TOCSY, and ROESY and tandem MS-MS analysis. The full glycan epitope structure is shown in Figure 1-4.<sup>56</sup> The full antigenic epitope is a 13-residue glycan composed of six monosaccharides connected in seven different linkages. The reducing terminal D-GlcNAc residue is believed to be linked to a Thr/Ser residue via phosphodiester bond and was assumed to be in alpha-anomeric linkage as a similar linkage was found in related *D. discoidium* proteinase I.<sup>57</sup> Another interesting structural detail of the glycan epitope is the presence of the fully glycosylated or ‘hyper-branched’ L-fucose and D-xylose core moieties, shaded in Figure 1-4. This kind of extensive branching in naturally occurring glycans is extremely rare and can only be found in a handful of structures. Ferguson also suggested that the glycan could possibly exist as phosphosaccharide repeats. The mature GP72 polypeptide has a

molecular mass of 59.4 kDa and that of the complete glycan epitope is ~2 kDa. Because the fully glycosylated GP72 is 50% carbohydrate by weight, it is estimated that each glycopeptide may contain up to 30 units of the glycan. The domain containing Thr/Ser residues predicted to be probable sites of attachment contains only 18 sites (17 Thr and 1 Ser residues), thus leading to the suggestion of phosphosaccharide repeats. This is further supported by the fact that a substantial ratio of terminal Galp residues are phosphorylated and hence, a possible point of connection for the phosphodiester bond with another reducing GlcNAc residue. With all the structural complexities and possible formation of repeats, this eukaryotic carbohydrate structure is considered as one of the most intricate protein-linked glycans ever described in the literature.<sup>56</sup>

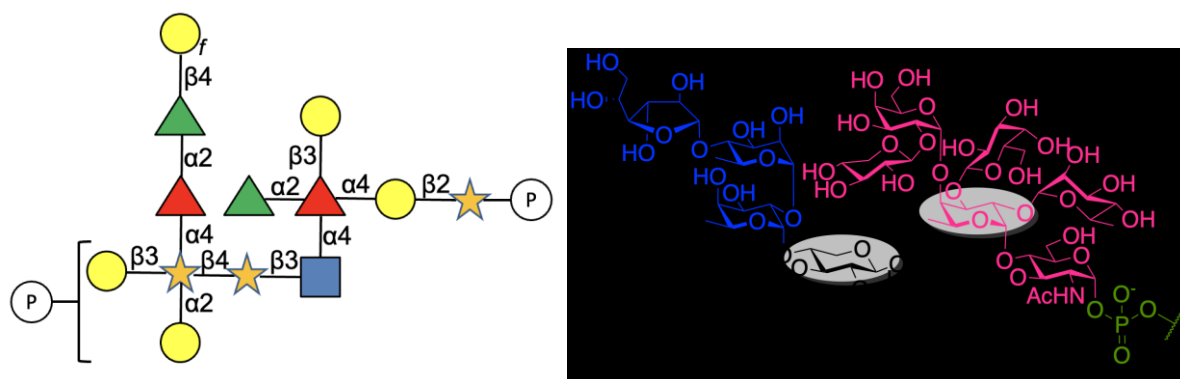


**Figure 1-4:** Structure of the WIC29.26 mAb glycan epitope found in *T. cruzi* GP72 glycoprotein in both pictorial and line-bond form. The ‘hyper-branched’ L-fucose and D-xylose residues are shaded in gray.

#### 1.4. Synthesis of highly congested oligosaccharides

As detailed below, my thesis topic is the synthesis of the GP72 glycan and some fragments. In developing a strategy to achieve these goals, I anticipated that the primary challenge would be the preparation of the ‘hyper-branched’ L-fucose and D-xylose residues. Unlike the synthesis of

other oligomeric biomolecules like peptides and nucleotides, the synthesis of carbohydrates is complicated not only by anomeric stereoisomerism but also the possibility of chain branching.<sup>58,59</sup> More branching in carbohydrate structures would require an increase in the number of orthogonal protecting groups during synthesis.<sup>59</sup> In addition to this, steric crowding among glycosylation partners can lead to low or no yields during reactions.

The synthesis of these highly sterically congested motifs like that in GP72 would require the correct glycosylation sequence to produce the desired products in good yields and stereoselectivity, if not the product might not be obtained at all.<sup>60-65</sup> In this section, I will discuss previous reports on synthesis of these highly branched sugar molecules (Figure 1-5) and the strategies employed by other investigators to overcome challenging synthetic problems.

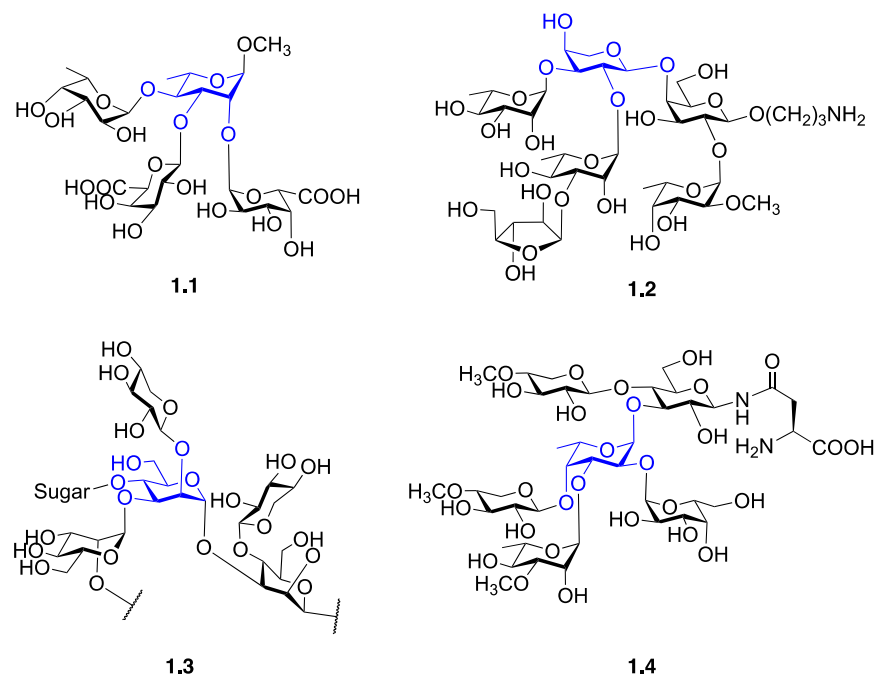
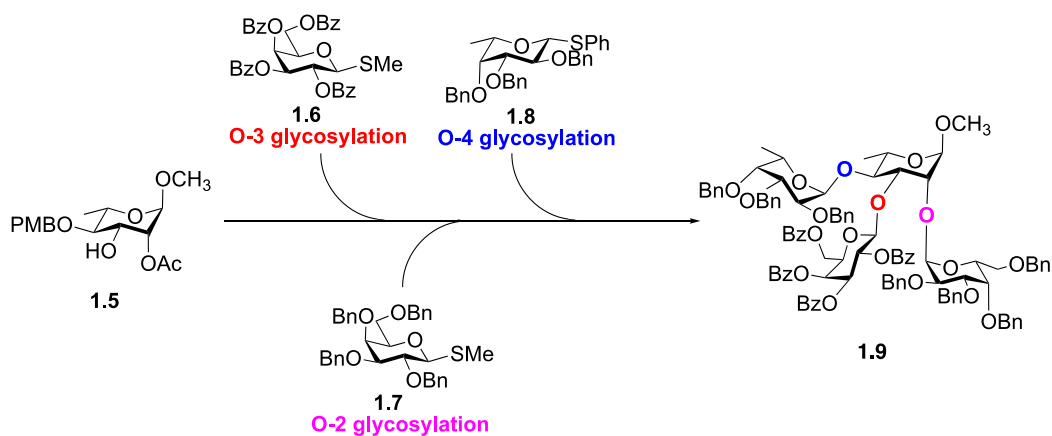


**Figure 1-5:** Structures of highly branched carbohydrate residues **1.1–1.4**, which have been previously synthesized.

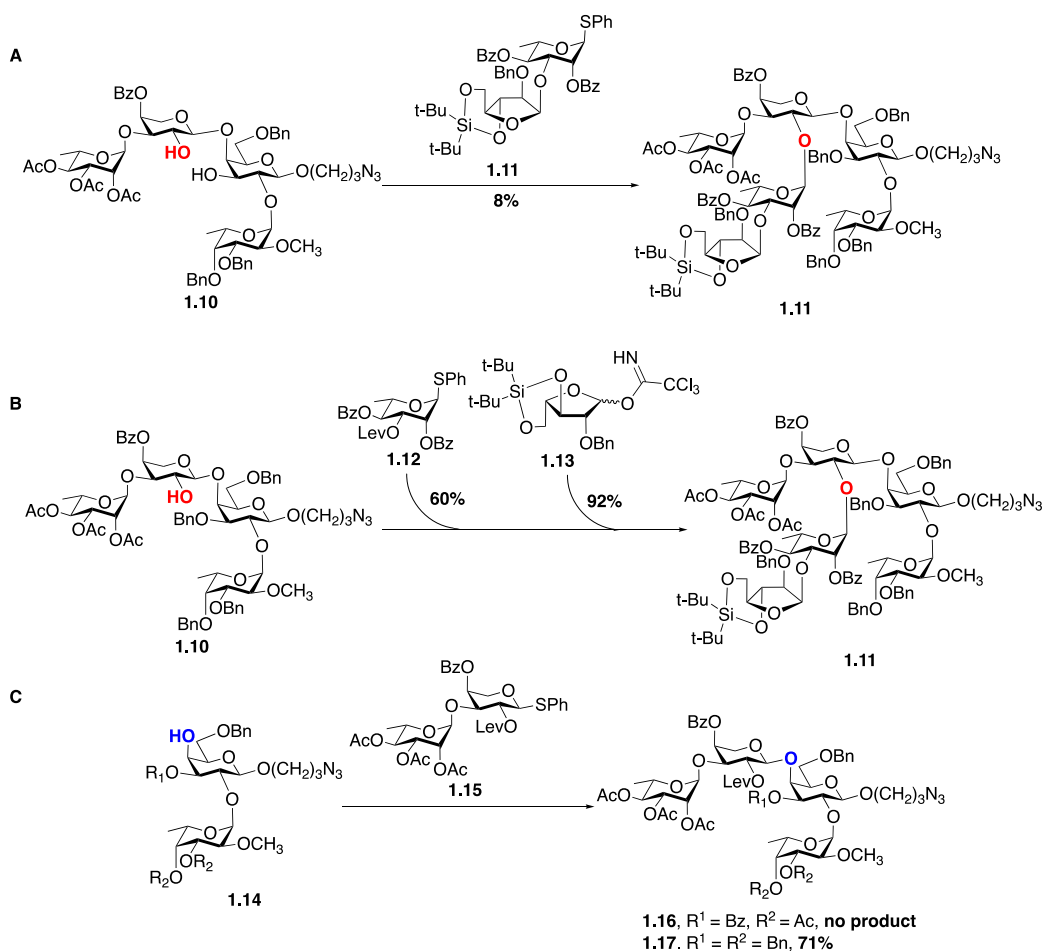
Rhamnogalacturonan (RGII) is an extremely complex polysaccharide found in plants composed of four distinctly different oligosaccharide side chains A–D. One of the side chains, side chain A, has a particularly interesting motif in which a core rhamnose is fully glycosylated in all its hydroxyl group. In 2005, the group of Field reported the synthesis of a tetrasaccharide fragment from side chain A containing the ‘hyper-branched’ rhamnose (Scheme 1-1). The strategy used was to employ the least number of steps and protecting group manipulation during the synthesis. The glycosylation sequence employed was to add monosaccharide first on O-3 followed by O-2 and lastly, on O-4.<sup>66</sup>



**Scheme 1-1:** Synthesis of side chain A rhamnogalacturonan (RGII) tetrasaccharide **1.9** by sequential addition of monosaccharide donors.

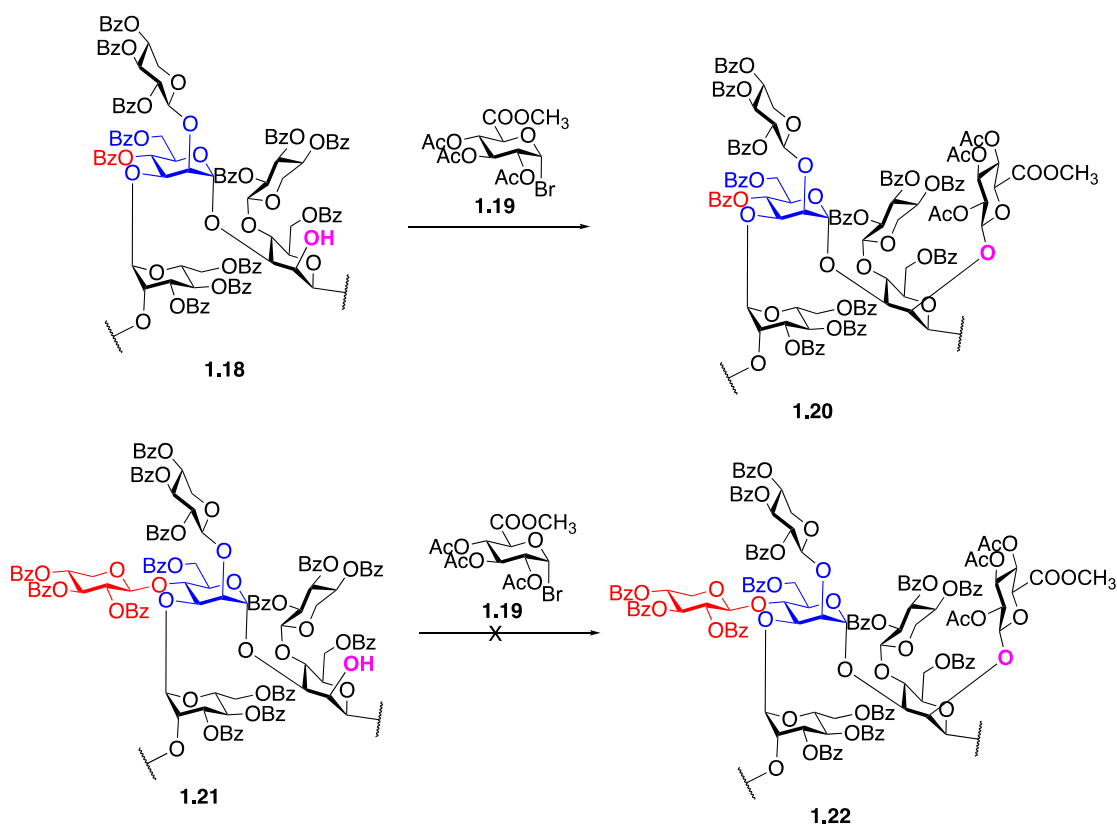
Another side chain of RGII, side chain B, also possesses a branched non-reducing arabinopyranose that is glycosylated at O-2 and O-3 positions. Boons and co-workers have reported the synthesis of a hexasaccharide fragment containing this rhamnose moiety derived from side chain B. When a [4+2] glycosylation was attempted, the desired hexasaccharide **1.11** was only obtained in low yield (Scheme 1-2A). The decision to employ a linear addition of the monosaccharides was found to be more efficient, yielding to the desired hexasaccharide in higher

yields (Scheme 1.2B). This shows that the size of the coupling partners is important in synthesizing highly congested molecules and the sequence that they are added is significant to obtain products in good yield. Another reaction in this paper shows how the reactivity of an acceptor can be improved by changing non-participating and distant protecting groups in the acceptor molecule. A [2+2] glycosylation was found to be only successful when the electron-withdrawing acetyl ester groups in the acceptor is replaced by benzyl ether groups (Scheme 1.2C).<sup>65</sup>



**Scheme 1-2:** Synthesis of a RGII side chain B fragment. A) Synthesis of **1.11** via [4+2] glycosylation; B) Synthesis of **1.11** through a linear addition of monosaccharide donors; C) The effect of protecting groups in the reactivity of an acceptor during the synthesis of tetrasaccharide **1.16** or **1.17**.

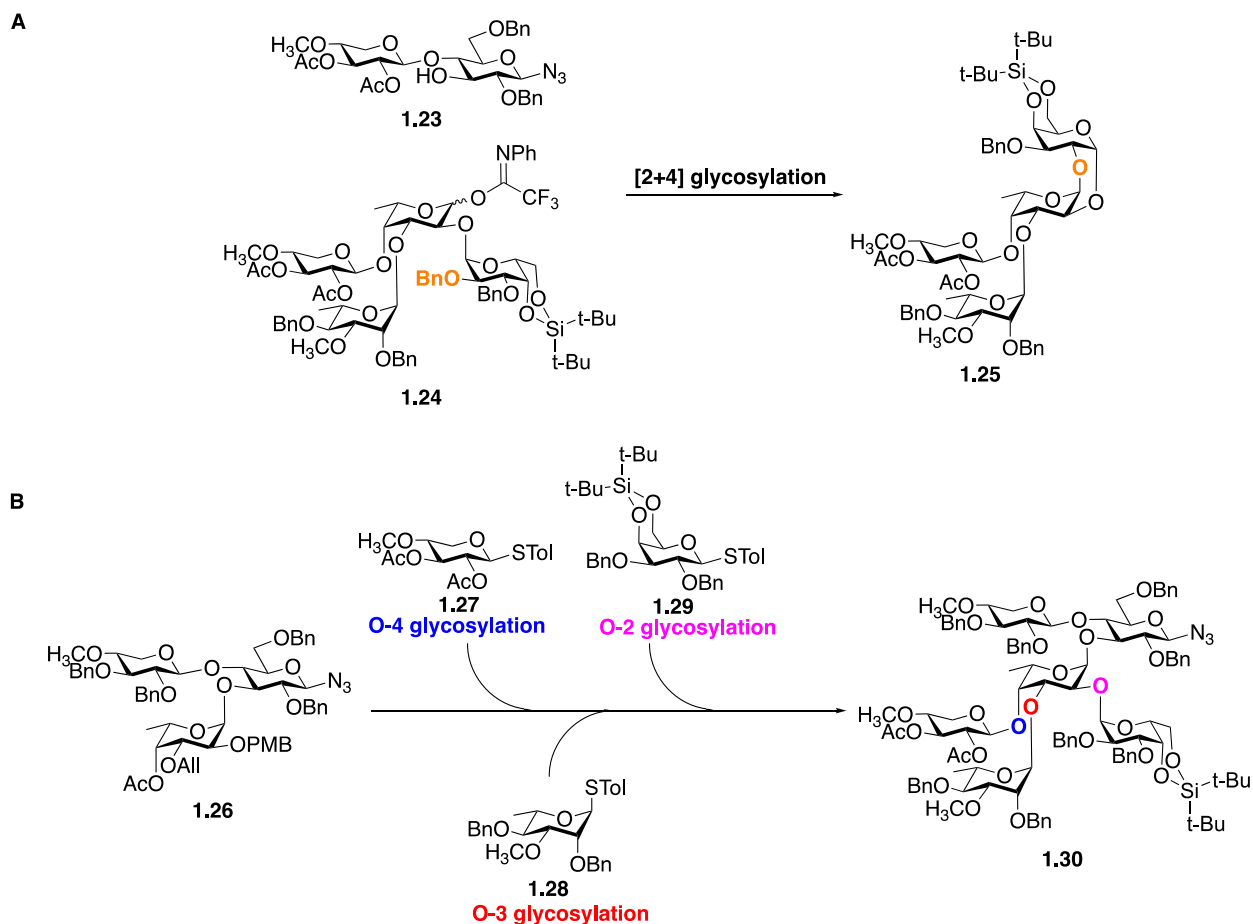
Another interesting example is the work of Kong and co-workers in their attempt to synthesize a 2,3,4-trisubstituted mannose residue from *Cryptococcus neoformans* serotype C capsular polysaccharide. The presence of a sugar residue, even distant from the glycosylation site, affected the result of the reaction. The presence of xylose vs a benzoyl group at C-4 of a mannose residue affects the reactivity of the hydroxyl group at C-2 of the other mannose residue (Scheme 1-3). It was speculated that there is an increase in steric crowding around the reacting hydroxyl group due to a change in the conformation of the acceptor when xylose is present instead of benzoyl.<sup>63,64</sup>



**Scheme 1-3:** Synthesis of a highly congested mannose residue in *C. neoformans*.

One of the examples of the synthesis of ‘hyper-branched’ sugar molecules is the work of Lin and co-workers in their syntheses of highly branched *N*-glycans from chlorella viruses.<sup>60</sup> The

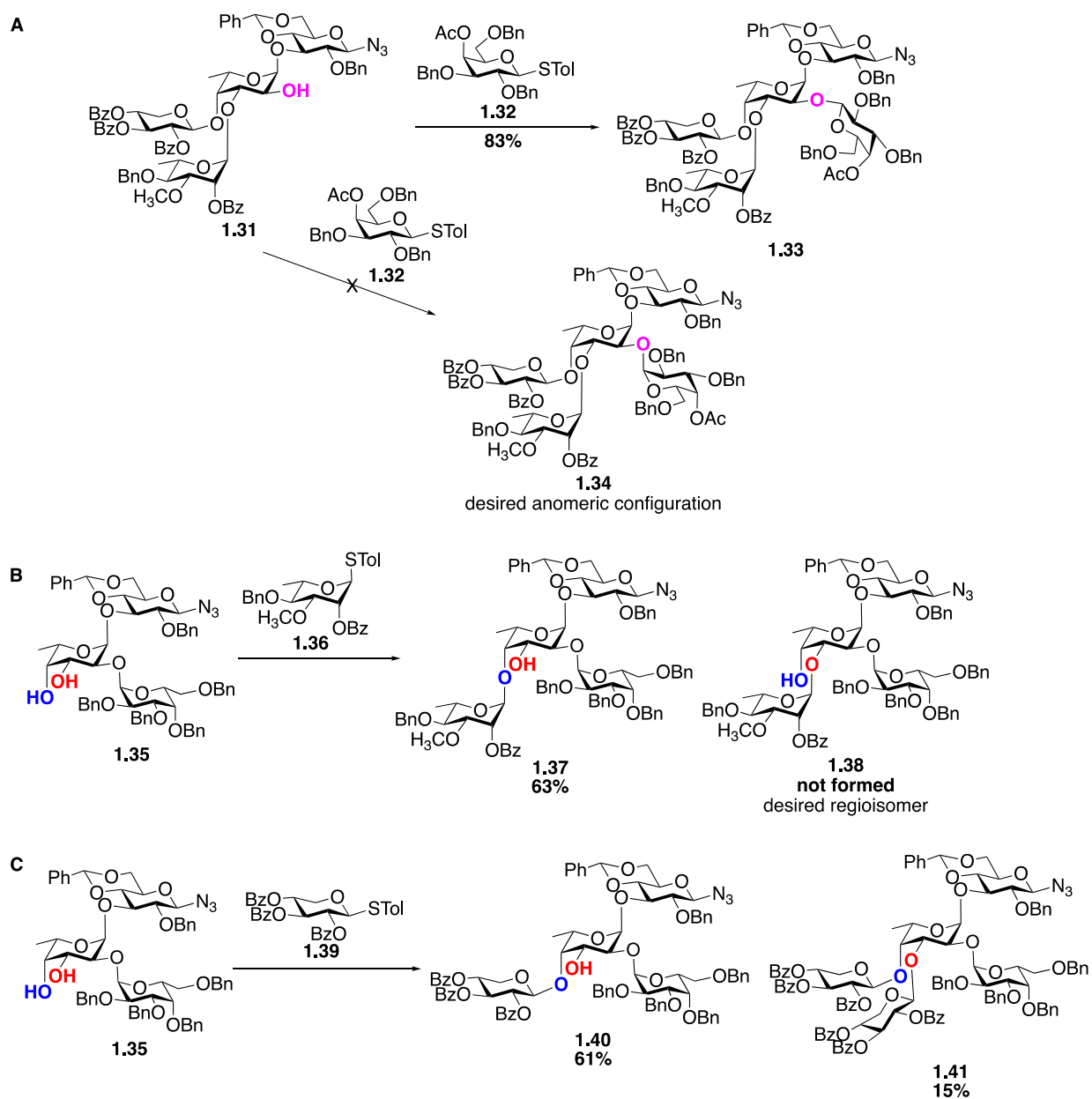
group synthesized a highly branched hexasaccharide structure found in *Acanthocystis turfacea* chlorovirus 1 (ACTV-1), which contains the conserved pentasaccharide present in all reported *N*-glycans produced by chlorella virus.<sup>67,68</sup> The first approach employed was a convergent [2+4] reaction between acceptor **1.23** and imidate donor **1.24** to access the hexasaccharide core (Scheme 1-4A). Unfortunately, when attempted, it was found that the reaction was unsuccessful, and the by-product **1.25** was obtained in 61% yield. This by-product was formed after the O-2 of the nearby galactose residue acts as a nucleophile and reacts with the oxocarbenium ion intermediate followed by the loss of a benzyl group. It is hypothesized that this intramolecular reaction occurred due to steric congestion in the highly branched donor **1.24** forcing an internal nucleophile to attack the oxocarbenium ion. The synthesis of the hexasaccharide **1.30** was successful following a linear synthetic strategy employing a fucose residue with three orthogonal protecting groups which would allow a versatile strategy in accessing several glycosylation sequences possible. The glycosylation sequence that gave the desired product was through a ‘counterclockwise’ addition of the monosaccharides around the fucose residue (Scheme 1-4B). The rationalization behind the success of this approach is the need to initially perform the glycosylation at the least reactive axial O-4. The addition of the monosaccharide at O-3 before O-2 was done considering that the opposite sequence would create a sterically hindered acceptor with two sugar units surrounding it.



**Scheme 1-4:** Synthesis of ACTV-1 hexasaccharide fragment **1.30** by Lin and Lowry. A) A convergent [2+4] glycosylation leads to an intramolecular reaction in the donor; B) Successful synthesis of a ‘hyper-branched’ fucose residue by ‘counterclockwise’ addition of sugar building blocks.

Another synthesis of the same ACTV-1 hexasaccharide by Ye and co-workers have shown a different glycosylation sequence in accessing the ‘hyper-branched’ fucose.<sup>62</sup> When trying to access the ‘hyper-branched’ fucose through a late stage O-2 glycosylation, it was found that the product obtained, though in high yield, bears the wrong  $\beta$ -configuration instead of the desired  $\alpha$ -configuration on the galactose moiety (Scheme 1-5A). This result shows that steric crowding can

also alter the stereoselectivity of glycosylation reactions. To circumvent this problem, it was strategized to perform O-2 glycosylation first followed by either O-3 or O-4. It was initially thought that the reactivity of the hydroxyl group at C-3 position is better than the one in C-4 hence their initial decision to do a regioselective glycosylation to a diol acceptor. However, the expected reactivity is reversed, and this could be attributed to the steric hindrance provided by the galactose residue at O-2 of the fucose acceptor (Scheme 1-5B). Knowing this reactivity, an initial O-4 glycosylation was found to be regioselective with a xylosyl donor to obtain **1.40** albeit with minor formation of di-O-glycosylation product **1.41**. It should be noted that they attached the proximal xylose moiety onto the reducing glucose moiety at the final stages of the synthesis.



**Scheme 1-5:** Synthesis of ACTV-1 congested glycans by Wang et. al. A) Glycosylation on a congested tetrasaccharide acceptor **1.31** yields to a product **1.33** with the incorrect anomeric configuration; B) The desired regioisomer **1.38** was not obtained after reversal of reactivity due to steric hindrance; C) The reversal of reactivity is used to obtain target tetrasaccharide **1.40** as the major product.

The counterclockwise approach formulated by Lin and co-workers was also applicable to the synthesis of a larger nonasaccharide *N*-glycan found in *Paramecium bursaria* chlorella virus 1 (PBCV-1), which bears the same hexasaccharide from ACTV-1. In the synthesis of this glycan, the counterclockwise approach was successful in accessing the ‘hyper-branched’ fucose moiety even if the glycosylation donors are larger than monosaccharide units.<sup>61</sup>

The examples given from above show the complexity of the structure and the synthesis of these highly congested and branched oligosaccharide targets. Yet, these examples have shown that through careful design of strategies and methodologies, these compounds could be synthesized in good yields and stereocontrol. The main hurdle in the synthesis of these congested oligosaccharide fragments is the increasing steric hindrance in the molecule after every glycosylation step. It leads to weak reactivity, formation of unwanted by-products and low stereocontrol. In addition, choosing the correct protecting groups and ensuring orthogonality among protecting groups is important during the synthesis of these molecules. Lastly, it is important to create a synthetic plan that is flexible, versatile, and adaptable to proficiently explore each glycosylation sequence possible during the synthesis.

### **1.5 Research objective – Synthesis of glycan fragments of the ‘hyper-branched’ WIC29.26 mAb glycan epitope from *T. cruzi* GP72**

The complex structure of the immunogenic glycan epitope from GP72 is important to the glycoprotein’s function, the parasite’s morphology and infectivity, and Chagas disease’s pathogenesis. The goal of this thesis research is to develop methods for the chemical synthesis of this glycan structure. The presence of the two ‘hyper-branched’ sugar residues is anticipated to pose a significant challenge in synthesizing the glycan structure. The proper chemical

glycosylation sequences would be essential to obtain these highly congested carbohydrate targets in good yield and stereoselectivity. The main aims of these research projects are: 1) synthesize smaller fragments of the glycan by developing versatile and efficient synthetic methodologies to obtain the ‘hyper-branched’ sugar residues. 2) synthesize the whole glycan epitope by using the strategies applied in creating the smaller fragments. 3) investigate the binding specificity of the antibody towards the glycan by performing binding analysis using the synthetic fragments.

**Aim 1.** The first aim is to synthesize the smaller fragments derived from the antigenic glycan epitope of GP72. In Chapter 2, I will describe my work on the synthesis of these fragments and the strategies employed. The structures of the small fragments are shown as below (Figure 1-6). The synthesis of hexasaccharide **2.2** and heptasaccharide **2.3** are of greater importance and challenge as these fragments each contain a ‘hyper-branched’ residue. I expected that the synthesis of these smaller fragments would shed some light on how to create sterically-congested sugar moieties using versatile methodologies.

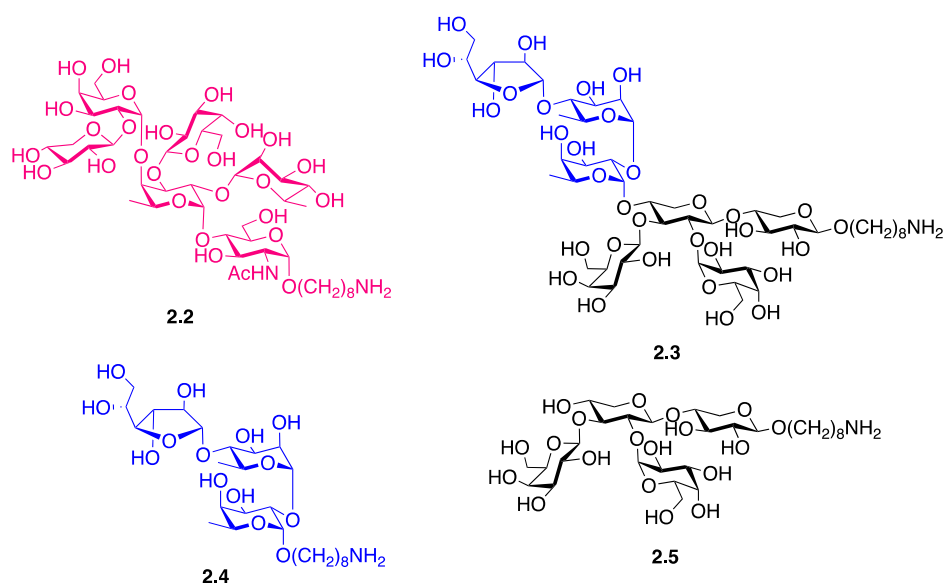


**Figure 1-6:** Structures of target fragments derived from the immunogenic glycan epitope from GP72.

**Aim 2.** The second aim is to synthesize the whole antigenic glycan epitope of GP72. In Chapter 3, I will describe my work on my efforts in synthesizing the whole tridecasaccharide structure GP72, which contains the two ‘hyper-branched’ residue (Figure 1-7). The synthetic route employed in this effort is an application of the methodologies from the previous chapter.

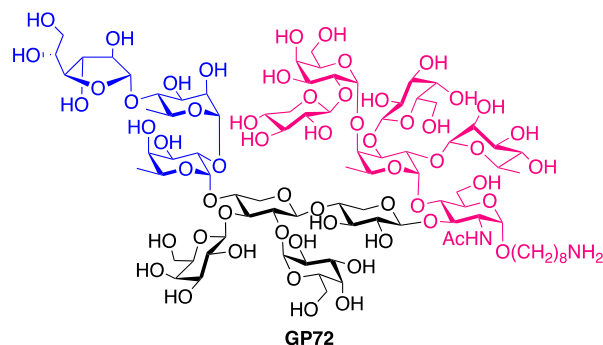


**Figure 1-7:** Structure of the target immunogenic glycan epitope from GP72.

**Aim 3.** The third aim is to find some insights on the glycan-antibody interaction by doing some binding analysis between the synthesized smaller fragments and the WIC29.26 mAb. These analyses were done using Bio-layer Interferometry (BLI) in an OctetRed96 machine. An additional dot blot assay was also performed to qualitatively analyze binding between the glycans and the mAb. The antibody sample was provided by the group of Dr. Michael Ferguson from the University of Dundee, UK.

## 1.6 References

- (1) *Chagas disease (American trypanosomiasis)*. <https://www.who.int/health-topics/chagas-disease>.
- (2) Mathers, C. D.; Ezzati, M.; Lopez, A. D. Measuring the Burden of Neglected Tropical Diseases: The Global Burden of Disease Framework. *PLoS Negl Trop Dis* **2007**, *1* (2), e114.
- (3) Moncayo, Á.; Silveira, A. C. Current Epidemiological Trends of Chagas Disease in Latin America and Future Challenges. In *American Trypanosomiasis Chagas Disease*; Elsevier, 2017; pp 59–88.
- (4) Rassi, A.; Rassi, A.; Marin-Neto, J. A. Chagas Disease. *Lancet* **2010**, *375* (9723), 1388–1402.
- (5) Chagas, C. Nova Tripanozomíaze Humana: Estudos Sobre a Morfologia e o Ciclo Evolutivo Do *Schizotrypanum cruzi* n. Gen., n. Sp., Ajente Etiológico de Nova Entidade Morbida Do Homem. *Mem. Inst. Oswaldo Cruz* **1909**, *1* (2), 159–218.
- (6) Miranda-Arboleda, A. F.; Zaidel, E. J.; Marcus, R.; Pinazo, M. J.; Echeverría, L. E.; Saldarriaga, C.; Sosa Liprandi, Á.; Baranchuk, A.; On Behalf of the Neglected Tropical Diseases and other Infectious Diseases affecting the Heart (NET-Heart) project. Roadblocks in Chagas Disease Care in Endemic and Nonendemic Countries: Argentina, Colombia, Spain, and the United States. The NET-Heart Project. *PLoS Negl Trop Dis* **2021**, *15* (12), e0009954.
- (7) Manne-Goehler, J.; Umeh, C. A.; Montgomery, S. P.; Wirtz, V. J. Estimating the Burden of Chagas Disease in the United States. *PLoS Negl Trop Dis* **2016**, *10* (11), e0005033.

- (8) *Neglected tropical diseases -- GLOBAL*. <https://www.who.int/health-topics/neglected-tropical-diseases>.
- (9) *American Trypanosomiasis Chagas Disease: One Hundred Years of Research*, Second edition.; Telleria, J., Tibayrenc, M., Eds.; Elsevier: Amsterdam, Netherlands, 2017.
- (10) Kropf, S. P.; Sá, M. R. The Discovery of *Trypanosoma cruzi* and Chagas Disease (1908-1909): Tropical Medicine in Brazil. *Hist. cienc. saude-Manguinhos* **2009**, *16* (suppl 1), 13–34.
- (11) Ballesteros-Rodea, G.; Santillán, M.; Martínez-Calvillo, S.; Manning-Cela, R. Flagellar Motility of *Trypanosoma cruzi* Epimastigotes. *J. Biomed. Biotechnol.* **2012**, *2012*, 1–9.
- (12) Zingales, B.; Andrade, S.; Briones, M.; Campbell, D.; Chiari, E.; Fernandes, O.; Guhl, F.; Lages-Silva, E.; Macedo, A.; Machado, C.; Miles, M.; Romanha, A.; Sturm, N.; Tibayrenc, M.; Schijman, A. A New Consensus for *Trypanosoma cruzi* Intraspecific Nomenclature: Second Revision Meeting Recommends TcI to TcVI. *Mem. Inst. Oswaldo Cruz* **2009**, *104* (7), 1051–1054.
- (13) Martín-Escolano, J.; Marín, C.; Rosales, M. J.; Tsaousis, A. D.; Medina-Carmona, E.; Martín-Escolano, R. An Updated View of the *Trypanosoma cruzi* Life Cycle: Intervention Points for an Effective Treatment. *ACS Infect. Dis.* **2022**, *8* (6), 1107–1115.
- (14) Bern, C. Chagas Disease. *N Engl J Med* **2015**, *373* (5), 456–466.
- (15) Tyler, K. M.; Engman, D. M. The Life Cycle of *Trypanosoma cruzi* Revisited. *Int. J. Parasitol.* **2001**, *31* (5–6), 472–481.
- (16) Jansen, A. M.; Xavier, S. C. D. C.; Roque, A. L. R. *Trypanosoma cruzi* Transmission in the Wild and Its Most Important Reservoir Hosts in Brazil. *Parasite Vector* **2018**, *11* (1), 502.

- (17) De Oliveira, A. B. B.; Alevi, K. C. C.; Imperador, C. H. L.; Madeira, F. F.; Azeredo-Oliveira, M. T. V. D. Parasite–Vector Interaction of Chagas Disease: A Mini-Review. *Am. J. Trop. Med. Hyg.* **2018**, *98* (3), 653–655.
- (18) Álvarez-Hernández, D.-A.; Franyuti-Kelly, G.-A.; Díaz-López-Silva, R.; González-Chávez, A.-M.; González-Hermosillo-Cornejo, D.; Vázquez-López, R. Chagas Disease: Current Perspectives on a Forgotten Disease. *Rev. Med. Hosp. Gen. (Mex)* **2018**, *81* (3), 154–164.
- (19) Nunes, M. C. P.; Dones, W.; Morillo, C. A.; Encina, J. J.; Ribeiro, A. L. Chagas Disease. *J. Am. Coll. Cardiol.* **2013**, *62* (9), 767–776.
- (20) Malik, L. H.; Singh, G. D.; Amsterdam, E. A. The Epidemiology, Clinical Manifestations, and Management of Chagas Heart Disease: Chagas Heart Disease. *Clin Cardiol* **2015**, *38* (9), 565–569.
- (21) Clark, E. H.; Bern, C. Chagas Disease in People with HIV: A Narrative Review. *TropicalMed* **2021**, *6* (4), 198. <https://doi.org/10.3390/tropicalmed6040198>.
- (22) Suárez, C.; Nolder, D.; García-Mingo, A.; Moore, D. A.; Chiodini, P. L. Diagnosis and Clinical Management of Chagas Disease: An Increasing Challenge in Non-Endemic Areas. *RRTM* **2022**, *13*, 25–40.
- (23) Rajão, M. A.; Furtado, C.; Alves, C. L.; Passos-Silva, D. G.; De Moura, M. B.; Schamber-Reis, B. L.; Kunrath-Lima, M.; Zuma, A. A.; Vieira-da-Rocha, J. P.; Garcia, J. B. F.; Mendes, I. C.; Pena, S. D. J.; Macedo, A. M.; Franco, G. R.; De Souza-Pinto, N. C.; De Medeiros, M. H. G.; Cruz, A. K.; Motta, M. C. M.; Teixeira, S. M. R.; Machado, C. R. Unveiling Benznidazole’s Mechanism of Action through Overexpression of DNA

- Repair Proteins in *Trypanosoma cruzi*: Unveiling Benznidazole's Mechanism. *Environ. Mol. Mutagen.* **2014**, *55* (4), 309–321.
- (24) Page, S. W. Antiparasitic Drugs. In *Small Animal Clinical Pharmacology*; Elsevier, 2008; pp 198–260.
- (25) Miller, D. A.; Hernandez, S.; Rodriguez De Armas, L.; Eells, S. J.; Traina, M. M.; Miller, L. G.; Meymandi, S. K. Tolerance of Benznidazole in a United States Chagas Disease Clinic. *Clin. Infect. Dis.* **2015**, *60* (8), 1237–1240.
- (26) Forsyth, C. J.; Hernandez, S.; Olmedo, W.; Abuhamidah, A.; Traina, M. I.; Sanchez, D. R.; Soverow, J.; Meymandi, S. K. Safety Profile of Nifurtimox for Treatment of Chagas Disease in the United States. *Clin. Infect. Dis.* **2016**, *63* (8), 1056–1062.
- (27) Sánchez-Valdéz, F. J.; Pérez Brandán, C.; Ferreira, A.; Basombrío, M. Á. Gene-Deleted Live-Attenuated *Trypanosoma cruzi* Parasites as Vaccines to Protect against Chagas Disease. *Expert Rev. Vaccines* **2015**, *14* (5), 681–697.
- (28) Quijano-Hernandez, I.; Dumonteil, E. Advances and Challenges towards a Vaccine against Chagas Disease. *Hum. Vaccines* **2011**, *7* (11), 1184–1191.
- (29) Gürtler, R. E.; Kitron, U.; Cecere, M. C.; Segura, E. L.; Cohen, J. E. Sustainable Vector Control and Management of Chagas Disease in the Gran Chaco, Argentina. *Proc. Natl. Acad. Sci. U.S.A.* **2007**, *104* (41), 16194–16199.
- (30) Cucunubá, Z. M.; Nouvellet, P.; Peterson, J. K.; Bartsch, S. M.; Lee, B. Y.; Dobson, A. P.; Basáñez, M.-G. Complementary Paths to Chagas Disease Elimination: The Impact of Combining Vector Control with Etiological Treatment. *Clin. Infect. Dis.* **2018**, *66* (4), S293–S300.

- (31) Sosa-Estani, S.; Segura, E. L. Integrated Control of Chagas Disease for Its Elimination as Public Health Problem - A Review. *Mem. Inst. Oswaldo Cruz* **2015**, *110* (3), 289–298.
- (32) Pech-Canul, Á. D. L. C.; Monteón, V.; Solís-Oviedo, R.-L. A Brief View of the Surface Membrane Proteins from *Trypanosoma cruzi*. *J. Parasitol. Res.* **2017**, *2017*, 1–13.
- (33) Moura E Castro, F. A.; Soares, R. P.; Almeida, I. C.; Freitas, G. F.; Torrecilhas, A. C.; Romanha, A. J.; Murta, S. M.; Assis, R. R.; Rocha, M. N.; Santos, S. L.; Marques, A. F. Intraspecies Variation in *Trypanosoma cruzi* GPI-Mucins: Biological Activities and Differential Expression of  $\alpha$ -Galactosyl Residues. *Am. J. Trop. Med. Hyg.* **2012**, *87* (1), 87–96.
- (34) Eugenia Giorgi, M.; De Lederkremer, R. M. Trans-Sialidase and Mucins of *Trypanosoma cruzi*: An Important Interplay for the Parasite. *Carbohydr. Res.* **2011**, *346* (12), 1389–1393.
- (35) Campetella, O.; Buscaglia, C. A.; Mucci, J.; Leguizamón, M. S. Parasite-Host Glycan Interactions during *Trypanosoma cruzi* Infection: Trans-Sialidase Rides the Show. *BBA. Molecular basis of disease* **2020**, *1866* (5), 165692.
- (36) Mattos, E. C.; Tonelli, R. R.; Colli, W.; Alves, M. J. M. The Gp85 Surface Glycoproteins from *Trypanosoma cruzi*. In *Proteins and Proteomics of Leishmania and Trypanosoma*; Santos, A. L. S., Branquinha, M. H., d'Avila-Levy, C. M., Kneipp, L. F., Sodré, C. L., Eds.; Subcellular Biochemistry; Springer Netherlands: Dordrecht, 2014; Vol. 74, pp 151–180.
- (37) Cortez, C.; Sobreira, T. J. P.; Maeda, F. Y.; Yoshida, N. The Gp82 Surface Molecule of *Trypanosoma cruzi* Metacyclic Forms. In *Proteins and Proteomics of Leishmania and Trypanosoma*; Santos, A. L. S., Branquinha, M. H., d'Avila-Levy, C. M., Kneipp, L. F.,

- Sodré, C. L., Eds.; Subcellular Biochemistry; Springer Netherlands: Dordrecht, 2014; Vol. 74, pp 137–150.
- (38) Cruz, M. C.; Souza-Melo, N.; Da Silva, C. V.; DaRocha, W. D.; Bahia, D.; Araújo, P. R.; Teixeira, S. R.; Mortara, R. A. *Trypanosoma cruzi*: Role of  $\delta$ -Amastin on Extracellular Amastigote Cell Invasion and Differentiation. *PLoS ONE* **2012**, 7 (12), e51804.
- (39) Sher, A.; Snary, D. Specific Inhibition of the Morphogenesis of *Trypanosoma cruzi* by a Monoclonal Antibody. *Nature* **1982**, 300 (5893), 639–640.
- (40) Cooper, R.; De Jesus, A.; Cross, G. Deletion of an Immunodominant *Trypanosoma cruzi* Surface Glycoprotein Disrupts Flagellum-Cell Adhesion. *J. Cell Biol.* **1993**, 122 (1), 149–156.
- (41) Nozaki, T. Characterization of the *Trypanosoma brucei* Homologue of a *Trypanosoma cruzi* Flagellum-Adhesion Glycoprotein. *Mol. Biochem. Parasitol.* **1996**, 82 (2), 245–255.
- (42) Rocha, G. M.; Seabra, S. H.; De Miranda, K. R.; Cunha-e-Silva, N.; De Carvalho, T. M. U.; De Souza, W. Attachment of Flagellum to the Cell Body Is Important to the Kinetics of Transferrin Uptake by *Trypanosoma cruzi*. *Parasitol. Int.* **2010**, 59 (4), 629–633.
- (43) Rocha, G. M.; Brandão, B. A.; Mortara, R. A.; Attias, M.; De Souza, W.; Carvalho, T. M. U. The Flagellar Attachment Zone of *Trypanosoma cruzi* Epimastigote Forms. *J. Struct. Biol.* **2006**, 154 (1), 89–99.
- (44) Sunter, J. D.; Gull, K. The Flagellum Attachment Zone: ‘The Cellular Ruler’ of Trypanosome Morphology. *Trends Parasitol.* **2016**, 32 (4), 309–324.
- (45) Basombrío, M. A.; Gómez, L.; Padilla, A. M.; Ciaccio, M.; Nozaki, T.; Cross, G. A. M. Targeted Deletion of the Gp72 Gene Decreases The Infectivity of *Trypanosoma cruzi* for Mice and Insect Vectors. *para* **2002**, 88 (3), 489–493.

- (46) Snary, D. Cell Surface Glycoproteins of *Trypanosoma cruzi*: Protective Immunity in Mice and Antibody Levels in Human Chagasic Sera. *Trans. R. Soc. Trop. Med. Hyg.* **1983**, *77* (1), 126–129.
- (47) Haynes, P. A.; Russell, D. G.; Cross, G. A. M. Subcellular Localization of *Trypanosoma cruzi* Glycoprotein Gp72. *J. Cell Sci.* **1996**, *109* (13), 2979–2988.
- (48) Dobson, D. E.; Kamhawi, S.; Lawyer, P.; Turco, S. J.; Beverley, S. M.; Sacks, D. L. Leishmania Major Survival in Selective *Phlebotomus papatasi* Sand Fly Vector Requires a Specific SCG-Encoded Lipophosphoglycan Galactosylation Pattern. *PLoS Pathog* **2010**, *6* (11), e1001185.
- (49) Kamhawi, S.; Modi, G. B.; Pimenta, P. F. P.; Rowton, E.; Sacks, D. L. The Vectorial Competence of *Phlebotomus sergenti* Is Specific for *Leishmania tropica* and is Controlled by Species-Specific, Lipophosphoglycan-Mediated Midgut Attachment. *Parasitology* **2000**, *121* (1), 25–33.
- (50) McConville, M. J.; Turco, S. J.; Ferguson, M. A.; Sacks, D. L. Developmental Modification of Lipophosphoglycan during the Differentiation of Leishmania Major Promastigotes to an Infectious Stage. *The EMBO Journal* **1992**, *11* (10), 3593–3600.
- (51) Nozaki, T.; Cross, G. A. M. Functional Complementation of Glycoprotein 72 in a *Trypanosoma cruzi* Glycoprotein 72 Null Mutant. *Molecular and Biochemical Parasitology* **1994**, *67* (1), 91–102.
- (52) Ferguson, M. A. J.; Allen, A. K.; Snary, D. Studies on the Structure of a Phosphoglycoprotein from the Parasitic Protozoan *Trypanosoma cruzi*. *Biochem. J.* **1983**, *213* (2), 313–319.

- (53) Ferguson, M. A. J.; Snary, D.; Allen, A. K. Comparative Compositions of Cell Surface Glycoconjugates Isolated from *Trypanosoma cruzi* Epimastigotes. *BBA - General Subjects* **1985**, *842* (1), 39–44.
- (54) Cooper, R.; Inverso, J. A.; Espinosa, M.; Nogueira, N.; Cross, G. A. M. Characterization of a Candidate Gene for GP72, an Insect Stage-Specific Antigen of *Trypanosoma cruzi*. *Mol. Biochem. Parasitol.* **1991**, *49* (1), 45–59.
- (55) Haynes, P. A.; Ferguson, A. J.; Cross, G. A. M. Structural Characterization of Novel Oligosaccharides of Cell-Surface Glycoproteins of *Trypanosoma cruzi*. *Glycobiology* **1996**, *6* (8), 869–878.
- (56) Allen, S.; Richardson, J. M.; Mehlert, A.; Ferguson, M. A. J. Structure of a Complex Phosphoglycan Epitope from Gp72 of *Trypanosoma cruzi*. *J. Biol. Chem.* **2013**, *288* (16), 11093–11105.
- (57) Gustafson, G. L.; Milner, L. A. Occurrence of *N*-Acetylglucosamine-1-Phosphate in Proteinase I from *Dictyostelium discoideum*. *J. Biol. Chem.* **1980**, *255* (15), 7208–7210.
- (58) Das, R.; Mukhopadhyay, B. Chemical O-Glycosylations: An Overview. *ChemistryOpen* **2016**, *5* (5), 401–433.
- (59) Ágoston, K.; Streicher, H.; Fügedi, P. Orthogonal Protecting Group Strategies in Carbohydrate Chemistry. *Tetrahedron: Asymmetry* **2016**, *27* (16), 707–728.
- (60) Lin, S.; Lowary, T. L. Synthesis of the Highly Branched Hexasaccharide Core of Chlorella Virus *N*-Linked Glycans. *Chem. Eur. J.* **2018**, *24* (64), 16992–16996.
- (61) Lin, S.; Lowary, T. L. Synthesis of a Highly Branched Nonasaccharide Chlorella Virus *N*-Glycan Using a “Counterclockwise” Assembly Approach. *Org. Lett.* **2020**, *22* (19), 7645–7649.

- (62) Wang, Y.; Wu, Y.; Xiong, D.; Ye, X. Total Synthesis of a Hyperbranched *N*-Linked Hexasaccharide Attached to ATCV-1 Major Capsid Protein without Precedent. *Chin. J. Chem.* **2019**, *37* (1), 42–48.
- (63) Zhao, W.; Kong, F. Facile Synthesis of the Heptasaccharide Repeating Unit of O-Deacetylated GXM of *C. neoformans* Serotype B. *Bioorg. Med. Chem.* **2005**, *13* (1), 121–130.
- (64) Zhao, W.; Kong, F. Synthesis of a Heptasaccharide Fragment of the O-Deacetylated GXM of *C. neoformans* Serotype C. *Carbohydr. Res.* **2005**, *340* (10), 1673–1681.
- (65) Rao, Y.; Boons, G.-J. A Highly Convergent Chemical Synthesis of Conformational Epitopes of Rhamnogalacturonan II. *Angew. Chem. Int. Ed.* **2007**, *46* (32), 6148–6151.
- (66) Chauvin, A.-L.; Nepogodiev, S. A.; Field, R. A. Synthesis of a 2,3,4-Triglycosylated Rhamnoside Fragment of Rhamnogalacturonan-II Side Chain A Using a Late Stage Oxidation Approach. *J. Org. Chem.* **2005**, *70* (3), 960–966.
- (67) De Castro, C.; Molinaro, A.; Piacente, F.; Gurnon, J. R.; Sturiale, L.; Palmigiano, A.; Lanzetta, R.; Parrilli, M.; Garozzo, D.; Tonetti, M. G.; Van Etten, J. L. Structure of *N*-Linked Oligosaccharides Attached to Chlorovirus PBCV-1 Major Capsid Protein Reveals Unusual Class of Complex *N*-Glycans. *Proc. Natl. Acad. Sci. U.S.A.* **2013**, *110* (34), 13956–13960.
- (68) De Castro, C.; Speciale, I.; Duncan, G.; Dunigan, D. D.; Agarkova, I.; Lanzetta, R.; Sturiale, L.; Palmigiano, A.; Garozzo, D.; Molinaro, A.; Tonetti, M.; Van Etten, J. L. *N*-Linked Glycans of Chloroviruses Sharing a Core Architecture without Precedent. *Angew. Chem. Int. Ed.* **2016**, *55* (2), 654–658.

## **Chapter 2**

### **Synthesis of Fragments Derived from the Immunogenic Glycan**

#### **Epitope of Glycoprotein GP72 of *T. cruzi***



D-xylose residues are in two different fragments, **2.2** and **2.3**, respectively. Compounds **2.4** and **2.5** are smaller fragments of heptasaccharide **2.3**. The synthesis of sterically congested ‘hyper-branched’ oligosaccharides, like **2.1** and its fragments, is challenging as the correct glycosylation reaction sequence must be used to ensure the products are obtained in good stereoselectivities and yields.<sup>11–16</sup> To synthesize the whole 13-residue glycan epitope, it was envisioned to prepare the smaller fragments described in this chapter first and then use similar intermediates to assemble the whole glycan. It was expected that the syntheses of the smaller fragments would shed light on efficient strategies that can be applied to synthesize the whole glycan structure, **2.1**.

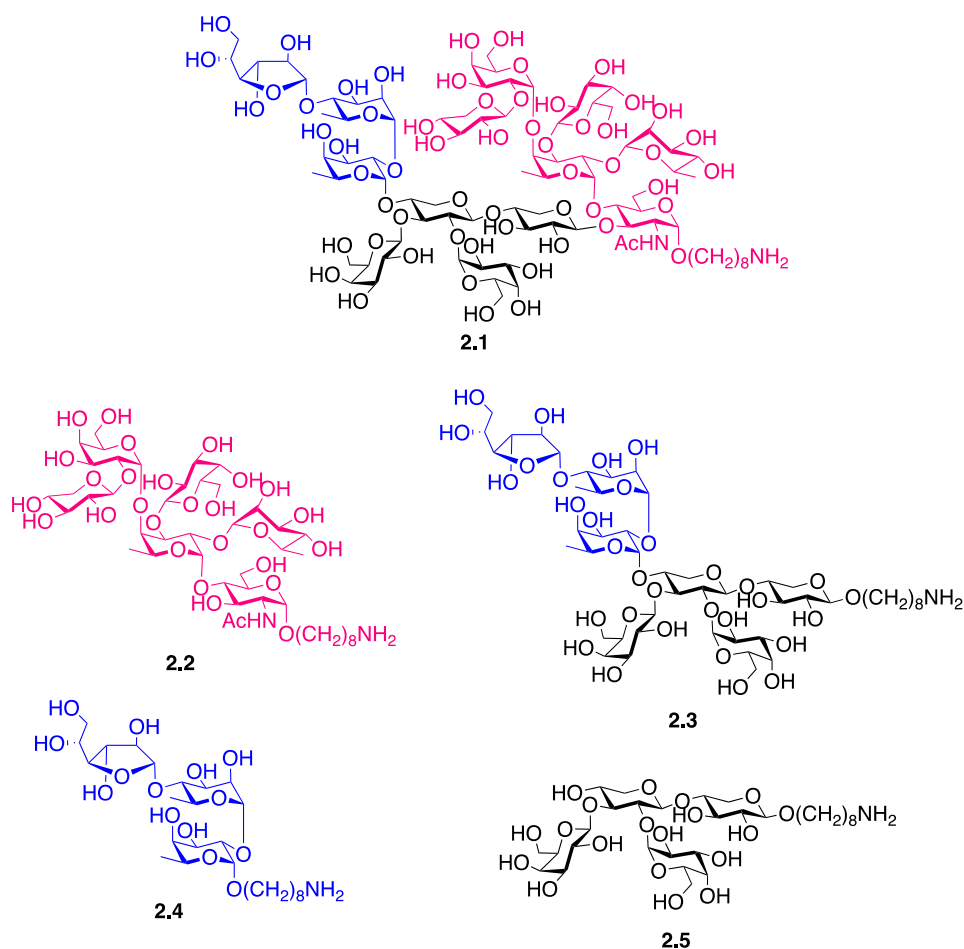


**Figure 2-2:** Structures of the synthetic targets derived from the immunogenic glycan epitope from GP72.

## 2.2 Results and discussion.

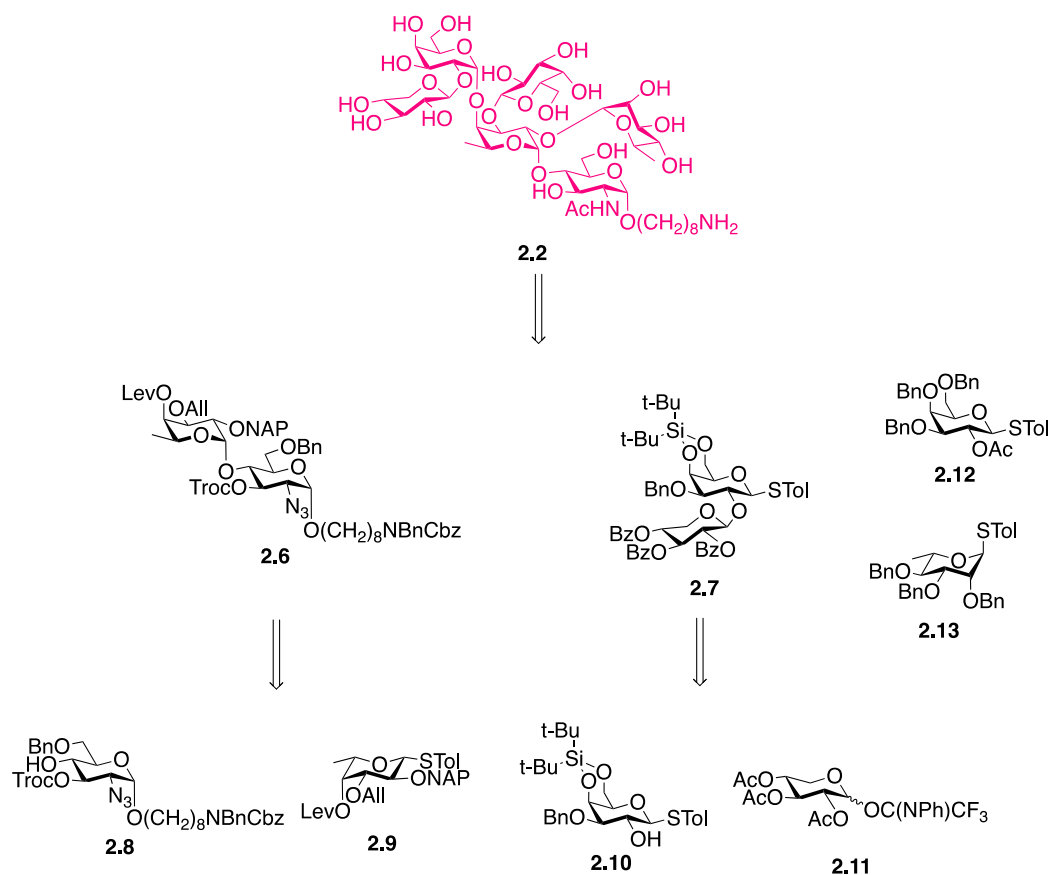
The main challenge in the syntheses of fragments **2.2** and **2.3** is anticipated to be the syntheses of the ‘hyper-branched’ residues. To be successful in this endeavor, my strategy must be versatile enough to allow me to explore several possible glycosylation sequences. There is an anticipation that some sequences might not be applicable to this system and thus, other sequences might need to be explored. Strategic selection and installation of orthogonal protecting groups in the building blocks is essential to the success of the synthesis. An additional challenge in the synthesis is the diversity of monosaccharides and linkages present in the molecules. Upon scrutiny of the structure, I established that almost all the 13 sugar residues (maybe except the two  $\beta$ -galactopyranoses present) in the whole glycan **2.1** must come from different building blocks. With all these challenges, a well-planned synthesis is a must.

In designing a synthetic strategy as well as building blocks, I employed some basic principles: 1) Sugar donors were usually chosen in the form of thioglycosides or imidates. Thioglycoside donors were chosen because of their stability to multiple conditions during protecting group manipulation.<sup>17</sup> They can also be activated using a variety of conditions. Finally, thioglycoside donors are also extremely versatile; they can be transformed to other donors in few steps. Imidate donors were usually chosen when a glycosylation reaction requires selective activation of the imidate donors over an acceptor containing a sulfur containing aglycon;<sup>18</sup> 2) Building blocks with orthogonal protecting groups must be accessed using the minimum number of steps possible; 3) Due to the high number of synthetic building blocks required, I synthesized building blocks of the same monosaccharide backbone using similar routes as much as possible and diverging only at the end to produce the target building block; 4) All the synthetic fragments are synthesized with an 8-amino-1-octyl linker, which will allow further conjugations through the

amine moiety. Other synthetic strategy decisions I made will be discussed further as I go through this chapter.

### **2.2.1 Synthesis of hexasaccharide 2.2.**

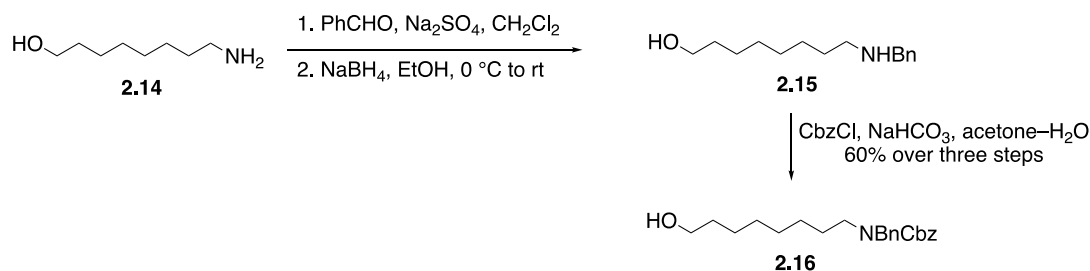
The main challenge in the synthesis of hexasaccharide **2.2** is anticipated to be the synthesis of the ‘hyper-branched’ L-fucose residue. Inspired by the success in the syntheses of similar ‘hyper-branched’ L-fucose residues found in chlorovirus *N*-glycans, I decided to employ a similar strategy highlighted by the ‘counterclockwise’ addition of sugar moieties around the L-fucose residue.<sup>11,12</sup> While similar, the synthesis **2.2** might not be like that of the chloroviruses *N*-glycans due to differences in the structures and linkages of the monosaccharide substituents. Anticipating this, I decided to create an L-fucose residue building block **2.9** with three orthogonal protecting groups: NAP (2-methylnaphthyl ether), All (allyl ether) and Lev (levulinoyl ester). Each orthogonal protecting group can be selectively cleaved without affecting other protecting groups and, thus, each possible glycosylation sequence is accessible. I envisioned to synthesize disaccharide **2.6** from monosaccharides **2.8** and **2.9** (Scheme 2-1). This compound would be the parent disaccharide where I will sequentially attach sugar donors **2.7**, **2.10**, and **2.11** to obtain the desired ‘hyper-branched’ hexasaccharide fragment **2.2** after global deprotection.



**Scheme 2-1:** Retrosynthetic analysis of hexasaccharide **2.2**.

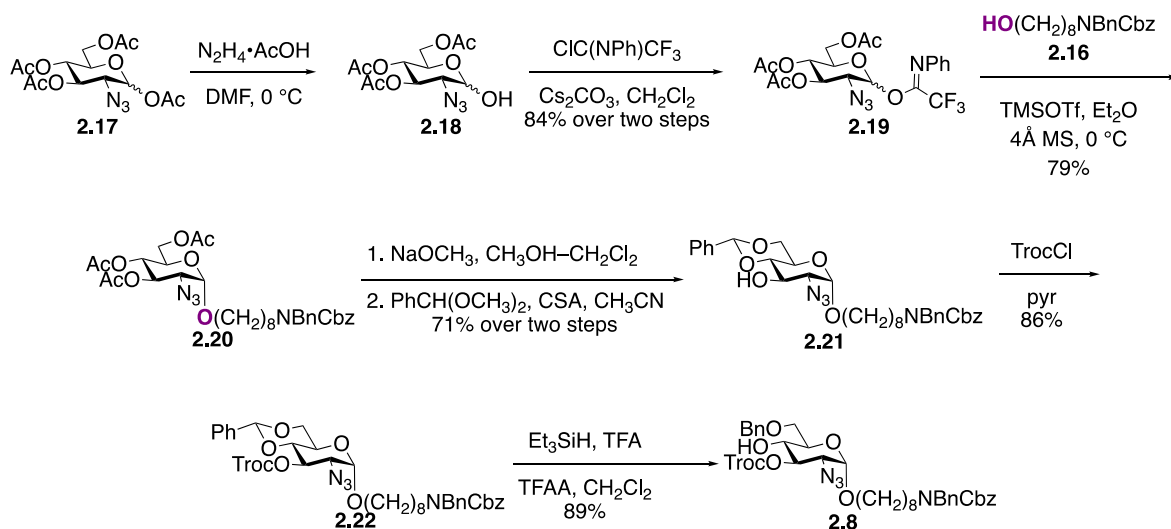
### 2.2.1.1 Synthesis of building blocks **2.8**–**2.13**.

Accessing building block **2.8** started with the synthesis of the 8-amino-1-octyl linker synthon **2.16**, which was prepared from 8-amino-1-octanol<sup>19</sup> (**2.14**, Scheme 2-2). The first step involved reductive amination between **2.14** and benzaldehyde using NaBH<sub>4</sub> to give secondary amine **2.15**. The crude product was carried to the next step where it was re-dissolved in an acetone–water mixture followed by addition of sodium bicarbonate and benzyl chloroformate to obtain linker **2.16** in 60% yield over three steps.



**Scheme 2-2:** Synthesis of linker **2.16**.

The linker **2.16** was then used in the subsequent glycosylation with *N*-phenyltrifluoroacetimidate donor **2.19**<sup>20</sup> (Scheme 2-3). The imidate donor **2.19** was synthesized in two steps from previously reported compound **2.17**.<sup>21</sup> Selective anomeric deacetylation was done using hydrazine acetate in DMF. The resulting hemiacetal was converted into imidate **2.19** using 2,2,2-trifluoro-*N*-phenylacetamidoyl chloride and cesium carbonate; the product was obtained in 84% yield over two steps. Once in hand, **2.19** was used to glycosylate **2.16** using TMSOTf as the activating agent to yield the desired  $\alpha$ -glycoside **2.20** as the major product in 79% yield. The  $\alpha$ -stereochemistry was confirmed by the coupling constant between H-1 and H-2 ( $^3J_{1,2} = 3.6$  Hz) in the  $^1\text{H}$  NMR spectrum. The stereochemical outcome of the reaction is mainly attributed to the kinetic anomeric effect.<sup>22</sup> Deprotection of acetyl groups in glycoside **2.20** using sodium methoxide followed by protection of 4,6-diol using benzaldehyde dimethyl acetal and camphorsulfonic acid gave **2.21** in 71% yield over two steps. Protection of the remaining hydroxyl group at C-3 with a Troc carbonate using 2,2,2-trichloroethoxycarbonyl chloride in pyridine afforded the fully protected sugar **2.22** in 86% yield. The final step involved the selective ring opening of the benzylidene acetal using trifluoroacetic acid and triethylsilane to produce the O-6 benzylated product **2.8** in 89% yield.

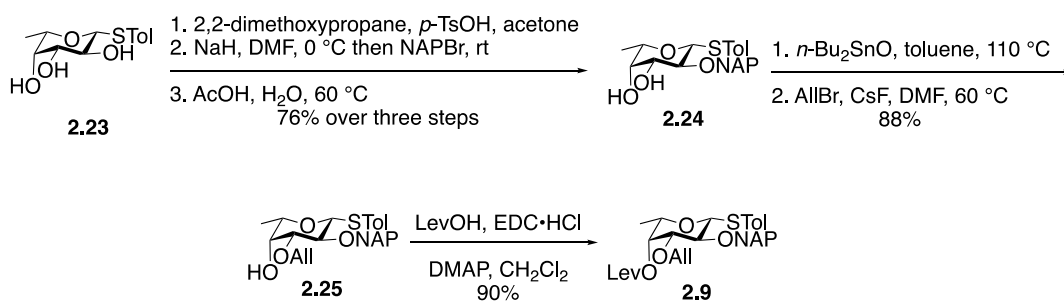


**Scheme 2-3:** Synthesis of building block **2.8**.

Compound **2.9** is an orthogonally protected L-fucose building block that would end up being the ‘hyper-branched’ fucose residue in the target fragment. The three orthogonal protecting groups chosen were NAP, All, and Lev for the hydroxyl groups at C-2, C-3, and C-4, respectively. These protecting groups are stable under multiple conditions including conditions for glycosylation reactions. The NAP and All ether protecting groups were chosen as they are non-participating groups during glycosylation reactions and their non-electron withdrawing nature do not compromise donor reactivity. On the other hand, the Lev ester group at O-4 was installed to assist  $\alpha$ -glycosylation by participation through a 6-membered ring transition state previously described.<sup>23</sup>

The synthesis of **2.9** (Scheme 2-4) started from the previously reported thiofucoside derivative **2.23**.<sup>24</sup> The reaction started with acetonide formation at O-3 and O-4 of the fucose residue using 2,2-dimethoxypropane, and *p*-toluenesulfonic acid in acetone. The hydroxyl group at C-2 was then protected with a NAP group by alkylation with 2-bromomethylnaphthalene and sodium hydride in DMF followed by acid hydrolysis of the isopropylidene ketal to obtain diol **2.24**

in 76% yield over three steps. The allyl ether protecting group was introduced regioselectively at the O-3 position by heating **2.24** to reflux with *n*-Bu<sub>2</sub>SnO in toluene to form the corresponding tin ketal. After cooling and concentration, the crude product was dissolved in DMF followed by the addition of allyl bromide and cesium fluoride and heating at 60 °C. This reaction gave the desired regioisomer **2.25** in 88% yield. The structure of the product was confirmed by a correlation of the Fuc-H-3 with the allyl -OCH<sub>2</sub> carbon in the HMBC spectrum. The Lev group was then finally introduced at O-4 using levulinic acid, EDC·HCl, and DMAP in CH<sub>2</sub>Cl<sub>2</sub> to yield target building block **2.9** in 90% yield.

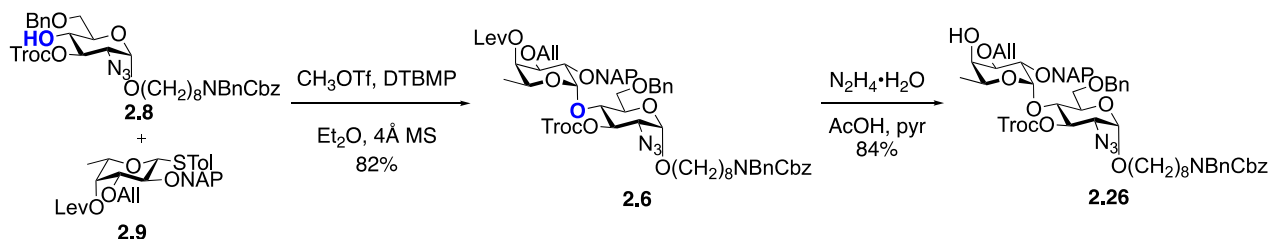


**Scheme 2-4:** Synthesis of building block **2.9**.

Building blocks **2.10**,<sup>25</sup> **2.11**,<sup>26</sup> **2.12**,<sup>24</sup> and **2.13**<sup>27</sup> were all prepared as described previously. The di-*t*-butylsilyl acetal (DTBS) protecting group in **2.10** was installed to promote  $\alpha$ -selectivity during the glycosylation reaction by blocking the  $\beta$ -face of the attack of the incoming acceptor.<sup>28</sup> Building blocks **2.11** and **2.12** have ester protecting group at O-2 to assist with the selective formation of 1,2-*trans*-glycosides during glycosylation reactions. Lastly, rhamnose thioglycoside **2.13** was protected with non-participating benzyl ether groups, although a 1,2-*trans*-glycosylation is desired. The decision to induce the stereoselectivity of the glycosylation reaction purely by the kinetic anomeric effect<sup>22</sup> will be further discussed in this chapter.

### 2.2.1.2 Attempted synthesis of hexasaccharide 2.2 using a ‘counterclockwise’ approach.

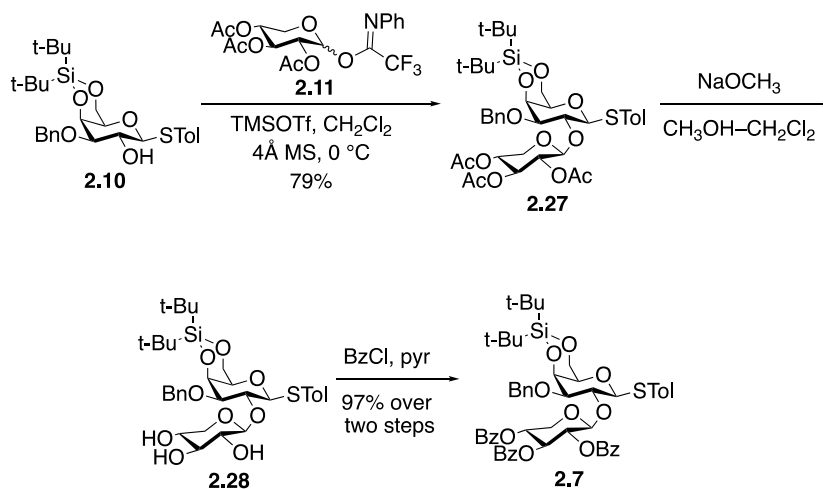
With all the desired building blocks in hand, disaccharide **2.6** containing the orthogonally protected L-fucose was assembled (Scheme 2-5). The synthesis of the disaccharide **2.6** proceeded by the glycosylation of acceptor **2.8** and thioglycoside donor **2.9** using MeOTf activation in 82% yield. This method was preferred over the more common NIS–AgOTf activation to avoid possible iodination of the allyl protecting group. In addition, a similar donor was successfully activated previously using the same method.<sup>11</sup> The desired  $\alpha$ -configuration on the L-fucose residue was confirmed by a small coupling constant between Fuc-H-1 and Fuc-H-2 ( $^3J_{1,2} = 3.7$  Hz), which is consistent with a 1,2-*cis*-linkage. I initially decided to use a counterclockwise approach as previously described by Lin and co-workers in their synthesis of similar ‘hyper-branched’ fucose residues.<sup>11</sup> This approach starts with a glycosylation at O-4 position of the fucose. Thus, the deprotection of the Lev group at O-4 using hydrazine hydrate in an acetic acid–pyridine mixture afforded the disaccharide acceptor **2.26** in 84% yield.



**Scheme 2-5:** Synthesis of disaccharide acceptor **2.26**.

I initially decided to perform a [2+2] glycosylation between acceptor **2.26** and disaccharide donor **2.7** to install the disaccharide moiety at O-4. This would save a number of steps when compared to adding each residue one at a time. To do this, disaccharide donor **2.27** was synthesized from acceptor **2.10** and imidate donor **2.11** using TMSOTf activation to provide the product in 79% yield (Scheme 2-6). In the <sup>1</sup>H NMR spectrum of compound **2.27**, the coupling constant

between Xyl-H-1 and Xyl-H-2 was  ${}^3J_{1,2} = 6.0$  Hz, which is unusually low for a 1,2-*trans*- $\beta$ -linkage in a  ${}^4C_1$  conformation. Similar observations were reported previously on similarly acylated  $\beta$ -xylopyranosides.<sup>29,30</sup> The unusual coupling constant likely arises due to the conformational flexibility of the xylose residue, presumably due to the absence of a C-5 hydroxymethyl group, allowing for it to adopt a conformation different from the expected  ${}^4C_1$  conformation, or a mixture of conformations that equilibrate rapidly on the NMR time scale.<sup>30–32</sup>

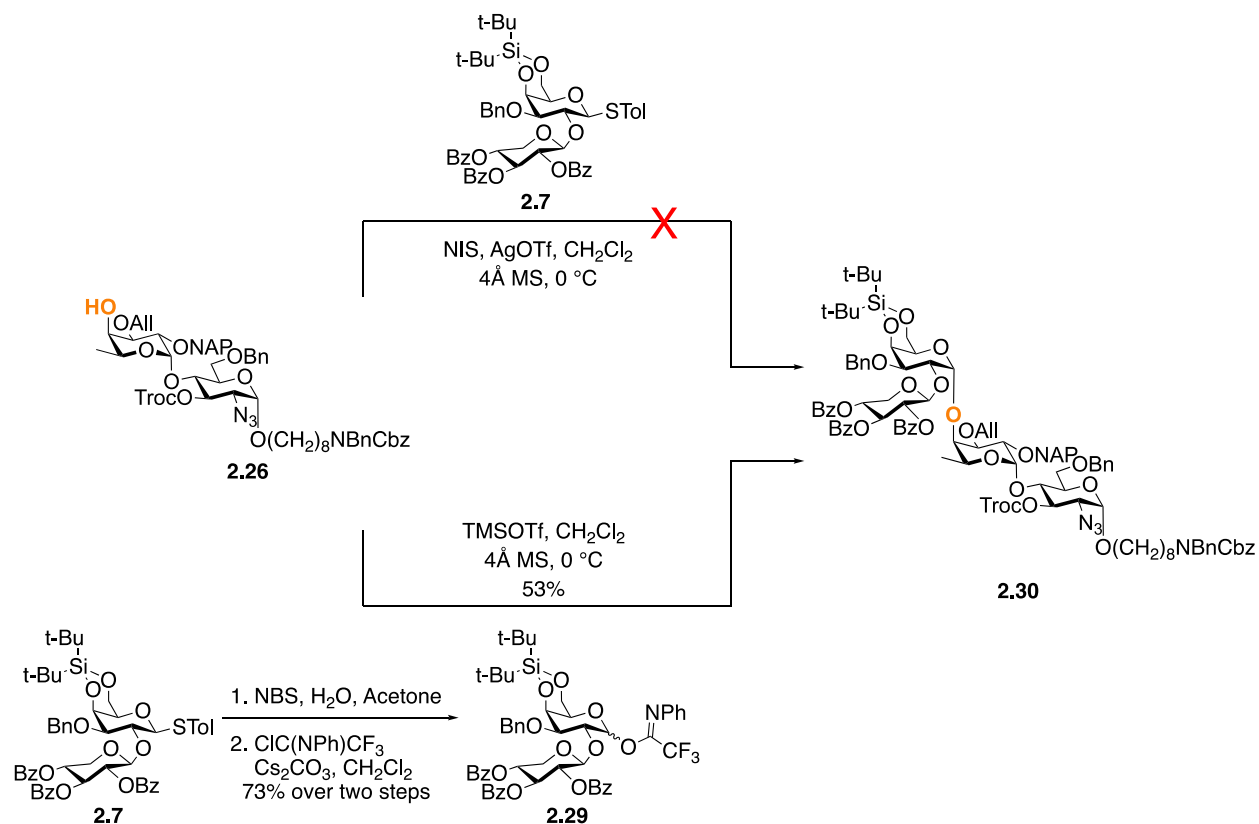


**Scheme 2-6:** Synthesis of disaccharide acceptor **2.7**.

At this stage, the acetyl protecting groups in **2.27** were replaced by less base-labile benzoyl groups to ensure selective deprotection of the Troc group using mild basic conditions instead of the usual reductive conditions to preserve the azido functional group later in the synthesis. The desired protecting group manipulation started with deacetylation using sodium methoxide to give triol **2.28**. Analysis of the  ${}^1\text{H}$  NMR spectrum of **2.28** showed the coupling constant between Xyl-H-1 and Xyl-H-2 was  ${}^3J_{1,2} = 7.0$  Hz, which is closer to the expected value for a  $\beta$ -xylopyranoside in a  ${}^4C_1$  conformation ( $\sim 8$  Hz). Compound **2.28** was then reacted with benzoyl chloride in pyridine to give desired disaccharide **2.7** in 97% yield over two steps.

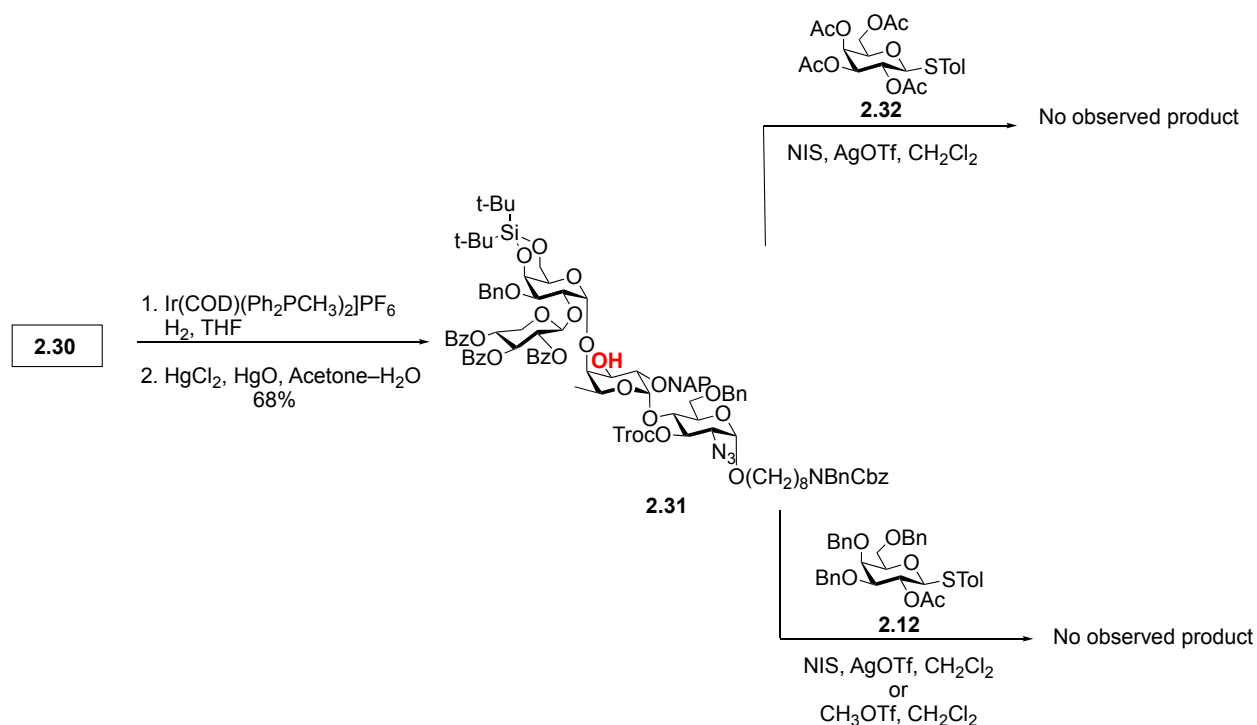
The introduction of benzoyl protecting groups changed the conformation of the xylose moiety from  ${}^4C_1$  to  ${}^1C_4$  as confirmed by a small coupling constant between Xyl-H-1 and Xyl-H-2 ( ${}^3J_{1,2} = 3.4$  Hz). The conditions applied to replace the acetate esters with benzoate esters are known not to cause isomerization of the anomeric center and thus the possibility of anomeric isomerization is not likely. The change in the conformation of the xylose residue was further established by the coupling constant between Xyl-H-1 and Xyl-C-1 ( ${}^1J_{C-H} = 170.9$  Hz) in the  ${}^1H$  coupled HSQC spectrum. Other coupling constant values among the sugar protons in **2.7** ( ${}^3J_{2,3} = 5.3$  Hz,  ${}^3J_{3,4} = 3.7$  Hz,  ${}^3J_{4,5a} = 3.2$  Hz,  ${}^3J_{4,5b} = 3.9$  Hz) are also indicative of a change of conformation to  ${}^1C_4$ . While aware of these changes in conformation, I decided to continue illustrating this xylose residue in a  ${}^4C_1$  confirmation of to avoid confusion throughout the discussion.

A [2+2] glycosylation reaction was attempted using acceptor **2.26** and thioglycoside donor **2.7** using the NIS–AgOTf promoter system but the reaction was unsuccessful (Scheme 2-7). I decided to transform the thioglycoside into a more reactive imidate donor in two steps. Thus, **2.7** was hydrolyzed in the presence of *N*-bromosuccinimide in an EtOAc–H<sub>2</sub>O mixture to produce the corresponding hemiacetal, which was reacted with 2,2,2-trifluoro-*N*-phenylacetamidoyl chloride and cesium carbonate to produce imidate **2.29** in 73% yield over two steps. Acceptor **2.26** and imidate donor **2.29** were reacted using TMSOTf activation to successfully synthesize the desired tetrasaccharide **2.30** in 53% yield. The DTBS group, as expected, induced high  $\alpha$ -selectivity as confirmed by a small coupling constant between Gal-H-1 and Gal-H-2 ( ${}^3J_{1,2} = 4.0$  Hz), which is consistent with an  $\alpha$ -linkage in galactopyranosides.



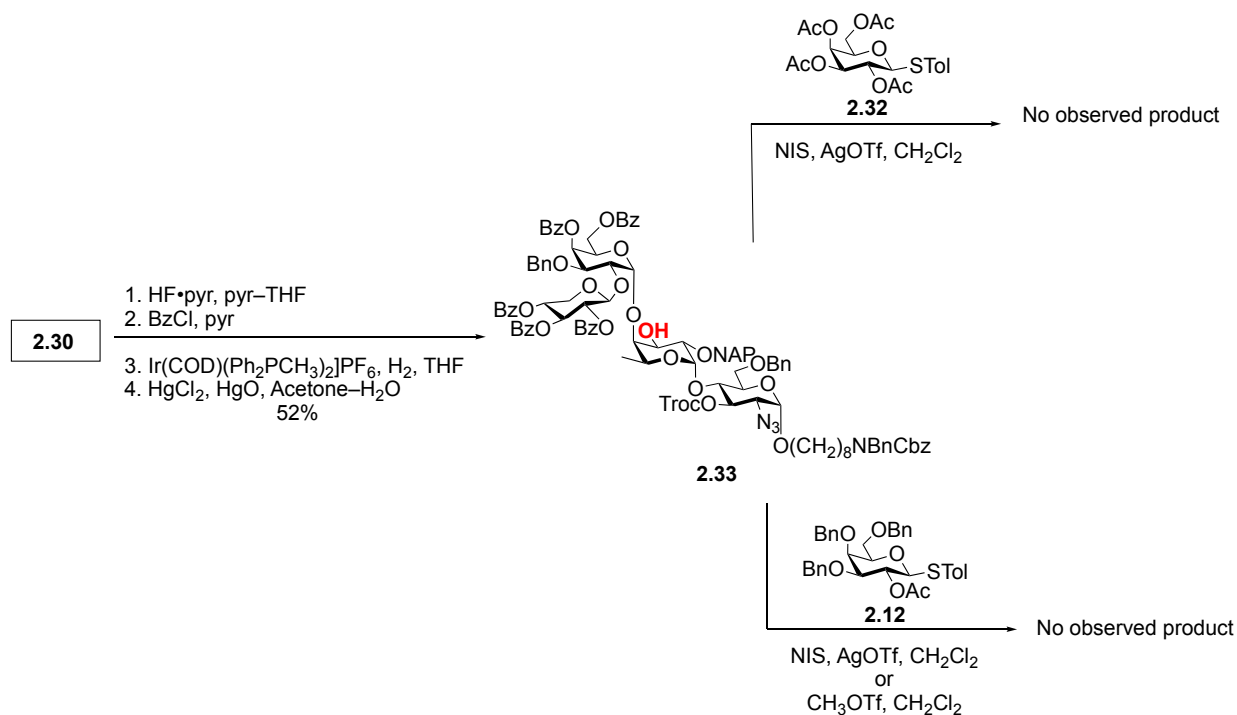
**Scheme 2-7:** Synthesis of tetrasaccharide **2.30**.

With this tetrasaccharide in hand, the allyl ether group was then deprotected (Scheme 2.8) using hydrogen-activated [Ir(COD)(CH<sub>3</sub>Ph<sub>2</sub>P)<sub>2</sub>]<sub>2</sub>PF<sub>6</sub> followed by cleavage of the resulting vinyl ether using mercuric chloride and mercuric oxide in an acetone–water mixture to give the tetrasaccharide acceptor **2.31** in 68% yield. An attempt to glycosylate at the C-3 hydroxyl group of the L-fucose in the acceptor with donor **2.32**<sup>33</sup> was unsuccessful, resulting only in the recovery of the acceptor and hydrolysis of the donor. A more armed donor, **2.12**, was used instead in the glycosylation with **2.31** but also did not give the desired product. It was postulated that this result could be attributed to the low reactivity of the acceptor due to steric crowding around the L-fucose C-3 hydroxyl group, possibly by the DTBS acetal.



**Scheme 2-8:** Failed O-3 glycosylation attempts on acceptor **2.31**.

To ease some steric hindrance near the reaction center, I decided to remove the bulky DTBS group in the galactose residue and introduce less bulky benzoyl ester groups (Scheme 2-9). To do this, tetrasaccharide **2.30** was treated with HF–pyridine in a pyridine–THF mixture followed by the addition of benzoyl chloride in pyridine to give the corresponding fully protected tetrasaccharide. Deallylation was then performed in similar fashion as previously described to give tetrasaccharide acceptor **2.33** in 52% yield over four steps. Attempts to glycosylate **2.33** with donors **2.32** or **2.12** were still unsuccessful, again only resulting to the recovery of acceptor and hydrolysis of the donor.



**Scheme 2-9:** Failed O-3 glycosylation attempts on acceptor **2.33**.

With these failed efforts, I decided to abandon the ‘counterclockwise’ addition of the donors onto the L-fucose residue. While the GP72 and ACTV-1 glycans both contains a similar ‘hyper-branched’ L-fucose residue, their chemical synthesis might differ due to, as hypothesized above, differences in the structures and linkages of the sugar residues surrounding them. Although the initial approach was not fruitful as hoped, my versatile approach allowed me to explore different glycosylation sequences.

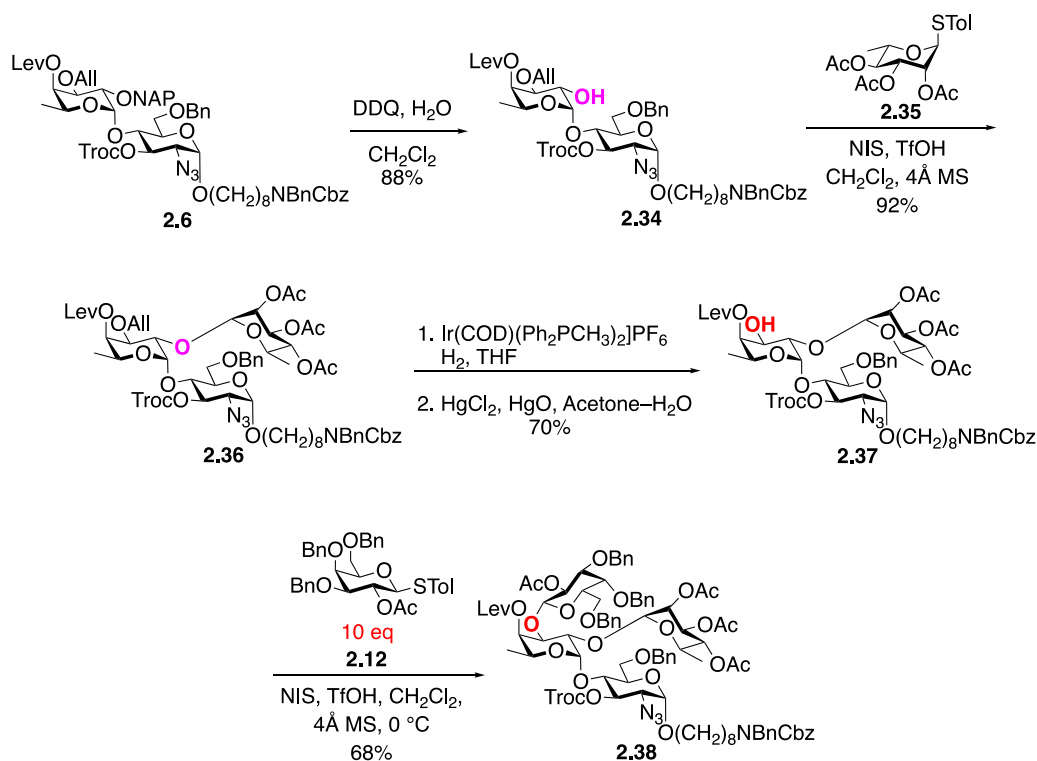
### 2.2.1.3 Synthesis of hexasaccharide **2.2** using a ‘clockwise’ and ‘pendulum’ approach.

#### 2.2.1.3.1 Synthesis using ‘clockwise’ approach.

The previous attempts to synthesize **2.2**, while unsuccessful, gave some insights on a possible sequence that might work. It was established that O-3 glycosylation at the L-fucose

residue seems to not work with O-4 glycosylation present. Another possible sequence, where an initial glycosylation at O-4 followed by O-2 and lastly at O-3 was not a sequence I considered as glycosylation at O-3 with two flanking residues at O-4 and O-2 would seem to result in failure. I therefore decided to try a ‘clockwise’ approach by initially performing a glycosylation at O-2 followed by O-3 and finally, at O-4.

This attempt started (Scheme 2-10) with the removal of the NAP group in disaccharide **2.6** using DDQ in wet CH<sub>2</sub>Cl<sub>2</sub> to obtain the desired disaccharide acceptor **2.34** in 88% yield. With this acceptor and thioglycoside donor **2.35**<sup>34</sup> using NIS–TfOH activation, trisaccharide **2.36** was obtained in 92% yield. The configuration at the anomeric center was confirmed to be the desired  $\alpha$ -linkage using the coupling constant between Rha-H-1 and Rha-C-1 ( $^1J_{C-H} = 174.2$  Hz) in the <sup>1</sup>H-coupled HSQC spectrum. Subsequent deprotection of the All group by isomerization to a vinyl ether using hydrogen-activated [Ir(COD)(CH<sub>3</sub>Ph<sub>2</sub>P)<sub>2</sub>]PF<sub>6</sub> followed by hydrolysis using mercuric chloride and mercuric oxide in an acetone–water mixture gave the trisaccharide acceptor **2.37** in 70% yield. The reaction of trisaccharide acceptor **2.37** and thioglycoside donor **2.12** was sluggish, which ultimately required the addition of 10 equiv of donor to afford tetrasaccharide **2.38** in a moderate yield of 68%. The acceptor **2.37** was found to be extremely unreactive, and rapid hydrolysis of the donor occurred before glycosylation. Nevertheless, the desired  $\beta$ -linkage was assigned using the coupling constant between Gal-H-1 and Gal-H-2 ( $^3J_{1,2} = 7.8$  Hz).

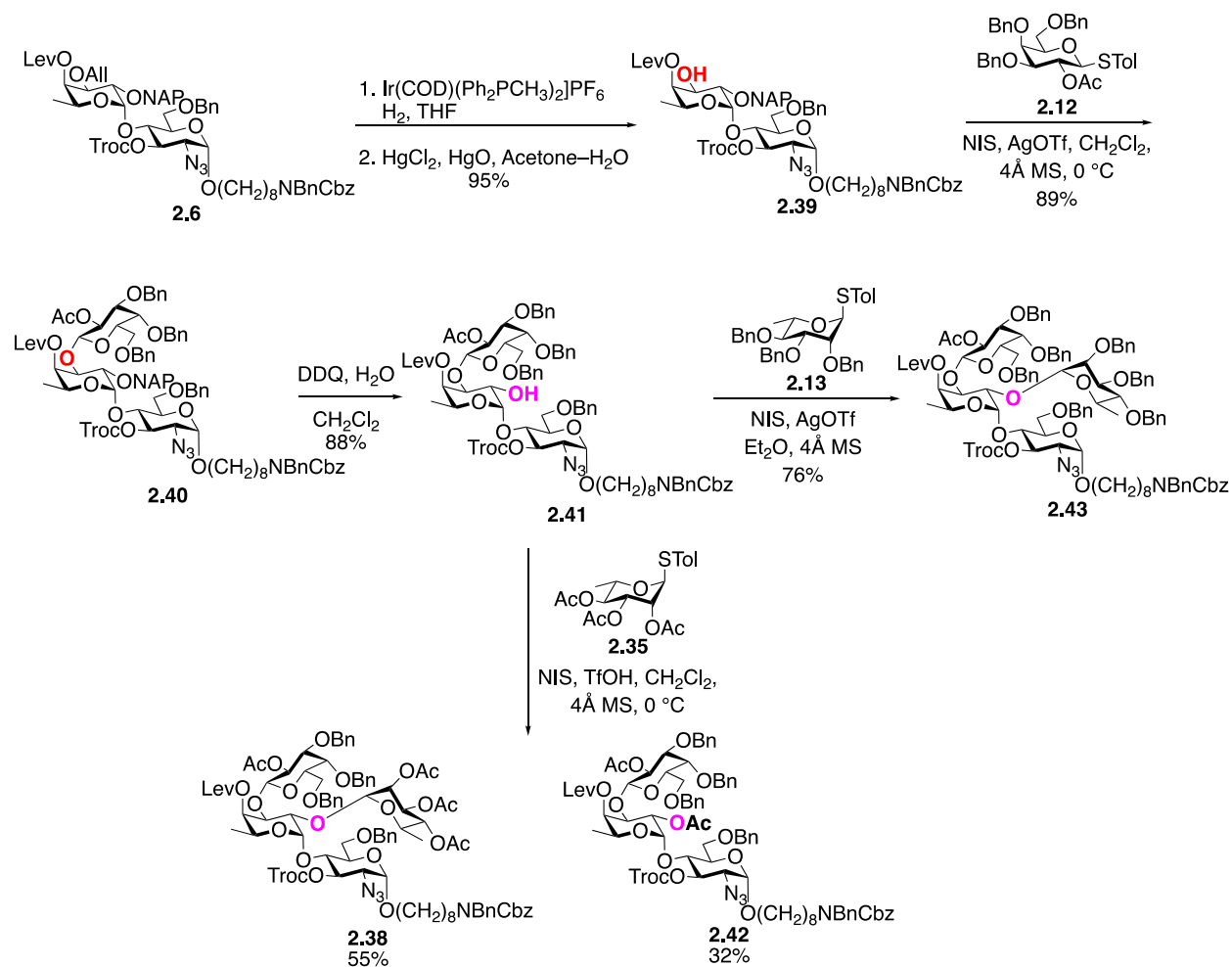


**Scheme 2-10:** Synthesis of tetrasaccharide **2.38**.

### 2.2.1.3.2 Synthesis using ‘pendulum’ approach.

Although the desired tetrasaccharide was obtained using the ‘clockwise’ approach, the large amount of donor required to obtain a moderate yield was discouraging and I ultimately chose to explore other routes to access the target compound. I decided to try out a sequence involving glycosylation at O-3 before at O-2 and whether this approach would give a more satisfactory results in both yields and material requirements. I call this a ‘pendulum’ approach (as I am already using clock directions). This attempt started (Scheme 2-11) with the removal of the All group in disaccharide **2.6** by Ir-mediated isomerization to the vinyl ether and then hydrolysis involving  $\text{Hg}^{2+}$  to give the disaccharide acceptor **2.39** in 95% yield. Glycosylation between acceptor **2.39** and donor **2.12** gave trisaccharide **2.40** in 89% yield in excellent  $\beta$ -selectivity. The configuration of the galactose residue was assigned from  $^3J_{1,2}$  of the newly introduced Gal residue; the 8.1 Hz

magnitude was consistent with a  $\beta$ -linkage. Selective deprotection of the NAP group using DDQ in wet  $\text{CH}_2\text{Cl}_2$  afforded acceptor **2.41** in 88% yield.



**Scheme 2-11:** Synthesis of tetrasaccharides **2.38** and **2.43**.

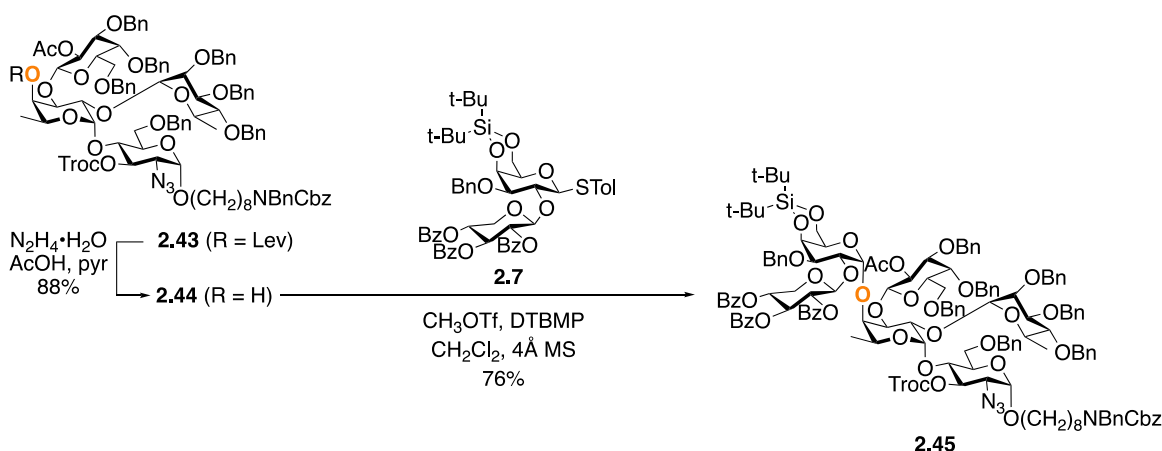
Glycosylation of **2.41** with peracetylated thioglycoside donor **2.35** yielded the desired product **2.38** in 55% yield, but also formed the acetylated acceptor **2.42** as a minor product in 32% yield. This side-product is produced from the orthoester intermediate, which can undergo rearrangement in two ways, one leading to the product, and one the other to the acetylated acceptor. To circumvent this unwanted side product, I changed the acetyl groups in **2.35** to benzyl groups; *i.e.*, thioglycoside **2.13**. The initial choice of using a donor with acetyl group on O-2 position was

to ensure the formation of  $\alpha$ -rhamnoside through neighboring group participation during glycosylation. Changing the acetyl groups to benzyl ethers would require the stereoselectivity to arise solely via the kinetic anomeric effect.<sup>22,35</sup> Fortunately, the reaction between acceptor **2.41** and perbenzylated donor **2.13** using NIS–AgOTf activation in Et<sub>2</sub>O gave the desired tetrasaccharide **2.43** with excellent selectivity for the  $\alpha$ -rhamnoside in 76% yield. A  $^1J_{C-1-H-1}$  of 169.3 Hz of the rhamnose residue confirmed the  $\alpha$ -stereochemistry. Given the better yield, this sequence was deemed to be more favorable than the previous one in accessing the desired tetrasaccharide intermediate.

To continue with the synthesis, deprotection of the Lev group at O-4 of the fucose residue of tetrasaccharide **2.43** (Scheme 2-12) using hydrazine monohydrate in acetic acid–pyridine led to formation of tetrasaccharide acceptor **2.44** in 88% yield. From here, a [4+2] glycosylation between tetrasaccharide acceptor **2.44** and disaccharide donor **2.7** using MeOTf activation was performed to give hexasaccharide **2.45**, the first synthetic intermediate containing the ‘hyper-branched’ fucose in 76% yield. Initially, the glycosylation was performed using NIS–AgOTf activation but this only resulted to the retrieval of the acceptor and hydrolysis of the donor.

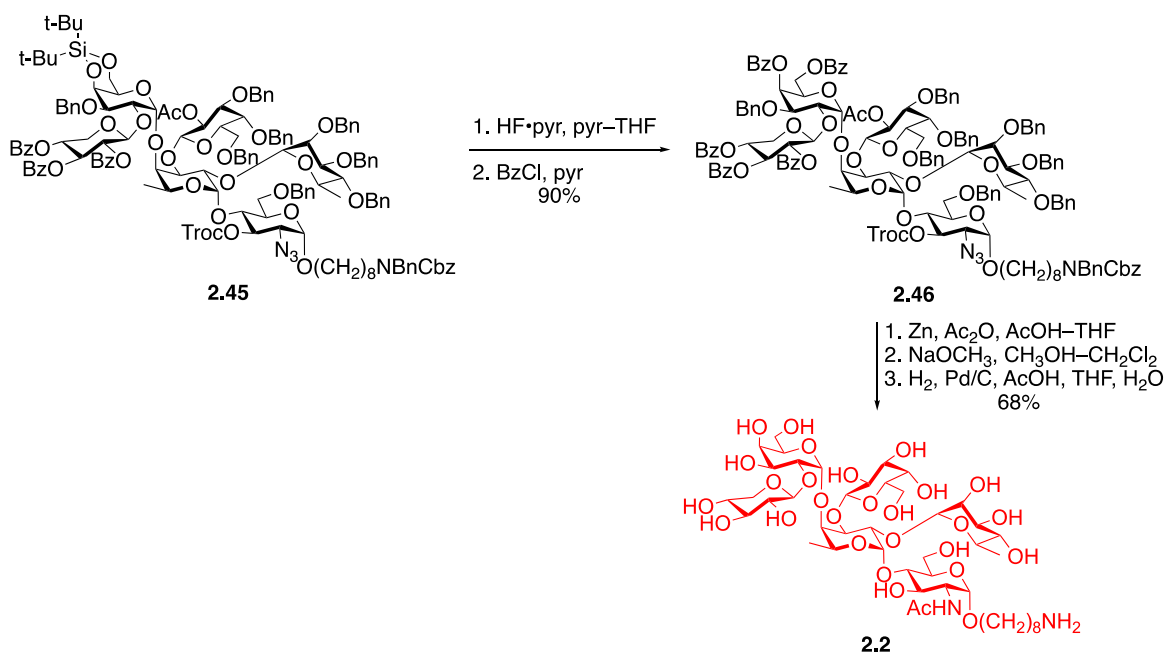
Upon examination of the  $^1H$  NMR and  $^{13}C$  NMR spectra of **2.45**, it was found that the peaks were broad, and some were missing. I hypothesized that due to the steric bulkiness within the compound, the molecule adopts multiple conformations that are too slow to equilibrate on the NMR time scale. An attempt to get a better NMR spectrum using VT-NMR experiments was not considered due to my concerns about heating the sample higher than 50 °C as I was unsure of the stability of these kind of highly branched sugar compounds. Due to this, the assignment of the linkage of the galactopyranose residue on the O-4 of fucose could not be determined at this point but could at a later stage (see below). To support that the synthesis of the compound was successful,

MALDI-MS analysis of the product was performed and it showed peak at  $m/z = 2783.9641$ , which correspond to compound **2.45**.



**Scheme 2-12:** Synthesis of hexasaccharide **2.45**.

The deprotection of the bulky DTBS group using HF–pyridine followed by protection of the resulting diol as benzoate esters using benzoyl chloride in pyridine gave compound **2.46** in 90% yield (Scheme 2-13). The decision to remove the bulky DTBS group was prompted by hopes that this would alleviate some of the steric bulk that might translate to an improvement in the resolution of the NMR analysis but unfortunately, this was found to be unsuccessful. Nevertheless, the switch of the DTBS acetal to benzoyl groups simplified the global deprotection process at the end of the synthesis.



**Scheme 2-13:** Synthesis of target hexasaccharide fragment **2.2**.

To access target hexasaccharide **2.2** from **2.46**, the initial step is to convert the 2-azido-2-deoxyglucose residue to an *N*-acetylglucosamine residue. This was done through a one-pot reduction–acetylation process using zinc dust in Ac<sub>2</sub>O in acetic acid–THF.<sup>36</sup> It is also expected that the Troc protecting group at O-3 of the 2-deoxyglucose residue was deprotected in this reaction. Still, the resulting crude material was subjected to ester group deprotection using sodium methoxide in CHCl<sub>3</sub>–MeOH at 60 °C. Increasing the temperature was vital to ensure the complete removal of all the ester groups. At lower temperatures the reaction was incomplete, even at extended reactions times, again pointing to the hindered nature of the molecule. Lastly, the benzyl ether and carbamate protecting groups were deprotected using 10% palladium on carbon in acetic acid in THF–H<sub>2</sub>O (1:1) to give the fully deprotected hexasaccharide fragment **2.2** in 68% yield over three steps. Analysis of the NMR spectrum of compound **2.2** showed well-defined peaks, unlike the previous hexasaccharide intermediates; this allowed me to assign properly the linkage

of the galactopyranose residue introduced in the final glycosylation. The desired  $\alpha$ -linkage was confirmed by the coupling constant between Gal-H-1 and Gal-H-2 ( $^3J_{1,2} = 3.9$  Hz). In addition, the linkage of the xylopyranose residue was confirmed to be the desired  $\beta$ -linkage using the coupling constant between Xyl-H-1 and Xyl-H-2 ( $^3J_{1,2} = 7.8$  Hz), suggesting that in **2.2** this residue is in the  $^4C_1$  conformation.

#### 2.2.1.4 Summary

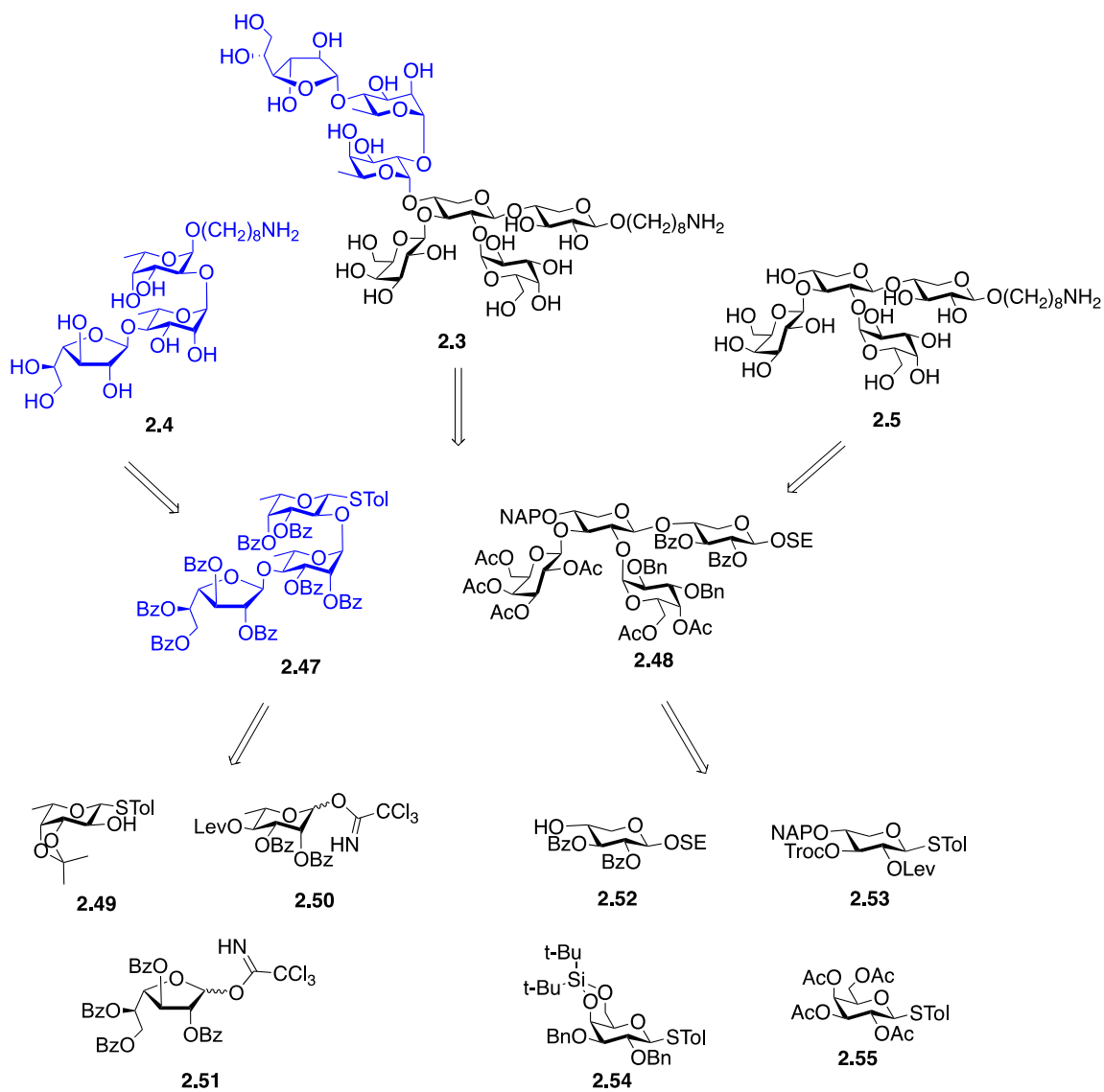
The ‘counterclockwise’ strategy, which is based on the previous report of the synthesis of ‘hyper-branched’ L-fucose residues in chlorovirus *N*-glycans was first attempted to synthesize hexasaccharide **2.2**. Unfortunately, this strategy was unsuccessful, presumably due to the steric hindrance presented by the glycans at O-4 of L-fucose during the glycosylation at the neighboring O-3 position. Multiple attempts of changing protecting groups both on the donor and acceptor leads to no product formation. It was concluded that the ‘counterclockwise’ strategy is not applicable to the synthesis of this ‘hyper-branched’ fucose from GP72. This is perhaps not surprising considering that the sugar compositions and linkages of the ‘hyper-branched’ fucoses in each of the glycan structures are different.

The versatile design of the L-fucose building block, with three orthogonal protecting groups, allowed me to access several glycosylation sequences. Taking into consideration the results from the attempted ‘counterclockwise’ approach, I tried a ‘clockwise’ approach where glycosylation starts at O-2 followed by O-3 and finally, at O-4. While this sequence afforded the desired tetrasaccharide intermediate, glycosylation at O-3 required large amounts of donor due to weak reactivity of the acceptor. To address this drawback, another sequence – a ‘pendulum’

approach – where glycosylation is performed at O-3 followed by O-2 and O-4 was explored. This approach succeeded in providing the desired hexasaccharide in high yield and stereoselectivity.

### **2.2.2 Synthesis of heptasaccharide 2.3**

As was the case for **2.2**, the main challenge in the synthesis of heptasaccharide **2.3** is expected to arise from the synthesis of the ‘hyper-branched’ D-xylose residue. My previous experience with the successful synthesis of hexasaccharide **2.2**, and its ‘hyper-branched’ L-fucose, provided several strategic insights on how to synthesize the similarly highly congested molecule in **2.3**. Although L-fucose and D-xylose are two different sugar residues, I hoped that I could apply some similar strategies from my previous work with hexasaccharide **2.2**. The most important thing that I learned from the previous synthesis is that the sequence of the glycosylation reactions is important to obtain the product in high yield and stereoselectivity. Having a versatile strategy to access several possible sequences in one intermediate is essential to the success of the synthesis. The use of three orthogonal protecting groups in D-xylose residue building block **2.53** (Scheme 2-14) will allow access to these possible sequences. In this case, the orthogonal protecting groups I decided to install on our molecule are Lev, Troc, and NAP. This set of protecting groups can be chemoselectively cleaved.



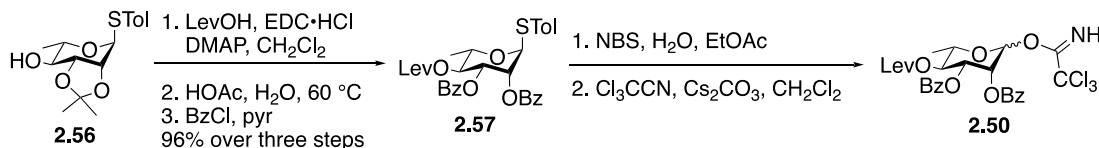
**Scheme 2-14:** Retrosynthetic analysis of heptasaccharide **2.3** and smaller fragments **2.4** and **2.5**.

Initially, I elected to divide the heptasaccharide **2.3** into two smaller pieces, trisaccharide **2.4** and tetrasaccharide **2.5**. These two fragments are also target molecules for the binding studies with GP72. I decided to synthesize these smaller fragments first and then do a possible [4+3] glycosylation with appropriate intermediates to build the heptasaccharide framework. Trisaccharide fragment **2.4** will be synthesized from trisaccharide **2.47**, which can be accessed from monosaccharides **2.49**, **2.50**, and **2.51**. On the other hand, tetrasaccharide fragment **2.5** can

be synthesized from tetrasaccharide **2.48** which can be obtained from monosaccharides **2.52**, **2.53**, **2.54**, and **2.55**.

### 2.2.2.1 Synthesis of trisaccharide **2.4**

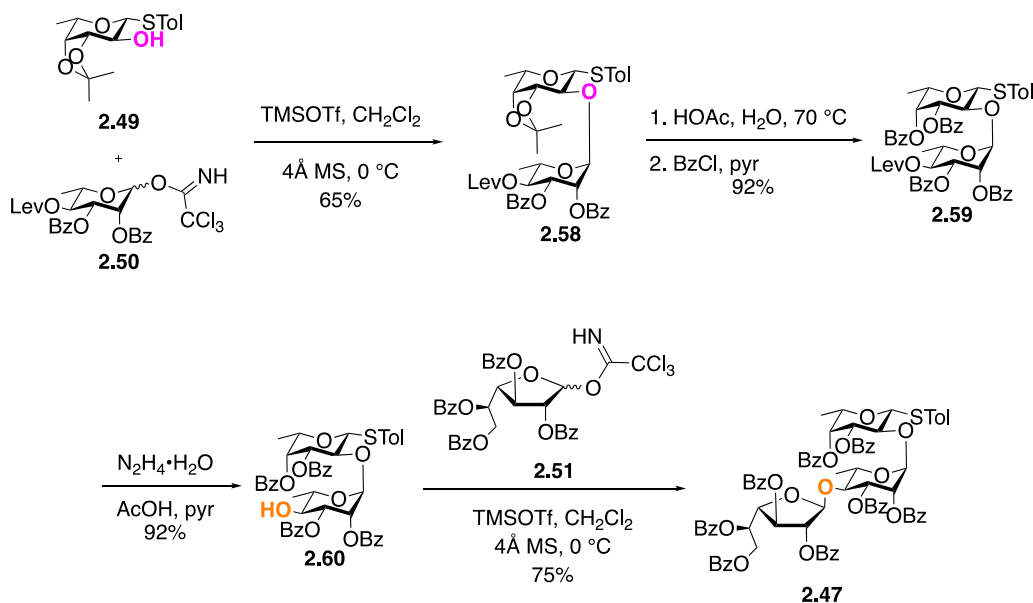
The synthesis of trisaccharide **2.4** starts with synthesis of the building blocks **2.49**–**2.51**. Building blocks **2.49**<sup>37</sup> and **2.51**<sup>38</sup> were synthesized as described in previous literature. On the other hand, building block **2.50** was obtained from reported compound **2.56**<sup>39</sup> in a total of five steps (Scheme 2-15). Alcohol **2.56** was protected with Lev group using levulinic acid, EDC·HCl, and DMAP in CH<sub>2</sub>Cl<sub>2</sub> to give the corresponding fully protected monosaccharide. The isopropylidene acetal was then hydrolyzed using acid to give the corresponding diol. The hydroxyl groups were then protected using benzoyl chloride in pyridine to afford compound **2.57** in 96% yield over three steps. Thioglycoside **2.57** was then hydrolyzed using *N*-bromosuccinimide in wet EtOAc, yielding the corresponding hemiacetal, which was transformed to a trichloroacetimidate **2.50** using trichloroacetonitrile and cesium carbonate in dichloromethane. After filtration of cesium carbonate through Celite and concentration of the mixture, the crude imidate was immediately used in the next step without further purification. The donors **2.50** and **2.51** both have ester protecting groups to ensure the desired 1,2-*trans*-linkage during glycosylation reactions.



**Scheme 2-15:** Synthesis of building block **2.50**.

With the building blocks in hand, the synthesis of **2.4** (Scheme 2-16) started with the reaction between acceptor **2.49** and crude imidate donor **2.50**, which was done using TMSOTf

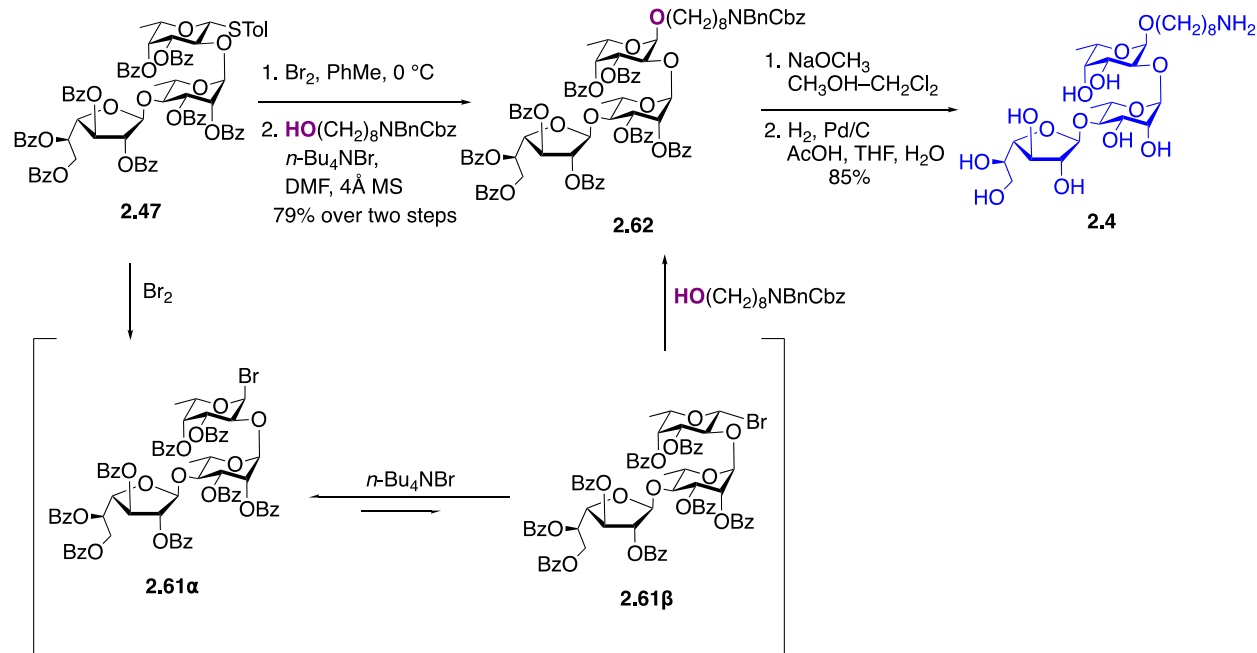
activation in  $\text{CH}_2\text{Cl}_2$  to give disaccharide **2.58** in 65% yield over three steps. The formation of the desired  $\alpha$ -linkage was confirmed by the coupling constant between Rha-H-1 and Rha-C-1 ( $^1J_{\text{C-H}} = 175.6 \text{ Hz}$ ). Removal of the acetonide protecting group and replacement with benzoyl groups was done at this point to avoid using acidic hydrolysis conditions once the acid sensitive GalF residue was introduced. This two-step process gave the disaccharide **2.59** in 92% yield over two steps. The Lev group was selectively cleaved using hydrazine monohydrate in acetic acid–pyridine mixture to give required acceptor **2.60** in 92% yield. This acceptor and GalF imidate donor **2.51** were used in a glycosylation reaction using TMSOTf activation in  $\text{CH}_2\text{Cl}_2$  to give trisaccharide **2.47** in 75% yield. The desired  $\beta$ -linkage was assigned using the peak corresponding to GalF-H-1, which appeared as a singlet ( $^3J_{1,2} = 0.0 \text{ Hz}$ ), consistent with values for 1,2-*trans*-furanosides.<sup>40</sup>



**Scheme 2-16:** Synthesis of trisaccharide **2.47**.

With trisaccharide **2.47** already in hand, the next step was to attach the linker at the reducing end. Multiple conditions were tested but most gave unsatisfactory stereoselectivity and a mixture of  $\alpha$  and  $\beta$  anomers. The most successful attempt used the Lemieux halide ion method.<sup>41</sup>

To do this, thioglycoside **2.47** was first converted to its corresponding  $\alpha$ -glycosyl bromide **2.61** by treatment with bromine in dichloromethane (Scheme 2-17). Without purification, **2.61** was added to a mixture containing linker alcohol **2.16** and tetra-*n*-butylammonium bromide in DMF and stirred overnight to yield the  $\alpha$ -product **2.62** in 70% yield over the two steps. The desired configuration was assigned using the coupling constant between Fuc-H-1 and Fuc-H-2 ( $^3J_{1,2} = 3.6$  Hz). The high stereoselectivity of the reaction can be explained by the mechanism shown below. The reaction proceeds by the way of the less stable  $\beta$ -glycosyl bromide **2.66 $\beta$** , which is in rapid equilibrium with the more stable  $\alpha$ -glycosyl bromide **2.66 $\alpha$** , in the presence of excess bromide ion. The reaction through the  $\beta$ -glycosyl bromide is faster due to the favorable antiparallel orientation of the incoming oxygen and ring oxygen lone pair in the bond making during glycosylation.<sup>22,41</sup>



**Scheme 2-17:** Synthesis of trisaccharide **2.4**.

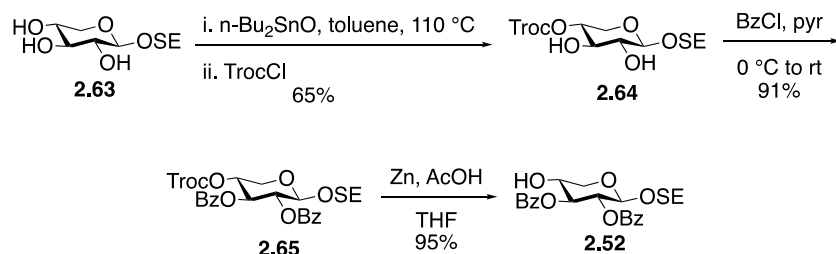
Trisaccharide **2.62** was subjected to a two-step global deprotection process. First, removal of the benzoyl ester protecting group was achieved using sodium methoxide in  $\text{CH}_2\text{Cl}_2\text{-CH}_3\text{OH}$

followed by deprotection of the benzyl and benzyl carbamate groups by hydrogenation over Pd–C in THF–H<sub>2</sub>O (1:1) to give **2.4** in 85% yield over two steps.

#### 2.2.2.2 Synthesis of tetrasaccharide **2.5**.

The synthesis of the tetrasaccharide **2.5** started with the preparation of the desired building blocks. The building block **2.52** for the D-xylose at the reducing end was designed to be a 2-trimethylsilylethyl glycoside. This decision was made to allow selective deprotection of the anomeric position to reveal the corresponding hemiacetal upon cleavage of the aglycon using anhydrous acid treatment.<sup>42</sup> The resulting hemiacetal can then be transformed to a suitable donor for glycosylation. To start, 2-trimethylsilylethyl glycoside **2.63** (Scheme 2-18), which was synthesized using a previous report,<sup>43</sup> was selectively protected at the *O*-4 position with a Troc group by first heating to reflux with *n*-Bu<sub>2</sub>SnO in toluene followed by the addition of 2,2,2-trichloroethoxycarbonyl chloride at 0 °C to give the desired product **2.64** in 65% yield. The regioselective formation of the product was confirmed by observing a correlation between of Xyl-H-4 and the Troc C=O in the HMBC spectrum. The regioselectivity of this reaction is similar to previously reported cases for similar D-xylose-containing molecules.<sup>29,44</sup> The remaining hydroxyl groups in **2.64** were protected with benzoyl protecting groups using benzoyl chloride in pyridine to obtain **2.65** in 91% yield. Finally, the Troc group was selectively deprotected upon treatment with zinc dust in acetic acid–THF to give the *O*-4 free xylose building block **2.52** in 95% yield. Upon examination of the NMR data for **2.52**, I found that the xylose residue, like the one in **2.7** and **2.27** (see above), appears to adopt a conformation different from the usual <sup>4</sup>C<sub>1</sub> because the coupling constant between H-1 and H-2 (<sup>3</sup>*J*<sub>1,2</sub> = 6.4 Hz) was unusually low for a 1,2-*trans*-glycoside. The conditions used during the synthesis of **2.52** from β-xylopyranoside **2.63** are not

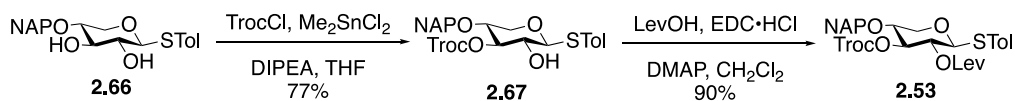
known to cause isomerization of the anomeric center and thus the possibility of anomeric isomerization is not likely. Similar  $^3J_{1,2}$  values were observed for the xylose residues in compounds **2.7** and **2.27**.



**Scheme 2-18:** Synthesis of building block **2.52**.

The next building block prepared was the orthogonally protected xylose donor **2.53** needed for the ‘hyper-branched’ residue (Scheme 2-19). The orthogonal protecting groups chosen to be installed in this molecule were Lev at O-2, Troc at O-3, and NAP at O-4. The installation of the Lev ester group at O-2 would ensure the formation of desired 1,2-*trans*-linkage during glycosylation reactions. The synthesis started with previously reported diol thioglycoside **2.66**.<sup>45</sup> Selective protection of either O-2 or O-3 in xylose residues is challenging as both have similar reactivity and are in a *trans* relationship. An attempt to selectively protect one of the hydroxyl groups using *n*-Bu<sub>2</sub>SnO in toluene at reflux followed by 2,2,2-trichloroethoxycarbonyl chloride gave a 2:3 mixture of O-2 and O-3 Troc protected products in 85% combined yield contaminated with the di-O-Troc protected product. The unsatisfactory result led me to try a method developed by Onomura that uses catalytic dimethyltin dichloride to regioselectively protect hydroxyl groups of sugars.<sup>44</sup> Using this method, compound **2.67** was mixed with dimethyltin dichloride, benzoyl chloride, diisopropylethylamine in THF to give the O-3 Troc protected sugar **2.67** in 77% yield. The reaction gave the O-2 Troc protected sugar in minor amounts and no di-O-Troc product was detected. Finally, the Lev group was installed at O-2 of the xylose intermediate **2.67** by adding

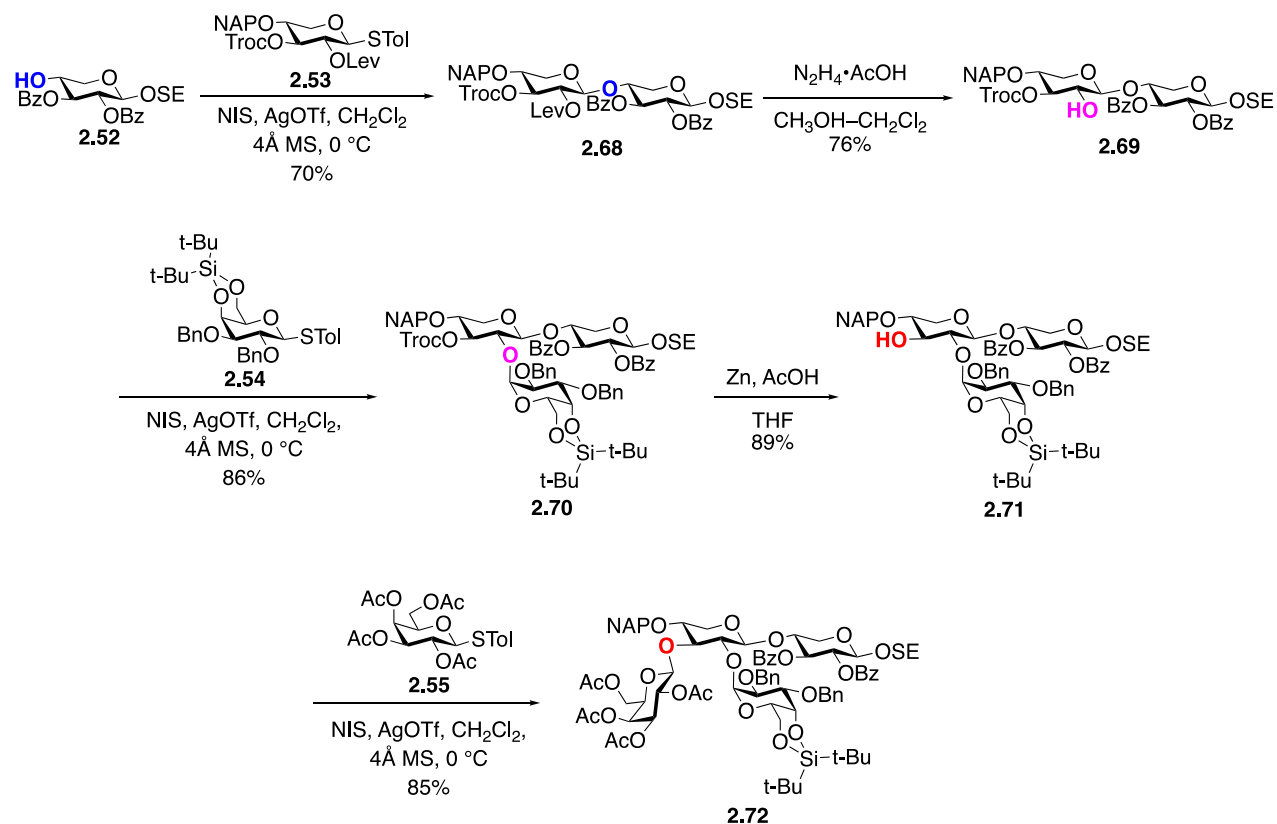
levulinic acid, EDC·HCl, and DMAP in CH<sub>2</sub>Cl<sub>2</sub> to give desired building block **2.53** in 90% yield. The desired positioning of the protecting group was confirmed by HMBC spectrum after observing correlations between H-2 and the Lev C=O. Similarly, analogous correlations were observed between H-3 and the Troc C=O in the same HMBC spectrum.



**Scheme 2-19:** Synthesis of building block **2.53**.

The two galactopyranose donor building blocks **2.54**<sup>46</sup> and **2.55**<sup>33</sup> were synthesized using previously reported literature. Again, the DTBS group on the galactopyranose donor **2.54** was installed to ensure the formation of the desired  $\alpha$ -linkage during the glycosylation.<sup>28</sup> The building block **2.55**, on the other hand, has an acetyl protecting group at O-2 to allow the formation of  $\beta$ -linked galactopyranose via neighboring group participation.

With the building blocks in hand, the synthesis of the tetrasaccharide started with the glycosylation reaction between xylose acceptor **2.52** and orthogonally protected xylose donor **2.53** using NIS–AgOTf activation in CH<sub>2</sub>Cl<sub>2</sub> to give desired disaccharide **2.68** in 70% yield (Scheme 2-20). The desired  $\beta$ -configuration was confirmed from the coupling constant between Xyl'-H-1 and Xyl'-H-2 ( $^3J_{1,2} = 7.3$  Hz).



**Scheme 2-20:** Synthesis of tetrasaccharide **2.72**.

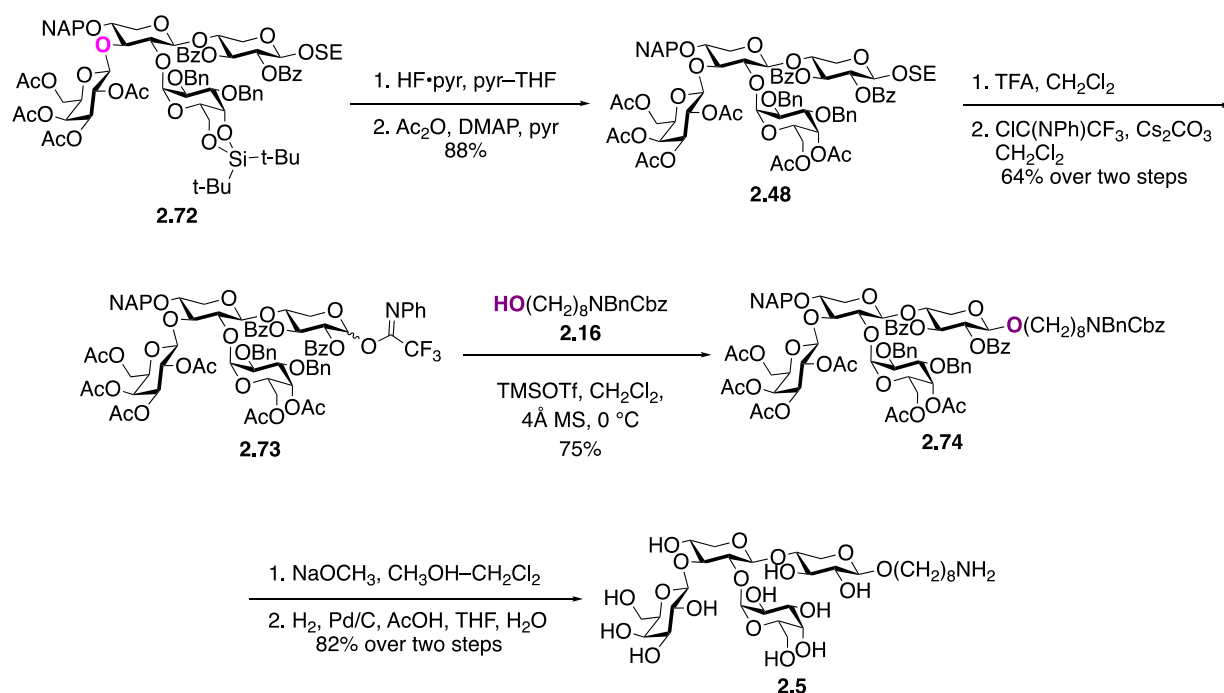
I decided to start the glycosylation sequence around the ‘hyper-branched’ xylose residue at O-2, followed by O-3, and lastly, at O-4. This decision was made through the following reasonings: 1) The selective Troc protection of xylose intermediate **2.66** shows that O-3 is more reactive than O-2. I hoped to glycosylate at the least reactive site first; 2) in the eventual synthesis of the heptasaccharide, I decided to do an end-stage [4+3] glycosylation at O-4 of the xylose using trisaccharide donor **2.47** and thus the same intermediate could be used; 3) It makes more sense to glycosylate at O-3 before O-4 as the reversed sequence would require reaction at an extremely hindered O-3 position flanked by two sugar substituents.

To start, the Lev group at O-2 was deprotected successfully using hydrazine acetate in  $\text{CH}_2\text{Cl}_2\text{-CH}_3\text{OH}$  producing disaccharide **2.69** in 76% yield. The reaction of this acceptor and

thioglycoside donor **2.54** in a NIS–AgOTf activated glycosylation gave the trisaccharide **2.70** in excellent  $\alpha$ -selectivity in 86% yield. The desired stereochemistry was assigned using the coupling constant between Gal-H-1 and Gal-H-2 ( $^3J_{1,2} = 3.7$  Hz). This excellent stereocontrol was attributed to the presence of the DTBS group in the donor. The Troc group was then deprotected using zinc dust in acetic acid–THF to give trisaccharide acceptor **2.70** in 89% yield. Trisaccharide acceptor **2.71** and donor **2.55** were reacted together using NIS–AgOTf system in a glycosylation reaction to give the tetrasaccharide product **2.72** in 85% yield. The desired  $\beta$ -configuration at the galactose was confirmed using the coupling constant between Gal-H-1 and Gal-H-2 ( $^3J_{1,2} = 7.9$  Hz). Upon analysis of the  $^1\text{H}$  NMR spectrum of **2.72**, it was discovered that the magnitude of the  $^3J_{1,2}$  of the ‘hyper-branched’ xylose residue was only 6.3 Hz. The xylose residues in previous intermediates in this sequence containing this residue (**2.68–2.71**) all have  $^3J_{1,2}$  values  $\sim 7.5$  Hz. It thus appears that the addition of another sugar residue, a considerably bulky substituent, forces the sugar to adopt an unusual structure to release steric congestion. This is possible because of the conformational flexibility of the xylose residue. I proceeded forward on the assumption that the stereochemistry was 1,2-*trans* as expected; the issue was resolved using data for the final compound (see below).

From here, I decided to replace the DTBS protecting group with acetate esters, to simplify the global deprotection at the end of the synthesis. The DTBS group was first cleaved using HF–pyridine in pyridine–THF and the resulting diol was acetylated using acetic anhydride in pyridine, giving **2.48** in 88% yield (Scheme 2-21). After the successful preparation of tetrasaccharide **2.48**, the following step was the attachment of the linker alcohol **2.16** to the reducing-end xylose residue. To achieve this, tetrasaccharide **2.48** must be converted first to a suitable donor for a glycosylation reaction with linker alcohol **2.16**. Thus, anomeric deblocking of the tetrasaccharide by selective

removal of the 2-trimethylsilylethyl aglycon was achieved by treatment with trifluoroacetic acid in CH<sub>2</sub>Cl<sub>2</sub>. Without further purification, the resulting hemiacetal was converted to the *N*-phenyl trifluoroacetimidate donor **2.73** using 2,2,2-trifluoro-*N*-phenylacetamidoyl chloride and cesium carbonate; the product was obtained in 64% yield over two steps. The imidate donor **2.73** was then activated with TMSOTf in the presence of linker alcohol **2.16** to form tetrasaccharide **2.74** in 75% yield. The configuration at the reducing xylose residue was found to be ambiguous as the coupling constant between Xyl-H-1 and Xyl-H-2 ( $^3J_{1,2} = 6.1$  Hz) was again unusually low for a 1,2-*trans*-xyloside in a <sup>4</sup>C<sub>1</sub> configuration. This slight deviation from the expected could be attributed to the flexibility of xylose residues. Interestingly, the branched xylose residue was also found to adopt an unexpected conformation other than <sup>4</sup>C<sub>1</sub> as the coupling constant between Xyl'-H-1 and Xyl'-H-2 ( $^3J_{1,2} = 6.3$  Hz) was also unusually low. However, the desired β-configuration in this residue was already confirmed during the synthesis of intermediate **2.68**. Isomerization of the anomeric center is unlikely on the conditions applied to the synthesis of **2.74**. Again, this observation is not surprising as similar observations were made upon NMR analysis of xylose residues in this thesis.

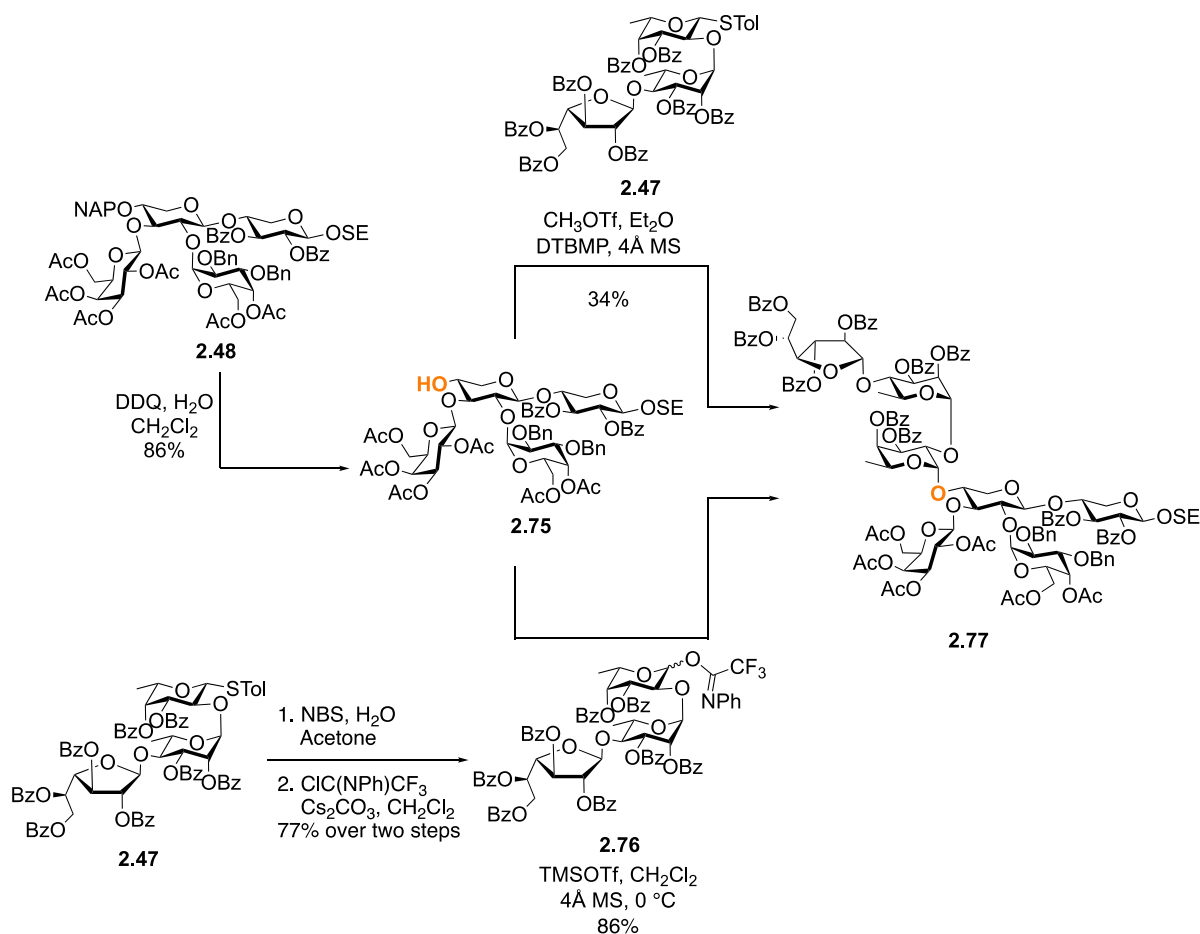


**Scheme 2-21:** Synthesis of tetrasaccharide **2.5**.

Tetrasaccharide **2.74** was subjected to a two-step global deprotection process. First, removal of the ester protecting groups was done using sodium methoxide in CH<sub>2</sub>Cl<sub>2</sub>–CH<sub>3</sub>OH. Next, deprotection of benzyl and benzyl carbamate groups was achieved by Pd–C catalyzed hydrogenation in THF–H<sub>2</sub>O (1:1). This reaction sequence gave the fully deprotected product **2.5** in 82% yield over two steps. The ambiguity regarding the configuration of the xylose residue at the reducing end (see above) was resolved at this point using the coupling constant between Xyl-H-1 and Xyl-H-2 (<sup>3</sup>J<sub>1,2</sub> = 7.9 Hz), which is consistent with a β-configuration. Interestingly, the branched xylose residue was found to deviate from the expected <sup>4</sup>C<sub>1</sub> configuration after an unexpectedly low <sup>3</sup>J<sub>1,2</sub> = 6.5 Hz. The β-configuration on this residue was established during the synthesis of intermediate **2.68**. I propose that the conformational changes by this inherently flexible monosaccharide are a mechanism to alleviate some of the steric crowding around the hyper-branched residues.

### 2.2.2.3 Synthesis of heptasaccharide **2.3** using a [4+3] glycosylation

With the successful syntheses of trisaccharide **2.4** and tetrasaccharide **2.5**, the focus shifted to synthesizing the larger heptasaccharide **2.3** containing the ‘hyper-branched’ xylose residue. The idea was to use the intermediates created during the synthesis of **2.4** and **2.5** in the synthesis of **2.3**. The most straightforward approach was to perform a [4+3] glycosylation reaction between tetrasaccharide acceptor **2.75** and trisaccharide donor **2.47** (Scheme 2-22).

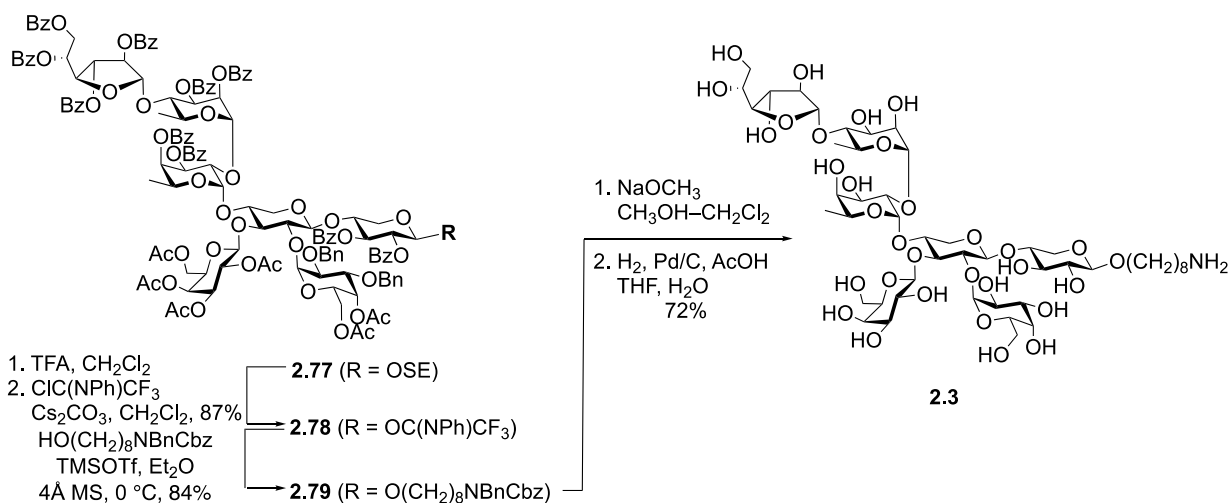


**Scheme 2-22:** Synthesis of heptasaccharide **2.77**.

To access tetrasaccharide acceptor **2.75**, the fully protected tetrasaccharide **2.48** was treated with DDQ in wet CH<sub>2</sub>Cl<sub>2</sub> to cleave the NAP group at O-4 of the xylose residue in 86% yield. An

attempt to glycosylate this acceptor using trisaccharide thioglycoside donor **2.47** with MeOTf activation in Et<sub>2</sub>O gave the desired heptasaccharide **2.77**, but only in 34% yield. A similar glycosylation was performed using NIS–AgOTf activation but this only resulted to the retrieval of the acceptor and hydrolysis of the donor. To increase the yield of the product, I converted **2.47** to a more reactive imidate donor **2.76**. This was done in two steps. First, **2.47** was hydrolyzed in the presence of *N*-bromosuccinimide in wet acetone resulting to the corresponding hemiacetal, which was then reacted with 2,2,2-trifluoro-*N*-phenylacetamidoyl chloride and cesium carbonate in CH<sub>2</sub>Cl<sub>2</sub> to obtain imidate donor **2.76** in 77% yield over the two steps. Using this prepared imidate donor, the glycosylation with acceptor **2.75** gave better results yielding heptasaccharide **2.77** in an excellent yield of 86%. The desired  $\alpha$ -configuration on the fucose residue was confirmed using the coupling constant between Fuc-H-1 and Fuc-H-2 ( $^3J_{1,2} = 3.5$  Hz). Heptasaccharide **2.77** is the first intermediate in this synthetic sequence that has the ‘hyper-branched’ xylose residue intact.

After the successful [4+3] glycosylation to form ‘hyper-branched’ xylose-containing heptasaccharide **2.77**, the installation of the linker was done. The 2-trimethylsilylethyl aglycon was cleaved using trifluoroacetic acid in CH<sub>2</sub>Cl<sub>2</sub> resulting in anomeric deblocking. The hemiacetal product was converted to the imidate using with 2,2,2-trifluoro-*N*-phenylacetamidoyl chloride and cesium carbonate in CH<sub>2</sub>Cl<sub>2</sub> providing donor **2.78** in 95% yield over two steps. Reaction of **2.78** with alcohol **2.16** was successful under TMSOTf activation giving the product **2.79** in 97% yield. The desired  $\beta$ -configuration at the reducing xylose residue was again confirmed using the coupling constant between Xyl-H-1 and Xyl-H-2 ( $^3J_{1,2} = 7.2$  Hz). With this heptasaccharide in hand, I performed a series of deprotection reactions to remove the protecting groups (Scheme 2-23). Deacylation using sodium methoxide in CH<sub>3</sub>OH–CH<sub>2</sub>Cl<sub>2</sub> followed by Pd–C catalyzed hydrogenation in THF–H<sub>2</sub>O provided the target heptasaccharide **2.3** in 72% yield.



**Scheme 2-23:** Synthesis of heptasaccharide **2.3**.

The conformations of the xylose residues in **2.3** were investigated using <sup>1</sup>H NMR spectroscopy. The xylose residue at the reducing end seems to adopt a <sup>4</sup>C<sub>1</sub> conformation as evident by the coupling constant between Xyl-H-1 and Xyl-H-2 (<sup>3</sup>J<sub>1,2</sub> = 7.8 Hz). On the other hand, and similar to observations made for tetrasaccharide **2.5**, the lower <sup>3</sup>J<sub>1,2</sub> for the ‘hyper-branched’ xylose (6.6 Hz), suggests this residue deviates from <sup>4</sup>C<sub>1</sub> conformation. This deviation from the expected conformation can be attributed to the flexibility of the xylose residue. In addition, the congestion around the ‘hyper-branched’ residue can be a significant driving force for the residue to adopt conformations different from <sup>4</sup>C<sub>1</sub> to alleviate steric crowding.

#### 2.2.2.4 Summary

A modular approach was used to synthesize target heptasaccharide **2.3**. The target was broken down into two smaller fragments, trisaccharide **2.4** and tetrasaccharide **2.5**. The syntheses of the smaller fragments were done in a linear fashion. The same approach was employed in synthesizing the building block corresponding to the ‘hyper-branched’ D-xylose, in which the

building block was designed to have three orthogonal protecting groups thus allowing for a versatile approach in accessing different glycosylation sequences. Luckily, the first and only sequence planned and attempted was successful. This ‘clockwise’ sequence starts with glycosylation of O-2, followed by O-3, and lastly, at O-4. The intermediates created during the synthesis of trisaccharide **2.4** and tetrasaccharide **2.5** were used to perform a successful end-stage [4+3] glycosylation forming the heptasaccharide with a ‘hyper-branched’ xylose residue in good yield and stereoselectivity.

### **2.3 <sup>1</sup>H NMR comparison between native GP72 and synthetic glycans**

The successful synthesis of hexasaccharide **2.2** and heptasaccharide **2.3** allowed me to provide some comparison between the <sup>1</sup>H NMR data between the synthetic glycan fragments and the native glycan isolated from GP72 of *T. cruzi*. The structures of these compounds are shown in Figure 2-3. Table 2-1 and 2-2 show the <sup>1</sup>H NMR data for anomeric protons (H-1) of each sugar residues in **2.2** and **2.3**, respectively. The <sup>1</sup>H NMR data of the native GP72 were also shown for comparison. In some cases, more than one value is reported for the native GP72 because the data provided from the literature were taken from a heterogenous sample of the glycan. Most of the <sup>1</sup>H NMR data for the anomeric peaks in **2.2** and **2.3** are close to that of the native GP72, but there are a few exceptions. The deviation of the data corresponding to the GluNAc<sub>p</sub> residue at the reducing end can be attributed to the fact that this residue was present at its hemiacetal form in the native GP72 while it is locked in its α-form in **2.2**. Another large difference was that the H-1 of the α-Galp residue of **2.2**, which appeared more downfield ( $\delta_{\text{H-1}} = 5.98$ ) compared to that of the native glycan ( $\delta_{\text{H-1}} = 5.40/5.35$ ). Lastly, the H-1 of β-Galf residue ( $\delta_{\text{H-1}} = 5.32$ ) in **2.3** also appeared to

be substantially more downfield compared to that of the native glycan ( $\delta_{H-1} = 5.09$ ). Resonances with large differences are highlighted in gray.

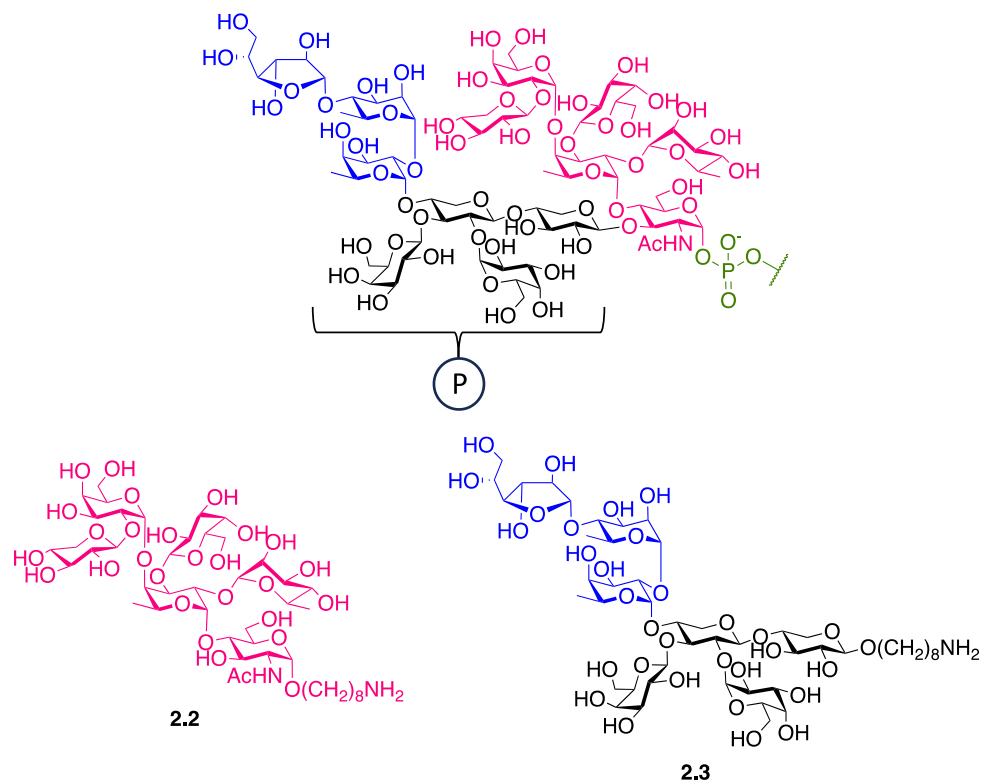


**Figure 2-3:** Structure of GP72 native glycan and synthetic fragments **2.2** and **2.3**.

**Table 2-1.** <sup>1</sup>H NMR data for the GP72 native glycan and synthetic hexasaccharide **2.2**.

Sugar	$\delta_{H-1}$ ; native GP72	$\delta_{H-1}$ ; <b>2.2</b>
$\alpha$ -GlcNAc <sub>p</sub>	4.74/5.23	4.91
$\beta$ -Xyl <sub>p</sub>	4.54/4.66	4.62
$\alpha$ -Gal <sub>p</sub>	5.40/5.35	5.98
$\alpha$ -Fuc <sub>p</sub>	5.18	5.22
$\alpha$ -Rhap	Not reported	5.01
$\beta$ -Gal <sub>p</sub>	4.81	4.83

**Table 2-2.** <sup>1</sup>H NMR data for the GP72 native glycan and synthetic heptasaccharide **2.3**.

Sugar	$\delta_{H-1}$ ; native GP72	$\delta_{H-1}$ ; <b>2.3</b>
$\beta$ -Xylp	4.48	4.43
$\beta$ -Xylp'	4.82	4.84
$\beta$ -Galp	4.68	4.67
$\alpha$ -Galp	5.46	5.46
$\alpha$ -Fucp	5.19	5.21
$\alpha$ -Rhap	4.91	4.93
$\beta$ -Galf	5.09	5.31

The differences in the chemical shifts of anomeric hydrogens observed in the spectra of synthetic compounds compared to the native glycan could be explained in several ways. First, it is possible that the smaller fragments **2.2** and **2.3** adopt conformations different than the native GP72 glycan. These differences might not exist if a synthetic version of the whole glycan structure (e.g., tridecasaccharide **2.1**) was compared to that of the native glycan. Another explanation for these differences is the fact that the native GP72 is phosphorylated at one or two galactose residues (both in the phosphomonoester and cyclic phosphodiester form) although the precise locations are unknown. The absence of the phosphorylation in the synthetic glycans **2.2** and **2.3** could cause chemical shift deviations compared to in the spectra of the native compound. The presence of the ionic phosphate functional group/s could both directly impact the chemical shifts of the monosaccharides to which they are attached through inductive effects, as well as indirectly by influencing the conformation these molecules adopt in solution. Finally, another possibility is that the reported structure of the target glycan of GP72 was incorrect.

## 2.4 Conclusions

In conclusion, the work presented in this chapter described the syntheses of four fragments of the antigenic glycan epitope of the *T. cruzi* glycoprotein GP72. This 13-residue glycan has a

unique and complex structure containing two hyper-branched residues, a fucose and a xylose. The synthesis of ‘hyper-branched’ oligosaccharides is challenging due to the increasing steric hindrance on the growing molecule that could affect both the yields and stereoselectivities of the reactions. The correct glycosylation sequence must be employed to obtain these highly congested oligosaccharide targets. The molecule was broken down into two fragments, hexasaccharide **2.2** and heptasaccharide **2.3**, each containing a ‘hyper-branched’ residue. A versatile approach of installing three orthogonal groups around the building block corresponding to the ‘hyper-branched’ residues was employed to access all possible glycosylation sequence during the synthesis.

The first attempt to synthesize hexasaccharide **2.2** using a ‘counterclockwise’ approach was found to be futile, as multiple attempts on glycosylation at O-3 failed when O-4 was glycosylated. On the other hand, a ‘clockwise’ approach was tried and gave the desired tetrasaccharide intermediate in moderate yield but required the addition a large amount of donor in the second glycosylation. Unsatisfied with this outcome, another sequence, which I call the ‘pendulum’ approach, proceeded in good yield by glycosylation of O-3 followed by O-2 and O-4. Although not explored in this chapter, I am hypothesizing that the ‘reversed pendulum’ approach would also work to synthesize the ‘hyper-branched’ fucose moiety. In this approach, glycosylation on O-3 comes first followed by O-4 and lastly on O-2. Some successful examples of this approach are shown in the next chapter.

The synthesis of the heptasaccharide **2.3** started with the synthesis of two other smaller fragments **2.4** and **2.5**. The ‘hyper-branched’ xylose residue was done using a ‘clockwise’ approach, requiring initial glycosylation at O-2, followed by O-3 and a final [4+3] glycosylation at O-4. This was the only sequence attempted and fortunately, gave the product in good yield and stereoselectivity. Interestingly, the conformation of the ‘hyper-branched’ xylose residue was found

to deviate significantly from the expected  ${}^4C_1$  based upon uncharacteristically low  ${}^3J_{1,2}$  values for this residue in both **2.3** and **2.5**. I proposed that congestion around these ‘hyper-branched’ residues is a significant driving force for the residue to adopting conformations other than  ${}^4C_1$  to alleviate steric crowding.

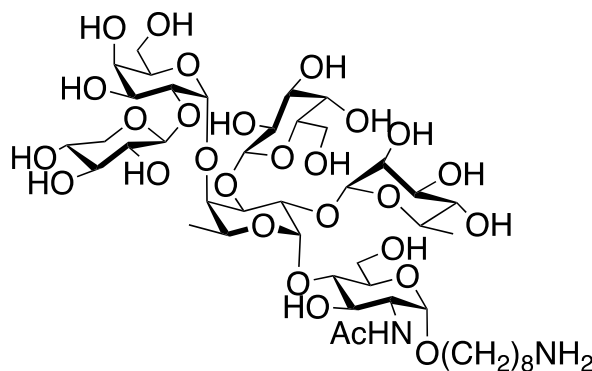
The syntheses of ‘hyper-branched’ carbohydrate structures are, as expected, not as straightforward. The work in this chapter showed the strategies employed in the synthesis of these compounds. Having a versatile strategy, allowing access to multiple possible glycosylation sequences was vital to the success of the synthetic plan. One successful sequence to one system might not be applicable to another target molecule despite having the same ‘hyper-branched’ residue. For example, the ACTV-1 *N*-glycan chlorovirus and hexasaccharide **2.6** both contains ‘hyper-branched’ L-fucose residues but the successful routes to obtain them are different. Such differences include more than just the glycosylation sequence; the identity of the donors and the effect of the glycosylation at a certain position on the acceptor are also important considerations.

## **2.5 Experimental section**

**General Methods:** All chemicals and reagents were purchased from commercial sources and were used without further purification unless noted. Reaction solvents (THF and  $CH_2Cl_2$ ) were taken from a solvent purification system in which the solvents were purified by successive passage through columns of alumina and copper under argon. Unless stated otherwise, all reactions were carried out at room temperature and under a positive pressure of argon and were monitored by TLC on Silica Gel G-25 F254 (0.25 mm, Merck). Visualization of the reaction components on TLC was achieved using UV light (254 nm) and/or by charring after treatment with a solution of *p*-anisaldehyde (3.7 mL) and glacial acetic acid (1.5 mL) and concentrated  $H_2SO_4$  (5 mL) in

ethanol (135 mL). Organic solvents were evaporated under reduced pressure, and the products were purified by column chromatography on silica gel (70 mesh). Optical rotations were measured on a Jasco P-2000 digital polarimeter at the sodium D line (589 nm) at  $25 \pm 2$  °C and are in units of (deg·mL)/(dm·g).  $^1\text{H}$  NMR spectra were recorded at 500 MHz or 600 MHz and the chemical shifts are referenced to residual  $\text{CHCl}_3$  (7.26 ppm,  $\text{CDCl}_3$ ) or HDO (4.78 ppm,  $\text{D}_2\text{O}$ ).  $^{13}\text{C}$  NMR spectra were recorded at 126 MHz or 151 MHz and are proton decoupled, and the chemical shifts are referenced to  $\text{CDCl}_3$  (77.0 ppm,  $\text{CDCl}_3$ ) or internal acetone (31.45 ppm,  $\text{D}_2\text{O}$ ). Standard splitting patterns are abbreviated: s (singlet), d (doublet), t (triplet), q (quartet), m (multiplet). To unequivocally assign the  $^1\text{H}$  and  $^{13}\text{C}$  NMR data, the protons and carbons corresponding to the monosaccharide at the reducing end were unprimed, while those corresponding to the next monosaccharide were labelled as  $\text{H}'$  and  $\text{C}'$ , and the next furthest from the reducing end  $\text{H}''$  and  $\text{C}''$ , and so on. For larger oligosaccharides (tetrasaccharides and/or larger) where assignment of all  $^1\text{H}$  and  $^{13}\text{C}$  NMR data cannot be done unambiguously due to overlapping peaks, only the anomeric data were reported. For example, the anomeric proton and carbon for an  $\alpha$ -L-rhamnopyranoside will be labelled as  $\alpha$ -Rhap-H-1 and  $\alpha$ -Rhap-C-1, respectively. In cases where more than one residue have the same sugar identity and anomeric configuration, e.g., two  $\beta$ -D-galactopyranosides, are present in the same molecule, the residue closest to the reducing end of the longest chain will be labelled as  $\beta$ -Galp-H-1 and  $\beta$ -Galp-C-1, and the next furthest from the reducing end  $\beta$ -Galp'-H-1 and  $\beta$ -Galp'-C-1. High resolution and high mass accuracy LC-MS experiments were done on a LTQFT Ultra (Linear quadrupole ion trap Fourier transform ion cyclotron resonance) mass spectrometer (Thermo Electron, San Jose, CA) equipped with a HESI-II source, an Agilent 1100 Series binary high-performance liquid chromatography pump (Agilent Technologies, Palo Alto, CA), and a Famos autosampler (LC Packings, San Francisco, CA). High

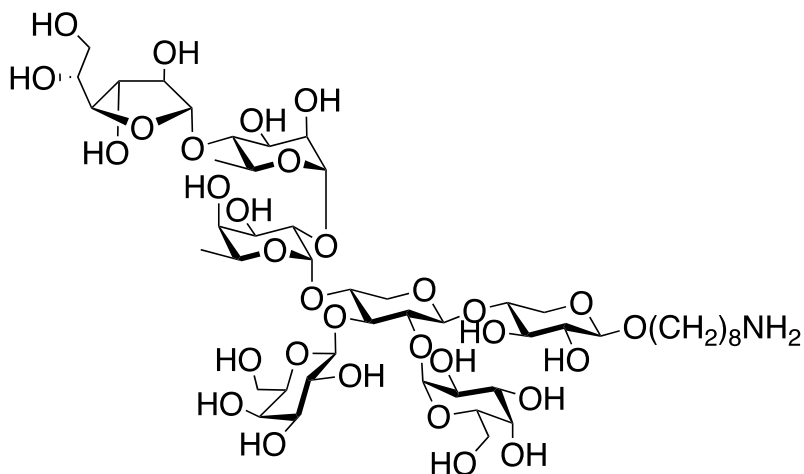
resolution MALDI–TOF mass spectra were conducted on a New ultrafleXtreme™ MALDI–TOF/TOF mass spectrometer (Bruker Corporation, Bremen, Germany) using DHB (2,5-dihydroxybenzoic acid) as the matrix.



**8-aminooctyl [ $\beta$ -D-galactopyranosyl-(1 $\rightarrow$ 3)-[ $\alpha$ -L-rhamnopyranosyl-(1 $\rightarrow$ 2)]-[ $\beta$ -D-xylopyranosyl-(1 $\rightarrow$ 2)]- $\alpha$ -D-galactopyranosyl-(1 $\rightarrow$ 4)]- $\alpha$ -L-fucopyranosyl-(1 $\rightarrow$ 4)]-N-acetyl-2-amino-2-deoxy- $\alpha$ -D-glucopyranoside (2.2)**

To a solution of compound **2.46** (30.0 mg, 0.0109 mmol) in AcOH–THF (20 mL, 1:1) was added freshly activated zinc dust (29.0 mg) and acetic anhydride (14.4 mL, 0.105  $\mu$ mol). After stirring overnight, the mixture was filtered through Celite. The filtrate was concentrated, dissolved in EtOAc (100 mL) and washed with water, saturated aqueous NaHCO<sub>3</sub> and brine. The organic layer was dried over Na<sub>2</sub>SO<sub>4</sub>, filtered and concentrated to dryness. The crude residue was dissolved in CH<sub>3</sub>OH–CH<sub>2</sub>Cl<sub>2</sub> (5.0 mL, 4:1) and then a solution of NaOCH<sub>3</sub> (0.5 M in CH<sub>3</sub>OH) was added until the solution pH = 12 (by wet pH paper). After stirring overnight, the reaction mixture was neutralized by the addition of prewashed Amberlite® IR-120 (H<sup>+</sup>) cation exchange resin, filtered and concentrated to dryness. The crude product was purified by flash chromatography (8:1 CH<sub>2</sub>Cl<sub>2</sub>–CH<sub>3</sub>OH) to give a white residue. This residue was dissolved in 1% AcOH in THF–H<sub>2</sub>O (4 mL, 1:1) and then 5% palladium on carbon (5.8 mg) was added. After stirring for 24 h under

an H<sub>2</sub> atmosphere (1 atm), the reaction mixture was filtered through Celite and concentrated. The crude residue was purified by a C18 reversed-phase chromatography (H<sub>2</sub>O to 9:1 H<sub>2</sub>O–MeOH) to afford a white solid that was redissolved in distilled water. The resulting solution was frozen and then lyophilized to afford **2.2** (7.9 mg, 68% over three steps) as a white fluffy solid: <sup>1</sup>H NMR (700 MHz, D<sub>2</sub>O) δ 5.98 (d, *J* = 3.9 Hz, 1H, α-Galp-H-1), 5.22 (d, *J* = 4.0 Hz, 1H, α-Fucp-H-1), 5.01 (s, 1H, α-Rhap-H-1), 4.91 (d, *J* = 3.7 Hz, 1H, α-GlcNAcp-H-1), 4.83 (d, *J* = 7.9 Hz, 1H, β-Galp-H-1), 4.62 (d, *J* = 7.8 Hz, 1H, β-Xylp-H-1), 4.52–4.44 (m, 2H), 4.33 (dd, *J* = 10.7, 3.9 Hz, 1H), 4.30–4.24 (m, 2H), 4.19 (dd, *J* = 10.4, 3.3 Hz, 1H), 4.05 (app dq, *J* = 7.7, 4.2 Hz, 3H), 4.01 (dd, *J* = 11.7, 5.5 Hz, 1H), 3.96 (dd, *J* = 10.6, 3.8 Hz, 1H), 3.95–3.92 (m, 3H), 3.91–3.85 (m, 4H), 3.81–3.67 (m, 8H), 3.65 (dd, *J* = 10.0, 3.4 Hz, 1H), 3.55–3.47 (m, 4H), 3.44 (app t, *J* = 9.4 Hz, 1H), 3.35 (app t, *J* = 11.2 Hz, 1H), 3.01 (app t, *J* = 7.6 Hz, 2H), 1.72–1.65 (m, 2H), 1.65–1.59 (m, 2H), 1.46–1.35 (m, 8H), 1.36 (d, *J* = 6.4 Hz, 3H), 1.27 (d, *J* = 6.5 Hz, 3H); <sup>13</sup>C NMR (126 MHz, D<sub>2</sub>O) δ 174.3, 103.2 (β-Galp-C-1), 100.8 (β-Xylp-C-1), 98.4 (α-Rhap-C-1), 96.8 (α-Fucp-C-1), 96.3 (α-GlcNAcp-C-1), 96.0 (α-Galp-C-1), 76.8, 76.7, 75.8, 75.2, 73.9, 73.3, 72.7, 72.4, 71.3, 71.3, 71.0, 70.6, 70.6, 70.3, 70.1, 69.6, 69.5, 69.1, 69.0, 68.2, 68.1, 67.7, 65.8, 65.0, 61.5, 61.2, 60.1, 54.2, 39.5, 28.3, 28.1 (2 x C), 26.6, 25.5, 25.0, 21.8, 16.8, 16.6, 14.1; HRMS (ESI–TOF) *m/z*: [M + H]<sup>+</sup> Calcd for C<sub>45</sub>H<sub>81</sub>N<sub>2</sub>O<sub>28</sub> 1097.4970; Found 1097.4962.

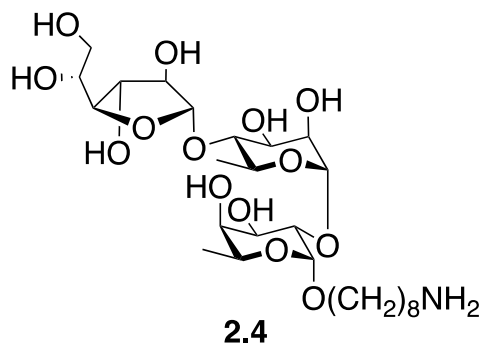


**2.3**

**8-amino-1-octyl [ $\beta$ -D-galactopyranosyl-(1 $\rightarrow$ 3)]-[ $\alpha$ -D-galactopyranosyl-(1 $\rightarrow$ 2)]-[[[ $\beta$ -D-galactofuranosyl-(1 $\rightarrow$ 4)]- $\alpha$ -L-rhamnopyranosyl]-(1 $\rightarrow$ 2)- $\alpha$ -L-fucopyranosyl-(1 $\rightarrow$ 4)]- $\beta$ -D-xylopyranosyl-(1 $\rightarrow$ 4)]- $\beta$ -D-xylopyranoside (2.3)**

To a stirred solution of **2.79** (29.0 mg, 0.0101 mmol) in CH<sub>3</sub>OH–CH<sub>2</sub>Cl<sub>2</sub> (5.0 mL, 4:1) was added a solution of NaOCH<sub>3</sub> (0.5 M in CH<sub>3</sub>OH) until the solution pH = 12. After stirring overnight, the reaction mixture was neutralized by the addition of prewashed Amberlite® IR-120 (H<sup>+</sup>) cation exchange resin, filtered and concentrated to dryness. The crude product was purified by flash chromatography (8:1 CH<sub>2</sub>Cl<sub>2</sub>–CH<sub>3</sub>OH) to give a white residue. This residue was dissolved in 1% AcOH in THF–H<sub>2</sub>O (4.0 mL, 1:1) and then 5% palladium on carbon (5.8 mg) was added. After stirring for 24 h under an H<sub>2</sub> atmosphere (1 atm), the reaction mixture was filtered through Celite and concentrated. The crude residue was purified by C18 reversed-phase chromatography (H<sub>2</sub>O to 9:1 H<sub>2</sub>O–MeOH) to afford a white solid that was redissolved in distilled water. The resulting solution was frozen and then lyophilized to afford **2.3** (8.6 mg, 72% over two steps) as a white fluffy solid: <sup>1</sup>H NMR (600 MHz, D<sub>2</sub>O)  $\delta$  5.46 (d,  $J$  = 3.7 Hz, 1H,  $\alpha$ -Gal $p$ -H-1), 5.31 (d,  $J$  = 1.9 Hz, 1H,  $\beta$ -Gal $f$ -H-1), 5.21 (d,  $J$  = 3.5 Hz, 1H,  $\alpha$ -Fuc $p$ -H-1), 4.93 (d,  $J$  = 1.9 Hz, 1H,  $\alpha$ -Rhap-H-1), 4.83 (d,  $J$  = 6.6 Hz, 1H,  $\beta$ -Xyl $p'$ -H-1), 4.67 (d,  $J$  = 7.8 Hz, 1H,  $\beta$ -Gal $p$ -H-1), 4.60 (app q,  $J$  = 6.7 Hz,

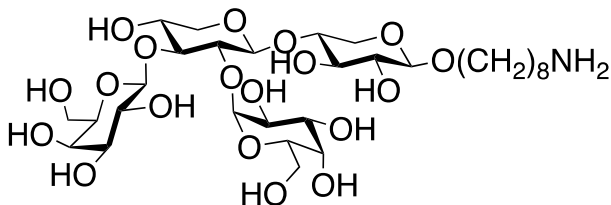
1H), 4.43 (d,  $J = 7.8$  Hz, 1H,  $\beta$ -Xylp-H-1), 4.23 (dd,  $J = 8.2, 4.3$  Hz, 1H), 4.20 (dd,  $J = 12.2, 4.4$  Hz, 1H), 4.18–4.15 (m, 2H), 4.14 (dd,  $J = 3.9, 1.8$  Hz, 1H), 4.09 (dd,  $J = 6.6, 3.8$  Hz, 1H), 4.02 (dd,  $J = 6.5, 3.9$  Hz, 1H), 4.00 (dd,  $J = 9.6, 3.4$  Hz, 1H), 3.99–3.95 (m, 2H), 3.95–3.90 (m, 3H), 3.90–3.78 (m, 9H), 3.78–3.69 (m, 5H), 3.70–3.57 (m, 6H), 3.53 (dd,  $J = 9.9, 7.7$  Hz, 1H), 3.51–3.42 (m, 2H), 3.28 (dd,  $J = 9.3, 7.8$  Hz, 1H), 3.04–2.95 (m, 2H), 1.70–1.57 (m, 4H), 1.43–1.32 (m, 8H), 1.31 (d,  $J = 6.2$  Hz, 3H), 1.22 (d,  $J = 6.6$  Hz, 3H);  $^{13}\text{C}$  NMR (126 MHz,  $\text{D}_2\text{O}$ )  $\delta$  108.4 ( $\beta$ -Galp-C-1), 102.8 ( $\beta$ -Xylp-C-1), 102.3 ( $\beta$ -Galp-C-1), 99.9 ( $\beta$ -Xylp'-C-1), 97.4 ( $\alpha$ -Rhap-C-1), 96.4 ( $\alpha$ -Galp-C-1), 94.4 ( $\alpha$ -Fucp-C-1), 82.8, 81.4, 78.1, 76.5, 75.1 (2 x C), 75.0, 73.7, 73.4, 73.0 (2 x C), 72.6, 71.9 (2 x C), 71.2, 70.9, 70.7, 70.7, 70.6, 70.4, 69.3, 69.2, 68.4, 68.1, 67.8, 67.5, 66.9, 62.8, 62.4, 61.6, 61.3, 61.3, 39.5, 28.7, 28.1, 28.0, 26.6, 25.4, 24.9, 17.1, 15.2; HRMS (ESI-TOF)  $m/z$ :  $[\text{M} + \text{H}]^+$  Calcd for  $\text{C}_{48}\text{H}_{86}\text{NO}_{32}$  1188.5133; Found 1188.5129.



**8-amino-1-octyl  $\beta$ -D-galactofuranosyl-(1 $\rightarrow$ 4)- $\alpha$ -L-rhamnopyranosyl-(1 $\rightarrow$ 2)- $\alpha$ -L-fucopyranoside (2.4)**

To a stirred solution of **2.62** (23.0 mg, 0.0139 mmol) in  $\text{CH}_3\text{OH}-\text{CH}_2\text{Cl}_2$  (8 mL, 3:1) was added a solution of  $\text{NaOCH}_3$  (0.5 M in  $\text{CH}_3\text{OH}$ ) until the solution pH = 12. After stirring overnight, the reaction mixture was neutralized by the addition of prewashed Amberlite® IR-120 ( $\text{H}^+$ ) cation exchange resin, filtered and concentrated to dryness. The crude product was purified by flash

chromatography (8:1 CH<sub>2</sub>Cl<sub>2</sub>–CH<sub>3</sub>OH) to give a white residue. This residue was dissolved in 1% AcOH in THF–H<sub>2</sub>O (4.0 mL, 1:1) and then 5% palladium on carbon (4.6 mg) was added. After stirring for 24 h under an H<sub>2</sub> atmosphere (1 atm), the reaction mixture was filtered through Celite and concentrated. The crude residue was purified by C18 reversed-phase chromatography (H<sub>2</sub>O to 9:1 H<sub>2</sub>O–MeOH) to afford a white solid that was redissolved in distilled water. The resulting solution was frozen and then lyophilized to afford **2.4** (7.1 mg, 85% over two steps) as a white fluffy solid: <sup>1</sup>H NMR (700 MHz, D<sub>2</sub>O) δ 5.32 (d, *J* = 1.9 Hz, 1H, β-Galf-H-1), 5.13 (d, *J* = 3.5 Hz, 1H, α-Rhap-H-1), 4.94 (d, *J* = 1.7 Hz, 1H, α-Fucp-H-1), 4.15 (dd, *J* = 4.1, 1.8 Hz, 1H, β-Galf-H-2), 4.10 (dd, *J* = 6.6, 3.9 Hz, 1H, β-Galf-H-3), 4.08 (app q, *J* = 6.7 Hz, 1H, α-Fucp-H-5), 4.04 (dd, *J* = 6.6, 3.9 Hz, 1H, β-Galf-H-4), 4.00 (dd, *J* = 9.7, 3.4 Hz, 1H, α-Rhap-H-3), 3.99–3.94 (m, 1H, α-Rhap-H-5), 3.94 (dd, *J* = 3.5, 1.7 Hz, 1H, α-Fucp-H-2), 3.91 (dd, *J* = 10.3, 3.3 Hz, 1H, α-Fucp-H-3), 3.88 (dd, *J* = 10.3, 3.6 Hz, 1H, α-Rhap-H-2), 3.86–3.83 (m, 2H, β-Galf-H-5, α-Fucp-H-4), 3.78–3.71 (m, 2H, octyl OCH<sub>2</sub>, β-Galf-H-6a), 3.68 (dd, *J* = 11.7, 7.5 Hz, 1H, β-Galf-H-6b), 3.62 (app t, *J* = 9.7 Hz, 1H, α-Rhap-H-4), 3.58 (app dt, *J* = 10.3, 6.4 Hz, 1H, octyl OCH<sub>2</sub>), 3.01 (app t, *J* = 7.6 Hz, 2H, octyl CH<sub>2</sub>NH<sub>2</sub>), 1.72–1.60 (m, 4H, OCH<sub>2</sub>CH<sub>2</sub>, NCH<sub>2</sub>CH<sub>2</sub>), 1.45–1.35 (m, 8H, 4 x CH<sub>2</sub>), 1.33 (d, *J* = 6.3 Hz, 3H, α-Rhap-H-6), 1.24 (d, *J* = 6.6 Hz, 3H, α-Fucp-H-6); <sup>13</sup>C NMR (176 MHz, D<sub>2</sub>O) δ 108.5 (β-Galf-C-1), 97.1 (α-Rhap-C-1), 95.1 (α-Fucp-C-1), 82.9 (β-Galf-C-4), 81.5 (β-Galf-C-2), 78.2 (α-Rhap-C-4), 76.6 (β-Galf-C-3), 71.9 (α-Rhap-C-2), 71.8 (α-Fucp-C-4), 70.8 (α-Fucp-C-2), 70.6 (β-Galf-C-5), 70.5 (α-Rhap-C-3), 68.1 (octyl OCH<sub>2</sub>), 68.1 (α-Fucp-C-3), 67.5 (α-Rhap-C-5), 66.5 (α-Fucp-C-5), 62.9 (β-Galf-C-6), 39.5 (octyl NCH<sub>2</sub>), 28.3 (CH<sub>2</sub>), 28.1 (CH<sub>2</sub>), 26.7 (CH<sub>2</sub>), 25.5 (CH<sub>2</sub>), 25.3 (CH<sub>2</sub>), 23.3 (CH<sub>2</sub>), 17.1 (α-Rhap-C-6), 15.3 (α-Fucp-C-6); HRMS (ESI–TOF) *m/z*: [M + H]<sup>+</sup> Calcd for C<sub>26</sub>H<sub>50</sub>NNaO<sub>14</sub> 600.3226; Found 600.3218.



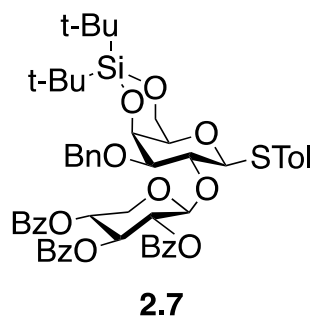
**2.5**

**8-amino-1-octyl                     $\beta$ -D-galactopyranosyl-(1 $\rightarrow$ 3)-[ $\alpha$ -D-galactopyranosyl-(1 $\rightarrow$ 2)]- $\beta$ -D-xylopyranosyl-(1 $\rightarrow$ 4)- $\beta$ -D-xylopyranoside (2.5)**

To a stirred solution of **2.74** (30.0 mg, 0.0173 mmol) in CH<sub>3</sub>OH–CH<sub>2</sub>Cl<sub>2</sub> (8 mL, 3:1) was added a solution of NaOCH<sub>3</sub> (0.5 M in CH<sub>3</sub>OH) until the solution pH = 12. After stirring overnight, the reaction mixture was neutralized by the addition of prewashed Amberlite® IR-120 (H<sup>+</sup>) cation exchange resin, filtered and concentrated to dryness. The crude product was purified by flash chromatography (8:1 CH<sub>2</sub>Cl<sub>2</sub>–CH<sub>3</sub>OH) to give a white residue. This residue was dissolved in 1% AcOH in THF–H<sub>2</sub>O (4.0 mL, 1:1) and then 5% palladium on carbon (6.0 mg) was added. After stirring for 24 h under an H<sub>2</sub> atmosphere (1 atm), the reaction mixture was filtered through Celite and concentrated. The crude residue was purified by C18 reversed-phase chromatography (H<sub>2</sub>O to 9:1 H<sub>2</sub>O–MeOH) to afford a white solid that was redissolved in distilled water. The resulting solution was frozen and then lyophilized to afford **2.5** (10.4 mg, 82% over two steps) as a white fluffy solid: <sup>1</sup>H NMR (500 MHz, D<sub>2</sub>O)  $\delta$  5.46 (d, *J* = 3.8 Hz, 1H,  $\alpha$ -Galp-H-1), 4.74 (d, *J* = 6.5 Hz, 1H,  $\beta$ -Xylp'-H-1), 4.63 (d, *J* = 7.6 Hz, 1H,  $\beta$ -Galp-H-1), 4.43 (d, *J* = 7.8 Hz, 1H,  $\beta$ -Xylp-H-1), 4.42–4.37 (m, 1H), 4.16 (dd, *J* = 11.7, 5.2 Hz, 1H), 4.13–4.08 (m, 1H), 3.99 (s, 1H), 3.96–3.70 (m, 13H), 3.70–3.64 (m, 2H), 3.63–3.55 (m, 2H), 3.52–3.39 (m, 2H), 3.32–3.25 (m, 1H), 3.00 (app t, *J* = 7.6 Hz, 3H), 1.71–1.58 (m, 4H), 1.44–1.34 (m, 8H); <sup>13</sup>C NMR (126 MHz, D<sub>2</sub>O)  $\delta$  102.8 ( $\beta$ -Xylp-C-1), 102.8 ( $\alpha$ -Galp-C-1), 100.6 ( $\beta$ -Xylp'-C-1), 96.7 ( $\beta$ -Galp-C-1), 81.0, 75.5, 75.4, 73.8, 73.0, 72.9, 72.5, 71.0, 70.9, 70.7, 69.4, 69.1, 68.6, 68.3, 68.2, 63.7, 62.7, 61.3, 61.0, 39.5, 28.7,



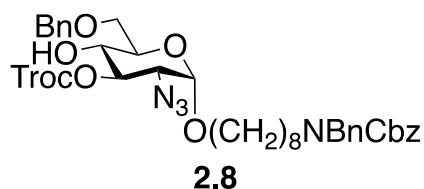
OCH<sub>2</sub>Ar), 4.15 (app ddt,  $J = 12.5, 5.4, 1.5$  Hz, 1H, OCH<sub>2</sub>CH=CH<sub>2</sub>), 4.10 (q,  $J = 6.6$  Hz, 1H, H-5'), 3.99 (dd,  $J = 12.5, 5.6$  Hz, 1H, OCH<sub>2</sub>CH=CH<sub>2</sub>), 3.94 (app t,  $J = 9.3$  Hz, 1H, H-5), 3.90–3.83 (m, 2H, H-4, H-6a), 3.81 (dd,  $J = 10.2, 3.2$  Hz, 1H, H-3'), 3.74 (dd,  $J = 10.3, 3.7$  Hz, 1H, H-2'), 3.71–3.64 (m, 2H, H-6b, octyl OCH<sub>2</sub>), 3.48–3.41 (m, 1H, octyl OCH<sub>2</sub>), 3.29–3.21 (m, 1H, octyl NCH<sub>2</sub>), 3.21–3.14 (m, 1H, octyl NCH<sub>2</sub>), 3.11 (dd,  $J = 10.6, 3.5$  Hz, 1H, H-2), 2.81–2.63 (m, 4H, COCH<sub>2</sub>CH<sub>2</sub>COCH<sub>3</sub>), 2.14 (s, 3H, COCH<sub>3</sub>), 1.66–1.55 (m, 2H, OCH<sub>2</sub>CH<sub>2</sub>), 1.55–1.42 (m, 2H, NCH<sub>2</sub>CH<sub>2</sub>), 1.35–1.15 (m, 8H, 4 x CH<sub>2</sub>), 1.12 (d,  $J = 6.5$  Hz, 3H, H-6'); <sup>13</sup>C NMR (126 MHz, CDCl<sub>3</sub>)  $\delta$  206.3 (C=O), 172.4 (C=O), 156.8 (C=O), 153.8 (C=O), 138.1 (Ar), 135.8 (Ar), 134.7 (OCH<sub>2</sub>CH=CH<sub>2</sub>), 133.3 (Ar), 133.0 (Ar), 128.5 (4 x Ar), 128.3 (2 x Ar), 128.2 (Ar), 127.9 (3 x Ar), 127.8 (2 x Ar), 127.7 (Ar), 127.5 (Ar), 127.4 (2 x Ar), 127.3 (Ar), 127.0 (Ar), 126.3 (Ar), 126.2 (Ar), 126.0 (Ar), 116.8 (OCH<sub>2</sub>CH=CH<sub>2</sub>), 99.5 (C-1'), 98.0 (C-1), 94.3 (OCH<sub>2</sub>CCl<sub>3</sub>), 77.3 (C-3), 77.1 (OCH<sub>2</sub>CCl<sub>3</sub>), 76.0 (C-3'), 75.1 (C-5), 75.1 (C-2'), 74.5 (OCH<sub>2</sub>Ar), 73.2 (OCH<sub>2</sub>Ar), 71.0 (C-4'), 70.4 (OCH<sub>2</sub>CH=CH<sub>2</sub>), 70.4 (C-4), 68.8 (octyl OCH<sub>2</sub>), 68.0 (C-6), 67.1 (OCH<sub>2</sub>Ar), 65.7 (C-5'), 61.3 (C-2), 50.5 (NC<sub>a</sub>H<sub>2</sub>Ph), 50.2 (NC<sub>b</sub>H<sub>2</sub>Ph), 47.3 (octyl NC<sub>a</sub>H<sub>2</sub>), 46.2 (octyl NC<sub>b</sub>H<sub>2</sub>), 38.0 (COCH<sub>2</sub>CH<sub>2</sub>COCH<sub>3</sub>), 29.8 (COCH<sub>3</sub>), 29.3 (OCH<sub>2</sub>CH<sub>2</sub>), 29.3 (CH<sub>2</sub>), 29.3 (CH<sub>2</sub>), 28.0 (COCH<sub>2</sub>CH<sub>2</sub>COCH<sub>3</sub>), 28.0 (NCH<sub>2</sub>C<sub>a</sub>H<sub>2</sub>), 27.7 (NCH<sub>2</sub>C<sub>b</sub>H<sub>2</sub>), 26.7 (CH<sub>2</sub>), 26.0 (CH<sub>2</sub>), 16.8 (C-6'); HRMS (ESI-TOF)  $m/z$ : [M + NH<sub>4</sub>]<sup>+</sup> Calcd for C<sub>64</sub>H<sub>79</sub>Cl<sub>3</sub>N<sub>5</sub>O<sub>15</sub> 1262.4633; Found 1262.4630.



***p*-Tolyl                      2,3,4-tri-*O*-benzoyl- $\beta$ -D-xylopyranosyl-(1 $\rightarrow$ 2)-3-*O*-benzyl-4,6-*O*-di-*tert*-butylsilylene-1-thio- $\beta$ -D-galactopyranoside (2.7)**

To a stirred solution of **2.27** (750 mg, 0.968 mmol) in CH<sub>3</sub>OH–CH<sub>2</sub>Cl<sub>2</sub> (25 mL, 4:1) was added a solution of NaOCH<sub>3</sub> (0.5 M in CH<sub>3</sub>OH) until the solution pH = 9. After stirring for 1 h, the reaction mixture was neutralized with addition of Amberlite® IR-120 (H<sup>+</sup>) cation exchange resin, filtered and concentrated to dryness. The crude product was dissolved in pyridine (5 mL) followed by dropwise addition of benzoyl chloride (0.410 mL, 3.48 mmol) at 0 °C. After stirring overnight, while warming to room temperature, ice water was added, and the solution was extracted with CH<sub>2</sub>Cl<sub>2</sub> (50 mL x 2). The combined organic layer was then washed successively with 1N HCl, saturated aqueous NaHCO<sub>3</sub>, water and brine. The organic layer was dried over Na<sub>2</sub>SO<sub>4</sub>, filtered, then concentrated and the resulting syrup was purified by flash chromatography (5:1 hexanes–EtOAc) to afford **2.7** (852 mg, 97% over two steps) as a fluffy white solid: *R*<sub>f</sub> = 0.32 (4:1 hexanes–EtOAc); [ $\alpha$ ]<sub>D</sub><sup>25</sup> –97.7 (*c* = 0.06, CHCl<sub>3</sub>); <sup>1</sup>H NMR (600 MHz, CDCl<sub>3</sub>)  $\delta$  8.04–7.99 (m, 4H, Ar), 7.99–7.94 (m, 2H, Ar), 7.55–7.44 (m, 5H, Ar), 7.34–7.28 (m, 4H, Ar), 7.27–7.23 (m, 2H, Ar), 7.23–7.19 (m, 2H, Ar), 7.16–7.07 (m, 5H, Ar), 5.70 (app t, *J* = 5.3 Hz, 1H, H-3'), 5.65 (d, *J* = 3.4 Hz, 1H, H-1'), 5.45 (dd, *J* = 5.5, 3.4 Hz, 1H, H-2'), 5.32 (app q, *J* = 3.7 Hz, 1H, H-4'), 5.00 (dd, *J* = 13.1, 3.2 Hz, 1H, H-5a'), 4.62 (d, *J* = 9.8 Hz, 1H, H-1), 4.60 (d, *J* = 11.3 Hz, 1H, OCH<sub>2</sub>Ph), 4.51 (d, *J* = 11.4 Hz, 1H, OCH<sub>2</sub>Ph), 4.46 (d, *J* = 3.0 Hz, 1H, H-4), 4.23–4.18 (m, 2H, H-2, H-6a), 4.15 (d, *J* = 12.3, 2.3 Hz, 1H, H-6b), 3.94 (dd, *J* = 13.1, 3.9 Hz, 1H, H-5b'), 3.44 (dd, *J* = 8.9, 3.0 Hz,

<sup>1</sup>H, H-3), 3.26 (app s, 1H, H-5), 2.36 (s, 3H, ArCH<sub>3</sub>), 1.13 (s, 9H, C(CH<sub>3</sub>)<sub>3</sub>), 1.04 (s, 9H, C(CH<sub>3</sub>)<sub>3</sub>); <sup>13</sup>C NMR (151 MHz, CDCl<sub>3</sub>) δ 165.8 (C=O), 165.2 (C=O), 165.1 (C=O), 137.9 (Ar), 137.6 (Ar), 133.3 (Ar), 133.3 (2 x Ar), 132.6 (3 x Ar), 130.9 (Ar), 130.1 (2 x Ar), 130.1 (4 x Ar), 129.7 (2 x Ar), 129.6 (Ar), 129.5 (2 x Ar), 128.6 (4 x Ar), 128.4 (2 x Ar), 128.4 (2 x Ar), 127.9 (Ar), 127.7 (Ar), 99.4 (C-1'), 87.4 (C-1), 83.8 (C-3), 74.7 (C-5), 73.4 (C-2), 70.8 (OCH<sub>2</sub>Ph), 69.5 (C-4), 69.3 (C-2'), 68.9 (C-4'), 68.5 (C-3'), 67.4 (C-6), 60.7 (C-5'), 27.8 (3 x C(CH<sub>3</sub>)<sub>3</sub>), 27.7 (3 x C(CH<sub>3</sub>)<sub>3</sub>), 23.5 (C(CH<sub>3</sub>)<sub>3</sub>), 21.3 (ArCH<sub>3</sub>), 20.8 (C(CH<sub>3</sub>)<sub>3</sub>); HRMS (ESI-TOF) *m/z*: [M + Na]<sup>+</sup> Calcd for C<sub>54</sub>H<sub>60</sub>NaO<sub>12</sub>SSi 983.3467; Found 983.3470.



***N*-benzyl-*N*-benzoxycarbonyl-8-aminoethyl 2-azido-6-*O*-benzyl-2-deoxy-3-*O*-(2,2,2-trichloroethoxycarbonyl)- $\alpha$ -D-glucopyranoside (**2.8**)**

To a stirred solution of **2.22** (465 mg, 0.567 mmol) in CH<sub>2</sub>Cl<sub>2</sub> (10 mL) was added triethylsilane (0.450 mL, 2.84 mmol), trifluoroacetic anhydride (80.0  $\mu$ L, 0.0567 mmol), and trifluoroacetic acid (0.220 mL, 2.84 mmol) successively at 0 °C. The reaction mixture was stirred for 2 h and then poured into saturated aqueous NaHCO<sub>3</sub>. The aqueous layer was extracted with CH<sub>2</sub>Cl<sub>2</sub> (100 mL  $\times$  3), and the combined organic layers were dried over Na<sub>2</sub>SO<sub>4</sub>, filtered and concentrated to dryness. The crude residue was purified by flash chromatography (4:1 hexane–EtOAc) to afford **2.8** (417 mg, 89%) as a colorless oil: *R*<sub>f</sub> = 0.19 (4:1 hexanes–EtOAc); [ $\alpha$ ]<sub>D</sub><sup>25</sup> +74.3 (*c* = 2.38, CHCl<sub>3</sub>); <sup>1</sup>H NMR (500 MHz, CDCl<sub>3</sub>) δ 7.39–7.21 (m, 14H, Ar), 7.21–7.14 (m, 1H, Ar), 5.26–5.21 (m, 1H, H-3), 5.17 (app d, *J* = 16.5 Hz, 2H, OCH<sub>2</sub>Ph), 4.97 (d, *J* = 3.5 Hz, 1H, H-1), 4.86 (d, *J* = 12.0 Hz,

1H, OCH<sub>2</sub>CCl<sub>3</sub>), 4.80 (d, *J* = 12.0 Hz, 1H, OCH<sub>2</sub>CCl<sub>3</sub>), 4.62 (d, *J* = 12.0 Hz, 1H, OCH<sub>2</sub>Ph), 4.55 (d, *J* = 12.0 Hz, 1H, OCH<sub>2</sub>Ph), 4.49 (app d, *J* = 8.0 Hz, 2H, NCH<sub>2</sub>Ph), 3.88–3.82 (m, 2H, H-4, H-5), 3.78 (dd, *J* = 10.5, 3.0 Hz, 1H, H-6a), 3.75–3.66 (m, 2H, H-6b, octyl OCH<sub>2</sub>), 3.51–3.44 (m, 1H, octyl OCH<sub>2</sub>), 3.29–3.23 (m, 1H, octyl NCH<sub>2</sub>), 3.23–3.16 (m, 1H, octyl NCH<sub>2</sub>), 3.21 (dd, *J* = 10.5, 3.5 Hz, 1H, H-2), 2.81–2.66 (m, 1H, 4-OH), 1.66–1.55 (m, 2H, OCH<sub>2</sub>CH<sub>2</sub>), 1.55–1.42 (m, 2H, NCH<sub>2</sub>CH<sub>2</sub>), 1.42–1.15 (m, 8H, 4 x CH<sub>2</sub>); <sup>13</sup>C NMR (126 MHz, CDCl<sub>3</sub>) δ 156.8 (C=O), 154.1 (C=O), 138.0 (Ar), 137.5 (Ar), 137.0 (Ar), 128.6 (2 x Ar), 128.5 (4 x Ar), 128.0 (Ar), 127.9 (Ar), 127.8 (5 x Ar), 127.3 (2 x Ar), 98.1 (C-1), 94.3 (OCH<sub>2</sub>CCl<sub>3</sub>), 78.2 (C-3), 77.1 (OCH<sub>2</sub>CCl<sub>3</sub>), 73.8 (OCH<sub>2</sub>Ph), 70.4 (C-4), 69.9 (C-5), 69.4 (C-6), 68.8 (octyl OCH<sub>2</sub>), 67.2 (OCH<sub>2</sub>Ph), 60.7 (C-2), 50.5 (NC<sub>a</sub>H<sub>2</sub>Ph), 50.2 (NC<sub>b</sub>H<sub>2</sub>Ph), 47.2 (octyl NC<sub>a</sub>H<sub>2</sub>), 46.3 (octyl NC<sub>b</sub>H<sub>2</sub>), 29.3 (OCH<sub>2</sub>CH<sub>2</sub>), 29.1 (2 x CH<sub>2</sub>), 28.0 (NCH<sub>2</sub>C<sub>a</sub>H<sub>2</sub>), 27.7 (NCH<sub>2</sub>C<sub>b</sub>H<sub>2</sub>), 26.7 (CH<sub>2</sub>), 26.0 (CH<sub>2</sub>); HRMS (ESI-TOF) *m/z*: [M + Na]<sup>+</sup> Calcd for C<sub>39</sub>H<sub>47</sub>Cl<sub>3</sub>N<sub>4</sub>NaO<sub>9</sub> 843.2301; Found 843.2299.

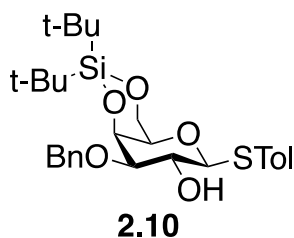


## 2.9

### *p*-Tolyl 3-*O*-allyl-4-*O*-levulinoyl-2-*O*-(2-naphthyl)methyl-1-thio-β-*L*-fucopyranoside (2.9)

To a stirred solution of **2.25** (1.68 g, 3.73 mmol) in dry CH<sub>2</sub>Cl<sub>2</sub> (25 mL) was added EDC·HCl (1.4 g, 7.46 mmol), 4-(dimethylamino)pyridine (910 mg, 7.46 mmol) and levulinic acid (650 mg, 5.60 mmol). The reaction mixture was stirred overnight before it was diluted with CH<sub>2</sub>Cl<sub>2</sub> (100 mL). The mixture was then washed successively with saturated aqueous NaHCO<sub>3</sub>, water and brine. The organic layer was dried over Na<sub>2</sub>SO<sub>4</sub>, filtered and concentrated to dryness. The crude residue was purified by flash chromatography (3:1 hexanes–EtOAc) to afford **2.9** (1.84 g, 90%) as a colorless oil: *R*<sub>f</sub> = 0.27 (3:1 hexanes–EtOAc); [α]<sub>D</sub><sup>25</sup> –4.5 (*c* = 0.98, CH<sub>2</sub>Cl<sub>2</sub>); <sup>1</sup>H NMR (600 MHz, CDCl<sub>3</sub>)

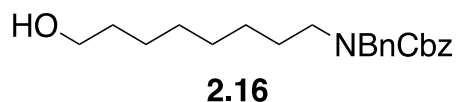
$\delta$  7.85–7.80 (m, 4H, Ar), 7.62–7.58 (m, 1H, Ar), 7.55–7.51 (m, 4H, Ar), 7.51–7.44 (m, 4H, Ar), 7.14–7.10 (m, 2H, Ar), 5.90 (ddt,  $J = 17.3, 10.4, 5.7$  Hz, 1H,  $\text{OCH}_2\text{CH}=\text{CH}_2$ ), 5.30–5.24 (m, 2H, H-4,  $\text{OCH}_2\text{CH}=\text{CH}_2$ ), 5.17 (dq,  $J = 10.4, 1.5$  Hz, 1H,  $\text{OCH}_2\text{CH}=\text{CH}_2$ ), 4.94 (d,  $J = 10.6$  Hz, 1H,  $\text{OCH}_2\text{Ar}$ ), 4.88 (d,  $J = 10.6$  Hz, 1H,  $\text{OCH}_2\text{Ar}$ ), 4.62 (d,  $J = 9.4$  Hz, 1H, H-1), 4.17 (ddt,  $J = 12.5, 5.5, 1.5$  Hz, 1H,  $\text{OCH}_2\text{CH}=\text{CH}_2$ ), 4.03 (ddt,  $J = 12.5, 5.8, 1.4$  Hz, 1H,  $\text{OCH}_2\text{CH}=\text{CH}_2$ ), 3.67 (q,  $J = 6.4$  Hz, 1H, H-5), 3.62 (app t,  $J = 9.3$  Hz, 1H, H-2), 3.57 (dd,  $J = 9.1, 3.3$  Hz, 1H, H-3), 2.86–2.63 (m, 4H,  $\text{COCH}_2\text{CH}_2\text{COCH}_3$ ), 2.34 (s, 3H,  $\text{ArCH}_3$ ), 2.20 (s, 3H,  $\text{COCH}_3$ ), 1.25 (d,  $J = 6.4$  Hz, 3H, H-6);  $^{13}\text{C}$  NMR (151 MHz,  $\text{CDCl}_3$ )  $\delta$  206.3 (C=O), 172.5 (C=O), 137.7 (Ar), 136.0 (Ar), 134.6 ( $\text{OCH}_2\text{CH}=\text{CH}_2$ ), 133.4 (Ar), 133.1 (Ar), 132.7 (2 x Ar), 130.0 (Ar), 129.6 (2 x Ar), 128.1 (Ar), 128.0 (Ar), 127.7 (Ar), 126.9 (Ar), 126.4 (Ar), 126.0 (Ar), 125.9 (Ar), 117.5 ( $\text{OCH}_2\text{CH}=\text{CH}_2$ ), 87.9 (C-1), 81.0 (C-3), 76.8 (C-2), 75.8 ( $\text{OCH}_2\text{Ar}$ ), 73.1 (C-5), 70.8 ( $\text{OCH}_2\text{CH}=\text{CH}_2$ ), 70.2 (C-4), 38.1 ( $\text{COCH}_2\text{CH}_2\text{COCH}_3$ ), 29.9 ( $\text{COCH}_3$ ), 28.1 ( $\text{COCH}_2\text{CH}_2\text{COCH}_3$ ), 21.2 ( $\text{ArCH}_3$ ), 16.9 (C-6); HRMS (ESI-TOF)  $m/z$ :  $[\text{M} + \text{Na}]^+$  Calcd for  $\text{C}_{32}\text{H}_{36}\text{NaO}_6\text{S}$  571.2125; Found 571.2122.



***p*-Tolyl 3-*O*-benzyl-4,6-*O*-di-*tert*-butylsilylene-1-thio- $\alpha$ -D-galactopyranoside (2.10)**

To a stirred solution of *p*-tolyl 3-*O*-benzyl-1-thio- $\alpha$ -D-galactopyranoside<sup>25</sup> (450 mg, 1.20 mmol) in dry pyridine (10 mL) was added di-*tert*-butylsilyl bis(trifluoromethanesulfonate) (0.428 mL, 1.32 mmol). The reaction mixture was stirred for 2 h before the addition of  $\text{CH}_3\text{OH}$  (1.5 mL) followed by removal of solvent by coevaporation with toluene. The crude residue was purified by flash chromatography (5:1 hexanes–EtOAc) to afford **2.10** (513 mg, 83%) as a white solid:  $R_f =$

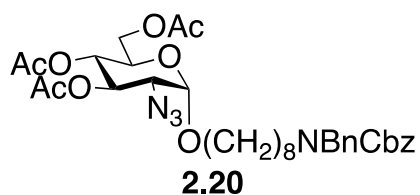
0.22 (5:1 hexanes–EtOAc);  $[\alpha]_D^{25} -16.2$  ( $c = 0.38$ ,  $\text{CH}_2\text{Cl}_2$ );  $^1\text{H NMR}$  (500 MHz,  $\text{CDCl}_3$ )  $\delta$  7.48–7.50 (m, 2H, Ar), 7.43–7.39 (m, 2H, Ar), 7.37–7.33 (m, 2H, Ar), 7.32–7.27 (m, 1H, Ar), 7.12–7.08 (m, 2H, Ar), 4.80 (d,  $J = 12.0$  Hz, 1H,  $\text{OCH}_2\text{Ph}$ ), 4.62 (d,  $J = 11.5$  Hz, 1H,  $\text{OCH}_2\text{Ph}$ ), 4.56 (d,  $J = 1.0$  Hz, 1H, H-4), 4.50 (d,  $J = 9.7$  Hz, 1H, H-1), 4.25 (d,  $J = 12.5$ , 1.0 Hz, 1H, H-6a), 4.21 (dd,  $J = 12.5$ , 2.5 Hz, 1H, H-6b), 4.00 (app td,  $J = 9.4$ , 1.6 Hz, 1H, H-2), 3.35 (dd,  $J = 9.0$ , 3.0 Hz, 1H, H-3), 3.34–3.32 (m, 1H, H-5), 2.56 (d,  $J = 2.0$  Hz, 1H, 2-OH), 2.33 (s, 3H,  $\text{ArCH}_3$ ), 1.06 (s, 18H,  $\text{C}(\text{CH}_3)_3$ );  $^{13}\text{C NMR}$  (126 MHz,  $\text{CDCl}_3$ )  $\delta$  138.0 (2 x Ar), 133.4 (2 x Ar), 129.6 (3 x Ar), 128.6 (2 x Ar), 127.9 (3 x Ar), 89.6 (C-1), 81.9 (C-5), 75.3 (C-3), 70.4 ( $\text{OCH}_2\text{Ph}$ ), 69.3 (C-4), 68.5 (C-2), 67.5 (C-6), 27.7 (3 x  $\text{C}(\text{CH}_3)_3$ ), 27.6 (3 x  $\text{C}(\text{CH}_3)_3$ ), 23.4 ( $\text{C}(\text{CH}_3)_3$ ), 21.2 ( $\text{ArCH}_3$ ), 20.7 ( $\text{C}(\text{CH}_3)_3$ ); HRMS (ESI–TOF)  $m/z$ :  $[\text{M} + \text{Na}]^+$  Calcd for  $\text{C}_{28}\text{H}_{40}\text{NaO}_5\text{SSi}$  539.2258; Found 539.2258.



### ***N*-benzyl-*N*-benzoxycarbonyl-8-amino-1-octanol (2.16)**

To a stirred solution of 8-amino-1-octanol<sup>19</sup> (2.11 g, 14.5 mmol) in dry  $\text{CH}_2\text{Cl}_2$  (30 mL) was added benzaldehyde (1.47 mL, 14.5 mmol) and anhydrous  $\text{Na}_2\text{SO}_4$  (2.05 g, 14.5 mmol). After being stirred overnight, the reaction mixture was filtered through Celite and the resulting filtrate was concentrated to dryness. The resulting crude imine product was dissolved in ethanol (30 mL) and then sodium borohydride (825 mg, 21.7 mmol) was added portionwise at 0 °C over an hour. After stirring overnight, the reaction mixture was then concentrated to dryness and then 1N HCl (40 mL) and  $\text{CH}_2\text{Cl}_2$  (40 mL) were added. The aqueous layer was then collected while the organic layer was extracted with water (20 mL x 2). The combined aqueous layers were then basified by the addition of 10N NaOH until precipitation of the product occurred. The resulting solution was then extracted with  $\text{CH}_2\text{Cl}_2$  (100 mL x 3). The combined organic layers were dried over  $\text{Na}_2\text{SO}_4$ , filtered

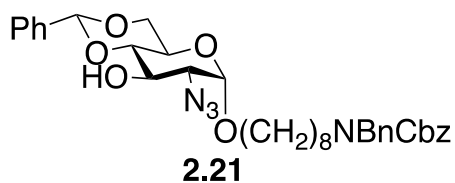
and concentrated to dryness to afford a white solid crude product. This product was resuspended in acetone–H<sub>2</sub>O (60 mL, 2:1) and then sodium bicarbonate (1.60 g, 15.9 mmol) and benzyl chloroformate (2.25 mL, 15.9 mmol) were added. After 1 h, the solution was concentrated, dissolved in EtOAc (100 mL) followed by washing with water and brine. The organic layer was dried over Na<sub>2</sub>SO<sub>4</sub>, filtered and concentrated to dryness. The crude residue was purified by flash chromatography (2:1 hexanes–EtOAc) to afford **2.16** (3.34 g, 60% over three steps) as a colorless oil: *R<sub>f</sub>* = 0.35 (2:1 hexanes–EtOAc); <sup>1</sup>H NMR (700 MHz, CDCl<sub>3</sub>) δ 7.40–7.34 (m, 2H, Ar), 7.34–7.22 (m, 7H, Ar), 7.21–7.14 (m, 1H, Ar), 5.22–5.11 (m, 2H, OCH<sub>2</sub>), 4.54–4.46 (m, 2H, OCH<sub>2</sub>Ph), 3.66–3.59 (m, 2H, OCH<sub>2</sub>), 3.30–3.16 (m, 2H, NCH<sub>2</sub>), 1.61–1.45 (m, 4H, 2 x CH<sub>2</sub>), 1.35–1.17 (m, 8H, 4 x CH<sub>2</sub>); <sup>13</sup>C NMR (176 MHz, CDCl<sub>3</sub>) δ 156.9 (C<sub>a</sub>=O), 156.3 (C<sub>b</sub>=O), 138.1 (Ar), 137.0 (Ar), 128.7 (2 x Ar), 128.6 (2 x Ar), 128.0 (2 x Ar), 127.8 (2 x Ar), 127.4 (2 x Ar), 67.3 (OCH<sub>2</sub>Ph), 63.2 (OCH<sub>2</sub>), 50.6 (NC<sub>a</sub>H<sub>2</sub>Ph), 50.3 (NC<sub>b</sub>H<sub>2</sub>Ph), 47.3 (octyl NC<sub>a</sub>H<sub>2</sub>), 46.4 (octyl NC<sub>b</sub>H<sub>2</sub>), 32.9 (CH<sub>2</sub>), 29.4 (CH<sub>2</sub>), 28.2 (CH<sub>2</sub>), 27.8 (CH<sub>2</sub>), 26.8 (CH<sub>2</sub>), 25.8 (CH<sub>2</sub>); HRMS (ESI–TOF) *m/z* [M + Na]<sup>+</sup> calcd for C<sub>23</sub>H<sub>31</sub>NNaO<sub>3</sub> 392.2196, found 392.2195.



***N*-benzyl-*N*-benzoxycarbonyl-8-amino-1-octyl 3,4,6-tri-*O*-acetyl-2-azido-2-deoxy- $\alpha$ -D-glucopyranoside (2.20)**

To a stirred solution of acceptor **2.16** (502 mg, 1.00 mmol) and donor **2.19**<sup>20</sup> (442 mg, 1.20 mmol) in dry diethyl ether (10 mL) was added 4Å molecular sieves powder (500 mg). After stirring for 30 min, the reaction mixture was cooled to 0 °C, and then trimethylsilyl trifluoromethanesulfonate

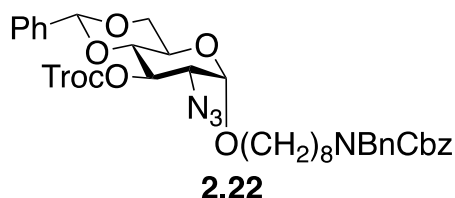
(18.0  $\mu$ L, 0.100 mmol) was added. The resulting solution was stirred for 1 h at 0  $^{\circ}$ C before triethylamine was added to the mixture and the solution was filtered through Celite and the filtrate was concentrated to dryness. The crude residue was purified by flash chromatography (3:1 hexanes–EtOAc) to afford **2.20** (547 mg, 79%) as a colorless oil:  $R_f$  = 0.31 (3:1 hexanes–EtOAc);  $[\alpha]_D^{25} +98.7$  ( $c$  = 2.05,  $\text{CH}_2\text{Cl}_2$ );  $^1\text{H}$  NMR (700 MHz,  $\text{CDCl}_3$ )  $\delta$  7.39–7.34 (m, 2H, Ar), 7.34–7.23 (m, 7H, Ar), 7.19–7.15 (m, 1H, Ar), 5.48 (dd,  $J$  = 10.6, 9.2 Hz, 1H, H-3), 5.21–5.13 (m, 2H,  $\text{OCH}_2\text{Ph}$ ), 5.04 (dd,  $J$  = 10.3, 9.2 Hz, 1H, H-4), 4.96 (d,  $J$  = 3.6 Hz, 1H, H-1), 4.53–4.46 (m, 2H,  $\text{NCH}_2\text{Ph}$ ), 4.28 (dd,  $J$  = 12.3, 4.6 Hz, 1H, H-6a), 4.08 (dd,  $J$  = 12.4, 2.4 Hz, 1H, H-6b), 4.02 (ddd,  $J$  = 10.2, 4.6, 2.3 Hz, 1H, H-5), 3.70 (appdt,  $J$  = 9.6, 6.7 Hz, 1H, octyl  $\text{OCH}_2$ ), 3.52–3.45 (m, 1H, octyl  $\text{OCH}_2$ ), 3.27 (dd,  $J$  = 10.6, 3.6 Hz, 1H, H-2), 3.29–3.23 (m, 1H, octyl  $\text{NCH}_2$ ), 3.23–3.15 (m, 1H, octyl  $\text{NCH}_2$ ), 2.08 (s, 3H,  $\text{COCH}_3$ ), 2.08 (s, 3H,  $\text{COCH}_3$ ), 2.04 (s, 3H,  $\text{COCH}_3$ ), 1.66–1.61 (m, 2H,  $\text{OCH}_2\text{CH}_2$ ), 1.55–1.44 (m, 2H,  $\text{NCH}_2\text{CH}_2$ ), 1.38–1.16 (m, 8H, 4 x  $\text{CH}_2$ );  $^{13}\text{C}$  NMR (176 MHz,  $\text{CDCl}_3$ )  $\delta$  170.7 (C=O), 170.2 (C=O), 169.8 (C=O), 156.3 (C=O), 138.1 (Ar), 137.1 (Ar), 128.6 (2 x Ar), 128.6 (2 x Ar), 128.0 (Ar), 127.9 (3 x Ar), 127.3 (2 x Ar), 98.0 (C-1), 70.5 (C-3), 69.1 (octyl  $\text{OCH}_2$ ), 68.8 (C-4), 67.7 (C-5), 67.2 ( $\text{OCH}_2\text{Ph}$ ), 62.0 (C-6), 61.0 (C-2), 50.6 ( $\text{NC}_a\text{H}_2\text{Ph}$ ), 50.3 ( $\text{NC}_b\text{H}_2\text{Ph}$ ), 47.3 (octyl  $\text{NC}_a\text{H}_2$ ), 46.4 (octyl  $\text{NC}_b\text{H}_2$ ), 29.4 ( $\text{OCH}_2\text{CH}_2$ ), 29.4 ( $\text{CH}_2$ ), 29.2 ( $\text{CH}_2$ ), 28.2 ( $\text{NCH}_2\text{C}_a\text{H}_2$ ), 27.8 ( $\text{NCH}_2\text{C}_b\text{H}_2$ ), 26.8 ( $\text{CH}_2$ ), 26.1 ( $\text{CH}_2$ ), 20.8 ( $\text{COCH}_3$ ), 20.7 ( $\text{COCH}_3$ ), 20.7 ( $\text{COCH}_3$ ); HRMS (ESI–TOF)  $m/z$ :  $[\text{M} + \text{Na}]^+$  Calcd for  $\text{C}_{35}\text{H}_{46}\text{N}_4\text{NaO}_{10}$  705.3106; Found 705.3109.



***N*-benzyl-*N*-benzoxycarbonyl-8-amino-1-octyl 2-azido-4,6-*O*-benzylidene-2-deoxy- $\alpha$ -D-glucopyranoside (2.21)**

To a stirred solution of **2.20** (547 mg, 0.802 mmol) in CH<sub>3</sub>OH–CH<sub>2</sub>Cl<sub>2</sub> (25 mL, 4:1) was added a solution of NaOCH<sub>3</sub> (0.5 M in CH<sub>3</sub>OH) until the solution was pH = 12. After stirring for 1 h, the reaction mixture was neutralized by the addition of prewashed Amberlite® IR-120 (H<sup>+</sup>) cation exchange resin, filtered and concentrated to dryness. The crude product was dissolved in CH<sub>3</sub>CN (8 mL) and then benzaldehyde dimethyl acetal (0.290 mL, 1.94 mmol) and 10-camphorsulfonic acid (11.0 mg, 0.0484 mmol) were added. After stirring overnight, the reaction mixture was added triethylamine, then concentrated to dryness and purified by flash chromatography (4:1 hexanes–EtOAc) to afford **2.21** (442 mg, 86% over 2 steps) as a colorless oil:  $R_f$  = 0.24 (4:1 hexanes–EtOAc);  $[\alpha]_D^{25}$  +62.7 ( $c$  = 0.91, CH<sub>2</sub>Cl<sub>2</sub>); <sup>1</sup>H NMR (500 MHz, CDCl<sub>3</sub>)  $\delta$  7.51–7.47 (m, 2H, Ar), 7.39–7.34 (m, 5H, Ar), 7.34–7.26 (m, 5H, Ar), 7.26–7.22 (m, 2H, Ar), 7.19–7.14 (m, 1H, Ar), 5.55 (s, 1H, PhCH(O)<sub>2</sub>), 5.17 (app d,  $J$  = 17.0 Hz, 2H, OCH<sub>2</sub>Ph), 4.96 (d,  $J$  = 3.5 Hz, 1H, H-1), 4.49 (app d,  $J$  = 12.5 Hz, 2H, NCH<sub>2</sub>Ph), 4.28 (dd,  $J$  = 10.0, 4.5 Hz, 1H, H-6a), 4.25–4.21 (m, 1H, H-3), 3.87 (ddd,  $J$  = 10.0, 10.0, 5.0 Hz, 1H, H-5), 3.74 (app t,  $J$  = 10.0 Hz, 1H, H-6b), 3.74–3.69 (m, 1H, octyl OCH<sub>2</sub>), 3.53 (app t,  $J$  = 9.5 Hz, 1H, H-4), 3.47 (app dt,  $J$  = 9.5, 6.5 Hz, 1H, octyl OCH<sub>2</sub>), 3.29–3.22 (m, 1H, octyl NCH<sub>2</sub>), 3.24 (dd,  $J$  = 10.0, 3.5 Hz, 1H, H-2), 3.22–3.16 (m, 1H, octyl NCH<sub>2</sub>), 1.66–1.57 (m, 2H, OCH<sub>2</sub>CH<sub>2</sub>), 1.55–1.44 (m, 2H, NCH<sub>2</sub>CH<sub>2</sub>), 1.40–1.22 (m, 8H, 4 x CH<sub>2</sub>); <sup>13</sup>C NMR (126 MHz, CDCl<sub>3</sub>)  $\delta$  156.2 (C=O), 138.0 (Ar), 137.0 (Ar), 129.4 (Ar), 128.5 (2 x Ar), 128.4 (2 x Ar), 128.4 (2 x Ar), 127.9 (Ar), 127.8 (3 x Ar), 127.2 (3 x Ar), 126.3 (2 x Ar), 102.1 (PhCH(O)<sub>2</sub>), 98.6 (C-1), 82.0 (C-4), 68.9 (C-6), 68.8 (octyl OCH<sub>2</sub>), 68.7 (C-3), 67.2 (OCH<sub>2</sub>Ph),

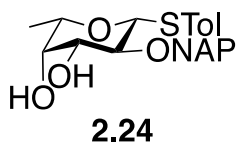
63.1 (C-2), 62.5 (C-5), 50.4 (NC<sub>a</sub>H<sub>2</sub>Ph), 50.2 (NC<sub>b</sub>H<sub>2</sub>Ph), 47.2 (octyl NC<sub>a</sub>H<sub>2</sub>), 46.2 (octyl NC<sub>b</sub>H<sub>2</sub>), 29.3 (OCH<sub>2</sub>CH<sub>2</sub>), 29.2 (CH<sub>2</sub>), 29.1 (CH<sub>2</sub>), 27.7 (NCH<sub>2</sub>CH<sub>2</sub>), 26.7 (CH<sub>2</sub>), 26.0 (CH<sub>2</sub>); HRMS (ESI-TOF) *m/z*: [M + Na]<sup>+</sup> Calcd for C<sub>36</sub>H<sub>44</sub>N<sub>4</sub>NaO<sub>7</sub> 667.3102; Found 667.3101.



***N*-benzyl-*N*-benzoxycarbonyl-8-amino-1-octyl 2-azido-4,6-*O*-benzylidene-2-deoxy-3-*O*-(2,2,2-trichloroethoxycarbonyl)- $\alpha$ -D-glucopyranoside (2.22)**

To a stirred solution of **2.21** (430 mg, 0.668 mmol) in dry pyridine (4 mL) was added 2,2,2-trichloroethoxycarbonyl chloride (0.140 mL, 0.839 mmol). The reaction mixture was stirred for 2 h before the addition of CH<sub>3</sub>OH (0.5 mL) followed by removal of solvent by coevaporation with toluene. The crude residue was purified by flash chromatography (20:1 toluene–EtOAc) to afford **2.22** (469 mg, 86%) as a colorless oil: *R<sub>f</sub>* = 0.29 (5:1 hexanes–EtOAc); [ $\alpha$ ]<sub>D</sub><sup>25</sup> +74.5 (*c* = 1.58, CH<sub>2</sub>Cl<sub>2</sub>); <sup>1</sup>H NMR (500 MHz, CDCl<sub>3</sub>)  $\delta$  7.45–7.42 (m, 2H, Ar), 7.45–7.26 (m, 11H, Ar), 7.26–7.23 (m, 1H, Ar), 7.19–7.14 (m, 1H, Ar), 5.53 (s, 1H, PhCH(O)<sub>2</sub>), 5.45 (dd, *J* = 10.0, 9.5 Hz, 1H, H-3), 5.17 (app d, *J* = 13.0 Hz, 2H, OCH<sub>2</sub>Ph), 5.00 (d, *J* = 3.5 Hz, 1H, H-1), 4.85 (d, *J* = 11.5 Hz, 1H, OCH<sub>2</sub>CCl<sub>3</sub>), 4.80 (d, *J* = 11.5 Hz, 1H, OCH<sub>2</sub>CCl<sub>3</sub>), 4.52–4.46 (m, 2H, NCH<sub>2</sub>Ph), 4.31 (dd, *J* = 10.5, 5.0 Hz, 1H, H-6a), 3.97 (ddd, *J* = 10.0, 10.0, 4.5 Hz, 1H, H-5), 3.80–3.69 (m, 3H, H-6b, octyl OCH<sub>2</sub>, H-4), 3.50 (ddd, *J* = 9.5, 6.5, 6.5 Hz, 1H, octyl OCH<sub>2</sub>), 3.29–3.22 (m, 1H, octyl NCH<sub>2</sub>), 3.28 (dd, *J* = 10.5, 4.0 Hz, 1H, H-2), 3.22–3.16 (m, 1H, octyl NCH<sub>2</sub>), 1.70–1.60 (m, 2H, OCH<sub>2</sub>CH<sub>2</sub>), 1.56–1.44 (m, 2H, NCH<sub>2</sub>CH<sub>2</sub>), 1.40–1.18 (m, 8H, 4 x CH<sub>2</sub>); <sup>13</sup>C NMR (126 MHz, CDCl<sub>3</sub>)  $\delta$  156.2 (C=O), 153.5 (C=O), 138.0 (Ar), 136.7 (Ar), 129.2 (Ar), 128.5 (4 x Ar), 128.2 (3 x Ar), 127.9 (Ar),

127.8 (3 x Ar), 127.3 (2 x Ar), 126.1 (2 x Ar), 101.7 (PhCH(O)<sub>2</sub>), 98.9 (C-1), 94.4 (OCH<sub>2</sub>CCl<sub>3</sub>), 79.2 (C-4), 77.0 (OCH<sub>2</sub>CCl<sub>3</sub>), 74.4 (C-3), 69.0 (octyl OCH<sub>2</sub>), 68.8 (C-6), 67.1 (OCH<sub>2</sub>Ph), 62.7 (C-5), 61.3 (C-2), 50.5 (NC<sub>a</sub>H<sub>2</sub>Ph), 50.2 (NC<sub>b</sub>H<sub>2</sub>Ph), 47.2 (octyl NC<sub>a</sub>H<sub>2</sub>), 46.3 (octyl NC<sub>b</sub>H<sub>2</sub>), 29.4 (OCH<sub>2</sub>CH<sub>2</sub>), 29.3 (2 x CH<sub>2</sub>), 28.1 (NCH<sub>2</sub>C<sub>a</sub>H<sub>2</sub>), 27.7 (NCH<sub>2</sub>C<sub>b</sub>H<sub>2</sub>), 26.7 (CH<sub>2</sub>), 26.0 (CH<sub>2</sub>); HRMS (ESI-TOF) *m/z*: [M + Na]<sup>+</sup> Calcd for C<sub>39</sub>H<sub>45</sub>Cl<sub>3</sub>N<sub>4</sub>NaO<sub>9</sub> 841.2144; Found 841.2132.



***p*-Tolyl 2-O-(2-naphthyl)methyl-1-thio-β-L-fucopyranoside (2.24)**

To a stirred solution of **2.23**<sup>24</sup> (1.50 g, 5.56 mmol) in acetone (25 mL) was added 2,2-dimethoxypropane (1.35 mL, 11.1 mmol) and 10-camphorsulfonic acid (130 mg, 0.556 mmol). After stirring for 3 h, the reaction mixture was added triethylamine and the solution was concentration to dryness. The resulting crude product was then dissolved in DMF (25 mL) and then sodium hydride (445 mg, 11.1 mmol, 60% dispersion in mineral oil) was added portionwise over 30 min at 0 °C. To the resulting mixture was added 2-(bromomethyl)naphthalene (1.47 g, 6.67 mmol) and the solution was stirred while warming to room temperature. After stirring for 2 h, the reaction mixture was slowly added to an ice-water mixture and was extracted with diethyl ether (100 mL x 2). The combined organic layers were dried over Na<sub>2</sub>SO<sub>4</sub>, filtered, concentrated and the resulting syrup was stirred in 80% aqueous AcOH (40 mL) at 60 °C for 3 h. The reaction mixture was cooled to room temperature and then concentrated to dryness. The resulting crude was purified with flash chromatography (2:1 hexane–EtOAc) to afford **2.24** (1.74 g, 76% over three steps) as a colorless oil: *R<sub>f</sub>* = 0.21 (2:1 hexanes–EtOAc); [α]<sub>D</sub><sup>25</sup> –16.2 (*c* = 0.23, CH<sub>2</sub>Cl<sub>2</sub>); <sup>1</sup>H NMR (600 MHz, CDCl<sub>3</sub>) δ 7.86–7.80 (m, 3H, Ar), 7.78–7.76 (m, 1H, Ar), 7.57–7.39 (m, 1H, Ar),

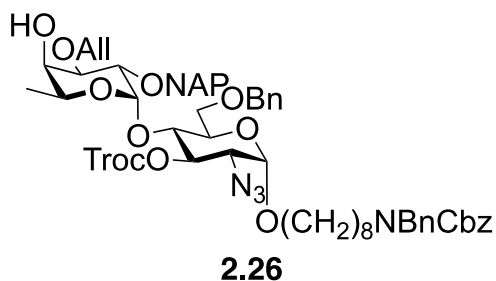
7.51–7.46 (m, 4H, Ar), 7.15–7.11 (m, 2H, Ar), 5.12 (d,  $J = 11.2$  Hz, 1H,  $\text{OCH}_2\text{Ar}$ ), 4.87 (d,  $J = 11.2$  Hz, 1H,  $\text{OCH}_2\text{Ar}$ ), 4.58 (d,  $J = 9.6$  Hz, 1H, H-1), 3.76–3.72 (m, 1H, H-4), 3.70–3.65 (m, 1H, H-3), 3.63 (q,  $J = 6.3$  Hz, 1H, H-5), 3.56 (app t,  $J = 9.2$  Hz, 1H, H-2), 2.45 (d,  $J = 5.4$  Hz, 1H, 3-OH), 2.36 (s, 3H,  $\text{ArCH}_3$ ), 2.05 (d,  $J = 5.3$  Hz, 1H, 4-OH), 1.35 (d,  $J = 6.4$  Hz, 3H, H-6);  $^{13}\text{C}$  NMR (151 MHz,  $\text{CDCl}_3$ )  $\delta$  137.9 (Ar), 135.6 (Ar), 133.5 (Ar), 133.3 (Ar), 132.6 (2 x Ar), 130.2 (Ar), 129.9 (2 x Ar), 128.7 (Ar), 128.1 (Ar), 127.9 (Ar), 127.4 (Ar), 126.4 (Ar), 126.2 (2 x Ar), 87.8 (C-1), 78.1 (C-2), 75.5 (C-3), 75.4 ( $\text{OCH}_2\text{Ar}$ ), 74.6 (C-5), 71.9 (C-4), 21.3 ( $\text{ArCH}_3$ ), 16.8 (C-6); HRMS (ESI–TOF)  $m/z$ :  $[\text{M} + \text{Na}]^+$  Calcd for  $\text{C}_{24}\text{H}_{26}\text{NaO}_4\text{S}$  433.1444; Found 433.1443.



***p*-Tolyl 3-O-allyl-2-O-(2-naphthyl)methyl-1-thio- $\beta$ -L-fucopyranoside (2.25)**

To a stirred solution of **2.24** (1.74 g, 4.24 mmol) in dry toluene (70 mL) was added di-*n*-butyltin oxide (1.27 g, 5.09 mmol). The reaction mixture was heated at reflux overnight at 120 °C. The reaction mixture was cooled to room temperature, concentrated and dried under high vacuum for 5 h. To a solution of the tin acetal in dry DMF (10 mL) was added cesium fluoride (966 mg, 6.36 mmol) and allyl bromide (0.720 mL, 8.48 mmol) successively. The reaction mixture was stirred overnight at 60 °C. After cooling to room temperature, the reaction mixture was diluted with EtOAc (100 mL x 2) and washed with brine. The combined organic layers were dried over  $\text{Na}_2\text{SO}_4$ , filtered and concentrated. The crude residue was purified by flash chromatography (3:1 hexanes–EtOAc) to afford **2.25** (1.69 g, 88%) as a colorless oil:  $R_f = 0.31$  (3:1 hexanes–EtOAc);  $[\alpha]_D^{25} +6.8$  ( $c = 0.82$ ,  $\text{CH}_2\text{Cl}_2$ );  $^1\text{H}$  NMR (600 MHz,  $\text{CDCl}_3$ )  $\delta$  7.85–7.80 (m, 4H, Ar), 7.61–7.56 (m, 1H, Ar), 7.52–7.45 (m, 4H, Ar), 7.13–7.09 (m, 2H, Ar), 5.94 (app ddt,  $J = 16.4, 10.2, 5.7$  Hz, 1H,

OCH<sub>2</sub>CH=CH<sub>2</sub>), 5.30 (app dq,  $J = 17.2, 1.6$  Hz, 1H, OCH<sub>2</sub>CH=CH<sub>2</sub>), 5.20 (app dq,  $J = 10.4, 1.5$  Hz, 1H, OCH<sub>2</sub>CH=CH<sub>2</sub>), 4.98 (d,  $J = 10.6$  Hz, 1H, OCH<sub>2</sub>Ar), 4.89 (d,  $J = 10.6$  Hz, 1H, OCH<sub>2</sub>Ar), 4.57 (d,  $J = 9.8$  Hz, 1H, H-1), 4.20 (app ddt,  $J = 12.5, 6.0, 1.5$  Hz, 1H, OCH<sub>2</sub>CH=CH<sub>2</sub>), 4.18 (app ddt,  $J = 12.5, 5.5, 1.5$  Hz, 1H, OCH<sub>2</sub>CH=CH<sub>2</sub>), 3.84 (app t,  $J = 3.0$  Hz, 1H, H-4), 3.67 (app t,  $J = 9.3$  Hz, 1H, H-2), 3.58 (q,  $J = 6.4$  Hz, 1H, H-5), 3.51 (dd,  $J = 9.0, 3.3$  Hz, 1H, H-3), 2.33 (s, 3H, ArCH<sub>3</sub>), 2.25 (d,  $J = 3.5$  Hz, 1H, 4-OH), 1.38 (d,  $J = 6.5$  Hz, 3H, H-6); <sup>13</sup>C NMR (151 MHz, CDCl<sub>3</sub>)  $\delta$  137.8 (Ar), 136.0 (Ar), 134.6 (OCH<sub>2</sub>CH=CH<sub>2</sub>), 133.5 (Ar), 133.2 (Ar), 132.8 (2 x Ar), 130.1 (Ar), 129.8 (2 x Ar), 128.2 (Ar), 128.1 (Ar), 127.8 (Ar), 127.0 (Ar), 126.5 (Ar), 126.1 (Ar), 126.0 (Ar), 117.8 (OCH<sub>2</sub>CH=CH<sub>2</sub>), 87.9 (C-1), 82.9 (C-3), 77.0 (C-2), 75.9 (OCH<sub>2</sub>Ar), 74.3 (C-5), 71.3 (OCH<sub>2</sub>CH=CH<sub>2</sub>), 69.6 (C-4), 21.3 (ArCH<sub>3</sub>), 16.9 (C-6); HRMS (ESI-TOF)  $m/z$ : [M + Na]<sup>+</sup> Calcd for C<sub>27</sub>H<sub>30</sub>NaO<sub>4</sub>S 473.1757; Found 473.1757.

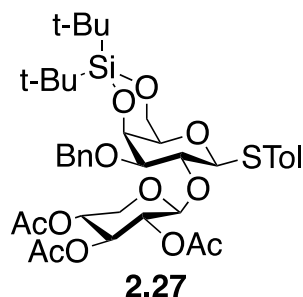


*N*-benzyl-*N*-benzoxycarbonyl-8-aminooctyl                      3-*O*-allyl-2-*O*-(2-naphthyl)methyl- $\alpha$ -L-fucopyranosyl-(1 $\rightarrow$ 4)-2-azido-6-*O*-benzyl-2-deoxy-3-*O*-(2,2,2-trichloroethoxycarbonyl)- $\alpha$ -D-glucopyranoside (**2.26**)

To a stirred solution of **2.6** (56 mg, 0.0449 mmol) in pyridine–AcOH (5 mL, 3:2) was added hydrazine monohydrate (6.5  $\mu$ L, 2.93 mmol). After stirring for 3 h, the reaction mixture was diluted with CH<sub>2</sub>Cl<sub>2</sub> (50 mL) and washed with 1N HCl, saturated aqueous NaHCO<sub>3</sub> and brine. The combined organic layers were dried over Na<sub>2</sub>SO<sub>4</sub>, filtered and concentrated to dryness. The crude

residue was purified by flash chromatography (2:1 hexanes–EtOAc) to afford **2.26** (43.0 mg, 84%) as a white solid:  $R_f = 0.24$  (2:1 hexanes–EtOAc);  $[\alpha]_D^{25} +122.0$  ( $c = 0.02$ ,  $\text{CHCl}_3$ );  $^1\text{H NMR}$  (600 MHz,  $\text{CDCl}_3$ )  $\delta$  7.85–7.73 (m, 4H, Ar), 7.73–7.69 (m, 1H, Ar), 7.50–7.44 (m, 2H, Ar), 7.42–7.38 (m, 1H, Ar), 7.38–7.26 (m, 7H, Ar), 7.726–7.23 (m, 5H, Ar), 7.13–7.08 (m, 2H, Ar), 5.96 (app ddt,  $J = 16.3, 10.8, 6.5$  Hz, 1H,  $\text{OCH}_2\text{CH}=\text{CH}_2$ ), 5.33 (dd,  $J = 17.3, 1.7$  Hz, 1H,  $\text{OCH}_2\text{CH}=\text{CH}_2$ ), 5.29 (dd,  $J = 10.6, 8.8$  Hz, 1H, H-3), 5.21 (dd,  $J = 10.4, 1.5$  Hz, 1H,  $\text{OCH}_2\text{CH}=\text{CH}_2$ ), 5.19–5.14 (m, 2H,  $\text{OCH}_2\text{Ar}$ ), 5.01 (d,  $J = 3.8$  Hz, 1H, H-1'), 4.98 (d,  $J = 3.5$  Hz, 1H, H-1), 4.95 (d,  $J = 11.8$  Hz, 1H,  $\text{OCH}_2\text{CCl}_3$ ), 4.88 (d,  $J = 11.7$  Hz, 1H,  $\text{OCH}_2\text{Ar}$ ), 4.70 (d,  $J = 11.9$  Hz, 1H,  $\text{OCH}_2\text{CCl}_3$ ), 4.67 (d,  $J = 11.7$  Hz, 1H,  $\text{OCH}_2\text{Ar}$ ), 4.53–4.45 (m, 2H,  $\text{NCH}_2\text{Ph}$ ), 4.28 (d,  $J = 12.2$  Hz, 1H,  $\text{OCH}_2\text{Ar}$ ), 4.23 (d,  $J = 12.2$  Hz, 1H,  $\text{OCH}_2\text{Ar}$ ), 4.15 (d,  $J = 5.7$  Hz, 1H,  $\text{OCH}_2\text{CH}=\text{CH}_2$ ), 4.19–4.10 (m, 1H, H-2'), 4.04–3.98 (m, 1H, H-5'), 3.94 (app t,  $J = 9.3$  Hz, 1H, H-4), 3.89–3.82 (m, 2H, H-5, H-4'), 3.82–3.79 (m, 2H, H-2', H-6a), 3.72 (dd,  $J = 10.2, 2.8$  Hz, 1H, H-3'), 3.70–3.64 (m, 2H, H-6b, octyl  $\text{OCH}_2$ ), 3.70–3.64 (m, 2H, H-6b, octyl  $\text{OCH}_2$ ), 3.48–3.39 (m, 1H, octyl  $\text{OCH}_2$ ), 3.29–3.21 (m, 1H, octyl  $\text{NCH}_2$ ), 3.21–3.14 (m, 1H, octyl  $\text{NCH}_2$ ), 3.10 (dd,  $J = 10.5, 3.5$  Hz, 1H, H-2), 1.66–1.55 (m, 2H,  $\text{OCH}_2\text{CH}_2$ ), 1.55–1.42 (m, 2H,  $\text{NCH}_2\text{CH}_2$ ), 1.35–1.15 (m, 8H, 4 x  $\text{CH}_2$ ), 1.28 (d,  $J = 6.6$  Hz, 3H, H-6');  $^{13}\text{C NMR}$  (151 MHz,  $\text{CDCl}_3$ )  $\delta$  156.9 (C=O), 154.0 (C=O), 138.1 (Ar), 135.8 (Ar), 134.7 ( $\text{OCH}_2\text{CH}=\text{CH}_2$ ), 133.4 (Ar), 133.2 (Ar), 129.1 (Ar), 128.7 (2 x Ar), 128.6 (Ar), 128.6 (Ar), 128.4 (2 x Ar), 128.3 (Ar), 128.0 (2x Ar), 128.0 (2 x Ar), 127.8 (Ar), 127.6 (Ar), 127.5 (2 x Ar), 127.4 (2 x Ar), 127.0 (Ar), 127.0 (Ar), 126.3 (Ar), 126.2 (Ar), 126.2 (Ar), 125.8 (Ar), 117.5 ( $\text{OCH}_2\text{CH}=\text{CH}_2$ ), 99.3 (C-1'), 98.1 (C-1), 94.5 ( $\text{OCH}_2\text{CCl}_3$ ), 78.1 (C-3'), 77.3 (C-3), 76.9 ( $\text{OCH}_2\text{CCl}_3$ ), 75.4 (C-2'), 75.0 (C-4), 74.6 ( $\text{OCH}_2\text{Ar}$ ), 73.3 ( $\text{OCH}_2\text{Ar}$ ), 71.1 ( $\text{OCH}_2\text{CH}=\text{CH}_2$ ), 70.6 (C-5), 70.1 (C-4'), 68.9 (octyl  $\text{OCH}_2$ ), 68.2 (C-6), 67.2 ( $\text{OCH}_2\text{Ar}$ ), 66.2 (C-5'), 61.4 (C-2), 50.6 ( $\text{NC}_a\text{H}_2\text{Ph}$ ), 50.3 ( $\text{NC}_b\text{H}_2\text{Ph}$ ), 47.4 (octyl  $\text{NC}_a\text{H}_2$ ), 46.4 (octyl  $\text{NC}_b\text{H}_2$ ), 29.4 ( $\text{OCH}_2\text{CH}_2$ ), 29.4

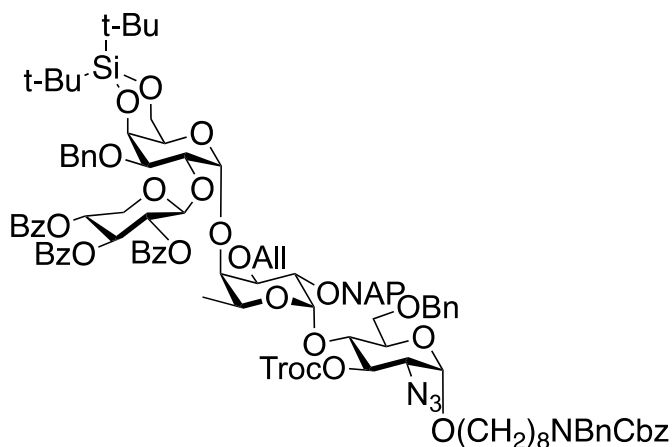
(CH<sub>2</sub>), 29.3 (CH<sub>2</sub>), 28.0 (NCH<sub>2</sub>C<sub>a</sub>H<sub>2</sub>), 27.7 (NCH<sub>2</sub>C<sub>b</sub>H<sub>2</sub>), 26.7 (CH<sub>2</sub>), 26.0 (CH<sub>2</sub>), 16.3 (C-6'); HRMS (MALDI-TOF) *m/z*: [M + Na]<sup>+</sup> Calcd for C<sub>59</sub>H<sub>69</sub>Cl<sub>3</sub>N<sub>4</sub>NaO<sub>13</sub> 1169.3822; Found 1169.3798.



***p*-Tolyl 2,3,4-tri-*O*-acetyl- $\beta$ -D-xylopyranosyl-(1 $\rightarrow$ 2)-3-*O*-benzyl-4,6-*O*-di-*tert*-butylsilylene-1-thio- $\beta$ -D-galactopyranoside (2.27)**

To a stirred solution of acceptor **2.10** (380 mg, 0.735 mmol) and donor **2.11** (380 mg, 0.882 mmol) in dry CH<sub>2</sub>Cl<sub>2</sub> (10 mL) was added 4Å molecular sieves powder (500 mg). After stirring for 30 min, the reaction mixture was cooled to 0 °C and then trimethylsilyl trifluoromethanesulfonate (13.0  $\mu$ L, 0.0735 mmol) was added. The resulting solution was stirred for 1 h at 0 °C before triethylamine was added to the mixture and the solution was filtered through Celite and the filtrate was concentrated to dryness. The crude residue was purified by flash chromatography (3:1 hexanes–EtOAc) to afford **2.27** (445 mg, 78%) as a white solid: *R<sub>f</sub>* = 0.26 (4:1 hexanes–EtOAc); [ $\alpha$ ]<sub>D</sub><sup>25</sup> – 15.3 (*c* = 0.21, CH<sub>2</sub>Cl<sub>2</sub>); <sup>1</sup>H NMR (500 MHz, CDCl<sub>3</sub>)  $\delta$  7.45–7.34 (m, 6H, Ar), 7.32–7.28 (m, 1H, Ar), 7.11–7.06 (m, 2H, Ar), 5.25 (d, *J* = 5.9 Hz, 1H, H-1'), 5.14 (dd, *J* = 8.4, 7.4 Hz, 1H, H-3'), 5.04 (dd, *J* = 8.4, 5.9 Hz, 1H, H-2'), 5.01 (app td, *J* = 7.0, 4.7 Hz, 1H, H-4'), 4.67 (d, *J* = 11.5 Hz, 1H, OCH<sub>2</sub>Ph), 4.58 (d, *J* = 11.5 Hz, 1H, OCH<sub>2</sub>Ph), 4.50 (d, *J* = 9.8 Hz, 1H, H-1), 4.45 (dd, *J* = 3.1, 1.0 Hz, 1H, H-4), 4.38 (dd, *J* = 12.4, 4.8 Hz, 1H, H-5a'), 4.16 (dd, *J* = 12.4, 1.7 Hz, 1H, H-6a), 4.16 (d, *J* = 12.6 Hz, 1H, H-6b), 4.09 (dd, *J* = 9.9, 9.1 Hz, 1H, H-2), 3.49 (dd, *J* = 12.4, 6.8 Hz,

1H, H-5b'), 3.41 (dd,  $J = 9.0, 3.1$  Hz, 1H, H-3), 3.23–3.20 (m, 1H, H-5), 2.32 (s, 3H, ArCH<sub>3</sub>), 2.05 (s, 3H, COCH<sub>3</sub>), 2.03 (s, 3H, COCH<sub>3</sub>), 1.99 (s, 3H, COCH<sub>3</sub>), 1.10 (s, 9H, C(CH<sub>3</sub>)<sub>3</sub>), 1.04 (s, 9H, C(CH<sub>3</sub>)<sub>3</sub>); <sup>13</sup>C NMR (126 MHz, CDCl<sub>3</sub>)  $\delta$  170.0 (2 x C=O), 169.4 (C=O), 138.0 (Ar), 137.7 (Ar), 133.2 (3 x Ar), 130.7 (Ar), 129.5 (Ar), 128.6 (Ar), 127.9 (4 x Ar), 100.2 (C-1'), 87.8 (C-1), 83.5 (C-3), 74.7 (C-5), 73.4 (C-2), 71.3 (C-3'), 71.1 (C-2'), 70.8 (OCH<sub>2</sub>Ph), 69.5 (C-4'), 69.5 (C-4), 67.3 (C-6), 62.2 (C-5'), 27.7 (3 x C(CH<sub>3</sub>)<sub>3</sub>), 27.6 (3 x C(CH<sub>3</sub>)<sub>3</sub>), 23.4 (C(CH<sub>3</sub>)<sub>3</sub>), 21.1 (ArCH<sub>3</sub>), 20.8 (2 x COCH<sub>3</sub>), 20.7 (COCH<sub>3</sub>), 20.8 (C(CH<sub>3</sub>)<sub>3</sub>); HRMS (ESI-TOF)  $m/z$ : [M + Na]<sup>+</sup> Calcd for C<sub>39</sub>H<sub>54</sub>NaO<sub>12</sub>SSi 797.2997; Found 797.2991.



**2.30**

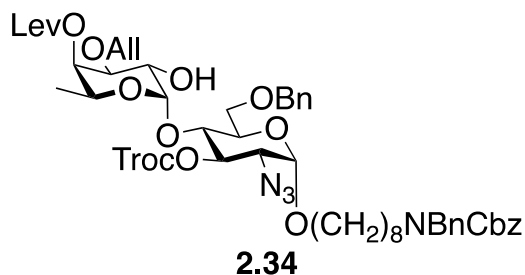
***N*-benzyl-*N*-benzoxycarbonyl-8-aminooctyl 2,3,4-tri-*O*-benzoyl- $\beta$ -D-xylopyranosyl-(1 $\rightarrow$ 2)-3-*O*-benzyl-4,6-*O*-di-*tert*-butylsilylene-1-thio- $\beta$ -D-galactopyranosyl-(1 $\rightarrow$ 4)-3-*O*-allyl-2-*O*-(2-naphthyl)methyl- $\alpha$ -L-fucopyranosyl-(1 $\rightarrow$ 4)-2-azido-6-*O*-benzyl-2-deoxy-3-*O*-(2,2,2-trichloroethoxycarbonyl)- $\alpha$ -D-glucopyranoside (2.30)**

To a stirred solution of **2.7** (100. mg, 0.104 mmol) in acetone–H<sub>2</sub>O (6 mL, 2:1) was added *N*-bromosuccinimide (93.0 mg, 0.520 mmol). The reaction mixture was stirred for 3 h before triethylamine was added. The mixture was diluted with EtOAc and washed successively with

saturated aqueous NaHCO<sub>3</sub>, water and brine. The organic layer was dried over Na<sub>2</sub>SO<sub>4</sub>, filtered and concentrated to dryness. The crude residue was purified using a short silica column (3:1 hexanes–EtOAc) to afford the corresponding hemiacetal product. The product was then dissolved in dry CH<sub>2</sub>Cl<sub>2</sub> (5 mL) before cesium carbonate (50.7 mg, 0.156 mmol) and 2,2,2-trifluoro-*N*-phenylacetamidoyl chloride (25.4 μL, 0.156 mmol) were added. After stirring overnight, the solution was filtered through Celite and the filtrate was concentrated to dryness. The crude product was purified using a short silica column (4:1 hexanes–EtOAc) to yield the imidate product **2.29** (75 mg, 73%) which was carried to the next step without further purification.

To a stirred solution of acceptor **2.26** (15.5 mg, 0.0147 mmol) and donor **2.29** (15 mg, 0.0176 mmol) in dry CH<sub>2</sub>Cl<sub>2</sub> (1 mL) was added 4Å molecular sieves powder (100 mg). After stirring for 30 min, the reaction mixture was cooled to 0 °C, and then trimethylsilyl trifluoromethanesulfonate (0.67 μL, 2.94 μmol) was added. The resulting solution was stirred for 1 h at 0 °C before triethylamine was added to the mixture and the solution was filtered through Celite and the filtrate was concentrated to dryness. The crude residue was purified by flash chromatography (3:1 hexanes–EtOAc) to afford **2.30** (15.5 mg, 53%) as a white solid: *R*<sub>f</sub> = 0.25 (3:1 hexanes–EtOAc); <sup>1</sup>H NMR (600 MHz, CDCl<sub>3</sub>) δ 7.94–7.88 (m, 5H), 7.82–7.74 (m, 3H), 7.65–7.57 (m, 3H), 7.52–7.47 (m, 1H), 7.47–7.38 (m, 4H), 7.82–7.74 (m, 3H), 7.37–7.32 (m, 5H), 7.32–7.26 (m, 5H), 7.23–7.19 (m, 3H), 7.18–7.14 (m, 3H), 7.14–7.10 (m, 2H), 7.10–7.06 (m, 2H), 7.00–6.95 (m, 2H), 6.02 (app ddt, *J* = 17.4, 10.6, 5.3 Hz, 1H), 5.83 (app t, *J* = 8.8 Hz, 1H), 5.77 (d, *J* = 4.0 Hz, 1H, H-1''), 5.59 (dd, *J* = 9.2, 6.7 Hz, 1H), 5.42 (dd, *J* = 17.2, 1.7 Hz, 1H), 5.32–5.28 (m, 2H), 5.27–5.24 (m, 1H), 5.22 (dd, *J* = 10.4, 6.0 Hz, 1H), 5.21 (d, *J* = 6.8 Hz, 1H, H-1'''), 5.20–5.14 (m, 3H, H-1'), 5.09 (d, *J* = 11.1 Hz, 1H), 4.97 (d, *J* = 3.6 Hz, 1H, H-1), 4.89 (d, *J* = 11.9 Hz, 1H), 4.75 (d, *J* = 11.9 Hz, 1H), 4.53–4.45 (m, 5H), 4.44 (d, *J* = 12.4 Hz, 1H), 4.34–4.28 (m, 4H), 4.21 (d, *J* = 5.7

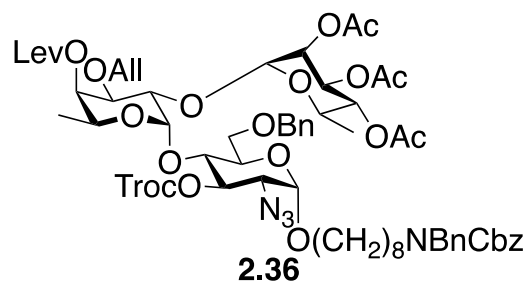
Hz, 3H), 4.20–4.13 (m, 3H), 4.09–4.03 (m, 3H), 3.94 (app t,  $J = 9.3$  Hz, 1H), 3.91–3.85 (m, 1H), 3.74–3.69 (m, 2H), 3.74–3.70 (m, 2H), 3.70–3.61 (m, 3H), 3.46–3.38 (m, 1H), 3.29–3.20 (m, 1H), 3.20–3.14 (m, 2H), 3.12 (dd,  $J = 10.6, 3.5$  Hz, 1H), 1.64–1.55 (m, 2H), 1.55–1.42 (m, 2H), 1.35–1.15 (m, 8H), 1.12 (d,  $J = 6.4$  Hz, 3H), 1.06 (s, 9H), 1.03 (s, 9H);  $^{13}\text{C}$  NMR (151 MHz,  $\text{CDCl}_3$ )  $\delta$  165.7, 165.6, 165.2, 154.0, 138.9, 138.2, 136.7, 135.0, 133.6, 133.4, 133.1, 130.0, 129.9, 129.7, 129.1, 128.7, 128.5, 128.5, 128.4, 128.4, 128.2, 128.0, 127.8, 127.6, 127.5, 127.4, 126.9, 126.7, 126.0, 125.8, 116.8, 102.2 (C-1'''), 99.7 (C-1'), 98.2 (C-1''), 98.1 (C-1), 94.6, 79.9, 75.9, 75.5, 74.7, 73.9, 73.2 (2 x C), 73.1, 72.1, 72.0, 71.9 (2 x C), 71.8, 71.7, 70.9, 70.6, 68.7, 68.1, 67.6, 67.6, 67.3, 67.2, 62.4, 61.5, 50.4, 50.3, 47.3, 46.4, 32.1, 29.5, 29.4, 26.8, 26.1, 23.6, 22.8, 20.9, 17.9; HRMS (MALDI-TOF)  $m/z$   $[\text{M} + \text{Na}]^+$  calcd for  $\text{C}_{106}\text{H}_{121}\text{Cl}_3\text{N}_4\text{NaO}_{25}\text{Si}$  2005.7051, found 2007.7095.



***N*-benzyl-*N*-benzoxycarbonyl-8-aminooctyl 3-*O*-allyl-4-*O*-levulinoyl- $\alpha$ -L-fucopyranosyl-(1 $\rightarrow$ 4)-2-azido-6-*O*-benzyl-2-deoxy-3-*O*-(2,2,2-trichloroethoxycarbonyl)- $\alpha$ -D-glucopyranoside (2.34)**

To a stirred biphasic solution of **2.6** (380 mg, 0.305 mmol) in  $\text{CH}_2\text{Cl}_2$ – $\text{H}_2\text{O}$  (11 mL, 10:1) was added 2,3-dichloro-5,6-dicyano-1,4-benzoquinone (169 mg, 0.610 mmol). The reaction mixture was stirred overnight before diluting it with  $\text{CH}_2\text{Cl}_2$  (100 mL). The mixture was then washed successively with 1N NaOH, water and brine. The organic layer was dried over  $\text{Na}_2\text{SO}_4$ , filtered

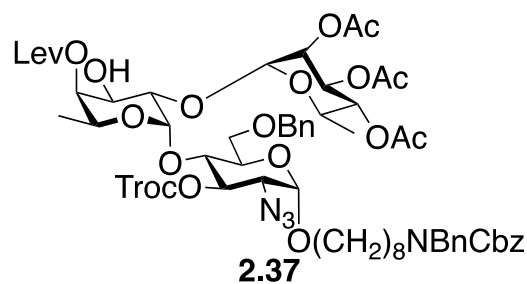
and concentrated to dryness. The crude residue was purified by flash chromatography (2:1 hexanes–EtOAc) to afford **2.34** (295 mg, 88%) as a colorless oil:  $R_f = 0.35$  (3:2 hexanes–EtOAc);  $^1\text{H NMR}$  (500 MHz,  $\text{CDCl}_3$ )  $\delta$  7.39–7.24 (m, 14H, Ar), 7.21–7.13 (m, 1H, Ar), 5.83 (app ddt,  $J = 16.5, 10.9, 5.8$  Hz, 1H,  $\text{OCH}_2\text{CH}=\text{CH}_2$ ), 5.28 (app t,  $J = 9.0$  Hz, 1H, H-3), 5.26–5.13 (m, 5H, Ar, H-4'), 2 x  $\text{OCH}_2\text{Ph}$ , 2 x  $\text{OCH}_2\text{CH}=\text{CH}_2$ ), 5.04 (d,  $J = 3.9$  Hz, 1H, H-1'), 4.98 (d,  $J = 3.6$  Hz, 1H, H-1), 4.96 (d,  $J = 11.9$  Hz, 1H,  $\text{OCH}_2\text{CCl}_3$ ), 4.69 (d,  $J = 11.9$  Hz, 1H,  $\text{OCH}_2\text{CCl}_3$ ), 4.62 (d,  $J = 12.0$  Hz, 1H,  $\text{OCH}_2\text{Ph}$ ), 4.57 (d,  $J = 12.0$  Hz, 1H,  $\text{OCH}_2\text{Ph}$ ), 4.52–4.46 (m, 2H,  $\text{NCH}_2\text{Ph}$ ), 4.11–4.03 (m, 2H,  $\text{OCH}_2\text{CH}=\text{CH}_2$ , H-5'), 4.00 (app t,  $J = 9.8$  Hz, 1H, H-4), 3.98 (dd,  $J = 11.2, 3.1$  Hz, 1H, H-6a), 3.91–3.84 (m, 2H,  $\text{OCH}_2\text{CH}=\text{CH}_2$ , H-5), 3.79 (ddd,  $J = 9.8, 5.5, 3.9$  Hz, 1H, H-2'), 3.71 (dd,  $J = 11.1, 2.7$  Hz, 1H, H-6b), 3.70–3.67 (m, 1H, octyl  $\text{OCH}_2$ ), 3.53 (dd,  $J = 10.2, 3.3$  Hz, 1H, H-3'), 3.50–3.44 (m, 1H, octyl  $\text{OCH}_2$ ), 3.29–3.22 (m, 1H, octyl  $\text{NCH}_2$ ), 3.22–3.16 (m, 1H, octyl  $\text{NCH}_2$ ), 3.13 (dd,  $J = 10.5, 3.6$  Hz, 1H, H-2), 2.83–2.58 (m, 4H,  $\text{COCH}_2\text{CH}_2\text{COCH}_3$ ), 2.39–2.32 (m, 1H, 2-OH'), 2.18 (s, 3H,  $\text{COCH}_3$ ), 1.69–1.57 (m, 2H,  $\text{OCH}_2\text{CH}_2$ ), 1.56–1.43 (m, 2H,  $\text{NCH}_2\text{CH}_2$ ), 1.35–1.19 (m, 8H, 4 x  $\text{CH}_2$ ), 1.14 (d,  $J = 6.5$  Hz, 3H, H-6');  $^{13}\text{C NMR}$  (126 MHz,  $\text{CDCl}_3$ )  $\delta$  206.2 (C=O), 172.4 (C=O), 156.8 (C=O), 153.9 (C=O), 138.0 (Ar), 137.6 (2 x Ar), 134.4 ( $\text{OCH}_2\text{CH}=\text{CH}_2$ ), 128.5 (3 x Ar), 128.4 (3 x Ar), 128.1 (2 x Ar), 127.9 (3 x Ar), 127.8 (2 x Ar), 127.3 (2 x Ar), 117.6 ( $\text{OCH}_2\text{CH}=\text{CH}_2$ ), 99.9 (C-1'), 98.1 (C-1), 94.3 ( $\text{OCH}_2\text{CCl}_3$ ), 77.0 (C-3), 76.9 ( $\text{OCH}_2\text{CCl}_3$ ), 75.5 (C-4), 75.5 (C-3'), 73.6 ( $\text{OCH}_2\text{Ph}$ ), 70.2 ( $\text{OCH}_2\text{CH}=\text{CH}_2$ ), 70.0 (C-4'), 70.0 (C-5), 68.9 (octyl  $\text{OCH}_2$ ), 68.1 (C-6'), 68.1 (C-2') 67.2 ( $\text{OCH}_2\text{Ph}$ ), 66.0 (C-5'), 61.3 (C-2), 50.5 ( $\text{NC}_a\text{H}_2\text{Ph}$ ), 50.2 ( $\text{NC}_b\text{H}_2\text{Ph}$ ), 47.2 (octyl  $\text{NC}_a\text{H}_2$ ), 46.3 (octyl  $\text{NC}_b\text{H}_2$ ), 38.0 ( $\text{COCH}_2\text{CH}_2\text{COCH}_3$ ), 29.9 ( $\text{COCH}_3$ ), 29.3 ( $\text{OCH}_2\text{CH}_2$ ), 29.3 ( $\text{CH}_2$ ), 29.3 ( $\text{CH}_2$ ), 28.1 ( $\text{NCH}_2\text{C}_a\text{H}_2$ ), 28.0 ( $\text{COCH}_2\text{CH}_2\text{COCH}_3$ ), 27.7 ( $\text{NCH}_2\text{C}_b\text{H}_2$ ), 26.7 ( $\text{CH}_2$ ), 26.0 ( $\text{CH}_2$ ), 16.2 (C-6'); HRMS (ESI–TOF)  $m/z$ :  $[\text{M} + \text{Na}]^+$  Calcd for  $\text{C}_{53}\text{H}_{67}\text{Cl}_3\text{N}_4\text{NaO}_{15}$  1127.3561; Found 1127.3556.



***N*-benzyl-*N*-benzoxycarbonyl-8-aminooctyl 2,3,4-tri-*O*-acetyl- $\alpha$ -L-rhamnopyranosyl-(1 $\rightarrow$ 2)-3-*O*-allyl-4-*O*-levulinoyl- $\alpha$ -L-fucopyranosyl-(1 $\rightarrow$ 4)-2-azido-6-*O*-benzyl-2-deoxy-3-*O*-(2,2,2-trichloroethoxycarbonyl)- $\alpha$ -D-glucopyranoside (2.36)**

To a stirred solution of acceptor **2.34** (59.0 mg, 53.3  $\mu$ mol) and donor **2.35**<sup>34</sup> (32.0 mg, 80.0  $\mu$ mol) in dry CH<sub>2</sub>Cl<sub>2</sub> (2 mL) was added 4Å molecular sieves powder (200 mg). After stirring for 30 min, the reaction mixture was cooled to 0 °C and then *N*-iodosuccinimide (14.0 mg, 64.0  $\mu$ mol) and silver trifluoromethanesulfonate (1.4 mg, 5.3  $\mu$ mol) were added successively. The resulting solution was stirred for 1 h at 0 °C before triethylamine was added to the mixture and the solution was filtered through Celite and the filtrate was washed with saturated aqueous Na<sub>2</sub>S<sub>2</sub>O<sub>3</sub> and saturated aqueous NaHCO<sub>3</sub>. The organic layer was dried over Na<sub>2</sub>SO<sub>4</sub>, filtered and concentrated to dryness. The crude residue was purified by flash chromatography (2:1 hexanes–EtOAc) to afford **2.36** (68.0 mg, 92%) as a colorless oil: *R*<sub>f</sub> = 0.29 (3:2 hexanes–EtOAc); <sup>1</sup>H NMR (500 MHz, CDCl<sub>3</sub>)  $\delta$  7.39–7.13 (m, 15H, Ar), 5.83 (app ddt, *J* = 16.5, 10.4, 5.8 Hz, 1H, OCH<sub>2</sub>CH=CH<sub>2</sub>), 5.29–5.24 (m, 4H, H-3, H-4', H-3''), OCH<sub>2</sub>CH=CH<sub>2</sub>), 5.21 (m, 1H, H-2''), 5.20–5.14 (m, 2H, OCH<sub>2</sub>Ar), 5.16 (app dq, *J* = 10.5, 1.4 Hz, 1H, OCH<sub>2</sub>CH=CH<sub>2</sub>), 5.06 (d, *J* = 3.6 Hz, 1H, H-1'), 5.04 (app t, *J* = 10.0 Hz, 1H, H-4''), 4.98 (d, *J* = 3.6 Hz, 1H, H-1), 4.94 (d, *J* = 11.9 Hz, 1H, OCH<sub>2</sub>CCl<sub>3</sub>), 4.71 (br s, 1H, H-1''), 4.69 (d, *J* = 11.9 Hz, 1H, OCH<sub>2</sub>CCl<sub>3</sub>), 4.65 (d, *J* = 12.2 Hz, 1H, OCH<sub>2</sub>Ph), 4.54 (d, *J* = 12.1 Hz, 1H, OCH<sub>2</sub>Ph), 4.52–4.45 (m, 2H, NCH<sub>2</sub>Ph), 4.28 (dq, *J* = 10.0, 6.3 Hz, 1H, H-5''), 4.16–4.09 (m, 1H, H-5'), 4.05 (app ddt, *J* = 10.7, 5.5, 1.5 Hz, 1H, OCH<sub>2</sub>CH=CH<sub>2</sub>), 3.96–3.84

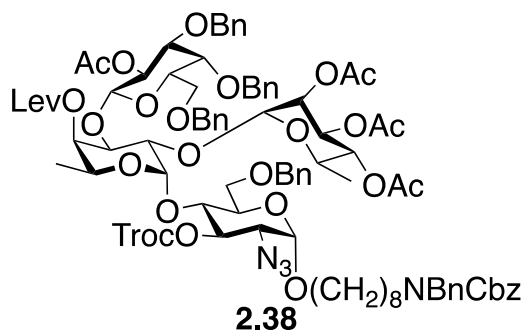
(m, 6H, H-2', H-4, H-6a, H-6b, H-5, OCH<sub>2</sub>CH=CH<sub>2</sub>), 3.76 (app dt,  $J = 9.7, 6.6$  Hz, 1H, octyl OCH<sub>2</sub>), 3.68 (dd,  $J = 10.5, 3.4$  Hz, 1H, H-3'), 3.47 (app dt,  $J = 9.1, 7.8$  Hz, 1H, octyl OCH<sub>2</sub>), 3.29–3.22 (m, 1H, octyl NCH<sub>2</sub>), 3.22–3.15 (m, 1H, octyl NCH<sub>2</sub>), 3.08 (dd,  $J = 10.6, 3.5$  Hz, 1H, H-2), 2.81–2.57 (m, 4H, COCH<sub>2</sub>CH<sub>2</sub>COCH<sub>3</sub>), 2.18 (s, 3H, COCH<sub>3</sub>), 2.07 (s, 3H, COCH<sub>3</sub>), 2.02 (s, 3H, COCH<sub>3</sub>), 1.97 (s, 3H, COCH<sub>3</sub>), 1.69–1.59 (m, 2H, OCH<sub>2</sub>CH<sub>2</sub>), 1.55–1.42 (m, 2H, NCH<sub>2</sub>CH<sub>2</sub>), 1.34–1.19 (m, 8H, 4 x CH<sub>2</sub>), 1.14 (d,  $J = 6.2$  Hz, 3H, H-6''), 1.13 (d,  $J = 6.5$  Hz, 3H, H-6'); <sup>13</sup>C NMR (126 MHz, CDCl<sub>3</sub>) δ 206.1 (C=O), 172.2 (C=O), 170.1 (C=O), 170.0 (C=O), 169.8 (C=O), 156.2 (C=O), 153.7 (C=O), 138.5 (Ar), 138.0 (Ar), 134.3 (OCH<sub>2</sub>CH=CH<sub>2</sub>), 128.5 (4 x Ar), 128.3 (3 x Ar), 127.9 (Ar), 127.8 (3 x Ar), 127.5 (Ar), 127.4 (2 x Ar), 127.3 (2 x Ar), 117.3 (OCH<sub>2</sub>CH=CH<sub>2</sub>), 97.9 (C-1), 97.3 (C-1'), 95.4 (C-1''), <sup>1</sup>J<sub>C-H</sub> = 174.2 Hz), 94.3 (OCH<sub>2</sub>CCl<sub>3</sub>), 77.5 (C-3), 76.9 (OCH<sub>2</sub>CCl<sub>3</sub>), 75.3 (C-5), 73.6 (OCH<sub>2</sub>Ph), 73.3 (C-3'), 71.5 (C-2'), 70.9 (C-4'), 70.9 (C-4), 70.7 (C-4''), 70.6 (OCH<sub>2</sub>CH=CH<sub>2</sub>), 69.8 (C-2''), 69.1 (C-3''), 68.8 (C-6), 68.6 (octyl OCH<sub>2</sub>), 67.1 (OCH<sub>2</sub>Ph), 66.3 (C-5''), 65.8 (C-5'), 61.2 (C-2), 50.5 (NC<sub>a</sub>H<sub>2</sub>Ph), 50.2 (NC<sub>b</sub>H<sub>2</sub>Ph), 47.2 (octyl NC<sub>a</sub>H<sub>2</sub>), 46.3 (octyl NC<sub>b</sub>H<sub>2</sub>), 38.0 (COCH<sub>2</sub>CH<sub>2</sub>COCH<sub>3</sub>), 29.9 (COCH<sub>3</sub>), 29.3 (OCH<sub>2</sub>CH<sub>2</sub>), 29.3 (CH<sub>2</sub>), 29.3 (CH<sub>2</sub>), 28.0 (NCH<sub>2</sub>C<sub>a</sub>H<sub>2</sub>), 27.9 (COCH<sub>2</sub>CH<sub>2</sub>COCH<sub>3</sub>), 27.7 (NCH<sub>2</sub>C<sub>b</sub>H<sub>2</sub>), 26.7 (CH<sub>2</sub>), 26.0 (CH<sub>2</sub>), 20.8 (3 x COCH<sub>3</sub>), 17.3 (C-6''), 16.0 (C-6'); HRMS (ESI-TOF)  $m/z$ : [M + H]<sup>+</sup> Calcd for C<sub>65</sub>H<sub>84</sub>Cl<sub>3</sub>N<sub>4</sub>O<sub>22</sub> 1377.4637; Found 1377.4637.



***N*-benzyl-*N*-benzoxycarbonyl-8-aminooctyl 2,3,4-tri-*O*-acetyl- $\alpha$ -L-rhamnopyranosyl-(1 $\rightarrow$ 2)-4-*O*-levulinoyl- $\alpha$ -L-fucopyranosyl-(1 $\rightarrow$ 4)-2-azido-6-*O*-benzyl-2-deoxy-3-*O*-(2,2,2-trichloroethoxycarbonyl)- $\alpha$ -D-glucopyranoside (**2.37**)**

To a stirred solution of **2.36** (63.0 mg, 45.7  $\mu$ mol) in dry THF (5 mL), degassed under vacuum, and under an Ar atmosphere, (1,5-cyclooctadiene)bis-(methyldiphenylphosphine)iridium I hexafluorophosphate (1.90 mg, 2.29  $\mu$ mol) was added, followed by further degassing of the reaction mixture. The suspension was stirred for 15 min at 0 °C and the catalyst was then activated with hydrogen (2 min under a hydrogen atmosphere). The excess of hydrogen was removed by three cycles of vacuum and flushing with Ar. The reaction mixture was then stirred for 2 h. The solvent was then evaporated, and the residue was dissolved in acetone–water (3.3 mL, 10:1) and HgO (15.0 mg, 68.6  $\mu$ mol) and HgCl<sub>2</sub> (15.0 mg, 54.8  $\mu$ mol) were added. The reaction mixture was stirred for 2 h, then the solvent was evaporated, and the residue was diluted with EtOAc (25 mL), washed with 10% KI, saturated aqueous Na<sub>2</sub>S<sub>2</sub>O<sub>3</sub> and water. The aqueous layers were extracted with EtOAc (25 mL), and the combined organic layers were dried over Na<sub>2</sub>SO<sub>4</sub>, filtered and concentrated. The crude residue was purified by flash chromatography (3:2 hexane–EtOAc) to afford **2.37** (43.3 mg, 70%) as a colorless oil:  $R_f$  = 0.16 (3:2 hexanes–EtOAc); <sup>1</sup>H NMR (700 MHz, CDCl<sub>3</sub>)  $\delta$  7.39–7.22 (m, 14H, Ar), 7.19–7.14 (m, 1H, Ar), 5.28 (dd,  $J$  = 10.7, 8.4 Hz, 1H, H-3), 5.22–5.13 (m, 5H, H-3'', H-2'', H-4', 2 x OCH<sub>2</sub>Ar), 5.11 (app t,  $J$  = 11.3 Hz, 1H, H-4'), 5.00 (d,  $J$  = 3.5 Hz, 1H, H-1), 4.94 (d,  $J$  = 3.9 Hz, 1H, H-1'), 4.90 (d,  $J$  = 11.8 Hz, 1H, OCH<sub>2</sub>CCl<sub>3</sub>), 4.73

(d,  $J = 11.8$  Hz, 1H,  $\text{OCH}_2\text{CCl}_3$ ), 4.71 (d,  $J = 12.1$  Hz, 1H,  $\text{OCH}_2\text{Ph}$ ), 4.66 (d,  $J = 1.5$  Hz, 1H, H-1''), 4.51 (d,  $J = 12.2$  Hz, 1H,  $\text{OCH}_2\text{Ph}$ ), 4.51–4.46 (m, 2H,  $\text{NCH}_2\text{Ph}$ ), 4.18 (dq,  $J = 9.8, 6.2$  Hz, 1H, H-5''), 4.10 (q,  $J = 6.5$  Hz, 1H, H-5'), 3.98–3.91 (m, 2H, H-5, H-4), 3.88 (dd,  $J = 11.6, 3.5$  Hz, 1H, H-6a), 3.88–3.85 (m, 1H, H-3'), 3.83 (d,  $J = 11.9$  Hz, 1H, H-6b), 3.77 (dt,  $J = 9.7, 6.7$  Hz, 1H, octyl  $\text{OCH}_2$ ), 3.56 (dd,  $J = 10.1, 3.8$  Hz, 1H, H-2'), 3.51–3.44 (m, 1H, octyl  $\text{OCH}_2$ ), 3.27–3.21 (m, 1H, octyl  $\text{NCH}_2$ ), 3.21–3.15 (m, 1H, octyl  $\text{NCH}_2$ ), 3.10 (dd,  $J = 10.6, 3.5$  Hz, 1H, H-2), 2.85–2.76 (m, 2H,  $\text{COCH}_2\text{CH}_2\text{COCH}_3$ ), 2.66–2.60 (m, 2H,  $\text{COCH}_2\text{CH}_2\text{COCH}_3$ ), 2.19 (s, 3H,  $\text{COCH}_3$ ), 2.15 (s, 3H,  $\text{COCH}_3$ ), 2.04 (s, 3H,  $\text{COCH}_3$ ), 1.96 (s, 3H,  $\text{COCH}_3$ ), 1.66–1.57 (m, 2H,  $\text{OCH}_2\text{CH}_2$ ), 1.55–1.44 (m, 2H,  $\text{NCH}_2\text{CH}_2$ ), 1.34–1.19 (m, 8H, 4 x  $\text{CH}_2$ ) 1.22 (d,  $J = 6.2$  Hz, 3H, H-6''), 1.13 (d,  $J = 6.5$  Hz, 3H, H-6');  $^{13}\text{C}$  NMR (126 MHz,  $\text{CDCl}_3$ )  $\delta$  204.3 (C=O), 172.6 (C=O), 170.0 (C=O), 169.9 (C=O), 169.6 (C=O), 156.0 (C=O), 153.8 (C=O), 138.1 (Ar), 138.0 (Ar), 136.8 (Ar), 128.4 (2 x Ar), 128.3 (2 x Ar), 128.0 (2 x Ar), 127.9 (2 x Ar), 127.8 (2 x Ar), 127.6 (Ar), 127.2 (2 x Ar), 97.8 (C-1), 97.8 (C-1''), 97.4 (C-1'), 94.2 ( $\text{OCH}_2\text{CCl}_3$ ), 78.5 (C-2'), 77.0 (C-3), 76.9 ( $\text{OCH}_2\text{CCl}_3$ ), 74.0 (C-5), 73.6 (C-4'), 73.4 ( $\text{OCH}_2\text{Ph}$ ), 70.5 (C-4), 70.4 (C-4''), 69.8 (C-2''), 68.7 (C-6), 68.5 (octyl  $\text{OCH}_2$ ), 67.9 (C-5''), 67.4 ( $\text{OCH}_2\text{Ph}$ ), 67.2 (C-3''), 67.1 (C-3'), 65.6 (C-5'), 61.2 (C-2), 50.5 ( $\text{NC}_a\text{H}_2\text{Ph}$ ), 50.1 ( $\text{NC}_b\text{H}_2\text{Ph}$ ), 47.2 (octyl  $\text{NC}_a\text{H}_2$ ), 46.2 (octyl  $\text{NC}_b\text{H}_2$ ), 38.3 ( $\text{COCH}_2\text{CH}_2\text{COCH}_3$ ), 29.8 ( $\text{COCH}_3$ ), 29.3 ( $\text{CH}_2$ ), 29.3 ( $\text{CH}_2$ ), 29.2 ( $\text{OCH}_2\text{CH}_2$ ), 28.0 ( $\text{NCH}_2\text{C}_a\text{H}_2$ ), 28.0 ( $\text{COCH}_2\text{CH}_2\text{COCH}_3$ ), 27.7 ( $\text{NCH}_2\text{C}_b\text{H}_2$ ), 26.7 ( $\text{CH}_2$ ), 26.0 ( $\text{CH}_2$ ), 20.8 ( $\text{COCH}_3$ ), 20.7 ( $\text{COCH}_3$ ), 20.6 ( $\text{COCH}_3$ ), 17.1 (C-6''), 16.0 (C-6'); HRMS (ESI-TOF)  $m/z$ :  $[\text{M} + \text{H}]^+$  Calcd for  $\text{C}_{62}\text{H}_{80}\text{Cl}_3\text{N}_4\text{O}_{22}$  1337.4324; Found 1337.4346.

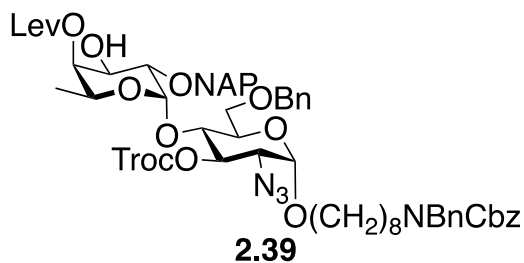


***N*-benzyl-*N*-benzoxycarbonyl-8-aminooctyl 2-*O*-acetyl-3,4,6-tri-*O*-benzyl- $\beta$ -D-galactopyranosyl-(1 $\rightarrow$ 3)-[2,3,4-tri-*O*-acetyl- $\alpha$ -L-rhamnopyranosyl-(1 $\rightarrow$ 2)]-4-*O*-levulinoyl- $\alpha$ -L-fucopyranosyl-(1 $\rightarrow$ 4)-2-azido-6-*O*-benzyl-2-deoxy-3-*O*-(2,2,2-trichloroethoxycarbonyl)- $\alpha$ -D-glucopyranoside (**2.38**)**

*Method A:* To a stirred solution of acceptor **2.37** (145 mg, 0.108 mmol) and donor **2.12**<sup>24</sup> (647 mg, 1.08 mmol) in dry CH<sub>2</sub>Cl<sub>2</sub> (5 mL) was added 4Å molecular sieves powder (300 mg). After stirring for 30 min, the reaction mixture was cooled to 0 °C and then *N*-iodosuccinimide (365 mg, 1.62 mmol) and trifluoromethanesulfonic acid (9.6  $\mu$ L, 0.108 mmol) were added successively. The resulting solution was stirred for 1 h at 0 °C before triethylamine was added to the mixture and the solution was filtered through Celite and the filtrate was washed with saturated aqueous Na<sub>2</sub>S<sub>2</sub>O<sub>3</sub> and saturated aqueous NaHCO<sub>3</sub>. The organic layer was dried over Na<sub>2</sub>SO<sub>4</sub>, filtered and concentrated to dryness. The crude residue was purified by flash chromatography (2:1 hexanes–EtOAc) to afford **2.38** (115 mg, 59%) as a white solid.

*Method B:* To a stirred solution of acceptor **2.41** (100 mg, 0.0649 mmol) and donor **2.35**<sup>34</sup> (77 mg, 0.195 mmol) in dry CH<sub>2</sub>Cl<sub>2</sub> (4 mL) was added 4Å molecular sieves powder (300 mg). After stirring for 30 min, the reaction mixture was cooled to 0 °C and then *N*-iodosuccinimide (58 mg, 0.260 mmol) and trifluoromethanesulfonic acid (0.57  $\mu$ L, 6.5  $\mu$ mol) were added successively. The resulting solution was stirred for 1 h at 0 °C before triethylamine was added to the mixture and the

solution was filtered through Celite and the filtrate was washed with saturated aqueous  $\text{Na}_2\text{S}_2\text{O}_3$  and saturated aqueous  $\text{NaHCO}_3$ . The organic layer was dried over  $\text{Na}_2\text{SO}_4$ , filtered and concentrated to dryness. The crude residue was purified by flash chromatography (2:1 hexanes–EtOAc) to afford **2.38** (65.3 mg, 55%) as a white solid:  $R_f = 0.29$  (2:1 hexanes–EtOAc);  $[\alpha]_D^{25} - 12.0$  ( $c = 0.5$ ,  $\text{CH}_2\text{Cl}_2$ );  $^1\text{H NMR}$  (600 MHz,  $\text{CDCl}_3$ )  $\delta$  7.41–7.22 (m, 22H, Ar), 7.22–7.13 (m, 8H, Ar), 5.42 (s, 1H, H-2''), 5.41 (app t,  $J = 3.4$  Hz, H-3''), 5.30 (dd,  $J = 9.4, 8.3$  Hz, 1H, H-2'''), 5.26 (dd,  $J = 10.5, 8.8$  Hz, 1H, H-3), 5.22–5.14 (m, 3H, 2 x  $\text{OCH}_2\text{Ar}$ , H-4'), 5.11 (d,  $J = 3.4$  Hz, 1H, H-1'), 5.09–5.04 (m, 1H, H-4''), 4.99 (d,  $J = 11.8$  Hz, 1H,  $\text{OCH}_2\text{CCl}_3$ ), 4.97 (d,  $J = 3.6$  Hz, 1H, H-1), 4.78 (s, 1H, H-1''), 4.73 (d,  $J = 12.2$  Hz, 1H,  $\text{OCH}_2\text{Ar}$ ), 4.69 (d,  $J = 12.5$  Hz, 1H,  $\text{OCH}_2\text{Ar}$ ), 4.66 (d,  $J = 12.2$  Hz, 1H,  $\text{OCH}_2\text{Ar}$ ), 4.63 (d,  $J = 12.0$  Hz, 1H,  $\text{OCH}_2\text{CCl}_3$ ), 4.62 (d,  $J = 12.3$  Hz, 1H,  $\text{OCH}_2\text{Ar}$ ), 4.52 (d,  $J = 12.2$  Hz, 1H,  $\text{OCH}_2\text{Ar}$ ), 4.51–4.45 (m, 3H, 2 x  $\text{NCH}_2\text{Ph}$ , H-5''), 4.40 (d,  $J = 7.9$  Hz, 1H, H-1'''), 4.37 (d,  $J = 12.2$  Hz, 1H,  $\text{OCH}_2\text{Ar}$ ), 4.36 (d,  $J = 11.9$  Hz, 1H,  $\text{OCH}_2\text{Ar}$ ), 4.34 (d,  $J = 11.7$  Hz, 1H,  $\text{OCH}_2\text{Ar}$ ), 4.22 (d,  $J = 10.8$  Hz, 1H, H-3'), 4.15–4.08 (m, 1H, H-5'), 4.08 (dd,  $J = 10.7, 3.4$  Hz, 1H, H-2'), 3.97–3.87 (m, 4H, H-5, H-6a, H-4''', H-6a'''), 3.86 (app t,  $J = 9.3$  Hz, 1H, H-4), 3.76–3.68 (m, 2H, H-6b''', octyl  $\text{OCH}_2$ ), 3.53 (app t,  $J = 6.7$  Hz, 1H, H-5'''), 3.45 (dd,  $J = 10.0, 3.1$  Hz, 1H, H-3'''), 3.48–3.41 (m, 1H, octyl  $\text{OCH}_2$ ), 3.29–3.22 (m, 1H, octyl  $\text{NCH}_2$ ), 3.22–3.14 (m, 1H, octyl  $\text{NCH}_2$ ), 2.83–2.75 (m, 1H,  $\text{COCH}_2\text{CH}_2\text{COCH}_3$ ), 2.74–2.65 (m, 2H,  $\text{COCH}_2\text{CH}_2\text{COCH}_3$ ,  $\text{COCH}_2\text{CH}_2\text{COCH}_3$ ), 2.56–2.47 (m, 1H,  $\text{COCH}_2\text{CH}_2\text{COCH}_3$ ), 2.18 (s, 3H,  $\text{COCH}_3$ ), 2.04 (s, 3H,  $\text{COCH}_3$ ), 1.98 (s, 3H,  $\text{COCH}_3$ ), 1.92 (s, 3H,  $\text{COCH}_3$ ), 1.81 (s, 3H,  $\text{COCH}_3$ ), 1.69–1.58 (m, 2H,  $\text{OCH}_2\text{CH}_2$ ), 1.57–1.42 (m, 2H,  $\text{NCH}_2\text{CH}_2$ ), 1.41–1.21 (m, 8H, 4 x  $\text{CH}_2$ ), 1.19 (d,  $J = 6.2$  Hz, 3H, H-6''), 1.08 (d,  $J = 6.5$  Hz, 3H, H-6'); HRMS (MALDI–TOF)  $m/z$ :  $[\text{M} + \text{Na}]^+$  Calcd for  $\text{C}_{91}\text{H}_{109}\text{Cl}_3\text{N}_4\text{NaO}_{28}$  1833.6190; Found 1833.6196.



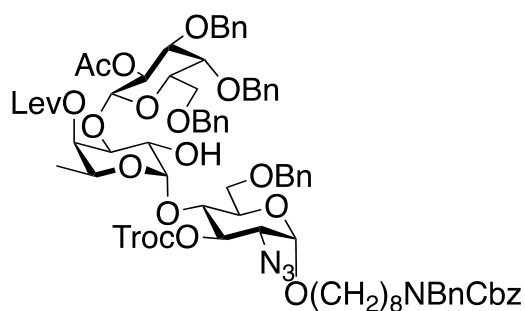
***N*-benzyl-*N*-benzoxycarbonyl-8-aminooctyl 3-*O*-allyl-4-*O*-levulinoyl- $\alpha$ -L-fucopyranosyl-(1 $\rightarrow$ 4)-2-azido-6-*O*-benzyl-2-deoxy-3-*O*-(2,2,2-trichloroethoxycarbonyl)- $\alpha$ -D-glucopyranoside (2.39)**

To a stirred solution of **2.6** (250 mg, 0.201 mmol) in dry THF (10 mL), degassed under vacuum and under an Ar atmosphere, (1,5-cyclooctadiene)bis-(methyldiphenylphosphine)iridium I hexafluorophosphate (8.5 mg, 10.0  $\mu$ mol) was added, followed by further degassing of the reaction mixture. The suspension was stirred for 15 min at 0 °C, and the catalyst was then activated with hydrogen (2 min under hydrogen atmosphere). The excess of hydrogen was removed by three cycles of vacuum and flushing with Ar. The reaction mixture was then stirred for 2 h. The solvent was then evaporated, and the residue was dissolved in acetone–water (10 mL, 9:1) and HgO (66.0 mg, 0.302 mmol) and HgCl<sub>2</sub> (66.0 mg, 0.241 mmol) were added. The reaction mixture was stirred for 2 h, then the solvent was evaporated, and the residue was diluted with EtOAc (50 mL), washed with 10% KI, saturated aqueous Na<sub>2</sub>S<sub>2</sub>O<sub>3</sub> and water. The aqueous layers were extracted with EtOAc (50 mL), and the combined organic layers were dried over Na<sub>2</sub>SO<sub>4</sub>, filtered and concentrated. The crude residue was purified by flash chromatography (2:1 hexane–EtOAc) to afford **2.39** (230 mg, 95%) as a colorless oil:  $R_f$  = 0.12 (2:1 hexanes–EtOAc);  $[\alpha]_D^{25}$  +34.1 ( $c$  = 1.29, CH<sub>2</sub>Cl<sub>2</sub>); <sup>1</sup>H NMR (500 MHz, CDCl<sub>3</sub>)  $\delta$  7.83–7.74 (m, 3H, Ar), 7.76–7.72 (m, 1H, Ar), 7.49–7.43 (m, 2H, Ar), 7.46–7.39 (m, 1H, Ar), 7.40–7.21 (m, 12H, Ar), 7.18–7.14 (m, 3H, Ar), 5.27 (dd,  $J$  = 10.5, 8.4 Hz, 1H, H-3), 5.20–5.13 (m, 3H, H-4', 2 x OCH<sub>2</sub>Ar), 5.08 (d,  $J$  = 3.6 Hz, 1H, H-1'),

4.98 (d,  $J = 3.6$  Hz, 1H, H-1), 4.98 (d,  $J = 11.9$  Hz, 1H,  $\text{OCH}_2\text{CCl}_3$ ), 4.83 (d,  $J = 11.8$  Hz, 1H,  $\text{OCH}_2\text{Ar}$ ), 4.76 (d,  $J = 11.9$  Hz, 1H,  $\text{OCH}_2\text{Ar}$ ), 4.63 (d,  $J = 11.8$  Hz, 1H,  $\text{OCH}_2\text{CCl}_3$ ), 4.52–4.46 (m, 2H,  $\text{NCH}_2\text{Ph}$ ), 4.36 (d,  $J = 12.3$  Hz, 1H,  $\text{OCH}_2\text{Ar}$ ), 4.33 (d,  $J = 12.3$  Hz, 1H,  $\text{OCH}_2\text{Ar}$ ), 4.13 (app t,  $J = 7.3$  Hz, 1H, H-5'), 4.13–4.06 (m, 1H, H-3'), 3.96–3.80 (m, 3H, H-4, H-5, H-6a), 3.74–3.66 (m, 2H, H-6b, octyl  $\text{OCH}_2$ ), 3.67 (dd,  $J = 10.2, 3.5$  Hz, 1H, H-2'), 3.49–3.42 (m, 1H, octyl  $\text{OCH}_2$ ), 3.27–3.21 (m, 1H, octyl  $\text{NCH}_2$ ), 3.21–3.14 (m, 1H, octyl  $\text{NCH}_2$ ), 3.11 (dd,  $J = 10.6, 3.5$  Hz, 1H, H-2), 2.77–2.72 (m, 2H,  $\text{COCH}_2\text{CH}_2\text{COCH}_3$ ), 2.62–2.55 (m, 2H,  $\text{COCH}_2\text{CH}_2\text{COCH}_3$ ), 2.14 (s, 3H,  $\text{COCH}_3$ ), 1.66–1.56 (m, 2H,  $\text{OCH}_2\text{CH}_2$ ), 1.56–1.42 (m, 2H,  $\text{NCH}_2\text{CH}_2$ ), 1.35–1.15 (m, 8H, 4 x  $\text{CH}_2$ ), 1.11 (d,  $J = 6.4$  Hz, 3H, H-6');  $^{13}\text{C}$  NMR (126 MHz,  $\text{CDCl}_3$ )  $\delta$  212.7 (C=O), 172.9 (C=O), 156.7 (C=O), 153.7 (C=O), 138.1 (Ar), 138.0 (Ar), 133.2 (Ar), 133.1 (Ar), 128.5 (4 x Ar), 128.4 (2 x Ar), 128.3 (3 x Ar), 127.9 (3 x Ar), 127.8 (4 x Ar), 127.5 (Ar), 127.4 (3 x Ar), 127.2 (2 x Ar), 127.0 (Ar), 126.3 (Ar), 126.1 (Ar), 126.0 (Ar), 99.1 (C-1'), 98.0 (C-1), 94.3 ( $\text{OCH}_2\text{CCl}_3$ ), 77.5 (C-3), 77.1 ( $\text{OCH}_2\text{CCl}_3$ ), 76.4 (C-2'), 75.6 (C-5), 74.2 (C-4'), 73.8 ( $\text{OCH}_2\text{Ar}$ ), 73.3 ( $\text{OCH}_2\text{Ar}$ ), 70.4 (C-4), 68.7 (C-3'), 68.7 (octyl  $\text{OCH}_2$ ), 68.1 (C-6), 67.2 ( $\text{OCH}_2\text{Ar}$ ), 66.0 (C-5'), 61.2 (C-2), 50.2 ( $\text{NCH}_2\text{Ph}$ ), 47.3 ( $\text{NCH}_2$ ), 38.3 ( $\text{COCH}_2\text{CH}_2\text{COCH}_3$ ), 29.8 ( $\text{COCH}_3$ ), 29.3 ( $\text{OCH}_2\text{CH}_2$ ), 29.3 ( $\text{CH}_2$ ), 29.3 ( $\text{CH}_2$ ), 28.1 ( $\text{COCH}_2\text{CH}_2\text{COCH}_3$ ), 27.7 ( $\text{NCH}_2\text{CH}_2$ ), 26.7 ( $\text{CH}_2$ ), 26.0 ( $\text{CH}_2$ ), 16.0 (C-6'); HRMS (ESI-TOF)  $m/z$ :  $[\text{M} + \text{Na}]^+$  Calcd for  $\text{C}_{61}\text{H}_{71}\text{Cl}_3\text{N}_4\text{NaO}_{15}$  1227.3874; Found 1227.3870.



$\text{OCH}_2\text{Ar}$ ), 4.67 (d,  $J = 12.2$  Hz, 1H,  $\text{OCH}_2\text{Ar}$ ), 4.66 (d,  $J = 11.9$  Hz, 1H,  $\text{OCH}_2\text{CCl}_3$ ), 4.62 (d,  $J = 11.5$  Hz, 1H,  $\text{OCH}_2\text{Ar}$ ), 4.51 (d,  $J = 11.6$  Hz, 1H,  $\text{OCH}_2\text{Ar}$ ), 4.51 (d,  $J = 12.7$  Hz, 1H,  $\text{OCH}_2\text{Ar}$ ), 4.49 (d,  $J = 8.1$  Hz, 1H, H-1''), 4.54–4.47 (m, 2H,  $\text{NCH}_2\text{Ph}$ ), 4.25 (d,  $J = 12.3$  Hz, 1H,  $\text{OCH}_2\text{Ar}$ ), 4.24 (dd,  $J = 7.0, 3.2$  Hz, 1H, H-3'), 4.17 (d,  $J = 12.2$  Hz, 1H,  $\text{OCH}_2\text{Ar}$ ), 4.14 (d,  $J = 11.9$  Hz, 1H,  $\text{OCH}_2\text{Ar}$ ), 4.10 (d,  $J = 11.7$  Hz, 1H,  $\text{OCH}_2\text{Ar}$ ), 4.03 (q,  $J = 6.6$  Hz, 1H, H-5'), 3.97 (d,  $J = 2.9$  Hz, 1H, H-4''), 3.91 (app t,  $J = 9.3$  Hz, 1H, H-4), 3.85–3.78 (m, 2H, H-5, H-6a), 3.72 (dd,  $J = 10.2, 3.8$  Hz, 1H, H-2'), 3.67–3.60 (m, 2H, H-6b, octyl  $\text{OCH}_2$ ), 3.58–3.49 (m, 3H, H-5'', H-3'', H-6a''), 3.44–3.38 (m, 1H, octyl  $\text{OCH}_2$ ), 3.38 (dd,  $J = 8.6, 4.8$  Hz, 1H, H-6b''), 3.27–3.20 (m, 1H, octyl  $\text{NCH}_2$ ), 3.20–3.14 (m, 1H, octyl  $\text{NCH}_2$ ), 3.09 (dd,  $J = 10.6, 3.5$  Hz, 1H, H-2), 2.78–2.53 (m, 4H,  $\text{COCH}_2\text{CH}_2\text{COCH}_3$ ), 2.09 (s, 3H,  $\text{COCH}_3$ ), 2.04 (s, 3H,  $\text{COCH}_3$ ), 1.66–1.54 (m, 2H,  $\text{OCH}_2\text{CH}_2$ ), 1.54–1.42 (m, 2H,  $\text{NCH}_2\text{CH}_2$ ), 1.29–1.19 (m, 8H, 4 x  $\text{CH}_2$ ), 1.07 (d,  $J = 6.5$  Hz, 3H, H-6');  $^{13}\text{C}$  NMR (126 MHz,  $\text{CDCl}_3$ )  $\delta$  206.2 (C=O), 172.1 (C=O), 169.8 (C=O), 156.0 (C=O), 153.9 (C=O), 138.7 (Ar), 138.1 (Ar), 138.0 (Ar), 137.9 (Ar), 136.3 (Ar), 133.3 (Ar), 133.0 (Ar), 128.5 (2 x Ar), 128.4 (5 x Ar), 128.3 (2 x Ar), 128.2 (2 x Ar), 128.0 (Ar), 127.9 (4 x Ar), 127.8 (3 x Ar), 127.7 (3 x Ar), 127.5 (2 x Ar), 127.4 (2 x Ar), 127.3 (3 x Ar), 127.0 (Ar), 126.7 (Ar), 125.9 (Ar), 125.7 (Ar), 100.0 (C-1'), 99.2 (C-1''), 97.9 (C-1), 94.4 ( $\text{OCH}_2\text{CCl}_3$ ), 80.7 (C-3''), 77.3 (C-3), 77.1 ( $\text{OCH}_2\text{CCl}_3$ ), 75.4 (C-3'), 75.4 (C-4), 74.6 ( $\text{OCH}_2\text{Ar}$ ), 74.3 ( $\text{OCH}_2\text{Ar}$ ), 73.9 (C-2'), 73.4 (C-5''), 73.2 ( $\text{OCH}_2\text{Ar}$ ), 73.1 ( $\text{OCH}_2\text{Ar}$ ), 72.7 (C-4''), 72.1 ( $\text{OCH}_2\text{Ar}$ ), 71.8 (C-2''), 71.3 (C-4'), 70.4 (C-5), 68.7 (octyl  $\text{OCH}_2$ ), 68.1 (C-6''), 68.0 (C-6), 67.1 ( $\text{OCH}_2\text{Ar}$ ), 66.0 (C-5'), 61.2 (C-2), 50.5 ( $\text{NC}_a\text{H}_2\text{Ph}$ ), 50.2 ( $\text{NC}_b\text{H}_2\text{Ph}$ ), 47.2 (octyl  $\text{NC}_a\text{H}_2$ ), 46.3 (octyl  $\text{NC}_b\text{H}_2$ ), 37.9 ( $\text{COCH}_2\text{CH}_2\text{COCH}_3$ ), 29.7 ( $\text{COCH}_3$ ), 29.3 ( $\text{CH}_2$ ), 29.3 ( $\text{CH}_2$ ), 29.1 ( $\text{OCH}_2\text{CH}_2$ ), 28.0 ( $\text{NCH}_2\text{C}_a\text{H}_2$ ), 28.1 ( $\text{COCH}_2\text{CH}_2\text{COCH}_3$ ), 27.7 ( $\text{NCH}_2\text{C}_b\text{H}_2$ ), 26.7 ( $\text{CH}_2$ ), 26.0 ( $\text{CH}_2$ ), 21.2 ( $\text{COCH}_3$ ), 16.1 (C-6'); HRMS (ESI-TOF)  $m/z$ :  $[\text{M} + \text{Na}]^+$  Calcd for  $\text{C}_{90}\text{H}_{101}\text{Cl}_3\text{N}_4\text{NaO}_{21}$  1701.5903; Found 1701.5913.

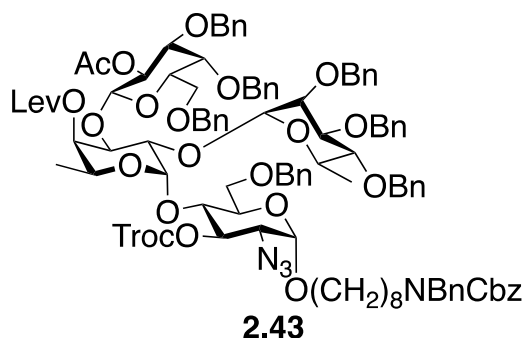


**2.41**

***N*-benzyl-*N*-benzoxycarbonyl-8-aminooctyl 2-*O*-acetyl-3,4,6-tri-*O*-benzyl- $\beta$ -D-galactopyranosyl-(1 $\rightarrow$ 3)-[2,3,4-tri-*O*-acetyl- $\alpha$ -L-rhamnopyranosyl-(1 $\rightarrow$ 2)]-4-*O*-levulinoyl- $\alpha$ -L-fucopyranosyl-(1 $\rightarrow$ 4)-2-azido-6-*O*-benzyl-2-deoxy-3-*O*-(2,2,2-trichloroethoxycarbonyl)- $\alpha$ -D-glucopyranoside (2.41)**

To a stirred biphasic solution of **2.40** (130 mg, 77.3  $\mu$ mol) in CH<sub>2</sub>Cl<sub>2</sub>–H<sub>2</sub>O (5.5 mL, 10:1) was added 2,3-dichloro-5,6-dicyano-1,4-benzoquinone (32.0 mg, 0.116 mmol). The reaction mixture was stirred overnight before being diluted with CH<sub>2</sub>Cl<sub>2</sub> (50 mL). The mixture was then washed successively with 1N NaOH, water and brine. The organic layer was dried over Na<sub>2</sub>SO<sub>4</sub>, filtered and concentrated to dryness. The crude residue was purified by flash chromatography (2:1 hexanes–EtOAc) to afford **2.41** (105 mg, 88%) as a white solid:  $R_f$  = 0.21 (2:1 hexanes–EtOAc);  $[\alpha]_D^{25} +16.6$  ( $c$  = 3.58, CHCl<sub>3</sub>); <sup>1</sup>H NMR (500 MHz, CDCl<sub>3</sub>)  $\delta$  7.38–7.22 (m, 29H, Ar), 7.19–7.14 (m, 1H, Ar), 5.30 (dd,  $J$  = 10.2, 7.9 Hz, 1H, H-2''), 5.26 (dd,  $J$  = 10.5, 9.0 Hz, 1H, H-3), 5.24–5.13 (m, 3H, 2 x OCH<sub>2</sub>Ar, H-4'), 5.05 (d,  $J$  = 3.9 Hz, 1H, H-1'), 4.98 (d,  $J$  = 3.6 Hz, 1H, H-1), 4.96 (d,  $J$  = 11.9 Hz, 1H, OCH<sub>2</sub>CCl<sub>3</sub>), 4.90 (d,  $J$  = 11.6 Hz, 1H, OCH<sub>2</sub>Ar), 4.66 (d,  $J$  = 11.9 Hz, 1H, OCH<sub>2</sub>CCl<sub>3</sub>), 4.65 (d,  $J$  = 12.2 Hz, 1H, OCH<sub>2</sub>Ar), 4.55 (d,  $J$  = 11.9 Hz, 1H, OCH<sub>2</sub>Ar), 4.54 (d,  $J$  = 12.0 Hz, 1H, OCH<sub>2</sub>Ar), 4.51 (d,  $J$  = 12.6 Hz, 1H, OCH<sub>2</sub>Ar), 4.50 (d,  $J$  = 11.9 Hz, 1H, OCH<sub>2</sub>Ar), 4.52–4.45 (m, 2H, NCH<sub>2</sub>Ph), 4.41 (d,  $J$  = 11.9 Hz, 1H, OCH<sub>2</sub>Ar), 4.51 (d,  $J$  = 11.9 Hz, 1H, OCH<sub>2</sub>Ar), 4.29 (d,  $J$  = 8.0 Hz, 1H, H-1''), 4.06–4.00 (m, 2H, H-5', H-6a), 3.97 (app t,  $J$  = 9.6 Hz,

1H, H-4), 3.88 (d,  $J = 2.8$  Hz, 1H, H-4''), 3.86–3.82 (m, 2H, H-5, 2-OH'), 3.82 (dd,  $J = 9.9, 4.0$  Hz, 1H, H-2'), 3.73–3.65 (m, 3H, H-3', octyl OCH<sub>2</sub>, H-6b), 3.61–3.56 (m, 1H, H-5''), 3.57 (app t,  $J = 6.0$  Hz, 1H, H-6a''), 3.52–3.48 (m, 1H, H-6b''), 3.45 (dd,  $J = 10.2, 3.1$  Hz, 1H, H-3''), 3.47–3.41 (m, 1H, octyl OCH<sub>2</sub>), 3.29–3.21 (m, 1H, octyl NCH<sub>2</sub>), 3.21–3.15 (m, 1H, octyl NCH<sub>2</sub>), 3.13 (dd,  $J = 10.6, 3.6$  Hz, 1H, H-2), 2.90–2.81 (m, 1H, COCH<sub>2</sub>CH<sub>2</sub>COCH<sub>3</sub>), 2.71–2.67 (m, 1H, COCH<sub>2</sub>CH<sub>2</sub>COCH<sub>3</sub>), 2.67–2.63 (m, 1H, COCH<sub>2</sub>CH<sub>2</sub>COCH<sub>3</sub>), 2.59–2.50 (m, 1H, COCH<sub>2</sub>CH<sub>2</sub>COCH<sub>3</sub>), 2.18 (s, 3H, COCH<sub>3</sub>), 2.05 (s, 3H, COCH<sub>3</sub>), 1.65–1.56 (m, 2H, OCH<sub>2</sub>CH<sub>2</sub>), 1.56–1.44 (m, 2H, NCH<sub>2</sub>CH<sub>2</sub>), 1.35–1.14 (m, 8H, 4 x CH<sub>2</sub>), 1.10 (d,  $J = 6.5$  Hz, 3H, H-6'); <sup>13</sup>C NMR (126 MHz, CDCl<sub>3</sub>) δ 206.8 (C=O), 172.5 (C=O), 169.7 (C=O), 156.8 (C=O), 154.0 (C=O), 138.1 (Ar), 138.0 (Ar), 137.7 (Ar), 137.6 (Ar), 128.5 (3 x Ar), 128.5 (3 x Ar), 128.5 (3 x Ar), 128.4 (3 x Ar), 128.4 (3 x Ar), 128.3 (3 x Ar), 127.9 (3 x Ar), 127.9 (3 x Ar), 127.8 (3 x Ar), 127.7 (3 x Ar), 127.6 (Ar), 127.5 (2 x Ar), 102.1 (C-1''), 99.9 (C-1'), 98.0 (C-1), 94.3 (OCH<sub>2</sub>CCl<sub>3</sub>), 80.3 (C-3'), 80.2 (C-3''), 77.3 (C-3), 77.1 (OCH<sub>2</sub>CCl<sub>3</sub>), 74.9 (C-4), 74.7 (OCH<sub>2</sub>Ph), 73.9 (C-5''), 73.6 (OCH<sub>2</sub>Ph), 73.3 (OCH<sub>2</sub>Ph), 72.4 (C-4''), 72.3 (OCH<sub>2</sub>Ph), 71.5 (C-4'), 70.6 (C-2''), 70.5 (C-5), 68.7 (octyl OCH<sub>2</sub>), 68.4 (C-6''), 67.8 (C-6), 67.6 (C-2'), 67.1 (OCH<sub>2</sub>Ph), 65.6 (C-5'), 61.3 (C-2), 50.4 (NC<sub>a</sub>H<sub>2</sub>Ph), 50.2 (NC<sub>b</sub>H<sub>2</sub>Ph), 47.2 (octyl NC<sub>a</sub>H<sub>2</sub>), 46.5 (octyl NC<sub>b</sub>H<sub>2</sub>), 38.0 (COCH<sub>2</sub>CH<sub>2</sub>COCH<sub>3</sub>), 29.9 (COCH<sub>3</sub>), 29.7 (CH<sub>2</sub>), 29.7 (CH<sub>2</sub>), 29.3 (OCH<sub>2</sub>CH<sub>2</sub>), 28.0 (NCH<sub>2</sub>C<sub>a</sub>H<sub>2</sub>), 28.1 (COCH<sub>2</sub>CH<sub>2</sub>COCH<sub>3</sub>), 27.7 (NCH<sub>2</sub>C<sub>b</sub>H<sub>2</sub>), 26.7 (CH<sub>2</sub>), 26.0 (CH<sub>2</sub>), 21.1 (COCH<sub>3</sub>), 15.8 (C-6'); HRMS (ESI-TOF)  $m/z$ : [M + Na]<sup>+</sup> Calcd for C<sub>79</sub>H<sub>93</sub>Cl<sub>3</sub>N<sub>4</sub>NaO<sub>21</sub> 1561.5290; Found 1561.5290.

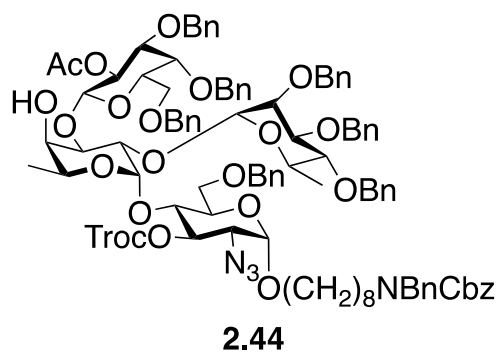


***N*-benzyl-*N*-benzoxycarbonyl-8-aminooctyl 2-*O*-acetyl-3,4,6-tri-*O*-benzyl- $\beta$ -D-galactopyranosyl-(1 $\rightarrow$ 3)-[2,3,4-tri-*O*-benzyl- $\alpha$ -L-rhamnopyranosyl-(1 $\rightarrow$ 2)]-4-*O*-levulinoyl- $\alpha$ -L-fucopyranosyl-(1 $\rightarrow$ 4)-2-azido-6-*O*-benzyl-2-deoxy-3-*O*-(2,2,2-trichloroethoxycarbonyl)- $\alpha$ -D-glucopyranoside (2.43)**

To a stirred solution of acceptor **2.41** (95 mg, 0.0616 mmol) and donor **2.13**<sup>27</sup> (67 mg, 0.123 mmol) in dry CH<sub>2</sub>Cl<sub>2</sub> (5 mL) was added 4Å molecular sieves powder (500 mg). After stirring for 30 min, the reaction mixture was cooled to 0 °C and then *N*-iodosuccinimide (42.0 mg, 0.185 mmol) and silver trifluoromethanesulfonate (3.2 mg, 0.0123 μmol) were added successively. The resulting solution was stirred for 1 h at 0 °C before triethylamine was added to the mixture and the solution was filtered through Celite and the filtrate was washed with saturated aqueous Na<sub>2</sub>S<sub>2</sub>O<sub>3</sub> and saturated aqueous NaHCO<sub>3</sub>. The organic layer was dried over Na<sub>2</sub>SO<sub>4</sub>, filtered and concentrated to dryness. The crude residue was purified by flash chromatography (2:1 hexanes–EtOAc) to afford **2.43** (110 mg, 91%) as a colorless oil: *R*<sub>f</sub> = 0.41 (3:2 hexanes–EtOAc); [α]<sub>D</sub><sup>25</sup> –10.3 (*c* = 0.08, CHCl<sub>3</sub>); <sup>1</sup>H NMR (600 MHz, CDCl<sub>3</sub>) δ 7.37–7.23 (m, 22H, Ar), 7.26–7.19 (m, 11H, Ar), 7.20–7.12 (m, 4H, Ar), 7.12–7.07 (m, 4H, Ar), 7.07–7.00 (m, 4H, Ar), 5.30 (dd, *J* = 10.2, 7.9 Hz, 1H, H-2'''), 5.21–5.14 (m, 4H, H-3, 2 x OCH<sub>2</sub>Ar, H-4'), 5.05 (d, *J* = 3.0 Hz, 1H, H-1'), 4.96 (d, *J* = 3.5 Hz, 1H, H-1), 4.91 (d, *J* = 11.7 Hz, 1H, OCH<sub>2</sub>CCl<sub>3</sub>), 4.84–4.79 (m, 2H, OCH<sub>2</sub>Ar, H-1''), 4.73 (d, *J* = 12.4 Hz, 1H, OCH<sub>2</sub>Ar), 4.71 (d, *J* = 11.7 Hz, 1H, OCH<sub>2</sub>CCl<sub>3</sub>), 4.66 (d, *J* = 11.5 Hz,

1H, OCH<sub>2</sub>Ar), 4.65 (d, *J* = 11.5 Hz, 1H, OCH<sub>2</sub>Ar), 4.59 (d, *J* = 11.4 Hz, 1H, OCH<sub>2</sub>Ar), 4.57 (d, *J* = 11.4 Hz, 1H, OCH<sub>2</sub>Ar), 4.53–4.45 (m, 7H, 5 x OCH<sub>2</sub>Ar, 2 x NCH<sub>2</sub>Ph), 4.43 (d, *J* = 7.8 Hz, 1H, H-1''), 4.35 (d, *J* = 12.0 Hz, 1H, OCH<sub>2</sub>Ar), 4.24–4.17 (m, 1H, H-5''), 4.14–4.11 (m, 2H, 2 x OCH<sub>2</sub>Ar), 4.11–4.06 (m, 2H, H-3', H-5'), 4.05 (dd, *J* = 10.1, 3.1 Hz, 1H, H-2'), 3.91 (dd, *J* = 9.1, 3.0 Hz, 1H, H-3''), 3.85 (d, *J* = 2.8 Hz, 1H, H-4'''), 3.84 (app t, *J* = 2.4 Hz, 1H, H-2''), 3.81 (dd, *J* = 10.3, 5.2 Hz, 1H, H-5), 3.76 (d, *J* = 11.2 Hz, 1H, H-6a), 3.67 (app dt, *J* = 9.7, 6.6 Hz, 1H, octyl OCH<sub>2</sub>), 3.65–3.57 (m, 2H, H-4'', H-6a'''), 3.54–3.46 (m, 4H, H-4, H-6b'', H-6b, H-5''), 3.47–3.39 (m, 1H, octyl OCH<sub>2</sub>), 3.44 (dd, *J* = 10.0, 2.8 Hz, 1H, H-3'''), 3.27–3.21 (m, 1H, octyl NCH<sub>2</sub>), 3.21–3.14 (m, 1H, octyl NCH<sub>2</sub>), 3.03 (dd, *J* = 10.6, 3.5 Hz, 1H, H-2), 2.80 (app dt, *J* = 18.4, 7.1 Hz, 1H, COCH<sub>2</sub>CH<sub>2</sub>COCH<sub>3</sub>), 2.72 (app dt, *J* = 18.3, 6.2 Hz, 1H, COCH<sub>2</sub>CH<sub>2</sub>COCH<sub>3</sub>), 2.64 (ddd, *J* = 17.0, 7.6, 6.1 Hz, 1H, COCH<sub>2</sub>CH<sub>2</sub>COCH<sub>3</sub>), 2.72 (app dt, *J* = 17.0, 6.5 Hz, 1H, COCH<sub>2</sub>CH<sub>2</sub>COCH<sub>3</sub>), 2.17 (s, 3H, COCH<sub>3</sub>), 1.99 (s, 3H, COCH<sub>3</sub>), 1.55–1.47 (m, 2H, OCH<sub>2</sub>CH<sub>2</sub>), 1.47–1.32 (m, 2H, NCH<sub>2</sub>CH<sub>2</sub>), 1.31 (d, *J* = 6.5 Hz, 3H, H-6'), 1.35–1.16 (m, 8H, 4 x CH<sub>2</sub>), 1.08 (d, *J* = 6.5 Hz, 3H, H-6'); <sup>13</sup>C NMR (151 MHz, CDCl<sub>3</sub>) δ 206.4 (C=O), 172.0 (C=O), 169.5 (C=O), 156.8 (C=O), 153.8 (C=O), 139.2 (Ar), 139.0 (Ar), 138.8 (Ar), 138.6 (Ar), 138.1 (Ar), 138.1 (Ar), 128.7 (Ar), 128.5 (Ar), 128.5 (Ar), 128.5 (Ar), 128.4 (Ar), 128.2 (Ar), 128.1 (Ar), 128.0 (Ar), 128.0 (Ar), 127.8 (Ar), 127.8 (Ar), 127.5 (Ar), 127.5 (Ar), 127.5 (Ar), 127.4 (Ar), 127.3 (Ar), 99.6 (C-1'''), 98.0 (C-1), 97.5 (C-1'), 97.1 (C-1'', <sup>1</sup>*J*<sub>C-H</sub> = 169.3 Hz), 94.6 (OCH<sub>2</sub>CCL<sub>3</sub>), 81.3 (C-3'''), 80.9 (C-4''), 80.1 (C-3''), 77.2 (C-3), 77.1 (OCH<sub>2</sub>CCL<sub>3</sub>), 75.6 (C-2''), 75.4 (C-4), 74.7 (OCH<sub>2</sub>Ar), 73.8 (OCH<sub>2</sub>Ar), 73.6 (C-5'''), 73.2 (OCH<sub>2</sub>Ar), 72.9 (OCH<sub>2</sub>Ar), 72.8 (OCH<sub>2</sub>Ar), 72.6 (C-3'), 72.2 (OCH<sub>2</sub>Ar), 71.5 (C-2'''), 71.0 (C-4'), 71.0 (C-4'''), 70.6 (C-5), 70.5 (C-2'), 69.0 (C-6), 68.9 (octyl OCH<sub>2</sub>), 68.7 (C-5''), 68.5 (C-6'''), 67.3 (OCH<sub>2</sub>Ph), 66.8 (C-5'), 61.1 (C-2), 50.4 (NC<sub>a</sub>H<sub>2</sub>Ph), 50.2 (NC<sub>b</sub>H<sub>2</sub>Ph), 47.2 (octyl NC<sub>a</sub>H<sub>2</sub>), 46.5 (octyl NC<sub>b</sub>H<sub>2</sub>), 38.2 (COCH<sub>2</sub>CH<sub>2</sub>COCH<sub>3</sub>), 30.0 (COCH<sub>3</sub>),

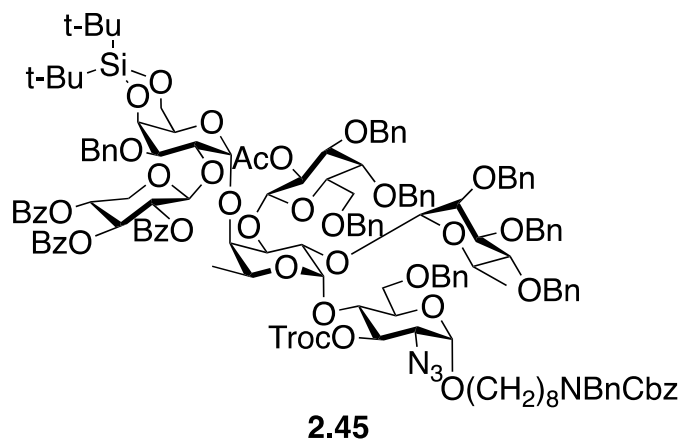
29.9 (2 x CH<sub>2</sub>), 29.4 (OCH<sub>2</sub>CH<sub>2</sub>), 28.2 (COCH<sub>2</sub>CH<sub>2</sub>COCH<sub>3</sub>), 27.9 (NCH<sub>2</sub>CH<sub>2</sub>), 26.9 (CH<sub>2</sub>), 26.1 (CH<sub>2</sub>), 21.3 (COCH<sub>3</sub>), 18.2 (C-6''), 15.9 (C-6'); HRMS (MALDI-TOF) *m/z*: [M + Na]<sup>+</sup> Calcd for C<sub>106</sub>H<sub>121</sub>Cl<sub>3</sub>N<sub>4</sub>NaO<sub>25</sub> 1977.7281; Found 1977.7294.



***N*-benzyl-*N*-benzoxycarbonyl-8-aminooctyl 2-*O*-acetyl-3,4,6-tri-*O*-benzyl- $\beta$ -D-galactopyranosyl-(1 $\rightarrow$ 3)-[2,3,4-tri-*O*-benzyl- $\alpha$ -L-rhamnopyranosyl-(1 $\rightarrow$ 2)]- $\alpha$ -L-fucopyranosyl-(1 $\rightarrow$ 4)-2-azido-6-*O*-benzyl-2-deoxy-3-*O*-(2,2,2-trichloroethoxycarbonyl)- $\alpha$ -D-glucopyranoside (2.44)**

To a stirred solution of **2.43** (210 mg, 0.107 mmol) in pyridine–AcOH (25 mL, 3:2) was added hydrazine monohydrate (10.4  $\mu$ L, 0.215 mmol). After stirring for 3 h, the reaction mixture was diluted with CH<sub>2</sub>Cl<sub>2</sub> (100 mL) and washed with 1N HCl, saturated aqueous NaHCO<sub>3</sub>, and brine. The combined organic layers were dried over Na<sub>2</sub>SO<sub>4</sub>, filtered and concentrated to dryness. The crude residue was purified by flash chromatography (2:1 hexanes–EtOAc) to afford **2.44** (162 mg, 81%) as a white solid: *R<sub>f</sub>* = 0.24 (2:1 hexanes–EtOAc); [ $\alpha$ ]<sub>D</sub><sup>25</sup> +40.8 (*c* = 0.8, CH<sub>2</sub>Cl<sub>2</sub>); <sup>1</sup>H NMR (600 MHz, CDCl<sub>3</sub>)  $\delta$  7.38–7.26 (m, 22H, Ar), 7.25–7.22 (m, 6H, Ar), 7.22–7.14 (m, 15H, Ar), 7.14–7.11 (m, 2H, Ar), 5.39 (dd, *J* = 10.0, 8.0 Hz, 1H, H-2'''), 5.19 (dd, *J* = 10.5, 9.0 Hz, 1H, H-3), 5.21–5.17 (m, 2H, 2 x OCH<sub>2</sub>Ar), 4.98 (d, *J* = 3.9 Hz, 1H, H-1), 4.96 (d, *J* = 12.0 Hz, 1H, OCH<sub>2</sub>CCl<sub>3</sub>), 4.79 (d, *J* = 11.3 Hz, 1H, OCH<sub>2</sub>Ar), 4.79 (d, *J* = 2.5 Hz, 1H, H-1'), 4.74 (d, *J* = 12.1

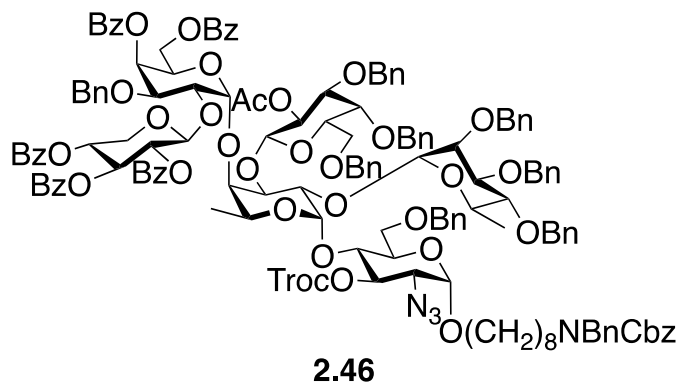
Hz, 1H, OCH<sub>2</sub>Ar), 4.73 (d, *J* = 12.1 Hz, 1H, OCH<sub>2</sub>Ar), 4.70 (d, *J* = 1.6 Hz, 1H, H-1''), 4.66 (d, *J* = 11.8 Hz, 1H, OCH<sub>2</sub>CCl<sub>3</sub>), 4.60 (d, *J* = 11.0 Hz, 1H, OCH<sub>2</sub>Ar), 4.60–4.59 (m, 2H, 2 x OCH<sub>2</sub>Ar), 4.54 (d, *J* = 12.4 Hz, 1H, OCH<sub>2</sub>Ar), 4.50 (d, *J* = 11.7 Hz, 1H, OCH<sub>2</sub>Ar), 4.49 (d, *J* = 8.0 Hz, 1H, H-1'''), 4.49–4.45 (m, 2H, 2 x NCH<sub>2</sub>Ph), 4.19–4.08 (m, 3H, 2 x OCH<sub>2</sub>Ar, H-5''), 3.99–3.89 (m, 4H, H-5', H-3', H-2', H-4'''), 3.85 (dd, *J* = 10.1, 4.7 Hz, H-5), 3.82–3.77 (m, 3H, H-6a, H-2'', H-3''), 3.76 (app t, 1H, *J* = 2.4 Hz, H-4'), 3.70 (app dt, *J* = 9.9, 6.7 Hz, 1H, octyl OCH<sub>2</sub>), 3.63–3.56 (m, 2H, H-6a''', H-4''), 3.55–3.49 (m, 3H, H-6b, H-6b''', H-5'''), 3.47 (dd, *J* = 10.0, 2.7 Hz, H-3'''), 3.47–3.42 (m, 2H, H-4, octyl OCH<sub>2</sub>), 3.27–3.21 (m, 1H, octyl NCH<sub>2</sub>), 3.21–3.14 (m, 1H, octyl NCH<sub>2</sub>), 3.02 (dd, *J* = 10.6, 3.4 Hz, 1H, H-2), 1.99 (s, 3H, COCH<sub>3</sub>), 1.58–1.50 (m, 2H, OCH<sub>2</sub>CH<sub>2</sub>), 1.50–1.41 (m, 2H, NCH<sub>2</sub>CH<sub>2</sub>), 1.38–1.19 (m, 8H, 4 x CH<sub>2</sub>), 1.26 (d, *J* = 6.5 Hz, 3H, H-6''), 1.20 (d, *J* = 6.5 Hz, 3H, H-6'); <sup>13</sup>C NMR (151 MHz, CDCl<sub>3</sub>) δ 169.8 (C=O), 156.8 (C=O), 153.8 (C=O), 139.2 (Ar), 138.9 (Ar), 138.6 (Ar), 138.5 (Ar), 138.1 (Ar), 138.0 (Ar), 128.7 (Ar), 128.6 (Ar), 128.6 (Ar), 128.5 (Ar), 128.5 (Ar), 128.5 (Ar), 128.3 (Ar), 128.3 (Ar), 128.1 (Ar), 128.1 (Ar), 128.0 (Ar), 128.0 (Ar), 128.0 (Ar), 127.9 (Ar), 127.8 (Ar), 127.6 (Ar), 127.5 (Ar), 127.5 (Ar), 127.4 (Ar), 127.4 (Ar), 99.9 (C-1'''), 98.0 (C-1), 97.8 (C-1'), 97.8 (C-1''), 94.6 (OCH<sub>2</sub>CCl<sub>3</sub>), 80.8 (C-4''), 80.5 (C-3'''), 80.5 (C-3''), 77.2 (C-3), 76.8 (OCH<sub>2</sub>CCl<sub>3</sub>), 75.7 (C-4), 75.3 (C-3'), 75.0 (C-2''), 74.3 (OCH<sub>2</sub>Ar), 73.9 (OCH<sub>2</sub>Ar), 73.8 (C-5'''), 73.4 (OCH<sub>2</sub>Ar), 73.1 (OCH<sub>2</sub>Ar), 72.5 (OCH<sub>2</sub>Ar), 71.9 (OCH<sub>2</sub>Ar), 71.9 (OCH<sub>2</sub>Ar), 71.9 (C-2'), 71.6 (C-4'), 71.1 (C-2'''), 70.5 (C-5), 69.7 (C-4'''), 69.5 (C-6), 68.9 (octyl OCH<sub>2</sub>), 68.5 (C-5''), 68.4 (C-6'''), 67.3 (OCH<sub>2</sub>Ph), 66.8 (C-5'), 61.1 (C-2), 50.6 (NC<sub>a</sub>H<sub>2</sub>Ph), 50.3 (NC<sub>b</sub>H<sub>2</sub>Ph), 47.4 (octyl NC<sub>a</sub>H<sub>2</sub>), 46.3 (octyl NC<sub>b</sub>H<sub>2</sub>), 29.9 (2 x CH<sub>2</sub>), 29.4 (OCH<sub>2</sub>CH<sub>2</sub>), 28.2 (NCH<sub>2</sub>CH<sub>2</sub>), 26.9 (CH<sub>2</sub>), 26.1 (CH<sub>2</sub>), 21.1 (COCH<sub>3</sub>), 18.0 (C-6''), 14.3 (C-6'); HRMS (MALDI-TOF) *m/z*: [M + Na]<sup>+</sup> Calcd for C<sub>101</sub>H<sub>115</sub>Cl<sub>3</sub>N<sub>4</sub>NaO<sub>23</sub> 1879.6914; Found 1879.6904.



***N*-benzyl-*N*-benzoxycarbonyl-8-aminooctyl 2-*O*-acetyl-3,4,6-tri-*O*-benzyl- $\beta$ -D-galactopyranosyl-(1 $\rightarrow$ 3)-[2,3,4-tri-*O*-benzyl- $\alpha$ -L-rhamnopyranosyl-(1 $\rightarrow$ 2)]-[[2,3,4-tri-*O*-benzoyl- $\beta$ -D-xylopyranosyl-(1 $\rightarrow$ 2)]-3-*O*-benzyl-4,6-*O*-di-*tert*-butylsilylene- $\alpha$ -D-galactopyranosyl-(1 $\rightarrow$ 4)]- $\alpha$ -L-fucopyranosyl-(1 $\rightarrow$ 4)-2-azido-6-*O*-benzyl-2-deoxy-3-*O*-(2,2,2-trichloroethoxycarbonyl)- $\alpha$ -D-glucopyranoside (**2.45**)**

To a stirred solution of acceptor **2.44** (50 mg, 0.0269 mmol) and donor **2.7** (103 mg, 0.108 mmol) in CH<sub>2</sub>Cl<sub>2</sub> (3 mL) was added 4Å molecular sieves powder (300 mg). After stirring for 30 min, di-*tert*-butylmethylpyridine (11.0 mg, 0.0538 mmol) and methyl trifluoromethanesulfonate (18.2  $\mu$ L, 0.161 mmol) were added. The resulting solution was stirred for 24 h before triethylamine was added to the mixture and the solution was filtered through Celite and the filtrate was concentrated to dryness. The crude residue was purified by flash chromatography (3:1 hexanes–EtOAc) to afford **2.45** (54 mg, 76%) as a colorless oil:  $R_f$  = 0.32 (2:1 hexanes–EtOAc);  $[\alpha]_D^{25}$  +25.6 ( $c$  = 0.16, CHCl<sub>3</sub>); <sup>1</sup>H NMR (500 MHz, CDCl<sub>3</sub>)  $\delta$  7.95–7.87 (m, 3H), 7.88–7.80 (m, 2H), 7.79–7.72 (m, 1H), 7.54–7.49 (m, 1H), 7.46–7.26 (m, 26H), 7.26–7.00 (m, 31H), 7.00–6.92 (m, 1H), 5.81 (app t,  $J$  = 9.7 Hz, 1H), 5.71–5.61 (m, 1H), 5.54–5.37 (m, 2H), 5.29–5.02 (m, 5H), 5.01–4.86 (m, 4H), 4.83 (d,  $J$  = 11.0 Hz, 1H), 4.81–4.72 (m, 4H), 4.72–4.62 (m, 4H), 4.62–4.52 (m, 4H), 4.52–4.40 (m, 4H), 4.39–4.27 (m, 4H), 4.27–4.06 (m, 8H), 4.05–3.94 (m, 3H), 3.91–3.81 (m, 4H), 3.81–3.67 (m,

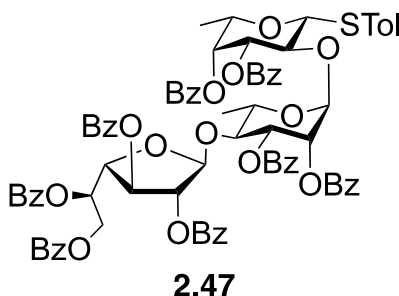
3H), 3.67–3.51 (m, 5H), 3.51–3.27 (m, 4H), 3.27–3.20 (m, 1H), 3.20–3.10 (m, 1H), 1.78 (br s, 3H), 1.46–1.35 (m, 4H), 1.35–1.19 (m, 8H), 1.10 (d,  $J = 6.5$  Hz, 3H), 1.10 (s, 9H), 1.01 (d,  $J = 6.2$  Hz, 3H), 1.00 (s, 9H); HRMS (MALDI–TOF)  $m/z$ :  $[M + Na]^+$  Calcd for  $C_{148}H_{167}Cl_3N_4NaO_{35}Si$  2716.0142; Found 2716.0103.



***N*-benzyl-*N*-benzoxycarbonyl-8-aminooctyl 2-*O*-acetyl-3,4,6-tri-*O*-benzyl- $\beta$ -D-galactopyranosyl-(1 $\rightarrow$ 3)-[2,3,4-tri-*O*-benzyl- $\alpha$ -L-rhamnopyranosyl-(1 $\rightarrow$ 2)]-[2,3,4-tri-*O*-benzoyl- $\beta$ -D-xylopyranosyl-(1 $\rightarrow$ 2)]-3-*O*-benzyl-4,6-di-*O*-benzoyl- $\alpha$ -D-galactopyranosyl-(1 $\rightarrow$ 4)]- $\alpha$ -L-fucopyranosyl-(1 $\rightarrow$ 4)-2-azido-6-*O*-benzyl-2-deoxy-3-*O*-(2,2,2-trichloroethoxycarbonyl)- $\alpha$ -D-glucopyranoside (2.46)**

To a stirred solution of **2.45** (50.0 mg, 0.0185 mmol) in THF–pyridine (2 mL, 1:1) was added HF–pyridine (0.05 mL, pyridine ~30%, hydrogen fluoride ~70%) at 0 °C. The reaction mixture was stirred for 1.5 h at 0 °C and then poured into saturated aqueous NaHCO<sub>3</sub>. The aqueous layer was extracted with EtOAc (50 mL  $\times$  2), dried over Na<sub>2</sub>SO<sub>4</sub>, filtered and concentrated to dryness. The resulting crude product was then dissolved in pyridine (10 mL) and then benzoyl chloride (0.20 mL, 1.72  $\mu$ mol) was added dropwise at 0 °C. After stirring overnight, while warming to room temperature, ice water was added, and the solution was extracted with CH<sub>2</sub>Cl<sub>2</sub> (50 mL  $\times$  2). The combined organic layer was then washed successively with 1N HCl, saturated aqueous NaHCO<sub>3</sub>,

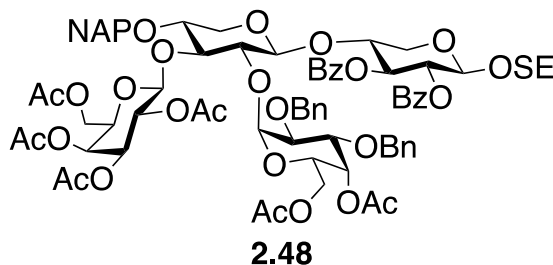
water and brine. The organic layer was dried over Na<sub>2</sub>SO<sub>4</sub>, filtered, concentrated and the resulting syrup was purified by flash chromatography (2:1 hexane–EtOAc) to afford **2.46** (42.0 mg, 82% over two steps) as a white solid:  $R_f = 0.21$  (2:1 hexanes–EtOAc);  $[\alpha]_D^{25} +47.3$  ( $c = 0.03$ , CHCl<sub>3</sub>); <sup>1</sup>H NMR (500 MHz, CDCl<sub>3</sub>)  $\delta$  8.14–7.82 (m, 9H), 7.81–7.63 (m, 2H), 7.62–7.57 (m, 1H), 7.56–7.26 (m, 29H), 7.26–6.82 (m, 34H), 6.05–5.93 (m, 1H), 5.86–5.76 (m, 2H), 5.74–5.66 (m, 1H), 5.66–5.56 (m, 1H), 5.51 (app t,  $J = 9.1$  Hz, 1H), 5.46–5.09 (m, 5H), 5.10–4.89 (m, 1H), 5.06 (s, 1H), 4.97 (d,  $J = 3.5$  Hz, 1H), 4.85 (d,  $J = 11.1$  Hz, 1H), 4.88–4.70 (m, 4H), 4.71–4.45 (m, 12H), 4.45–4.26 (m, 6H), 4.26–4.17 (m, 2H), 4.22 (d,  $J = 11.3$  Hz, 1H), 4.17–3.69 (m, 13H), 3.66 (app dt,  $J = 9.9, 6.8$  Hz, 1H), 3.69–3.61 (m, 1H), 3.61–3.48 (m, 2H), 3.48–3.30 (m, 3H), 3.30–3.23 (m, 1H), 3.24–3.09 (m, 2H), 3.08–2.83 (m, 1H), 1.95–1.67 (m, 3H), 1.59–1.47 (m, 4H), 1.34–1.10 (m, 14H); <sup>13</sup>C NMR (151 MHz, CDCl<sub>3</sub>)  $\delta$  170.5, 169.5, 166.1, 165.9, 165.6, 165.3, 165.3, 156.9, 156.3, 153.8, 138.6, 138.2, 138.1, 137.6, 137.0, 136.9, 136.5, 134.7, 133.7, 133.4, 133.3, 133.2, 130.7, 130.3, 130.0, 129.8, 129.8, 129.6, 129.5, 129.0, 128.6, 128.6, 128.5, 128.5, 128.4, 128.4, 128.3, 128.1, 128.0, 127.9, 127.9, 127.8, 127.7, 127.5, 127.4, 127.3, 126.9, 125.2, 101.4, 97.9, 94.5, 92.3, 85.2, 81.6, 80.3, 77.4, 77.2, 76.9, 75.2, 74.3, 73.6, 72.2, 72.0, 71.7, 70.8, 70.4, 68.8, 68.1, 67.3, 63.3, 61.0, 50.6, 50.2, 47.3, 46.4, 36.8, 33.2, 32.1, 29.8, 29.5, 29.4, 29.3, 28.5, 28.2, 27.8, 26.8, 26.0, 24.8, 24.7, 24.0, 23.5, 22.8, 21.1, 20.7, 18.6, 17.9; HRMS (MALDI–TOF)  $m/z$ :  $[M + Na]^+$  Calcd for C<sub>154</sub>H<sub>159</sub>Cl<sub>3</sub>N<sub>4</sub>NaO<sub>37</sub> 2783.9644; Found 2783.9641.



***p*-Tolyl 2,3,5,6-tetra-*O*-benzoyl- $\beta$ -D-galactofuranosyl-(1 $\rightarrow$ 4)-2,3-di-*O*-benzoyl- $\alpha$ -L-rhamnopyranosyl-(1 $\rightarrow$ 2)-3,4-di-*O*-benzoyl-1-thio- $\beta$ -L-fucopyranoside (2.47)**

To a stirred solution of acceptor **2.60** (666 mg, 0.800 mmol) and trichloroacetimidate donor **2.51**<sup>38</sup> (884 mg, 1.19 mmol) in dry CH<sub>2</sub>Cl<sub>2</sub> (25 mL) was added 4Å molecular sieves powder (1.5 g). After stirring for 30 min, the reaction mixture was cooled to 0 °C and then trimethylsilyl trifluoromethanesulfonate (22.0  $\mu$ L, 0.119 mmol) was added. The resulting solution was stirred for 1 h at 0 °C before triethylamine was added to the mixture and the solution was filtered through Celite and the filtrate was concentrated to dryness. The crude residue was purified by flash chromatography (3:1 hexanes–EtOAc) to afford **2.47** (853 mg, 75%) as a white solid:  $R_f$  = 0.28 (2:1 hexanes–EtOAc);  $[\alpha]_D^{25}$  +1.8 ( $c$  = 0.11, CHCl<sub>3</sub>); <sup>1</sup>H NMR (700 MHz, CDCl<sub>3</sub>)  $\delta$  8.05–8.00 (m, 4H, Ar), 8.00–7.94 (m, 4H, Ar), 7.92–7.88 (m, 2H, Ar), 7.86–7.80 (m, 2H, Ar), 7.74–7.68 (m, 2H, Ar), 7.67–7.61 (m, 4H, Ar), 7.61–7.57 (m, 1H, Ar), 7.56–7.51 (m, 2H, Ar), 7.51–7.42 (m, 6H, Ar), 7.42–7.36 (m, 2H, Ar), 7.36–7.30 (m, 4H, Ar), 7.25–7.18 (m, 3H, Ar), 7.14–7.05 (m, 8H, Ar), 5.98–5.95 (m, 2H, H-5'', H-2'), 5.75 (dd,  $J$  = 9.7, 3.3 Hz, 1H, H-3'), 5.65 (dd,  $J$  = 3.4, 0.9 Hz, 1H, H-4), 5.53 (dd,  $J$  = 9.4, 3.5 Hz, 1H, H-3), 5.51 (dd,  $J$  = 5.4, 1.6 Hz, 1H, H-3''), 5.44 (s, 1H, H-1''), 5.30 (d,  $J$  = 1.7 Hz, 1H, H-2'), 5.10 (d,  $J$  = 2.0 Hz, 1H, H-1'), 4.79 (d,  $J$  = 9.6 Hz, 1H, H-1), 4.63 (dd,  $J$  = 11.8, 2.9 Hz, 1H, H-6a''), 4.60 (dd,  $J$  = 10.2, 5.2 Hz, 1H, H-6b''), 4.43 (dd,  $J$  = 5.5, 3.8 Hz, 1H, H-4''), 4.10 (app t,  $J$  = 9.4 Hz, 1H, H-2), 4.06 (qd,  $J$  = 6.9, 1.1 Hz, 1H, H-5), 3.90 (app t,  $J$  = 9.7 Hz, 1H, H-4'), 3.77 (dq,  $J$  = 9.4, 6.0 Hz, 1H, H-5'), 2.36 (s, 3H, ArCH<sub>3</sub>), 1.36 (d,  $J$  = 6.4

Hz, 3H, H-6), 0.69 (d,  $J = 6.2$  Hz, 3H, H-6');  $^{13}\text{C}$  NMR (126 MHz,  $\text{CDCl}_3$ )  $\delta$  166.0 (C=O), 165.8 (C=O), 165.6 (C=O), 165.5 (2 x C=O), 165.1 (C=O), 165.1 (C=O), 164.6 (C=O), 138.1 (Ar), 133.6 (Ar), 133.4 (3 x Ar), 133.3 (Ar), 133.2 (Ar), 133.1 (Ar), 133.1 (Ar), 132.9 (Ar), 132.6 (Ar), 132.3 (Ar), 130.0 (2 x Ar), 129.9 (3 x Ar), 129.8 (4 x Ar), 129.7 (2 x Ar), 129.6 (3 x Ar), 129.5 (4 x Ar), 129.4 (3 x Ar), 129.3 (Ar), 128.8 (Ar), 128.6 (3 x Ar), 128.5 (5 x Ar), 128.3 (5 x Ar), 128.3 (2 x Ar), 128.2 (2 x Ar), 128.1 (2 x Ar), 127.9 (2 x Ar), 107.2 (C-1''), 100.1 (C-1'), 87.6 (C-1), 82.1 (C-2'), 82.0 (C-4''), 77.2 (C-3''), 76.8 (C-4'), 76.5 (C-2), 73.7 (C-3), 73.4 (C-5), 72.0 (C-3'), 71.4 (C-4), 70.9 (C-2'), 70.3 (C-5''), 67.7 (C-5'), 63.4 (C-6''), 21.3 (ArCH<sub>3</sub>), 17.5 (C-6'), 16.7 (C-6); HRMS (ESI-TOF)  $m/z$ :  $[\text{M} + \text{Na}]^+$  Calcd for  $\text{C}_{81}\text{H}_{70}\text{NaO}_{21}\text{S}$  1433.4023; Found 1433.4026.



**2-Trimethylsilylethyl 2,3,4,6-tetra-*O*-acetyl- $\beta$ -D-galactopyranosyl-(1 $\rightarrow$ 3)-[4,6-di-*O*-acetyl-2,3-di-*O*-benzyl- $\alpha$ -D-galactopyranosyl-(1 $\rightarrow$ 2)]-4-*O*-(2-naphthyl)methyl- $\beta$ -D-xylopyranosyl-(1 $\rightarrow$ 4)-2,3-di-*O*-benzoyl- $\beta$ -D-xylopyranoside (2.48)**

To a stirred solution of **2.72** (78 mg, 0.051 mmol) in THF-pyridine (2.0 mL, 1:1) was added HF-pyridine (0.10 mL, pyridine ~30%, hydrogen fluoride ~70%) at 0 °C. The reaction mixture was stirred for 1.5 h at 0 °C, and then poured into saturated aqueous  $\text{NaHCO}_3$ . The aqueous layer was extracted with EtOAc (20 mL  $\times$  2), dried over  $\text{Na}_2\text{SO}_4$ , filtered and concentrated to dryness. The crude residue was dissolved in pyridine (1.0 mL) followed by the addition of acetic anhydride (19  $\mu\text{mol}$ , 0.20 mmol) and catalytic 4-(dimethylamino)pyridine. The reaction mixture was stirred

overnight before the addition of CH<sub>3</sub>OH (0.1 mL) followed by removal of solvent by coevaporation with toluene. The resulting residue was purified by flash chromatography (2:1 hexanes–EtOAc) to afford **2.48** (66.3 mg, 88%) as a white solid:  $R_f = 0.31$  (3:2 hexanes–EtOAc);  $[\alpha]_D^{25} +41.7$  ( $c = 0.42$ , CH<sub>2</sub>Cl<sub>2</sub>); <sup>1</sup>H NMR (700 MHz, CDCl<sub>3</sub>)  $\delta$  8.00–7.95 (m, 4H, Ar), 7.85–7.76 (m, 3H, Ar), 7.66–7.63 (m, 1H, Ar), 7.54–7.58 (m, 3H, Ar), 7.48–7.44 (m, 1H, Ar), 7.42–7.38 (m, 2H, Ar), 7.38–7.31 (m, 9H, Ar), 7.30–7.24 (m, 4H, Ar), 5.68 (d,  $J = 1.9$  Hz, 1H, H-4''), 5.48 (app t,  $J = 8.0$  Hz, 1H, H-3), 5.44 (d,  $J = 3.6$  Hz, 1H, H-1''), 5.20 (dd,  $J = 8.2, 6.4$  Hz, 1H, H-2), 5.18 (d,  $J = 3.6$  Hz, 1H, H-4'''), 5.04–5.00 (m, 2H, H-1''', H-2'''), 4.94 (d,  $J = 11.7$  Hz, 1H, OCH<sub>2</sub>Ar), 4.83 (ddd,  $J = 8.1, 3.5, 1.9$  Hz, 1H, H-3'''), 4.76 (d,  $J = 12.2$  Hz, 1H, OCH<sub>2</sub>Ar), 4.76 (d,  $J = 12.2$  Hz, 1H, OCH<sub>2</sub>Ar), 4.63 (d,  $J = 6.3$  Hz, 1H, H-1'), 4.56 (d,  $J = 6.3$  Hz, 1H, H-1), 4.57–4.51 (m, 2H, OCH<sub>2</sub>Ar), 4.50–4.47 (m, 1H, H-5''), 4.48 (d,  $J = 11.1$  Hz, 1H, OCH<sub>2</sub>Ar), 4.29 (dd,  $J = 11.4, 5.0$  Hz, 1H, H-6a''), 4.10 (dd,  $J = 11.3, 7.0$  Hz, 1H, H-6b''), 3.98 (d,  $J = 12.1, 4.7$  Hz, 1H, H-5a), 4.00–3.95 (m, 2H, H-6a''', H-6b'''), 3.94–3.90 (m, 4H, H-4, H-3', OCH<sub>2</sub>CH<sub>2</sub>Si, H-3''), 3.88 (dd,  $J = 10.2, 3.6$  Hz, 1H, H-2''), 3.67 (dd,  $J = 9.2, 6.2$  Hz, 1H, H-2'), 3.64–3.61 (m, 2H, H-4', H-5a'), 3.55 (app td,  $J = 10.1, 6.3$  Hz, 1H, OCH<sub>2</sub>CH<sub>2</sub>Si), 3.41 (app td,  $J = 6.7, 1.2$  Hz, 1H, H-5'''), 3.33 (dd,  $J = 12.2, 8.3$  Hz, 1H, H-5b), 3.16 (dd,  $J = 13.9, 6.9$  Hz, 1H, H-5b'), 2.12 (s, 3H, COCH<sub>3</sub>), 2.12 (s, 3H, COCH<sub>3</sub>), 2.09 (s, 3H, COCH<sub>3</sub>), 1.98 (s, 3H, COCH<sub>3</sub>), 1.96 (s, 3H, COCH<sub>3</sub>), 1.90 (s, 3H, COCH<sub>3</sub>), 0.94 (ddd,  $J = 14.0, 10.7, 6.3$  Hz, 1H, OCH<sub>2</sub>CH<sub>2</sub>Si), 0.87 (ddd,  $J = 14.0, 10.4, 5.7$  Hz, 1H, OCH<sub>2</sub>CH<sub>2</sub>Si), –0.04 (s, 9H, 3 x Si(CH<sub>3</sub>)<sub>3</sub>); <sup>13</sup>C NMR (176 MHz, CDCl<sub>3</sub>)  $\delta$  170.7 (C=O), 170.5 (C=O), 170.4 (C=O), 170.2 (C=O), 170.2 (C=O), 169.5 (C=O), 165.5 (C=O), 165.3 (C=O), 138.6 (Ar), 138.3 (Ar), 135.2 (Ar), 133.3 (Ar), 133.1 (3 x Ar), 130.0 (2 x Ar), 129.9 (2 x Ar), 129.8 (Ar), 128.6 (Ar), 128.5 (3 x Ar), 128.4 (3 x Ar), 128.4 (2 x Ar), 128.4 (2 x Ar), 128.1 (3 x Ar), 128.0 (3 x Ar), 127.9 (Ar), 127.9 (Ar), 127.8 (Ar), 127.6 (Ar), 126.6 (Ar), 126.3 (Ar), 126.0 (Ar),

125.2 (Ar), 102.3 (C-1'), 100.1 (C-1), 99.6 (C-1'''), 97.5 (C-1''), 79.5 (C-3'), 78.1 (C-4'), 76.7 (C-3''), 75.3 (C-2'), 74.9 (C-2''), 74.2 (OCH<sub>2</sub>Ar), 74.0 (C-4), 72.3 (C-3), 71.5 (OCH<sub>2</sub>Ar), 71.4 (OCH<sub>2</sub>Ar), 71.4 (C-3'''), 71.2 (C-2), 70.5 (C-5'''), 70.0 (C-2'''), 68.1 (C-4''), 67.0 (OCH<sub>2</sub>CH<sub>2</sub>Si), 67.0 (C-5''), 66.8 (C-4'''), 62.9 (C-6''), 62.3 (C-5), 61.9 (C-5'), 61.1 (C-6'''), 21.1 (2 x COCH<sub>3</sub>), 20.9 (COCH<sub>3</sub>), 20.7 (COCH<sub>3</sub>), 20.7 (COCH<sub>3</sub>), 20.6 (COCH<sub>3</sub>), 18.1 (OCH<sub>2</sub>CH<sub>2</sub>Si), -1.3 (3 x Si(CH<sub>3</sub>)<sub>3</sub>); HRMS (ESI-TOF) *m/z*: [M + Na]<sup>+</sup> calcd for C<sub>78</sub>H<sub>90</sub>NaO<sub>27</sub>Si 1509.5331; Found 1509.5327.



**2.52**

### 2-Trimethylsilylethyl 2,3-di-*O*-benzoyl- $\beta$ -D-xylopyranoside (2.52)

To a solution of compound **2.65** (1.09 g, 2.38 mmol) in AcOH-THF (20 mL, 1:1) was added freshly activated zinc dust (1.00 g). After stirring for 2 h, the mixture was filtered through Celite. The filtrate was concentrated, dissolved in CH<sub>2</sub>Cl<sub>2</sub> (100 mL) and washed with water, saturated aqueous NaHCO<sub>3</sub> and brine. The organic layer was dried over Na<sub>2</sub>SO<sub>4</sub>, filtered and concentrated to dryness. The crude residue was purified by flash chromatography (3:1 hexanes-EtOAc) to afford **2.52** (750 mg, 95%) as a colorless oil: *R<sub>f</sub>* = 0.22 (3:1 hexanes-EtOAc); [ $\alpha$ ]<sub>D</sub><sup>25</sup> +47.8 (*c* = 1.13, CH<sub>2</sub>Cl<sub>2</sub>); <sup>1</sup>H NMR (400 MHz, CDCl<sub>3</sub>)  $\delta$  8.02–7.96 (m, 4H, Ar), 7.56–7.49 (m, 2H, Ar), 7.43–7.35 (m, 4H, Ar), 5.35 (dd, *J* = 8.4, 6.4 Hz, 1H, H-2), 5.27 (dd, *J* = 8.4, 7.6 Hz, 1H, H-3), 4.71 (d, *J* = 6.4 Hz, 1H, H-1), 4.22 (dd, *J* = 12.0, 4.8 Hz, 1H, H-5a), 4.05–3.97 (m, 1H, H-4), 3.97 (ddd, *J* = 10.8, 9.6, 6.0 Hz, 1H, OCH<sub>2</sub>CH<sub>2</sub>Si), 3.59 (ddd, *J* = 10.4, 9.6, 6.4 Hz, 1H, OCH<sub>2</sub>CH<sub>2</sub>Si), 3.52 (dd, *J* = 12.0, 8.4 Hz, 1H, H-5b), 3.09 (d, *J* = 5.6 Hz, 1H, 4-OH), 0.95 (ddd, *J* = 14.0, 10.4, 6.4 Hz, 1H, OCH<sub>2</sub>CH<sub>2</sub>Si), 0.87 (ddd, *J* = 14.0, 10.4, 6.0 Hz, 1H, OCH<sub>2</sub>CH<sub>2</sub>Si), -0.05 (s, 9H, 3 x Si(CH<sub>3</sub>)<sub>3</sub>);

$^{13}\text{C}$  NMR (126 MHz,  $\text{CDCl}_3$ )  $\delta$  167.5 (C=O), 165.3 (C=O), 133.7 (Ar), 133.4 (Ar), 130.2 (2 x Ar), 129.9 (2 x Ar), 129.7 (Ar), 129.1 (Ar), 128.6 (2 x Ar), 128.5 (2 x Ar), 100.4 (C-1), 76.5 (C-3), 70.9 (C-2), 69.1 (C-4), 67.3 ( $\text{OCH}_2\text{CH}_2\text{Si}$ ), 64.9 (C-5), 18.2 ( $\text{OCH}_2\text{CH}_2\text{Si}$ ),  $-1.3$  (3 x  $\text{Si}(\text{CH}_3)_3$ ); HRMS (ESI-TOF)  $m/z$ :  $[\text{M} + \text{Na}]^+$  Calcd for  $\text{C}_{24}\text{H}_{30}\text{NaO}_7\text{Si}$  481.1653; found 481.1653.

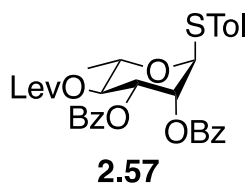


**2.53**

***p*-Tolyl 2-*O*-levulinoyl-4-*O*-(2-naphthyl)methyl-3-*O*-(2,2,2-trichloroethoxycarbonyl)-1-thio- $\beta$ -D-xylopyranoside (2.53)**

To a stirred solution of **2.67** (1.04 g, 1.81 mmol) in dry  $\text{CH}_2\text{Cl}_2$  (20 mL) was added EDC·HCl (696 mg, 3.63 mmol), 4-(dimethylamino)pyridine (443 mg, 3.63 mmol) and levulinic acid (315 mg, 2.72 mmol). The reaction mixture was stirred overnight before it was diluted with  $\text{CH}_2\text{Cl}_2$  (100 mL). The mixture was then washed successively with saturated aqueous  $\text{NaHCO}_3$ , water and brine. The organic layer was dried over  $\text{Na}_2\text{SO}_4$ , filtered and concentrated to dryness. The crude residue was purified by flash chromatography (3:1 hexanes–EtOAc) to afford **2.53** (1.09 g, 90%) as a colorless oil:  $R_f = 0.27$  (3:1 hexanes–EtOAc);  $[\alpha]_{\text{D}}^{25} -22.1$  ( $c = 0.57$ ,  $\text{CH}_2\text{Cl}_2$ );  $^1\text{H}$  NMR (400 MHz,  $\text{CDCl}_3$ )  $\delta$  7.84–7.79 (m, 3H, Ar), 7.72–7.70 (m, 1H, Ar), 7.50–7.45 (m, 2H, Ar), 7.40–7.37 (m, 1H, Ar), 7.37–7.33 (m, 2H, Ar), 7.12–7.08 (m, 2H, Ar), 5.06 (app t,  $J = 9.1$  Hz, 1H, H-3), 4.93 (app t,  $J = 9.4$  Hz, 1H, H-2), 4.86 (d,  $J = 11.9$  Hz, 1H,  $\text{OCH}_2\text{CCl}_3$ ), 4.82–4.77 (m, 3H, 2 x  $\text{OCH}_2\text{Ar}$ ,  $\text{OCH}_2\text{CCl}_3$ ), 4.59 (d,  $J = 9.7$  Hz, 1H, H-1), 4.08 (dd,  $J = 11.6, 5.4$  Hz, 1H, H-5a), 3.74 (ddd,  $J = 10.3, 9.1, 5.4$  Hz, 1H, H-4), 3.32 (dd,  $J = 11.7, 10.3$  Hz, 1H, H-5b), 2.83 (ddd,  $J = 18.9, 8.2, 6.0$  Hz, 1H,  $\text{COCH}_2\text{CH}_2\text{COCH}_3$ ), 2.75–2.51 (m, 3H,  $\text{COCH}_2\text{CH}_2\text{COCH}_3$ ), 2.33 (s, 3H,  $\text{ArCH}_3$ ), 2.18 (s, 3H,  $\text{COCH}_3$ );  $^{13}\text{C}$  NMR (126 MHz,  $\text{CDCl}_3$ )  $\delta$  206.1 (C=O), 171.3 (C=O), 153.8 (C=O), 138.8

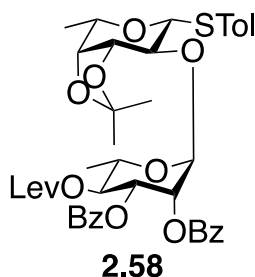
(Ar), 135.0 (Ar), 133.8 (2 x Ar), 133.3 (Ar), 133.3 (Ar), 129.9 (2 x Ar), 128.6 (Ar), 128.1 (Ar), 128.0 (Ar), 127.9 (Ar), 126.8 (Ar), 126.3 (Ar), 125.7 (Ar), 94.6 (OCH<sub>2</sub>CCl<sub>3</sub>), 86.8 (C-1), 80.7 (C-3), 77.2 (OCH<sub>2</sub>CCl<sub>3</sub>), 74.8 (C-4), 73.6 (OCH<sub>2</sub>Ar), 70.2 (C-2), 67.9 (C-5), 37.9 (COCH<sub>2</sub>CH<sub>2</sub>COCH<sub>3</sub>), 30.0 (COCH<sub>3</sub>), 28.1 (COCH<sub>2</sub>CH<sub>2</sub>COCH<sub>3</sub>), 21.3 (ArCH<sub>3</sub>); HRMS (ESI-TOF) *m/z*: [M + NH<sub>4</sub>]<sup>+</sup> Calcd for C<sub>31</sub>H<sub>35</sub>Cl<sub>3</sub>NO<sub>8</sub>S 686.1143; Found 686.1135.



***p*-Tolyl 2,3-di-*O*-benzoyl-4-*O*-levulinoyl-1-thio- $\alpha$ -L-rhamnopyranoside (2.57)**

Compound **2.56**<sup>39</sup> (1.60 g, 3.91 mmol) was stirred in 80% aqueous AcOH (40 mL) at 60 °C for 3 h. The reaction mixture was cooled to room temperature and then concentrated. The resulting crude product was then dissolved in pyridine (10 mL), before benzoyl chloride (1.82 mL, 15.6 mmol) was added dropwise at 0 °C. After stirring overnight, while warming to room temperature, ice-water was added, and the solution was extracted with CH<sub>2</sub>Cl<sub>2</sub> (50 mL x 2). The combined organic layer was then washed successively with 1N HCl, saturated aqueous NaHCO<sub>3</sub>, water and brine. The organic layer was dried over Na<sub>2</sub>SO<sub>4</sub>, filtered, then concentrated and the resulting syrup was purified with flash chromatography (3:1 hexane–EtOAc) to afford **2.57** (2.15 g, 96% over two steps) as a white solid: *R*<sub>f</sub> = 0.13 (4:1 hexanes–EtOAc); [ $\alpha$ ]<sub>D</sub><sup>25</sup> +13.5 (*c* = 0.19, CHCl<sub>3</sub>); <sup>1</sup>H NMR (500 MHz, CDCl<sub>3</sub>)  $\delta$  8.06–7.98 (m, 2H, Ar), 7.92–7.88 (m, 2H, Ar), 7.60–7.56 (m, 1H, Ar), 7.53–7.49 (m, 1H, Ar), 7.48–7.40 (m, 4H, Ar), 7.38–7.33 (m, 2H, Ar), 7.17–7.12 (m, 2H, Ar), 5.86 (dd, *J* = 3.3, 1.6 Hz, 1H, H-2), 5.65 (dd, *J* = 10.1, 3.3 Hz, 1H, H-3), 5.56 (d, *J* = 1.6 Hz, 1H, H-1), 5.48 (app t, *J* = 9.9 Hz, 1H, H-4), 4.56 (dq, *J* = 9.7, 6.2 Hz, 1H, H-5), 2.75–2.65 (m, 1H, COCH<sub>2</sub>CH<sub>2</sub>COCH<sub>3</sub>), 2.65–2.53 (m, 2H, COCH<sub>2</sub>CH<sub>2</sub>COCH<sub>3</sub>, COCH<sub>2</sub>CH<sub>2</sub>COCH<sub>3</sub>), 2.47–2.38 (m,

<sup>1</sup>H, COCH<sub>2</sub>CH<sub>2</sub>COCH<sub>3</sub>), 2.34 (s, 3H, ArCH<sub>3</sub>), 2.08 (s, 3H, COCH<sub>3</sub>), 1.36 (d, *J* = 6.2 Hz, 3H, H-6); <sup>13</sup>C NMR (101 MHz, CDCl<sub>3</sub>) δ 206.1 (C=O), 172.2 (C=O), 165.6 (C=O), 138.4 (Ar), 133.6 (Ar), 133.4 (Ar), 132.7 (2 x Ar), 130.1 (2 x Ar), 130.0 (2 x Ar), 130.0 (2 x Ar), 129.6 (Ar), 129.5 (Ar), 129.4 (Ar), 128.7 (2 x Ar), 128.6 (2 x Ar), 86.3 (C-1), 72.4 (C-2), 71.8 (C-4), 70.4 (C-3), 68.0 (C-5), 38.0 (COCH<sub>2</sub>CH<sub>2</sub>COCH<sub>3</sub>), 29.7 (COCH<sub>3</sub>), 28.1 (COCH<sub>2</sub>CH<sub>2</sub>COCH<sub>3</sub>), 21.3 (ArCH<sub>3</sub>), 17.6 (C-6); HRMS (ESI-TOF) *m/z*: [M + Na]<sup>+</sup> Calcd for C<sub>32</sub>H<sub>32</sub>O<sub>8</sub>NaS 599.1710; Found 599.1706.



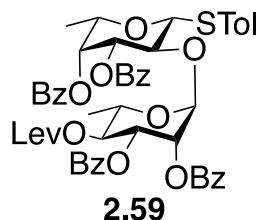
***p*-Tolyl 2,3-di-*O*-benzoyl-4-*O*-levulinoyl- $\alpha$ -L-rhamnopyranosyl-(1→2)-3,4-*O*-isopropylidene-1-thio- $\beta$ -L-fucopyranoside (2.58)**

To a stirred biphasic solution of **2.57** (2.935 g, 5.09 mmol) in EtOAc–H<sub>2</sub>O (40 mL, 3:1) was added *N*-bromosuccinimide (4.53 g, 25.4 mmol). The reaction mixture was stirred for 3 h before triethylamine was added. The mixture was diluted with EtOAc, and the organic layer was then washed successively with saturated aqueous NaHCO<sub>3</sub>, water and brine. The organic layer was dried over Na<sub>2</sub>SO<sub>4</sub>, filtered and concentrated to dryness. The crude residue was purified using a short silica column (3:1 hexanes–EtOAc) to afford the corresponding hemiacetal product (2.395 g, 67%). A portion of the product (998 mg, 2.12 mmol) was then dissolved in dry CH<sub>2</sub>Cl<sub>2</sub> (50 mL) before cesium carbonate (3.70 g, 10.6 mmol) and trichloroacetonitrile (0.640 mL, 6.36 mmol) were added. After stirring overnight, the solution was filtered through Celite and the filtrate was

concentrated to dryness. The crude product **2.50** was carried to the next step without further purification.

To a stirred solution of acceptor **2.49**<sup>37</sup> (516 mg, 1.66 mmol) and donor **2.50** in dry CH<sub>2</sub>Cl<sub>2</sub> (20 mL) was added 4Å molecular sieves powder (1 g). After stirring for 30 min, the reaction mixture was cooled to 0 °C, and then trimethylsilyl trifluoromethanesulfonate (19.0 μL, 0.106 mmol) was added. The resulting solution was stirred for 1 h at -78 °C before triethylamine was added to the mixture and the solution was filtered through Celite and the filtrate was concentrated to dryness. The crude residue was purified by flash chromatography (2:1 hexanes–EtOAc) to afford **2.58** (819 mg, 65%) as a white solid:  $R_f = 0.25$  (2:1 hexanes–EtOAc);  $[\alpha]_D^{25} +17.8$  ( $c = 0.53$ , CHCl<sub>3</sub>); <sup>1</sup>H NMR (700 MHz, CDCl<sub>3</sub>) δ 8.09–8.06 (m, 2H, Ar), 7.89–7.85 (m, 2H, Ar), 7.61–7.56 (m, 1H, Ar), 7.52–7.45 (m, 5H, Ar), 7.36–7.31 (m, 2H, Ar), 7.10–7.05 (m, 2H, Ar), 5.73 (dd,  $J = 3.4, 1.7$  Hz, 1H, H-2'), 5.66 (dd,  $J = 10.2, 3.4$  Hz, 1H, H-3'), 5.42 (app t,  $J = 10.1$  Hz, 1H, H-4'), 5.30 (d,  $J = 1.7$  Hz, 1H, H-1'), 4.47 (d,  $J = 10.2$  Hz, 1H, H-1), 4.37 (dq,  $J = 9.9, 6.2$  Hz, 1H, H-5'), 4.17 (dd,  $J = 6.9, 5.3$  Hz, 1H, H-3), 4.06 (dd,  $J = 5.2, 2.1$  Hz, 1H, H-4), 3.84 (qd,  $J = 6.5, 2.1$  Hz, 1H, H-5), 3.71 (dd,  $J = 10.0, 6.7$  Hz, 1H, H-2), 2.69–2.64 (m, 1H, COCH<sub>2</sub>CH<sub>2</sub>COCH<sub>3</sub>), 2.59–2.52 (m, 2H, COCH<sub>2</sub>CH<sub>2</sub>COCH<sub>3</sub>, COCH<sub>2</sub>CH<sub>2</sub>COCH<sub>3</sub>), 2.40–2.35 (m, 1H, COCH<sub>2</sub>CH<sub>2</sub>COCH<sub>3</sub>), 2.30 (s, 3H, ArCH<sub>3</sub>), 2.06 (s, 3H, COCH<sub>3</sub>), 1.51 (s, 3H, (O)<sub>2</sub>C(CH<sub>3</sub>)<sub>2</sub>), 1.44 (d,  $J = 6.6$  Hz, 3H, H-6), 1.38 (s, 3H, C(O)<sub>2</sub>(CH<sub>3</sub>)<sub>2</sub>), 1.31 (d,  $J = 6.2$  Hz, 3H, H-6'); <sup>13</sup>C NMR (126 MHz, CDCl<sub>3</sub>) δ 206.0 (C=O), 172.1 (C=O), 165.5 (C=O), 165.2 (C=O), 137.8 (Ar), 133.3 (Ar), 133.1 (Ar), 132.6 (2 x Ar), 129.9 (3 x Ar), 129.8 (2 x Ar), 129.7 (2 x Ar), 129.5 (Ar), 129.4 (Ar), 128.5 (2 x Ar), 128.3 (2 x Ar), 109.7 ((O)<sub>2</sub>C(CH<sub>3</sub>)<sub>2</sub>), 98.2 (C-1'), 87.8 (C-1), 78.7 (C-3), 76.7 (C-2), 76.5 (C-4), 72.4 (C-5), 71.6 (C-4'), 70.3 (C-2'), 70.1 (C-3'), 66.8 (C-5'), 37.8 (COCH<sub>2</sub>CH<sub>2</sub>COCH<sub>3</sub>), 29.6 (COCH<sub>3</sub>), 28.2

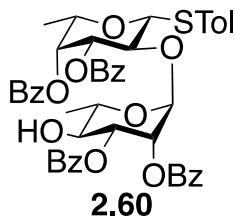
((O)<sub>2</sub>C(CH<sub>3</sub>)<sub>2</sub>), 27.9 (COCH<sub>2</sub>CH<sub>2</sub>COCH<sub>3</sub>), 26.5 ((O)<sub>2</sub>C(CH<sub>3</sub>)<sub>2</sub>), 21.1 (ArCH<sub>3</sub>), 17.3 (C-6'), 16.9 (C-6); HRMS (ESI-TOF) *m/z*: [M + Na]<sup>+</sup> Calcd for C<sub>41</sub>H<sub>46</sub>NaO<sub>12</sub>S 785.2602; Found 785.2595.



***p*-Tolyl 2,3-di-*O*-benzoyl-4-*O*-levulinoyl- $\alpha$ -L-rhamnopyranosyl-(1 $\rightarrow$ 2)-3,4-di-*O*-benzoyl-1-thio- $\beta$ -L-fucopyranoside (2.59)**

Compound **2.58** (819 mg, 1.07 mmol) was stirred in 80% aqueous AcOH (25 mL) at 60 °C for 4 h. The reaction mixture was cooled to room temperature and then concentrated. The resulting crude product was then dissolved in pyridine (5 mL) before benzoyl chloride (1.00 mL, 8.59 mmol) was added dropwise at 0 °C. After stirring overnight, while warming to room temperature, ice water was added, and the solution was extracted with CH<sub>2</sub>Cl<sub>2</sub> (50 mL x 2). The combined organic layer was then washed successively with 1N HCl, saturated aqueous NaHCO<sub>3</sub>, water and brine. The organic layer was dried over Na<sub>2</sub>SO<sub>4</sub>, filtered, concentrated and the resulting syrup was purified by flash chromatography (2:1 hexane–EtOAc) to afford **2.59** (921 mg, 92% over two steps) as a white solid: *R<sub>f</sub>* = 0.20 (2:1 hexanes–EtOAc); [ $\alpha$ ]<sub>D</sub><sup>25</sup> +14.5 (*c* = 1.08, CHCl<sub>3</sub>); <sup>1</sup>H NMR (700 MHz, CDCl<sub>3</sub>)  $\delta$  8.05–8.00 (m, 2H, Ar), 7.97–7.93 (m, 2H, Ar), 7.88–7.81 (m, 4H, Ar), 7.66–7.61 (m, 3H, Ar), 7.61–7.56 (m, 1H, Ar), 7.52–7.42 (m, 6H, Ar), 7.35–7.31 (m, 2H, Ar), 7.30–7.26 (m, 2H, Ar), 7.16–7.11 (m, 2H, Ar), 5.93 (dd, *J* = 3.3, 2.0 Hz, 1H, H-2'), 5.63 (dd, *J* = 3.6, 1.0 Hz, 1H, H-4), 5.53 (dd, *J* = 10.2, 3.3 Hz, 1H, H-3'), 5.50 (dd, *J* = 9.4, 3.4 Hz, 1H, H-3), 5.21 (d, *J* = 2.2 Hz, 1H, H-1'), 5.20 (app t, *J* = 10.0 Hz, 1H, H-4'), 4.76 (d, *J* = 9.6 Hz, 1H, H-1), 4.13 (app t, *J* = 9.5 Hz, 1H, H-2), 4.05 (qd, *J* = 6.0, 1.1 Hz, 1H, H-5), 3.75 (dq, *J* = 9.9, 6.1 Hz, 1H, H-5'), 2.53 (ddd,

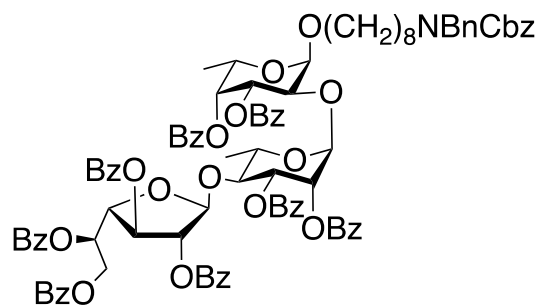
$J = 18.4, 8.1, 6.0$  Hz, 1H,  $\text{COCH}_2\text{CH}_2\text{COCH}_3$ ), 2.45 (app dt,  $J = 18.4, 6.2$  Hz, 1H,  $\text{COCH}_2\text{CH}_2\text{COCH}_3$ ), 2.35 (ddd,  $J = 17.2, 7.9, 5.8$  Hz, 1H,  $\text{COCH}_2\text{CH}_2\text{COCH}_3$ ), 2.36 (s, 3H, Ar $\text{CH}_3$ ), 2.24 (app dt,  $J = 17.0, 6.2$  Hz, 1H,  $\text{COCH}_2\text{CH}_2\text{COCH}_3$ ), 2.00 (s, 3H,  $\text{COCH}_3$ ), 1.35 (d,  $J = 6.4$  Hz, 3H, H-6), 0.61 (d,  $J = 6.2$  Hz, 3H, H-6');  $^{13}\text{C}$  NMR (126 MHz,  $\text{CDCl}_3$ )  $\delta$  205.8 (C=O), 171.7 (C=O), 165.8 (C=O), 165.6 (C=O), 165.3 (C=O), 165.2 (C=O), 138.2 (Ar), 133.4 (3 x Ar), 133.3 (2 x Ar), 133.1 (Ar), 129.9 (6 x Ar), 129.8 (4 x Ar), 129.5 (Ar), 129.4 (Ar), 129.3 (Ar), 129.2 (Ar), 128.6 (Ar), 128.5 (4 x Ar), 128.3 (4 x Ar), 99.7 (C-1'), 87.5 (C-1), 75.8 (C-2), 73.8 (C-3), 73.4 (C-5), 71.3 (C-4), 71.3 (C-4'), 70.6 (C-2'), 69.7 (C-3'), 67.2 (C-5'), 37.7 ( $\text{COCH}_2\text{CH}_2\text{COCH}_3$ ), 29.7 ( $\text{COCH}_3$ ), 27.8 ( $\text{COCH}_2\text{CH}_2\text{COCH}_3$ ), 21.3 (Ar $\text{CH}_3$ ), 16.9 (C-6'), 16.7 (C-6); HRMS (ESI-TOF)  $m/z$ :  $[\text{M} + \text{Na}]^+$  Calcd for  $\text{C}_{52}\text{H}_{50}\text{NaO}_{14}\text{S}$  953.2814; Found 953.2819.



***p*-Tolyl 2,3-di-*O*-benzoyl- $\alpha$ -L-rhamnopyranosyl-(1 $\rightarrow$ 2)-3,4-di-*O*-benzoyl-1-thio- $\beta$ -L-fucopyranoside (2.60)**

To a stirred solution of **2.59** (910 mg, 0.977 mmol) in pyridine-AcOH (25 mL, 3:2) was added hydrazine monohydrate (0.142 mL, 2.93 mmol). After stirring for 3 h, the reaction mixture was diluted with  $\text{CH}_2\text{Cl}_2$  (100 mL) and then washed with 1N HCl, saturated aqueous  $\text{NaHCO}_3$  and brine. The combined organic layers were dried over  $\text{Na}_2\text{SO}_4$ , filtered and concentrated to dryness. The crude residue was purified by flash chromatography (2:1 hexanes-EtOAc) to afford **2.60** (692 mg, 85%) as a white solid:  $R_f = 0.28$  (2:1 hexanes-EtOAc);  $[\alpha]_{\text{D}}^{25} -9.8$  ( $c = 1.47$ ,  $\text{CHCl}_3$ );  $^1\text{H}$  NMR (700 MHz,  $\text{CDCl}_3$ )  $\delta$  8.08–8.04 (m, 2H, Ar), 7.98–7.95 (m, 2H, Ar), 7.93–7.88 (m, 2H, Ar), 7.86–

7.82 (m, 2H, Ar), 7.65–7.57 (m, 4H, Ar), 7.52–7.44 (m, 6H, Ar), 7.36–7.31 (m, 2H, Ar), 7.31–7.27 (m, 2H, Ar), 7.14–7.09 (m, 2H, Ar), 5.93 (dd,  $J = 3.2, 1.9$  Hz, 1H, H-2'), 5.65 (dd,  $J = 3.5, 1.0$  Hz, 1H, H-4), 5.50 (dd,  $J = 9.4, 3.5$  Hz, 1H, H-3), 5.41 (dd,  $J = 9.9, 3.3$  Hz, 1H, H-3'), 5.17 (d,  $J = 1.9$  Hz, 1H, H-1'), 4.75 (d,  $J = 9.6$  Hz, 1H, H-1), 4.14 (app t,  $J = 9.5$  Hz, 1H, H-2), 4.06 (qd,  $J = 6.4, 1.1$  Hz, 1H, H-5), 3.70 (app td,  $J = 9.6, 5.5$  Hz, 1H, H-4'), 3.64 (dq,  $J = 9.4, 6.0$  Hz, 1H, H-5'), 2.36 (s, 3H, ArCH<sub>3</sub>), 2.16 (d,  $J = 5.7$  Hz, 1H, 4-OH'), 1.36 (d,  $J = 6.4$  Hz, 3H, H-6), 0.73 (d,  $J = 6.0$  Hz, 3H, H-6'); <sup>13</sup>C NMR (126 MHz, CDCl<sub>3</sub>) δ 167.0 (C=O), 165.8 (C=O), 165.6 (C=O), 165.2 (C=O), 138.1 (Ar), 133.4 (2 x Ar), 133.3 (Ar), 133.3 (2 x Ar), 133.2 (2 x Ar), 129.9 (8 x Ar), 129.8 (2 x Ar), 129.6 (Ar), 129.4 (Ar), 129.3 (2 x Ar), 128.6 (Ar), 128.5 (4 x Ar), 128.3 (4 x Ar), 99.9 (C-1'), 87.5 (C-1), 75.8 (C-2), 73.7 (C-3), 73.4 (C-5), 72.9 (C-3'), 72.0 (C-4'), 71.4 (C-4), 70.9 (C-2'), 69.6 (C-5'), 21.2 (ArCH<sub>3</sub>), 17.2 (C-6'), 16.7 (C-6); HRMS (ESI-TOF)  $m/z$ : [M + Na]<sup>+</sup> Calcd for C<sub>47</sub>H<sub>44</sub>NaO<sub>12</sub>S 855.2446; Found 855.2444.



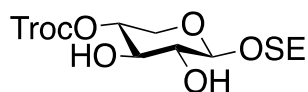
**2.62**

***N*-benzyl-*N*-benzoxycarbonyl-8-amino-1-octyl 2,3,5,6-tetra-*O*-benzoyl-β-*D*-galactofuranosyl-(1→4)-2,3-di-*O*-benzoyl-α-*L*-rhamnopyranosyl-(1→2)-3,4-di-*O*-benzoyl-α-*L*-fucopyranoside (2.62)**

To a stirred solution of **2.47** (140 mg, 0.0992 mmol) in dry CH<sub>2</sub>Cl<sub>2</sub> (10 mL) was added bromine (10.2 μL, 0.198 mmol) at 0 °C. After stirring for 1 h, the reaction mixture was concentrated to

dryness. The resulting crude product was redissolved in CH<sub>2</sub>Cl<sub>2</sub> (2 mL) and then **2.16** (110 mg, 0.298 mmol), tetrabutylammonium bromide (160 mg, 0.496 mmol) and 4Å molecular sieves powder (200 mg) were added. After stirring for 48 h, the reaction mixture was diluted with CH<sub>2</sub>Cl<sub>2</sub> (50 mL) and washed with saturated aqueous NaHCO<sub>3</sub> and brine. The combined organic layers were dried over Na<sub>2</sub>SO<sub>4</sub>, filtered and concentrated to dryness. The crude residue was purified by flash chromatography (2:1 hexanes–EtOAc) to afford **2.62** (131 mg, 79%) as a colorless oil: *R<sub>f</sub>* = 0.30 (2:1 hexanes–EtOAc); [ $\alpha$ ]<sub>D</sub><sup>25</sup> –30.4 (*c* = 0.40, CH<sub>2</sub>Cl<sub>2</sub>); <sup>1</sup>H NMR (500 MHz, CDCl<sub>3</sub>)  $\delta$  8.10–8.04 (m, 2H, Ar), 8.02–7.96 (m, 4H, Ar), 7.96–7.92 (m, 2H, Ar), 7.91–7.87 (m, 2H, Ar), 7.83–7.74 (m, 4H, Ar), 7.63–7.50 (m, 3H, Ar), 7.49–7.41 (m, 6H, Ar), 7.41–7.38 (m, 3H, Ar), 7.37–7.31 (m, 6H, Ar), 7.31–7.26 (m, 7H, Ar), 7.25–7.16 (m, 8H, Ar), 7.16–7.08 (m, 4H, Ar), 7.08–7.01 (m, 2H, Ar), 5.95 (app dt, *J* = 7.8, 4.2 Hz, 1H, H-5''), 5.78 (dd, *J* = 10.4, 3.4 Hz, 1H, H-3), 5.73 (d, *J* = 3.5, 1H, H-4), 5.65 (dd, *J* = 11.5, 3.9 Hz, 1H, H-3'), 5.53 (dd, *J* = 3.5, 1.8 Hz, 1H, H-2'), 5.51 (dd, *J* = 5.8, 1.9 Hz, 1H, H-3''), 5.46 (s, 1H, H-1''), 5.21 (d, *J* = 1.9 Hz, 1H, H-2''), 5.17 (d, *J* = 3.5 Hz, 1H, H-1), 5.17 (m, 2H, 2 x OCH<sub>2</sub>Ph), 5.09 (d, *J* = 1.8 Hz, 1H, H-1'), 4.70 (dd, *J* = 11.9, 4.4 Hz, 1H, H-6a''), 4.65 (dd, *J* = 11.8, 7.1 Hz, 1H, H-6b''), 4.50–4.43 (m, 3H, 2 x NCH<sub>2</sub>Ph, H-4''), 4.43–4.36 (m, 2H, H-2, H-5), 4.01–4.91 (m, 2H, H-4', H-5'), 3.78 (app dt, *J* = 9.6, 6.7 Hz, 1H, octyl OCH<sub>2</sub>), 3.61 (app dt, *J* = 9.5, 6.5 Hz, 1H, octyl OCH<sub>2</sub>), 3.26–3.19 (m, 1H, octyl NCH<sub>2</sub>), 3.19–3.11 (m, 1H, octyl NCH<sub>2</sub>), 1.52–1.34 (m, 4H, OCH<sub>2</sub>CH<sub>2</sub>, NCH<sub>2</sub>CH<sub>2</sub>), 1.37–1.15 (m, 8H, 4 x CH<sub>2</sub>), 1.24 (d, *J* = 6.4 Hz, 3H, H-6), 1.10 (d, *J* = 4.9 Hz, 3H, H-6'); <sup>13</sup>C NMR (126 MHz, CDCl<sub>3</sub>)  $\delta$  166.2 (C=O), 166.1 (C=O), 165.8 (C=O), 165.7 (C=O), 165.6 (C=O), 165.6 (C=O), 164.8 (C=O), 164.7 (C=O), 156.8 (C=O), 138.2 (Ar), 133.7 (Ar), 133.5 (Ar), 133.4 (Ar), 133.4 (Ar), 133.3 (Ar), 133.1 (Ar), 132.9 (Ar), 132.8 (Ar), 130.0 (4 x Ar), 130.0 (2 x Ar), 129.9 (2 x Ar), 129.9 (Ar), 129.8 (2 x Ar), 129.7 (2 x Ar), 129.7 (2 x Ar), 129.7 (Ar), 129.6 (2 x Ar), 129.5 (2 x Ar), 129.5 (Ar),

128.9 (Ar), 128.7 (4 x Ar), 128.6 (4 x Ar), 128.6 (4 x Ar), 128.5 (3 x Ar), 128.5 (Ar), 128.3 (2 x Ar), 128.2 (2 x Ar), 128.2 (2 x Ar), 127.9 (5 x Ar), 127.4 (2 x Ar), 107.4 (C-1''), 96.8 (C-1), 96.3 (C-1'), 82.3 (C-2''), 81.6 (C-4''), 77.4 (C-3''), 76.9 (C-4'), 72.7 (C-2), 72.4 (C-4), 72.1 (C-3'), 71.5 (C-2'), 70.3 (C-5''), 69.9 (C-3), 69.3 (octyl OCH<sub>2</sub>), 67.2 (C-5'), 64.9 (C-5), 63.4 (C-6''), 50.5 (NC<sub>a</sub>H<sub>2</sub>Ph), 50.2 (NC<sub>b</sub>H<sub>2</sub>Ph), 47.5 (octyl NC<sub>a</sub>H<sub>2</sub>), 46.4 (octyl NC<sub>b</sub>H<sub>2</sub>), 29.9 (CH<sub>2</sub>), 29.6 (CH<sub>2</sub>), 29.5 (CH<sub>2</sub>), 28.2 (NCH<sub>2</sub>C<sub>a</sub>H<sub>2</sub>), 28.0 (NCH<sub>2</sub>C<sub>b</sub>H<sub>2</sub>), 27.0 (CH<sub>2</sub>), 26.3 (CH<sub>2</sub>), 17.9 (C-6'), 16.3 (C-6); HRMS (ESI-TOF) *m/z*: [M + Na]<sup>+</sup> Calcd for C<sub>97</sub>H<sub>93</sub>NNaO<sub>24</sub> 1678.5980; Found 1678.6015.

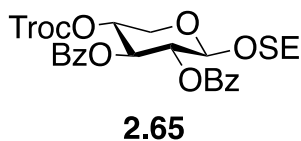


**2.64**

### 2-Trimethylsilylethyl 4-*O*-(2,2,2-trichloroethoxycarbonyl)- $\beta$ -D-xylopyranoside (**2.64**)

To a stirred solution of **2.63**<sup>43</sup> (1.06 g, 4.42 mmol) in dry toluene (25 mL) was added di-*n*-butyltin oxide (1.32 g, 5.31 mmol). The reaction mixture was heated at reflux at 110 °C for 1 h. The reaction mixture was cooled to 0 °C, followed by dropwise addition of 2,2,2-trichloroethoxycarbonyl chloride (0.640 mL, 4.64 mmol). The reaction mixture was stirred for 1 h then diluted with EtOAc (100 mL) and washed with brine. The aqueous layer was extracted with EtOAc (50 mL  $\times$  2), and the combined organic layers were dried over Na<sub>2</sub>SO<sub>4</sub>, filtered and concentrated to dryness. The crude residue was purified by flash chromatography (2:1 hexanes–EtOAc) to afford **2.64** (1.23 g, 65%) as a white solid: *R<sub>f</sub>* = 0.17 (2:1 hexanes–EtOAc); [ $\alpha$ ]<sub>D</sub><sup>25</sup> –46.3 (*c* = 1.62, CH<sub>2</sub>Cl<sub>2</sub>); <sup>1</sup>H NMR (400 MHz, CDCl<sub>3</sub>)  $\delta$  4.82 (d, *J* = 12.0 Hz, 1H, OCH<sub>2</sub>CCl<sub>3</sub>), 4.76 (app td, *J* = 12.0, 4.4 Hz, 1H, H-4), 4.76 (d, *J* = 12.0 Hz, 1H, OCH<sub>2</sub>CCl<sub>3</sub>), 4.42 (d, *J* = 6.0 Hz, 1H, H-1), 4.16 (dd, *J* = 12.0, 4.8 Hz, 1H, H-5a), 3.95 (ddd, *J* = 11.2, 10.0, 6.4 Hz, 1H, OCH<sub>2</sub>CH<sub>2</sub>Si), 3.82 (app td, *J* = 7.6, 4.8 Hz, 1H, H-3), 3.59 (ddd, *J* = 10.8, 9.6, 6.4 Hz, 1H, OCH<sub>2</sub>CH<sub>2</sub>Si), 3.52–3.44 (m, 2H, H-2, H-5b), 3.04 (d,

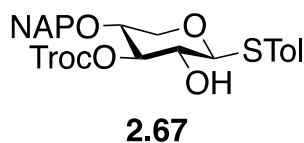
$J = 5.0$  Hz, 1H, 3-OH), 2.65 (d,  $J = 4.9$  Hz, 1H, 2-OH), 1.06–0.92 (m, 2H,  $\text{OCH}_2\text{CH}_2\text{Si}$ ), 0.03 (s, 9H, 3 x  $\text{Si}(\text{CH}_3)_3$ );  $^{13}\text{C}$  NMR (126 MHz,  $\text{CDCl}_3$ )  $\delta$  153.3 (C=O), 101.7 (C-1), 94.2 ( $\text{OCH}_2\text{CCl}_3$ ), 77.1 ( $\text{OCH}_2\text{CCl}_3$ ), 75.6 (C-4), 72.2 (C-2), 71.9 (C-3), 67.3 ( $\text{OCH}_2\text{CH}_2\text{Si}$ ), 61.1 (C-5), 18.3 ( $\text{OCH}_2\text{CH}_2\text{Si}$ ),  $-1.4$  (3 x  $\text{Si}(\text{CH}_3)_3$ ); HRMS (ESI-TOF)  $m/z$ :  $[\text{M} + \text{NH}_4]^+$  Calcd for  $\text{C}_{13}\text{H}_{27}\text{Cl}_3\text{NO}_7\text{Si}$  442.0617; Found 442.0616.



**2-Trimethylsilylethyl 2,3-di-*O*-benzoyl-4-*O*-(2,2,2-trichloroethoxycarbonyl)- $\beta$ -D-xylopyranoside (2.65)**

To a stirred solution of **2.64** (800 mg, 1.88 mmol) in pyridine (10 mL) was added benzoyl chloride (0.875 mL, 7.53 mmol) at 0 °C. After stirring overnight, while warming to room temperature,  $\text{CH}_3\text{OH}$  (2 mL) was added, and the solution was concentrated. The residue was dissolved in EtOAc (100 mL) and then washed with 1N HCl, saturated aqueous  $\text{NaHCO}_3$ , water and brine. The organic layer was dried over  $\text{Na}_2\text{SO}_4$ , filtered and concentrated to dryness. The crude residue was purified by flash chromatography (5:1 hexanes–EtOAc) to afford **2.65** (1.09 g, 91%) as a white solid:  $R_f = 0.35$  (4:1 hexanes–EtOAc);  $[\alpha]_{\text{D}}^{25} +17.2$  ( $c = 1.80$ ,  $\text{CH}_2\text{Cl}_2$ );  $^1\text{H}$  NMR (400 MHz,  $\text{CDCl}_3$ )  $\delta$  8.06–8.02 (m, 2H, Ar), 8.02–7.98 (m, 2H, Ar), 7.57–7.50 (m, 2H, Ar), 7.43–7.37 (m, 4H, Ar), 5.60 (app t,  $J = 6.8$  Hz, 1H, H-3), 5.30 (dd,  $J = 7.2, 5.2$  Hz, 1H, H-2), 5.05 (app td,  $J = 6.8, 4.4$  Hz, 1H, H-4), 4.80 (d,  $J = 5.2$  Hz, 1H, H-1), 4.75–4.70 (m, 2H,  $\text{OCH}_2\text{CCl}_3$ ), 4.33 (dd,  $J = 12.4, 4.0$  Hz, 1H, H-5a), 3.95 (ddd,  $J = 10.8, 9.6, 5.6$  Hz, 1H,  $\text{OCH}_2\text{CH}_2\text{Si}$ ), 3.76 (dd,  $J = 12.4, 6.8$  Hz, 1H, H-5b), 3.59 (ddd,  $J = 10.4, 9.6, 6.4$  Hz, 1H,  $\text{OCH}_2\text{CH}_2\text{Si}$ ), 0.98 (ddd,  $J = 14.0, 10.8, 6.4$  Hz, 1H,  $\text{OCH}_2\text{CH}_2\text{Si}$ ), 0.91 (ddd,  $J = 14.0, 10.4, 6.0$  Hz, 1H,  $\text{OCH}_2\text{CH}_2\text{Si}$ ),  $-0.03$  (s, 9H, 3 x  $\text{Si}(\text{CH}_3)_3$ );

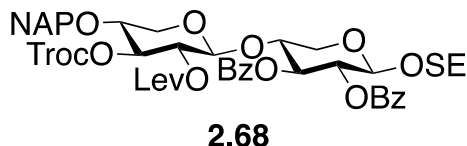
$^{13}\text{C}$  NMR (126 MHz,  $\text{CDCl}_3$ )  $\delta$  165.3 (C=O), 165.3 (C=O), 153.4 (C=O), 133.6 (Ar), 133.4 (Ar), 130.1 (2 x Ar), 130.1 (2 x Ar), 129.5 (Ar), 129.2 (Ar), 128.5 (4 x Ar), 99.3 (C-1), 94.2 ( $\text{OCH}_2\text{CCl}_3$ ), 77.1 ( $\text{OCH}_2\text{CCl}_3$ ), 72.8 (C-4), 70.2 (C-3), 70.0 (C-2), 67.1 ( $\text{OCH}_2\text{CH}_2\text{Si}$ ), 60.6 (C-5), 18.2 ( $\text{OCH}_2\text{CH}_2\text{Si}$ ), -1.3 (3 x  $\text{Si}(\text{CH}_3)_3$ ); HRMS (ESI-TOF)  $m/z$ :  $[\text{M} + \text{NH}_4]^+$  Calcd for  $\text{C}_{27}\text{H}_{35}\text{Cl}_3\text{NO}_9\text{Si}$  650.1141; Found 650.1132.



***p*-Tolyl 4-*O*-(2-naphthyl)methyl-3-*O*-(2,2,2-trichloroethoxycarbonyl)-1-thio- $\beta$ -D-xylopyranoside (2.67)**

To a stirred solution of **2.66**<sup>45</sup> (980 mg, 2.47 mmol) in dry THF (25 mL) was added dimethyltin dichloride (271 mg, 1.24 mmol), DIPEA (0.860 mL, 4.94 mmol), and 2,2,2-trichloroethoxycarbonyl chloride (0.409 mL, 2.97 mmol). The reaction mixture was stirred for 2 h and then 1N HCl was added before being extracted with EtOAc (100 mL) and washed with brine. The organic layer was dried over  $\text{Na}_2\text{SO}_4$ , filtered and concentrated to dryness. The crude residue was purified by flash chromatography (3:1 hexanes–EtOAc) to afford **2.67** (1.09 g, 77%) as a colorless oil:  $R_f$  = 0.31 (3:1 hexanes–EtOAc);  $[\alpha]_{\text{D}}^{25}$  -46.4 ( $c$  = 0.68,  $\text{CH}_2\text{Cl}_2$ );  $^1\text{H}$  NMR (400 MHz,  $\text{CDCl}_3$ )  $\delta$  7.85–7.77 (m, 3H, Ar), 7.73–7.70 (m, 1H, Ar), 7.51–7.44 (m, 2H, Ar), 7.42–7.37 (m, 3H, Ar), 7.14–7.10 (m, 2H, Ar), 4.98 (app t,  $J$  = 8.6 Hz, 1H, H-3), 4.83 (d,  $J$  = 11.9 Hz, 1H,  $\text{OCH}_2\text{CCl}_3$ ), 4.79–4.75 (m, 2H,  $\text{OCH}_2\text{Ar}$ ), 4.74 (d,  $J$  = 11.9 Hz, 1H,  $\text{OCH}_2\text{CCl}_3$ ), 4.52 (d,  $J$  = 8.8 Hz, 1H, H-1), 4.14 (dd,  $J$  = 11.7, 5.0 Hz, 1H, H-5a), 3.67 (ddd,  $J$  = 9.6, 8.6, 5.0 Hz, 1H, H-4), 3.51 (app td,  $J$  = 8.7, 3.7 Hz, 1H, H-2), 3.38 (dd,  $J$  = 11.8, 9.6 Hz, 1H, H-5b), 2.62 (d,  $J$  = 3.8 Hz, 1H, 2-OH), 2.34 (s, 3H,  $\text{ArCH}_3$ );  $^{13}\text{C}$  NMR (126 MHz,  $\text{CDCl}_3$ )  $\delta$  154.0 (C=O), 139.1 (Ar), 135.0 (Ar),

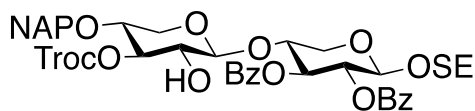
133.9 (2 x Ar), 133.3 (Ar), 133.3 (Ar), 130.1 (2 x Ar), 128.6 (Ar), 128.1 (Ar), 127.9 (Ar), 127.3 (Ar), 126.7 (Ar), 126.4 (Ar), 126.3 (Ar), 125.6 (Ar), 94.5 (OCH<sub>2</sub>CCl<sub>3</sub>), 89.2 (C-1), 81.5 (C-3), 77.2 (OCH<sub>2</sub>CCl<sub>3</sub>), 74.6 (C-4), 73.3 (OCH<sub>2</sub>Ar), 70.2 (C-2), 67.2 (C-5), 21.3 (ArCH<sub>3</sub>); HRMS (ESI-TOF) *m/z*: [M + NH<sub>4</sub>]<sup>+</sup> Calcd for C<sub>26</sub>H<sub>29</sub>Cl<sub>3</sub>NO<sub>6</sub>S 588.0776; Found 588.0772.



**2-Trimethylsilylethyl 2-*O*-levulinoyl-4-*O*-(2-naphthyl)methyl-3-*O*-(2,2,2-trichloroethoxycarbonyl)- $\beta$ -D-xylopyranosyl-(1 $\rightarrow$ 4)-2,3-di-*O*-benzoyl- $\beta$ -D-xylopyranoside (2.68)**

To a stirred solution of acceptor **2.52** (640 mg, 1.40 mmol) and donor **2.53** (1.03 g, 1.54 mmol) in dry CH<sub>2</sub>Cl<sub>2</sub> (15 mL) was added 4Å molecular sieves powder (750 mg). After stirring for 30 min, the reaction mixture was cooled to 0 °C and then *N*-iodosuccinimide (378 mg, 1.68 mmol) and silver trifluoromethanesulfonate (36.0 mg, 0.14 mmol) were added successively. The resulting solution was stirred for 1 h at 0 °C before triethylamine was added to the mixture and the solution was filtered through Celite and the filtrate was washed with saturated aqueous Na<sub>2</sub>S<sub>2</sub>O<sub>3</sub> and saturated aqueous NaHCO<sub>3</sub>. The organic layer was dried over Na<sub>2</sub>SO<sub>4</sub>, filtered and concentrated to dryness. The crude residue was purified by flash chromatography (3:1 hexanes–EtOAc) to afford **2.68** (990 mg, 70%) as a colorless oil: *R*<sub>f</sub> = 0.25 (3:1 hexanes–EtOAc); [ $\alpha$ ]<sub>D</sub><sup>25</sup> –0.6 (*c* = 0.18, CH<sub>2</sub>Cl<sub>2</sub>); <sup>1</sup>H NMR (700 MHz, CDCl<sub>3</sub>)  $\delta$  7.96–7.93 (m, 2H, Ar), 7.93–7.90 (m, 2H, Ar), 7.82–7.80 (m, 1H, Ar), 7.80–7.75 (m, 2H, Ar), 7.63–7.59 (m, 1H, Ar), 7.50–7.45 (m, 3H, Ar), 7.42–7.39 (m, 1H, Ar), 7.37–7.34 (m, 2H, Ar), 7.30–7.36 (m, 3H, Ar), 5.53 (app t, *J* = 8.2 Hz, 1H, H-3), 5.22 (dd, *J* = 8.5, 6.6 Hz, 1H, H-2), 4.93 (app t, *J* = 9.2 Hz, 1H, H-3'), 4.84 (dd, *J* = 9.5, 7.3 Hz, 1H, H-

2'), 4.81 (d,  $J = 12.0$  Hz, 1H,  $\text{OCH}_2\text{CCl}_3$ ), 4.73 (d,  $J = 12.0$  Hz, 1H,  $\text{OCH}_2\text{CCl}_3$ ), 4.66 (d,  $J = 6.5$  Hz, 1H, H-1), 4.64 (d,  $J = 12.2$  Hz, 1H,  $\text{OCH}_2\text{Ar}$ ), 4.56 (d,  $J = 12.2$  Hz, 1H,  $\text{OCH}_2\text{Ar}$ ), 4.49 (d,  $J = 7.3$  Hz, 1H, H-1'), 4.12 (dd,  $J = 12.2, 4.9$  Hz, 1H, H-5a), 3.96 (app td,  $J = 8.3, 4.9$  Hz, 1H, H-4), 3.93 (ddd,  $J = 10.7, 9.6, 5.5$  Hz, 1H,  $\text{OCH}_2\text{CH}_2\text{Si}$ ), 3.58–3.48 (m, 3H,  $\text{OCH}_2\text{CH}_2\text{Si}$ , H-4, H-5b), 3.41 (dd,  $J = 12.0, 5.4$  Hz, 1H, H-5a'), 2.97 (dd,  $J = 12.0, 9.9$  Hz, 1H, H-5b'), 2.72 (ddd,  $J = 18.4, 7.7, 5.4$  Hz, 1H,  $\text{COCH}_2\text{CH}_2\text{COCH}_3$ ), 2.66 (ddd,  $J = 18.4, 7.0, 5.1$  Hz, 1H,  $\text{COCH}_2\text{CH}_2\text{COCH}_3$ ), 2.53 (ddd,  $J = 17.3, 7.4, 5.0$  Hz, 1H,  $\text{COCH}_2\text{CH}_2\text{COCH}_3$ ), 2.48 (ddd,  $J = 17.4, 7.0, 5.4$  Hz, 1H,  $\text{COCH}_2\text{CH}_2\text{COCH}_3$ ), 2.17 (s, 3H,  $\text{COCH}_3$ ), 0.92 (ddd,  $J = 14.0, 10.9, 6.3$  Hz, 1H,  $\text{OCH}_2\text{CH}_2\text{Si}$ ), 0.84 (ddd,  $J = 14.0, 10.3, 5.6$  Hz, 1H,  $\text{OCH}_2\text{CH}_2\text{Si}$ ),  $-0.07$  (s, 9H, 3 x  $\text{Si}(\text{CH}_3)_3$ );  $^{13}\text{C}$  NMR (126 MHz,  $\text{CDCl}_3$ )  $\delta$  206.1 (C=O), 171.1 (C=O), 165.5 (C=O), 165.4 (C=O), 153.8 (C=O), 134.9 (Ar), 133.3 (Ar), 133.2 (Ar), 133.1 (Ar), 133.1 (Ar), 130.0 (2 x Ar), 130.0 (Ar), 130.0 (3 x Ar), 128.5 (Ar), 128.4 (2 x Ar), 128.3 (2 x Ar), 128.1 (Ar), 127.8 (Ar), 126.7 (Ar), 126.4 (Ar), 126.3 (Ar), 125.6 (Ar), 101.7 (C-1'), 100.4 (C-1), 94.6 ( $\text{OCH}_2\text{CCl}_3$ ), 79.3 (C-3'), 77.4 ( $\text{OCH}_2\text{CCl}_3$ ), 76.9 (C-4), 74.6 (C-4'), 73.4 ( $\text{OCH}_2\text{Ar}$ ), 72.6 (C-3), 71.8 (C-2'), 71.3 (C-2), 67.3 ( $\text{OCH}_2\text{CH}_2\text{Si}$ ), 63.5 (C-5'), 62.9 (C-5), 37.7 ( $\text{COCH}_2\text{CH}_2\text{COCH}_3$ ), 29.9 ( $\text{COCH}_3$ ), 27.8 ( $\text{COCH}_2\text{CH}_2\text{COCH}_3$ ), 18.2 ( $\text{OCH}_2\text{CH}_2\text{Si}$ ),  $-1.3$  (3 x  $\text{Si}(\text{CH}_3)_3$ ); HRMS (ESI-TOF)  $m/z$ :  $[\text{M} + \text{Na}]^+$  Calcd for  $\text{C}_{48}\text{H}_{53}\text{Cl}_3\text{NaO}_{15}\text{Si}$  1025.2112; Found 1025.2097.

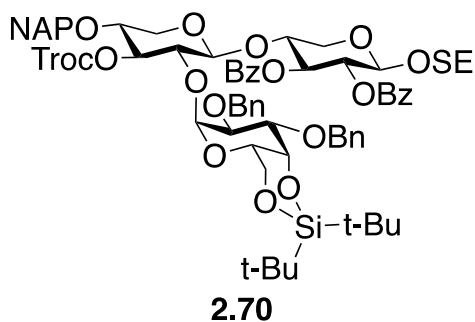


**2.69**

**2-Trimethylsilylethyl 4-*O*-(2-naphthyl)methyl-3-*O*-(2,2,2-trichloroethoxycarbonyl)- $\beta$ -D-xylopyranosyl-(1 $\rightarrow$ 4)-2,3-di-*O*-benzoyl- $\beta$ -D-xylopyranoside (2.69)**

To a stirred solution of **2.68** (409 mg, 0.407 mmol) in  $\text{CH}_2\text{Cl}_2$ – $\text{CH}_3\text{OH}$  (10.5 mL, 20:1) was added hydrazine acetate (56.2 mg, 0.611 mmol). After stirring for 2 h, the reaction mixture was concentrated and the crude residue was purified by flash chromatography (3:1 hexanes–EtOAc) to afford **2.69** (279 mg, 76%) as a colorless oil:  $R_f = 0.28$  (3:1 hexanes–EtOAc);  $[\alpha]_D^{25} +13.2$  ( $c = 0.18$ ,  $\text{CH}_2\text{Cl}_2$ );  $^1\text{H NMR}$  (500 MHz,  $\text{CDCl}_3$ )  $\delta$  7.98–7.90 (m, 4H, Ar), 7.84–7.77 (m, 3H, Ar), 7.65 (s, 1H, Ar), 7.51–7.46 (m, 3H, Ar), 7.45–7.40 (m, 1H, Ar), 7.38–7.27 (m, 5H, Ar), 5.55 (app t,  $J = 7.9$  Hz, 1H, H-3), 5.24 (dd,  $J = 8.2, 6.2$  Hz, 1H, H-2), 4.88 (app t,  $J = 8.8$  Hz, 1H, H-3'), 4.80 (d,  $J = 11.9$  Hz, 1H,  $\text{OCH}_2\text{CCl}_3$ ), 4.71 (d,  $J = 11.9$  Hz, 1H,  $\text{OCH}_2\text{CCl}_3$ ), 4.70 (d,  $J = 6.2$  Hz, 1H, H-1), 4.68 (d,  $J = 12.1$  Hz, 1H,  $\text{OCH}_2\text{Ar}$ ), 4.64 (d,  $J = 12.1$  Hz, 1H,  $\text{OCH}_2\text{Ar}$ ), 4.41 (d,  $J = 6.9$  Hz, 1H, H-1'), 4.19 (dd,  $J = 12.1, 4.6$  Hz, 1H, H-5a), 4.04 (app td,  $J = 8.0, 4.6$  Hz, 1H, H-4), 3.94 (ddd,  $J = 10.6, 9.7, 5.7$  Hz, 1H,  $\text{OCH}_2\text{CH}_2\text{Si}$ ), 3.61 (dd,  $J = 12.0, 5.0$  Hz, 1H, H-5a'), 3.59–3.53 (m, 2H,  $\text{OCH}_2\text{CH}_2\text{Si}$ , H-5b), 3.51–3.44 (m, 2H, H-2', H-4'), 3.12 (dd,  $J = 11.9, 9.4$  Hz, 1H, H-5b'), 2.58 (dd,  $J = 4.3$  Hz, 1H, 2'-OH), 0.94 (ddd,  $J = 13.9, 10.5, 6.4$  Hz, 1H,  $\text{OCH}_2\text{CH}_2\text{Si}$ ), 0.87 (ddd,  $J = 13.9, 10.3, 5.8$  Hz, 1H,  $\text{OCH}_2\text{CH}_2\text{Si}$ ),  $-0.06$  (s, 9H, 3 x  $\text{Si}(\text{CH}_3)_3$ );  $^{13}\text{C NMR}$  (126 MHz,  $\text{CDCl}_3$ )  $\delta$  165.6 (C=O), 165.2 (C=O), 153.9 (C=O), 134.8 (Ar), 133.1 (3 x Ar), 133.0 (Ar), 129.8 (2 x Ar), 129.7 (3 x Ar), 129.6 (Ar), 128.4 (Ar), 128.3 (2 x Ar), 128.2 (2 x Ar), 127.9 (Ar), 127.7 (Ar), 126.6 (Ar), 126.3 (Ar), 126.2 (Ar), 125.4 (Ar), 102.4 (C-1), 100.1 (C-1'), 94.4 ( $\text{OCH}_2\text{CCl}_3$ ), 79.9 (C-3'), 76.9 ( $\text{OCH}_2\text{CCl}_3$ ), 75.0 (C-4), 74.3 (C-4'), 73.0 ( $\text{OCH}_2\text{Ar}$ ), 72.1 (C-3), 71.5 (C-2'), 71.0 (C-2),

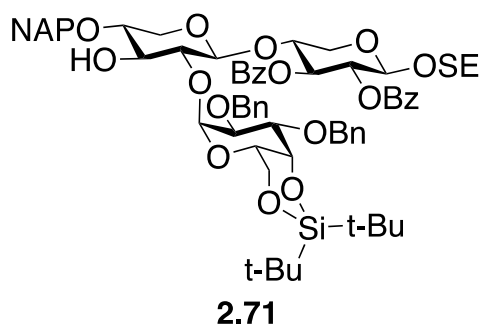
67.1 (OCH<sub>2</sub>CH<sub>2</sub>Si), 63.0 (C-5'), 62.3 (C-5), 18.0 (OCH<sub>2</sub>CH<sub>2</sub>Si), -1.5 (3 x Si(CH<sub>3</sub>)<sub>3</sub>); HRMS (ESI-TOF) *m/z*: [M + Na]<sup>+</sup> Calcd for C<sub>43</sub>H<sub>47</sub>Cl<sub>3</sub>NaO<sub>13</sub>Si 927.1744; Found 927.1748.



**2-Trimethylsilylethyl 2,3-di-*O*-benzyl-4,6-*O*-di-*tert*-butylsilylene- $\alpha$ -D-galactopyranosyl-(1 $\rightarrow$ 2)-4-*O*-(2-naphthyl)methyl-3-*O*-(2,2,2-trichloroethoxycarbonyl)- $\beta$ -D-xylopyranosyl-(1 $\rightarrow$ 4)-2,3-di-*O*-benzoyl- $\beta$ -D-xylopyranoside (2.70)**

To a stirred solution of acceptor **2.69** (70 mg, 0.077 mmol) and donor **2.54**<sup>46</sup> (70 mg, 0.12 mmol) in dry CH<sub>2</sub>Cl<sub>2</sub> (4 mL) was added 4Å molecular sieves powder (200 mg). After stirring for 30 min, the reaction mixture was cooled to 0 °C and then *N*-iodosuccinimide (35 mg, 0.15 mmol) and silver trifluoromethanesulfonate (6.0 mg, 0.023 mmol) were added successively. The resulting solution was stirred for 1 h at 0 °C before triethylamine was added to the mixture and the solution was filtered through Celite and the filtrate was washed with saturated aqueous Na<sub>2</sub>S<sub>2</sub>O<sub>3</sub> and saturated aqueous NaHCO<sub>3</sub>. The organic layer was dried over Na<sub>2</sub>SO<sub>4</sub>, filtered and concentrated to dryness. The crude residue was purified by flash chromatography (5:1 hexanes–EtOAc) to afford **2.70** (92 mg, 86%) as a white solid: *R*<sub>f</sub> = 0.34 (4:1 hexanes–EtOAc); [ $\alpha$ ]<sub>D</sub><sup>25</sup> +41.2 (*c* = 0.57, CH<sub>2</sub>Cl<sub>2</sub>); <sup>1</sup>H NMR (700 MHz, CDCl<sub>3</sub>)  $\delta$  7.98–7.95 (m, 2H, Ar), 7.95–7.91 (m, 2H, Ar), 7.83–7.80 (m, 1H, Ar), 7.79–7.74 (m, 2H, Ar), 7.61–7.58 (m, 1H, Ar), 7.50–7.46 (m, 3H, Ar), 7.45–7.39 (m, 5H, Ar), 7.38–7.36 (m, 2H, Ar), 7.35–7.32 (m, 4H, Ar), 7.32–7.27 (m, 2H, Ar), 7.27–7.23 (m, 3H, Ar), 5.46 (app t, *J* = 7.9 Hz, 1H, H-3), 5.33 (d, *J* = 3.7 Hz, 1H, H-1''), 5.15 (dd, *J* = 8.1, 6.3 Hz, 1H, H-2),

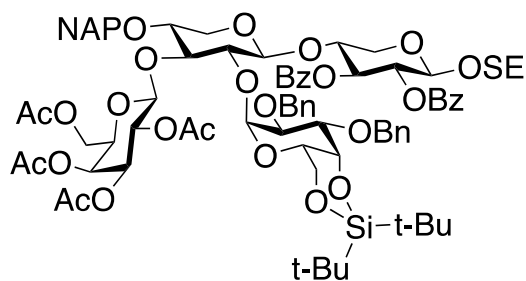
4.93 (d,  $J = 11.6$  Hz, 1H,  $\text{OCH}_2\text{Ar}$ ), 4.89 (app t,  $J = 9.4$  Hz, 1H, H-3'), 4.80 (d,  $J = 11.6$  Hz, 1H,  $\text{OCH}_2\text{Ar}$ ), 4.70 (d,  $J = 11.8$  Hz, 1H,  $\text{OCH}_2\text{Ar}$ ), 4.65 (d,  $J = 12.0$  Hz, 1H,  $\text{OCH}_2\text{Ar}$ ), 4.65 (d,  $J = 12.0$  Hz, 1H,  $\text{OCH}_2\text{CCl}_3$ ), 4.56 (d,  $J = 12.2$  Hz, 1H,  $\text{OCH}_2\text{Ar}$ ), 4.53 (d,  $J = 12.3$  Hz, 1H,  $\text{OCH}_2\text{Ar}$ ), 4.50 (d,  $J = 12.0$  Hz, 1H,  $\text{OCH}_2\text{CCl}_3$ ), 4.46–4.44 (m, 1H, H-4''), 4.45 (d,  $J = 6.4$  Hz, 1H, H-1), 4.44 (d,  $J = 7.4$  Hz, 1H, H-1'), 4.19 (dd,  $J = 12.7, 2.2$  Hz, 1H, H-6a''), 4.14 (dd,  $J = 12.7, 1.6$  Hz, 1H, H-6b''), 4.09 (dd,  $J = 10.0, 3.7$  Hz, 1H, H-2''), 3.97 (dd,  $J = 12.3, 4.7$  Hz, 1H, H-5a), 3.90 (ddd,  $J = 10.9, 9.7, 5.6$  Hz, 1H,  $\text{OCH}_2\text{CH}_2\text{Si}$ ), 3.87 (app td,  $J = 8.0, 4.7$  Hz, 1H, H-4), 3.75 (dd,  $J = 10.2, 2.9$  Hz, 1H, H-3''), 3.73–3.68 (m, 1H, H-5''), 3.61 (dd,  $J = 9.7, 7.4$  Hz, 1H, H-2'), 3.52 (app td,  $J = 9.7, 6.2$  Hz, 1H,  $\text{OCH}_2\text{CH}_2\text{Si}$ ), 3.48 (dd,  $J = 11.7, 5.2$  Hz, 1H, H-5a'), 3.40 (app td,  $J = 9.5, 5.2$  Hz, 1H, H-4'), 3.23 (dd,  $J = 12.3, 8.4$  Hz, 1H, H-5b), 3.00 (dd,  $J = 11.8, 9.9$  Hz, 1H, H-5b'), 1.05 (s, 9H,  $\text{C}(\text{CH}_3)_3$ ), 1.02 (s, 9H,  $\text{C}(\text{CH}_3)_3$ ), 0.92 (ddd,  $J = 14.0, 10.7, 6.2$  Hz, 1H,  $\text{OCH}_2\text{CH}_2\text{Si}$ ), 0.86 (ddd,  $J = 14.0, 10.6, 5.6$  Hz, 1H,  $\text{OCH}_2\text{CH}_2\text{Si}$ ),  $-0.05$  (s, 9H, 3 x  $\text{Si}(\text{CH}_3)_3$ );  $^{13}\text{C}$  NMR (126 MHz,  $\text{CDCl}_3$ )  $\delta$  165.6 (C=O), 165.4 (C=O), 153.6 (C=O), 138.8 (2 x Ar), 135.0 (Ar), 133.3 (Ar), 133.2 (Ar), 133.1 (Ar), 133.0 (Ar), 130.0 (Ar), 130.0 (2 x Ar), 129.9 (2 x Ar), 129.9 (Ar), 128.6 (2 x Ar), 128.5 (2 x Ar), 128.4 (4 x Ar), 128.3 (2 x Ar), 128.0 (Ar), 127.9 (4 x Ar), 127.8 (Ar), 127.7 (Ar), 126.5 (Ar), 126.4 (Ar), 126.3 (Ar), 125.4 (Ar), 103.0 (C-1'), 100.1 (C-1), 98.3 (C-1''), 94.5 ( $\text{OCH}_2\text{CCl}_3$ ), 80.1 (C-3'), 77.8 (C-3''), 76.9 ( $\text{OCH}_2\text{CCl}_3$ ), 76.0 (C-4'), 75.3 (C-4), 74.9 (C-2'), 74.3 (C-2''), 74.2 ( $\text{OCH}_2\text{Ar}$ ), 73.0 ( $\text{OCH}_2\text{Ar}$ ), 72.1 (C-3), 71.1 (C-2), 71.0 (C-4''), 71.0 ( $\text{OCH}_2\text{Ar}$ ), 67.8 (C-5''), 67.0 (C-6''), 67.0 ( $\text{OCH}_2\text{CH}_2\text{Si}$ ), 63.2 (C-5), 62.3 (C-5'), 27.8 (3 x  $\text{C}(\text{CH}_3)_3$ ), 27.5 (3 x  $\text{C}(\text{CH}_3)_3$ ), 23.6 ( $\text{C}(\text{CH}_3)_3$ ), 20.8 ( $\text{C}(\text{CH}_3)_3$ ), 18.2 ( $\text{OCH}_2\text{CH}_2\text{Si}$ ),  $-1.3$  (3 x  $\text{Si}(\text{CH}_3)_3$ ); HRMS (ESI-TOF)  $m/z$ :  $[\text{M} + \text{Na}]^+$  Calcd for  $\text{C}_{71}\text{H}_{85}\text{Cl}_3\text{NaO}_{18}\text{Si}_2$  1409.4232; Found 1409.4247.



**2-Trimethylsilylethyl 2,3-di-*O*-benzyl-4,6-*O*-di-*tert*-butylsilylene- $\alpha$ -D-galactopyranosyl-(1 $\rightarrow$ 2)-4-*O*-(2-naphthyl)methyl- $\beta$ -D-xylopyranosyl-(1 $\rightarrow$ 4)-2,3-di-*O*-benzoyl- $\beta$ -D-xylopyranoside (2.71)**

To a solution of compound **2.70** (410 mg) in AcOH–THF (20 mL, 1:1) was added freshly activated zinc dust (400 mg) and, after stirring for 2 h, the mixture was filtered through Celite. The filtrate was concentrated, dissolved in CH<sub>2</sub>Cl<sub>2</sub> (100 mL) and washed with water, saturated aqueous NaHCO<sub>3</sub> and brine. The organic layer was dried over Na<sub>2</sub>SO<sub>4</sub>, filtered and concentrated to dryness. The crude residue was purified by flash chromatography (3:1 hexanes–EtOAc) to afford **2.71** (321 mg, 89%) as a white solid:  $R_f = 0.31$  (8:1 hexanes–EtOAc);  $[\alpha]_D^{25} +36.6$  ( $c = 0.18$ , CH<sub>2</sub>Cl<sub>2</sub>); <sup>1</sup>H NMR (700 MHz, CDCl<sub>3</sub>)  $\delta$  7.98–7.95 (m, 2H, Ar), 7.94–7.91 (m, 2H, Ar), 7.84–7.81 (m, 1H, Ar), 7.80–7.77 (m, 2H, Ar), 7.67–7.65 (m, 1H, Ar), 7.51–7.46 (m, 5H, Ar), 7.45–7.43 (m, 2H, Ar), 7.42–7.40 (m, 1H, Ar), 7.39–7.34 (m, 7H, Ar), 7.31–7.26 (m, 4H, Ar), 5.44 (app t,  $J = 8.5$  Hz, 1H, H-3), 5.16 (dd,  $J = 8.8, 6.8$  Hz, 1H, H-2), 5.11 (d,  $J = 3.7$  Hz, 1H, H-1''), 4.89 (d,  $J = 11.6$  Hz, 1H, OCH<sub>2</sub>Ar), 4.81 (d,  $J = 11.6$  Hz, 1H, OCH<sub>2</sub>Ar), 4.78 (d,  $J = 12.2$  Hz, 1H, OCH<sub>2</sub>Ar), 4.72 (d,  $J = 12.0$  Hz, 1H, OCH<sub>2</sub>Ar), 4.71 (d,  $J = 12.1$  Hz, 1H, OCH<sub>2</sub>Ar), 4.62 (d,  $J = 12.0$  Hz, 1H, OCH<sub>2</sub>Ar), 4.53 (d,  $J = 2.6$  Hz, 1H, H-4''), 4.35 (d,  $J = 7.3$  Hz, 1H, H-1'), 4.24 (d,  $J = 6.8$  Hz, 1H, H-1), 4.18 (dd,  $J = 12.8, 2.2$  Hz, 1H, H-6a''), 4.10 (dd,  $J = 12.8, 2.0$  Hz, 1H, H-6b''), 4.08 (dd,  $J = 10.1, 3.7$  Hz, 1H, H-2''), 3.99–3.97 (m, 1H, H-5''), 3.97 (dd,  $J = 12.0, 5.0$  Hz, 1H, H-5a), 3.91–3.84 (m, 2H, H-4, OCH<sub>2</sub>CH<sub>2</sub>Si), 3.81 (dd,  $J = 10.1, 2.9$  Hz, 1H, H-3''), 3.53 (app td,  $J = 8.7, 2.1$  Hz, 1H,

H-3'), 3.48 (app td,  $J = 10.0, 6.3$  Hz, 1H, OCH<sub>2</sub>CH<sub>2</sub>Si), 3.44 (dd,  $J = 11.7, 5.1$  Hz, 1H, H-5a'), 3.40 (d,  $J = 2.2$  Hz, 1H, 3-OH'), 3.29 (dd,  $J = 9.0, 7.3$  Hz, 1H, H-2'), 3.25 (ddd,  $J = 9.6, 8.5, 5.1$  Hz, 1H, H-4'), 3.20 (dd,  $J = 12.2, 9.1$  Hz, 1H, H-5b), 2.93 (dd,  $J = 11.8, 9.7$  Hz, 1H, H-5b'), 1.06 (s, 9H, C(CH<sub>3</sub>)<sub>3</sub>), 1.01 (s, 9H, C(CH<sub>3</sub>)<sub>3</sub>), 0.90 (ddd,  $J = 14.0, 10.7, 6.4$  Hz, 1H, OCH<sub>2</sub>CH<sub>2</sub>Si), 0.83 (ddd,  $J = 14.0, 10.4, 5.7$  Hz, 1H, OCH<sub>2</sub>CH<sub>2</sub>Si), -0.05 (s, 9H, 3 x Si(CH<sub>3</sub>)<sub>3</sub>); <sup>13</sup>C NMR (126 MHz, CDCl<sub>3</sub>) δ 165.8 (C=O), 165.4 (C=O), 138.9 (Ar), 138.9 (Ar), 135.6 (Ar), 133.4 (Ar), 133.2 (Ar), 133.1 (Ar), 132.9 (Ar), 130.1 (Ar), 130.0 (2 x Ar), 129.9 (2 x Ar), 128.6 (2 x Ar), 128.5 (2 x Ar), 128.5 (4 x Ar), 128.4 (2 x Ar), 128.2 (2 x Ar), 128.1 (Ar), 127.8 (2 x Ar), 127.7 (3 x Ar), 126.7 (Ar), 126.3 (Ar), 126.2 (Ar), 125.8 (Ar), 102.2 (C-1'), 100.4 (C-1), 99.3 (C-1''), 81.5 (C-2'), 77.4 (C-4'), 77.2 (C-3''), 75.5 (C-4), 75.1 (C-3'), 74.6 (C-2''), 73.9 (OCH<sub>2</sub>Ar), 73.2 (OCH<sub>2</sub>Ar), 72.7 (C-3), 71.4 (C-2), 70.9 (C-4''), 70.8 (OCH<sub>2</sub>Ar), 68.2 (C-5''), 67.3 (C-6''), 67.1 (OCH<sub>2</sub>CH<sub>2</sub>Si), 63.3 (C-5'), 62.8 (C-5), 27.8 (3 x C(CH<sub>3</sub>)<sub>3</sub>), 27.5 (3 x C(CH<sub>3</sub>)<sub>3</sub>), 23.6 (C(CH<sub>3</sub>)<sub>3</sub>), 20.9 (C(CH<sub>3</sub>)<sub>3</sub>), 18.2 (OCH<sub>2</sub>CH<sub>2</sub>Si), -1.3 (3 x Si(CH<sub>3</sub>)<sub>3</sub>); HRMS (ESI-TOF)  $m/z$ : [M + NH<sub>4</sub>]<sup>+</sup> Calcd for C<sub>68</sub>H<sub>88</sub>NO<sub>16</sub>Si<sub>2</sub> 1230.5636; Found 1230.5629.

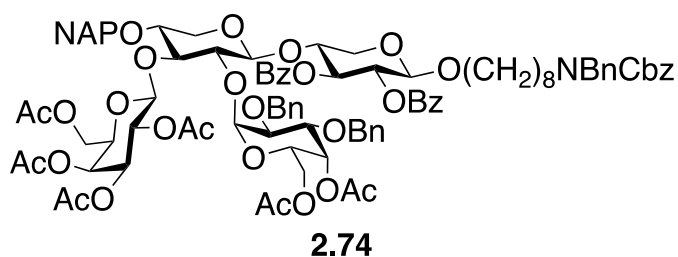


**2.72**

**2-Trimethylsilylethyl 2,3,4,6-tetra-*O*-acetyl-β-D-galactopyranosyl-(1→3)-[2,3-di-*O*-benzyl-4,6-*O*-di-tert-butylsilylene-α-D-galactopyranosyl-(1→2)]-4-*O*-(2-naphthyl)methyl-β-D-xylopyranosyl-(1→4)-2,3-di-*O*-benzoyl-β-D-xylopyranoside (2.72)**

To a stirred solution of acceptor **2.71** (60 mg, 0.049 mmol) and donor **2.55**<sup>33</sup> (90 mg, 0.20 mmol) in dry CH<sub>2</sub>Cl<sub>2</sub> (3 mL) was added 4Å molecular sieves powder (200 mg). After stirring for 30 min, the reaction mixture was cooled to 0 °C and then *N*-iodosuccinimide (66 mg, 0.29 mmol) and silver trifluoromethanesulfonate (5.1 mg, 0.020 mmol) were added successively. The resulting solution was stirred for 1 h at 0 °C before triethylamine was added to the mixture and the solution was filtered through Celite and the filtrate was washed with saturated aqueous Na<sub>2</sub>S<sub>2</sub>O<sub>3</sub> and saturated aqueous NaHCO<sub>3</sub>. The organic layer was dried over Na<sub>2</sub>SO<sub>4</sub>, filtered and concentrated to dryness. The crude residue was purified by flash chromatography (2:1 hexanes–EtOAc) to afford **2.72** (65 mg, 85%) as a white solid: *R*<sub>f</sub> = 0.26 (2:1 hexanes–EtOAc); [α]<sub>D</sub><sup>25</sup> +12.5 (*c* = 0.26, CHCl<sub>3</sub>); <sup>1</sup>H NMR (700 MHz, CDCl<sub>3</sub>) δ 7.99–7.95 (m, 4H, Ar), 7.86–7.81 (m, 2H, Ar), 7.81–7.77 (m, 1H, Ar), 7.64–7.61 (m, 1H, Ar), 7.52–7.44 (m, 4H, Ar), 7.43–7.37 (m, 6H, Ar), 7.37–7.30 (m, 7H, Ar), 7.28–7.23 (m, 2H, Ar), 5.49 (app t, *J* = 8.1 Hz, 1H, H-3), 5.24 (d, *J* = 3.8 Hz, 1H, H-1''), 5.18 (dd, *J* = 8.3, 6.4 Hz, 1H, H-2), 5.10 (dd, *J* = 3.3, 1.1 Hz, 1H, H-4'''), 4.97 (d, *J* = 11.7 Hz, 1H, OCH<sub>2</sub>Ar), 4.85 (dd, *J* = 9.9, 8.0 Hz, 1H, H-2'''), 4.82 (d, *J* = 7.9 Hz, 1H, H-1'''), 4.81 (d, *J* = 11.8 Hz, 1H, OCH<sub>2</sub>Ar), 4.77 (d, *J* = 12.0 Hz, 1H, OCH<sub>2</sub>Ar), 4.75 (dd, *J* = 9.9, 3.4 Hz, 1H, H-3'''), 4.63 (d, *J* = 3.0 Hz, 1H, H-4''), 4.58 (d, *J* = 11.8 Hz, 1H, OCH<sub>2</sub>Ar), 4.58 (d, *J* = 6.3 Hz, 1H, H-1'), 4.55 (d, *J* = 12.1 Hz, 1H, OCH<sub>2</sub>Ar), 4.53 (d, *J* = 6.7 Hz, 1H, H-1), 4.46 (d, *J* = 11.8 Hz, 1H, OCH<sub>2</sub>Ar), 4.23 (dd, *J* = 12.3, 2.0 Hz, 1H, H-6a''), 4.20 (dd, *J* = 12.3, 1.8 Hz, 1H, H-6b''), 4.06 (dd, *J* = 10.1, 3.9 Hz, 1H, H-2''), 4.04–4.03 (m, 1H, H-5''), 3.98 (dd, *J* = 12.0, 4.8 Hz, 1H, H-5a), 3.94–3.91 (m, 2H, H-4, OCH<sub>2</sub>CH<sub>2</sub>Si), 3.92 (app t, *J* = 5.8 Hz, 1H, H-6a'''), 3.89–3.85 (m, 2H, H-3', H-6b'''), 3.79 (dd, *J* = 10.1, 2.9 Hz, 1H, H-3''), 3.64 (dd, *J* = 12.3, 4.6 Hz, 1H, H-5a'), 3.62 (dd, *J* = 8.7, 6.2 Hz, 1H, H-2'), 3.61–3.59 (m, 1H, H-4'), 3.55 (ddd, *J* = 10.5, 9.7, 6.2 Hz, 1H, OCH<sub>2</sub>CH<sub>2</sub>Si), 3.31 (dd, *J* = 12.1, 8.4 Hz, 1H, H-5b), 3.20 (app t, *J* = 6.7 Hz, 1H, H-5'''), 3.11 (dd, *J* = 12.3, 6.0

Hz, 1H, H-5b'), 2.12 (s, 3H, COCH<sub>3</sub>), 1.95 (s, 3H, COCH<sub>3</sub>), 1.94 (s, 3H, COCH<sub>3</sub>), 1.92 (s, 3H, COCH<sub>3</sub>), 1.06 (s, 9H, C(CH<sub>3</sub>)<sub>3</sub>), 1.02 (s, 9H, C(CH<sub>3</sub>)<sub>3</sub>), 0.95–0.83 (m, 2H, OCH<sub>2</sub>CH<sub>2</sub>Si), –0.04 (s, 9H, 3 x Si(CH<sub>3</sub>)<sub>3</sub>); <sup>13</sup>C NMR (126 MHz, CDCl<sub>3</sub>) δ 170.2 (2 x C=O), 170.1 (C=O), 169.6 (C=O), 165.5 (C=O), 165.4 (C=O), 139.2 (Ar), 138.9 (Ar), 135.0 (Ar), 133.3 (Ar), 133.1 (2 x Ar), 130.0 (2 x Ar), 130.0 (2 x Ar), 129.9 (Ar), 128.7 (Ar), 128.5 (9 x Ar), 128.4 (3 x Ar), 128.0 (2 x Ar), 127.7 (Ar), 127.6 (2 x Ar), 127.5 (Ar), 126.7 (Ar), 126.5 (Ar), 126.5 (Ar), 125.7 (Ar), 102.4 (C-1'), 100.2 (C-1), 98.7 (C-1'''), 98.3 (C-1''), 79.2 (C-3'), 78.3 (C-3''), 76.1 (C-2'), 76.1 (C-4'), 74.2 (OCH<sub>2</sub>Ar), 74.2 (C-2''), 74.2 (C-4), 72.4 (C-3), 71.4 (C-2), 71.2 (OCH<sub>2</sub>Ar), 71.1 (C-3'''), 70.4 (C-5'''), 70.2 (C-4''), 69.9 (OCH<sub>2</sub>Ar), 69.3 (C-2'''), 67.3 (C-6''), 67.3 (C-4'''), 67.1 (C-5''), 67.1 (OCH<sub>2</sub>CH<sub>2</sub>Si), 62.5 (C-5), 61.9 (C-5'), 61.2 (C-6'''), 27.9 (3 x C(CH<sub>3</sub>)<sub>3</sub>), 27.6 (3 x C(CH<sub>3</sub>)<sub>3</sub>), 23.5 (C(CH<sub>3</sub>)<sub>3</sub>), 21.0 (COCH<sub>3</sub>), 20.9 (C(CH<sub>3</sub>)<sub>3</sub>), 20.7 (COCH<sub>3</sub>), 20.7 (COCH<sub>3</sub>), 20.6 (COCH<sub>3</sub>), 18.2 (OCH<sub>2</sub>CH<sub>2</sub>Si), –1.3 (3 x Si(CH<sub>3</sub>)<sub>3</sub>); HRMS (ESI-TOF) *m/z*: [M + Na]<sup>+</sup> Calcd for C<sub>82</sub>H<sub>102</sub>NaO<sub>25</sub>Si<sub>2</sub> 1565.6141; Found 1565.6132.



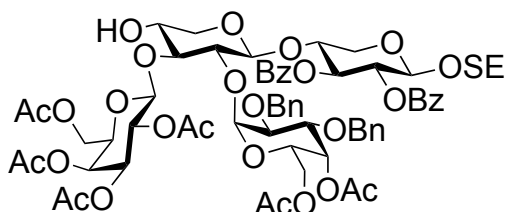
***N*-benzyl-*N*-benzoxycarbonyl-8-amino-1-octyl 2,3,4,6-tetra-*O*-acetyl-β-*D*-galactopyranosyl-(1→3)-[4,6-di-*O*-acetyl-2,3-di-*O*-benzyl-α-*D*-galactopyranosyl-(1→2)]-4-*O*-(2-naphthyl)methyl-β-*D*-xylopyranosyl-(1→4)-2,3-di-*O*-benzoyl-β-*D*-xylopyranoside (2.74)**

To a stirred solution of **2.48** (115 mg, 0.0819 mmol) in CH<sub>2</sub>Cl<sub>2</sub> (5.0 mL) was added trifluoroacetic acid (0.1 mL) at 0 °C. The reaction mixture was stirred overnight before concentration to dryness. The crude product was then dissolved in dry CH<sub>2</sub>Cl<sub>2</sub> (5.0 mL) before cesium carbonate (40.0 mg,

0.123 mmol) and 2,2,2-trifluoro-*N*-phenylacetamidoyl chloride (40  $\mu$ L, 0.246 mmol) were added. After stirring overnight, the solution was filtered through Celite and the filtrate was concentrated to dryness. The crude product was purified using a short silica column (3:2 hexanes–EtOAc) to yield the imidate product **2.73** (75 mg, 64%), which was carried to the next step without further purification.

To a stirred solution of acceptor **2.16** (38.0 mg, 0.102 mmol) and donor **2.73** (50.0 mg, 0.0339 mmol) in dry  $\text{CH}_2\text{Cl}_2$  (3 mL) was added 4 $\text{\AA}$  molecular sieves powder (300 mg). After stirring for 30 min, the reaction mixture was cooled to  $-30\text{ }^\circ\text{C}$ , and then trimethylsilyl trifluoromethanesulfonate (34.0  $\mu$ L, 0.199 mmol) was added and the resulting solution was stirred for 1h. Triethylamine was added to the mixture, the solution was filtered through Celite and the filtrate was concentrated to dryness. The crude residue was purified by flash chromatography (3:2 hexanes–EtOAc) to afford **2.74** (44.3 mg, 75%) as a white solid:  $R_f = 0.35$  (3:2 hexanes–EtOAc);  $[\alpha]_D^{25} +40.9$  ( $c = 0.13$ ,  $\text{CH}_2\text{Cl}_2$ );  $^1\text{H NMR}$  (600 MHz,  $\text{CDCl}_3$ )  $\delta$  8.00–7.94 (m, 4H, Ar), 7.87–7.77 (m, 3H, Ar), 7.67–7.63 (m, 1H, Ar), 7.52–7.43 (m, 4H, Ar), 7.40–7.21 (m, 24H, Ar), 7.19–7.14 (m, 1H, Ar), 5.68 (dd,  $J = 3.0, 1.3$  Hz, 1H, H-4''), 5.48 (app t,  $J = 7.7$  Hz, 1H, H-3), 5.45 (d,  $J = 3.6$  Hz, 1H, H-1'), 5.21–5.12 (m, 4H, 2 x  $\text{OCH}_2\text{Ar}$ , H-2, H-4'''), 5.03 (d,  $J = 8.6$  Hz, 1H, H-1'''), 5.01 (app t,  $J = 8.1$  Hz, 1H, H-2'''), 4.94 (d,  $J = 11.6$  Hz, 1H,  $\text{OCH}_2\text{Ar}$ ), 4.83 (ddd,  $J = 8.3, 3.5, 1.7$  Hz, 1H, H-3'''), 4.76 (d,  $J = 11.3$  Hz, 1H,  $\text{OCH}_2\text{Ar}$ ), 4.76 (d,  $J = 11.3$  Hz, 1H,  $\text{OCH}_2\text{Ar}$ ), 4.63 (d,  $J = 6.3$  Hz, 1H, H-1'), 4.56–4.52 (m, 2H,  $\text{OCH}_2\text{Ar}$ ), 4.54–4.44 (m, 4H, 2 x  $\text{NCH}_2\text{Ph}$ , H-5'',  $\text{OCH}_2\text{Ar}$ ), 4.52 (d,  $J = 6.1$  Hz, 1H, H-1), 4.29 (dd,  $J = 11.4, 4.9$  Hz, 1H, H-6a''), 4.10 (dd,  $J = 11.4, 7.1$  Hz, 1H, H-6b''), 4.00–3.95 (m, 3H, H-5a, H-6a''', H-6b'''), 3.93–3.85 (m, 4H, H-4, H-3', H-3''', H-2'''), 3.79 (app dt,  $J = 9.6, 6.3$  Hz, 1H, octyl  $\text{OCH}_2$ ), 3.67 (dd,  $J = 9.2, 6.3$  Hz, 1H, H-2'), 3.65–3.59 (m, 2H, H-5a', H-4'), 3.44 (app dt,  $J = 9.6, 6.3$  Hz, 1H, octyl  $\text{OCH}_2$ ), 3.43–3.38 (m, 1H,

H-5'''), 3.33 (dd,  $J = 12.1, 7.9$  Hz, 1H, H-5b), 3.26–3.19 (m, 1H, octyl NCH<sub>2</sub>), 3.19–3.10 (m, 1H, octyl NCH<sub>2</sub>), 3.15 (dd,  $J = 12.2, 7.3$  Hz, 1H, H-5b'), 2.12 (s, 3H, COCH<sub>3</sub>), 2.12 (s, 3H, COCH<sub>3</sub>), 2.09 (s, 3H, COCH<sub>3</sub>), 1.98 (s, 3H, COCH<sub>3</sub>), 1.96 (s, 3H, COCH<sub>3</sub>), 1.90 (s, 3H, COCH<sub>3</sub>), 1.56–1.35 (m, 4H, OCH<sub>2</sub>CH<sub>2</sub>, NCH<sub>2</sub>CH<sub>2</sub>), 1.32–1.12 (m, 8H, 4 x CH<sub>2</sub>); <sup>13</sup>C NMR (126 MHz, CDCl<sub>3</sub>) δ 170.7 (C=O), 170.5 (C=O), 170.4 (C=O), 170.2 (C=O), 170.2 (C=O), 169.5 (C=O), 165.5 (C=O), 165.3 (C=O), 156.9 (C=O), 138.6 (Ar), 138.3 (Ar), 138.1 (Ar), 137.0 (Ar), 135.2 (Ar), 133.3 (Ar), 133.2 (Ar), 133.2 (Ar), 133.1 (Ar), 130.0 (2 x Ar), 129.9 (2 x Ar), 129.9 (Ar), 129.8 (Ar), 128.6 (2 x Ar), 128.6 (Ar), 128.6 (Ar), 128.5 (2 x Ar), 128.4 (3 x Ar), 128.4 (2 x Ar), 128.1 (2 x Ar), 128.0 (Ar), 128.0 (3 x Ar), 128.0 (2 x Ar), 127.9 (3 x Ar), 127.8 (Ar), 127.7 (Ar), 127.4 (2 x Ar), 126.6 (Ar), 126.4 (Ar), 126.0 (Ar), 125.2 (Ar), 102.4 (C-1'), 100.6 (C-1), 99.7 (C-1'''), 97.5 (C-1''), 79.5 (C-3'), 78.2 (C-4'), 76.6 (C-3''), 75.3 (C-2'), 74.9 (C-2''), 74.2 (OCH<sub>2</sub>Ar), 74.0 (C-4), 72.0 (C-3), 71.5 (OCH<sub>2</sub>Ar), 71.4 (OCH<sub>2</sub>Ar), 71.4 (C-3'''), 71.0 (C-2), 70.6 (C-5'''), 70.0 (C-2'''), 69.6 (octyl OCH<sub>2</sub>), 68.1 (C-4''), 67.2 (OCH<sub>2</sub>Ar), 67.1 (C-5''), 66.8 (C-4'''), 62.9 (C-6''), 62.1 (C-5), 62.0 (C-5'), 61.1 (C-6'''), 50.6 (NC<sub>a</sub>H<sub>2</sub>Ph), 50.3 (NC<sub>b</sub>H<sub>2</sub>Ph), 47.4 (octyl NC<sub>a</sub>H<sub>2</sub>), 46.4 (octyl NC<sub>b</sub>H<sub>2</sub>), 29.8 (CH<sub>2</sub>), 29.6 (CH<sub>2</sub>), 29.4 (CH<sub>2</sub>), 28.2 (NCH<sub>2</sub>C<sub>a</sub>H<sub>2</sub>), 27.8 (NCH<sub>2</sub>C<sub>b</sub>H<sub>2</sub>), 26.8 (CH<sub>2</sub>), 26.3 (CH<sub>2</sub>), 21.1 (2 x COCH<sub>3</sub>), 21.0 (COCH<sub>3</sub>), 20.7 (2 x COCH<sub>3</sub>), 20.6 (COCH<sub>3</sub>); HRMS (ESI-TOF)  $m/z$ : [M + NH<sub>4</sub>]<sup>+</sup> Calcd for C<sub>96</sub>H<sub>111</sub>N<sub>2</sub>O<sub>29</sub> 1755.7267; Found 1755.7266.

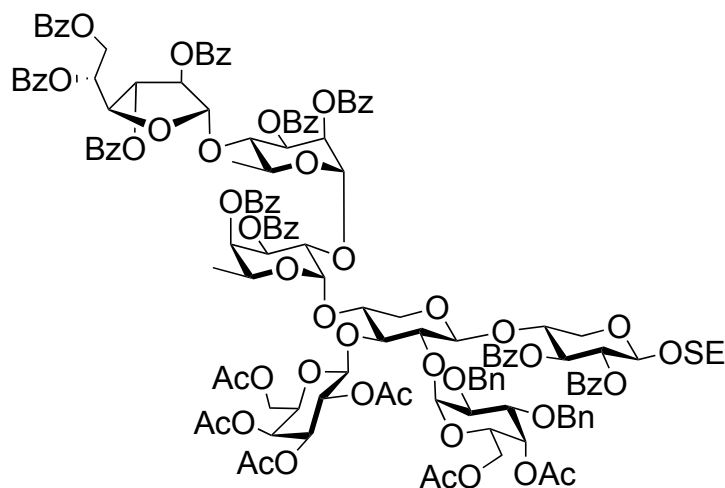


**2.75**

**2-Trimethylsilylethyl 2,3,4,6-tetra-*O*-acetyl- $\beta$ -D-galactopyranosyl-(1 $\rightarrow$ 3)-[4,6-di-*O*-acetyl-2,3-di-*O*-benzyl- $\alpha$ -D-galactopyranosyl-(1 $\rightarrow$ 2)]- $\beta$ -D-xylopyranosyl-(1 $\rightarrow$ 4)-2,3-di-*O*-benzoyl- $\beta$ -D-xylopyranoside (2.75)**

To a stirred biphasic solution of **2.48** (160 mg, 0.108 mmol) in CH<sub>2</sub>Cl<sub>2</sub>–H<sub>2</sub>O (10 mL, 4:1) was added 2,3-dichloro-5,6-dicyano-1,4-benzoquinone (36.6 mg, 0.162 mmol). The reaction mixture was stirred overnight before being diluted with CH<sub>2</sub>Cl<sub>2</sub> (50 mL). The mixture was then washed successively with 1N NaOH, water and brine. The organic layer was dried over Na<sub>2</sub>SO<sub>4</sub>, filtered and concentrated to dryness. The crude residue was purified by flash chromatography (2:1 hexanes–EtOAc) to afford **2.75** (140 mg, 97%) as a colorless oil: *R*<sub>f</sub> = 0.19 (3:2 hexanes–EtOAc); [α]<sub>D</sub><sup>25</sup> +25.9 (*c* = 0.34, CHCl<sub>3</sub>); <sup>1</sup>H NMR (600 MHz, CDCl<sub>3</sub>) δ 8.00–7.95 (m, 4H, Ar), 7.53–7.48 (m, 2H, Ar), 7.42–7.35 (m, 8H, Ar), 7.35–7.29 (m, 5H, Ar), 7.28–7.26 (m, 1H, Ar), 5.63 (dd, *J* = 2.9, 1.3 Hz, 1H, H-4''), 5.49 (app t, *J* = 8.3 Hz, 1H, H-3), 5.35 (d, *J* = 3.2 Hz, 1H, H-1'), 5.32 (dd, *J* = 3.5, 1.1 Hz, 1H, H-4'''), 5.21 (dd, *J* = 8.7, 6.8 Hz, 1H, H-2), 5.12 (dd, *J* = 8.7, 6.8, 1H, H-2'''), 4.97 (dd, *J* = 10.2, 3.5 Hz, 1H, H-3'''), 4.86 (d, *J* = 11.6 Hz, 1H, OCH<sub>2</sub>Ar), 4.81 (d, *J* = 7.9 Hz, 1H, H-1'''), 4.79 (d, *J* = 11.2 Hz, 1H, OCH<sub>2</sub>Ar), 4.73 (d, *J* = 11.6 Hz, 1H, OCH<sub>2</sub>Ar), 4.53 (d, *J* = 11.1 Hz, 1H, OCH<sub>2</sub>Ar), 4.52 (d, *J* = 5.9 Hz, 1H, H-1'), 4.44 (d, *J* = 6.8 Hz, 1H, H-1), 4.29 (app t, *J* = 5.8 Hz, 1H, H-5''), 4.22 (dd, *J* = 11.3, 5.4 Hz, 1H, H-6a''), 4.11 (dd, *J* = 11.5, 5.9 Hz, 1H, H-6b''), 4.11 (dd, *J* = 11.5, 4.0 Hz, 1H, H-6a'''), 4.04 (dd, *J* = 11.5, 7.9 Hz, 1H, H-6b'''), 3.98 (d, *J* = 11.8, 4.9 Hz, 1H, H-5a), 3.95–3.92 (m, 1H, H-4), 3.90 (ddd, *J* = 9.6, 6.3, 4.9 Hz, 1H,

OCH<sub>2</sub>CH<sub>2</sub>Si), 3.87–3.81 (m, 3H, H-3'', H-5''', H-2''), 3.62 (dd, *J* = 8.0, 6.2 Hz, 1H, H-3'), 3.60–3.49 (m, 4H, H-5a', H-2', H-4', OCH<sub>2</sub>CH<sub>2</sub>Si), 3.28 (dd, *J* = 11.9, 8.6 Hz, 1H, H-5b), 3.00 (dd, *J* = 11.5, 6.6 Hz, 1H, H-5b'), 2.16 (s, 3H, COCH<sub>3</sub>), 2.14 (s, 3H, COCH<sub>3</sub>), 2.08 (s, 3H, COCH<sub>3</sub>), 2.01 (s, 3H, COCH<sub>3</sub>), 1.97 (s, 3H, COCH<sub>3</sub>), 1.97 (s, 3H, COCH<sub>3</sub>), 0.96–0.81 (m, 2H, 2 x OCH<sub>2</sub>CH<sub>2</sub>Si), –0.06 (s, 9H, 3 x Si(CH<sub>3</sub>)<sub>3</sub>); <sup>13</sup>C NMR (151 MHz, CDCl<sub>3</sub>) δ 170.7 (C=O), 170.4 (C=O), 170.4 (C=O), 170.3 (C=O), 170.1 (C=O), 169.7 (C=O), 165.4 (2 x C=O), 138.5 (Ar), 138.1 (Ar), 133.2 (2 x Ar), 130.0 (3 x Ar), 129.9 (2 x Ar), 129.8 (Ar), 128.6 (Ar), 128.5 (3 x Ar), 128.4 (3 x Ar), 128.4 (2 x Ar), 128.4 (2 x Ar), 128.1 (3 x Ar), 128.0 (3 x Ar), 127.9 (Ar), 127.9 (Ar), 127.8 (Ar), 127.6 (Ar), 126.6 (Ar), 126.3 (Ar), 126.0 (Ar), 125.2 (Ar), 128.6 (2 x Ar), 128.6 (2 x Ar), 128.4 (4 x Ar), 128.3 (2 x Ar), 128.0 (2 x Ar), 127.9 (Ar), 127.8 (Ar), 101.5 (C-1'), 100.5 (C-1'''), 100.4 (C-1), 97.3 (C-1''), 83.6 (C-3'), 76.3 (C-3''), 76.3 (C-2'), 76.1 (C-2''), 75.4 (C-4), 74.8 (OCH<sub>2</sub>Ar), 74.1 (C-3), 72.5 (OCH<sub>2</sub>Ar), 71.2 (C-2), 71.3 (C-5'''), 71.2 (C-3'''), 69.8 (C-2'''), 69.3 (C-4'), 67.9 (C-4''), 67.4 (C-5''), 67.2 (OCH<sub>2</sub>CH<sub>2</sub>Si), 67.2 (C-4'''), 64.3 (C-5'), 62.8 (C-6''), 62.7 (C-5), 62.2 (C-6'''), 21.1 (COCH<sub>3</sub>), 21.1 (COCH<sub>3</sub>), 20.9 (COCH<sub>3</sub>), 20.7 (COCH<sub>3</sub>), 20.7 (COCH<sub>3</sub>), 20.7 (COCH<sub>3</sub>), 18.2 (OCH<sub>2</sub>CH<sub>2</sub>Si), –1.3 (3 x Si(CH<sub>3</sub>)<sub>3</sub>); HRMS (MALDI–TOF) *m/z*: [M + Na]<sup>+</sup> Calcd for C<sub>67</sub>H<sub>82</sub>NaO<sub>27</sub>Si 1369.4610; Found 1369.4692.



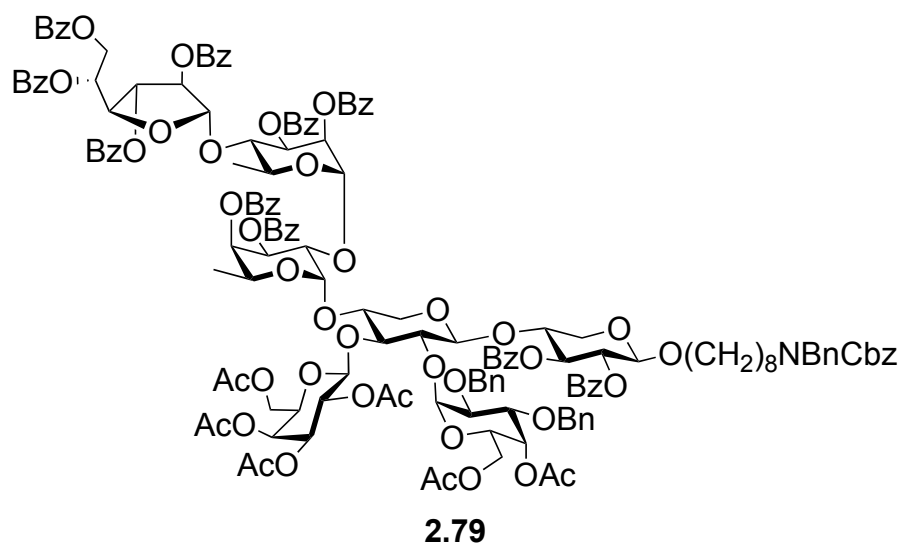
**2.77**

**2-Trimethylsilylethyl 2,3,4,6-tetra-*O*-acetyl- $\beta$ -D-galactopyranosyl-(1 $\rightarrow$ 3)-[4,6-di-*O*-acetyl-2,3-di-*O*-benzyl- $\alpha$ -D-galactopyranosyl-(1 $\rightarrow$ 2)]-[2,3,5,6-tetra-*O*-benzoyl- $\beta$ -D-galactofuranosyl-(1 $\rightarrow$ 4)-2,3-di-*O*-benzoyl- $\alpha$ -L-rhamnopyranosyl-(1 $\rightarrow$ 2)-3,4-di-*O*-benzoyl- $\alpha$ -L-fucopyranosyl-(1 $\rightarrow$ 4)]- $\beta$ -D-xylopyranosyl-(1 $\rightarrow$ 4)-2,3-di-*O*-benzoyl- $\beta$ -D-xylopyranoside (2.77)**

To a stirred biphasic solution of **2.47** (370 mg, 0.262 mmol) in EtOAc–H<sub>2</sub>O (10 mL, 1:1) was added *N*-bromosuccinimide (233 mg, 1.311 mmol). The reaction mixture was stirred for 3 h before triethylamine was added and the solution was diluted with EtOAc. The mixture was then washed successively with saturated aqueous NaHCO<sub>3</sub>, water and brine. The organic layer was dried over Na<sub>2</sub>SO<sub>4</sub>, filtered and concentrated to dryness. The crude residue was purified using a short silica column (3:1 hexanes–EtOAc) to afford the corresponding hemiacetal product. The product was then dissolved in dry CH<sub>2</sub>Cl<sub>2</sub> (30 mL) before cesium carbonate (122 mg, 0.374 mmol) and 2,2,2-trifluoro-*N*-phenylacetamidoyl chloride (61.0  $\mu$ L, 4.71 mmol) were added. After stirring overnight, the solution was filtered through Celite and the filtrate was concentrated to dryness. The crude product was purified using a short silica column (3:1 hexanes–EtOAc) to yield the imidate product **2.76** (272 mg, 70%), which was carried to the next step without further purification.

To a stirred solution of acceptor **2.75** (165 mg, 0.123 mmol) and donor **2.76** (272 mg, 0.184 mmol) in dry CH<sub>2</sub>Cl<sub>2</sub> (5 mL) was added 4Å molecular sieves powder (500 mg). After stirring for 30 min, the reaction mixture was cooled to 0 °C and then trifluoromethanesulfonic acid (5.0 μL, 0.025 mmol) was added. The resulting solution was stirred for 1 h at 0 °C before triethylamine was added to the mixture and the solution was filtered through Celite and the filtrate was concentrated to dryness. The crude residue was purified by flash chromatography (3:2 hexanes–EtOAc) to afford **2.77** (292 mg, 90%) as a white solid:  $R_f = 0.15$  (3:2 hexanes–EtOAc);  $[\alpha]_D^{25} -39.0$  ( $c = 0.02$ , CHCl<sub>3</sub>); <sup>1</sup>H NMR (600 MHz, CDCl<sub>3</sub>) δ 8.11–8.06 (m, 2H), 8.06–8.02 (m, 2H), 8.02–7.98 (m, 2H), 7.97–7.89 (m, 8H), 7.87–7.81 (m, 2H), 7.79–7.75 (m, 2H), 7.63–7.58 (m, 2H), 7.57–7.53 (m, 1H), 7.52–7.45 (m, 7H), 7.45–7.33 (m, 17H), 7.32–7.29 (m, 2H), 7.28–7.21 (m, 7H), 7.16–7.07 (m, 6H), 5.96 (app dt,  $J = 7.2, 4.2$  Hz, 1H), 5.72 (dd,  $J = 3.5, 1.3$  Hz, 1H), 5.70–5.66 (m, 2H), 5.65 (dd,  $J = 9.8, 3.4$  Hz, 1H), 5.54 (dd,  $J = 5.9, 1.9$  Hz, 1H), 5.51 (s, 1H, β-Galf-H-1), 5.51 (appt,  $J = 8.7$  Hz, 1H), 5.52–5.49 (m, 2H), 5.43 (d,  $J = 3.6$  Hz, 1H, α-Galp-H-1), 5.37 (dd,  $J = 3.5, 1.8$  Hz, 1H), 5.35 (dd,  $J = 3.6, 1.1$  Hz, 1H), 5.24 (d,  $J = 1.9$  Hz, 1H), 5.19 (dd,  $J = 9.0, 7.1$  Hz, 1H), 5.15 (dd,  $J = 10.5, 8.2$  Hz, 1H), 5.02 (d,  $J = 8.2$  Hz, 1H, β-Galp-H-1), 4.99 (d,  $J = 1.7$  Hz, 1H, α-Rhap-H-1), 4.95 (d,  $J = 12.4$  Hz, 1H), 4.95–4.90 (m, 1H), 4.91 (dd,  $J = 10.5, 3.5$  Hz, 1H), 4.86 (d,  $J = 3.5$  Hz, 1H, α-Fucp-H-1), 4.79 (d,  $J = 11.6$  Hz, 1H), 4.73–4.64 (m, 3H), 4.61 (d,  $J = 11.7$  Hz, 1H), 4.57 (d,  $J = 6.3$  Hz, 1H, β-Xylp'-H-1), 4.56 (dd,  $J = 11.4, 6.5$  Hz, 1H), 4.50 (d,  $J = 7.1$  Hz, 1H, β-Xylp-H-1), 4.47 (dd,  $J = 5.9, 3.9$  Hz, 1H), 4.37 (dd,  $J = 11.5, 7.0$  Hz, 1H), 4.29 (dd,  $J = 10.4, 3.5$  Hz, 1H), 4.24 (app t,  $J = 6.5$  Hz, 1H), 4.21–4.18 (m, 1H), 4.18–4.15 (m, 2H), 4.05–3.95 (m, 4H), 3.95–3.88 (m, 2H), 3.86 (dd,  $J = 9.8, 3.6$  Hz, 1H), 3.73 (app t,  $J = 6.9$  Hz, 1H), 3.70–3.64 (m, 2H), 3.62 (dd,  $J = 8.7, 6.3$  Hz, 1H), 3.53 (app td,  $J = 10.1, 6.3$  Hz, 1H), 3.48 (app td,  $J = 10.4, 3.4$  Hz, 1H), 3.31 (app td,  $J = 10.7, 2.9$  Hz, 1H), 2.25 (s, 3H), 2.16 (s, 3H), 2.11 (s, 3H), 2.05 (s, 3H), 2.03 (s, 3H),

1.97 (s, 3H), 1.28 (d,  $J = 6.6$  Hz, 3H), 1.00 (d,  $J = 6.1$  Hz, 3H), 0.90 (ddd,  $J = 13.9, 10.7, 6.3$  Hz, 1H), 0.83 (ddd,  $J = 13.9, 10.5, 5.6$  Hz, 1H),  $-0.06$  (s, 9H);  $^{13}\text{C}$  NMR (151 MHz,  $\text{CDCl}_3$ )  $\delta$  170.8, 170.8, 170.5 (2 x C), 169.9, 169.3, 166.2, 166.1, 165.8, 165.8, 165.6, 165.6, 165.3, 165.3, 165.0, 164.8, 138.8, 138.2, 133.7, 133.4, 133.3, 133.1, 133.0, 132.9, 130.0, 130.0, 129.9, 129.9, 129.9, 129.8, 129.8, 129.7, 129.6, 129.5, 128.8, 128.7, 128.6, 128.6, 128.5, 128.4, 128.2, 128.2, 128.0, 127.9, 127.8, 127.6, 107.4 ( $\beta$ -Gal $f$ -C-1), 101.2 ( $\beta$ -Xyl $p'$ -C-1), 100.7 ( $\beta$ -Xyl $p$ -C-1), 100.2 ( $\beta$ -Gal $p$ -C-1), 96.9 ( $\alpha$ -Rhap-C-1), 95.7 ( $\alpha$ -Gal $p$ -C-1), 94.4 ( $\alpha$ -Fuc $p$ -C-1), 82.3, 81.6, 77.8, 77.2, 76.3, 76.2, 75.4, 73.9, 73.7, 73.6, 72.8, 72.6, 72.2, 71.9, 71.8 (2 x C), 71.7, 71.2, 71.1, 70.4, 69.7, 69.5, 67.6, 67.5 (2 x C), 67.3, 67.2, 65.1, 63.4, 62.9, 62.2, 61.9, 61.2, 21.1, 21.0, 21.0, 20.9, 20.8, 20.7, 18.1, 17.8, 16.1,  $-1.3$  (3 x C); HRMS (MALDI-TOF)  $m/z$ :  $[\text{M} + \text{Na}]^+$  Calcd for  $\text{C}_{141}\text{H}_{144}\text{NaO}_{48}\text{Si}$  2655.8494; Found 2655.8450.



*N*-benzyl-*N*-benzoxycarbonyl-8-amino-1-octyl 2,3,4,6-tetra-*O*-acetyl- $\beta$ -D-galactopyranosyl-(1 $\rightarrow$ 3)-[4,6-di-*O*-acetyl-2,3-di-*O*-benzyl- $\alpha$ -D-galactopyranosyl-(1 $\rightarrow$ 2)]-[2,3,5,6-tetra-*O*-benzoyl- $\beta$ -D-galactofuranosyl-(1 $\rightarrow$ 4)-2,3-di-*O*-benzoyl- $\alpha$ -L-rhamnopyranosyl-(1 $\rightarrow$ 2)-3,4-di-*O*-benzoyl- $\alpha$ -L-fucopyranosyl-(1 $\rightarrow$ 4)]- $\beta$ -D-xylopyranosyl-(1 $\rightarrow$ 4)-2,3-di-*O*-benzoyl- $\beta$ -D-xylopyranoside (**2.79**)

To a stirred solution of **2.77** (99 mg, 0.0375 mmol) in CH<sub>2</sub>Cl<sub>2</sub> (5.0 mL) was added trifluoroacetic acid (0.50 mL) at 0 °C. The reaction mixture was stirred overnight before concentration to dryness. The crude product was then dissolved in dry CH<sub>2</sub>Cl<sub>2</sub> (2.0 mL) before cesium carbonate (18 mg, 0.0562 mmol) and 2,2,2-trifluoro-*N*-phenylacetamidoyl chloride (9.1  $\mu$ L, 0.0562 mmol) were added. After stirring overnight, the solution was filtered through Celite and the filtrate was concentrated to dryness. The crude product was purified using a short silica column (3:2 hexanes–EtOAc) to yield the imidate product **2.78** (88 mg, 87%), which was carried to the next step without further purification.

To a stirred solution of acceptor **2.16** (9.0 mg, 0.025 mmol) and donor **2.78** (13.0 mg, 0.0050 mmol) in dry CH<sub>2</sub>Cl<sub>2</sub> (2.0 mL) was added 4Å molecular sieves powder (200 mg). After stirring for 30 min, the reaction mixture was cooled to 0 °C and then trimethylsilyl trifluoromethanesulfonate

(0.10  $\mu$ L, 0.50 mmol) was added. The resulting solution was stirred for 1 h at 0  $^{\circ}$ C before triethylamine was added to the mixture and the solution was filtered through Celite and the filtrate was concentrated to dryness. The crude residue was purified by flash chromatography (3:2 hexanes–EtOAc) to afford **2.79** (10.2 mg, 84%) as a white solid:  $R_f$  = 0.10 (3:2 hexanes–EtOAc);  $[\alpha]_D^{25}$   $-18.6$  ( $c$  = 0.07,  $\text{CHCl}_3$ );  $^1\text{H}$  NMR (600 MHz,  $\text{CDCl}_3$ )  $\delta$  8.11–8.05 (m, 2H), 8.05–8.02 (m, 2H), 8.02–7.98 (m, 2H), 7.97–7.91 (m, 5H), 7.91–7.88 (m, 2H), 7.86–7.83 (m, 2H), 7.80–7.74 (m, 2H), 7.62–7.57 (m, 2H), 7.57–7.52 (m, 1H), 7.53–7.44 (m, 7H), 7.45–7.19 (m, 36H), 7.19–7.14 (m, 1H), 7.14–7.06 (m, 6H), 5.96 (app dt,  $J$  = 7.9, 4.2 Hz, 1H), 5.73 (d,  $J$  = 3.6 Hz, 1H), 5.68 (app dt,  $J$  = 10.2, 3.5 Hz, 1H), 5.68–5.67 (m, 1H), 5.64 (dd,  $J$  = 9.8, 3.4 Hz, 1H), 5.54 (dd,  $J$  = 5.9, 1.9 Hz, 1H), 5.51 (s, 1H,  $\beta$ -Gal $f$ -H-1), 5.51 (app t,  $J$  = 8.2 Hz, 1H), 5.43 (d,  $J$  = 3.6 Hz, 1H,  $\alpha$ -Gal $p$ -H-1), 5.38 (dd,  $J$  = 3.5, 1.7 Hz, 1H), 5.35 (d,  $J$  = 3.7 Hz, 1H), 5.24 (d,  $J$  = 2.0 Hz, 1H), 5.21–5.13 (m, 4H), 5.02 (d,  $J$  = 8.2 Hz, 1H,  $\beta$ -Gal $p$ -H-1), 4.99 (d,  $J$  = 1.7 Hz, 1H,  $\alpha$ -Rhap-H-1), 4.95 (d,  $J$  = 12.4 Hz, 1H), 4.95–4.91 (m, 1H), 4.91 (dd,  $J$  = 10.5, 3.5 Hz, 1H), 4.86 (d,  $J$  = 3.5 Hz, 1H,  $\alpha$ -Fuc $p$ -H-1), 4.79 (d,  $J$  = 11.6 Hz, 1H), 4.73–4.65 (m, 3H), 4.61 (d,  $J$  = 11.6 Hz, 1H), 4.57 (d,  $J$  = 6.2 Hz, 1H,  $\beta$ -Xyl $p'$ -H-1), 4.55 (dd,  $J$  = 11.4, 6.5 Hz, 1H), 4.49–4.43 (m, 3H), 4.47 (d,  $J$  = 6.5 Hz, 1H,  $\beta$ -Xyl $p$ -H-1), 4.37 (dd,  $J$  = 11.5, 7.0 Hz, 1H), 4.29 (dd,  $J$  = 10.4, 3.5 Hz, 1H), 4.25 (app t,  $J$  = 6.1 Hz, 1H), 4.21–4.14 (m, 3H), 4.04–3.96 (m, 4H), 3.91 (dq,  $J$  = 9.6, 6.3 Hz, 1H), 3.86 (dd,  $J$  = 9.8, 3.6 Hz, 1H), 3.78 (app dt,  $J$  = 9.7, 6.3 Hz, 1H), 3.73 (app t,  $J$  = 6.8 Hz, 1H), 3.70–3.63 (m, 2H), 3.62 (dd,  $J$  = 8.6, 6.3 Hz, 1H), 3.48 (app td,  $J$  = 10.4, 3.4 Hz, 1H), 3.40 (app dt,  $J$  = 9.6, 6.7 Hz, 1H), 3.31 (dd,  $J$  = 13.2, 10.6 Hz, 1H), 3.23–3.16 (m, 1H), 3.16–3.08 (m, 1H), 2.25 (s, 3H), 2.16 (s, 3H), 2.10 (s, 3H), 2.05 (s, 3H), 2.03 (s, 3H), 1.97 (s, 3H), 1.59–1.38 (m, 4H), 1.33–1.18 (m, 8H), 1.28 (d,  $J$  = 6.7 Hz, 3H), 1.01 (d,  $J$  = 6.1 Hz, 3H);  $^{13}\text{C}$  NMR (151 MHz,  $\text{CDCl}_3$ )  $\delta$  170.8, 170.8, 170.5, 170.5, 169.9, 169.3, 166.2, 166.1, 165.8, 165.8, 165.6 (2 x C), 165.3, 165.3, 165.0, 164.8, 138.8,

138.2, 138.1, 133.7, 133.4, 133.4, 133.3, 133.1, 133.0, 132.9, 130.0, 120.0, 129.9, 129.8, 129.7, 129.6, 129.5, 129.5, 128.8, 128.7, 128.7, 128.6, 128.5, 128.4, 128.2, 128.2, 128.2, 128.0, 128.0, 127.9, 127.8, 127.6, 127.4, 127.4, 127.3, 107.4 ( $\beta$ -Gal $f$ -C-1), 101.3 ( $\beta$ -Xyl $p$ -C-1), 101.2 ( $\beta$ -Xyl $p$ '-C-1), 100.2 ( $\beta$ -Gal $p$ -C-1), 96.8 ( $\alpha$ -Rhap-C-1), 95.8 ( $\alpha$ -Gal $p$ -C-1), 94.3 ( $\alpha$ -Fuc $p$ -C-1), 82.3, 81.6, 77.8, 77.0, 77.0, 76.4, 76.3, 75.4, 73.9 (2 x C), 73.7, 73.5, 72.6, 72.5, 72.2, 71.9, 71.8 (2 x C), 71.5, 71.2, 71.1, 70.3, 69.8, 69.7, 69.5, 67.6, 67.5 (2 x C), 67.3 (2 x C), 65.1, 63.4, 62.8, 62.2, 61.9, 61.2, 50.5, 50.3, 47.4, 46.4, 32.1, 30.3, 29.8, 29.6, 29.5, 29.3, 28.2, 26.8, 25.9, 22.8, 21.1, 21.0, 21.0, 20.9, 20.8, 20.7, 17.8, 16.1; HRMS (MALDI-TOF)  $m/z$ :  $[M + Na]^+$  Calcd for C<sub>159</sub>H<sub>161</sub>NNaO<sub>50</sub> 2906.9984; Found 2907.0031.

## 2.6 References

- (1) *Chagas disease (American trypanosomiasis)*. <https://www.who.int/health-topics/chagas-disease>.
- (2) *Neglected tropical diseases -- GLOBAL*. <https://www.who.int/health-topics/neglected-tropical-diseases>.
- (3) Martín-Escolano, J.; Marín, C.; Rosales, M. J.; Tsaousis, A. D.; Medina-Carmona, E.; Martín-Escolano, R. An Updated View of the *Trypanosoma cruzi* Life Cycle: Intervention Points for an Effective Treatment. *ACS Infect. Dis.* **2022**, *8* (6), 1107–1115.
- (4) Basombrío, M. A.; Gómez, L.; Padilla, A. M.; Ciaccio, M.; Nozaki, T.; Cross, G. A. M. Targeted Deletion of the Gp72 Gene Decreases the Infectivity of *Trypanosoma cruzi* for Mice and Insect Vectors. *para* **2002**, *88* (3), 489–493.
- (5) Rocha, G. M.; Seabra, S. H.; De Miranda, K. R.; Cunha-e-Silva, N.; De Carvalho, T. M. U.; De Souza, W. Attachment of Flagellum to the Cell Body is Important to the Kinetics of Transferrin Uptake by *Trypanosoma cruzi*. *Parasitol. Int.* **2010**, *59* (4), 629–633.
- (6) Rocha, G. M.; Brandão, B. A.; Mortara, R. A.; Attias, M.; De Souza, W.; Carvalho, T. M. U. The Flagellar Attachment Zone of *Trypanosoma cruzi* Epimastigote Forms. *J. Struct. Biol.* **2006**, *154* (1), 89–99.
- (7) Cooper, R.; De Jesus, A.; Cross, G. Deletion of an Immunodominant *Trypanosoma cruzi* Surface Glycoprotein Disrupts Flagellum-Cell Adhesion. *J. Cell Biol.* **1993**, *122* (1), 149–156.
- (8) Nozaki, T. Characterization of the *Trypanosoma brucei* Homologue of a *Trypanosoma cruzi* Flagellum-Adhesion Glycoprotein. *Mol. Biochem. Parasitol.* **1996**, *82* (2), 245–255.

- (9) Sher, A.; Snary, D. Specific Inhibition of the Morphogenesis of *Trypanosoma cruzi* by a Monoclonal Antibody. *Nature* **1982**, *300* (5893), 639–640.
- (10) Allen, S.; Richardson, J. M.; Mehlert, A.; Ferguson, M. A. J. Structure of a Complex Phosphoglycan Epitope from Gp72 of *Trypanosoma cruzi*. *J. Biol. Chem.* **2013**, *288* (16), 11093–11105.
- (12) Lin, S.; Lowary, T. L. Synthesis of a Highly Branched Nonasaccharide Chlorella Virus *N*-Glycan Using a “Counterclockwise” Assembly Approach. *Org. Lett.* **2020**, *22* (19), 7645–7649.
- (13) Wang, Y.; Wu, Y.; Xiong, D.; Ye, X. Total Synthesis of a Hyperbranched *N*-Linked Hexasaccharide Attached to ATCV-1 Major Capsid Protein without Precedent. *Chin. J. Chem.* **2019**, *37* (1), 42–48.
- (14) Zhao, W.; Kong, F. Facile Synthesis of the Heptasaccharide Repeating Unit of O-Deacetylated GXM of *C. neoformans* Serotype B. *Bioorg. Med. Chem.* **2005**, *13* (1), 121–130.
- (15) Zhao, W.; Kong, F. Synthesis of a Heptasaccharide Fragment of the O-Deacetylated GXM of *C. neoformans* Serotype C. *Carbohydr. Res.* **2005**, *340* (10), 1673–1681.
- (16) Rao, Y.; Boons, G.-J. A Highly Convergent Chemical Synthesis of Conformational Epitopes of Rhamnogalacturonan II. *Angew. Chem. Int. Ed.* **2007**, *46* (32), 6148–6151.
- (17) Lian, G.; Zhang, X.; Yu, B. Thioglycosides in Carbohydrate Research. *Carbohydr. Res.* **2015**, *403*, 13–22.
- (18) Christensen, H. M.; Oscarson, S.; Jensen, H. H. Common Side Reactions of the Glycosyl Donor in Chemical Glycosylation. *Carbohydr. Res.* **2015**, *408*, 51–95.

- (19) Sommer, R.; Neres, J.; Piton, J.; Dhar, N.; Van Der Sar, A.; Mukherjee, R.; Laroche, T.; Dyson, P. J.; McKinney, J. D.; Bitter, W.; Makarov, V.; Cole, S. T. Fluorescent Benzothiazinone Analogues Efficiently and Selectively Label Dpre1 in Mycobacteria and Actinobacteria. *ACS Chem. Biol.* **2018**, *13* (11), 3184–3192.
- (20) Walvoort, M. T. C.; Moggré, G.-J.; Lodder, G.; Overkleeft, H. S.; Codée, J. D. C.; Van Der Marel, G. A. Stereoselective Synthesis of 2,3-Diamino-2,3-dideoxy- $\beta$ -D-mannopyranosyl Uronates. *J. Org. Chem.* **2011**, *76* (18), 7301–7315.
- (21) Glibstrup, E.; Pedersen, C. M. Scalable Synthesis of Anomerically Pure Orthogonal-Protected GlcN<sub>3</sub> and GalN<sub>3</sub> from D-Glucosamine. *Org. Lett.* **2016**, *18* (17), 4424–4427.
- (22) Cumpstej, I. On a So-Called “Kinetic Anomeric Effect” in Chemical Glycosylation. *Org. Biomol. Chem.* **2012**, *10* (13), 2503.
- (23) Gerbst, A. G.; Ustuzhanina, N. E.; Grachev, A. A.; Khatuntseva, E. A.; Tsvetkov, D. E.; Whitfield, D. M.; Berces, A.; Nifantiev, N. E. Synthesis, NMR, and Conformational Studies of Fucoidan Fragments. III. Effect of Benzoyl Group at O-3 on Stereoselectivity of Glycosylation by 3-O- And 3,4-Di-O-Benzoylated 2-O-Benzylfucosyl Bromides. *J. Carbohydr. Chem.* **2001**, *20* (9), 821–831.
- (24) Wang, Z.; Zhou, L.; El-Boubbou, K.; Ye, X.; Huang, X. Multi-Component One-Pot Synthesis of the Tumor-Associated Carbohydrate Antigen Globo-H Based on Preactivation of Thioglycosyl Donors. *J. Org. Chem.* **2007**, *72* (17), 6409–6420.
- (25) Ding, N.; Li, C.; Liu, Y.; Zhang, Z.; Li, Y. Concise Synthesis of Clarhamnoside, a Novel Glycosphingolipid Isolated from the Marine Sponge *Agela clathrodes*. *Carbohydr. Res.* **2007**, *342* (14), 2003–2013.

- (26) Mori, M.; Ito, Y.; Ogawa, T. Total Synthesis of the Mollu-Series Glycosyl Ceramides  $\alpha$ -D-Manp-(1 $\rightarrow$ 3)- $\beta$ -D-Manp-(1 $\rightarrow$ 4)- $\beta$ -D-Glcp-(1 $\rightarrow$ 1)-Cer and  $\alpha$ -D-Manp-(1 $\rightarrow$ 3)-[ $\beta$ -D-Xylp-(1 $\rightarrow$ 2)]- $\beta$ -D-Manp-(1 $\rightarrow$ 4)- $\beta$ -D-Glcp-(1 $\rightarrow$ 1)-Cer. *Carbohydr. Res.* **1990**, *195* (2), 199–224.
- (27) Furukawa, J.; Kobayashi, S.; Nomizu, M.; Nishi, N.; Sakairi, N. Total Synthesis of Calonyctin A2, a Macrolidic Glycolipid with Plant Growth-Promoting Activity. *Tetrahedron Lett.* **2000**, *41* (18), 3453–3457.
- (28) Imamura, A.; Matsuzawa, N.; Sakai, S.; Udagawa, T.; Nakashima, S.; Ando, H.; Ishida, H.; Kiso, M. The Origin of High Stereoselectivity in Di-*tert*-Butylsilylene-Directed  $\alpha$ -Galactosylation. *J. Org. Chem.* **2016**, *81* (19), 9086–9104.
- (29) Shen, K.; Bai, B.; Liu, Y.; Lowary, T. L. Synthesis of a Tridecasaccharide Lipooligosaccharide Antigen from the Opportunistic Pathogen *Mycobacterium kansasii*. *Angew. Chem.* **2021**, *133* (47), 25063–25067.
- (30) Holland, C. V.; Horton, D.; Jewell, J. S. Favored Conformation of Tri-O-Acetyl-beta-D-xylopyranosyl Chloride. An All-Axial Tetrasubstituted Six-Membered Ring. *J. Org. Chem.* **1967**, *32* (6), 1818–1821.
- (31) Yuasa, H.; Hashimoto, H. Bending Trisaccharides by a Chelation-Induced Ring Flip of a Hinge-Like Monosaccharide Unit. *J. Am. Chem. Soc.* **1999**, *121* (21), 5089–5090.
- (32) Jaeschke, S. O.; Lindhorst, T. K.; Auer, A. Between Two Chairs: Combination of Theory and Experiment for the Determination of the Conformational Dynamics of Xylosides. *Chem. Eur. J.* **2022**, *28* (56), e202201544.
- (33) Fu, J.; Laval, S.; Yu, B. Total Synthesis of Nucleoside Antibiotics Plicacetin and Streptocytosine A. *J. Org. Chem.* **2018**, *83* (13), 7076–7084.

- (34) Long, D. E.; Karmakar, P.; Wall, K. A.; Sucheck, S. J. Synthesis of  $\alpha$ -L-Rhamnosyl Ceramide and Evaluation of Its Binding with Anti-Rhamnose Antibodies. *Bioorg. Med. Chem.* **2014**, *22* (19), 5279–5289.
- (35) Bérces, A.; Whitfield, D. M.; Nukada, T.; Do Santos Z., I.; Obuchowska, A.; Krepinsky, J. J. Is Acyl Migration to the Aglycon Avoidable in 2-Acyl Assisted Glycosylation Reactions? *Can. J. Chem.* **2004**, *82* (7), 1157–1171.
- (36) Lin, W.; Zhang, X.; He, Z.; Jin, Y.; Gong, L.; Mi, A. Reduction of Azides to Amines or Amides with Zinc and Ammonium Chloride As Reducing Agent. *Synth. Commun.* **2002**, *32* (21), 3279–3284.
- (37) Verma, P. R.; Mukhopadhyay, B. Concise Synthesis of a Tetra- and a Trisaccharide Related to the Repeating Unit of the O-Antigen from *Providencia rustigianii* O34 in the form of their *p*-Methoxyphenyl Glycosides. *RSC Adv.* **2013**, *3* (1), 201–207.
- (38) Gallo-Rodriguez, C.; Gandolfi, L.; De Lederkremer, R. M. Synthesis of  $\beta$ -D-Galf-(1–3)-D-GlcNAc by the Trichloroacetamidate Method and of  $\beta$ -D-Galf-(1–6)-D-GlcNAc by SnCl<sub>4</sub>-Promoted Glycosylation. *Org. Lett.* **1999**, *1* (2), 245–248.
- (39) Rajput, V. K.; Mukhopadhyay, B. Concise Synthesis of a Pentasaccharide Related to the Anti-Leishmanial Triterpenoid Saponin Isolated from *Maesa balansae*. *J. Org. Chem.* **2008**, *73* (17), 6924–6927.
- (40) Cyr, N.; Perlin, A. S. The Conformations of Furanosides. A <sup>13</sup>C Nuclear Magnetic Resonance Study. *Can. J. Chem.* **1979**, *57* (18), 2504–2511.
- (41) Lemieux, R. U.; Hendriks, K. B.; Stick, R. V.; James, K. Halide Ion Catalyzed Glycosidation Reactions. Syntheses of Alpha-Linked Disaccharides. *J. Am. Chem. Soc.* **1975**, *97* (14), 4056–4062.

- (42) Jansson, K.; Frejd, T.; Kihlberg, J.; Magnusson, G. 2-Trimethylsilylethyl Glycosides. Anomeric Deblocking of Mono- and Disaccharides. *Tetrahedron Lett.* **1988**, *29* (3), 361–362.
- (43) Wilstermann, M.; Magnusson, G. Synthesis of Xyl $\beta$ Cer, Gal $\beta$ 1–4Xyl $\beta$ Cer, NeuAca2–3Gal $\beta$ 1–4Xyl $\beta$ Cer and the Corresponding Lactone and Lactam Trisaccharides. *J. Org. Chem.* **1997**, *62* (23), 7961–7971.
- (44) Demizu, Y.; Kubo, Y.; Miyoshi, H.; Maki, T.; Matsumura, Y.; Moriyama, N.; Onomura, O. Highly Regioselective Protection of Sugars Catalyzed by Dimethyltin Dichloride. *Org. Lett.* **2008**, *10*, 21, 5075–5077
- (45) Bai, S.; Wu, Z.; Huang, Q.; Zhang, L.; Chen, P.; Wang, C.; Zhang, X.; Wang, P.; Li, M. Efforts to Total Synthesis of Philinopside E: Convergent Synthesis of the Sulfated Lanostane-Type Tetraglycoside. *RSC Adv.* **2016**, *6* (7), 5442–5455.
- (46) Shiozaki, M.; Tashiro, T.; Koshino, H.; Shigeura, T.; Watarai, H.; Taniguchi, M.; Mori, K. Synthesis and Biological Activity of Hydroxylated Analogues of KRN7000 ( $\alpha$ -Galactosylceramide). *Carbohydr. Res.* **2013**, *370*, 46–66.

## **Chapter 3**

### **Synthesis of a Highly Branched Immunogenic Glycan Epitope of Glycoprotein GP72 of *T. cruzi***

### 3.1 Background

GP72 is a cell surface glycoprotein of *Trypanosoma cruzi*, the etiological agent of Chagas disease.<sup>1</sup> This glycoprotein plays important roles in the parasite's infectivity and morphology.<sup>2-6</sup> The glycoprotein was found to be recognized by a monoclonal antibody WIC29.26 which in turn prevented the transformation of *T. cruzi* epimastigotes to human-infectious trypomastigotes.<sup>7</sup> The portion of the glycoprotein being recognized by the antibody was found to be a phosphoglycan molecule of unusual and complex structure. The complexity of this 13 residue-glycan can be attributed to the presence of two 'hyper-branched' residues which means that these sugars are fully glycosylated on all its available hydroxyl groups.<sup>8</sup> This type of branching is rare in naturally occurring glycans and having two of these residues in one single glycan structure makes this target molecule one of the most complex protein-linked glycan structures found in the literature.

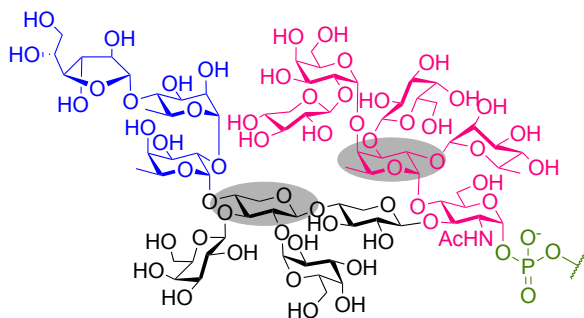


**Figure 3-1:** Structure of the immunogenic glycan epitope of GP72.

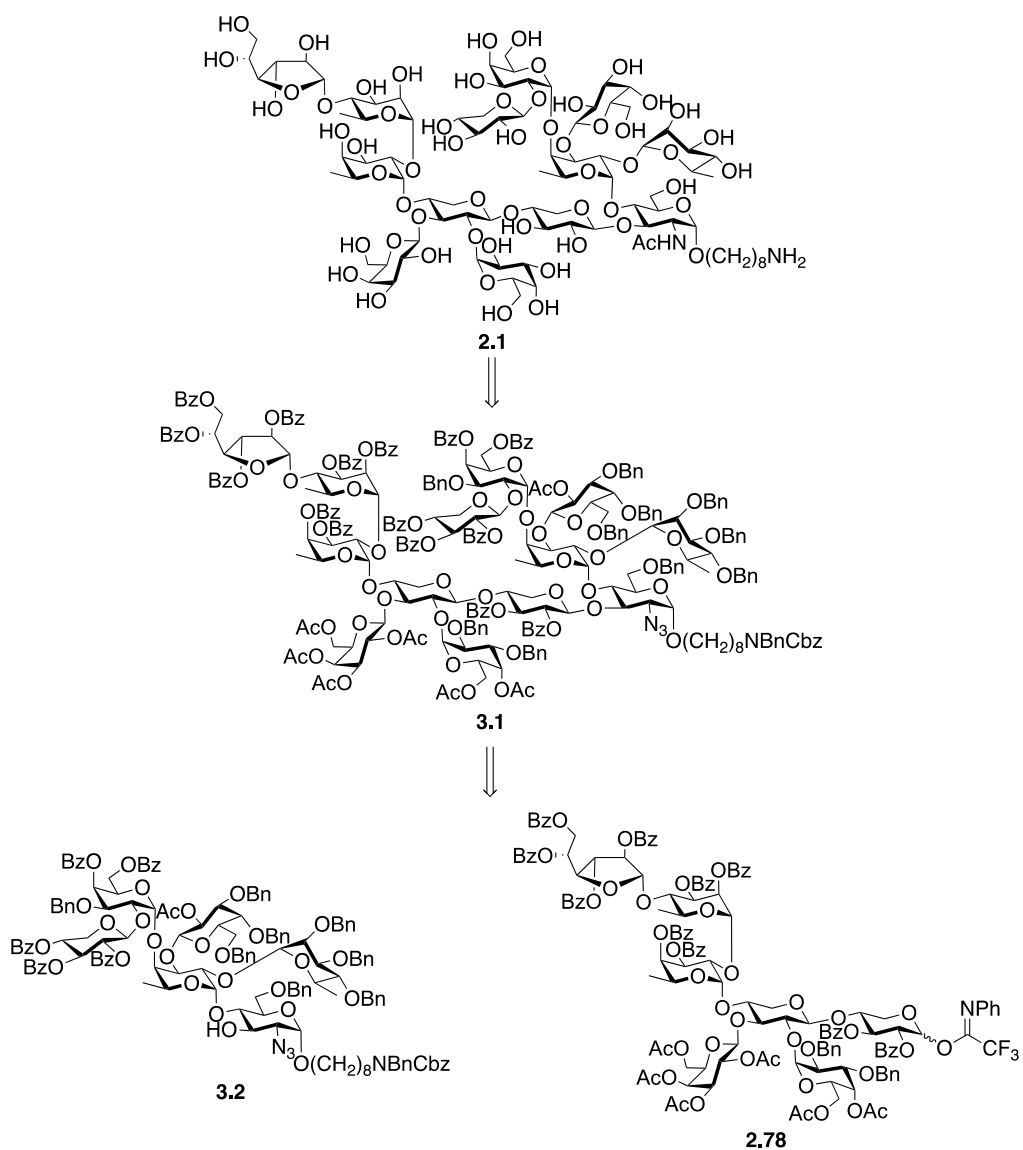
### 3.2 Results and discussion

The syntheses of similarly complex oligosaccharides have been rarely described in the literature due to the challenges in the synthesis of 'hyper-branched' molecules.<sup>9-14</sup> This chapter will focus on my efforts to synthesize the whole tridecasaccharide immunogenic glycan epitope of GP72. In the previous chapter, I described my successful synthesis of the hexasaccharide **2.2** and heptasaccharide **2.3**, each containing the 'hyper-branched' residues. This work highlighted

strategies I could use to make the larger compound, specifically the appropriate glycosylation sequences to access these highly congested sugar residues. The intermediates described in the previous chapter can also be used to investigate the synthesis of the whole glycan fragment.

### **3.2.1 Attempted glycosylations with heptasaccharide donor 2.78**

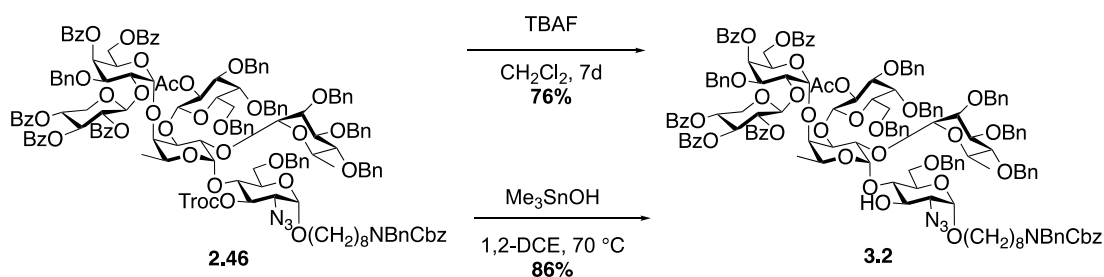
The initial strategy formulated to access the whole glycan fragment epitope was to perform a [6+7] glycosylation reaction between hexasaccharide acceptor **3.2** and heptasaccharide donor **2.78**. Hexasaccharide **3.2** could be accessed from intermediate **2.46** by selective deprotection of the Troc protecting group. On the other hand, heptasaccharide donor **2.78** was synthesized during the synthesis of heptasaccharide **2.3** as described from the previous chapter. If the glycosylation worked, the resulting tridecasaccharide **3.1** would be subjected to azido to *N*-acetamido transformation followed by global deprotection of the rest of the protecting groups to obtain target glycan fragment **2.1**.



**Scheme 3-1:** Retrosynthetic analysis of tridecasaccharide **2.1** through a [6+7] glycosylation.

The proposed [6+7] glycosylation approach started with the synthesis of hexasaccharide acceptor **3.2** (Scheme 3-2). The selective deprotection of the Troc group in **2.46** was initially planned to be carried out using reducing conditions but as previously shown in Chapter 2, these conditions (Zn, AcOH, Ac<sub>2</sub>O, THF) also reduced the azido group to an amino group. Knowing this, I decided to selectively cleave the Troc group using other methods. I initially employed mild

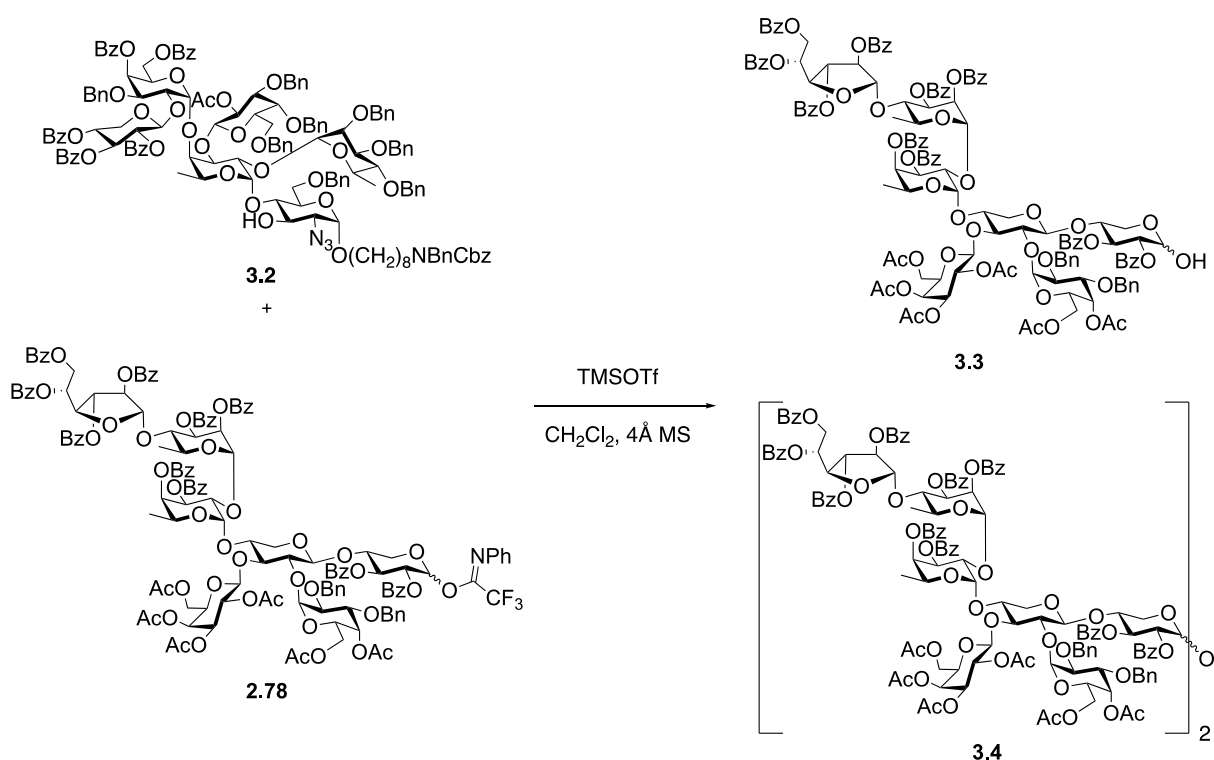
basic conditions using TBAF in  $\text{CH}_2\text{Cl}_2$ <sup>15</sup> but the reaction was extremely slow to reach completion, giving the desired compound **3.2** in 76% after seven days, while starting material remained. Thinking that the reaction time was too long, I explored another reported chemoselective Troc deprotection using trimethyltin oxide,<sup>16</sup> as a mildly basic reagent, and heating. Employing this strategy, the Troc group was selectively cleaved to give compound **3.2** in 86% yield after an overnight reaction. Upon examination of the  $^1\text{H}$  NMR and  $^{13}\text{C}$  NMR spectra of **3.2**, it was found that the peaks were broad, and some were missing, like that of compounds **2.45** and **2.46**. All these three compounds are protected hexasaccharides containing the ‘hyper-branched’ fucose residue. I hypothesized that due to the steric bulkiness within these compounds, these molecules adopt multiple conformations that are too slow to equilibrate on the NMR time scale. To support that the synthesis of the compound was successful, MALDI-MS analysis of the product was performed and it showed peak at  $m/z = 2610.0615$ , which correspond to compound **3.2**.



**Scheme 3-2:** Synthesis of target hexasaccharide fragment **3.2**.

With the hexasaccharide acceptor **3.2** and heptasaccharide donor **2.78** on hand, I decided to investigate the plausibility of a [6+7] glycosylation (Scheme 3-3). Unfortunately, multiple attempts and conditions led to failed reactions. All my attempts resulted in hydrolysis of the donor to form an inseparable mixture of the corresponding hemiacetal **3.3** and the donor dimer **3.4**, which were characterized by LRMS–MALDI. Dimer **3.4** can be formed from glycosylation of hemiacetal

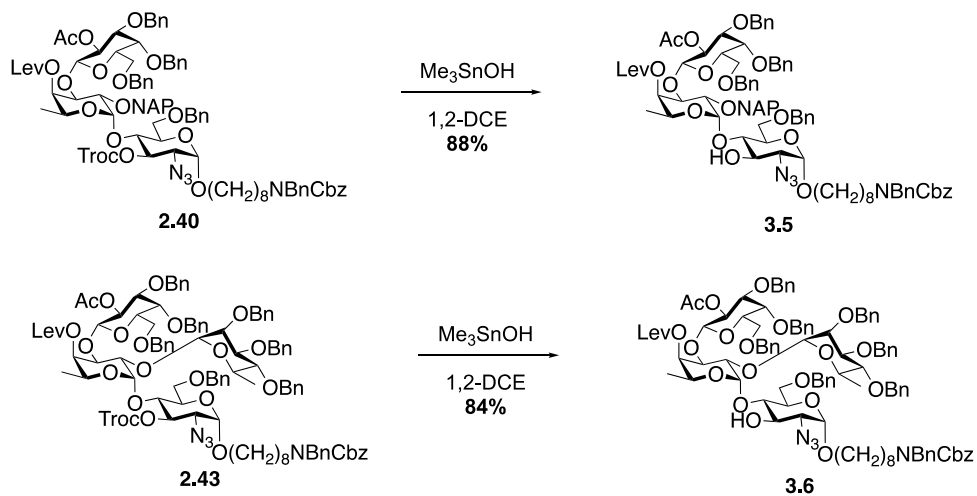
**3.3** with donor **2.78**. The formation of this by-product signifies the low reactivity of the acceptor, as a usually weakly reactive hemiacetal acted as a better nucleophile than the desired acceptor. The low reactivity of the acceptor might be attributed to the electron withdrawing nature of the neighboring azido functional group. In addition to this, the steric hindrance surrounding the GlcN<sub>3</sub> C-3 hydroxyl group in **3.3** could also affect the reactivity of the hydroxyl group. In particular, the bulky ‘hyper-branched’ fucose residue on the neighboring oxygen could hinder productive collision between the two molecules.



**Scheme 3-3:** Unsuccessful attempt on [6+7] glycosylation.

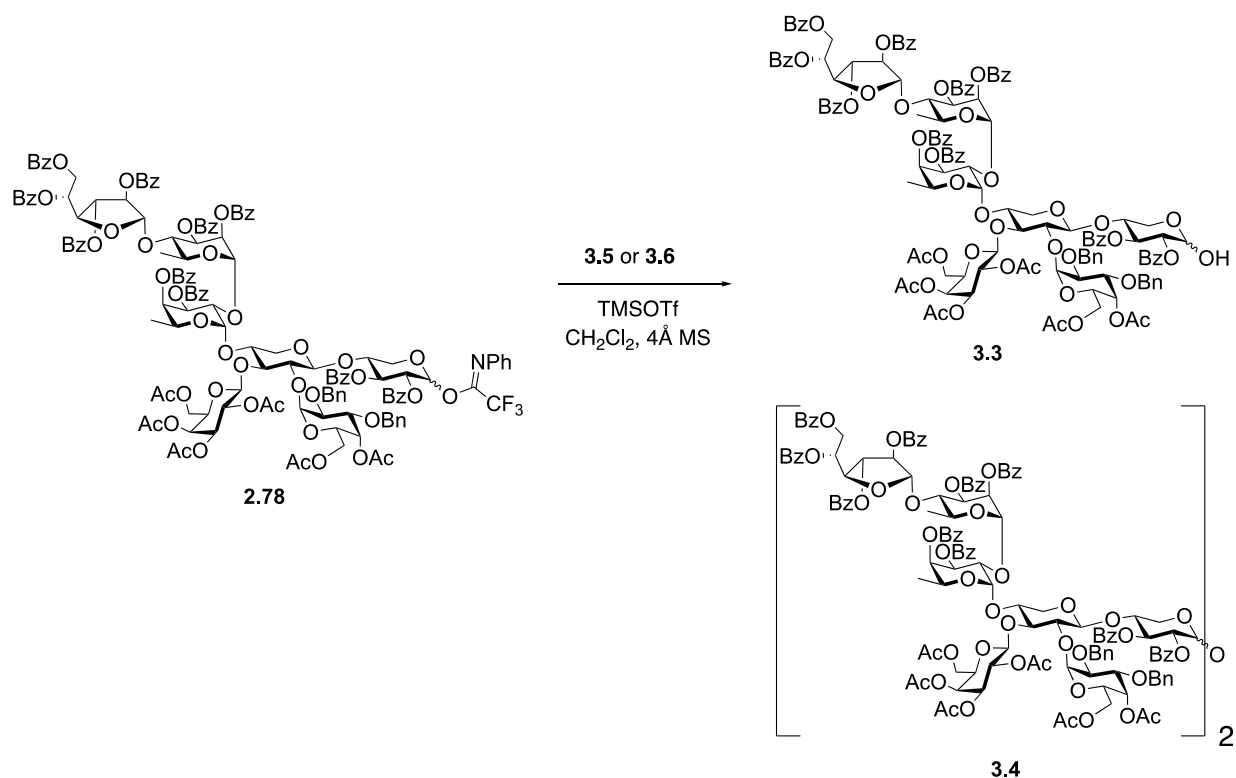
With the undesirable results from the attempted [6+7] glycosylation reactions, I decided to perform some test glycosylation reactions with smaller reacting partners. Previous reactions, specifically during the synthesis of heptasaccharide **2.79**, showed that heptasaccharide donor **2.78** reacts if a properly reactive acceptor (the linker alcohol **2.16**) is present. With this knowledge, I

decided to maintain the identity of the donor and react it with easily accessible acceptors – **3.5** and **3.6** (Scheme 3-4) – which could easily be accessed from the corresponding Troc-protected intermediates **2.40** and **2.43** (the syntheses of these compounds were described in Chapter 2). It was planned to use acceptors **3.5** and **3.6** to attempt [3+7] and [4+7] glycosylation, respectively.



**Scheme 3-4:** Synthesis of acceptors **3.5** and **3.6**.

Applying the trimethyltin oxide-mediated method to chemoselectively remove the Troc group, acceptors **3.5** and **3.6** were obtained in 88% and 84% yield from fully protected starting materials **2.40** and **2.43**, respectively (Scheme 3-4). Both acceptors were used in glycosylation reactions with heptasaccharide donor **2.78** (Scheme 3-5). Unluckily, both acceptors did not react to form the desired products but only gave the same by-products as that of the [6+7] glycosylation attempts – the unreacted acceptors and a mixture of hydrolyzed donor and donor dimer.

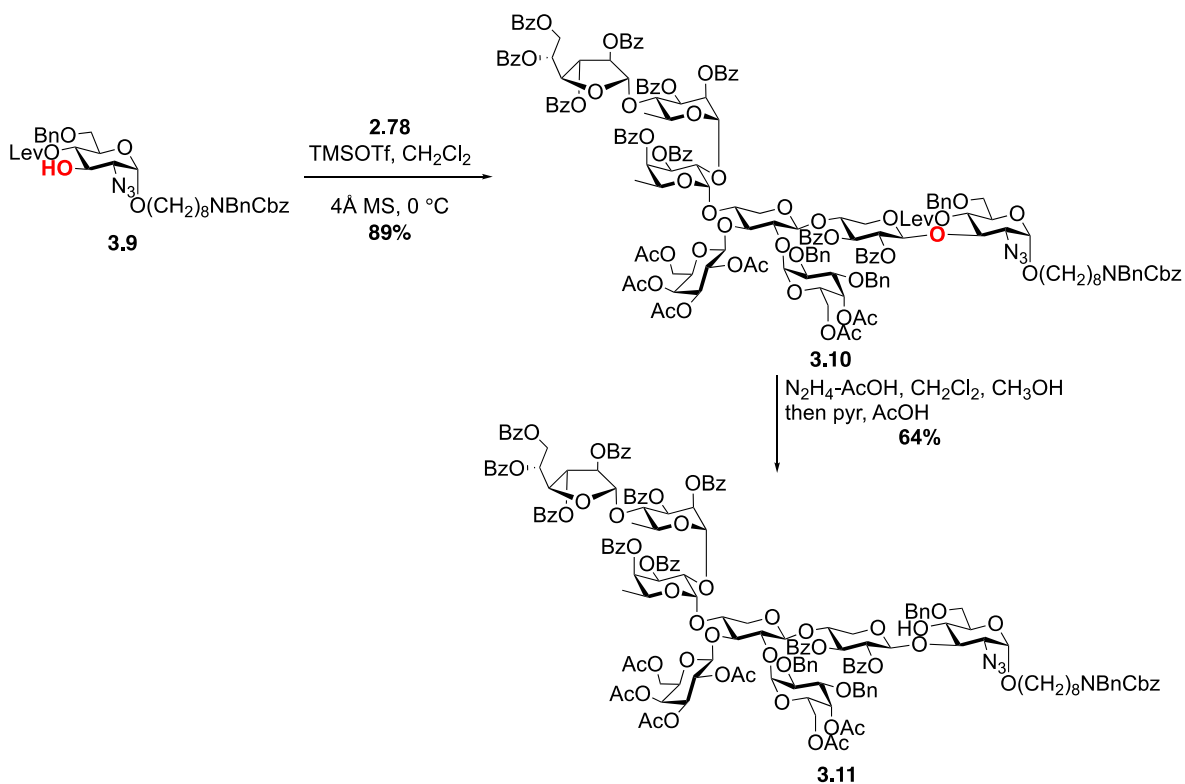


**Scheme 3-5:** Unsuccessful attempt on [3+7] and [4+7] glycosylation.

### 3.2.2 Synthesis of octasaccharide 3.11

After these failed attempts to use heptasaccharide donor **2.78** in glycosylation reactions with acceptors of varying sizes, I thought that the size of the donor might be too big for any successful reaction to occur with a carbohydrate alcohol. To test this hypothesis, I attempted a test reaction involving trisaccharide acceptor **3.5** and xylosyl thioglycoside donor **3.7**<sup>17</sup> (Scheme 3-6). However, even with this monosaccharide donor, the desired glycosylation product was not obtained. I therefore concluded that a glycosylation reaction at O-3 of the 2-azido-2-deoxyglucoside moiety is not feasible using any appropriate donor if there was an existing O-4 glycosylation. Due to this conclusion, I decided to change the glycosylation sequence on the 2-azido-2-deoxyglucoside moiety to glycosylate at O-3 before O-4.

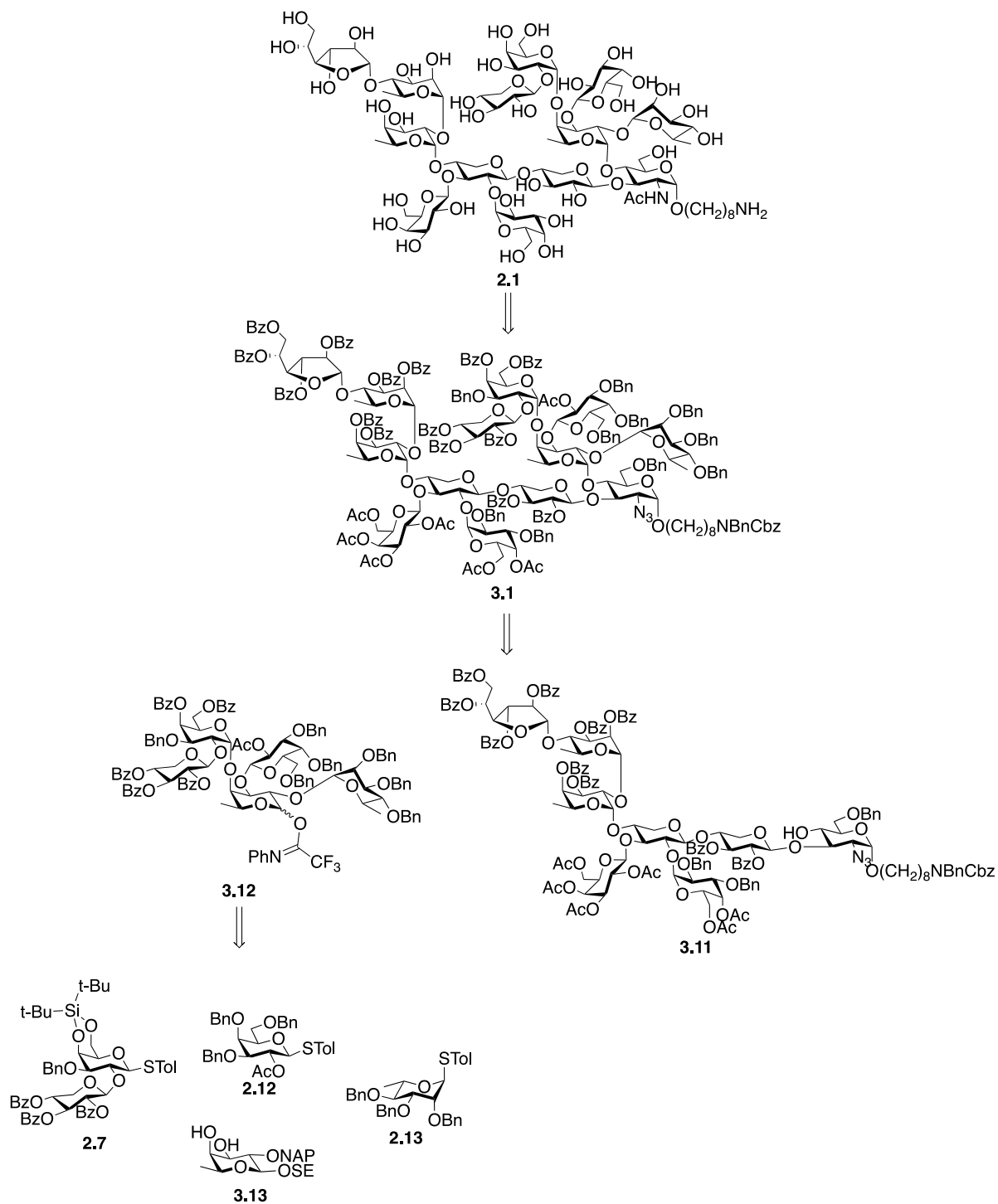




**Scheme 3-8:** Successful [1+7] glycosylation between **2.78** and **3.9** and synthesis of acceptor **3.11**.

### 3.2.3 Attempted [8+5] glycosylations.

With the successful synthesis of octasaccharide acceptor **3.11**, I pursued a [8+5] glycosylation which required the synthesis of a pentasaccharide donor, **3.12** (Scheme 3-9). Compound **3.12** contains a ‘hyper-branched’ fucose sugar without the 2-azido-2-deoxyglucose reducing end. Because of this, I hoped to employ a strategy based on the successful synthesis of the ‘hyper-branched’ fucose residue in **2.2** (shown again in Scheme 3-9 to help comparison). My successful synthesis of **2.2** employed a ‘pendulum’ approach; glycosylation initially on O-3 followed by O-2 and O-4 resulted in the desired product. The same approach was planned for the synthesis of **3.12**.



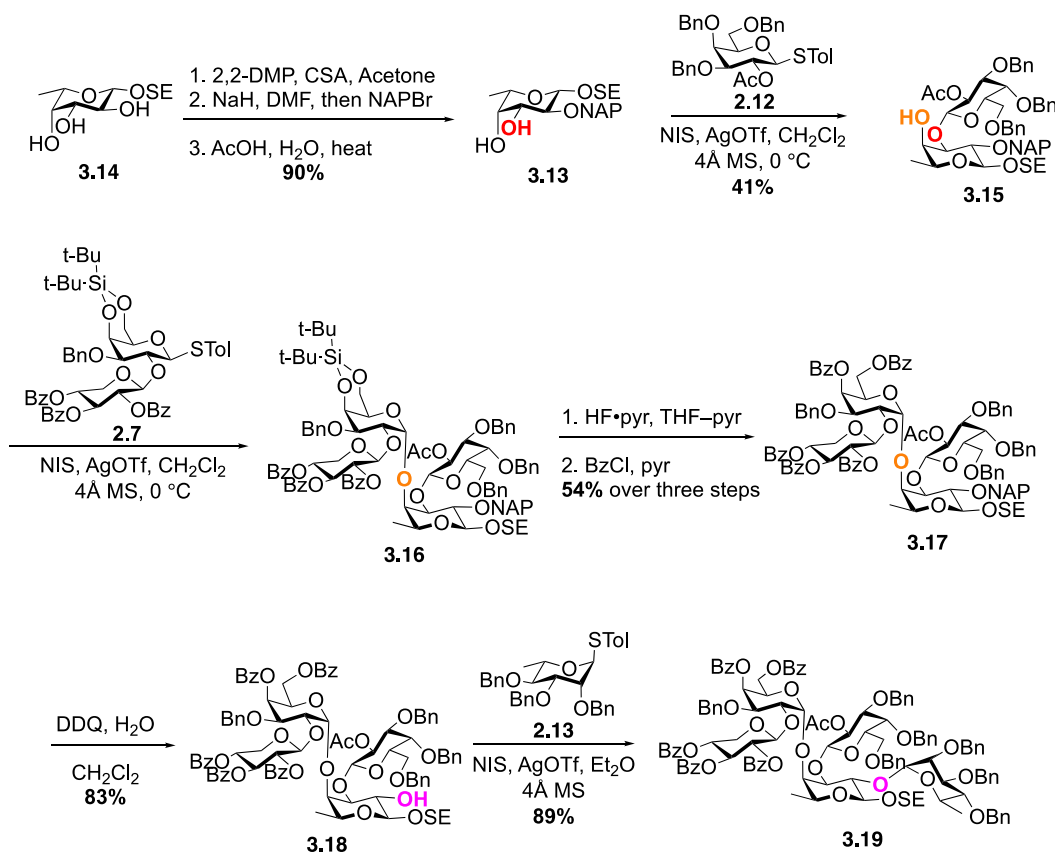
**Scheme 3-9:** Retrosynthetic analysis of tridecasaccharide **2.1** through a [8+5] glycosylation.

Pentasaccharide **3.12** could be synthesized using the building blocks **3.13**, **2.7**, **2.12** and **2.13**. Notably, monosaccharide **3.13** is a 3,4-diol fucosyl acceptor. I chose to employ a regioselective glycosylation at O-3 then followed by glycosylation at O-4. This route was chosen as this would allow me to skip multiple protection and deprotection steps. It was envisioned that the ‘reversed pendulum’ approach would also be applicable in synthesizing this ‘hyper-branched’ fucose residue.

### 3.2.3.1 Synthesis of pentasaccharide **3.12**

The synthesis of pentasaccharide **3.12** started by preparing its 2-trimethylsilylethyl glycoside **3.19** counterpart from diol acceptor **3.13**, which was synthesized from **3.14**<sup>18</sup> in 90% over three steps (Scheme 3-10). To shorten the route, I first attempted a regioselective monoglycosylation of diol **3.13** with thioglycoside **2.12**<sup>19</sup> to form disaccharide **3.15**. The idea that the reaction would proceed regioselectively at O-3 and not at O-4 of the fucose acceptor was based on the observations in Chapter 2 that the axial hydroxyl group at C-4 was less reactive during acylation and glycosylation during the synthesis of hexasaccharide **2.2**. The glycosylation reaction was performed using NIS–AgOTf activation, which gave the desired disaccharide **3.15** as the major product in a moderate yield of 41%. The O-3 regioselectivity was confirmed after observing a correlation between Gal-H-1 and the Fuc-C-3 in the HMBC spectrum. In addition, the desired  $\beta$ -stereoselectivity of the reaction was shown by the coupling constant between Gal-H-1 and Gal-H-2 ( $^3J_{1,2} = 7.9$  Hz). The moderate yield arose from the formation of other undesired products and unreacted acceptor. While the yield is lower than hoped, this route enabled me to avoid protection and deprotection steps (at least two) thus increasing efficiency. I further postulated that if the [8+5]

approach was successful, I could return to the preparation of **3.15** to improve its yield by optimization of the glycosylation.



**Scheme 3-10:** Synthesis of pentasaccharide **3.19** using the ‘reversed pendulum’ approach.

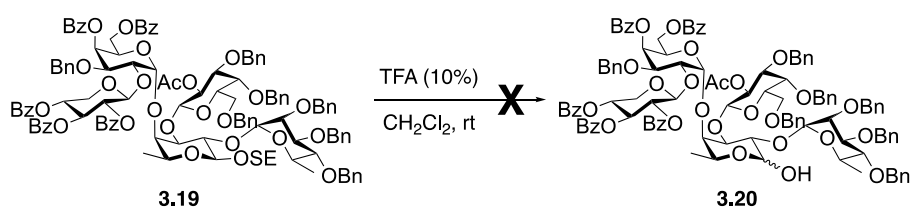
With disaccharide **3.15** in hand, I performed a glycosylation between **3.15** and disaccharide donor **2.7** using NIS–AgOTf activation; this reaction gave the desired tetrasaccharide **3.16**. Unfortunately, the product could not be purified using column chromatography due to contamination by other by-products. I therefore subjected the crude material containing **3.16** to treatment with HF–pyridine to cleave the DTBS group and protect the resulting diol with benzoyl groups which gave **3.17**. This tetrasaccharide was successfully separated from the unwanted contaminants in 54% yield over three steps, including the glycosylation. The reaction proceeded

with  $\alpha$ -selectivity as evident by the coupling constant between Gal-H-1 and Gal-H-2 ( $^3J_{1,2} = 3.8$  Hz).

After the successful synthesis of this tetrasaccharide **3.17**, the NAP group at O-2 was deprotected using DDQ in wet  $\text{CH}_2\text{Cl}_2$  to give acceptor **3.18** in 83% yield. This acceptor and donor **2.13**<sup>20</sup> were then coupled using NIS–AgOTf activation in  $\text{Et}_2\text{O}$  to give the desired pentasaccharide **3.19** in 89% yield. The resulting glycosidic linkage was established to be the desired  $\alpha$ -linkage using the coupling constant between Rha-H-1 and Rha-C-1 ( $^1J_{\text{C-1-H-1}} = 170.9$  Hz) from the  $^1\text{H}$  coupled HSQC spectrum. Thus, the synthesis of pentasaccharide **3.19**, which contains a ‘hyper-branched’ fucose residue, was successful using the ‘reversed pendulum’ approach where in the glycosylation was initially performed on O-3 followed by O-4 then lastly on O-2. My success in accessing **3.19**, together with the success of the synthesis of hexasaccharide **2.2** using the ‘pendulum’ approach showed that the ‘hyper-branched’ fucose residue in the GP72 glycan can be synthesized if the O-3 is glycosylated first. The glycosylation sequence of the remaining hydroxyl groups is not critical in obtaining the desired final products.

With pentasaccharide **3.19** already in-hand, I proceeded to transform this compound to a suitable imidate donor **3.12** in two steps. The plan was to first chemoselectively cleave the 2-trimethylsilylethyl aglycon using anhydrous acid<sup>21</sup> producing the corresponding hemiacetal, which could be converted to an imidate donor. Following this plan, pentasaccharide **3.19** was subjected to trifluoroacetic acid in dichloromethane but, unfortunately, this reaction did not give the desired hemiacetal but instead a complex mixture of multiple unwanted side products was produced. The mixture was analyzed using mass spectrometry. The expected mass ion peak ( $m/z = 1981.7$ ) corresponding for the product was not found. One of the main  $m/z$  ion peaks observed was at  $m/z = 1547.5$ , which corresponds to the compound with the 2-trimethylsilylethyl aglycon

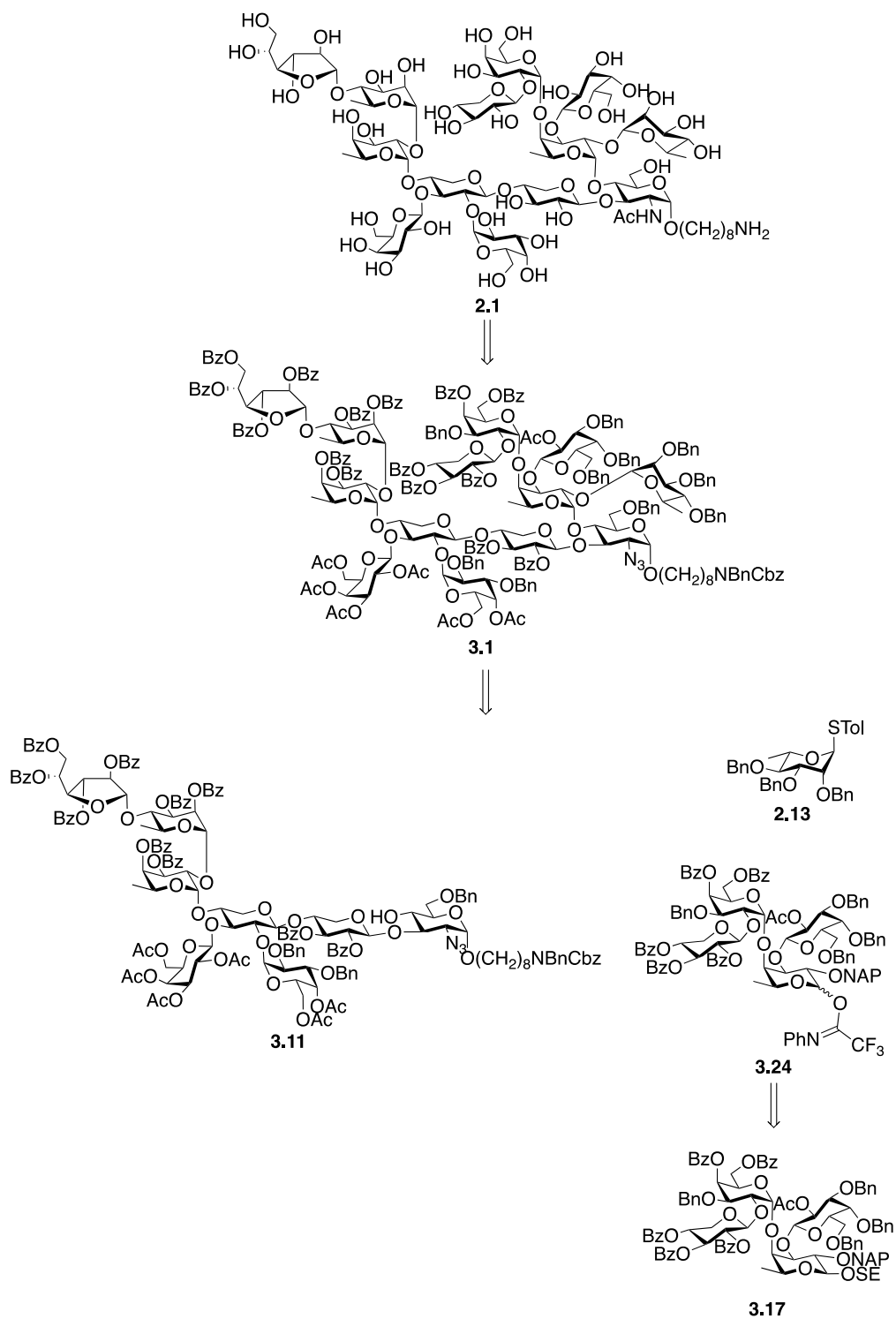
cleaved but also lacking the rhamnosyl residue and a water molecule. Another peak at  $m/z = 1565.5$ , corresponding to a compound with both the aglycon and rhamnosyl residue cleaved, was also present. The formation of these undesirable side products can be attributed to the lability of the rhamnosyl residue in acidic media. Glycosides of 6-deoxysugars are known to be more acid sensitive than their fully oxygenated counterparts<sup>22</sup> and it appears that the rhamnose in **3.19** is particularly sensitive. I propose that the driving force for the ease of release of the rhamnosyl residue from the molecule is that its removal decreases congestion in the molecule.



**Scheme 3-11:** Failed attempt to synthesize **3.20** from **3.19**.

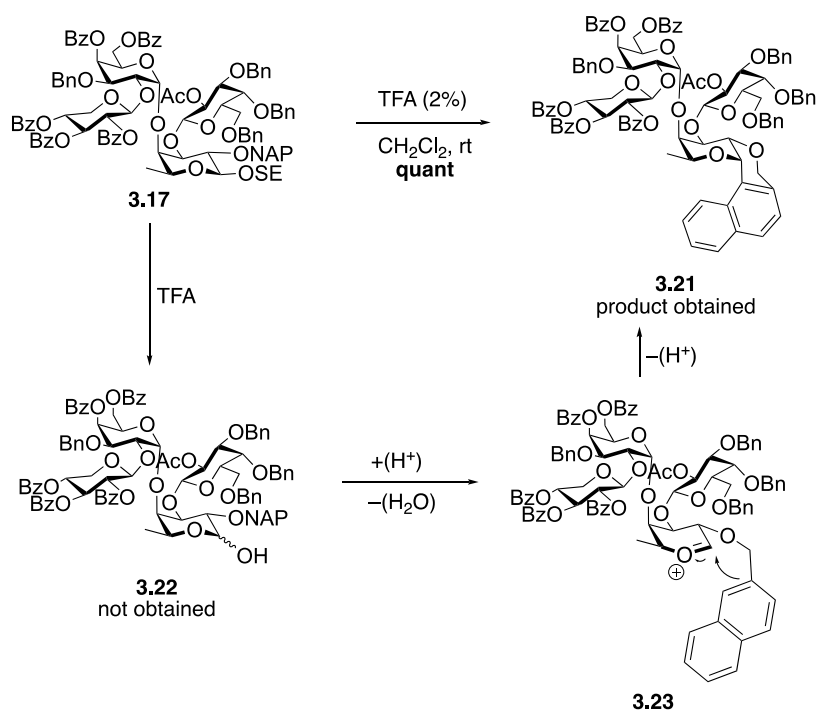
### 3.2.3.2 Synthesis of tetrasaccharide **3.24** and attempted [8+4] glycosylation.

Knowing that the route to convert pentasaccharide **3.19** into a suitable donor did not seem possible, I decided instead to create a donor from tetrasaccharide **3.17** and perform an [8+4] glycosylation and, after that reaction, add the rhamnose residue (Scheme 3-12). The idea for this approach is that **3.17** does not have the acid-labile rhamnose residue yet and this might avoid the formation of unwanted side products.



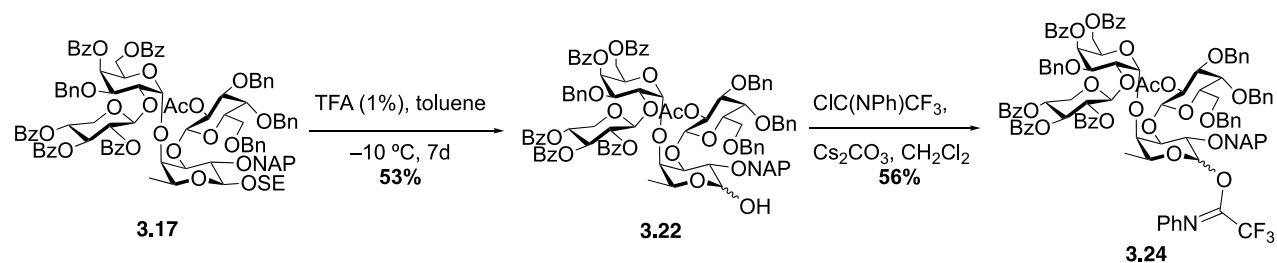
**Scheme 3-12:** Retrosynthetic analysis of tridecasaccharide **3.1** through a [8+4] glycosylation.

The first step in this conversion is the selective removal of the 2-trimethylsilylethyl aglycon in the tetrasaccharide by treatment of **3.17** with trifluoroacetic acid in CH<sub>2</sub>Cl<sub>2</sub> (Scheme 3-13). The product obtained from this reaction was not the desired hemiacetal but an unwanted less polar side product. Upon ESI-MS analysis, a peak at  $m/z = 1687.6$ , corresponding to a molecule lacking the 2-trimethylsilylmethyl aglycon and a water molecule, was observed. After NMR analysis, the structure of the side product was found to be **3.21**. The anomeric proton of the resulting carbasugar ( $\delta_{\text{H}} = 5.39$  ppm) was found to correlate with two aromatic carbons ( $\delta_{\text{C}} = 133.7$  and 127.3 ppm) in the NAP group. The regioselectivity of the reaction to the C-1 of the NAP group was confirmed after the loss of the usual broad singlet peak corresponding to the proton in the NAP protecting group. The formation of **3.21** can be explained through an intramolecular Friedel Crafts alkylation on the desired hemiacetal **3.22**. I hypothesized that the hemiacetal was formed during the reaction, but, due to the acidity of the solution, that it instantly loses water to give the corresponding oxocarbenium ion **3.23**. Subsequent nucleophilic attack of the pi electrons of the O-2 NAP group forms a bicyclic structure that, upon loss of a proton restores aromaticity to form **3.21**. Similar by-products were previously described in the work of Lin during an attempt to synthesize a ‘hyper-branched’ fucose residue found in ACTV-1 *N*-glycan.<sup>9</sup>



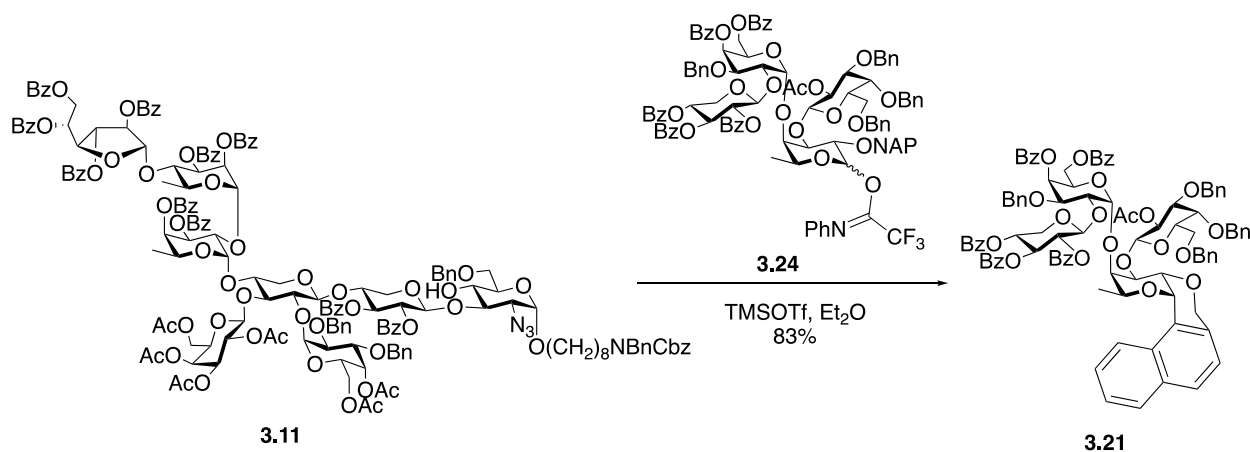
**Scheme 3-13:** Formation of unwanted product **3.21** and proposed mechanism for its formation.

If the proposed mechanism for the formation of the side product is correct, then in theory, the product can be isolated if the formation of the oxocarbenium ion or the attack of the NAP group can be suppressed. The acid concentration of the reaction mixture was decreased hoping that this would prevent the protonation of the hemiacetal but unfortunately, **3.21** was still the sole product. I then changed the solvent from dichloromethane to toluene hoping that the non-polar nature of the solvent medium would prevent the formation of charged intermediates.<sup>23</sup> This approach worked to give the desired hemiacetal, but only in 53% yield after seven days of reaction time. Nevertheless, this allowed me to proceed with the plan of transforming this tetrasaccharide into a *N*-phenyl trifluoroacetimidate donor **3.24** using 2,2,2-trifluoro-*N*-phenylacetimidoyl chloride and cesium carbonate in 56% yield (Scheme 3-14).



**Scheme 3-14:** Synthesis of **3.24** from **3.17**.

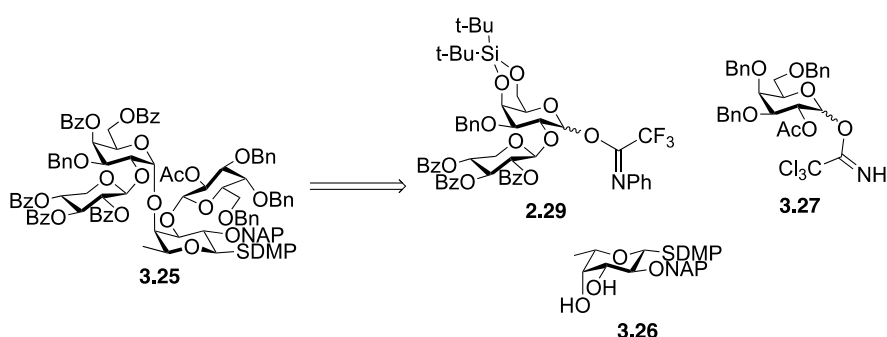
With tetrasaccharide donor **3.24** and octasaccharide acceptor **3.11** in hand, I moved forward with the planned [8+4] glycosylation (Scheme 3-15). The reaction was performed under TMSOTf activation but, unfortunately, the reaction did not give the desired product but instead gave the same Friedel-Crafts side product **3.21** in 83%. Presumably, the reaction proceeded by activation of the imidate donor to produce the oxocarbenium ion, which was followed by intramolecular attack of the nearby NAP group. Considering this failed glycosylation as well as the difficulty in synthesizing this imidate, I chose to abandon this route and looked for another one.



**Scheme 3-15:** An [8+4] glycosylation attempt between **3.11** and **3.24**.

### 3.2.3.3 Synthesis of tetrasaccharide **3.25** and attempted [8+4] glycosylation.

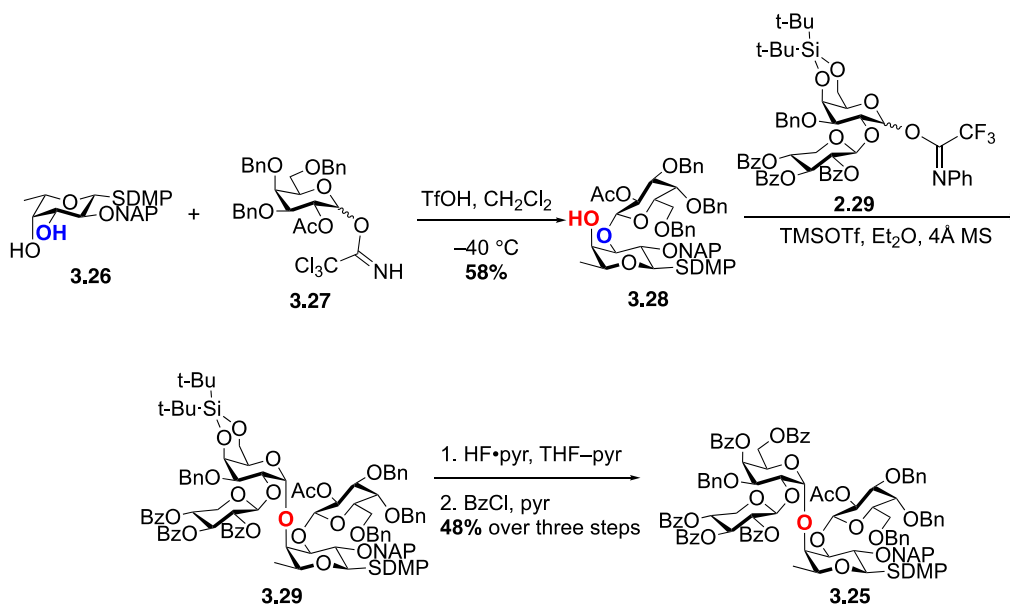
The previous [8+4] glycosylation route was unsuccessful, mainly due to the inefficient cleavage of the 2-trimethylsilylethyl aglycon. I therefore, decided to synthesize thioglycoside donor **3.25** so the need for conversion is not necessary (Scheme 3-16). I planned to synthesize **3.25** as a 2,6-dimethylphenyl thioglycoside to prevent unwanted aglycon transfer during glycosylation<sup>24</sup> reactions. The synthesis of compound **3.25** was envisioned to be done similarly with that of compound **3.24**.



**Scheme 3-16:** Retrosynthetic analysis of trisaccharide donor **3.25**.

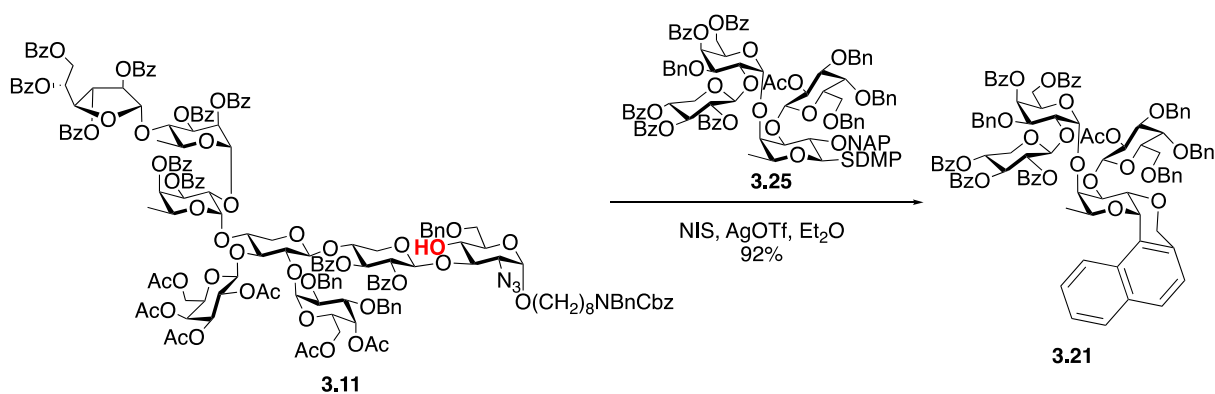
The synthesis started with diol thioglycoside acceptor **3.26**<sup>25</sup> and imidate donor **3.27**<sup>26</sup>, which were coupled using TfOH activation to afford **3.28**, in which O-3 of the acceptor is regioselective glycosylated, in 58% yield (Scheme 3-17). While this yield is relatively modest, I deemed it as acceptable considering the number of steps that were avoided. The regioselectivity was confirmed from the HMBC spectrum after observing a correlation between of Gal-H-1 and the Fuc-C-3. In addition, the  $\beta$ -stereoselectivity of the reaction was established by the coupling constant between Gal-H-1 and Gal-H-2 ( $^3J_{1,2} = 9.3$  Hz). Disaccharide **3.28** was then reacted with disaccharide imidate donor **2.29** and TMSOTf to produce tetrasaccharide **3.29**. Purification of **3.29** was unsuccessful and I decided to perform protecting group manipulations to separate the desired tetrasaccharide from the impurities. Thus, the DTBS protecting group was cleaved using HF–

pyridine and the hydroxyl groups of the resulting diol were protected as benzoyl groups using benzoyl chloride in pyridine. After purification, the desired tetrasaccharide **3.25** was obtained in 48% yield over three steps, including the glycosylation. The  $\alpha$ -selectivity of the glycosylation reaction was established by the coupling constant between Gal-H-1 and Gal-H-2 ( $^3J_{1,2} = 3.2$  Hz).



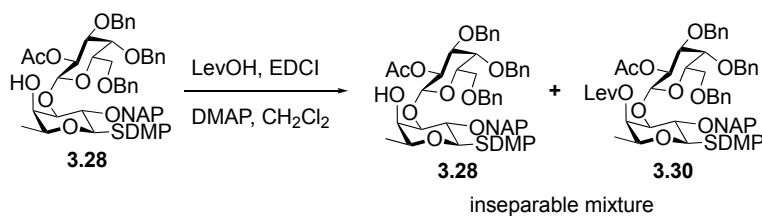
**Scheme 3-17:** Synthesis of donor **3.25**.

With this tetrasaccharide donor in hand, I proceeded with another [8+4] glycosylation attempt with octasaccharide acceptor **3.11** (Scheme 3-18). The reaction was performed with NIS-AgOTf activation in  $\text{Et}_2\text{O}$  but unfortunately, was unsuccessful. The main product was the bicyclic side product **3.21** in 92%, resulting from an intramolecular Friedel-Crafts reaction of the donor.



**Scheme 3-18:** An [8+4] glycosylation attempt between **3.11** and **3.25**.

These failed [8+4] glycosylation attempts led me to consider trying smaller donors for the glycosylation with **3.11**. My first idea was to create disaccharide thioglycoside donor **3.30** from **3.28** by Lev protection of the fucose C-4 hydroxyl group (Scheme 3-19). Attempts to perform this protection did not succeed. The reaction did not go to completion, even after a week, and the starting material and the product were inseparable in different eluent systems for column chromatography. It is important to have a pure donor for the glycosylation reactions and any trace of alcohol **3.28** could lead to multiple side products. Due to these reasons, I abandoned this route.

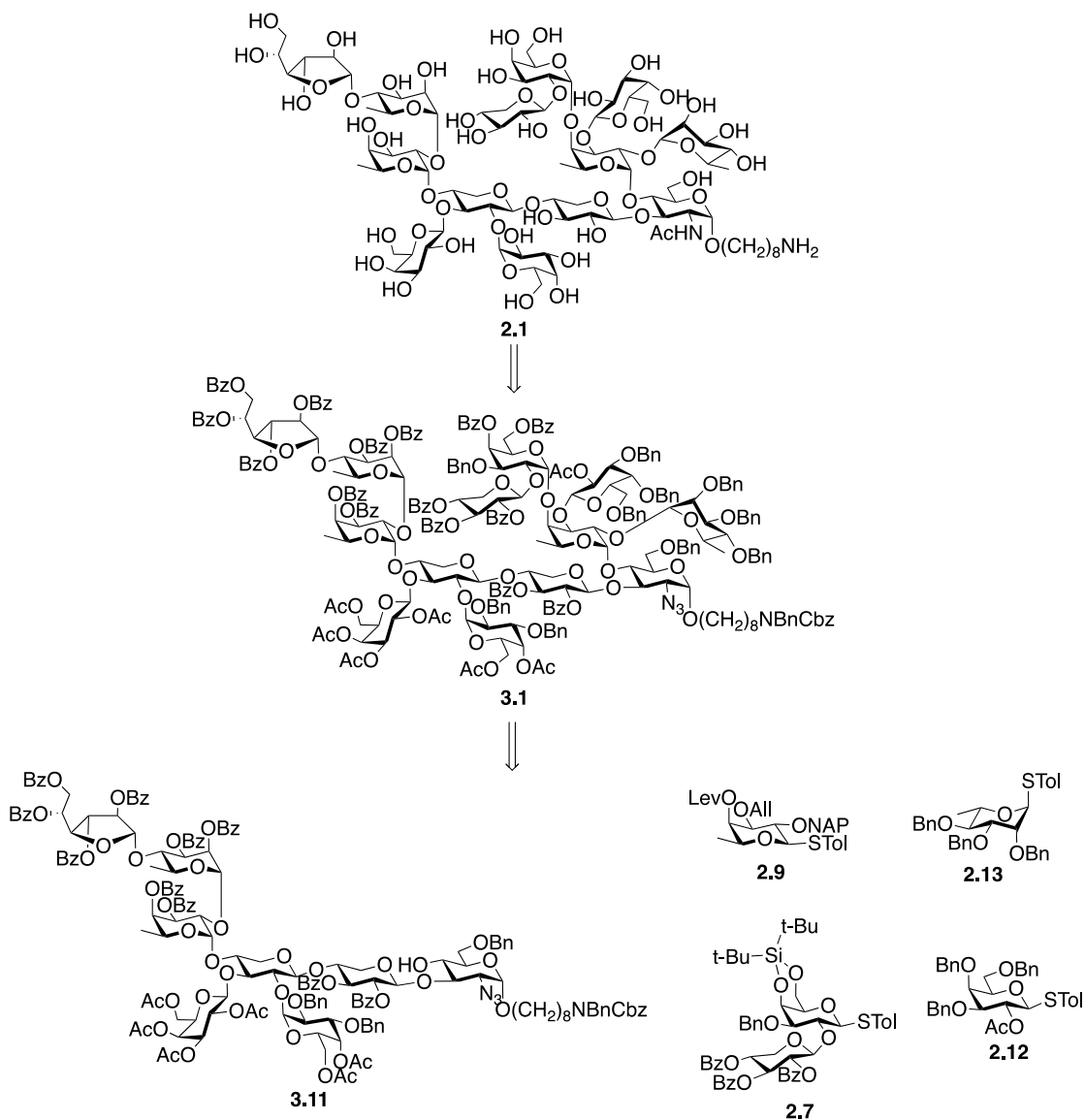


**Scheme 3-19:** Unsuccessful synthesis of disaccharide **3.30**.

### 3.2.4 Attempted linear synthesis towards the whole glycan structure.

With these failed attempts to perform a modular synthesis of **3.1**, I decided to add the remaining sugar residues in a linear fashion, starting with an [8+1] glycosylation between **3.11** and

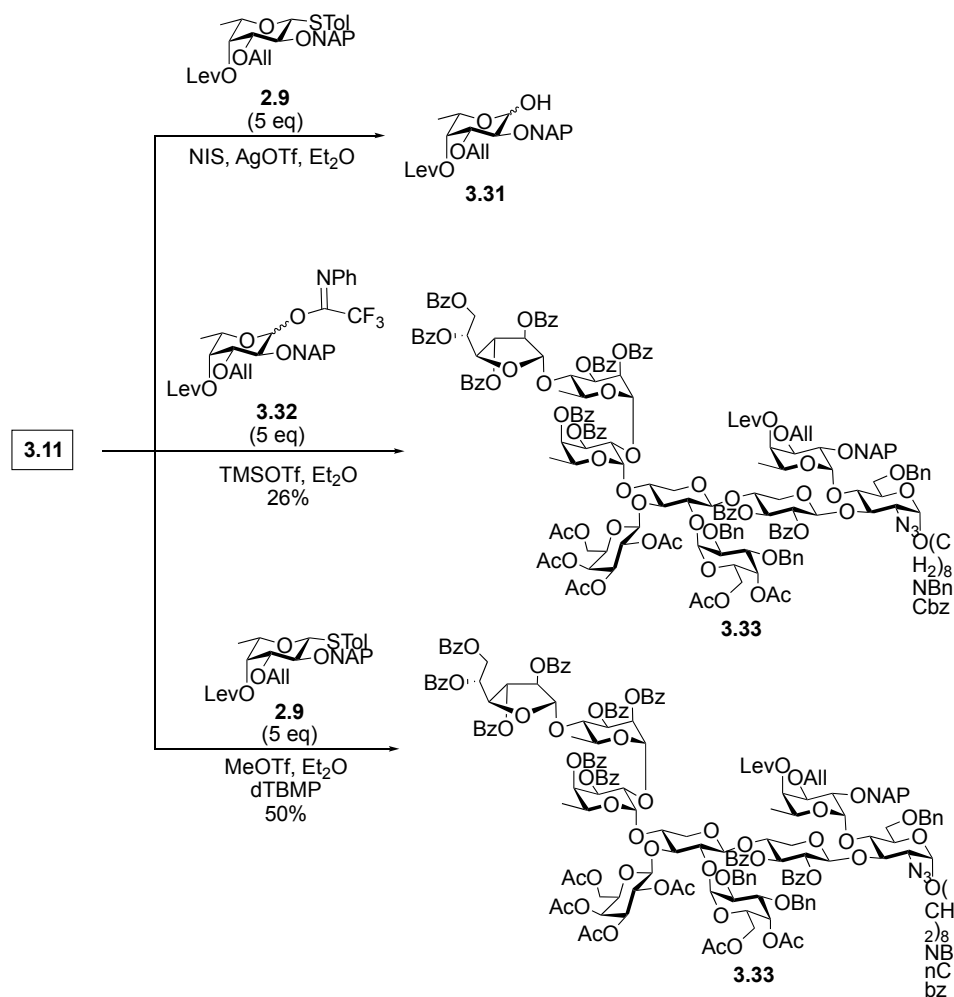
orthogonally protected fucose donor **2.9** (Scheme 3-20). The other sugar residues would be added to the fucose using donors **2.7**, **2.12**, and **2.13**. The glycosylation sequence to be used would be the ‘pendulum’ approach previously successfully employed to synthesize hexasaccharide **2.2**.



**Scheme 3-20:** Retrosynthetic analysis of tridecasaccharide **2.1** via a linear synthesis from **3.11**.

### 3.2.4.1 Synthesis of undecasaccharide 3.38.

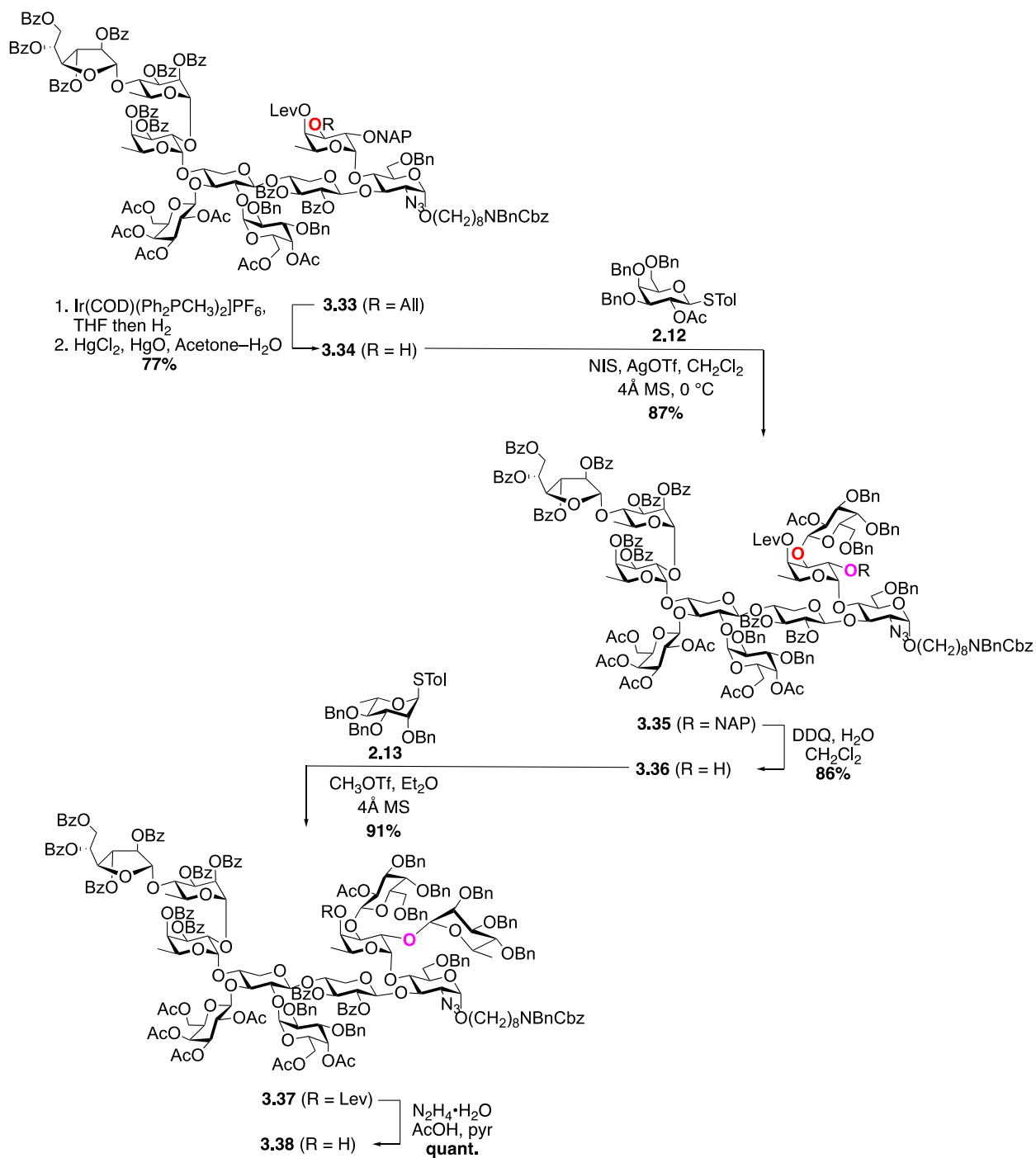
The linear synthesis of the whole glycan fragment started with the glycosylation of octasaccharide acceptor **3.11** with fucose donor **2.9** (Scheme 3-21). Activation with NIS–AgOTf was unsuccessful; only **3.11** and the hydrolyzed donor **3.31** were recovered, even after addition of five equivalents of the donor. With the recovered hydrolyzed donor in hand, I transformed it into imidate **3.32** in quantitative yield by treatment with 2,2,2-trifluoro-*N*-phenylacetamidoyl chloride and cesium carbonate. I then performed another [8+1] glycosylation with acceptor **3.11** and five equivalents of **3.32** using TMSOTf activation. This reaction gave the desired nonasaccharide **3.33** in 26% yield (52% based on recovered starting material) with 50% of the recovered acceptor. The reaction required a high equivalence of the donor because the donor hydrolyzed faster than its reaction with the acceptor. This yield was unsatisfactory and thus, I explored other methods for this glycosylation. Another method, which used MeOTf activation of thioglycosides with 2,6-di-*tert*-butyl-4-methylpyridine as an acid quencher, was explored with thioglycoside donor **2.9** and acceptor **3.11**. Again, this required five equivalents of the donor to obtain the desired product in 50% yield. However, the unreacted acceptor can be recovered increasing the reaction yield to 67% based on the recovered starting material. While this yield is not ideal at this stage of the synthesis, I accepted this result, and this was the first time I could make this bond using **3.11** and the acceptor could be recovered and be subjected again to the reaction. Although low yielding, the glycosylation proceeded with excellent  $\alpha$ -selectivity as evident by the coupling constant between Fuc-H-1 and Fuc-H-2 ( $^3J_{1,2} = 3.6$  Hz).



**Scheme 3-21:** Synthesis of **3.33** using acceptor **3.11** and donors **2.9** and **3.32**.

With the orthogonally protected fucose residue installed, I moved forward to employ the ‘pendulum’ approach to create the ‘hyper-branched’ fucose residue. The planned route required glycosylation first on O-3 followed by O-2 then lastly on O-4. Initially, nonasaccharide **3.33** was transformed to the desired acceptor **3.34** by the deprotection of allyl group at O-3 using hydrogen-activated  $[\text{Ir}(\text{COD})(\text{CH}_3\text{Ph}_2\text{P})_2]\text{PF}_6$  followed by cleavage of the resulting vinyl ether using mercuric chloride and mercuric oxide in acetone–water mixture to give the **3.34** in 77% yield (Scheme 3-22). With this acceptor in hand, the glycosylation reaction with galactosyl donor **2.12** was performed with NIS–AgOTf activation to give decasaccharide **3.35** in 87% yield. The desired

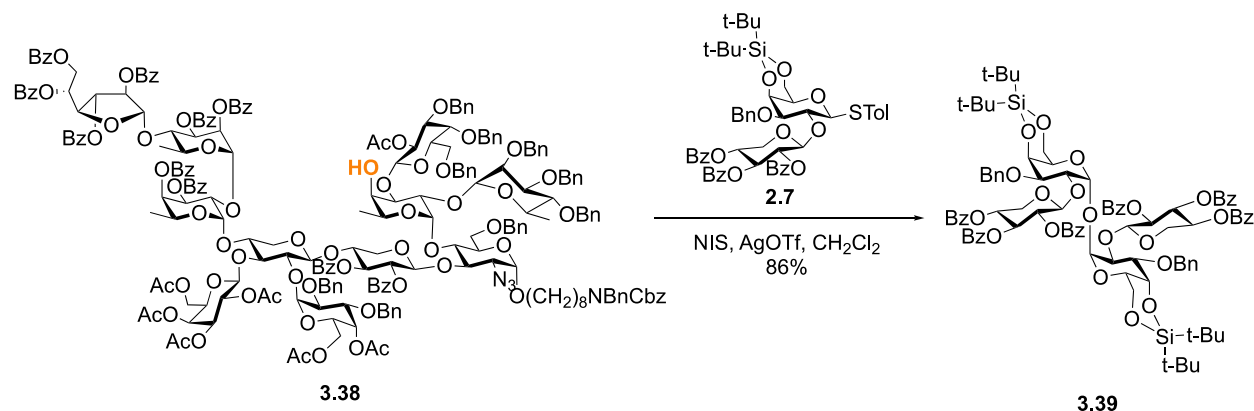
$\beta$ -linkage was assigned using the coupling constant between Gal-H-1 and Gal-H-2 ( ${}^3J_{1,2} = 7.8$  Hz). Subsequent deprotection of the NAP group at O-2 using DDQ in wet  $\text{CH}_2\text{Cl}_2$  afforded the desired decasaccharide acceptor **3.36** in 86% yield. Using this acceptor and rhamnosyl donor **2.13**, a NIS–AgOTf-promoted glycosylation was performed, giving the desired undecasaccharide **3.37** in 91% yield. The stereochemistry at the anomeric linkage was determined to be  $\alpha$ -linkage from the coupling constant between Rha-H-1 and Rha-C-1 ( ${}^1J_{\text{C-1-H-1}} = 170.6$  Hz) in the  ${}^1\text{H}$  coupled HSQC spectrum. Compound **3.37** was then subjected to a Lev deprotection under the usual conditions of hydrazine monohydrate in an acetic acid–pyridine mixture, which gave undecasaccharide acceptor **3.38** in quantitative yield.



**Scheme 3-22:** Synthesis of undecasaccharide **3.38**.

### 3.2.4.2 Attempted [11+2] glycosylation with undecasaccharide acceptor **3.38**.

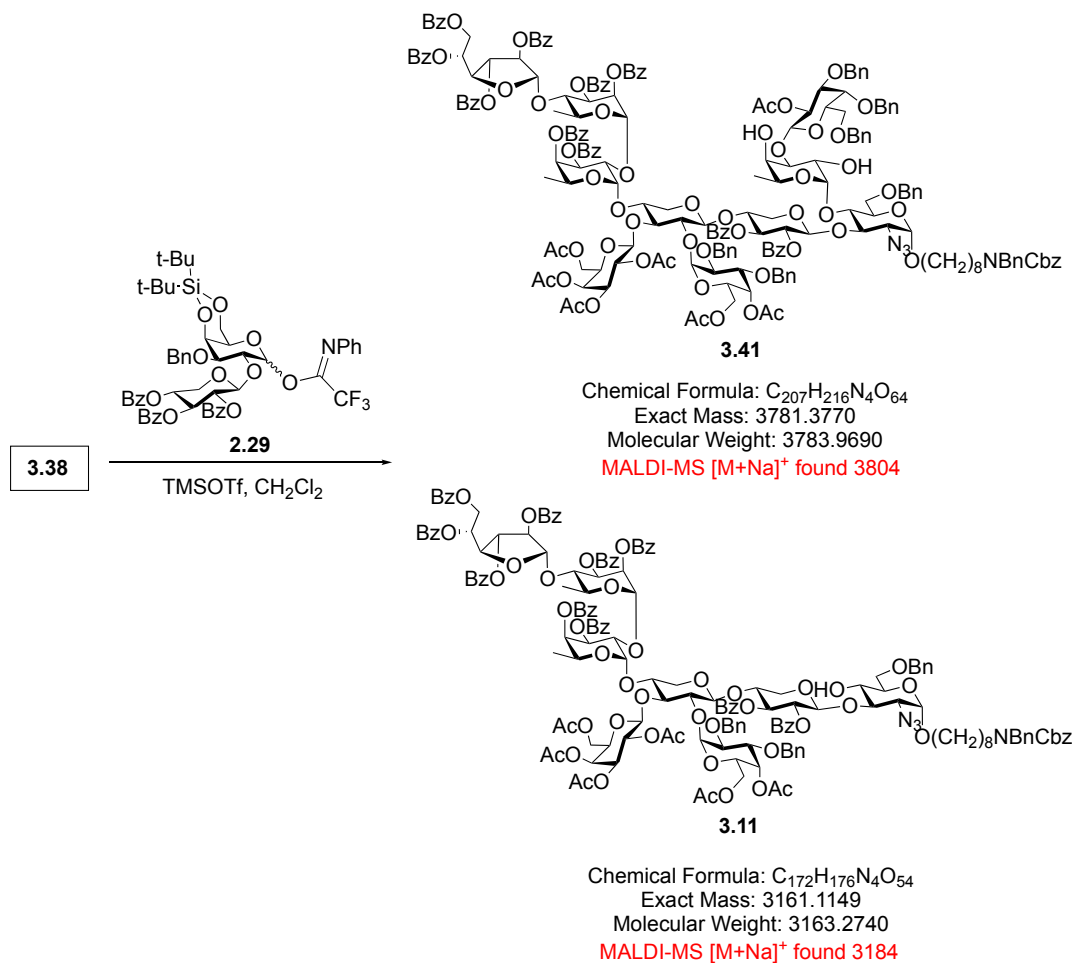
With acceptor **3.38** in hand, I attempted a possible final [11+2] glycosylation to create the 13-residue glycan framework. The glycosylation attempt started with undecasaccharide acceptor **3.38** and disaccharide thioglycoside donor **2.7** with NIS–AgOTf activation (Scheme 3-23). However, this attempt was unsuccessful; no desired product was formed and only dimerized donor **3.40** was recovered along with the unreacted acceptor **3.38**.



**Scheme 3-23:** Attempted [11+2] glycosylation with acceptor **3.38** and donor **2.7**.

Using a more reactive imidate donor **2.29** was hypothesized to improve the reaction outcome as seen in the synthesis of **2.30** in the previous chapter. Thus, acceptor **3.38** and imidate donor **2.29** were used in another glycosylation attempt using TMSOTf activation, but this reaction also did not succeed (Scheme 3-24). The acceptor was completely consumed but the desired product was not formed; instead, some acid labile residues were cleaved. MALDI-MS analysis of the products obtained from this reaction showed peaks at  $m/z = 3804.4$  and  $m/z = 3184.1$ , which correspond to compounds **3.41** and **3.11**, respectively. The cleavage of the rhamnosyl residue to give compound **3.41** was not surprising as it was observed previously in work described in this chapter. The fucose residue was also cleaved to give compound **3.11**. 6-deoxypyranosides are

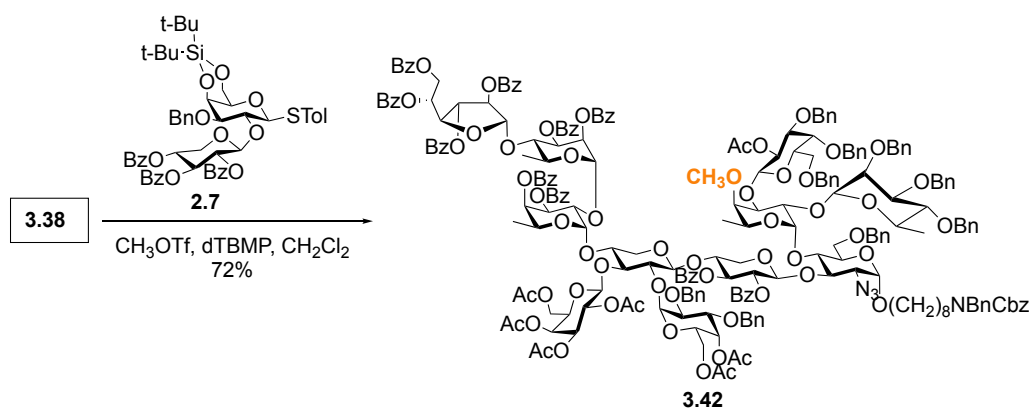
known to be more acid labile than their fully oxygenated pyranoside counterparts.<sup>22</sup> The sterically-crowded nature of this region of the molecule likely exacerbates this acid-lability as the cleavage of these motifs would be expected to relieve this congestion. Dimer **3.39** was also formed in 82% yield.



**Scheme 3-24:** Attempted [1+2] glycosylation with acceptor **3.38** and donor **2.29**.

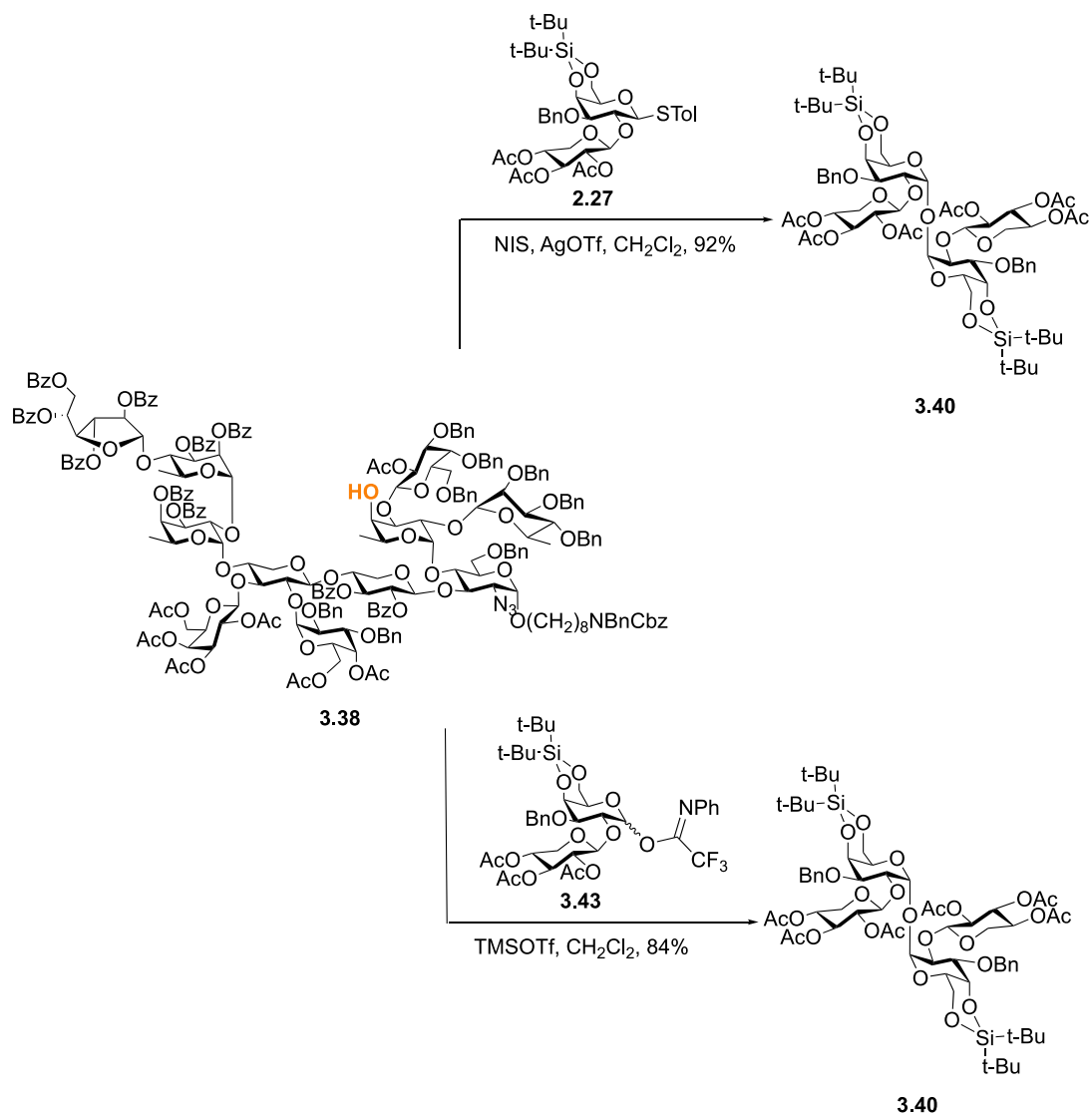
Observing that these residues in **3.38** appear to be extremely sensitive to acid, I performed a glycosylation with thioglycoside donor **2.7** under neutral conditions with MeOTf as the activator and dTBMP as an acid scavenger (Scheme 3-25). The glycosylation was performed but,

unfortunately, the desired product was not obtained. Instead, the reaction only gave the methylated acceptor **3.42** in 72% yield.



**Scheme 3-25:** Attempted [11+2] glycosylation with acceptor **3.38** and donor **2.7** under neutral conditions.

Another disaccharide thioglycoside, **2.27**, was available so I explored using this as a donor for this glycosylation (Scheme 3-26). As discussed previously, compounds **2.7** and **2.27** have different ring conformations in their xylose residue and this difference might change their properties as a donor. I performed glycosylation with either  $\text{NIS-AgOTf}$  and  $\text{MeOTf-dTBMP}$  activation systems but both reactions were unsuccessful to give the desired product but instead just gave dimerized donor **3.40**. Thioglycoside **2.27** was then converted to a more reactive imidate **3.43** in two steps. The thioglycoside donor was hydrolyzed using *N*-bromosuccinimide in wet  $\text{EtOAc}$  giving the corresponding hemiacetal, which was reacted with 2,2,2-trifluoro-*N*-phenylacetamidoyl chloride and cesium carbonate producing **3.43** in 73% yield over two steps. Attempted coupling of **3.43** and **3.38** with  $\text{TMSOTf}$  activation, unfortunately, still failed to give the desired product and only gave **3.40**.

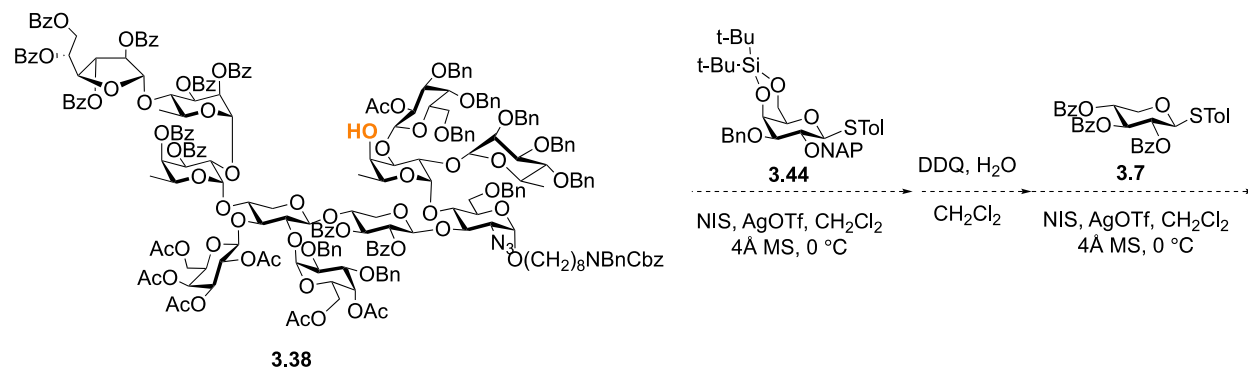


**Scheme 3-26:** Attempted [11+2] glycosylation with acceptor **3.38** and donors **2.27** and **3.43**.

### 3.2.5 Proposed synthetic routes towards synthesis of the whole glycan structure.

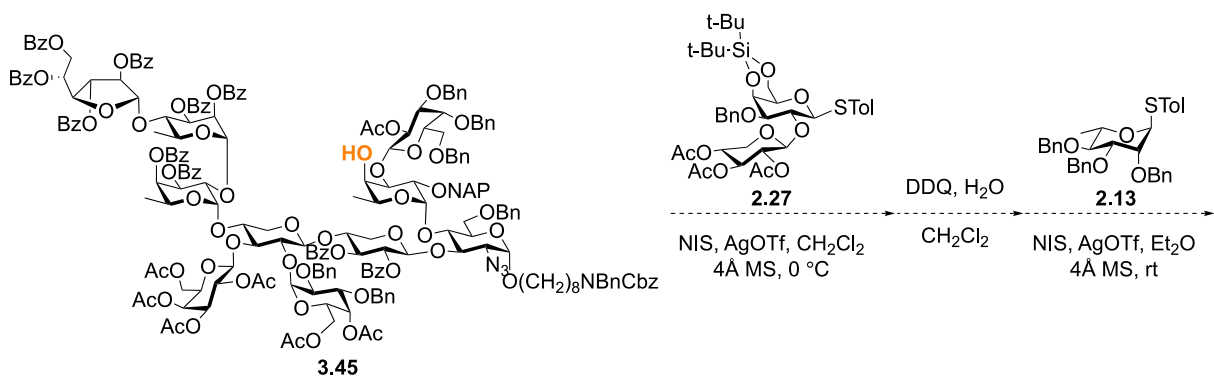
Unfortunately, my attempts to synthesize the whole glycan fragment **3.1** came to an end due to the limited amount of undecasaccharide **3.11** and time limitations. Given the multiple failed attempts on the final [11+2] glycosylation, there was not enough material to keep moving forward with the synthesis. If there were more time and materials, it would be worth to attempting other approaches to create the whole glycan structure. One of the approaches that could be successful is

to explore adding the last two residues one at a time instead as a disaccharide (Scheme 3-27). Using acceptor **3.38**, the last two sugar residues could be added stepwise using galactosyl donor **3.34** and xylosyl donor **3.7**. This strategy might allow the reaction to occur with smaller reacting partners. Compound **3.44** can be prepared from **2.10** in one step.



**Scheme 3-27:** Proposed synthesis of tridecasaccharide using linear addition of monosaccharide donors.

Another possible approach is to add the residues around the fucose residue in a different sequence. I have shown during the synthesis of the pentasaccharide **3.19** that a ‘reversed pendulum’ approach can also be employed to access the ‘hyper-branched’ fucose residue. In this approach (Scheme 3-28), the glycosylation at O-4 with donor **2.27** would be done first before at O-2 with donor **2.13**. Decasaccharide acceptor **3.45** could be synthesized from the previously described **3.35**.



**Scheme 3-28:** Proposed synthesis of tridecasaccharide by glycosylation on O-4 then O-2 at the fucose residue.

### 3.3 Summary and conclusions.

The work presented in this chapter described the attempted synthesis of the full antigenic glycan epitope of the *T. cruzi* glycoprotein GP72. This 13-residue glycan has a unique and complex structure containing two ‘hyper-branched’ residues, a fucose and a xylose. The synthesis of ‘hyper-branched’ oligosaccharides is challenging due to the increasing steric hindrance on the growing molecule, which affects both the yields and stereoselectivities of the reactions. The correct glycosylation sequence must be employed to obtain these highly congested carbohydrate targets.

The first attempt to synthesize the whole glycan fragment was to perform a [6+7] glycosylation between a hexasaccharide acceptor **3.2** and heptasaccharide donor **2.78**. Unfortunately, this attempt was futile. Smaller acceptors like trisaccharide acceptor **3.5** and tetrasaccharide acceptor **3.5** also did not react with donor **2.78** using multiple reaction conditions. Based on these failed attempts, I hypothesized that O-3 glycosylation of the 2-azido-2-deoxyglucose residue is not feasible if an existing glycosylation is at O-4. To circumvent this issue, glycosylation of O-3 of the 2-azido-2-deoxyglucose residue was performed first before O-4.

Glycosylation of acceptor **3.9** with donor **2.78** successfully provided octasaccharide **3.10**, which was transformed to acceptor **3.11** in a single step.

Following the success of the synthesis of octasaccharide acceptor **3.11**, I envisioned synthesizing the target glycan through an [8+5] glycosylation with pentasaccharide **3.12**, which I hoped to synthesize from 2-trimethylsilylethyl glycoside **3.19**. Pentasaccharide **3.19** contained a ‘hyper-branched’ residue and was successfully synthesized using the ‘reversed pendulum’ approach. However, the attempted synthesis of **3.12** from **3.19** was unsuccessful due to the lability of the rhamnose residue under the acidic conditions. Because of the failure to synthesize pentasaccharide donor **3.12**, I decided to rather perform a [8+4] glycosylation with tetrasaccharide donors **3.24** or **3.25**. Glycosylation of **3.11** with either **3.24** or **3.25** was unsuccessful, not giving the desired product but instead only producing the bicyclic side product **3.21**. Compound **3.21** was proposed to form as a result of an intramolecular Friedel-Crafts reaction of the oxocarbenium ion intermediate derived from the donor and the adjacent NAP ether.

The failed attempts to glycosylate octasaccharide **3.11** with a penta- or tetrasaccharide led me to the linear addition of the rest of the sugar residues. A successful reaction between **3.11** and orthogonally protected fucosyl donor **2.9** gave desired nonasaccharide **3.33**. The rest of the sugar residues on the ‘hyper-branched’ fucose residue were planned to be added in the same ‘pendulum’ glycosylation sequence as previously applied for similar hexasaccharide **2.2**. Glycosylations on O-3 followed by on O-2 were successful to give eventually undecasaccharide **3.38**. The proposed final [11+2] glycosylation reaction was attempted using various donors and reaction conditions, but all the attempts were unsuccessful. One of the reasons for the failure of some of the attempts is the weak reactivity of the acceptor **3.38** causing the donor to either undergo hydrolysis or form

the donor dimer. In addition, some sugar residues in acceptor **3.38** were prone to cleavage in the acidic conditions of the glycosylation.

Due to the limited and depleted amount of undecasaccharide **3.38** and the number of steps required to synthesize it, I have decided to finish my work at this point but have proposed other synthetic routes to be investigated in the future. The addition of the last two residues onto **3.38** in a stepwise manner might give the desired product. Another possible approach is to investigate another glycosylation sequence wherein glycosylation on O-4 of the fucose residue is done before on O-2.

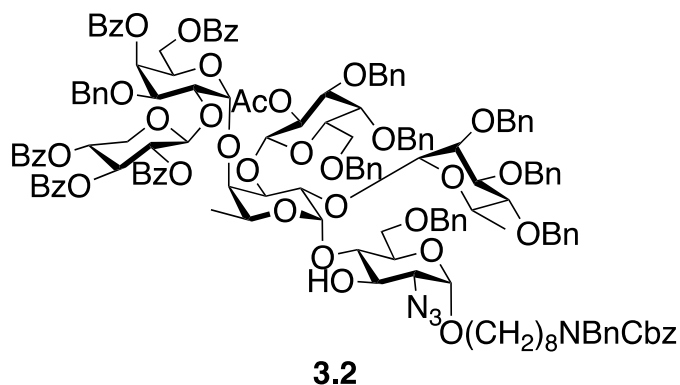
While the synthesis of the whole glycan structure was not fully achieved, this research has still described significant progress on the synthesis of a complex glycan structure containing two ‘hyper-branched’ sugar residues. My findings could be employed in the synthesis of similar complex glycans containing ‘hyper-branched’ residues. While each of these glycans are composed of different sugar residue and linkages, the strategies used in this research can be explored and applied to see their feasibility in the syntheses of other glycans.

### **3.4 Experimental methods**

**General Methods:** All chemicals and reagents were purchased from commercial sources and were used without further purification unless noted. Reaction solvents (THF and CH<sub>2</sub>Cl<sub>2</sub>) were taken from a solvent purification system in which the solvents were purified by successive passage through columns of alumina and copper under argon. Unless stated otherwise, all reactions were carried out at room temperature and under a positive pressure of argon and were monitored by TLC on Silica Gel G-25 F254 (0.25 mm, Merck). Visualization of the reaction components on TLC was achieved using UV light (254 nm) and/or by charring after treatment with a solution of

*p*-anisaldehyde (3.7 mL) and glacial acetic acid (1.5 mL) and concentrated H<sub>2</sub>SO<sub>4</sub> (5 mL) in ethanol (135 mL). Organic solvents were evaporated under reduced pressure, and the products were purified by column chromatography on silica gel (70 mesh). Optical rotations were measured on a Jasco P-2000 digital polarimeter at the sodium D line (589 nm) at 25 ± 2 °C and are in units of (deg·mL)/(dm·g). <sup>1</sup>H NMR spectra were recorded at 500 MHz or 600 MHz and the chemical shifts are referenced to residual CHCl<sub>3</sub> (7.26 ppm, CDCl<sub>3</sub>) or HDO (4.78 ppm, D<sub>2</sub>O). <sup>13</sup>C NMR spectra were recorded at 126 MHz or 151 MHz and are proton decoupled, and the chemical shifts are referenced to CDCl<sub>3</sub> (77.0 ppm, CDCl<sub>3</sub>) or internal acetone (31.45 ppm, D<sub>2</sub>O). Standard splitting patterns are abbreviated: s (singlet), d (doublet), t (triplet), q (quartet), m (multiplet). To unequivocally assign the <sup>1</sup>H and <sup>13</sup>C NMR data, the protons and carbons corresponding to the monosaccharide at the reducing end were unprimed, while those corresponding to the next monosaccharide were labelled as H' and C', and the next furthest from the reducing end H'' and C'', and so on. For larger oligosaccharides (tetrasaccharides and/or larger) where assignment of all <sup>1</sup>H and <sup>13</sup>C NMR data cannot be done unambiguously due to overlapping peaks, only the anomeric data were reported. For example, the anomeric proton and carbon for an α-L-rhamnopyranoside will be labelled as α-Rhap-H-1 and α-Rhap-C-1, respectively. In cases where more than one residue have the same sugar identity and anomeric configuration, e.g., two β-D-galactopyranosides, are present in the same molecule, the residue closest to the reducing end of the longest chain will be labelled as β-Galp-H-1 and β-Galp-C-1, and the next furthest from the reducing end β-Galp'-H-1 and β-Galp'-C-1. High resolution and high mass accuracy LC-MS experiments were done on a LTQFT Ultra (Linear quadrupole ion trap Fourier transform ion cyclotron resonance) mass spectrometer (Thermo Electron, San Jose, CA) equipped with a HESI-II source, an Agilent 1100 Series binary high-performance liquid chromatography pump (Agilent

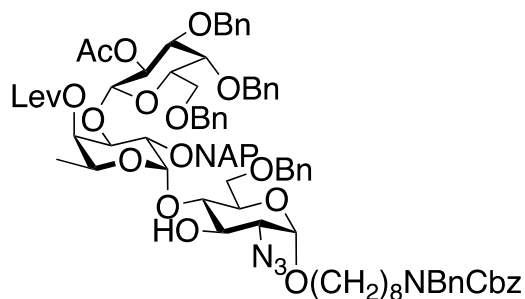
Technologies, Palo Alto, CA), and a Famos autosampler (LC Packings, San Francisco, CA). High resolution MALDI-TOF mass spectra were conducted on a New ultrafleXtreme™ MALDI-TOF/TOF mass spectrometer (Bruker Corporation, Bremen, Germany) using DHB (2,5-dihydroxybenzoic acid) as the matrix.



***N*-benzyl-*N*-benzoxycarbonyl-8-aminooctyl 2-*O*-acetyl-3,4,6-tri-*O*-benzyl- $\beta$ -D-galactopyranosyl-(1 $\rightarrow$ 3)-[2,3,4-tri-*O*-benzyl- $\alpha$ -L-rhamnopyranosyl-(1 $\rightarrow$ 2)]-[2,3,4-tri-*O*-benzoyl- $\beta$ -D-xylopyranosyl-(1 $\rightarrow$ 2)]-3-*O*-benzyl-4,6-di-*O*-benzoyl- $\alpha$ -D-galactopyranosyl-(1 $\rightarrow$ 4)]- $\alpha$ -L-fucopyranosyl-(1 $\rightarrow$ 4)-2-azido-6-*O*-benzyl-2-deoxy- $\alpha$ -D-glucopyranoside (**3.2**)**

To a stirred solution of **2.46** (15.0 mg, 0.00548 mmol) in dry 1,2-dichloroethane (0.06 mL) at 70 °C was added trimethyltin hydroxide (10.0 mg, 0.0548 mmol). The reaction mixture was stirred overnight before it was cooled to room temperature and then diluted with CH<sub>2</sub>Cl<sub>2</sub> (10 mL). The solution was filtered through Celite and the filtrate was concentrated to dryness. The crude residue was purified by flash chromatography (2:1 hexanes-EtOAc) to afford **3.2** (12.2 mg, 86%) as a colorless oil: *R<sub>f</sub>* = 0.18 (2:1 hexanes-EtOAc); <sup>1</sup>H NMR (500 MHz, CDCl<sub>3</sub>)  $\delta$  8.13–8.00 (m, 4H), 7.99–7.84 (m, 5H), 7.83–7.64 (m, 2H), 7.64–7.57 (m, 2H), 7.54–7.42 (m, 7H), 7.41–7.26 (m, 25H), 7.26–6.95 (m, 29H), 6.94–6.82 (m, 1H), 5.82 (app t, *J* = 9.5 Hz, 1H), 5.78–5.66 (m, 2H), 5.66–5.41 (m, 2H), 5.38–5.22 (m, 1H), 5.22–5.11 (m, 3H), 5.06 (s, 1H), 5.06–4.92 (m, 2H), 4.86 (d, *J* =

3.7 Hz, 1H), 4.92–4.74 (m, 2H), 4.74–4.54 (m, 8H), 4.54–4.46 (m, 2H), 4.42 (d,  $J = 11.5$  Hz, 1H), 4.54–4.31 (m, 7H), 4.31–4.08 (m, 8H), 4.08–3.91 (m, 4H), 3.90–3.69 (m, 6H), 3.70–3.56 (m, 5H), 3.56–3.43 (m, 3H), 3.42 (app q,  $J = 7.8$  Hz, 1H), 3.31–3.20 (m, 1H), 3.20–3.11 (m, 1H), 3.18 (dd,  $J = 10.3, 3.5$  Hz, 1H), 1.97–1.83 (m, 3H), 1.52–1.41 (m, 4H), 1.32–1.17 (m, 14H);  $^{13}\text{C}$  NMR (126 MHz,  $\text{CDCl}_3$ )  $\delta$  170.1, 166.2, 165.9, 165.6, 165.4, 156.9, 138.7, 138.1, 137.5, 136.9, 133.8, 133.5, 133.2, 130.3, 130.0, 130.0, 129.7, 129.6, 129.5, 129.3, 128.7, 128.7, 128.6, 128.6, 128.5, 128.4, 128.4, 128.3, 128.2, 128.2, 128.0, 127.9, 127.8, 127.7, 127.7, 127.6, 127.4, 127.3, 127.0, 77.4, 77.2, 76.9, 75.4, 73.5, 73.3, 72.2, 71.9, 69.5, 68.7, 67.3, 60.6, 50.6, 50.3, 47.3, 46.4, 36.8, 33.8, 33.3, 32.1, 29.9, 29.5, 29.4, 28.6, 28.2, 27.8, 26.9, 26.0, 24.8, 23.5, 22.8, 21.3, 21.2, 18.4, 14.3; HRMS (MALDI–TOF)  $m/z$ :  $[\text{M} + \text{Na}]^+$  Calcd for  $\text{C}_{151}\text{H}_{158}\text{N}_4\text{NaO}_{35}$  2610.0603; Found 2610.0615.



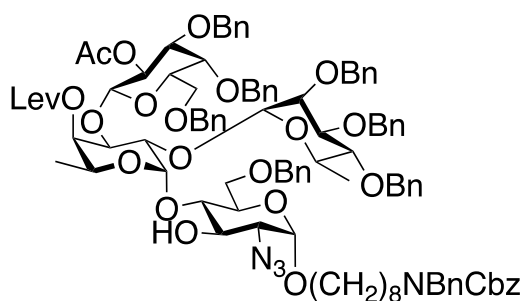
**3.5**

***N*-benzyl-*N*-benzoxycarbonyl-8-aminooctyl 2-*O*-acetyl-3,4,6-tri-*O*-benzyl- $\beta$ -D-galactopyranosyl-(1 $\rightarrow$ 3)-4-*O*-levulinoyl-2-*O*-(2-naphthyl)methyl- $\alpha$ -L-fucopyranosyl-(1 $\rightarrow$ 4)-2-azido-6-*O*-benzyl-2-deoxy- $\alpha$ -D-glucopyranoside (3.5)**

To a stirred solution of **2.40** (20.0 mg, 0.0119 mmol) in dry 1,2-dichloroethane (0.12 mL) at 70 °C was added trimethyltin hydroxide (21.5 mg, 0.119 mmol). The reaction mixture was stirred overnight before it was cooled to room temperature and then diluted with  $\text{CH}_2\text{Cl}_2$  (10 mL). The solution was filtered through Celite and the filtrate was concentrated to dryness. The crude residue

was purified by flash chromatography (3:2 hexanes–EtOAc) to afford **3.5** (16.0 mg, 88%) as a white solid:  $R_f = 0.28$  (1:1 hexanes–EtOAc);  $[\alpha]_D^{25} +15.0$  ( $c = 0.02$ ,  $\text{CHCl}_3$ );  $^1\text{H NMR}$  (600 MHz,  $\text{CDCl}_3$ )  $\delta$  7.76–7.71 (m, 2H, Ar), 7.71–7.67 (m, 1H, Ar), 7.60–7.56 (m, 1H, Ar), 7.50–7.47 (m, 1H, Ar), 7.46–7.38 (m, 2H, Ar), 7.38–7.31 (m, 4H, Ar), 7.32–7.26 (m, 10H, Ar), 7.25–7.15 (m, 12H, Ar), 7.15–7.11 (m, 2H, Ar), 7.10–7.06 (m, 2H, Ar), 5.39 (dd,  $J = 10.0, 7.7$  Hz, 1H, H-2''), 5.21–5.12 (m, 3H, H-4', 2 x  $\text{OCH}_2\text{Ar}$ ), 5.04 (d,  $J = 11.6$  Hz, 1H,  $\text{OCH}_2\text{Ar}$ ), 4.95 (d,  $J = 4.6$  Hz, 1H, H-1'), 4.94 (d,  $J = 11.6$  Hz, 1H,  $\text{OCH}_2\text{Ar}$ ), 4.85 (d,  $J = 3.5$  Hz, 1H, H-1), 4.75 (d,  $J = 11.6$  Hz, 1H,  $\text{OCH}_2\text{Ar}$ ), 4.68 (d,  $J = 12.1$  Hz, 1H,  $\text{OCH}_2\text{Ar}$ ), 4.54 (d,  $J = 11.8$  Hz, 1H,  $\text{OCH}_2\text{Ar}$ ), 4.52 (d,  $J = 12.1$  Hz, 1H,  $\text{OCH}_2\text{Ar}$ ), 4.52 (d,  $J = 7.5$  Hz, 1H, H-1''), 4.51–4.46 (m, 2H,  $\text{NCH}_2\text{Ph}$ ), 4.31 (dd,  $J = 10.0, 3.7$  Hz, 1H, H-3'), 4.28 (d,  $J = 12.3$  Hz, 1H,  $\text{OCH}_2\text{Ar}$ ), 4.25 (d,  $J = 12.0$  Hz, 1H,  $\text{OCH}_2\text{Ar}$ ), 4.25 (d,  $J = 12.0$  Hz, 1H,  $\text{OCH}_2\text{Ar}$ ), 4.21 (d,  $J = 12.0$  Hz, 1H,  $\text{OCH}_2\text{Ar}$ ), 4.21 (d,  $J = 12.0$  Hz, 1H,  $\text{OCH}_2\text{Ar}$ ), 4.06–4.03 (m, 1H, H-5'), 4.00 (app td,  $J = 9.9, 1.5$  Hz, 1H, H-3), 3.97 (d,  $J = 2.8$  Hz, 1H, H-4''), 3.78 (dd,  $J = 10.2, 4.3$  Hz, 1H, H-2'), 3.78–3.74 (m, 1H, H-5), 3.72 (dd,  $J = 10.8, 4.3$  Hz, 1H, H-6a), 3.66–3.56 (m, 4H, H-6b, H-6a'', H-4, H-5''), 3.55 (dd,  $J = 10.0, 2.8$  Hz, 1H, H-3''), 3.51–3.46 (m, 1H, H-6b''), 3.42–3.35 (m, 1H, octyl  $\text{OCH}_2$ ), 3.28–3.20 (m, 1H, octyl  $\text{NCH}_2$ ), 3.20–3.14 (m, 1H, octyl  $\text{NCH}_2$ ), 3.16 (dd,  $J = 10.2, 3.5$  Hz, 1H, H-2), 2.76–2.52 (m, 4H,  $\text{COCH}_2\text{CH}_2\text{COCH}_3$ ), 2.07 (s, 3H,  $\text{COCH}_3$ ), 2.05 (s, 3H,  $\text{COCH}_3$ ), 1.66–1.54 (m, 2H,  $\text{OCH}_2\text{CH}_2$ ), 1.54–1.42 (m, 2H,  $\text{NCH}_2\text{CH}_2$ ), 1.29–1.19 (m, 8H, 4 x  $\text{CH}_2$ ), 1.07 (d,  $J = 6.5$  Hz, 3H, H-6');  $^{13}\text{C NMR}$  (151 MHz,  $\text{CDCl}_3$ )  $\delta$  206.2 (C=O), 172.2 (C=O), 169.9 (C=O), 157.2 (C=O), 138.7 (Ar), 138.0 (Ar), 138.0 (Ar), 137.9 (Ar), 136.0 (Ar), 133.4 (Ar), 133.2 (Ar), 128.7 (Ar), 128.6 (Ar), 128.5 (Ar), 128.4 (Ar), 128.3 (Ar), 128.2 (Ar), 128.1 (Ar), 128.0 (Ar), 127.9 (Ar), 127.8 (Ar), 127.7 (Ar), 127.5 (Ar), 127.5 (Ar), 127.4 (Ar), 126.8 (Ar), 126.0 (Ar), 125.9 (Ar), 99.4 (C-1'), 99.2 (C-1''), 97.8 (C-1), 81.4 (C-4), 80.7 (C-3''), 74.7 ( $\text{OCH}_2\text{Ar}$ ), 74.7 (C-3'), 74.5 ( $\text{OCH}_2\text{Ar}$ ),

73.9 (C-5''), 73.6 (C-2'), 73.2 (OCH<sub>2</sub>Ar), 73.2 (OCH<sub>2</sub>Ar), 72.9 (C-4''), 72.3 (OCH<sub>2</sub>Ar), 71.8 (OCH<sub>2</sub>Ar), 71.5 (C-2''), 71.3 (C-4'), 69.8 (C-3), 69.4 (C-5), 68.7 (octyl OCH<sub>2</sub>), 68.5 (C-6''), 68.5 (C-6), 67.3 (OCH<sub>2</sub>Ar), 66.6 (C-5'), 62.6 (C-2), 50.3 (NCH<sub>2</sub>Ph), 46.2 (octyl NCH<sub>2</sub>), 37.8 (COCH<sub>2</sub>CH<sub>2</sub>COCH<sub>3</sub>), 29.9 (COCH<sub>3</sub>), 29.3 (CH<sub>2</sub>), 29.3 (CH<sub>2</sub>), 29.1 (OCH<sub>2</sub>CH<sub>2</sub>), 28.0 (NCH<sub>2</sub>CH<sub>2</sub>), 28.2 (COCH<sub>2</sub>CH<sub>2</sub>COCH<sub>3</sub>), 26.7 (CH<sub>2</sub>), 26.0 (CH<sub>2</sub>), 21.3 (COCH<sub>3</sub>), 16.3 (C-6'); HRMS (MALDI-TOF) *m/z*: [M + Na]<sup>+</sup> Calcd for C<sub>87</sub>H<sub>100</sub>N<sub>4</sub>NaO<sub>19</sub> 1527.6879; Found 1527.6848.

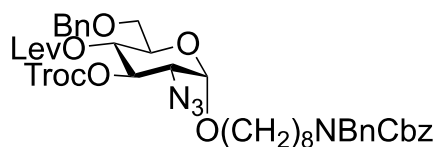


**3.6**

***N*-benzyl-*N*-benzoxycarbonyl-8-aminooctyl 2-*O*-acetyl-3,4,6-tri-*O*-benzyl-β-*D*-galactopyranosyl-(1→3)-[2,3,4-tri-*O*-benzyl-α-*L*-rhamnopyranosyl-(1→2)]-4-*O*-levulinoyl-α-*L*-fucopyranosyl-(1→4)-2-azido-6-*O*-benzyl-2-deoxy-α-*D*-glucopyranoside (3.6)**

To a stirred solution of **2.43** (25.0 mg, 0.0128 mmol) in dry 1,2-dichloroethane (0.13 mL) at 70 °C was added trimethyltin hydroxide (23.0 mg, 0.128 mmol). The reaction mixture was stirred overnight before it was cooled to room temperature and then diluted with CH<sub>2</sub>Cl<sub>2</sub> (10 mL). The solution was filtered through Celite and the filtrate was concentrated to dryness. The crude residue was purified by flash chromatography (3:2 hexanes–EtOAc) to afford **3.6** (19.0 mg, 88%) as a white solid: *R<sub>f</sub>* = 0.14 (3:2 hexanes–EtOAc); [α]<sub>D</sub><sup>25</sup> +10.5 (*c* = 0.04, CHCl<sub>3</sub>); <sup>1</sup>H NMR (500 MHz, CDCl<sub>3</sub>) δ 7.40–7.22 (m, 34H), 7.20–7.15 (m, 5H), 7.15–7.11 (m, 3H), 7.11–7.07 (m, 3H), 5.33 (dd, *J* = 10.0, 7.9 Hz, 1H), 5.22–5.13 (m, 3H), 4.91 (d, *J* = 2.8 Hz, 1H, α-Fucp-H-1), 4.87 (d, *J* = 10.2

Hz, 1H), 4.86 (d,  $J = 3.0$  Hz, 1H,  $\alpha$ -Rhap-H-1), 4.86 (d,  $J = 3.1$  Hz, 1H,  $\alpha$ -GlcN<sub>3p</sub>-H-1), 4.90–4.85 (m, 3H), 4.72 (d,  $J = 12.6$  Hz, 1H), 4.69–4.65 (m, 2H), 4.62 (d,  $J = 11.7$  Hz, 1H), 4.60–4.53 (m, 2H), 4.53–4.45 (m, 6H), 4.44 (d,  $J = 8.0$  Hz, 1H,  $\beta$ -Galp-H-1), 4.40 (d,  $J = 12.0$  Hz, 1H), 4.26–4.17 (m, 3H), 4.17–4.10 (m, 2H), 3.94 (app t,  $J = 9.2$  Hz, 1H), 3.91–3.84 (m, 3H), 3.81 (dd,  $J = 10.3, 5.3$  Hz, 1H), 3.74–3.58 (m, 4H), 3.59–3.51 (m, 3H), 3.48 (dd,  $J = 10.0, 2.7$  Hz, 1H), 3.46–3.36 (m, 1H), 3.30–3.21 (m, 2H), 3.21–3.12 (m, 2H), 2.87–2.53 (m, 4H), 2.19 (s, 3H), 2.00 (s, 3H), 1.61–1.47 (m, 4H), 1.37–1.17 (m, 8H), 1.31 (d,  $J = 6.2$  Hz, 3H), 1.17 (d,  $J = 6.7$  Hz, 3H); <sup>13</sup>C NMR (126 MHz, CDCl<sub>3</sub>)  $\delta$  206.3, 172.0, 169.6, 156.9, 156.3, 139.1, 138.9, 138.6, 138.5, 138.2, 138.1, 138.0, 138.0, 137.1, 134.6, 129.9, 129.2, 128.7, 128.6, 128.5, 128.5, 128.3, 128.2, 128.1, 128.0, 128.0, 127.9, 127.9, 127.9, 127.8, 127.8, 127.7, 127.5, 127.5, 127.4, 100.1 ( $\beta$ -Galp-H-1), 97.6 ( $\alpha$ -GlcN<sub>3p</sub>-C-1), 97.5 ( $\alpha$ -Rhap-C-1), 97.3 ( $\alpha$ -Fucp-C-1), 81.6, 81.0, 80.6, 80.3, 75.4, 75.0, 73.9, 73.8 (2 x C), 73.4, 73.0 (2 x C), 72.6, 72.2, 71.4, 71.1, 70.6, 70.4, 69.9, 69.1, 68.8, 68.7, 68.7, 67.8, 67.3, 62.5, 50.6, 50.3, 47.4, 46.4, 38.1, 29.9, 29.9, 29.4, 29.1, 28.1, 26.9, 26.0, 22.8, 21.3, 18.1, 15.8; HRMS (MALDI-TOF)  $m/z$ :  $[M + Na]^+$  Calcd for C<sub>103</sub>H<sub>120</sub>N<sub>4</sub>NaO<sub>23</sub> 1803.8240; Found 1803.8248.

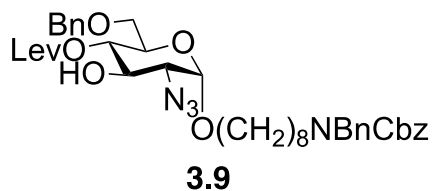


**3.8**

***N*-benzyl-*N*-benzoxycarbonyl-8-aminooctyl 2-azido-6-*O*-benzyl-2-deoxy-4-*O*-levulinoyl-3-*O*-(2,2,2-trichloroethoxycarbonyl)- $\alpha$ -D-glucopyranoside (3.8)**

To a stirred solution of **2.8** (210 mg, 0.258 mmol) in dry CH<sub>2</sub>Cl<sub>2</sub> (5 mL) was added EDC·HCl (74.0 mg, 0.383 mmol), 4-(dimethylamino)pyridine (6.2 mg, 0.051 mmol) and levulinic acid (44.0 mg,

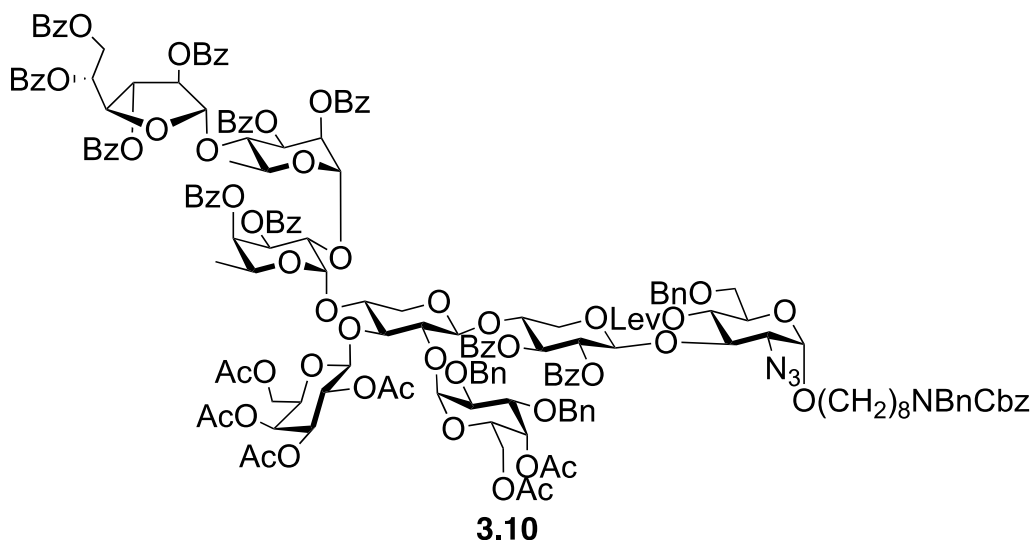
0.383 mmol). The reaction mixture was stirred overnight before it was diluted with CH<sub>2</sub>Cl<sub>2</sub> (50 mL). The mixture was then washed successively with saturated aqueous NaHCO<sub>3</sub>, water and brine. The organic layer was dried over Na<sub>2</sub>SO<sub>4</sub>, filtered and concentrated to dryness. The crude residue was purified by flash chromatography (2:1 hexanes–EtOAc) to afford **3.8** (228 mg, 97%) as a colorless oil: *R<sub>f</sub>* = 0.29 (2:1 hexanes–EtOAc); [ $\alpha$ ]<sub>D</sub><sup>25</sup> +99.4 (*c* = 1.39, CHCl<sub>3</sub>); <sup>1</sup>H NMR (600 MHz, CDCl<sub>3</sub>)  $\delta$  7.40–7.22 (m, 14H, Ar), 7.22–7.14 (m, 1H, Ar), 5.34 (dd, *J* = 10.6, 9.2 Hz, 1H, H-3), 5.25 (app t, *J* = 9.7 Hz, 1H, H-4), 5.17 (m, 2H, OCH<sub>2</sub>Ph), 5.01 (d, *J* = 3.5 Hz, 1H, H-1), 4.87 (d, *J* = 11.9 Hz, 1H, OCH<sub>2</sub>CCl<sub>3</sub>), 4.83 (d, *J* = 11.9 Hz, 1H, OCH<sub>2</sub>CCl<sub>3</sub>), 4.56–4.45 (m, 4H, 2x OCH<sub>2</sub>Ph, 2 x NCH<sub>2</sub>Ph), 3.97 (ddd, *J* = 10.1, 4.3, 2.7 Hz, 1H, H-5), 3.73 (app dt, *J* = 9.6, 6.7 Hz, 1H, octyl OCH<sub>2</sub>), 3.60 (dd, *J* = 10.9, 2.7 Hz, 1H, H-6a), 3.54 (dd, *J* = 10.9, 4.4 Hz, 1H, H-6b), 3.51–3.46 (m, 1H, octyl OCH<sub>2</sub>), 3.33 (dd, *J* = 10.6, 3.5 Hz, 1H, H-2), 3.29–3.22 (m, 1H, octyl NCH<sub>2</sub>), 3.23–3.16 (m, 1H, octyl NCH<sub>2</sub>), 2.70–2.64 (m, 2H, COCH<sub>2</sub>CH<sub>2</sub>COCH<sub>3</sub>), 2.46–2.36 (m, 2H, COCH<sub>2</sub>CH<sub>2</sub>COCH<sub>3</sub>), 2.15 (s, 3H, COCH<sub>3</sub>), 1.67–1.57 (m, 2H, OCH<sub>2</sub>CH<sub>2</sub>), 1.56–1.44 (m, 2H, NCH<sub>2</sub>CH<sub>2</sub>), 1.38–1.15 (m, 8H, 4 x CH<sub>2</sub>); <sup>13</sup>C NMR (151 MHz, CDCl<sub>3</sub>)  $\delta$  206.2 (C=O), 171.4 (C=O), 156.8 (C=O), 153.8 (C=O), 138.1 (Ar), 137.9 (Ar), 137.1 (Ar), 128.7 (3 x Ar), 128.6 (Ar), 128.5 (3 x Ar), 128.1 (3 x Ar), 128.0 (Ar), 128.0 (2 x Ar), 127.8 (Ar), 127.4 (Ar), 97.9 (C-1), 94.5 (OCH<sub>2</sub>CCl<sub>3</sub>), 77.4 (OCH<sub>2</sub>CCl<sub>3</sub>), 76.0 (C-3), 73.8 (OCH<sub>2</sub>Ph), 69.0 (octyl OCH<sub>2</sub>), 68.9 (C-4), 68.9 (C-5), 68.2 (C-6), 67.3 (OCH<sub>2</sub>Ph), 60.9 (C-2), 50.6 (NC<sub>a</sub>H<sub>2</sub>Ph), 50.3 (NC<sub>b</sub>H<sub>2</sub>Ph), 47.4 (octyl NC<sub>a</sub>H<sub>2</sub>), 46.4 (octyl NC<sub>b</sub>H<sub>2</sub>), 37.8 (COCH<sub>2</sub>CH<sub>2</sub>COCH<sub>3</sub>), 29.9 (COCH<sub>3</sub>), 29.9 (OCH<sub>2</sub>CH<sub>2</sub>), 29.8 (CH<sub>2</sub>), 29.4 (CH<sub>2</sub>), 28.2 (COCH<sub>2</sub>CH<sub>2</sub>COCH<sub>3</sub>), 28.2 (NCH<sub>2</sub>C<sub>a</sub>H<sub>2</sub>), 27.8 (NCH<sub>2</sub>C<sub>b</sub>H<sub>2</sub>), 26.9 (CH<sub>2</sub>), 26.1 (CH<sub>2</sub>); HRMS (ESI–TOF) *m/z*: [M + Na]<sup>+</sup> Calcd for C<sub>44</sub>H<sub>53</sub>N<sub>4</sub>NaO<sub>11</sub>Cl<sub>3</sub> 941.2669; Found 941.2678.



***N*-benzyl-*N*-benzoxycarbonyl-8-amino-octyl 2-azido-6-*O*-benzyl-2-deoxy-4-*O*-levulinoyl- $\alpha$ -*D*-glucopyranoside (3.9)**

To a stirred solution of **3.8** (220 mg, 0.239 mmol) in dry 1,2-dichloroethane (2.4 mL) at 70 °C was added trimethyltin hydroxide (65.0 mg, 0.359 mmol). The reaction mixture was stirred overnight before it was cooled to room temperature and then diluted with CH<sub>2</sub>Cl<sub>2</sub> (20 mL). The solution was filtered through Celite and the filtrate was concentrated to dryness. The crude residue was purified by flash chromatography (2:1 hexanes–EtOAc) to afford **3.9** (172 mg, 97%) as a white solid:  $R_f$  = 0.13 (2:1 hexanes–EtOAc);  $[\alpha]_D^{25} +75.9$  ( $c = 0.78$ , CHCl<sub>3</sub>); <sup>1</sup>H NMR (600 MHz, CDCl<sub>3</sub>)  $\delta$  7.40–7.22 (m, 14H, Ar), 7.22–7.14 (m, 1H, Ar), 5.17 (m, 2H, OCH<sub>2</sub>Ph), 5.01 (dd,  $J = 10.2, 9.0$  Hz, 1H, H-4), 4.91 (d,  $J = 3.5$  Hz, 1H, H-1), 4.55 (d,  $J = 11.9$  Hz, 1H, OCH<sub>2</sub>Ph), 4.51 (d,  $J = 11.9$  Hz, 1H, OCH<sub>2</sub>Ph), 4.54–4.45 (m, 2H, 2 x NCH<sub>2</sub>Ph), 4.15 (dd,  $J = 10.4, 9.0$  Hz, 1H, H-3), 3.90 (ddd,  $J = 10.2, 4.6, 2.7$  Hz, 1H, H-5), 3.70 (app dt,  $J = 9.6, 6.6$  Hz, 1H, octyl OCH<sub>2</sub>), 3.57 (dd,  $J = 10.8, 2.7$  Hz, 1H, H-6a), 3.53 (dd,  $J = 10.8, 4.7$  Hz, 1H, H-6b), 3.49–3.43 (m, 1H, octyl OCH<sub>2</sub>), 3.27 (dd,  $J = 10.4, 3.5$  Hz, 1H, H-2), 3.27–3.21 (m, 1H, octyl NCH<sub>2</sub>), 3.21–3.15 (m, 1H, octyl NCH<sub>2</sub>), 2.82–2.70 (m, 2H, COCH<sub>2</sub>CH<sub>2</sub>COCH<sub>3</sub>), 2.54–2.36 (m, 2H, COCH<sub>2</sub>CH<sub>2</sub>COCH<sub>3</sub>), 2.17 (s, 3H, COCH<sub>3</sub>), 1.64–1.57 (m, 2H, OCH<sub>2</sub>CH<sub>2</sub>), 1.56–1.43 (m, 2H, NCH<sub>2</sub>CH<sub>2</sub>), 1.39–1.16 (m, 8H, 4 x CH<sub>2</sub>); <sup>13</sup>C NMR (151 MHz, CDCl<sub>3</sub>)  $\delta$  207.6 (C=O), 172.7 (C=O), 156.9 (C=O), 138.0 (2 x Ar), 137.1 (Ar), 128.6 (3 x Ar), 128.6 (Ar), 128.4 (3 x Ar), 128.0 (Ar), 128.0 (3 x Ar), 127.9 (2 x Ar), 127.8 (Ar), 127.3 (Ar), 97.9 (C-1), 73.7 (OCH<sub>2</sub>Ph), 72.5 (C-4), 70.5 (C-3), 68.8 (C-5), 68.8 (octyl OCH<sub>2</sub>), 68.7 (C-6), 67.3 (OCH<sub>2</sub>Ph), 63.0 (C-2), 50.6 (NC<sub>a</sub>H<sub>2</sub>Ph), 50.3 (NC<sub>b</sub>H<sub>2</sub>Ph), 47.4 (octyl NC<sub>a</sub>H<sub>2</sub>), 46.3

(octyl NC<sub>6</sub>H<sub>2</sub>), 38.5 (COCH<sub>2</sub>CH<sub>2</sub>COCH<sub>3</sub>), 29.9 (COCH<sub>3</sub>), 29.8 (OCH<sub>2</sub>CH<sub>2</sub>), 29.4 (CH<sub>2</sub>), 29.3 (2 x CH<sub>2</sub>), 28.2 (COCH<sub>2</sub>CH<sub>2</sub>COCH<sub>3</sub>), 28.2 (NCH<sub>2</sub>C<sub>6</sub>H<sub>2</sub>), 27.8 (NCH<sub>2</sub>C<sub>6</sub>H<sub>2</sub>), 26.8 (CH<sub>2</sub>), 26.1 (CH<sub>2</sub>); HRMS (ESI-TOF) *m/z*: [M + Na]<sup>+</sup> Calcd for C<sub>41</sub>H<sub>52</sub>N<sub>4</sub>NaO<sub>9</sub> 767.3627; Found 767.3618.

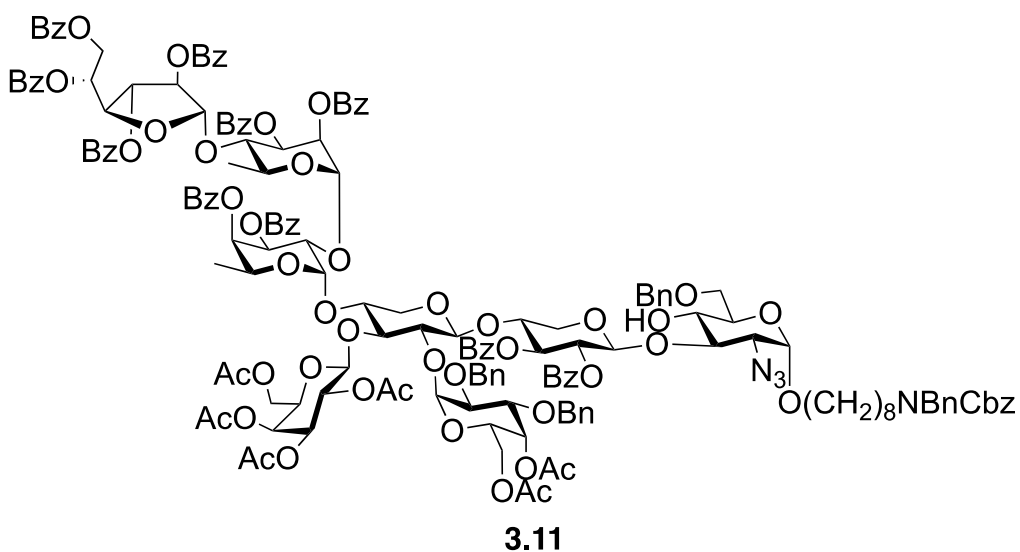


*N*-benzyl-*N*-benzoxycarbonyl-8-amino-1-octyl 2,3,4,6-tetra-*O*-acetyl- $\beta$ -D-galactopyranosyl-(1 $\rightarrow$ 3)-[4,6-di-*O*-acetyl-2,3-di-*O*-benzyl- $\alpha$ -D-galactopyranosyl-(1 $\rightarrow$ 2)]-[2,3,5,6-tetra-*O*-benzoyl- $\beta$ -D-galactofuranosyl-(1 $\rightarrow$ 4)-2,3-di-*O*-benzoyl- $\alpha$ -L-rhamnopyranosyl-(1 $\rightarrow$ 2)-3,4-di-*O*-benzoyl- $\alpha$ -L-fucopyranosyl-(1 $\rightarrow$ 4)]- $\beta$ -D-xylopyranosyl-(1 $\rightarrow$ 4)-2,3-di-*O*-benzoyl- $\beta$ -D-xylopyranosyl-(1 $\rightarrow$ 3)-2-azido-6-*O*-benzyl-2-deoxy-4-*O*-levulinoyl- $\alpha$ -D-glucopyranoside (3.10)

To a stirred solution of acceptor **3.9** (133 mg, 0.179 mmol) and donor **2.78** (97 mg, 0.0358 mmol) in dry CH<sub>2</sub>Cl<sub>2</sub> (5.0 mL) was added 4Å molecular sieves powder (500 mg). After stirring for 30 min, the reaction mixture was cooled to -30 °C, and then trimethylsilyl trifluoromethanesulfonate (18.0  $\mu$ L, 0.100 mmol) was added. The resulting solution was stirred for 1 h at 0 °C and then triethylamine was added to the mixture, the solution was filtered through Celite and the filtrate was concentrated to dryness. The crude residue was purified by flash chromatography (3:2

hexanes–EtOAc) to afford **3.10** (101 mg, 89%) as a white solid:  $R_f = 0.14$  (3:2 hexanes–EtOAc);  $[\alpha]_D^{25} -15.9$  ( $c = 0.10$ ,  $\text{CHCl}_3$ );  $^1\text{H NMR}$  (600 MHz,  $\text{CDCl}_3$ )  $\delta$  8.11–8.07 (m, 2H), 8.05–8.02 (m, 2H), 8.02–7.99 (m, 2H), 7.99–7.96 (m, 2H), 7.95–7.92 (m, 2H), 7.91–7.87 (m, 4H), 7.86–7.81 (m, 2H), 7.79–7.75 (m, 2H), 7.65–7.58 (m, 2H), 7.58–7.53 (m, 1H), 7.53–7.44 (m, 7H), 7.44–7.33 (m, 18H), 7.32–7.26 (m, 13H), 7.24–7.21 (m, 6H), 7.19–7.05 (m, 10H), 5.96 (app dt,  $J = 7.9, 4.1$  Hz, 1H), 5.72 (d,  $J = 3.5$  Hz, 1H), 5.68 (d,  $J = 3.4$  Hz, 1H), 5.68 (dd,  $J = 10.4, 3.4$  Hz, 1H), 5.63 (dd,  $J = 9.8, 3.4$  Hz, 1H), 5.54 (dd,  $J = 6.0, 2.0$  Hz, 1H), 5.51 (app t,  $J = 8.7$  Hz, 1H), 5.49 (s, 1H,  $\beta$ -Gal $f$ -H-1), 5.46 (d,  $J = 3.6$  Hz, 1H,  $\alpha$ -Gal $p$ -H-1), 5.37 (dd,  $J = 3.5, 1.7$  Hz, 1H), 5.35 (d,  $J = 3.7$  Hz, 1H), 5.21 (d,  $J = 1.9$  Hz, 1H), 5.20–5.12 (m, 4H), 5.03 (app t,  $J = 9.9$  Hz, 1H), 5.01 (d,  $J = 8.1$  Hz, 1H,  $\beta$ -Gal $p$ -H-1), 4.98 (d,  $J = 1.7$  Hz, 1H,  $\alpha$ -Rhap-H-1), 4.96–4.88 (m, 3H), 4.85 (d,  $J = 3.5$  Hz, 1H,  $\alpha$ -Glc $N_3p$ -H-1), 4.82 (d,  $J = 3.5$  Hz, 1H,  $\alpha$ -Fuc $p$ -H-1), 4.79 (d,  $J = 11.6$  Hz, 1H), 4.74–4.63 (m, 3H), 4.66 (d,  $J = 7.2$  Hz, 1H,  $\beta$ -Xyl $p$ -H-1), 4.63 (d,  $J = 6.2$  Hz, 1H,  $\beta$ -Xyl $p'$ -H-1), 4.60 (d,  $J = 11.7$  Hz, 1H), 4.55 (dd,  $J = 11.4, 6.5$  Hz, 1H), 4.52–4.44 (m, 3H), 4.46 (dd,  $J = 6.9, 2.8$  Hz, 1H), 4.37 (dd,  $J = 11.5, 7.2$  Hz, 1H), 4.30 (dd,  $J = 10.4, 3.4$  Hz, 1H), 4.25 (app t,  $J = 6.7$  Hz, 1H), 4.22–4.15 (m, 3H), 4.05–3.99 (m, 2H), 3.98 (d,  $J = 9.5$  Hz, 1H), 3.94–3.84 (m, 3H), 3.72 (app t,  $J = 7.2$  Hz, 1H), 3.70–3.60 (m, 3H), 3.56 (dd,  $J = 11.0, 2.5$  Hz, 1H), 3.49 (dd,  $J = 11.0, 5.0$  Hz, 1H), 3.47–3.37 (m, 2H), 3.34–3.27 (m, 1H), 3.27–3.20 (m, 1H), 3.20–3.14 (m, 1H), 3.08 (dd,  $J = 10.3, 3.5$  Hz, 1H), 2.64–2.48 (m, 1H), 2.47–2.32 (m, 3H), 2.25 (s, 3H), 2.16 (s, 3H), 2.10 (s, 3H), 2.04 (s, 3H), 2.03 (s, 3H), 1.97 (s, 3H), 1.93 (s, 3H), 1.59–1.42 (m, 4H), 1.33–1.18 (m, 8H), 1.28 (d,  $J = 6.7$  Hz, 3H), 1.03 (d,  $J = 6.1$  Hz, 3H);  $^{13}\text{C NMR}$  (151 MHz,  $\text{CDCl}_3$ )  $\delta$  206.6, 171.4, 170.8, 170.7, 170.5 (2 x C), 169.9, 169.2, 166.2, 166.1, 165.8 (2 x C), 165.6, 165.5, 165.3, 165.2, 165.0, 164.7, 138.8, 138.2, 138.2, 138.0, 133.8, 133.8, 133.4, 133.3, 133.2, 133.1, 133.1, 133.0, 132.9, 130.0, 129.9, 129.8, 129.8, 129.7, 129.6, 129.5, 129.5, 129.2, 128.9, 128.8, 128.7, 128.7, 128.6, 128.5,

128.4, 128.2, 128.0, 128.0, 127.9, 127.8, 127.7, 127.3, 125.4, 107.5 ( $\beta$ -Gal $f$ -C-1), 102.3 ( $\beta$ -Xyl $p$ -C-1), 101.4 ( $\beta$ -Xyl $p'$ -C-1), 100.2 ( $\beta$ -Gal $p$ -C-1), 97.7 ( $\alpha$ -Glc $N_3p$ -C-1), 96.6 ( $\alpha$ -Rhap-C-1), 95.7 ( $\alpha$ -Gal $p$ -C-1), 94.3 ( $\alpha$ -Fuc $p$ -C-1), 82.3, 81.6, 78.4, 77.7, 77.5, 77.3, 77.3, 76.4, 76.2, 75.4, 73.7 (2 x C), 73.7, 73.2, 72.6, 72.6, 72.3, 71.9, 71.8, 71.7, 71.6, 71.2, 71.0, 70.3, 69.7, 69.5, 69.4, 69.3, 68.7 (2 x C), 67.6, 67.5 (2 x C), 67.3 (2 x C), 67.3, 65.1, 63.4, 63.1, 62.5, 62.2, 62.0, 61.2, 50.6, 50.3, 47.4, 46.4, 37.6, 32.1, 29.8, 29.5, 29.4, 27.9, 26.9, 26.1, 21.6, 21.1, 21.0, 21.0, 20.9, 20.8, 20.7, 17.8, 16.1; HRMS (MALDI-TOF)  $m/z$ :  $[M + Na]^+$  Calcd for  $C_{177}H_{182}N_4NaO_{56}$  3282.1414; Found 3282.1365.

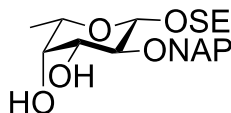


*N*-benzyl-*N*-benzoxycarbonyl-8-amino-1-octyl 2,3,4,6-tetra-*O*-acetyl- $\beta$ -D-galactopyranosyl-(1 $\rightarrow$ 3)-[4,6-di-*O*-acetyl-2,3-di-*O*-benzyl- $\alpha$ -D-galactopyranosyl-(1 $\rightarrow$ 2)]-[2,3,5,6-tetra-*O*-benzoyl- $\beta$ -D-galactofuranosyl-(1 $\rightarrow$ 4)-2,3-di-*O*-benzoyl- $\alpha$ -L-rhamnopyranosyl-(1 $\rightarrow$ 2)-3,4-di-*O*-benzoyl- $\alpha$ -L-fucopyranosyl-(1 $\rightarrow$ 4)]- $\beta$ -D-xylopyranosyl-(1 $\rightarrow$ 4)-2,3-di-*O*-benzoyl- $\beta$ -D-xylopyranosyl-(1 $\rightarrow$ 3)-2-azido-6-*O*-benzyl-2-deoxy- $\alpha$ -D-glucopyranoside (**3.11**)

To a stirred solution of **3.10** (84 mg, 0.0258 mmol) in pyridine-AcOH (5 mL, 3:2) was added hydrazine monohydrate (3.7  $\mu$ L, 0.0773 mmol). After stirring for 3 h, the reaction mixture was

diluted with CH<sub>2</sub>Cl<sub>2</sub> (50 mL) and washed with 1N HCl, saturated aqueous NaHCO<sub>3</sub> and brine. The combined organic layers were dried over Na<sub>2</sub>SO<sub>4</sub>, filtered and concentrated to dryness. The crude residue was purified by flash chromatography (3:2 hexanes–EtOAc) to afford **3.11** (52.0 mg, 64%) as a white solid:  $R_f = 0.18$  (3:2 hexanes–EtOAc);  $[\alpha]_D^{25} -5.7$  ( $c = 0.07$ , CHCl<sub>3</sub>); <sup>1</sup>H NMR (600 MHz, CDCl<sub>3</sub>)  $\delta$  8.13–8.07 (m, 2H), 8.06–8.02 (m, 2H), 8.02–7.99 (m, 2H), 7.99–7.96 (m, 2H), 7.96–7.87 (m, 6H), 7.87–7.83 (m, 1H), 7.80–7.77 (m, 2H), 7.65–7.58 (m, 2H), 7.58–7.53 (m, 1H), 7.53–7.44 (m, 7H), 7.44–7.20 (m, 41H), 7.20–7.15 (m, 1H), 7.15–7.07 (m, 6H), 5.96 (app dt,  $J = 7.8, 4.2$  Hz, 1H), 5.72 (d,  $J = 3.5$  Hz, 1H), 5.68 (d,  $J = 3.4$  Hz, 1H), 5.67 (dd,  $J = 10.4, 3.4$  Hz, 1H), 5.63 (dd,  $J = 9.8, 3.4$  Hz, 1H), 5.54 (dd,  $J = 6.0, 1.9$  Hz, 1H), 5.52 (app t,  $J = 9.4$  Hz, 1H), 5.50 (s, 1H,  $\beta$ -Gal $f$ -H-1), 5.38 (dd,  $J = 3.5, 1.7$  Hz, 1H), 5.36 (d,  $J = 3.5$  Hz, 1H), 5.27 (dd,  $J = 9.7, 7.8$  Hz, 1H), 5.23 (d,  $J = 3.9$  Hz, 1H,  $\alpha$ -Gal $p$ -H-1), 5.23 (d,  $J = 3.2$  Hz, 1H), 5.19–5.14 (m, 2H), 5.14 (dd,  $J = 10.9, 8.3$  Hz, 1H), 5.00 (d,  $J = 7.8$  Hz, 1H,  $\beta$ -Gal $p$ -H-1), 4.99 (d,  $J = 11.9$  Hz, 1H), 4.97 (d,  $J = 1.7$  Hz, 1H,  $\alpha$ -Rhap-H-1), 4.92 (dd,  $J = 7.8, 3.6$  Hz, 1H), 4.92–4.88 (m, 1H), 4.83 (d,  $J = 3.5$  Hz, 1H,  $\alpha$ -GlcN<sub>3</sub> $p$ -H-1), 4.80 (d,  $J = 11.2$  Hz, 1H), 4.79 (d,  $J = 3.0$  Hz, 1H,  $\alpha$ -Fuc $p$ -H-1), 4.71 (dd,  $J = 11.9, 4.4$  Hz, 1H), 4.67 (dd,  $J = 11.8, 7.2$  Hz, 1H), 4.63 (d,  $J = 12.3$  Hz, 1H), 4.62–4.55 (m, 4H), 4.53 (d,  $J = 6.3$  Hz, 1H,  $\beta$ -Xyl $p$ -H-1), 4.53 (d,  $J = 6.3$  Hz, 1H,  $\beta$ -Xyl $p'$ -H-1), 4.51–4.45 (m, 3H), 4.37 (dd,  $J = 11.4, 7.2$  Hz, 1H), 4.28 (dd,  $J = 10.4, 3.5$  Hz, 1H), 4.22 (q,  $J = 6.4$  Hz, 1H), 4.20–4.14 (m, 3H), 4.04–3.98 (m, 3H), 3.92 (dd,  $J = 9.6, 6.1$  Hz, 1H), 3.88 (d,  $J = 13.5$  Hz, 1H), 3.85 (dd,  $J = 9.9, 3.6$  Hz, 1H), 3.81 (dd,  $J = 11.7, 5.4$  Hz, 1H), 3.79–3.66 (m, 5H), 3.63 (app td,  $J = 7.9, 5.4$  Hz, 1H), 3.60–3.53 (m, 3H), 3.43 (dd,  $J = 12.1, 7.7$  Hz, 1H), 3.41–3.35 (m, 1H), 3.27–3.20 (m, 2H), 3.20–3.14 (m, 1H), 3.03 (dd,  $J = 10.4, 3.5$  Hz, 1H), 2.25 (s, 3H), 2.17 (s, 3H), 2.11 (s, 3H), 2.05 (s, 3H), 2.03 (s, 3H), 1.97 (s, 3H), 1.59–1.42 (m, 4H), 1.33–1.18 (m, 8H), 1.28 (d,  $J = 6.7$  Hz, 3H), 1.03 (d,  $J = 6.2$  Hz, 3H); <sup>13</sup>C NMR (151 MHz, CDCl<sub>3</sub>)  $\delta$  170.8, 170.7, 170.5 (2 x C),

169.9, 169.2, 166.2, 166.1, 165.8, 165.8, 165.6, 165.5, 165.3, 165.3, 165.0, 164.8, 138.9, 138.3, 138.2, 138.1, 133.8, 133.7, 133.4, 133.3, 133.2, 133.1, 132.9, 130.0, 129.9, 129.8, 129.7, 129.6, 129.5, 129.4, 128.9, 128.8, 128.6, 128.6, 128.5, 128.4, 128.3, 128.3, 128.2, 128.2, 128.0, 127.9, 127.8, 127.7, 127.6, 127.6, 127.4, 107.4 ( $\beta$ -Gal $f$ -C-1), 102.7 ( $\beta$ -Xyl $p$ -C-1), 101.0 ( $\beta$ -Xyl $p'$ -C-1), 100.2 ( $\beta$ -Gal $p$ -C-1), 98.0 ( $\alpha$ -GlcN $_3p$ -C-1), 96.7 ( $\alpha$ -Rhap-C-1), 96.0 ( $\alpha$ -Gal $p$ -C-1), 94.2 ( $\alpha$ -Fuc $p$ -C-1), 83.3, 82.3, 81.5, 78.0, 77.2, 77.0, 76.4, 76.3, 75.7, 74.2, 73.6 (2 x C), 73.3, 72.8, 72.6, 72.1, 71.9, 71.8, 71.7, 71.4, 71.2, 71.2, 71.0, 70.3, 69.7, 69.5, 69.2, 69.1, 68.5, 67.6, 67.5, 67.5, 67.2 (3 x C), 65.1, 63.4, 63.4, 62.0, 61.9, 61.5, 61.2, 60.5, 50.6, 50.3, 47.3, 46.3, 29.8, 29.5, 29.4, 28.2, 27.8, 26.9, 26.1, 22.8, 21.1, 21.0, 21.0, 20.9, 20.8, 20.7, 17.8, 16.1; HRMS (MALDI-TOF)  $m/z$ : [M + Na] $^+$  Calcd for C $_{172}$ H $_{176}$ N $_4$ NaO $_{54}$  3184.1047; Found 3184.1096.

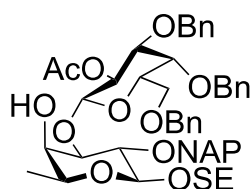


**3.13**

### **2-Trimethylsilylethyl 2-O-(2-naphthyl)methyl- $\beta$ -L-fucopyranoside (3.13)**

To a stirred solution of **3.14**<sup>18</sup> (400 mg, 1.52 mmol) in acetone (10 mL) was added 2,2-dimethoxypropane (0.37 mL, 3.0 mmol) and 10-camphorsulfonic acid (35.0 mg, 0.152 mmol). After stirring for 3 h, to the reaction mixture was added triethylamine and the solution was concentrated to dryness. The resulting crude product was then dissolved in DMF (25 mL) and then sodium hydride (182 mg, 4.56 mmol, 60% dispersion in mineral oil) was added portionwise over 30 min at 0 °C. To the resulting mixture was added 2-(bromomethyl)naphthalene (504 mg, 2.28 mmol) and the solution was stirred while warming to room temperature. After stirring for 2 h, the reaction mixture was slowly added to an ice-water mixture and was extracted with diethyl ether (100 mL x 2). The combined organic layers were dried over Na $_2$ SO $_4$ , filtered, concentrated and the

resulting syrup was stirred in 80% aqueous AcOH (25 mL) at 60 °C for 3 h. The reaction mixture was cooled to room temperature and then concentrated to dryness. The resulting crude product was purified with flash chromatography (2:1 hexane–EtOAc) to afford **3.13** (560 mg, 90% over three steps) as a colorless oil:  $R_f = 0.13$  (2:1 hexanes–EtOAc);  $[\alpha]_D^{25} -32.9$  ( $c = 0.56$ ,  $\text{CHCl}_3$ );  $^1\text{H NMR}$  (600 MHz,  $\text{CDCl}_3$ )  $\delta$  7.86–7.79 (m, 4H, Ar), 7.55–7.42 (m, 3H, Ar), 5.12 (d,  $J = 11.9$  Hz, 1H,  $\text{OCH}_2\text{Ar}$ ), 4.87 (d,  $J = 11.9$  Hz, 1H,  $\text{OCH}_2\text{Ar}$ ), 4.38 (d,  $J = 7.6$  Hz, 1H, H-1), 4.03 (ddd,  $J = 11.0$ , 9.5, 6.6 Hz, 1H,  $\text{OCH}_2\text{CH}_2\text{Si}$ ), 3.72 (dd,  $J = 3.5$ , 1.2 Hz, 1H, H-4), 3.64–3.56 (m, 3H, H-5, H-3,  $\text{OCH}_2\text{CH}_2\text{Si}$ ), 3.47 (dd,  $J = 9.2$ , 7.7 Hz, 1H, H-2), 1.34 (d,  $J = 6.6$  Hz, 3H, H-6), 1.11–0.99 (m, 2H, 2 x  $\text{OCH}_2\text{CH}_2\text{Si}$ ), 0.03 (s, 9H, 3 x  $\text{Si}(\text{CH}_3)_3$ );  $^{13}\text{C NMR}$  (126 MHz,  $\text{CDCl}_3$ )  $\delta$  136.1 (Ar), 133.5 (Ar), 133.2 (Ar), 128.5 (Ar), 128.1 (Ar), 127.9 (Ar), 127.1 (Ar), 126.3 (Ar), 126.1 (2 x Ar), 103.2 (C-1), 79.2 (C-2), 74.7 ( $\text{OCH}_2\text{Ar}$ ), 73.7 (C-5), 71.5 (C-4), 70.4 (C-3), 67.4 ( $\text{OCH}_2\text{CH}_2\text{Si}$ ), 18.7 ( $\text{OCH}_2\text{CH}_2\text{Si}$ ), 16.4 (C-6),  $-1.3$  (3 x  $\text{Si}(\text{CH}_3)_3$ ); HRMS (ESI–TOF)  $m/z$ :  $[\text{M} + \text{Na}]^+$  Calcd for  $\text{C}_{22}\text{H}_{32}\text{NaO}_5\text{Si}$  427.1911; Found 427.1909.

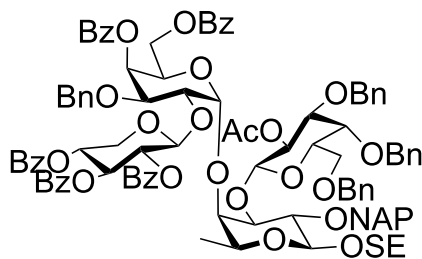


**3.15**

**2-Trimethylsilylethyl 2-O-acetyl-3,4,6-tri-O-benzyl- $\beta$ -D-galactopyranosyl-(1→3)-2-O-(2-naphthyl)methyl- $\beta$ -L-fucopyranoside (3.15)**

To a stirred solution of acceptor **3.13** (303 mg, 0.750 mmol) and donor **2.12**<sup>19</sup> (300 mg, 0.500 mmol) in dry  $\text{CH}_2\text{Cl}_2$  (10 mL) was added 4Å molecular sieves powder (1.0 g). After stirring for 30 min, the reaction mixture was cooled to 0 °C and then *N*-iodosuccinimide (58 mg, 0.260 mmol) and trifluoromethanesulfonic acid (4.4  $\mu\text{L}$ , 50.  $\mu\text{mol}$ ) were added successively. The resulting

solution was stirred for 1 h at 0 °C before triethylamine was added to the mixture and the solution was filtered through Celite and the filtrate was washed with saturated aqueous Na<sub>2</sub>S<sub>2</sub>O<sub>3</sub> and saturated aqueous NaHCO<sub>3</sub>. The organic layer was dried over Na<sub>2</sub>SO<sub>4</sub>, filtered and concentrated to dryness. The crude residue was purified by flash chromatography (2:1 hexanes–EtOAc) to afford **3.15** (180 mg, 41%) as a white solid:  $R_f = 0.24$  (2:1 hexanes–EtOAc);  $[\alpha]_D^{25} +0.4$  ( $c = 1.54$ , CHCl<sub>3</sub>); <sup>1</sup>H NMR (600 MHz, CDCl<sub>3</sub>)  $\delta$  7.80–7.78 (m, 1H, Ar), 7.77–7.73 (m, 2H, Ar), 7.68–7.64 (m, 1H, Ar), 7.57–7.53 (m, 1H, Ar), 7.45–7.41 (m, 1H, Ar), 7.41–7.38 (m, 1H, Ar), 7.38–7.32 (m, 4H, Ar), 7.32–7.23 (m, 9H, Ar), 7.17–7.13 (m, 2H, Ar), 5.46 (dd,  $J = 10.1, 7.9$  Hz, 1H, H-2'), 5.00 (d,  $J = 11.5$  Hz, 1H, OCH<sub>2</sub>Ar), 4.98–4.91 (m, 2H, 2 x OCH<sub>2</sub>Ar), 4.68 (d,  $J = 12.3$  Hz, 1H, OCH<sub>2</sub>Ar), 4.60 (d,  $J = 7.9$  Hz, 1H, H-1'), 4.60 (d,  $J = 11.5$  Hz, 1H, OCH<sub>2</sub>Ar), 4.50 (d,  $J = 12.3$  Hz, 1H, OCH<sub>2</sub>Ar), 4.33 (d,  $J = 7.7$  Hz, 1H, H-1), 4.25–4.23 (m, 2H, 2 x OCH<sub>2</sub>Ar), 4.05–3.97 (m, 2H, OCH<sub>2</sub>CH<sub>2</sub>Si, H-4'), 4.81 (dd,  $J = 9.5, 3.4$  Hz, 1H, H-3), 3.69 (d,  $J = 3.3$  Hz, 1H, H-4), 3.64–3.47 (m, 6H, H-6a', H-2, OCH<sub>2</sub>CH<sub>2</sub>Si, H-5', H-3', H-5), 3.40 (dd,  $J = 8.8, 5.2$  Hz, 1H, H-6b'), 2.05 (s, 3H, COCH<sub>3</sub>), 1.34 (d,  $J = 6.4$  Hz, 3H, H-6), 1.07–0.99 (m, 2H, 2 x OCH<sub>2</sub>CH<sub>2</sub>Si), 0.01 (s, 9H, 3 x Si(CH<sub>3</sub>)<sub>3</sub>); <sup>13</sup>C NMR (126 MHz, CDCl<sub>3</sub>)  $\delta$  170.0 (C=O), 138.7 (Ar), 138.0 (Ar), 137.9 (Ar), 136.8 (Ar), 133.4 (Ar), 133.1 (Ar), 128.6 (2 x Ar), 128.5 (2 x Ar), 128.4 (2 x Ar), 128.1 (2 x Ar), 128.1 (Ar), 128.0 (2 x Ar), 127.9 (2 x Ar), 127.8 (Ar), 127.7 (Ar), 127.7 (Ar), 127.6 (2 x Ar), 126.6 (Ar), 126.5 (Ar), 125.8 (Ar), 125.6 (Ar), 103.0 (C-1), 100.0 (C-1'), 81.1 (C-3), 80.3 (C-3), 77.7 (C-2), 75.1 (OCH<sub>2</sub>Ar), 74.8 (OCH<sub>2</sub>Ar), 73.8 (C-5'), 73.6 (OCH<sub>2</sub>Ar), 72.7 (C-4'), 72.0 (OCH<sub>2</sub>Ar), 71.7 (C-2'), 69.8 (C-4), 69.7 (C-5), 68.3 (C-6'), 67.4 (OCH<sub>2</sub>CH<sub>2</sub>Si), 21.1 (COCH<sub>3</sub>), 18.6 (OCH<sub>2</sub>CH<sub>2</sub>Si), 16.6 (C-6), –1.3 (3 x Si(CH<sub>3</sub>)<sub>3</sub>); HRMS (ESI–TOF)  $m/z$ :  $[M + Na]^+$  Calcd for C<sub>51</sub>H<sub>62</sub>NaO<sub>11</sub>Si 901.3954; Found 901.3963.



**3.17**

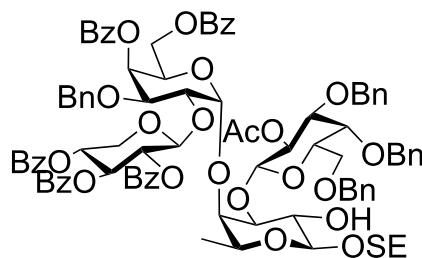
**2-Trimethylsilylethyl 2-*O*-acetyl-3,4,6-tri-*O*-benzyl- $\beta$ -D-galactopyranosyl-(1 $\rightarrow$ 3)-[[2,3,4-tri-*O*-benzoyl- $\beta$ -D-xylopyranosyl-(1 $\rightarrow$ 2)]-3-*O*-benzyl-4,6-di-*O*-benzoyl- $\alpha$ -D-galactopyranosyl-(1 $\rightarrow$ 4)]-2-*O*-(2-naphthyl)methyl- $\beta$ -L-fucopyranoside (3.17)**

To a stirred solution of acceptor **3.15** (90.0 mg, 0.102 mmol) and donor **2.7** (197 mg, 0.205 mmol) in dry CH<sub>2</sub>Cl<sub>2</sub> (10 mL) was added 4Å molecular sieves powder (1.0 g). After stirring for 30 min at room temperature, the reaction mixture was cooled to 0 °C and then *N*-iodosuccinimide (46.0 mg, 0.205 mmol) and silver trifluoromethanesulfonate (10.5 mg, 0.0408 mmol) were added successively at 0 °C. The reaction mixture was stirred for 1 h before triethylamine was added to the mixture. The solution was filtered through Celite and the filtrate was washed with saturated aqueous Na<sub>2</sub>S<sub>2</sub>O<sub>3</sub> and saturated aqueous NaHCO<sub>3</sub>. The organic layer was dried over Na<sub>2</sub>SO<sub>4</sub>, filtered and concentrated to dryness. The crude residue was purified by flash chromatography (4:1 hexanes–EtOAc) to afford **3.16**, which was used without further purification.

To a stirred solution of **3.16** in THF–pyridine (7 mL, 5:2) was added HF–pyridine (0.10 mL, pyridine ~30%, hydrogen fluoride ~70%) at 0 °C under an Ar atmosphere. The reaction mixture was stirred for 1.5 h at 0 °C and then poured into saturated aqueous NaHCO<sub>3</sub>. The aqueous layer was extracted with EtOAc (50 mL  $\times$  2), dried over Na<sub>2</sub>SO<sub>4</sub>, filtered and concentrated to dryness. The resulting crude product was then dissolved in pyridine (5.0 mL) and then benzoyl chloride (40.0  $\mu$ L, 0.340 mmol) was added dropwise at 0 °C. After stirring overnight, while warming to

room temperature, ice water was added, and the solution was extracted with  $\text{CH}_2\text{Cl}_2$  (50 mL x 2). The combined organic layer was then washed successively with 1N HCl, saturated aqueous  $\text{NaHCO}_3$ , water and brine. The organic layer was dried over  $\text{Na}_2\text{SO}_4$ , filtered, concentrated and the resulting syrup was purified by flash chromatography (2:1 hexane–EtOAc) to afford **3.17** (133 mg, 73% over two steps) as a white solid:  $R_f = 0.22$  (2:1 hexanes–EtOAc);  $[\alpha]_D^{25} +8.2$  ( $c = 0.64$ ,  $\text{CHCl}_3$ );  $^1\text{H NMR}$  (600 MHz,  $\text{CDCl}_3$ )  $\delta$  8.10–8.06 (m, 2H, Ar), 8.01–7.94 (m, 3H, Ar), 7.88–7.84 (m, 2H, Ar), 7.83–7.77 (m, 5H, Ar), 7.75–7.71 (m, 2H, Ar), 7.70–7.66 (m, 1H, Ar), 7.64–7.59 (m, 1H, Ar), 7.55–7.51 (m, 1H, Ar), 7.51–7.44 (m, 3H, Ar), 7.41–7.37 (m, 4H, Ar), 7.36–7.28 (m, 7H, Ar), 7.25–7.21 (m, 6H, Ar), 7.15–7.16 (m, 11H, Ar), 7.05–7.02 (m, 2H, Ar), 7.00–6.95 (m, 2H, Ar), 5.96 (d,  $J = 3.8$  Hz, 1H, H-1''), 5.75 (d,  $J = 3.5$  Hz, 1H, H-4''), 5.73 (dd,  $J = 9.1, 8.0$  Hz, 1H, H-3'''), 5.58 (dd,  $J = 9.1, 6.5$  Hz, 1H, H-2'''), 5.47–5.42 (m, 2H, H-4''', H-2''), 5.29 (d,  $J = 11.6$  Hz, 1H,  $\text{OCH}_2\text{Ar}$ ), 5.24 (d,  $J = 11.6$  Hz, 1H,  $\text{OCH}_2\text{Ar}$ ), 5.13 (d,  $J = 6.4$  Hz, 1H, H-1'''), 4.80 (d,  $J = 11.7$  Hz, 1H,  $\text{OCH}_2\text{Ar}$ ), 4.59 (d,  $J = 8.2$  Hz, 1H, H-1'), 4.58–4.53 (m, 3H, 2 x  $\text{OCH}_2\text{Ar}$ , H-5a'''), 4.53–4.48 (m, 2H,  $\text{OCH}_2\text{Ar}$ , H-6a''), 4.47–4.40 (m, 1H, H-5), 4.39 (d,  $J = 12.2$  Hz, 1H,  $\text{OCH}_2\text{Ar}$ ), 4.38 (d,  $J = 7.5$  Hz, 1H, H-1), 4.29 (d,  $J = 12.2$  Hz, 1H,  $\text{OCH}_2\text{Ar}$ ), 4.26 (dd,  $J = 11.1, 5.5$  Hz, 1H, H-6b''), 4.17 (d,  $J = 10.3, 3.8$  Hz, 1H, H-2''), 4.13–4.08 (m, 2H, H-3'', H-2), 4.03 (d,  $J = 11.5$  Hz, 1H,  $\text{OCH}_2\text{Ar}$ ), 4.03–3.96 (m, 1H,  $\text{OCH}_2\text{CH}_2\text{Si}$ ), 3.96 (d,  $J = 11.5$  Hz, 1H,  $\text{OCH}_2\text{Ar}$ ), 3.92 (d,  $J = 2.5$  Hz, 1H, H-4), 3.90 (d,  $J = 2.5$  Hz, 1H, H-4'), 3.83 (dd,  $J = 10.0, 2.5$  Hz, 1H, H-3), 3.73 (dd,  $J = 12.5, 7.3$  Hz, 1H, H-5b'''), 3.63–3.56 (m, 3H, H-6a',  $\text{OCH}_2\text{CH}_2\text{Si}$ , H-5), 3.46 (dd,  $J = 10.1, 2.8$  Hz, 1H, H-3'), 3.40–3.35 (m, 1H, H-5'), 3.22 (dd,  $J = 9.0, 5.1$  Hz, 1H, H-6b'), 2.03 (s, 3H,  $\text{COCH}_3$ ), 1.33 (d,  $J = 6.4$  Hz, 3H, H-6), 1.08–0.97 (m, 2H, 2 x  $\text{OCH}_2\text{CH}_2\text{Si}$ ), 0.01 (s, 9H, 3 x  $\text{Si}(\text{CH}_3)_3$ );  $^{13}\text{C NMR}$  (126 MHz,  $\text{CDCl}_3$ )  $\delta$  169.8 (C=O), 166.1 (C=O), 165.8 (C=O), 165.8 (C=O), 165.2 (C=O), 165.0 (C=O), 138.7 (Ar), 138.3 (Ar), 138.1 (Ar), 138.0 (Ar), 137.7 (Ar), 133.6 (Ar), 133.3 (Ar),

133.3 (2 x Ar), 133.1 (Ar), 133.0 (Ar), 132.9 (Ar), 132.9 (Ar), 130.1 (Ar), 130.0 (2 x Ar), 130.0 (3 x Ar), 129.9 (2 x Ar), 129.8 (2 x Ar), 129.7 (Ar), 129.6 (Ar), 129.4 (Ar), 128.6 (Ar), 128.6 (2 x Ar), 128.5 (Ar), 128.5 (2 x Ar), 128.4 (2 x Ar), 128.4 (2 x Ar), 128.3 (2 x Ar), 128.2 (6 x Ar), 128.2 (2 x Ar), 128.1 (2 x Ar), 127.9 (2 x Ar), 127.8 (Ar), 127.8 (2 x Ar), 127.7 (Ar), 127.5 (4 x Ar), 127.4 (2 x Ar), 127.2 (Ar), 126.5 (Ar), 126.0 (Ar), 125.7 (Ar), 125.3 (Ar), 103.8 (C-1), 102.5 (C-1'''), 102.3 (C-1'), 97.6 (C-1''), 84.2 (C-3), 80.9 (C-3'), 78.2 (H-3''), 76.3 (C-2''), 75.3 (OCH<sub>2</sub>Ar), 74.4 (OCH<sub>2</sub>Ar), 73.9 (C-2), 73.5 (C-5'), 73.2 (C-4), 72.7 (OCH<sub>2</sub>Ar), 72.1 (C-3'''), 72.1 (C-2'), 72.1 (OCH<sub>2</sub>Ar), 71.8 (C-2'''), 71.8 (C-4'), 71.8 (OCH<sub>2</sub>Ar), 70.5 (C-4'''), 70.2 (C-5), 69.1 (C-4''), 68.3 (C-6'), 67.7 (OCH<sub>2</sub>CH<sub>2</sub>Si), 67.2 (C-5''), 63.4 (C-6''), 62.6 (C-5'''), 21.2 (COCH<sub>3</sub>), 18.6 (OCH<sub>2</sub>CH<sub>2</sub>Si), 18.0 (C-6), -1.2 (3 x Si(CH<sub>3</sub>)<sub>3</sub>); HRMS (MALDI-TOF) *m/z*: [M + Na]<sup>+</sup> Calcd for C<sub>104</sub>H<sub>106</sub>NaO<sub>25</sub>Si 1805.6690; Found 1805.6674.



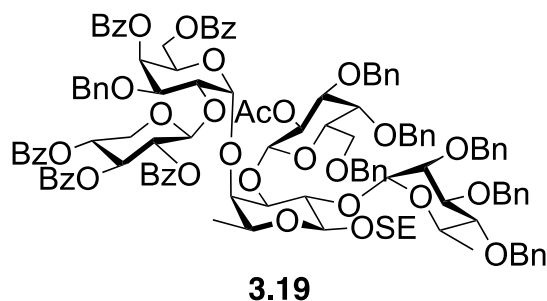
**3.18**

**2-Trimethylsilylethyl 2-*O*-acetyl-3,4,6-tri-*O*-benzyl- $\beta$ -D-galactopyranosyl-(1 $\rightarrow$ 3)-[[2,3,4-tri-*O*-benzoyl- $\beta$ -D-xylopyranosyl-(1 $\rightarrow$ 2)]-3-*O*-benzyl-4,6-di-*O*-benzoyl- $\alpha$ -D-galactopyranosyl-(1 $\rightarrow$ 4)]- $\beta$ -L-fucopyranoside (3.18)**

To a stirred biphasic solution of **3.17** (46.0 mg, 0.0258 mmol) in CH<sub>2</sub>Cl<sub>2</sub>-H<sub>2</sub>O (5 mL, 9:1) was added 2,3-dichloro-5,6-dicyano-1,4-benzoquinone (12.0 mg, 0.0516 mmol). The reaction mixture was stirred overnight before being diluted with CH<sub>2</sub>Cl<sub>2</sub> (50 mL). The mixture was then washed successively with 1N NaOH, water and brine. The organic layer was dried over Na<sub>2</sub>SO<sub>4</sub>, filtered

and concentrated to dryness. The crude residue was purified by flash chromatography (2:1 hexanes–EtOAc) to afford **3.18** (35.0 mg, 83%) as a colorless oil:  $R_f = 0.20$  (2:1 hexanes–EtOAc);  $[\alpha]_D^{25} +32.7$  ( $c = 0.73$ ,  $\text{CHCl}_3$ );  $^1\text{H NMR}$  (600 MHz,  $\text{CDCl}_3$ )  $\delta$  8.13–8.07 (m, 2H, Ar), 7.97–7.92 (m, 2H, Ar), 7.92–7.86 (m, 4H, Ar), 7.86–7.81 (m, 2H, Ar), 7.62–7.57 (m, 1H, Ar), 7.56–7.52 (m, 1H, Ar), 7.52–7.48 (m, 2H, Ar), 7.48–7.44 (m, 1H, Ar), 7.44–7.37 (m, 3H, Ar), 7.37–7.26 (m, 15H, Ar), 7.18–7.10 (m, 7H, Ar), 7.09–7.02 (m, 5H, Ar), 5.78 (d,  $J = 3.9$  Hz, 1H, H-1''), 5.73 (d,  $J = 3.3$  Hz, 1H, H-4''), 5.68 (dd,  $J = 9.2, 8.1$  Hz, 1H, H-3'''), 5.58 (dd,  $J = 9.2, 6.6$  Hz, 1H, H-2'''), 5.50 (dd,  $J = 10.1, 8.0$  Hz, 1H, H-2'), 5.48 (dd,  $J = 8.0, 5.3$  Hz, 1H, H-4'''), 5.09 (d,  $J = 6.6$  Hz, 1H, H-1'''), 4.75 (d,  $J = 11.8$  Hz, 1H,  $\text{OCH}_2\text{Ar}$ ), 4.60 (d,  $J = 12.3$  Hz, 1H,  $\text{OCH}_2\text{Ar}$ ), 4.59 (d,  $J = 11.8$  Hz, 1H,  $\text{OCH}_2\text{Ar}$ ), 4.53 (d,  $J = 8.0$  Hz, 1H, H-1'), 4.52 (d,  $J = 12.3$  Hz, 1H,  $\text{OCH}_2\text{Ar}$ ), 4.47–4.40 (m, 5H, 2 x  $\text{OCH}_2\text{Ar}$ , H-5'', H-6a'', H-6a'''), 4.39 (d,  $J = 11.7$  Hz, 1H,  $\text{OCH}_2\text{Ar}$ ), 4.29 (d,  $J = 11.5$  Hz, 1H,  $\text{OCH}_2\text{Ar}$ ), 4.27 (d,  $J = 7.7$  Hz, 1H, H-1), 4.26–4.21 (m, 1H, H-6b''), 4.19 (d,  $J = 10.3, 3.9$  Hz, 1H, H-2''), 4.08 (d,  $J = 2.7$  Hz, 1H, 2-OH), 4.07–4.00 (m, 2H, H-2, H-3''), 3.96 (ddd,  $J = 12.4, 9.3, 5.2$  Hz, 1H,  $\text{OCH}_2\text{CH}_2\text{Si}$ ), 3.92 (d,  $J = 2.5$  Hz, 1H, H-4'), 3.84 (d,  $J = 2.2$  Hz, 1H, H-4), 3.79–3.72 (m, 2H, H-6a', H-6b'), 3.65 (dd,  $J = 12.4, 8.1$  Hz, 1H, H-5b'''), 3.63 (app t,  $J = 5.9$  Hz, H-5'), 3.61–3.55 (m, 2H,  $\text{OCH}_2\text{CH}_2\text{Si}$ , H-5), 3.55 (dd,  $J = 9.9, 2.7$  Hz, 1H, H-3), 3.52 (dd,  $J = 10.1, 2.8$  Hz, 1H, H-3'), 2.08 (s, 3H,  $\text{COCH}_3$ ), 1.29 (d,  $J = 6.4$  Hz, 3H, H-6), 1.11 (ddd,  $J = 13.7, 12.4, 5.4$  Hz, 1H,  $\text{OCH}_2\text{CH}_2\text{Si}$ ), 0.99 (ddd,  $J = 13.7, 12.2, 5.4$  Hz, 1H,  $\text{OCH}_2\text{CH}_2\text{Si}$ ), 0.02 (s, 9H, 3 x  $\text{Si}(\text{CH}_3)_3$ );  $^{13}\text{C NMR}$  (126 MHz,  $\text{CDCl}_3$ )  $\delta$  169.8 (C=O), 166.1 (C=O), 166.0 (C=O), 165.8 (C=O), 165.6 (C=O), 165.3 (C=O), 138.3 (Ar), 138.2 (Ar), 138.1 (Ar), 138.0 (Ar), 133.3 (Ar), 133.3 (Ar), 133.1 (Ar), 133.0 (Ar), 132.9 (Ar), 130.1 (Ar), 130.0 (4 x Ar), 130.0 (2 x Ar), 129.9 (Ar), 129.7 (2 x Ar), 129.7 (Ar), 129.6 (Ar), 128.7 (Ar), 128.5 (5 x Ar), 128.4 (3 x Ar), 128.4 (Ar), 128.2 (5 x Ar), 128.2 (3 x Ar), 128.2 (Ar), 127.9 (2 x Ar), 127.7 (2 x Ar), 127.6 (2 x Ar), 127.5

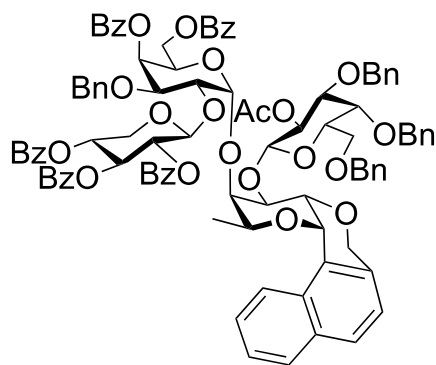
(Ar), 127.4 (Ar), 103.2 (C-1), 103.0 (C-1'), 102.0 (C-1'''), 98.2 (C-1''), 87.1 (C-3), 80.7 (C-3'), 75.2 (C-4), 75.2 (C-2''), 75.0 (C-3''), 74.6 (C-5'), 74.2 (OCH<sub>2</sub>Ar), 73.7 (OCH<sub>2</sub>Ar), 73.7 (OCH<sub>2</sub>Ar), 72.8 (OCH<sub>2</sub>Ar), 72.2 (C-3'''), 72.1 (OCH<sub>2</sub>Ar), 72.1 (OCH<sub>2</sub>Ar), 71.9 (C-4'), 71.5 (C-2'''), 71.3 (C-2'), 70.4 (C-4'''), 70.2 (C-5), 69.3 (C-2), 69.0 (C-4''), 68.8 (C-6'), 67.2 (OCH<sub>2</sub>CH<sub>2</sub>Si), 67.2 (C-5''), 63.4 (C-6''), 62.7 (C-5'''), 21.2 (COCH<sub>3</sub>), 18.4 (OCH<sub>2</sub>CH<sub>2</sub>Si), 17.8 (C-6), -1.2 (3 x Si(CH<sub>3</sub>)<sub>3</sub>); HRMS (MALDI-TOF) *m/z*: [M + Na]<sup>+</sup> Calcd for C<sub>93</sub>H<sub>98</sub>NaO<sub>25</sub>Si 1665.6063; Found 1665.6042.



**2-Trimethylsilylethyl 2-*O*-acetyl-3,4,6-tri-*O*-benzyl- $\beta$ -D-galactopyranosyl-(1 $\rightarrow$ 3)-[2,3,4-tri-*O*-benzyl- $\alpha$ -L-rhamnopyranosyl-(1 $\rightarrow$ 2)]-[[2,3,4-tri-*O*-benzoyl- $\beta$ -D-xylopyranosyl-(1 $\rightarrow$ 2)]-3-*O*-benzyl-4,6-di-*O*-benzoyl- $\alpha$ -D-galactopyranosyl-(1 $\rightarrow$ 4)]- $\beta$ -L-fucopyranoside (3.19)**

To a stirred solution of acceptor **3.18** (25.0 mg, 0.0152 mmol) and donor **2.13**<sup>20</sup> (41.0 mg, 0.0760 mmol) in dry Et<sub>2</sub>O (5.0 mL) was added 4Å molecular sieves powder (500 mg). After stirring for 30 min, the reaction mixture was cooled to 0 °C and then *N*-iodosuccinimide (17.0 mg, 0.0760 mmol) and silver trifluoromethanesulfonate (0.4 mg, 1.5  $\mu$ mol) were added successively. The resulting solution was stirred overnight at room temperature. Triethylamine was added to the mixture, the solution was filtered through Celite and the filtrate was washed with saturated aqueous Na<sub>2</sub>S<sub>2</sub>O<sub>3</sub> and saturated aqueous NaHCO<sub>3</sub>. The organic layer was dried over Na<sub>2</sub>SO<sub>4</sub>, filtered and concentrated to dryness. The crude residue was purified by flash chromatography (3:1 hexanes–

EtOAc) to afford **3.19** (28.0 mg, 89%) as a colorless oil:  $R_f = 0.31$  (2:1 hexanes–EtOAc);  $[\alpha]_D^{25} +36.9$  ( $c = 0.44$ ,  $\text{CHCl}_3$ );  $^1\text{H NMR}$  (600 MHz,  $\text{CDCl}_3$ )  $\delta$  8.05–8.00 (m, 2H), 8.00–7.97 (m, 2H), 7.97–7.94 (m, 2H), 7.94–7.90 (m, 2H), 7.81–7.76 (m, 2H), 7.62–7.57 (m, 1H), 7.55–7.49 (m, 2H), 7.47–7.43 (m, 2H), 7.41–7.35 (m, 7H), 7.35–7.26 (m, 12H), 7.26–7.22 (m, 4H), 7.22–7.07 (m, 20H), 7.05–6.98 (m, 2H), 6.02 (d,  $J = 3.9$  Hz, 1H,  $\alpha$ -Rhap-H-1), 5.78 (d,  $J = 3.4$  Hz, 1H), 5.76 (dd,  $J = 9.5, 7.2$  Hz, 1H), 5.65 (s, 1H,  $\alpha$ -Galp-H-1), 5.65 (dd,  $J = 9.1, 6.4$  Hz, 1H), 5.60 (app q,  $J = 6.0$  Hz, 1H), 5.47 (dd,  $J = 10.0, 8.0$  Hz, 1H), 5.22 (d,  $J = 6.5$  Hz, 1H,  $\beta$ -Xylp-H-1), 4.89 (d,  $J = 11.0$  Hz, 1H), 4.81 (d,  $J = 13.4$  Hz, 1H), 4.75 (d,  $J = 13.4$  Hz, 1H), 4.75–4.69 (m, 1H), 4.70 (d,  $J = 12.3$  Hz, 1H), 4.62 (d,  $J = 12.0$  Hz, 1H), 4.56 (d,  $J = 12.3$  Hz, 1H), 4.56 (d,  $J = 12.3$  Hz, 1H), 4.53 (d,  $J = 12.3$  Hz, 1H), 4.51–4.42 (m, 3H), 4.49 (d,  $J = 9.2$  Hz, 1H,  $\beta$ -Galp-H-1), 4.34 (d,  $J = 12.3$  Hz, 1H), 4.31 (d,  $J = 11.6$ , 1H), 4.31 (d,  $J = 12.3$ , 1H), 4.28–4.22 (m, 2H), 4.22–4.17 (m, 2H), 4.15 (d,  $J = 7.4$  Hz, 1H,  $\beta$ -Fucp-H-1), 4.12 (dd,  $J = 10.2, 3.3$  Hz, 1H), 3.97 (d,  $J = 2.1$  Hz, 1H), 3.94 (d,  $J = 2.7$  Hz, 1H), 3.86–3.76 (m, 4H), 3.72 (d,  $J = 10.2$  Hz, 1H), 3.66 (dd,  $J = 10.3, 6.5$  Hz, 1H), 3.65 (app t,  $J = 9.7$  Hz, 1H), 3.57 (dd,  $J = 9.8, 6.0$  Hz, 1H), 3.53–3.49 (m, 1H), 3.49–3.39 (m, 4H), 2.17 (s, 3H), 1.32 (d,  $J = 6.1$  Hz, 3H), 1.31 (d,  $J = 6.8$  Hz, 3H), 0.86–0.79 (m, 1H), 0.75 (td,  $J = 13.1, 5.6$  Hz, 1H), –0.07 (s, 9H);  $^{13}\text{C NMR}$  (151 MHz,  $\text{CDCl}_3$ )  $\delta$  169.4, 166.1, 166.0, 165.7, 165.3, 164.7, 139.9, 139.7, 139.4, 138.7, 138.4, 138.0, 133.4, 133.3, 133.0, 132.8, 130.1, 130.1, 130.0, 129.9, 129.8, 129.8, 129.7, 129.4, 128.8, 128.6, 128.6, 128.5, 128.5, 128.4, 128.3, 128.3, 128.3, 128.2, 128.2, 128.1, 127.8, 127.7, 127.6, 127.5, 127.5, 127.4, 127.4, 127.3, 127.0, 103.5 ( $\beta$ -Fucp-C-1), 101.8 ( $\beta$ -Xylp-C-1), 99.8 ( $\alpha$ -Galp-C-1), 99.6 ( $\beta$ -Galp-C-1), 96.9 ( $\alpha$ -Rhap-C-1), 81.7, 81.3, 81.2, 80.5, 77.8, 75.9, 75.4, 75.1, 74.7, 74.0, 73.8, 73.4, 72.9, 72.1, 71.9 (3 x C), 71.7, 71.6, 71.3, 71.1, 70.8, 70.2, 69.5, 68.8, 68.4, 67.2, 66.9, 63.4, 62.9, 21.1, 18.5, 18.4, 18.1, 14.3, –1.3 (3 x C); HRMS (MALDI–TOF)  $m/z$ :  $[\text{M} + \text{Na}]^+$  Calcd for  $\text{C}_{120}\text{H}_{126}\text{NaO}_{29}\text{Si}$  2081.8052; Found 2081.8062.



**3.21**

**(2S,3S,4R,4aS,12cS)-4-(2-O-acetyl-3,4,6-tri-O-benzyl-β-D-galactopyranosyl)-3-((2,3,4-tri-O-benzoyl-β-D-xylopyranosyl-(1→2))-3-O-benzyl-4,6-di-O-benzoyl-α-D-galactopyranosyl)-2-methyl-2,3,4,4a,6,12c-hexahydrobenzo[f]pyrano[3,2-c]isochromene (3.21)**

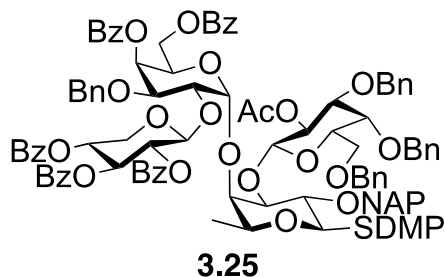
*Method A:* To a stirred solution of **3.17** (26.0 mg, 0.0146 mmol) in CH<sub>2</sub>Cl<sub>2</sub> (25 mL) was added trifluoroacetic acid (0.25 mL) at 0 °C. The reaction mixture was stirred for 2 h before concentration to dryness. The crude product was purified by chromatography (2:1 hexanes–EtOAc) to yield **3.21** (24.0 mg, quant) as a white solid.

*Method B:* To a stirred solution of **3.17** (83.0 mg, 0.0466 mmol) in toluene (25 mL) was added trifluoroacetic acid (0.25 mL) at –10 °C. The reaction mixture was stirred for 7 d before concentration to dryness. The crude product was purified by chromatography (1:1:0.01 hexanes–EtOAc–Et<sub>3</sub>N) to yield **3.22** (41.0 mg, 53%) as a colorless oil. The product was then dissolved in dry CH<sub>2</sub>Cl<sub>2</sub> (5 mL) before cesium carbonate (12.0 mg, 0.0370 mmol) and 2,2,2-trifluoro-*N*-phenylacetamidoyl chloride (6.0 μL, 0.0370 mmol) were added. After stirring overnight, the solution was filtered through Celite and the filtrate was concentrated to dryness. The crude product was purified by chromatography (2:1:0.01 hexanes–EtOAc–Et<sub>3</sub>N) to yield the imidate product **3.24** (22.0 mg, 56%) which was carried to the next step without further purification. To a stirred solution of acceptor **3.11** (29.0 mg, 0.0092 mmol) and donor **3.24** (22.0 mg, 0.0138 mmol) in dry

CH<sub>2</sub>Cl<sub>2</sub> (1 mL) was added 4Å molecular sieves powder (100 mg). After stirring for 30 min, the reaction mixture was cooled to 0 °C, and then trimethylsilyl trifluoromethanesulfonate (0.5 μL, 2.76 μmol) was added. The resulting solution was stirred for 1 h at 0 °C before triethylamine was added, and then the solution was filtered through Celite and the filtrate was concentrated to dryness. The crude residue was purified by flash chromatography (2:1 hexanes–EtOAc) to afford **3.21** (19.0 mg, 83%) as a white solid.

*Method C:* To a stirred solution of acceptor **3.11** (8.0 mg, 0.0025 mmol) and donor **3.25** (14.0 mg, 0.00750 mmol) in dry CH<sub>2</sub>Cl<sub>2</sub> (2 mL) was added 4Å molecular sieves powder (200 mg). After stirring for 30 min, the reaction mixture was cooled to 0 °C and then *N*-iodosuccinimide (2.3 mg, 0.010 mmol) and silver trifluoromethanesulfonate (0.60 mg, 2.5 μmol) were added successively. The resulting solution was stirred for 1 h at 0 °C and then triethylamine was added to the mixture before the solution was filtered through Celite and the filtrate was washed with saturated aqueous Na<sub>2</sub>S<sub>2</sub>O<sub>3</sub> and saturated aqueous NaHCO<sub>3</sub>. The organic layer was dried over Na<sub>2</sub>SO<sub>4</sub>, filtered and concentrated to dryness. The crude residue was purified by flash chromatography (2:1 hexanes–EtOAc) to afford **3.21** (11.5 mg, 92%) as a white solid:  $R_f = 0.23$  (2:1 hexanes–EtOAc);  $[\alpha]_D^{25} +33.9$  ( $c = 0.28$ , CHCl<sub>3</sub>); <sup>1</sup>H NMR (600 MHz, CDCl<sub>3</sub>) δ 8.11–8.07 (m, 2H), 8.07–8.03 (m, 1H), 7.96–7.90 (m, 4H), 7.82–7.75 (m, 5H), 7.63–7.58 (m, 1H), 7.56–7.51 (m, 2H), 7.51–7.45 (m, 3H), 7.41–7.37 (m, 2H), 7.37–7.32 (m, 3H), 7.32–7.27 (m, 8H), 7.25–7.19 (m, 7H), 7.19–7.14 (m, 3H), 7.14–7.10 (m, 2H), 7.10–7.05 (m, 4H), 7.05–7.01 (m, 2H), 6.93–6.89 (m, 2H), 5.85 (app t,  $J = 9.5$  Hz, 1H), 5.78 (d,  $J = 3.5$  Hz, 1H), 5.71 (app t,  $J = 8.8$  Hz, 1H), 5.55 (dd,  $J = 10.2, 7.9$  Hz, 1H), 5.49 (app td,  $J = 9.5, 5.6$  Hz, 1H), 5.45 (s, 1H, α-Galp-H-1), 5.35 (s, 1H, α-carbaFucp-H-1), 5.07 (d,  $J = 7.6$  Hz, 1H, β-Xylp-H-1), 4.99 (d,  $J = 9.0$  Hz, 1H, β-Galp-H-1), 5.02–4.97 (m, 1H), 4.95–4.89 (m, 2H), 4.70 (d,  $J = 11.8$  Hz, 1H), 4.62 (d,  $J = 11.5$  Hz, 1H), 4.58 (d,  $J = 11.2$  Hz, 1H), 4.48

(d,  $J = 11.8$  Hz, 1H), 4.45 (dd,  $J = 11.9, 5.8$  Hz, 1H), 4.42 (d,  $J = 12.1$  Hz, 1H), 4.40–4.32 (m, 3H), 4.30 (d,  $J = 6.8$  Hz, 1H), 4.24 (d,  $J = 12.1$  Hz, 1H), 4.21 (s, 1H), 4.16 (dd,  $J = 10.1, 3.6$  Hz, 1H), 4.10 (d,  $J = 3.0$  Hz, 1H), 3.95 (dd,  $J = 10.1, 3.5$  Hz, 1H), 3.87 (d,  $J = 10.2$  Hz, 1H), 3.80 (dd,  $J = 9.5, 5.7$  Hz, 1H), 3.71 (app t,  $J = 8.3$  Hz, 1H), 3.66 (dd,  $J = 11.7, 10.0$  Hz, 1H), 1.97 (s, 3H), 1.59 (d,  $J = 7.3$  Hz, 3H);  $^{13}\text{C}$  NMR (151 MHz,  $\text{CDCl}_3$ )  $\delta$  169.9, 166.3, 165.9, 165.7, 165.6, 138.7, 138.5, 137.7, 133.6, 133.5, 133.3, 133.2, 132.8, 132.5, 130.1, 130.0, 129.8, 129.5, 129.2, 128.9, 128.7, 128.6, 128.5, 128.4, 128.4, 128.3, 127.8, 127.7, 127.6, 127.4, 127.3, 127.0, 126.9, 125.6, 123.6, 122.2, 103.7 ( $\beta$ -Xylp-C-1), 103.0 ( $\beta$ -Galp-C-1), 100.6 ( $\alpha$ -Galp-C-1), 81.7, 78.5, 76.4, 76.2, 75.3, 74.5, 74.3, 74.2, 73.5, 73.5, 72.9, 72.7, 72.1 (3 x C), 71.9, 71.7, 70.0, 69.0, 68.8, 68.6, 68.0, 63.3, 63.1, 57.5 ( $\alpha$ -carbaFucp-C-1), 21.3, 13.7; HRMS (MALDI-TOF)  $m/z$ :  $[\text{M} + \text{Na}]^+$  Calcd for  $\text{C}_{99}\text{H}_{92}\text{NaO}_{24}$  1687.5876; Found 1687.5857.



**2,6-Dimethylphenyl 2-*O*-acetyl-3,4,6-tri-*O*-benzyl- $\beta$ -D-galactopyranosyl-(1 $\rightarrow$ 3)-[[2,3,4-tri-*O*-benzoyl- $\beta$ -D-xylopyranosyl-(1 $\rightarrow$ 2)]-3-*O*-benzyl-4,6-di-*O*-benzoyl- $\alpha$ -D-galactopyranosyl-(1 $\rightarrow$ 4)]-2-*O*-(2-naphthyl)methyl-1-thio- $\beta$ -L-fucopyranoside (3.25)**

To a stirred solution of acceptor **3.28** (28.0 mg, 0.0311 mmol) and donor **2.7** (70 mg, 0.0622 mmol) in dry  $\text{CH}_2\text{Cl}_2$  (5 mL) was added 4Å molecular sieves powder (500 mg). After stirring for 30 min at room temperature, the reaction mixture was cooled to 0 °C and then *N*-iodosuccinimide (21.0 mg, 0.093 mmol) and silver trifluoromethanesulfonate (3.2 mg, 0.012 mmol) were added

successively at 0 °C. The reaction mixture was stirred for 1 h before triethylamine was added to the mixture. The solution was filtered through Celite and the filtrate was washed with saturated aqueous Na<sub>2</sub>S<sub>2</sub>O<sub>3</sub> and saturated aqueous NaHCO<sub>3</sub>. The organic layer was dried over Na<sub>2</sub>SO<sub>4</sub>, filtered and concentrated to dryness. The crude residue was purified by flash chromatography (4:1 hexanes–EtOAc) to afford **3.29**, which was used without further purification.

To a stirred solution of **3.16** in THF–pyridine (5 mL, 1:1) was added HF–pyridine (0.10 mL, pyridine ~30%, hydrogen fluoride ~70%) at 0 °C. The reaction mixture was stirred for 1.5 h at 0 °C and then poured into saturated aqueous NaHCO<sub>3</sub>. The aqueous layer was extracted with EtOAc (25 mL × 2), dried over Na<sub>2</sub>SO<sub>4</sub>, filtered and concentrated to dryness. The resulting crude product was then dissolved in pyridine (5.0 mL) and then benzoyl chloride (17.5 μL, 0.156 mmol) was added dropwise at 0 °C. After stirring overnight, while warming to room temperature, ice water was added, and the solution was extracted with CH<sub>2</sub>Cl<sub>2</sub> (50 mL x 2). The combined organic layer was then washed successively with 1N HCl, saturated aqueous NaHCO<sub>3</sub>, water and brine. The organic layer was dried over Na<sub>2</sub>SO<sub>4</sub>, filtered, concentrated and the resulting syrup was purified by flash chromatography (3:1 hexane–EtOAc) to afford **3.25** (26.0 mg, 48% over two steps) as a white solid: *R<sub>f</sub>* = 0.35 (2:1 hexanes–EtOAc); [ $\alpha$ ]<sub>D</sub><sup>25</sup> –2.1 (*c* = 0.15, CHCl<sub>3</sub>); <sup>1</sup>H NMR (600 MHz, CDCl<sub>3</sub>)  $\delta$  8.09–8.05 (m, 3H), 8.01–7.98 (m, 1H), 7.96–7.88 (m, 6H), 7.84–7.81 (m, 2H), 7.81–7.78 (m, 1H), 7.71–7.67 (m, 2H), 7.58–7.54 (m, 1H), 7.52–7.41 (m, 7H), 7.41–7.34 (m, 5H), 7.34–7.31 (m, 4H), 7.31–7.27 (m, 2H), 7.25–7.16 (m, 10H), 7.09–7.04 (m, 6H), 7.02–6.98 (m, 2H), 6.98–6.93 (m, 3H), 5.85 (dd, *J* = 3.3, 1.4 Hz, 1H), 5.58 (d, *J* = 11.8 Hz, 1H), 5.52 (d, *J* = 3.2 Hz, 1H,  $\alpha$ -Galp-H-1), 5.48–5.43 (m, 2H), 5.21 (d, *J* = 11.9 Hz, 1H), 4.97 (app t, *J* = 7.7 Hz, 1H), 4.95 (d, *J* = 7.5 Hz, 1H,  $\beta$ -Galp-H-1), 4.81 (dd, *J* = 8.2, 4.2 Hz, 1H), 4.63 (d, *J* = 12.2, 1H), 4.63 (d, *J*

= 12.2, 1H), 4.53 (d,  $J = 12.2$  Hz, 1H), 4.48 (d,  $J = 10.2$  Hz, 1H), 4.45 (d,  $J = 12.1$  Hz, 1H), 4.42 (d,  $J = 8.0$  Hz, 1H,  $\beta$ -Xylp-H-1), 4.39 (d,  $J = 11.8$  Hz, 1H), 4.37–4.25 (m, 4H), 4.24 (d,  $J = 9.6$  Hz, 1H,  $\beta$ -Fucp-H-1), 4.20 (dd,  $J = 10.4, 3.3$  Hz, 1H), 4.16 (d,  $J = 10.2$  Hz, 1H), 3.93–3.85 (m, 2H), 3.79 (app t,  $J = 9.4$  Hz, 1H), 3.77–3.71 (m, 2H), 3.59 (dd,  $J = 7.9, 5.2$  Hz, 1H), 3.54 (app t,  $J = 7.9$  Hz, 1H), 3.51–3.46 (m, 2H), 3.13 (dd,  $J = 11.8, 9.4$  Hz, 1H), 3.13–3.07 (m, 1H), 2.43 (s, 6H), 2.19 (s, 3H), 0.95 (d,  $J = 6.6$  Hz, 3H);  $^{13}\text{C}$  NMR (151 MHz,  $\text{CDCl}_3$ )  $\delta$  169.6, 166.1, 165.9, 165.8, 165.2, 165.0, 144.6, 133.8, 138.4, 138.0, 137.8, 137.5, 133.8, 133.6, 133.5, 133.3, 133.2, 133.2, 132.9, 132.5, 130.3, 130.0, 130.0, 129.9, 129.8, 129.6, 128.7, 128.6, 128.5, 128.4, 128.4, 128.2, 128.2, 128.2, 128.1, 128.0, 128.0, 127.7, 127.5, 127.4, 126.2, 125.8, 101.7 ( $\beta$ -Xylp-C-1), 101.4 ( $\beta$ -Galp-C-1), 100.3 ( $\alpha$ -Galp-C-1), 90.7 ( $\beta$ -Fucp-C-1), 80.3, 80.1, 77.0, 76.2, 74.9, 74.1, 73.7, 73.3, 73.3, 73.1, 72.3, 72.1, 71.9, 71.9, 70.8, 70.0, 69.0, 68.0, 67.4, 63.7, 62.0, 22.5, 21.3, 17.2; HRMS (MALDI-TOF)  $m/z$ :  $[\text{M} + \text{Na}]^+$  Calcd for  $\text{C}_{107}\text{H}_{102}\text{NaO}_{24}\text{S}$  1825.6379; Found 1825.6346.

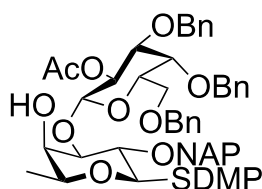


**3.26**

### **2,6-Dimethylphenyl 2-*O*-(2-naphthyl)methyl-1-thio- $\beta$ -L-fucopyranoside (3.26)**

To a stirred solution of 2,6-dimethylphenyl 3,4-*O*-isopropylidene-1-thio- $\beta$ -L-fucopyranoside<sup>25</sup> (650 mg, 2.01 mmol) in DMF (10 mL) was added sodium hydride (321 mg, 8.07 mmol, 60% dispersion in mineral oil) portionwise over 30 min at 0 °C. To the resulting mixture was added 2-(bromomethyl)naphthalene (665 mg, 3.01 mmol) and the solution was stirred while warming to room temperature. After stirring for 2 h, the reaction mixture was slowly added to an ice-water mixture and was extracted with EtOAc (50 mL x 2). The combined organic layers were dried over  $\text{Na}_2\text{SO}_4$ , filtered, concentrated and the resulting syrup was stirred in 75% aqueous AcOH (20 mL)

at 60 °C for 3 h. The reaction mixture was cooled to room temperature and then concentrated to dryness. The resulting crude product was purified with flash chromatography (2:1 hexane–EtOAc) to afford **3.26** (810 mg, 95% over two steps) as a colorless oil:  $R_f = 0.15$  (2:1 hexanes–EtOAc);  $[\alpha]_D^{25} -50.2$  ( $c = 0.11$ ,  $\text{CHCl}_3$ );  $^1\text{H NMR}$  (600 MHz,  $\text{CDCl}_3$ )  $\delta$  7.91–7.89 (m, 1H, Ar), 7.89–7.86 (m, 1H, Ar), 7.86–7.82 (m, 2H, Ar), 7.61–7.58 (m, 1H, Ar), 7.52–7.47 (m, 2H, Ar), 7.18–7.14 (m, 1H, Ar), 7.14–7.10 (m, 2H, Ar), 5.28 (d,  $J = 11.3$  Hz, 1H,  $\text{OCH}_2\text{Ar}$ ), 5.00 (d,  $J = 11.3$  Hz, 1H,  $\text{OCH}_2\text{Ar}$ ), 4.30 (d,  $J = 9.2$  Hz, 1H, H-1), 3.70 (dd,  $J = 5.2, 3.1$  Hz, 1H, H-4), 3.64–3.55 (m, 2H, H-3, H-2), 3.43 (app q,  $J = 6.4$  Hz, 1H, H-5), 2.61 (s, 6H, 2 x  $\text{ArCH}_3$ ), 2.47 (d,  $J = 4.7$  Hz, 1H, 3-OH), 2.14 (d,  $J = 5.3$  Hz, 1H, 4-OH), 1.24 (d,  $J = 6.4$  Hz, 3H, H-6);  $^{13}\text{C NMR}$  (151 MHz,  $\text{CDCl}_3$ )  $\delta$  144.5 (2 x Ar), 135.7 (Ar), 133.5 (Ar), 133.3 (Ar), 132.3 (Ar), 129.2 (Ar), 128.7 (Ar), 128.3 (2 x Ar), 128.2 (Ar), 127.9 (Ar), 127.4 (Ar), 126.4 (Ar), 126.3 (Ar), 126.3 (Ar), 90.4 (C-1), 79.3 (C-2), 75.9 (C-3), 75.6 ( $\text{OCH}_2\text{Ar}$ ), 74.2 (C-5), 71.8 (C-4), 22.8 (2 x  $\text{ArCH}_3$ ), 16.6 (C-6); HRMS (ESI–TOF)  $m/z$ :  $[\text{M} + \text{Na}]^+$  Calcd for  $\text{C}_{25}\text{H}_{28}\text{NaO}_4\text{S}$  447.1601; Found 447.1606.



**3.28**

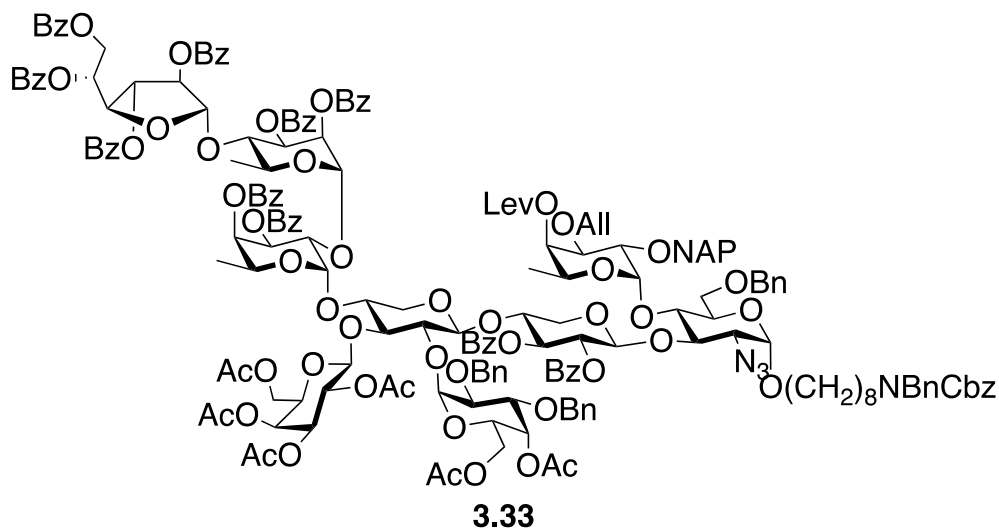
**2,6-Dimethylphenyl 2-O-acetyl-3,4,6-tri-O-benzyl- $\beta$ -D-galactopyranosyl-(1 $\rightarrow$ 3)-2-O-(2-naphthyl)methyl-1-thio- $\beta$ -L-fucopyranoside (3.28)**

To a stirred solution of 2-O-acetyl-3,4,6-tri-O-benzyl- $\beta$ -D-galactopyranose<sup>26</sup> (300 mg, 0.610 mmol) in dry  $\text{CH}_2\text{Cl}_2$  (10 mL) was added cesium carbonate (298 mg, 0.915 mmol) and trichloroacetonitrile (0.183 mL, 1.83 mmol). After stirring for 1 h, the solution was filtered through

Celite and the filtrate was concentrated to dryness. The crude imidate product **3.27** was carried to the next step without further purification.

To a stirred solution of acceptor **3.26** (233 mg, 0.550 mmol) and donor **3.27** in dry CH<sub>2</sub>Cl<sub>2</sub> (10 mL) was added 4Å molecular sieves powder (1.0 g). After stirring for 30 min, the reaction mixture was cooled to -40 °C, and then trifluoromethanesulfonic acid (5.0 µL, 0.061 mmol) was added. After stirring for 1 h, triethylamine was added to the mixture, the solution was filtered through Celite and the filtrate was concentrated to dryness. The crude residue was purified by flash chromatography (2:1 hexanes–EtOAc) to afford **3.28** (285 mg, 58%) as a white solid: *R<sub>f</sub>* = 0.25 (2:1 hexanes–EtOAc); [α]<sub>D</sub><sup>25</sup> -23.9 (*c* = 0.34, CHCl<sub>3</sub>); <sup>1</sup>H NMR (600 MHz, CDCl<sub>3</sub>) δ 7.91–7.88 (m, 1H, Ar), 7.83–7.77 (m, 3H, Ar), 7.66–7.62 (m, 1H, Ar), 7.46–7.41 (m, 2H, Ar), 7.38–7.35 (m, 2H, Ar), 7.35–7.30 (m, 9H, Ar), 7.30–7.26 (m, 4H, Ar), 7.13–7.04 (m, 3H), 5.52 (dd, *J* = 10.2, 8.0 Hz, 1H, H-2'), 5.09 (d, *J* = 10.7 Hz, 1H, OCH<sub>2</sub>Ar), 5.01 (d, *J* = 10.7 Hz, 1H, OCH<sub>2</sub>Ar), 4.97 (d, *J* = 11.6 Hz, 1H, OCH<sub>2</sub>Ar), 4.69 (d, *J* = 12.2 Hz, 1H, OCH<sub>2</sub>Ar), 4.59 (d, *J* = 11.6 Hz, 1H, OCH<sub>2</sub>Ar), 4.54 (d, *J* = 12.2 Hz, 1H, OCH<sub>2</sub>Ar), 4.47 (d, *J* = 11.8 Hz, 1H, OCH<sub>2</sub>Ar), 4.41 (d, *J* = 11.8 Hz, 1H, OCH<sub>2</sub>Ar), 4.38 (d, *J* = 8.0 Hz, 1H, H-1'), 4.28 (d, *J* = 9.3 Hz, 1H, H-1), 3.94 (d, *J* = 2.8 Hz, 1H, H-4'), 3.83 (d, *J* = 10.0 Hz, 1H, 4-OH), 3.66–3.59 (m, 3H, H-4, H-6a', H-3), 3.58 (dd, *J* = 9.7, 3.0 Hz, 1H, H-5'), 3.56–3.52 (m, 3H, H-6b', H-2, H-3'), 3.36 (q, *J* = 6.4 Hz, 1H, H-5), 2.54 (s, 6H, 2 x ArCH<sub>3</sub>), 2.07 (s, 3H, COCH<sub>3</sub>), 1.13 (d, *J* = 6.3 Hz, 3H, H-6); <sup>13</sup>C NMR (151 MHz, CDCl<sub>3</sub>) δ 169.4, (C=O), 144.7 (2 x Ar), 138.3 (Ar), 137.9 (Ar), 137.8 (Ar), 136.6 (Ar), 133.5 (Ar), 133.1 (Ar), 132.5 (Ar), 128.7 (Ar), 128.6 (4 x Ar), 128.6 (2 x Ar), 128.5 (2 x Ar), 128.4 (Ar), 128.2 (Ar), 128.1 (2 x Ar), 128.0 (2 x Ar), 128.0 (2 x Ar), 127.9 (Ar), 127.8 (Ar), 127.7 (2 x Ar), 126.9 (Ar), 126.7 (Ar), 125.9 (Ar), 125.7 (Ar), 103.1 (C-1'), 89.6 (C-1), 83.3 (C-3), 80.5 (C-2), 80.1 (C-3'),

76.0 (OCH<sub>2</sub>Ar), 75.4 (C-5'), 74.9 (OCH<sub>2</sub>Ar), 74.3 (C-4), 73.8 (C-5), 73.5 (OCH<sub>2</sub>Ar), 72.7 (C-4'), 72.3 (OCH<sub>2</sub>Ar), 71.5 (C-2'), 68.7 (C-6'), 22.7 (2 x ArCH<sub>3</sub>), 21.1 (COCH<sub>3</sub>), 16.6 (C-6); HRMS (ESI-TOF) *m/z*: [M + Na]<sup>+</sup> Calcd for C<sub>54</sub>H<sub>58</sub>NaO<sub>10</sub>S 921.3643; Found 921.3641.

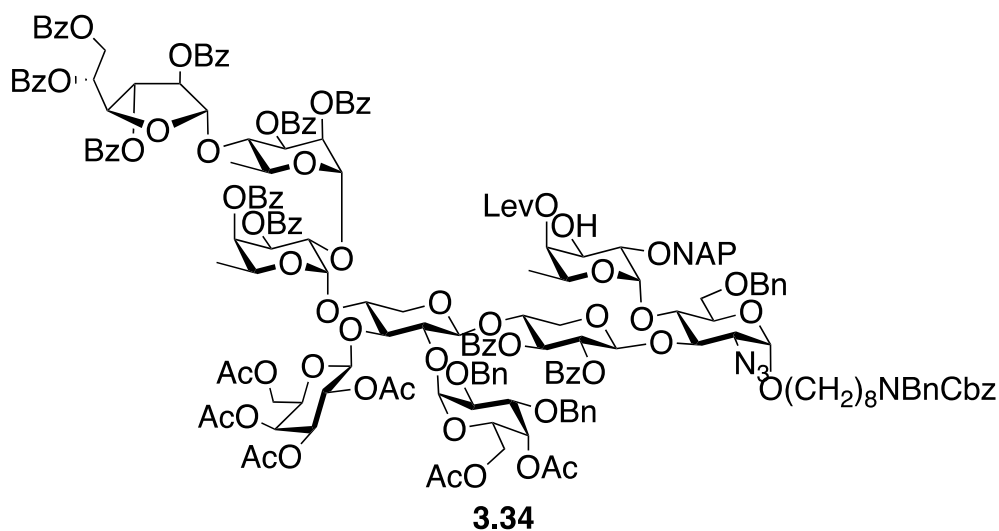


*N*-benzyl-*N*-benzoxycarbonyl-8-amino-1-octyl 2,3,4,6-tetra-*O*-acetyl-β-D-galactopyranosyl-(1→3)-[4,6-di-*O*-acetyl-2,3-di-*O*-benzyl-α-D-galactopyranosyl-(1→2)]-[2,3,5,6-tetra-*O*-benzoyl-β-D-galactofuranosyl-(1→4)-2,3-di-*O*-benzoyl-α-L-rhamnopyranosyl-(1→2)-3,4-di-*O*-benzoyl-α-L-fucopyranosyl-(1→4)]-β-D-xylopyranosyl-(1→4)-2,3-di-*O*-benzoyl-β-D-xylopyranosyl-(1→3)-[3-*O*-allyl-4-*O*-levulinoyl-2-*O*-(2-naphthyl)methyl-α-L-fucopyranosyl-(1→4)]-2-azido-6-*O*-benzyl-2-deoxy-α-D-glucopyranoside (3.33)

To a stirred solution of acceptor **3.11** (60.0 mg, 0.0190 mmol) and donor **2.9** (104 mg, 0.190 mmol) in Et<sub>2</sub>O (5.0 mL) was added 4Å molecular sieves powder (500 mg). After stirring for 30 min, di-tert-butylmethylpyridine (47.0 mg, 0.228 mmol) and methyl trifluoromethanesulfonate (41.6 μL, 0.379 mmol) were added. The resulting solution was stirred for 24 h and then triethylamine was added to the mixture and the solution was filtered through Celite. The filtrate was concentrated to dryness and the crude residue was purified by flash chromatography (3:1 toluene-EtOAc) to afford

**3.33** (34 mg, 50%) as a colorless oil:  $R_f = 0.08$  (3:2 hexanes–EtOAc);  $[\alpha]_D^{25} +10.0$  ( $c = 0.04$ ,  $\text{CHCl}_3$ );  $^1\text{H NMR}$  (600 MHz,  $\text{CDCl}_3$ )  $\delta$  8.12–8.05 (m, 4H), 8.02–7.96 (m, 4H), 7.96–7.89 (m, 4H), 7.89–7.86 (m, 2H), 7.82–7.70 (m, 8H), 7.63–7.56 (m, 2H), 7.56–7.26 (m, 38H), 7.26–7.15 (m, 12H), 7.15–7.10 (m, 4H), 7.10–7.04 (m, 4H), 5.95 (app dt,  $J = 7.9, 4.2$  Hz, 1H), 5.86–5.74 (m, 1H), 5.72 (d,  $J = 3.3$  Hz, 1H), 5.69 (dd,  $J = 10.4, 3.5$  Hz, 1H), 5.66 (d,  $J = 3.2$  Hz, 1H), 5.57 (d,  $J = 2.9$  Hz, 1H), 5.54 (d,  $J = 9.1$  Hz, 1H), 5.52 (dd,  $J = 6.0, 1.8$  Hz, 1H), 5.45 (s, 1H,  $\beta\text{-Gal}f\text{-H-1}$ ), 5.37 (d,  $J = 3.6$  Hz, 1H), 5.36–5.34 (m, 2H), 5.34 (d,  $J = 3.6$  Hz, 1H,  $\alpha\text{-Gal}p\text{-H-1}$ ), 5.29 (d,  $J = 3.2$  Hz, 1H), 5.24–5.10 (m, 6H), 5.06 (d,  $J = 3.0$  Hz, 1H,  $\alpha\text{-Fuc}p'\text{-H-1}$ ), 5.05 (s, 1H), 5.00 (d,  $J = 8.0$  Hz, 1H,  $\beta\text{-Gal}p\text{-H-1}$ ), 4.97 (d,  $J = 1.7$  Hz, 1H,  $\alpha\text{-Rhap-H-1}$ ), 4.95 (dd,  $J = 9.5, 6.4$  Hz, 1H), 4.93 (s, 1H), 4.91 (d,  $J = 8.5$  Hz, 1H,  $\beta\text{-Xyl}p\text{-H-1}$ ), 4.89 (d,  $J = 8.3$  Hz, 1H), 4.81 (d,  $J = 3.8$  Hz, 1H,  $\alpha\text{-GlcN}_3p\text{-H-1}$ ), 4.79 (s, 1H,  $\alpha\text{-Fuc}p\text{-H-1}$ ), 4.76 (d,  $J = 11.3$  Hz, 1H), 4.73–4.64 (m, 4H), 4.62 (d,  $J = 11.9$  Hz, 1H), 4.60 (d,  $J = 5.8$  Hz, 1H,  $\beta\text{-Xyl}p'\text{-H-1}$ ), 4.57–4.51 (m, 2H), 4.50–4.45 (m, 2H), 4.43 (dd,  $J = 5.9, 3.9$  Hz, 1H), 4.37 (dd,  $J = 11.6, 6.9$  Hz, 1H), 4.31 (d,  $J = 11.2$  Hz, 1H), 4.30 (d,  $J = 11.2$  Hz, 1H), 4.26–4.21 (m, 2H), 4.21–4.10 (m, 4H), 4.09–4.02 (m, 3H), 4.02–3.97 (m, 2H), 3.93 (dd,  $J = 11.6, 5.5$  Hz, 1H), 3.91–3.85 (m, 4H), 3.84–3.72 (m, 4H), 3.70 (dd,  $J = 10.2, 3.8$  Hz, 1H), 3.63–3.55 (m, 3H), 3.49 (d,  $J = 10.7$  Hz, 1H), 3.43 (dd,  $J = 12.1, 8.5$  Hz, 1H), 3.40–3.33 (m, 1H), 3.30–3.21 (m, 2H), 3.21–3.13 (m, 1H), 3.09 (dd,  $J = 10.0, 3.7$  Hz, 1H), 2.61–2.53 (m, 4H), 2.24 (s, 3H), 2.14 (s, 3H), 2.09 (s, 3H), 2.07 (s, 3H), 2.03 (s, 3H), 1.97 (s, 3H), 1.97 (s, 3H), 1.59–1.42 (m, 4H), 1.33–1.18 (m, 8H), 1.26 (d,  $J = 6.5$  Hz, 3H), 1.22 (d,  $J = 6.5$  Hz, 3H), 1.06 (d,  $J = 6.2$  Hz, 3H);  $^{13}\text{C NMR}$  (151 MHz,  $\text{CDCl}_3$ )  $\delta$  206.2, 172.2, 170.8, 170.7, 170.6, 170.5, 169.9, 169.2, 166.3, 166.1, 165.8, 165.7, 165.6 (2 x C), 165.3, 165.1, 164.7, 164.6, 139.4, 138.7, 138.2, 137.9, 136.1, 135.1, 133.7, 133.4, 133.1, 132.9, 130.0, 129.9, 129.8, 129.7, 129.6, 129.6, 129.5, 128.8, 128.8, 128.7, 128.6, 128.6, 128.5, 128.5, 128.4, 128.3, 128.2, 128.2, 128.2, 128.1, 128.0, 127.9,

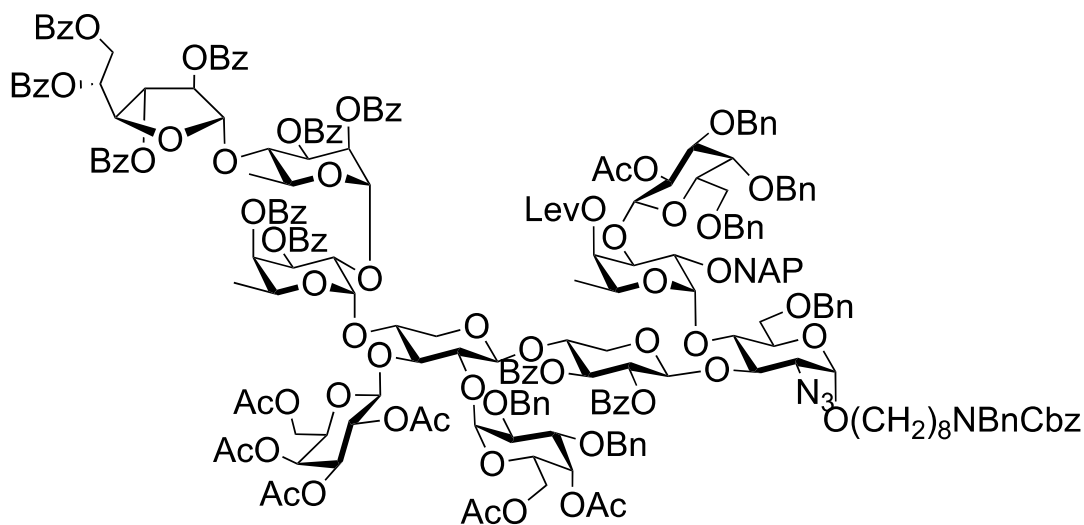
127.8, 127.7, 127.7, 127.6, 127.4, 127.1, 126.5, 126.3, 126.1, 107.4 ( $\beta$ -Gal $f$ -C-1), 101.4 ( $\beta$ -Xyl $p$ -C-1), 100.5 ( $\beta$ -Xyl $p'$ -C-1), 100.2 ( $\beta$ -Gal $p$ -C-1), 97.5 ( $\alpha$ -Glc $N_3p$ -C-1), 97.1 ( $\alpha$ -Fuc $p'$ -C-1), 95.8 ( $\alpha$ -Rhap-C-1), 95.7 ( $\alpha$ -Gal $p$ -C-1), 93.8 ( $\alpha$ -Fuc $p$ -C-1), 82.2, 81.5, 77.9, 77.6, 77.1, 76.5, 76.4, 76.2, 75.9, 75.4, 75.4, 74.6, 73.8, 73.7, 73.6, 73.2 (2 x C), 72.8, 72.4, 71.9, 71.9 (2 x C), 71.8, 71.7 (2 x C), 71.3, 71.0, 70.8, 70.4 (2 x C), 70.3 (2 x C), 69.8, 69.4, 68.6, 68.0, 67.5 (2 x C), 67.3, 67.3, 65.1, 64.9, 63.7, 63.4, 62.2, 62.0, 61.2, 50.3, 47.3, 38.2, 30.1, 29.6, 29.4, 29.4, 28.3, 28.2, 27.9, 26.7, 22.8, 21.0 (2 x C), 21.0, 20.9, 20.9, 20.7, 17.9, 16.4, 16.1; HRMS (MALDI-TOF)  $m/z$ :  $[M + Na]^+$  Calcd for  $C_{197}H_{204}N_4NaO_{60}$  3608.2932; Found 3608.2952.



*N*-benzyl-*N*-benzoxycarbonyl-8-amino-1-octyl 2,3,4,6-tetra-*O*-acetyl- $\beta$ -D-galactopyranosyl-(1 $\rightarrow$ 3)-[4,6-di-*O*-acetyl-2,3-di-*O*-benzyl- $\alpha$ -D-galactopyranosyl-(1 $\rightarrow$ 2)]-[2,3,5,6-tetra-*O*-benzoyl- $\beta$ -D-galactofuranosyl-(1 $\rightarrow$ 4)-2,3-di-*O*-benzoyl- $\alpha$ -L-rhamnopyranosyl-(1 $\rightarrow$ 2)-3,4-di-*O*-benzoyl- $\alpha$ -L-fucopyranosyl-(1 $\rightarrow$ 4)]- $\beta$ -D-xylopyranosyl-(1 $\rightarrow$ 4)-2,3-di-*O*-benzoyl- $\beta$ -D-xylopyranosyl-(1 $\rightarrow$ 3)-[4-*O*-levulinoyl-2-*O*-(2-naphthyl)methyl- $\alpha$ -L-fucopyranosyl-(1 $\rightarrow$ 4)]-2-azido-6-*O*-benzyl-2-deoxy- $\alpha$ -D-glucopyranoside (3.34)

To a stirred solution of **3.33** (30.0 mg, 8.36  $\mu\text{mol}$ ) in dry THF (5 mL), degassed under vacuum, and under an Ar atmosphere, (1,5-cyclooctadiene)bis-(methyldiphenylphosphine)iridium I hexafluorophosphate (0.71 mg, 0.84  $\mu\text{mol}$ ) was added, followed by further degassing of the reaction mixture. The suspension was stirred for 15 min at 0 °C and the catalyst was then activated with hydrogen (2 min under a hydrogen atmosphere). The excess hydrogen was removed by three cycles of vacuum and flushing with Ar. The reaction mixture was then stirred for 2 h before the solvent was evaporated and the residue was dissolved in acetone–water (5.0 mL, 9:1) and HgO (4.50 mg, 20.9  $\mu\text{mol}$ ) and HgCl<sub>2</sub> (4.50 mg, 16.7  $\mu\text{mol}$ ) were added. The reaction mixture was stirred for 2 h, the solvent was evaporated, and the residue was diluted with EtOAc (25 mL), washed with 10% KI, saturated aqueous Na<sub>2</sub>S<sub>2</sub>O<sub>3</sub> and water. The aqueous layers were extracted with EtOAc (25 mL), and the combined organic layers were dried over Na<sub>2</sub>SO<sub>4</sub>, filtered and concentrated. The crude residue was purified by flash chromatography (3:2 hexane–EtOAc) to afford **3.34** (23.0 mg, 77%) as a colorless oil:  $R_f = 0.20$  (1:1 hexanes–EtOAc);  $[\alpha]_D^{25} +14.0$  ( $c = 0.07$ , CHCl<sub>3</sub>); <sup>1</sup>H NMR (600 MHz, CDCl<sub>3</sub>)  $\delta$  8.10–8.03 (m, 4H), 8.02–7.96 (m, 4H), 7.96–7.89 (m, 4H), 7.89–7.85 (m, 2H), 7.82–7.69 (m, 8H), 7.63–7.27 (m, 41H), 7.26–7.14 (m, 13H), 7.13–7.03 (m, 6H), 5.94 (app dt,  $J = 7.8, 4.1$  Hz, 1H), 5.71 (s, 1H), 5.71 (dd,  $J = 9.3, 3.5$  Hz, 1H), 5.66 (d,  $J = 3.2$  Hz, 1H), 5.56 (dd,  $J = 9.8, 3.5$  Hz, 1H), 5.53 (app t,  $J = 8.7$  Hz, 1H), 5.52 (dd,  $J = 6.0, 2.0$  Hz, 1H), 5.45 (s, 1H,  $\beta$ -Gal $f$ -H-1), 5.39–5.36 (m, 2H), 5.32 (d,  $J = 3.6$  Hz, 1H,  $\alpha$ -Gal $p$ -H-1), 5.23–5.10 (m, 6H), 5.06 (d,  $J = 8.2$  Hz, 1H,  $\beta$ -Gal $p$ -H-1), 5.03 (d,  $J = 3.6$  Hz, 1H,  $\alpha$ -Fuc $p'$ -H-1), 4.95 (d,  $J = 7.1$  Hz, 1H,  $\beta$ -Xyl $p$ -H-1), 4.95 (d,  $J = 1.7$  Hz, 1H,  $\alpha$ -Rhap-H-1), 5.00–4.89 (m, 3H), 4.85–4.76 (m, 2H), 4.83 (s, 1H,  $\alpha$ -Fuc $p$ -H-1), 4.81 (d,  $J = 3.5$  Hz, 1H,  $\alpha$ -GlcN<sub>3</sub> $p$ -H-1), 4.76 (d,  $J = 11.5$  Hz, 1H), 4.72–4.62 (m, 4H), 4.59 (d,  $J = 6.7$  Hz, 1H,  $\beta$ -Xyl $p'$ -H-1), 4.57 (d,  $J = 11.5$  Hz, 1H), 4.52 (dd,  $J = 11.5, 6.5$  Hz, 1H), 4.48 (m, 2H), 4.43 (dd,  $J = 5.9, 3.9$  Hz, 1H), 4.38 (d,  $J = 12.3$

Hz, 1H), 4.36–4.30 (m, 2H), 4.29 (app t,  $J = 6.1$  Hz, 1H), 4.22–4.17 (m, 2H), 4.17–4.10 (m, 2H), 4.07 (app t,  $J = 9.4$  Hz, 1H), 4.04–3.96 (m, 2H), 3.93 (dd,  $J = 11.8, 5.7$  Hz, 1H), 3.91–3.86 (m, 2H), 3.85–3.76 (m, 2H), 3.78–3.71 (m, 3H), 3.66–3.53 (m, 4H), 3.49 (d,  $J = 10.7$  Hz, 1H), 3.43 (dd,  $J = 12.2, 8.6$  Hz, 1H), 3.42–3.32 (m, 1H), 3.27–3.13 (m, 3H), 3.08 (dd,  $J = 10.1, 3.7$  Hz, 1H), 2.67–2.52 (m, 2H), 2.52–2.40 (m, 2H), 2.24 (s, 3H), 2.15 (s, 3H), 2.09 (s, 3H), 2.08 (s, 3H), 2.02 (s, 3H), 1.97 (s, 3H), 1.97 (s, 3H), 1.59–1.42 (m, 4H), 1.33–1.18 (m, 11H), 1.22 (d,  $J = 6.5$  Hz, 3H), 1.06 (d,  $J = 6.2$  Hz, 3H);  $^{13}\text{C}$  NMR (151 MHz,  $\text{CDCl}_3$ )  $\delta$  207.2, 173.0, 170.8, 170.8, 170.6, 170.5, 169.9, 169.3, 166.2, 166.1, 165.8, 165.7, 165.6, 165.6, 165.3, 165.2, 164.8, 164.6, 138.8, 138.2, 137.9, 135.9, 133.7, 133.7, 133.4, 133.3, 133.3, 133.1, 132.9, 130.0, 129.9, 129.8, 129.7, 129.6, 129.5, 128.8, 128.8, 128.7, 128.6, 128.5, 128.4, 128.4, 128.3, 128.2, 128.2, 128.0, 128.0, 127.9, 127.8, 127.8, 127.6, 127.4, 127.1, 126.3, 126.2, 126.1, 107.4 ( $\beta$ -Gal $f$ -C-1), 101.4 ( $\beta$ -Xyl $p$ -C-1), 100.5 ( $\beta$ -Xyl $p'$ -C-1), 100.1 ( $\beta$ -Gal $p$ -C-1), 97.2 ( $\alpha$ -Glc $N_3p$ -C-1), 96.9 ( $\alpha$ -Fuc $p$ -C-1), 95.9 ( $\alpha$ -Rhap-C-1), 95.7 ( $\alpha$ -Gal $p$ -C-1), 93.9 ( $\alpha$ -Fuc $p'$ -C-1), 82.2, 81.5, 77.9, 77.6, 77.1, 76.3, 76.2, 76.1, 75.6, 74.1, 73.9 (2 x C), 73.6, 73.4 (2 x C), 72.8, 72.1, 71.9, 71.9 (2 x C), 71.7, 71.3, 70.9, 70.8, 70.3, 69.7, 69.4, 68.9, 68.6, 68.0, 67.6, 67.5, 67.4, 67.3, 65.1, 65.0, 63.6, 63.4, 62.1, 62.0, 61.3, 50.6, 50.3, 47.3, 46.3, 38.4, 30.3, 29.8, 29.5, 29.4, 28.2, 26.9, 26.0, 22.8, 21.1, 21.0, 21.0, 20.9 (2 x C), 20.7, 17.8, 16.3, 16.2; HRMS (MALDI-TOF)  $m/z$ :  $[\text{M} + \text{Na}]^+$  Calcd for  $\text{C}_{194}\text{H}_{200}\text{N}_4\text{NaO}_{60}$  3568.2615; Found 3568.2607.

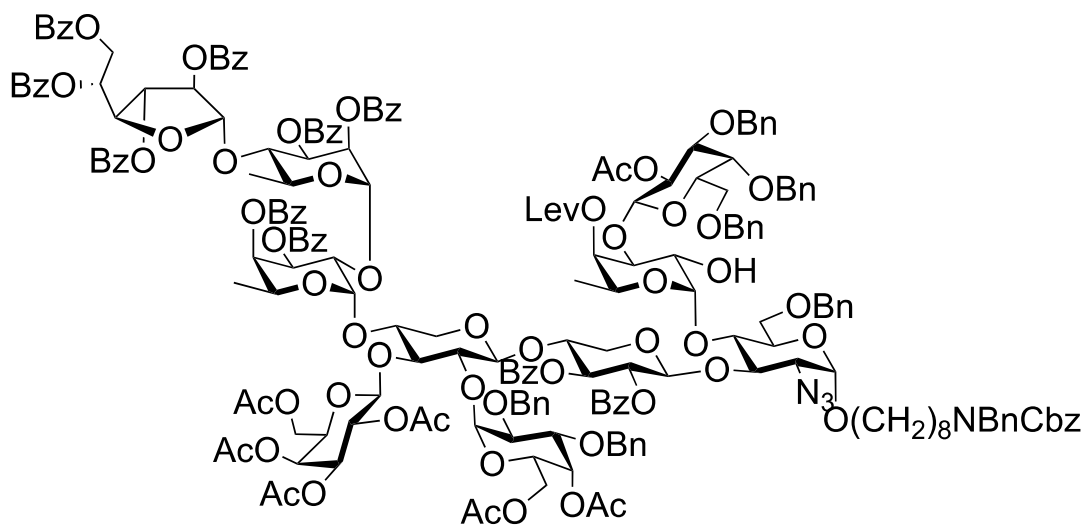


**3.35**

*N*-benzyl-*N*-benzoxycarbonyl-8-amino-1-octyl 2,3,4,6-tetra-*O*-acetyl- $\beta$ -D-galactopyranosyl-(1 $\rightarrow$ 3)-[4,6-di-*O*-acetyl-2,3-di-*O*-benzyl- $\alpha$ -D-galactopyranosyl-(1 $\rightarrow$ 2)]-[2,3,5,6-tetra-*O*-benzoyl- $\beta$ -D-galactofuranosyl-(1 $\rightarrow$ 4)-2,3-di-*O*-benzoyl- $\alpha$ -L-rhamnopyranosyl-(1 $\rightarrow$ 2)-3,4-di-*O*-benzoyl- $\alpha$ -L-fucopyranosyl-(1 $\rightarrow$ 4)]- $\beta$ -D-xylopyranosyl-(1 $\rightarrow$ 4)-2,3-di-*O*-benzoyl- $\beta$ -D-xylopyranosyl-(1 $\rightarrow$ 3)-[2-*O*-acetyl-3,4,6-tri-*O*-benzyl- $\beta$ -D-galactopyranosyl-(1 $\rightarrow$ 3)-4-*O*-levulinoyl-2-*O*-(2-naphthyl)methyl- $\alpha$ -L-fucopyranosyl-(1 $\rightarrow$ 4)]-2-azido-6-*O*-benzyl-2-deoxy- $\alpha$ -D-glucopyranoside (**3.35**)

To a stirred solution of acceptor **3.34** (23.0 mg, 6.48  $\mu$ mol) and donor **2.12**<sup>19</sup> (19.0 mg, 32.4  $\mu$ mol) in dry CH<sub>2</sub>Cl<sub>2</sub> (5 mL) was added 4Å molecular sieves powder (500 mg). After stirring for 30 min, the reaction mixture was cooled to 0 °C and then *N*-iodosuccinimide (12.0 mg, 51.8  $\mu$ mol) and silver trifluoromethanesulfonate (0.8 mg, 3.24  $\mu$ mol) were added successively. The resulting solution was stirred for 1 h at 0 °C before triethylamine was added. The solution was filtered through Celite and the filtrate was washed with saturated aqueous Na<sub>2</sub>S<sub>2</sub>O<sub>3</sub> and saturated aqueous NaHCO<sub>3</sub>. The organic layer was dried over Na<sub>2</sub>SO<sub>4</sub>, filtered and concentrated to dryness. The crude residue was purified by flash chromatography (2:1 hexanes–EtOAc) to afford **3.35** (22.2 mg,

87%) as a colorless oil:  $R_f = 0.32$  (2:1 hexanes–EtOAc);  $^1\text{H NMR}$  (600 MHz,  $\text{CDCl}_3$ )  $\delta$  8.13–8.09 (m, 2H), 8.08–8.03 (m, 2H), 8.03–7.95 (m, 4H), 7.95–7.89 (m, 4H), 7.88–7.84 (m, 2H), 7.80–7.74 (m, 4H), 7.73–7.69 (m, 1H), 7.68–7.65 (m, 1H), 7.64–7.56 (m, 3H), 7.54–7.44 (m, 9H), 7.44–7.26 (m, 32H), 7.26–7.22 (m, 7H), 7.21–7.14 (m, 16H), 7.14–7.02 (m, 8H), 7.00–6.96 (m, 2H), 5.95 (app dt,  $J = 7.8, 4.1$  Hz, 1H), 5.73 (d,  $J = 3.4$  Hz, 1H), 5.70–5.65 (m, 2H), 5.55 (dd,  $J = 9.7, 3.2$  Hz, 1H), 5.53 (app t,  $J = 8.6$  Hz, 1H), 5.51 (dd,  $J = 6.0, 1.7$  Hz, 1H), 5.44 (s, 1H,  $\beta\text{-Gal}f\text{-H-1}$ ), 5.38–5.33 (m, 2H), 5.29–5.25 (m, 1H), 5.27 (d,  $J = 3.0$  Hz, 1H,  $\alpha\text{-Gal}p\text{-H-1}$ ), 5.26–5.22 (m, 1H), 5.19 (d,  $J = 3.3$  Hz, 1H), 5.18–5.12 (m, 4H), 5.08 (d,  $J = 11.6$  Hz, 1H), 5.07 (d,  $J = 2.7$  Hz, 1H,  $\alpha\text{-Fuc}p'\text{-H-1}$ ), 5.05 (d,  $J = 8.0$  Hz, 1H,  $\beta\text{-Gal}p\text{-H-1}$ ), 5.02 (d,  $J = 8.2$  Hz, 1H,  $\beta\text{-Gal}p'\text{-H-1}$ ), 4.96–4.90 (m, 3H), 4.89 (d,  $J = 3.8$  Hz, 1H,  $\alpha\text{-Rhap}\text{-H-1}$ ), 4.82 (d,  $J = 11.6$  Hz, 1H), 4.78 (d,  $J = 3.5$  Hz, 1H,  $\alpha\text{-Glc}N_3p\text{-H-1}$ ), 4.77 (d,  $J = 11.6$  Hz, 1H), 4.71 (dd,  $J = 12.0, 4.4$  Hz, 1H), 4.69 (s, 1H,  $\alpha\text{-Fuc}p\text{-H-1}$ ), 4.68–4.62 (m, 2H), 4.54 (d,  $J = 5.8$  Hz, 1H,  $\beta\text{-Xyl}p'\text{-H-1}$ ), 4.62–4.52 (m, 4H), 4.51–4.45 (m, 3H), 4.44–4.35 (m, 4H), 4.42 (d,  $J = 6.4$  Hz, 1H,  $\beta\text{-Xyl}p\text{-H-1}$ ), 4.34 (d,  $J = 12.4$  Hz, 1H), 4.31 (dd,  $J = 10.7, 3.4$  Hz, 1H), 4.27–4.14 (m, 4H), 4.13 (dd,  $J = 7.9, 6.5$  Hz, 1H), 4.11 (dd,  $J = 7.8, 3.0$  Hz, 1H), 4.09–4.04 (m, 1H), 4.03–3.94 (m, 4H), 3.94–3.84 (m, 5H), 3.83–3.64 (m, 6H), 3.61 (dd,  $J = 8.3, 5.6$  Hz, 1H), 3.57–3.52 (m, 1H), 3.50–3.41 (m, 2H), 3.40–3.29 (m, 4H), 3.27–3.11 (m, 5H), 3.04 (dd,  $J = 9.9, 3.6$  Hz, 1H), 2.66–2.45 (m, 4H), 2.25 (s, 3H), 2.14 (s, 3H), 2.10 (s, 3H), 2.08 (s, 3H), 2.00 (s, 6H), 1.96 (s, 3H), 1.93 (s, 3H), 1.59–1.42 (m, 4H), 1.33–1.18 (m, 8H), 1.26 (d,  $J = 6.5$  Hz, 3H), 1.19 (d,  $J = 6.5$  Hz, 3H), 1.10 (d,  $J = 6.0$  Hz, 3H); HRMS (MALDI–TOF)  $m/z$ :  $[\text{M} + \text{Na}]^+$  Calcd for  $\text{C}_{223}\text{H}_{230}\text{N}_4\text{NaO}_{66}$  4042.4658; Found 4042.4695.

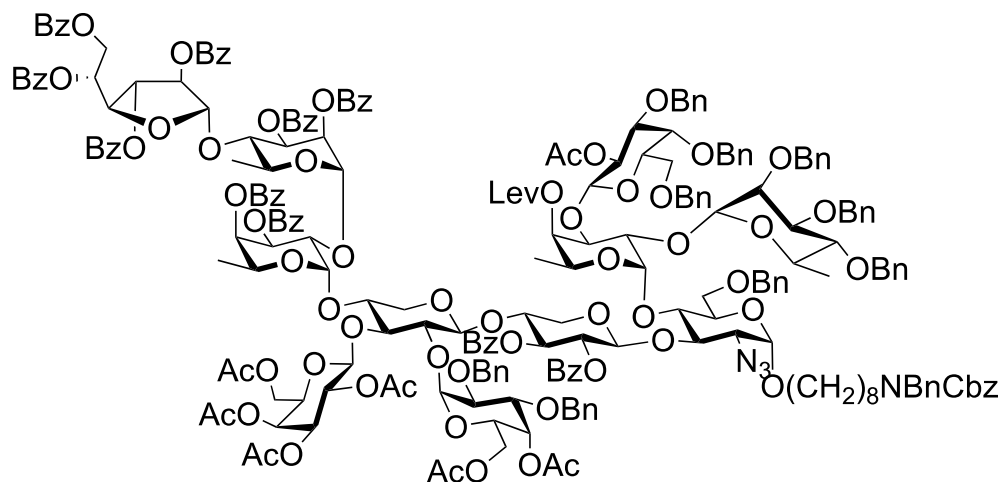


**3.36**

*N*-benzyl-*N*-benzoxycarbonyl-8-amino-1-octyl 2,3,4,6-tetra-*O*-acetyl- $\beta$ -D-galactopyranosyl-(1 $\rightarrow$ 3)-[4,6-di-*O*-acetyl-2,3-di-*O*-benzyl- $\alpha$ -D-galactopyranosyl-(1 $\rightarrow$ 2)]-[2,3,5,6-tetra-*O*-benzoyl- $\beta$ -D-galactofuranosyl-(1 $\rightarrow$ 4)-2,3-di-*O*-benzoyl- $\alpha$ -L-rhamnopyranosyl-(1 $\rightarrow$ 2)-3,4-di-*O*-benzoyl- $\alpha$ -L-fucopyranosyl-(1 $\rightarrow$ 4)]- $\beta$ -D-xylopyranosyl-(1 $\rightarrow$ 4)-2,3-di-*O*-benzoyl- $\beta$ -D-xylopyranosyl-(1 $\rightarrow$ 3)-[2-*O*-acetyl-3,4,6-tri-*O*-benzyl- $\beta$ -D-galactopyranosyl-(1 $\rightarrow$ 3)-4-*O*-levulinoyl- $\alpha$ -L-fucopyranosyl-(1 $\rightarrow$ 4)]-2-azido-6-*O*-benzyl-2-deoxy- $\alpha$ -D-glucopyranoside (3.36)

To a stirred biphasic solution of **3.35** (6.0 mg, 1.5  $\mu$ mol) in CH<sub>2</sub>Cl<sub>2</sub>-H<sub>2</sub>O (5 mL, 4:1) was added 2,3-dichloro-5,6-dicyano-1,4-benzoquinone (0.70 mg, 3.0 mmol) at room temperature. The reaction mixture was stirred overnight before being diluted with CH<sub>2</sub>Cl<sub>2</sub> (50 mL). The mixture was then washed successively with 1N NaOH, water and brine. The organic layer was dried over Na<sub>2</sub>SO<sub>4</sub>, filtered and concentrated to dryness. The crude residue was purified by flash chromatography (1:1 hexanes-EtOAc) to afford **3.36** (5.0 mg, 86%) as a colorless oil: *R*<sub>f</sub> = 0.12 (2:1 hexanes-EtOAc); *R*<sub>f</sub> = 0.21 (2:1 hexanes-EtOAc); <sup>1</sup>H NMR (600 MHz, CDCl<sub>3</sub>)  $\delta$  8.12–8.08 (m, 2H), 8.08–8.03 (m, 2H), 8.02–7.96 (m, 4H), 8.02–7.96 (m, 4H), 7.96–7.89 (m, 4H), 7.87–7.83

(m, 2H), 7.80–7.73 (m, 4H), 7.64–7.57 (m, 2H), 7.54–7.44 (m, 9H), 7.43–7.26 (m, 30H), 7.26–7.14 (m, 17H), 7.18–7.09 (m, 3H), 7.09–6.97 (m, 6H), 6.89–6.84 (m, 1H), 5.95 (app dt,  $J = 7.9$ , 4.2 Hz, 1H), 5.72 (s, 1H), 5.71–5.62 (m, 2H), 5.57–5.51 (m, 2H), 5.50 (dd,  $J = 5.9$ , 2.2 Hz, 1H), 5.44 (s, 1H,  $\beta$ -Gal $f$ -H-1), 5.38–5.28 (m, 3H), 5.26 (d,  $J = 3.6$  Hz, 1H,  $\alpha$ -Gal $p$ -H-1), 5.29–5.20 (m, 1H), 5.20–5.10 (m, 5H), 5.05 (d,  $J = 7.9$  Hz, 1H,  $\beta$ -Gal $p$ -H-1), 5.05 (d,  $J = 2.6$  Hz, 1H,  $\alpha$ -Fuc $p'$ -H-1), 5.02 (d,  $J = 9.8$  Hz, 1H,  $\beta$ -Gal $p'$ -H-1), 4.98–4.83 (m, 4H), 4.88 (s, 1H,  $\alpha$ -Rhap-H-1), 4.81 (d,  $J = 3.8$  Hz, 1H,  $\alpha$ -GlcN $_3p$ -H-1), 4.78–4.73 (m, 1H), 4.73–4.60 (m, 4H), 4.68 (s, 1H,  $\alpha$ -Fuc $p$ -H-1), 4.59–4.53 (m, 2H), 4.56 (d,  $J = 6.4$  Hz, 1H,  $\beta$ -Xyl $p'$ -H-1), 4.53–4.42 (m, 5H), 4.42 (dd,  $J = 6.0$ , 3.9 Hz, 1H), 4.40–4.28 (m, 4H), 4.26–4.07 (m, 6H), 4.24 (d,  $J = 6.9$  Hz, 1H,  $\beta$ -Xyl $p$ -H-1), 4.07–3.95 (m, 5H), 3.94–3.87 (m, 2H), 3.92 (dd,  $J = 12.0$ , 6.1 Hz, 1H), 3.85 (d,  $J = 3.7$  Hz, 1H), 3.83 (dd,  $J = 6.4$ , 3.1 Hz, 1H), 3.77 (dd,  $J = 9.9$ , 4.1 Hz, 1H), 3.75–3.62 (m, 4H), 3.62–3.50 (m, 4H), 3.50–3.42 (m, 2H), 3.40–3.33 (m, 2H), 3.29 (app t,  $J = 11.1$  Hz, 1H), 3.27–3.12 (m, 3H), 3.08 (dd,  $J = 9.8$ , 3.6 Hz, 1H), 2.72–2.42 (m, 4H), 2.25 (s, 3H), 2.15 (s, 3H), 2.11 (s, 3H), 2.08 (s, 3H), 2.06 (s, 3H), 2.01 (s, 3H), 1.97 (s, 3H), 1.89 (s, 3H), 1.59–1.42 (m, 4H), 1.33–1.18 (m, 8H), 1.28 (d,  $J = 6.5$  Hz, 3H), 1.22 (d,  $J = 6.6$  Hz, 3H), 1.10 (d,  $J = 6.1$  Hz, 3H); HRMS (MALDI–TOF)  $m/z$ :  $[M + Na]^+$  Calcd for C<sub>212</sub>H<sub>222</sub>N<sub>4</sub>NaO<sub>66</sub> 3902.4031; Found 3902.4025.

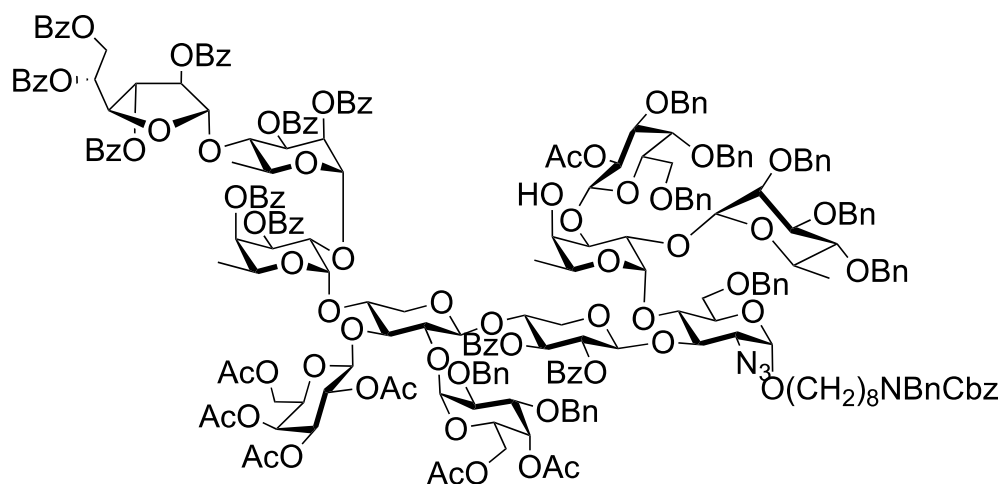


**3.37**

*N*-benzyl-*N*-benzoxycarbonyl-8-amino-1-octyl 2,3,4,6-tetra-*O*-acetyl- $\beta$ -D-galactopyranosyl-(1 $\rightarrow$ 3)-[4,6-di-*O*-acetyl-2,3-di-*O*-benzyl- $\alpha$ -D-galactopyranosyl-(1 $\rightarrow$ 2)]-[2,3,5,6-tetra-*O*-benzoyl- $\beta$ -D-galactofuranosyl-(1 $\rightarrow$ 4)-2,3-di-*O*-benzoyl- $\alpha$ -L-rhamnopyranosyl-(1 $\rightarrow$ 2)-3,4-di-*O*-benzoyl- $\alpha$ -L-fucopyranosyl-(1 $\rightarrow$ 4)]- $\beta$ -D-xylopyranosyl-(1 $\rightarrow$ 4)-2,3-di-*O*-benzoyl- $\beta$ -D-xylopyranosyl-(1 $\rightarrow$ 3)-[2-*O*-acetyl-3,4,6-tri-*O*-benzyl- $\beta$ -D-galactopyranosyl-(1 $\rightarrow$ 3)]-[2,3,4-tri-*O*-benzyl- $\alpha$ -L-rhamnopyranosyl-(1 $\rightarrow$ 2)]-4-*O*-levulinoyl- $\alpha$ -L-fucopyranosyl-(1 $\rightarrow$ 4)]-2-azido-6-*O*-benzyl-2-deoxy- $\alpha$ -D-glucopyranoside (3.37)

To a stirred solution of acceptor **3.36** (5.7 mg, 1.48  $\mu$ mol) and donor **2.13**<sup>20</sup> (4.0 mg, 7.41  $\mu$ mol) in dry CH<sub>2</sub>Cl<sub>2</sub> (2 mL) was added 4Å molecular sieves powder (200 mg). After stirring for 30 min, the reaction mixture was cooled to 0 °C and then *N*-iodosuccinimide (2.5 mg, 11.2  $\mu$ mol) and silver trifluoromethanesulfonate (0.19 mg, 0.74  $\mu$ mol) were added successively. The resulting solution was stirred for 1 h at 0 °C before triethylamine was added. The solution was filtered through Celite and the filtrate was washed with saturated aqueous Na<sub>2</sub>S<sub>2</sub>O<sub>3</sub> and saturated aqueous NaHCO<sub>3</sub>. The organic layer was dried over Na<sub>2</sub>SO<sub>4</sub>, filtered and concentrated to dryness and the crude residue was purified by flash chromatography (2:1 hexanes–EtOAc) to afford **3.37** (5.8 mg, 91%) as a colorless oil: *R*<sub>f</sub> = 0.32 (2:1 hexanes–EtOAc); <sup>1</sup>H NMR (600 MHz, CDCl<sub>3</sub>)  $\delta$  8.13–8.08

(m, 2H), 8.07–8.03 (m, 2H), 8.02–7.96 (m, 4H), 7.96–7.92 (m, 2H), 7.92–7.89 (m, 2H), 7.88–7.83 (m, 2H), 7.81–7.74 (m, 4H), 7.63–7.58 (m, 2H), 7.53–7.43 (m, 8H), 7.43–7.27 (m, 32H), 7.26–7.02 (m, 41H), 7.01–6.97 (m, 2H), 6.91–7.86 (m, 2H), 5.95 (app dt,  $J = 7.7, 4.1$  Hz, 1H), 5.72 (d,  $J = 3.4$  Hz, 1H), 5.71–5.63 (m, 2H), 5.59–5.52 (m, 2H), 5.51 (dd,  $J = 6.1, 1.9$  Hz, 1H), 5.45 (s, 1H,  $\beta$ -Gal $f$ -H-1), 5.39–5.31 (m, 2H), 5.38 (s, 1H,  $\alpha$ -Gal $p$ -H-1), 5.30–5.23 (m, 6H), 5.24 (s, 1H,  $\alpha$ -Fuc $p'$ -H-1), 5.02 (d,  $J = 8.0$  Hz, 1H,  $\beta$ -Gal $p$ -H-1), 5.00 (d,  $J = 8.9$  Hz, 1H,  $\beta$ -Gal $p'$ -H-1), 4.96–4.87 (m, 2H), 4.95 (s, 1H,  $\alpha$ -Rhap' $'$ -H-1), 4.94 (s, 1H,  $\alpha$ -Rhap-H-1), 4.81 (d,  $J = 11.2$  Hz, 1H), 4.78–4.53 (m, 10H), 4.75 (d,  $J = 3.6$  Hz, 1H,  $\alpha$ -GlcN $_3p$ -H-1), 4.73 (d,  $J = 3.5$  Hz, 1H,  $\alpha$ -Fuc $p$ -H-1), 4.62 (d,  $J = 6.8$  Hz, 1H,  $\beta$ -Xyl $p'$ -H-1), 4.53–4.44 (m, 6H), 4.44–4.40 (m, 1H), 4.43 (d,  $J = 5.8$  Hz, 1H,  $\beta$ -Xyl $p$ -H-1), 4.39–4.26 (m, 7H), 4.26–4.10 (m, 9H), 4.10–3.95 (m, 6H), 3.95–3.84 (m, 3H), 3.80 (s, 1H), 3.77–3.54 (m, 7H), 3.77–3.42 (m, 5H), 3.41–3.35 (m, 2H), 3.35–3.21 (m, 5H), 3.21–3.13 (m, 1H), 2.93 (d,  $J = 9.8$  Hz, 1H), 2.72–2.56 (m, 2H), 2.53–2.42 (m, 2H), 2.24 (s, 3H), 2.14 (s, 3H), 2.10 (s, 3H), 2.08 (s, 3H), 2.06 (s, 3H), 2.01 (s, 3H), 1.96 (s, 3H), 1.88 (s, 3H), 1.59–1.42 (m, 4H), 1.33–1.18 (m, 8H), 1.31 (d,  $J = 6.5$  Hz, 3H), 1.29 (d,  $J = 6.2$  Hz, 3H), 1.14 (d,  $J = 6.4$  Hz, 3H), 1.11 (d,  $J = 5.9$  Hz, 3H); HRMS (MALDI–TOF)  $m/z$ :  $[M + Na]^+$  Calcd for C $_{239}$ H $_{250}$ N $_4$ NaO $_{70}$  4318.6021; Found 4318.5985.

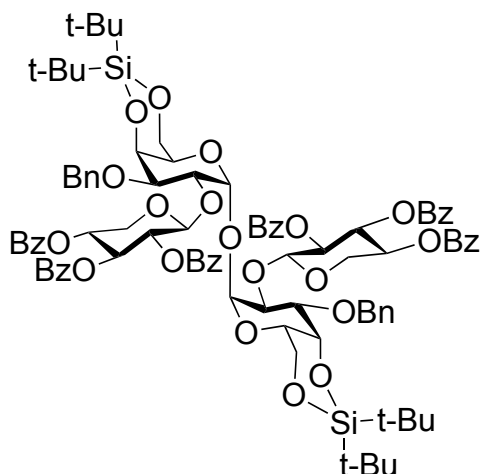


**3.38**

*N*-benzyl-*N*-benzoxycarbonyl-8-amino-1-octyl 2,3,4,6-tetra-*O*-acetyl- $\beta$ -D-galactopyranosyl-(1 $\rightarrow$ 3)-[4,6-di-*O*-acetyl-2,3-di-*O*-benzyl- $\alpha$ -D-galactopyranosyl-(1 $\rightarrow$ 2)]-[2,3,5,6-tetra-*O*-benzoyl- $\beta$ -D-galactofuranosyl-(1 $\rightarrow$ 4)-2,3-di-*O*-benzoyl- $\alpha$ -L-rhamnopyranosyl-(1 $\rightarrow$ 2)-3,4-di-*O*-benzoyl- $\alpha$ -L-fucopyranosyl-(1 $\rightarrow$ 4)]- $\beta$ -D-xylopyranosyl-(1 $\rightarrow$ 4)-2,3-di-*O*-benzoyl- $\beta$ -D-xylopyranosyl-(1 $\rightarrow$ 3)-[2-*O*-acetyl-3,4,6-tri-*O*-benzyl- $\beta$ -D-galactopyranosyl-(1 $\rightarrow$ 3)]-[2,3,4-tri-*O*-benzyl- $\alpha$ -L-rhamnopyranosyl-(1 $\rightarrow$ 2)]- $\alpha$ -L-fucopyranosyl-(1 $\rightarrow$ 4)]-2-azido-6-*O*-benzyl-2-deoxy- $\alpha$ -D-glucopyranoside (**3.38**)

To a stirred solution of **2.37** (5.2 mg, 1.3  $\mu$ mol) in pyridine–AcOH (2.5 mL, 3:2) was added hydrazine monohydrate (0.12  $\mu$ L, 2.4  $\mu$ mol). After stirring for overnight, the reaction mixture was diluted with CH<sub>2</sub>Cl<sub>2</sub> (50 mL) and washed with 1N HCl, saturated aqueous NaHCO<sub>3</sub> and brine. The combined organic layers were dried over Na<sub>2</sub>SO<sub>4</sub>, filtered and concentrated to dryness. The crude residue was purified by flash chromatography (2:1 hexanes–EtOAc) to afford **2.26** (5.2 mg, quant) as a white solid:  $R_f$  = 0.35 (2:1 hexanes–EtOAc); <sup>1</sup>H NMR (600 MHz, CDCl<sub>3</sub>)  $\delta$  8.14–8.09 (m, 2H), 8.06–8.02 (m, 2H), 8.02–7.98 (m, 2H), 7.98–7.96 (m, 2H), 7.96–7.92 (m, 2H), 7.92–7.88 (m, 2H), 7.88–7.82 (m, 2H), 7.81–7.74 (m, 4H), 7.64–7.58 (m, 2H), 7.55–7.43 (m, 8H), 7.43–7.26 (m, 29H), 7.26–6.98 (m, 48H), 5.95 (app dt,  $J$  = 7.7, 4.1 Hz, 1H), 5.72 (d,  $J$  = 3.5 Hz, 1H), 5.69–5.63

(m, 2H), 5.56 (dd,  $J = 10.1, 3.8$  Hz, 1H), 5.54–5.49 (m, 2H), 5.47 (s, 1H,  $\beta$ -Gal $f$ -H-1), 5.39–5.32 (m, 2H), 5.32 (d,  $J = 3.5$  Hz, 1H,  $\alpha$ -Gal $p$ -H-1), 5.30–5.25 (m, 2H), 5.21–5.11 (m, 4H), 5.11 (d,  $J = 2.4$  Hz, 1H,  $\alpha$ -Fuc $p$ -H-1), 5.01 (d,  $J = 7.9$  Hz, 1H,  $\beta$ -Gal $p$ -H-1), 4.99 (d,  $J = 8.2$  Hz, 1H,  $\beta$ -Gal $p'$ -H-1), 4.93 (d,  $J = 6.6$  Hz, 1H), 4.90 (d,  $J = 3.5$  Hz, 1H), 4.88 (s, 1H,  $\alpha$ -Rhap-H-1), 4.86 (s, 1H,  $\alpha$ -Rhap'-H-1), 4.84 (d,  $J = 12.0$  Hz, 1H), 4.77 (d,  $J = 3.5$  Hz, 1H,  $\alpha$ -GlcN $_3p$ -H-1), 4.76–4.69 (m, 4H), 4.67 (dd,  $J = 11.8, 7.3$  Hz, 1H), 4.63–4.59 (m, 2H), 4.63 (d,  $J = 3.8$  Hz, 1H,  $\alpha$ -Fuc $p$ -H-1), 4.59 (d,  $J = 7.8$  Hz, 1H,  $\beta$ -Xyl $p'$ -H-1), 4.57–4.52 (m, 4H), 4.52–4.34 (m, 13H), 4.46 (d,  $J = 6.7$  Hz, 1H,  $\beta$ -Xyl $p$ -H-1), 4.32–4.26 (m, 3H), 4.21–4.16 (m, 3H), 4.16–4.08 (m, 4H), 4.07–3.99 (m, 3H), 3.97 (dd,  $J = 10.0, 3.3$  Hz, 1H), 3.94–3.87 (m, 2H), 3.86 (dd,  $J = 9.9, 3.4$  Hz, 1H), 3.82 (dd,  $J = 9.0, 2.8$  Hz, 1H), 3.79–3.67 (m, 4H), 3.66–3.51 (m, 6H), 3.52–3.41 (m, 4H), 3.40–3.31 (m, 4H), 3.27–3.21 (m, 1H), 3.21–3.14 (m, 2H), 2.98 (dd,  $J = 9.6, 3.6$  Hz, 1H), 2.25 (s, 3H), 2.15 (s, 3H), 2.10 (s, 3H), 2.07 (s, 3H), 2.02 (s, 3H), 1.96 (s, 3H), 1.84 (s, 3H), 1.59–1.42 (m, 4H), 1.33–1.18 (m, 8H), 1.32 (d,  $J = 6.6$  Hz, 3H), 1.28 (d,  $J = 6.2$  Hz, 3H), 1.26 (d,  $J = 6.2$  Hz, 3H), 1.10 (d,  $J = 6.1$  Hz, 3H); HRMS (MALDI-TOF)  $m/z$ :  $[M + Na]^+$  Calcd for C<sub>234</sub>H<sub>244</sub>N<sub>4</sub>NaO<sub>68</sub> 4220.5649; Found 4220.5640.

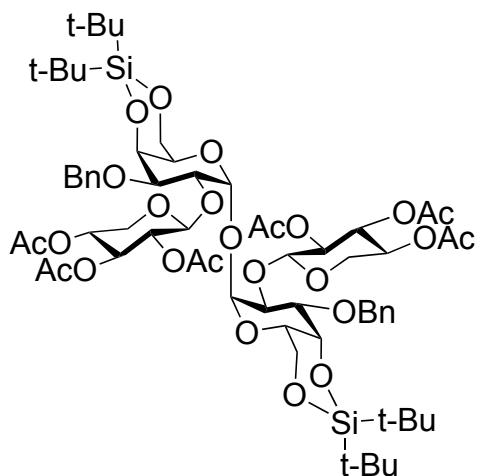


**3.39**

**2,3,4-Tri-*O*-benzoyl- $\beta$ -D-xylopyranosyl-(1 $\rightarrow$ 2)-3-*O*-benzyl-4,6-*O*-di-*tert*-butylsilylene- $\alpha$ -D-galactopyranosyl 2,3,4-tri-*O*-benzoyl- $\beta$ -D-xylopyranosyl-(1 $\rightarrow$ 2)-3-*O*-benzyl-4,6-*O*-di-*tert*-butylsilylene- $\alpha$ -D-galactopyranoside (3.39)**

To a stirred solution of acceptor **3.38** (2.1 mg, 0.50  $\mu$ mol) and donor **2.7** (4.8 mg, 5.0  $\mu$ mol) in dry  $\text{CH}_2\text{Cl}_2$  (2 mL) was added 4Å molecular sieves powder (200 mg). After stirring for 30 min, the reaction mixture was cooled to 0 °C and then *N*-iodosuccinimide (2.5 mg, 11.2  $\mu$ mol) and silver trifluoromethanesulfonate (0.19 mg, 0.74  $\mu$ mol) were added successively. The resulting solution was stirred for 1 h at 0 °C before triethylamine was added. The solution was filtered through Celite and the filtrate was washed with saturated aqueous  $\text{Na}_2\text{S}_2\text{O}_3$  and saturated aqueous  $\text{NaHCO}_3$ . The organic layer was dried over  $\text{Na}_2\text{SO}_4$ , filtered and concentrated to dryness. The crude residue was purified by flash chromatography (3:1 hexanes–EtOAc) to afford **3.39** (3.6 mg, 86%) as a colorless oil:  $R_f$  = 0.24 (3:1 hexanes–EtOAc);  $^1\text{H}$  NMR (600 MHz,  $\text{CDCl}_3$ )  $\delta$  7.97–7.91 (m, 4H, Ar), 7.90–7.84 (m, 4H, Ar), 7.84–7.77 (m, 4H, Ar), 7.56–7.49 (m, 2H, Ar), 7.42–7.35 (m, 10H, Ar), 7.35–7.26 (m, 10H, Ar), 7.21–7.15 (m, 6H, Ar), 5.79 (app t,  $J$  = 9.3 Hz, 2H, 2 x H-3'), 5.33 (d,  $J$  = 3.9 Hz, 2H, 2 x H-1), 5.30 (app td,  $J$  = 9.5, 5.7 Hz, 2H, 2 x H-4'), 5.19 (dd,  $J$  = 9.5, 7.5 Hz, 2H, 2 x H-2'), 5.13 (d,  $J$  = 7.5 Hz, 2H, 2 x H-1'), 4.61 (d,  $J$  = 3.0 Hz, 2H, 2 x H-4), 4.49 (dd,  $J$  = 12.6, 2.2

Hz, 2H, 2 x H-6a), 4.40–4.34 (m, 4H, 2 x H-5a', 2 x OCH<sub>2</sub>Ph), 4.33–4.28 (m, 4H, 2 x H-6b, 2 x H-2), 4.24 (app s, 2H, H-5), 4.21 (d, *J* = 11.8 Hz, 2H, 2 x OCH<sub>2</sub>Ph), 3.63 (dd, *J* = 10.0, 3.0 Hz, 2H, 2 x H-3), 3.59 (dd, *J* = 11.8, 9.7 Hz, 2H, 2 x H-5b'), 1.11 (s, 18H, 2 x C(CH<sub>3</sub>)<sub>3</sub>), 1.09 (s, 18H, 2 x C(CH<sub>3</sub>)<sub>3</sub>); <sup>13</sup>C NMR (151 MHz, CDCl<sub>3</sub>) δ 165.8 (2 x C=O), 165.5 (2 x C=O), 165.3 (2 x C=O), 138.9 (2 x Ar), 133.5 (2 x Ar), 133.3 (2 x Ar), 133.2 (2 x Ar), 129.9 (4 x Ar), 129.8 (4 x Ar), 129.7 (4 x Ar), 129.5 (2 x Ar), 129.2 (2 x Ar), 129.1 (2 x Ar), 128.5 (4 x Ar), 128.5 (8 x Ar), 128.4 (4 x Ar), 127.5 (2 x Ar), 127.2 (4 x Ar), 101.9 (2 x C-1'), 94.4 (2 x C-1), 78.3 (2 x C-3), 73.8 (2 x C-2), 72.2 (2 x C-3'), 72.0 (2 x C-2'), 70.8 (2 x OCH<sub>2</sub>Ph), 70.7 (2 x C-4), 70.3 (2 x C-4'), 67.7 (2 x C-5), 67.3 (2 x C-6), 62.8 (2 x C-5'), 27.8 (6 x C(CH<sub>3</sub>)<sub>3</sub>), 27.6 (6 x C(CH<sub>3</sub>)<sub>3</sub>), 23.5 (2 x C(CH<sub>3</sub>)<sub>3</sub>), 20.9 (2 x C(CH<sub>3</sub>)<sub>3</sub>); HRMS (MALDI–TOF) *m/z*: [M + Na]<sup>+</sup> Calcd for C<sub>94</sub>H<sub>106</sub>NaO<sub>25</sub>Si<sub>2</sub> 1713.6459; Found 1713.6440.

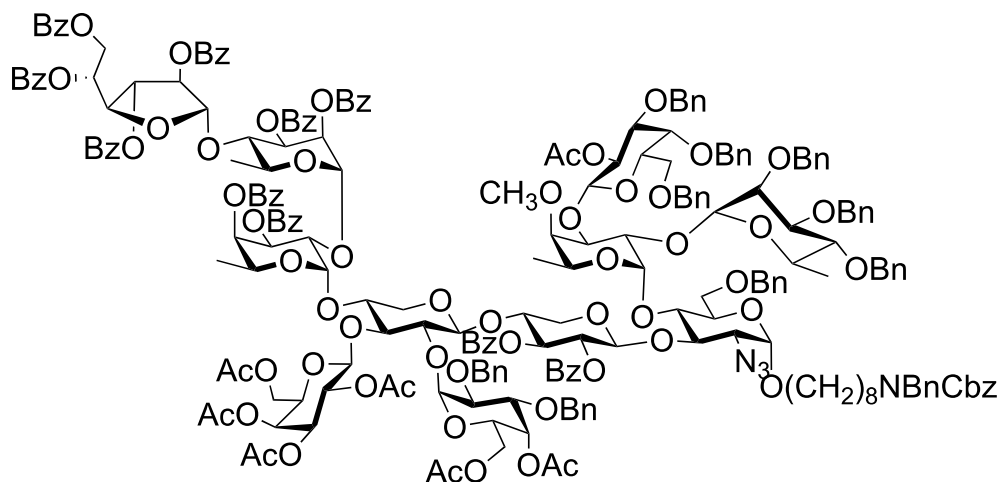


**3.40**

**2,3,4-Tri-*O*-acetyl- $\beta$ -D-xylopyranosyl-(1 $\rightarrow$ 2)-3-*O*-benzyl-4,6-*O*-di-*tert*-butylsilylene- $\alpha$ -D-galactopyranosyl 2,3,4-tri-*O*-acetyl- $\beta$ -D-xylopyranosyl-(1 $\rightarrow$ 2)-3-*O*-benzyl-4,6-*O*-di-*tert*-butylsilylene- $\alpha$ -D-galactopyranoside (3.40)**

To a stirred solution of acceptor **3.38** (2.1 mg, 0.50  $\mu$ mol) and donor **2.27** (3.9 mg, 5.0  $\mu$ mol) in dry  $\text{CH}_2\text{Cl}_2$  (2 mL) was added 4Å molecular sieves powder (200 mg). After stirring for 30 min, the reaction mixture was cooled to 0 °C and then *N*-iodosuccinimide (2.5 mg, 11.2  $\mu$ mol) and silver trifluoromethanesulfonate (0.19 mg, 0.74  $\mu$ mol) were added successively. The resulting solution was stirred for 1 h at 0 °C and then triethylamine was added before the solution was filtered through Celite and the filtrate was washed with saturated aqueous  $\text{Na}_2\text{S}_2\text{O}_3$  and saturated aqueous  $\text{NaHCO}_3$ . The organic layer was dried over  $\text{Na}_2\text{SO}_4$ , filtered and concentrated to dryness. The crude residue was purified by flash chromatography (2:1 hexanes–EtOAc) to afford **3.40** (3.0 mg, 92%) as a colorless oil:  $R_f$  = 0.29 (2:1 hexanes–EtOAc);  $^1\text{H NMR}$  (600 MHz,  $\text{CDCl}_3$ )  $\delta$  7.45–7.40 (m, 4H, Ar), 7.39–7.34 (m, 4H, Ar), 7.31–7.26 (m, 2H, Ar), 5.22 (d,  $J$  = 3.7 Hz, 2H, 2 x H-1), 5.15 (app t,  $J$  = 9.5 Hz, 2H, 2 x H-3'), 4.88 (app td,  $J$  = 9.9, 5.7 Hz, 2H, 2 x H-4'), 4.77 (d,  $J$  = 7.8 Hz, 2H, 2 x H-1'), 4.72 (dd,  $J$  = 9.7, 8.0 Hz, 2H, 2 x H-2'), 4.70 (d,  $J$  = 11.6 Hz, 2H, 2 x  $\text{OCH}_2\text{Ph}$ ), 4.66 (d,  $J$  = 3.0 Hz, 2H, 2 x H-4), 4.56 (d,  $J$  = 11.5 Hz, 2H, 2 x  $\text{OCH}_2\text{Ph}$ ), 4.32 (dd,  $J$  =

12.5, 2.2 Hz, 2H, 2 x H-6a), 4.16–4.11 (m, 4H, 2 x H-2, 2 x H-6b), 4.07 (d,  $J = 2.3$  Hz, 2H, 2 x H-5), 4.02 (dd,  $J = 11.7, 5.7$  Hz, 2H, 2 x H-5a), 3.74 (dd,  $J = 9.9, 3.0$  Hz, 2H, 2 x H-3), 3.30 (dd,  $J = 11.7, 10.3$  Hz, 2H, 2 x H-5b), 2.01 (s, 12H, 4 x COCH<sub>3</sub>), 1.79 (s, 6H, 2 x COCH<sub>3</sub>), 1.07 (s, 18H, 2 x C(CH<sub>3</sub>)<sub>3</sub>), 1.03 (s, 18H, 2 x C(CH<sub>3</sub>)<sub>3</sub>); <sup>13</sup>C NMR (151 MHz, CDCl<sub>3</sub>) δ 170.1 (2 x C=O), 169.9 (2 x C=O), 169.5 (2 x C=O), 138.7 (2 x Ar), 128.6 (4 x Ar), 127.7 (2 x Ar), 127.6 (4 x Ar), 102.0 (2 x C-1'), 93.7 (2 x C-1), 77.7 (2 x C-3), 74.4 (2 x C-2), 72.2 (2 x C-3'), 71.6 (2 x C-2'), 70.5 (2 x C-4), 70.4 (2 x OCH<sub>2</sub>Ph), 69.3 (2 x C-4'), 67.6 (2 x C-5), 67.2 (2 x C-6), 62.7 (2 x C-5'), 27.8 (6 x C(CH<sub>3</sub>)<sub>3</sub>), 27.5 (6 x C(CH<sub>3</sub>)<sub>3</sub>), 23.5 (2 x C(CH<sub>3</sub>)<sub>3</sub>), 20.9 (2 x COCH<sub>3</sub>) 20.8 (2 x COCH<sub>3</sub>), 20.8 (2 x COCH<sub>3</sub>), 20.7 (2 x C(CH<sub>3</sub>)<sub>3</sub>); HRMS (MALDI–TOF)  $m/z$ : [M + Na]<sup>+</sup> Calcd for C<sub>64</sub>H<sub>94</sub>NaO<sub>25</sub>Si<sub>2</sub> 1341.5519; Found 1341.5531.



**3.42**

*N*-benzyl-*N*-benzoxycarbonyl-8-amino-1-octyl 2,3,4,6-tetra-*O*-acetyl- $\beta$ -D-galactopyranosyl-(1 $\rightarrow$ 3)-[4,6-di-*O*-acetyl-2,3-di-*O*-benzyl- $\alpha$ -D-galactopyranosyl-(1 $\rightarrow$ 2)]-[2,3,5,6-tetra-*O*-benzoyl- $\beta$ -D-galactofuranosyl-(1 $\rightarrow$ 4)-2,3-di-*O*-benzoyl- $\alpha$ -L-rhamnopyranosyl-(1 $\rightarrow$ 2)-3,4-di-*O*-benzoyl- $\alpha$ -L-fucopyranosyl-(1 $\rightarrow$ 4)]- $\beta$ -D-xylopyranosyl-(1 $\rightarrow$ 4)-2,3-di-*O*-benzoyl- $\beta$ -D-xylopyranosyl-(1 $\rightarrow$ 3)-[2-*O*-acetyl-3,4,6-tri-*O*-benzyl- $\beta$ -D-galactopyranosyl-(1 $\rightarrow$ 3)]-[2,3,4-tri-*O*-benzyl- $\alpha$ -L-rhamnopyranosyl-(1 $\rightarrow$ 2)]-4-*O*-methyl- $\alpha$ -L-fucopyranosyl-(1 $\rightarrow$ 4)]-2-azido-6-*O*-benzyl-2-deoxy- $\alpha$ -D-glucopyranoside (3.42)

To a stirred solution of acceptor **3.38** (2.5 mg, 0.60  $\mu$ mol) and donor **2.7** (5.7 mg, 6.0  $\mu$ mol) in CH<sub>2</sub>Cl<sub>2</sub> (1.0 mL) was added 4Å molecular sieves powder (100 mg). After stirring for 30 min, di-tert-butylmethylpyridine (1.6 mg, 8.0  $\mu$ mol) and methyl trifluoromethanesulfonate (2.0  $\mu$ L, 18.0  $\mu$ mol) were added. The resulting solution was stirred for 24 h and then triethylamine was added to the mixture and the solution was filtered through Celite. The filtrate was concentrated to dryness and the crude residue was purified by flash chromatography (3:1 toluene–EtOAc) to afford **3.42** (1.8 mg, 72%) as a colorless oil: *R*<sub>f</sub> = 0.42 (2:1 hexanes–EtOAc); HRMS (MALDI–TOF) *m/z*: [M + Na]<sup>+</sup> Calcd for C<sub>234</sub>H<sub>244</sub>N<sub>4</sub>NaO<sub>68</sub> 4234.5812; Found 4234.5802.

### 3.5 References

- (1) *Chagas disease (American trypanosomiasis)*. <https://www.who.int/health-topics/chagas-disease> (accessed 2023-09-01).
- (2) Basombrío, M. A.; Gómez, L.; Padilla, A. M.; Ciaccio, M.; Nozaki, T.; Cross, G. A. M. Targeted Deletion of the Gp72 Gene Decreases The Infectivity of *Trypanosoma cruzi* For Mice and Insect Vectors. *para* **2002**, *88* (3), 489–493.
- (3) Rocha, G. M.; Seabra, S. H.; De Miranda, K. R.; Cunha-e-Silva, N.; De Carvalho, T. M. U.; De Souza, W. Attachment of Flagellum to the Cell Body Is Important to the Kinetics of Transferrin Uptake by *Trypanosoma cruzi*. *Parasitol. Int.* **2010**, *59* (4), 629–633.
- (4) Rocha, G. M.; Brandão, B. A.; Mortara, R. A.; Attias, M.; De Souza, W.; Carvalho, T. M. U. The Flagellar Attachment Zone of *Trypanosoma cruzi* Epimastigote Forms. *J. Struct. Biol.* **2006**, *154* (1), 89–99.
- (5) Cooper, R.; De Jesus, A.; Cross, G. Deletion of an Immunodominant *Trypanosoma cruzi* Surface Glycoprotein Disrupts Flagellum-Cell Adhesion. *J. Cell Biol.* **1993**, *122* (1), 149–156.
- (6) Nozaki, T. Characterization of the *Trypanosoma brucei* Homologue of a *Trypanosoma cruzi* Flagellum-Adhesion Glycoprotein. *Mol. Biochem. Parasitol.* **1996**, *82* (2), 245–255.
- (7) Sher, A.; Snary, D. Specific Inhibition of the Morphogenesis of *Trypanosoma cruzi* by a Monoclonal Antibody. *Nature* **1982**, *300* (5893), 639–640.
- (8) Allen, S.; Richardson, J. M.; Mehlert, A.; Ferguson, M. A. J. Structure of a Complex Phosphoglycan Epitope from Gp72 of *Trypanosoma cruzi*. *J. Biol. Chem.* **2013**, *288* (16), 11093–11105.

- (9) Lin, S.; Lowary, T. L. Synthesis of the Highly Branched Hexasaccharide Core of Chlorella Virus *N*-Linked Glycans. *Chem. Eur. J.* **2018**, *24* (64), 16992–16996.
- (10) Lin, S.; Lowary, T. L. Synthesis of a Highly Branched Nonasaccharide Chlorella Virus *N*-Glycan Using a “Counterclockwise” Assembly Approach. *Org. Lett.* **2020**, *22* (19), 7645–7649.
- (11) Wang, Y.; Wu, Y.; Xiong, D.; Ye, X. Total Synthesis of a Hyperbranched *N*-Linked Hexasaccharide Attached to ATCV-1 Major Capsid Protein without Precedent. *Chin. J. Chem.* **2019**, *37* (1), 42–48.
- (12) Zhao, W.; Kong, F. Facile Synthesis of the Heptasaccharide Repeating Unit of O-Deacetylated GXM of *C. neoformans* Serotype B. *Bioorg. Med. Chem.* **2005**, *13* (1), 121–130.
- (13) Zhao, W.; Kong, F. Synthesis of a Heptasaccharide Fragment of the O-Deacetylated GXM of *C. neoformans* Serotype C. *Carbohydr. Res.* **2005**, *340* (10), 1673–1681.
- (14) Rao, Y.; Boons, G.-J. A Highly Convergent Chemical Synthesis of Conformational Epitopes of Rhamnogalacturonan II. *Angew. Chem. Int. Ed.* **2007**, *46* (32), 6148–6151.
- (15) Huang, C.; Wang, N.; Fujiki, K.; Otsuka, Y.; Akamatsu, M.; Fujimoto, Y.; Fukase, K. Widely Applicable Deprotection Method of 2,2,2-Trichloroethoxycarbonyl (Troc) Group Using Tetrabutylammonium Fluoride. *J. Carbohydr. Chem.* **2010**, *29* (6), 289–298.
- (16) Trost, B. M.; Kalnmals, C. A.; Tracy, J. S.; Bai, W.-J. Highly Chemoselective Deprotection of the 2,2,2-Trichloroethoxycarbonyl (Troc) Protecting Group. *Org. Lett.* **2018**, *20* (24), 8043–8046.

- (17) Zhang, J.; Li, C.; Sun, L.; Yu, G.; Guan, H. Total Synthesis of Myrmekioside A, a Mono-*O*-alkyl-diglycosylglycerol from Marine Sponge *Myrmekioderma* Sp. *Eur J Org Chem* **2015**, *2015* (19), 4246–4253.
- (18) Hasegawa, A.; Ando, T.; Kato, M.; Ishida, H.; Kiso, M. Synthesis of the Methyl Thioglycosides of 2-,3-, and 4-Deoxy-L-Fucose. *Carbohydr. Res.* **1994**, *257* (1), 55–65.
- (19) Wang, Z.; Zhou, L.; El-Boubbou, K.; Ye, X.; Huang, X. Multi-Component One-Pot Synthesis of the Tumor-Associated Carbohydrate Antigen Globo-H Based on Preactivation of Thioglycosyl Donors. *J. Org. Chem.* **2007**, *72* (17), 6409–6420.
- (20) Furukawa, J.; Kobayashi, S.; Nomizu, M.; Nishi, N.; Sakairi, N. Total Synthesis of Calonyctin A2, a Macrolidic Glycolipid with Plant Growth-Promoting Activity. *Tetrahedron Lett.* **2000**, *41* (18), 3453–3457.
- (21) Jansson, K.; Frejd, T.; Kihlberg, J.; Magnusson, G. 2-Trimethylsilylethyl Glycosides. Anomeric Deblocking of Mono- and Disaccharides. *Tetrahedron Lett.* **1988**, *29* (3), 361–362.
- (22) Namchuk, M. N.; McCarter, J. D.; Becalski, A.; Andrews, T.; Withers, S. G. The Role of Sugar Substituents in Glycoside Hydrolysis. *J. Am. Chem. Soc.* **2000**, *122* (7), 1270–1277.
- (23) Mong, K. T.; Nokami, T.; Tran, N. T. T.; Nhi, P. B. Solvent Effect on Glycosylation. In *Selective Glycosylations: Synthetic Methods and Catalysts*; Bennett, C. S., Ed.; Wiley, 2017; pp 59–77.
- (24) Li, Z.; Gildersleeve, J. C. Mechanistic Studies and Methods to Prevent Aglycon Transfer of Thioglycosides. *J. Am. Chem. Soc.* **2006**, *128* (35), 11612–11619.

- (25) Arafuka, S.; Koshiba, N.; Takahashi, D.; Toshima, K. Systematic Synthesis of Sulfated Oligofucosides and Their Effect on Breast Cancer MCF-7 Cells. *Chem. Commun.* **2014**, 50 (69), 9831–9834.
- (26) Lay, L.; Nicotra, F.; Panza, L.; Russo, G.; Adobati, E. Oligosaccharides Related to Tumor-Associated Antigens. Part I. Synthesis of the Propyl Glycoside of the Trisaccharide  $\alpha$ -L-Fucp-(1→2)- $\beta$ -D-Galp-(1→3)- $\alpha$ -D-GalpNAc, Component of a Tumor Antigen Recognized by the Antibody MBr1. *Helv. Chim. Acta* **1994**, 77 (2), 509–514.

## **Chapter 4**

### **Study on the Binding of Synthetic Glycan Fragments of GP72 and WIC29.26 mAb**

#### 4.1 Protein–Glycan interactions

Glycans and their conjugates, which include glycoproteins, can be found on the cell surface of all life forms.<sup>1</sup> Their interactions with carbohydrate-recognizing and binding proteins play significant roles in several physiological processes including immunity, cellular transduction, cellular proliferation, and apoptosis.<sup>2–6</sup> For example, glycans of pathogenic microorganisms are important to their virulence and growth. These microbial glycans are unique and have unusual structures, which are often foreign to the host and thus can elicit a response from the immune system to produce protective anti-carbohydrate antibodies.<sup>7,8</sup> Due to this, these glycans can act as potent vaccine antigens and adjuvants.<sup>9–11</sup> Studying the interaction between carbohydrate-specific antibodies and these glycans has been one of the cornerstones of the field of glycoimmunology. Glycoprotein GP72 is a cell-surface glycoprotein found in *Trypanosoma cruzi*, the etiological agent of Chagas disease.<sup>12</sup> This glycoprotein has been shown to be important in the parasite's morphology and infectivity.<sup>13–18</sup> The antigenic glycan portion of GP72, a 13-residue glycan with an unusual structure, is recognized by a monoclonal antibody (mAb) WIC29.26 that prevents the transformation of the parasite to its human infectious form.<sup>19,20</sup> Studying the specificity of the interaction between glycoprotein GP72 and the WIC29.26 mAb could give valuable insights on future vaccines for Chagas disease.

Protein–carbohydrate interactions are of relatively low affinity compared to their protein–protein counterparts. For protein–carbohydrate interactions, the affinity is usually in the mM to nM range. Historically, measuring protein–carbohydrate binding has been performed using methods including isothermal titration calorimetry (ITC),<sup>21</sup> fluorescence spectroscopy,<sup>22</sup> NMR spectroscopy, surface plasmon resonance (SPR) spectroscopy,<sup>23</sup> bio-layer interferometry (BLI),<sup>24</sup> and mass spectrometry.<sup>25</sup>

Label-free techniques, like SPR and BLI have increased in use and popularity for studying biomolecular interactions due to their multiple advantages.<sup>26</sup> SPR and BLI detect real time interactions between analytes and ligands without the need to label the molecules and thus, have benefits over fluorescence methods. SPR and BLI, aside from being label-free techniques, share some conceptual likenesses in that a ligand is immobilized on a surface. Similar immobilization methods and techniques are employed in both techniques, and also allow the determination of kinetic binding rate constants, which are important in describing completely different molecular interactions. The main difference is that SPR uses a microfluidic system while BLI uses row of sensors dipped in a multi-well plate containing solutions. Additional information about BLI is provided below.

While both SPR and BLI are techniques applicable to the binding studies between the synthesized glycans **2.2–2.5** in Chapter 2 (See Figure **2-2**) of this thesis work and the WIC29.26 mAb, I decided to use BLI due to multiple advantages over SPR. For instance, due to its microfluidic set-up and the limited volume of analyte solution, SPR has limitations on the measurement time during association or dissociation steps which is not a problem in BLI. In addition, the ‘dip and read’ feature of BLI also allows recovery of precious samples for future use. The same feature also eliminates the complications associated with microfluidics like clogging of lines. BLI has been used for mapping interactions using analytes with molecular weight of 1.5–4 kDa and with affinities between 1 mM and 10 pM, which is the range where protein–carbohydrate interaction lie.<sup>27</sup>

### 4.1.1 Bio-layer Interferometry (BLI)

Bio-layer interferometry (BLI) is a relatively new technique that uses disposable biosensors containing an immobilized layer of ligands on the sensor's tip. The tips are then dipped in wells containing the analyte solution (in my case, the mAb) and the binding between the ligand and the analyte is measured using the change in the interference pattern of white light that is being reflected down the biosensor. The binding of the analyte to the ligand creates a secondary surface on which the light can reflect, thus creating a shift in the wavelength of light that is proportional to the optical thickness of the binding surface. The change in thickness is, in turn, directly proportional to the number of binding particles on the surface.<sup>28</sup> Some key considerations in the experimental design include the selection of the molecule to be immobilized and choosing a suitable method of immobilization. The most used BLI platform is the ForteBio OctetRed96, which is what is used in the experiments described in this chapter.

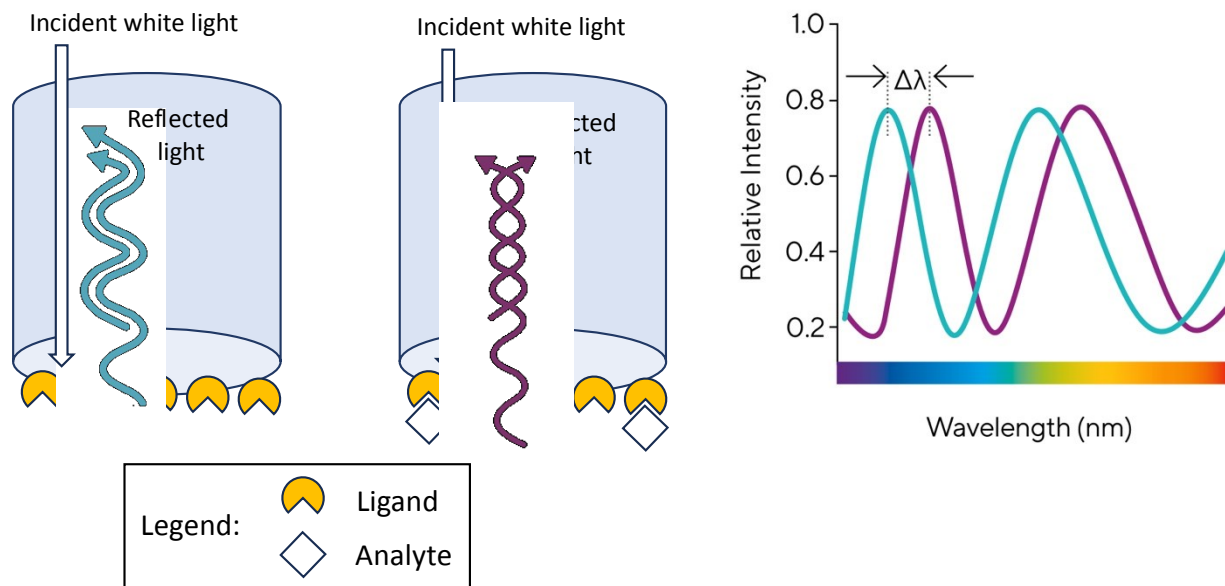


**Figure 4-1:** Schematic diagram illustrating BLI spectroscopy.

The results from BLI experiments are usually presented in a sensogram that shows the change in wavelength shift over time. Each portion of the sensogram describes different binding events during the experiment, including baseline, association, dissociation, and regeneration steps. The typical experiment starts with a baseline measurement after the biosensor tip, with an immobilized ligand, is dipped into a buffer solution. This is then followed by the association step where the sensor is then dipped into a solution containing the analyte. The binding of the analyte to the immobilized ligand is observed through an increase in the signal due to an increase in the optical thickness of the biosensor. This portion of the curve can be used to determine association kinetics. Over a period of time, if the concentration of analyte is sufficiently high, a steady state is achieved, in which the immobilized ligand is in equilibrium of saturation with the analyte. This part of the curve can give information about the binding affinity and equilibrium constant for the interaction. The biosensor tip is then removed from the analyte solution and then dipped into a buffer solution to commence the dissociation step. The signal will slowly decrease due to analyte molecules being released from the immobilized ligand. This portion can be used for determining the dissociation constant. The final portion of the sensogram shows the regeneration step where the biosensors is dipped into stripping buffers to completely remove all bound analyte molecules and to regenerate the biosensor surface for another round of experiments.<sup>29</sup>

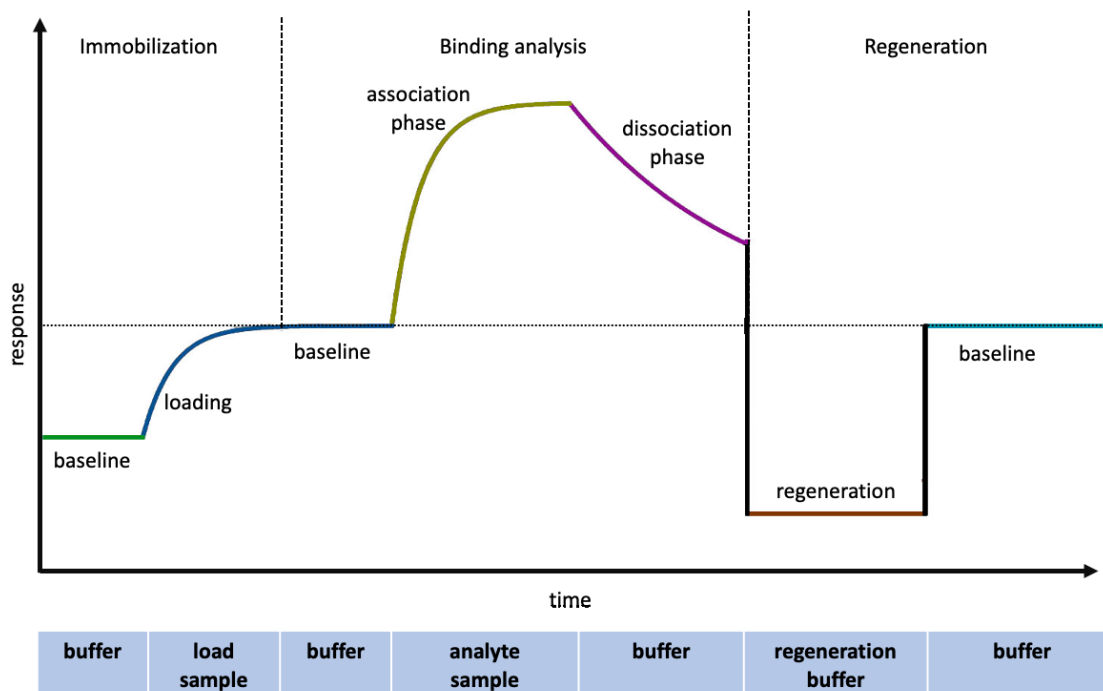


**Figure 4-2:** BLI sensogram showing the immobilization, association, dissociation, and regeneration phases.

One of the key aspects of BLI is the selection of the ligand immobilization method. It is necessary to make sure that the immobilization method does not affect the orientation or conformation of the molecule. There are a multitude of options for immobilization of molecules onto the biosensor surface. A few examples are carboxylate–amine coupling, biotin–streptavidin interaction, gold–thiol coupling, Staudinger ligation and bio-orthogonal click chemistry.<sup>30</sup>

In this chapter, I will discuss the binding studies I performed between the glycan fragments I synthesized in Chapter 2 of this thesis and the WIC29.26 mAb. The binding studies were done using BLI on a ForteBio OctetRed96 instrument. In addition, a dot blot assay was done to obtain qualitative analysis of the binding.

## **4.2 Results and Discussion**

One of the main objectives of my research was to gain insights into the specificity of the interaction between the antigenic glycan epitope of GP72 and the WIC29.26 mAb. I would like to determine if certain structural motifs in this huge and complex glycan structure are important for antibody recognition. In Chapter 2, I described the synthesis of glycan fragments derived from the whole antigenic glycan epitope of GP72. These fragments will be used in this chapter for binding studies with WIC29.26 mAb using the BLI technique. I was lucky to receive a supply of the mAb for the binding studies from our collaborator Dr. Michael Ferguson from the University of Dundee, United Kingdom.

### **4.2.2 Bio-layer Interferometry (BLI) binding analysis between synthetic glycans and WIC29.26 mAb**

#### **4.2.2.1 Immobilization of glycans onto biosensors**

Bio-layer interferometry binding experiments require the immobilization of one of the binding partners onto the tip surface of the biosensor. I decided to immobilize the glycans, and not the mAb, for a few important reasons. First, immobilization of the glycans and using the heavier antibody as the analyte would allow us to obtain a better signal-to-noise ratio during the measurements. Doing the reverse version of the experiment, where the low molecular weight glycans would be used as the analyte, would cause only a small amount of change in the optical thickness of the sensor tip and thus, weaker signals.<sup>24</sup> Second, the octylamine linker installed at the reducing end of the glycans is a versatile functional group to facilitate immobilization onto the sensors. Immobilization of the sugars at their reducing end would ensure that the carbohydrate portion of the molecule protrudes from the surface and available for mAb recognition.

Immobilization of the antibody might not only affect its conformation but also its orientation, which could greatly affect its binding capability. Lastly, the limited amount of the mAb compared to the glycans, pointed us to use the protein as the analyte, as this would allow it to be recovered for multiple uses. This is a great advantage of the ‘dip and read’ feature of BLI.

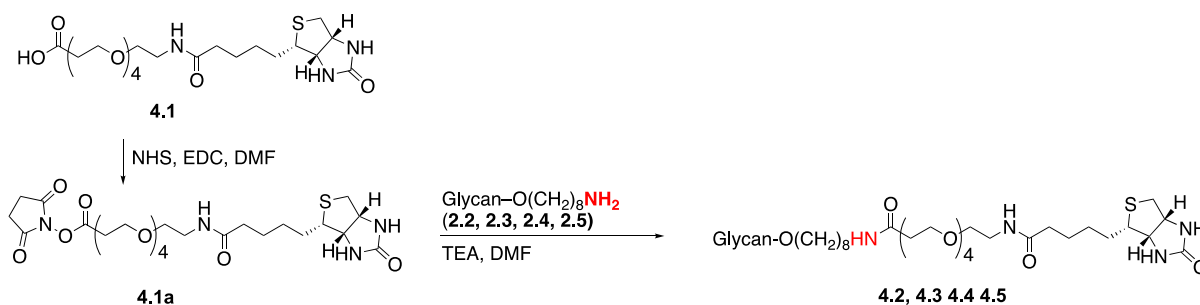
#### **4.2.2.1.1 Choice of the BLI biosensor and immobilization method**

The first step to achieve the goals set in this chapter was to design an effective way of loading the glycans onto the biosensor. The octylamine linker at the reducing end of the glycans is extremely useful to facilitate immobilization. A variety of immobilization methods can be employed that make use of the amine functional group. I decided to attach a biotin-containing linker to the glycans and employ a biotin–streptavidin interaction to immobilize them onto BLI biosensors coated with streptavidin. Streptavidin is a protein isolated from *Streptomyces avidinii* that has an extremely high affinity for biotin (dissociation constant of  $10^{-14}$  M), making it one of the strongest non-covalent interactions that exists in nature.<sup>31</sup> The biosensor used is the Octet SAX biosensor, a high precision streptavidin biosensor for quantitation and kinetic analysis.<sup>32</sup>

##### **4.2.2.1.1.1 Synthesis of biotin-tagged glycans**

Before loading the glycans into the sensors, they must be tagged with biotin. I chose to use the biotin-containing linker **4.1**, which has a hydrophilic PEG-4 spacer. This spacer would ensure that the glycans are projected far away from the surface of the biosensors to allow the much larger mAb room for binding. The installation of the biotin linker onto the glycans involves amide bond formation using the octylamino containing glycans and the linker **4.1** (Scheme 4-1). The protocol started with the conversion of the carboxylic acid in **4.1** into the reactive *N*-hydroxysuccinimide

ester **4.1a** by reaction with *N*-hydroxysuccinimide with 1-ethyl-3-(3-dimethylaminopropyl)carbodiimide hydrochloride (EDC·HCl) in DMF. In the same mixture, the glycan and triethylamine dissolved in DMF were added to give the desired biotinylated materials. The products were then purified by reversed phase and/or size-exclusion chromatography. Using this approach, the corresponding biotinylated glycans **4.2**, **4.3**, **4.4** and **4.5** were synthesized from **2.2**, **2.3**, **2.4**, and **2.5** in 76%, 62%, 82% and 79% yields, respectively. The structures of these biotinylated glycans are shown in Figure 4-3.



**Scheme 4-1:** Synthetic scheme for the synthesis of biotinylated glycans **4.2–4.5**.

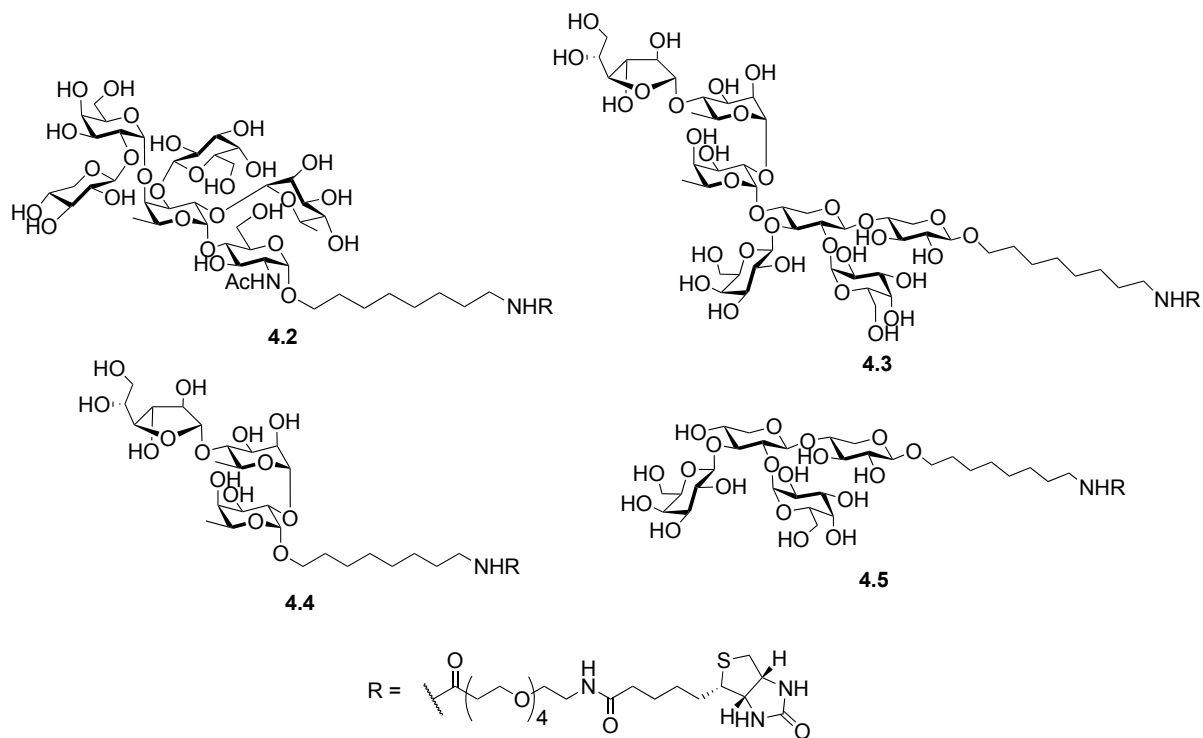


**Figure 4-3:** Structure of the biotinylated glycans to be used for binding experiments.

#### 4.2.2.1.1.2 Immobilization of biotin-tagged glycans on biosensors

With the biotinylated glycans in hand, their immobilization onto the SAX biosensors was tested. The immobilization process started by dipping a SAX biosensor into a solution containing one of the biotinylated glycans. After some time to allow binding, the loaded sensor was dipped into a buffer solution and then a solution containing biocytin, a biotin–lysine conjugate, to block any unoccupied streptavidin binding sites (Figure 4-4). The loading of the glycans was done using a loading protocol on the OctetRed96 instrument. In total, four biosensors were produced to be used in each binding experiment. The first two biosensors were loaded with the same glycan (*e.g.*, **4.2**), while the other two, which were used as referenced biosensors, were loaded with biocytin. Using these four biosensors, the experiment was done in double reference method, which is a reliable method to eliminate non-specific interaction between the sensor and the solution

components in the measurement.<sup>33</sup> One of the biosensors loaded with the glycan was used for analyte measurement while the other was used as for blank measurement.

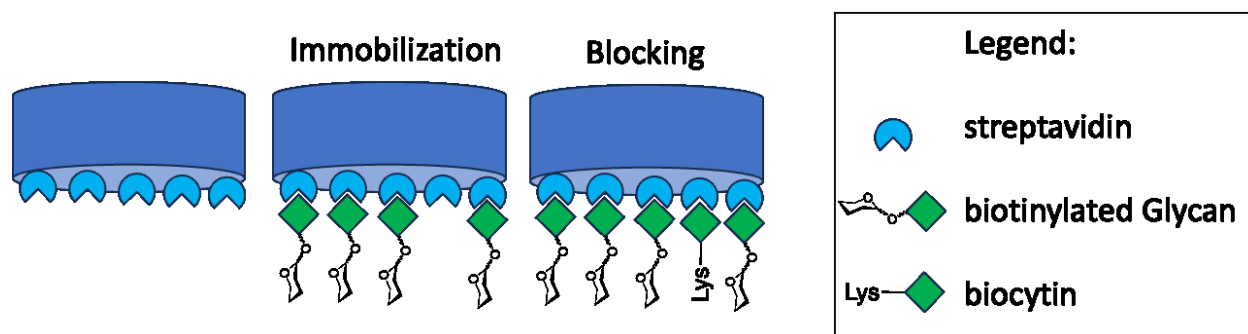


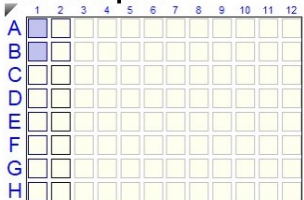
**Figure 4-4.** Immobilization of biotinylated glycans on SAX biosensors followed by blocking with biocytin.

The sample and biosensor plate design for the experiment with glycan **4.4** is shown in Figure 4-5A. The buffer used in these experiments was PBS (pH 7.4) containing 0.1% BSA and 0.05% Tween 20. The biosensors (biosensors A1/B1) were dipped first in wells containing the buffer solution (sample plate A1/B1) to establish a baseline and then transferred to wells containing 200 nM of **4.4** in buffer (sample plate A2/B2) to allow loading via biotin–streptavidin binding. The successful loading of the biotinylated glycan on each biosensor was evident based on the significant increase in the wavelength shift as the loading proceeded (Figure 4-5B). The biosensors were dipped back to the buffer solution (sample plate A3/B3) after loading to remove excess unbound biotinylated glycan. Any unreacted streptavidin on the surface of the already loaded biosensors were then blocked by dipping them into a biocytin solution (sample plate A4/B4). The streptavidin sites were blocked successfully as shown by the increase in wavelength shift as shown in Figure 4-6.

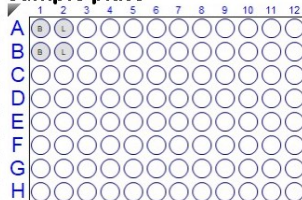
A

### Glycan 4.4 Immobilization (Plate details)

Biosensor plate

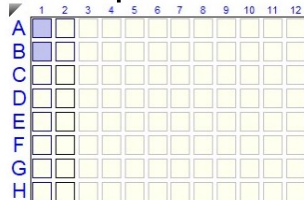


Sample plate

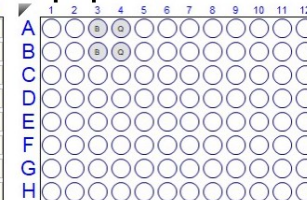


### Blocking with biocytin (Plate details)

Biosensor plate

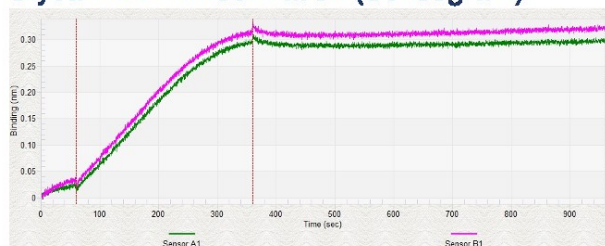


Sample plate



B

### Glycan 4.4 Immobilization (Sensogram)



### Blocking with biocytin (Sensogram)

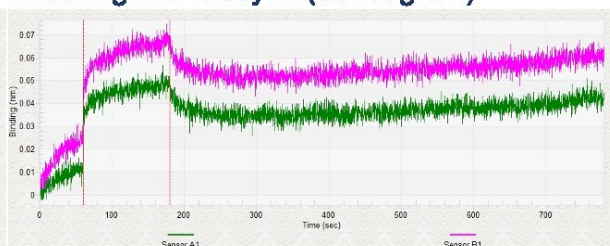


**Figure 4-5:** **A)** Biosensor and sample plate layout for glycan 4.4 immobilization and blocking with biocytin; B = buffer; L = ligand (glycan 4.4), Q = biocytin. **B)** Sensograms during the immobilization and blocking steps.

The same loading and blocking protocols were performed to load each of the biotinylated glycans onto the biosensors. Each biotinylated glycan was immobilized successfully as evident by the increase in the wavelength shift by about 0.35 nm. Another two SAX biosensors, blocked using biocytin, were used as another set of reference biosensors for the double reference method (Figure 4-6).

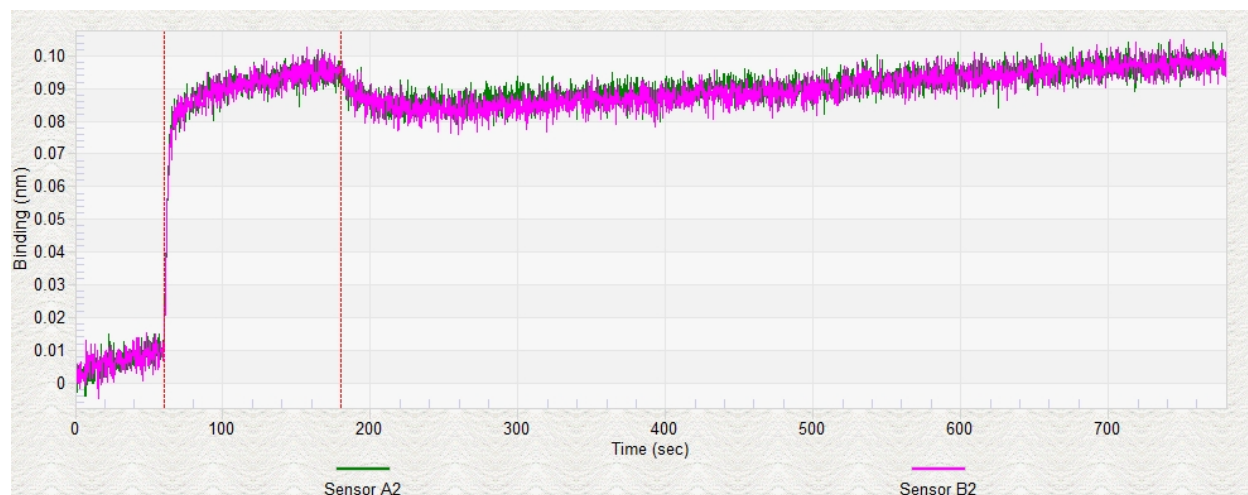


**Figure 4-6:** Sensograms during the biocytin loading on two reference SAX sensors.

#### 4.2.2.2 Binding analysis with WIC29.26 using BLI

With successful loading of the glycans onto the biosensors, I then proceeded to perform BLI analysis up on the OctetRed96 to see any binding between the mAb and the glycan fragments. All binding experiments were performed in PBS buffer. The binding experiment started with the biosensors being dipped in a buffer solution to establish a baseline followed by an association phase when the sensor was dipped in a solution containing the mAb. The sensors were then transferred to a buffer solution to proceed to the dissociation phase where some of the binding components will slowly dissociate from the biosensor. Finally, the sensor was regenerated by using acidic conditions. The regenerated biosensor could then be used for another round of analysis (Figure 4-7).

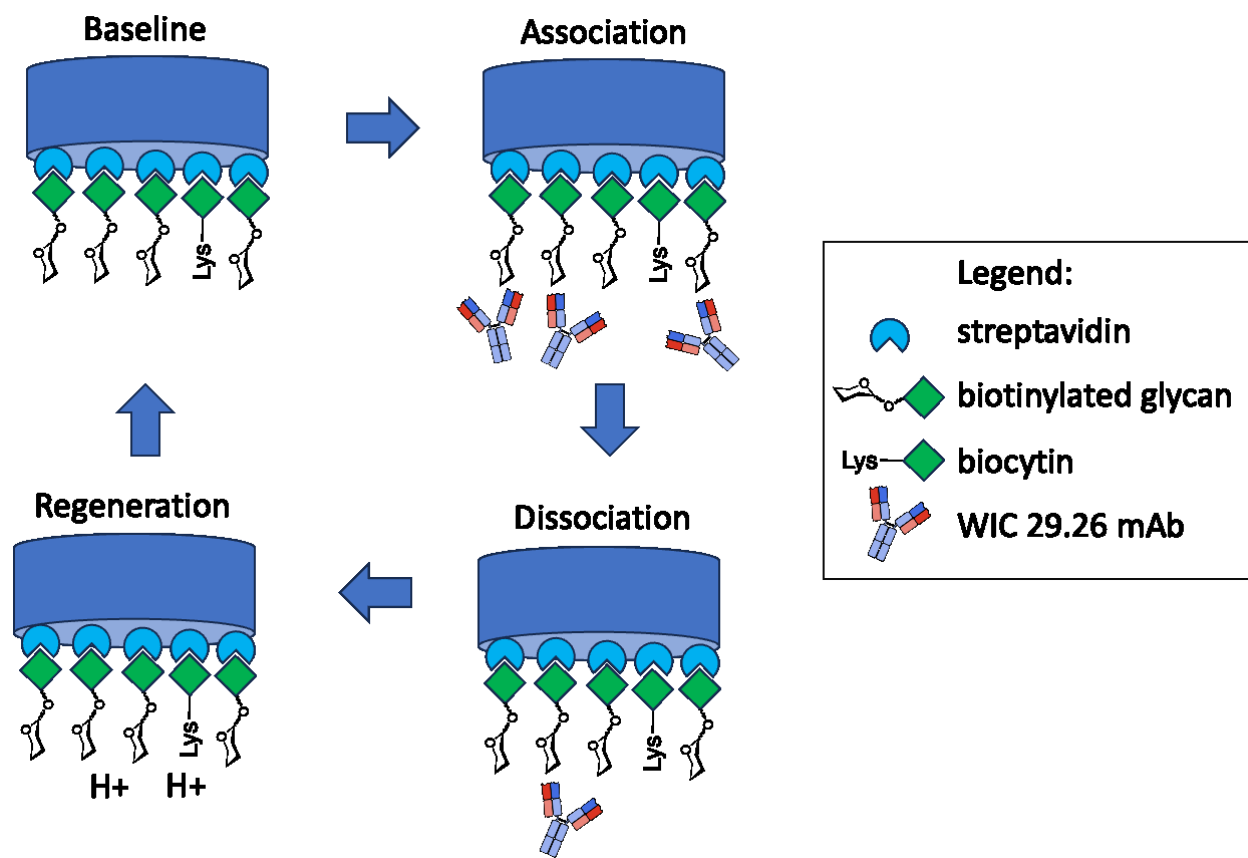
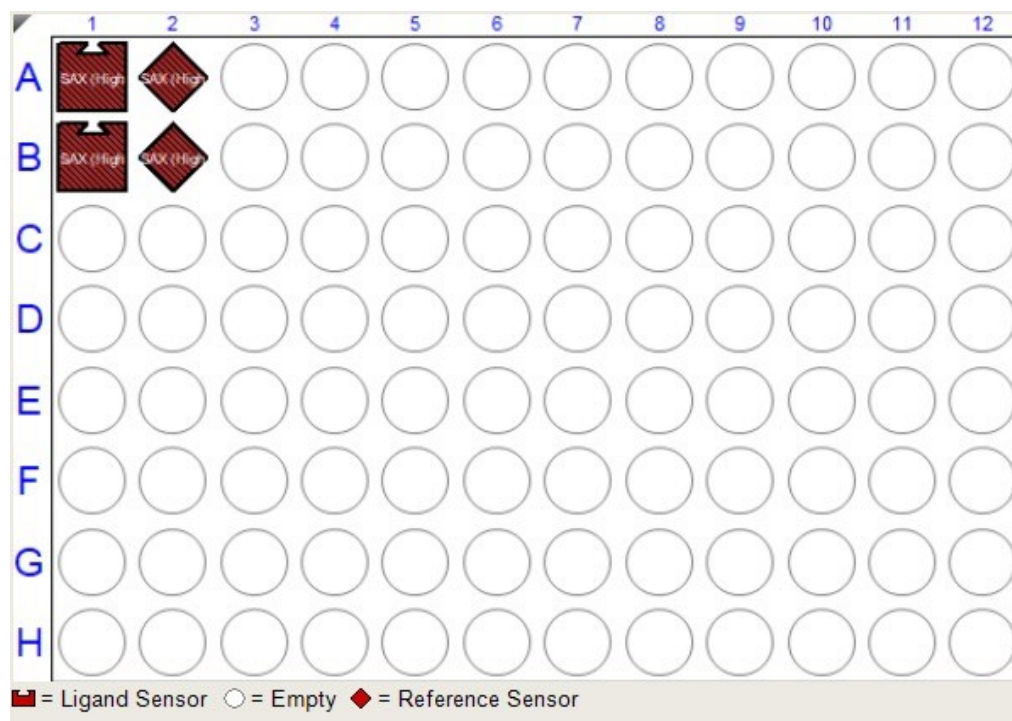


**Figure 4-7:** Process used for binding analysis between immobilized glycans and WIC29.26 mAb.

In each binding analysis, four biosensors were used: two were loaded with the glycan in question for binding and two were reference sensors that were blocked using biocytin. The experiment layout of the biosensor and the sample plates are shown in Figure 4-8. The first of the two glycan-loaded biosensors (biosensor A1) was subjected to the solution containing the antibody while the other (biosensor B1) was dipped in the blank buffer solution during the association phase. The binding analysis was done using two WIC29.26 mAb concentrations (667 nM and 1333 nM). The two biosensors loaded with biocytin were used as reference with the one (biosensor A2) being subjected to antibody solution while the second (biosensor B2) being dipped in the blank solution.

## Biosensor plate



## Sample plate

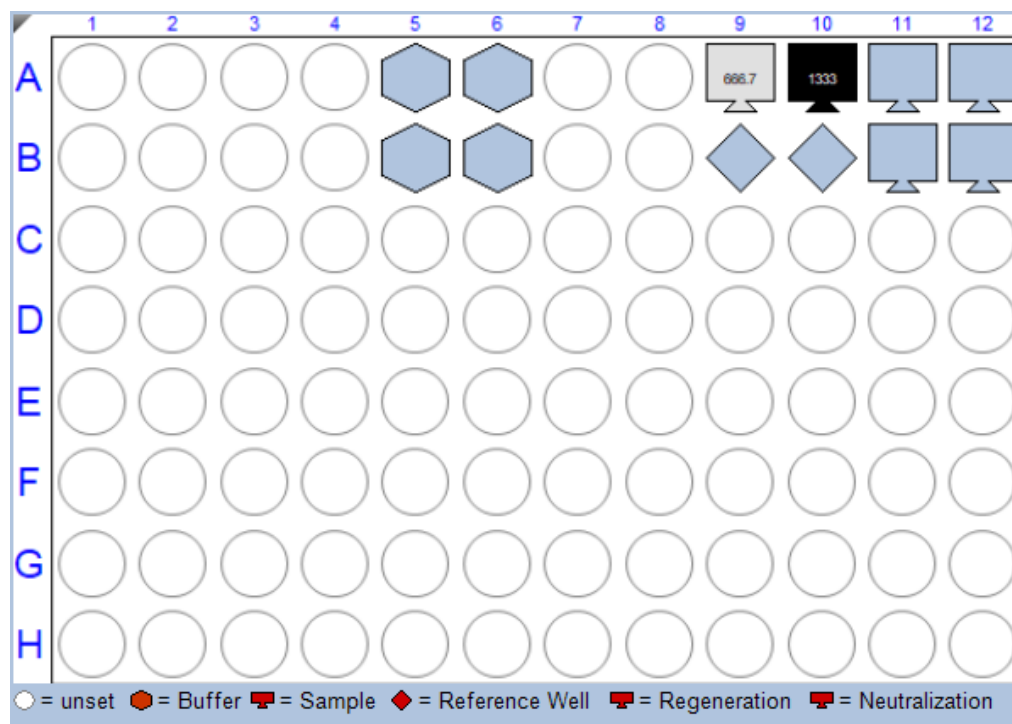
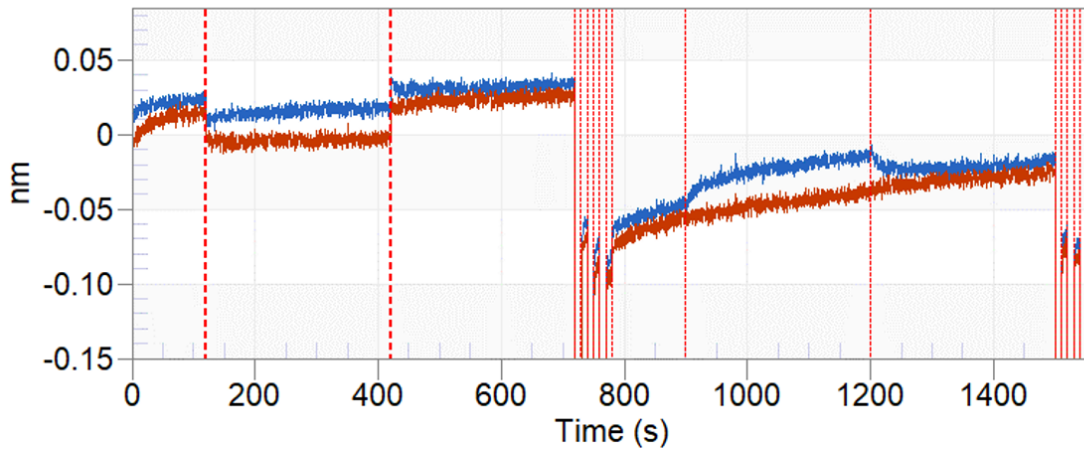


**Figure 4-8:** Biosensor and sample plate layouts during the binding analysis for glycan 4.4.

The binding experiment started with the equilibration of the biosensor on to the buffer solution (sample plate A5/B5) for 120 seconds to establish a baseline. This was followed by the association phase in which the first sensor was dipped into the solution containing the WIC29.26 mAb (sample plate A9), and the second sensor dipped into a blank buffer solution (sample plate B9). The association phase lasted for 300 seconds before both sensors were transferred to blank buffer solutions to start the dissociation phase that lasted for another 300 seconds. Both sensors were then subjected to three rounds of regeneration which included a 10 second interval on a glycine solution (pH = 2.5) followed by a 10 second interval on a neutralization buffer. After this, the whole process was repeated but instead using a different concentration of the antibody (sample plate A10) during the association phase. This exact binding analysis sequence was repeated for the two reference sensors (biosensors A2/B2). The analysis was monitored by measurement of wavelength shift during the experiment.

The sensogram for the binding analysis for glycan **4.4** is shown in Figure 4-9. Figure 4-9A corresponds to the experiments involving biosensors with immobilized glycans while Figure 4-9B corresponds to the experiments with the reference biosensors. The measurements were then processed by subtracting the readings from the reference sensors to that of the ligand sensors e.g. (A1-B1)-(A2-B2). The processed and stacked sensograms for each of the concentration are shown in Figure 4-10.

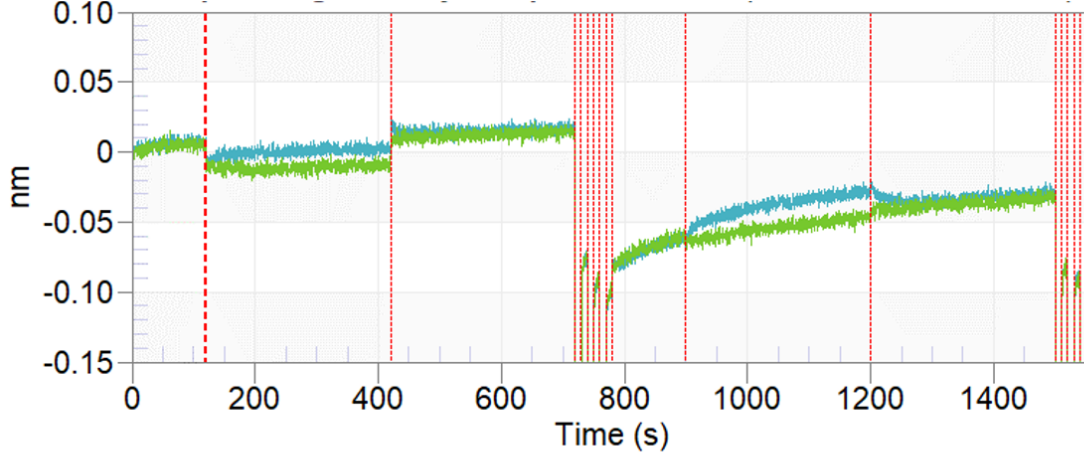
**A. Sensogram for Binding Analysis, Ligand (Glycan 4.4) sensors**



A1

B1

**B. Sensogram for Binding Analysis, Reference sensors**



A2

B2

**Figure 4-9:** **A)** Sensogram for the binding analysis using ligand sensors immobilized with glycan 4.4. Blue sensogram corresponds to experiment with mAb; Red sensogram corresponds to the experiment with blank. **B)** Sensogram for the binding analysis using reference sensors. Cyan sensogram corresponds to experiment with mAb; Green sensogram corresponds to the experiment with blank.

### Subtracted and Stacked Sensograms for glycan 4.4

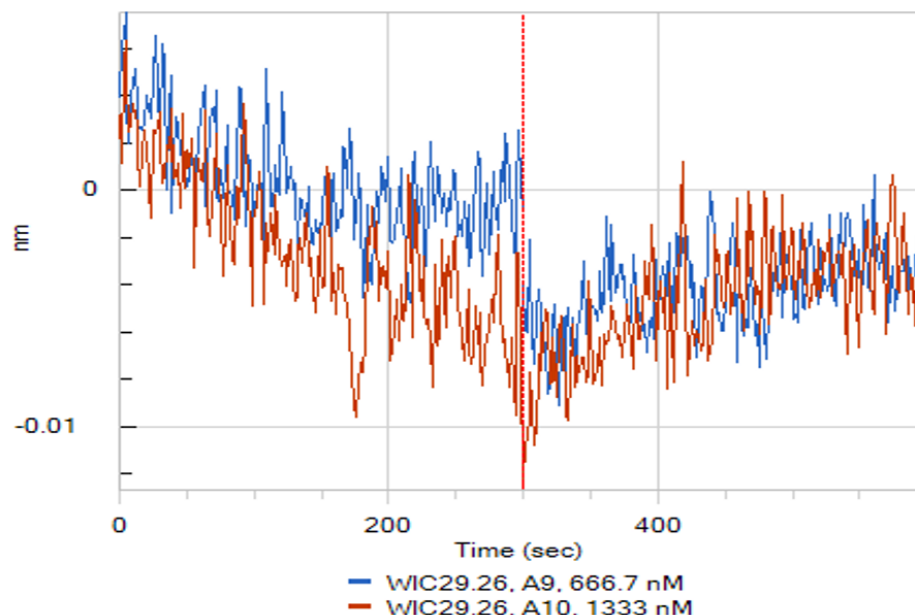


**Figure 4-10:** Subtracted and stacked sensograms for binding analysis with glycan 4.4.

As shown in Figure 4-9A, a gradual increase in the wavelength shift during the association phase when **A1** was dipped into antibody solution was observed as compared to **B1**, which was subjected to a blank solution. This change in wavelength shift corresponds to a measurable interaction between the biosensor and the antibody solution. The change in wavelength shift was  $<0.05$  nm, which is much smaller than what would be expected if the antibody was binding to the biosensor. The antibody has a molecular weight of  $\sim 150$  kDa,  $\sim 100$  times larger than the glycan. During the process of immobilization of the glycans (MW of 1 kDa) on the biosensors showed a change of around 0.35 nm. Thus, binding of the antibody (MW of  $\sim 150$  kDa) should show higher change in wavelength shift because the change in wavelength shift is directly proportional to the molecular weight of the binding partner. The interaction was found to be non-specific binding after the reading on reference biosensor A2 also showed the same change in wavelength shift was

observed. The processed sensogram after subtracting the measurements from the reference biosensors (Figure 4-10) showed an almost flat line, indicating that there is no specific interaction between glycan and the antibody solution. Unfortunately, this non-specific interaction between the biosensors and the mAb was observed with all the glycans I tested. I decided to perform the similar experiments but using Tris-buffer as the buffer solution, but the same results were obtained.

#### **4.2.2.3 Binding analysis with purified WIC29.26 mAb using BLI**

With these results from the initial binding experiments, I hypothesized that some components present in the antibody sample were capable of non-specifically interacting with the biosensor surface, possibly masking more specific interactions with the mAb. The antibody samples provided by our collaborators were freeze-dried ascites fluid containing the antibody and also a significant amount of serum albumin (67 kDa). An SDS PAGE of the antibody sample is shown in Figure 4-11A. The bands at 50 kDa and 23 kDa correspond to the heavy and light chains of the antibody while the band at 67 kDa corresponds to the serum albumin. I then decided to purify the antibody sample to remove some of these other components.

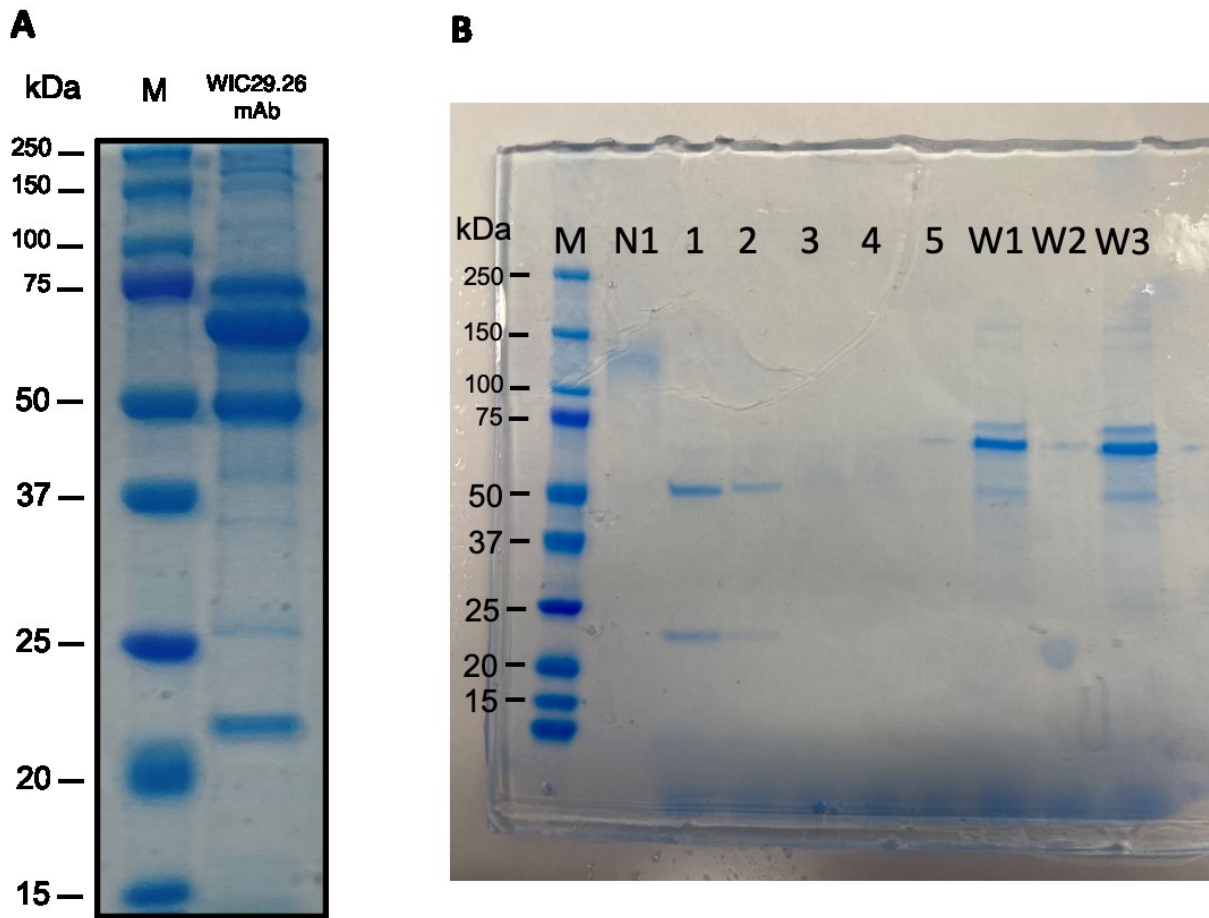


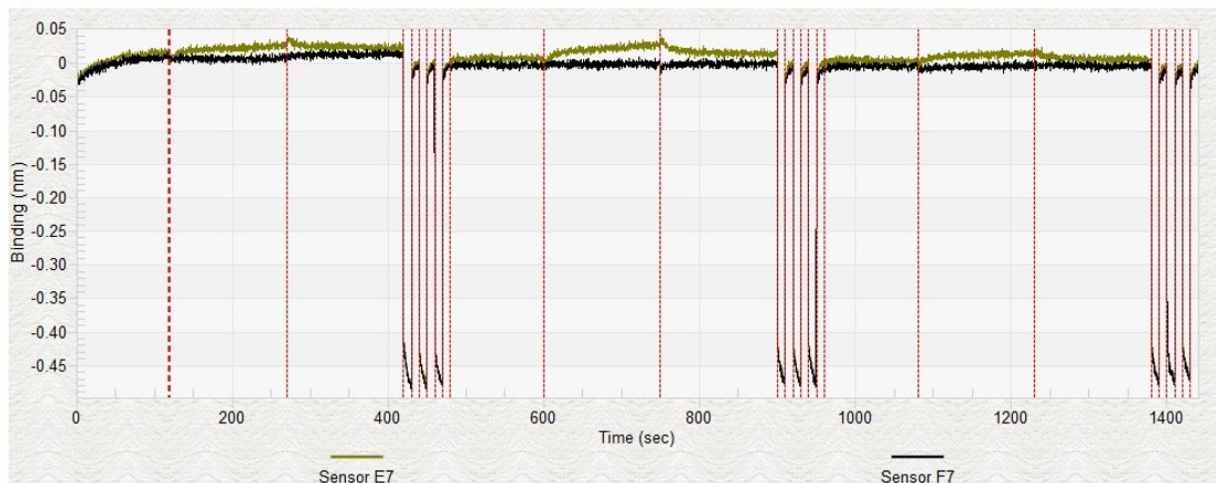
**Figure 4-11: A)** SDS PAGE of the WIC29.26 mAb sample. **B)** SDS PAGE profiles of each eluted fractions during Protein A agarose affinity gel chromatography. Legend: M = marker; N1 = undenatured fraction 1; 1, 2, 3, 4 = fractions 1, 2, 3, 4; W1, W2, W3 = PBS wash fractions 1, 2, 3.

The purification was performed using affinity chromatography with an agarose gel column functionalized with Protein A, which binds to the Fc region of antibodies. The antibody sample was first loaded into the column followed by elution of unbound components using PBS solution. After this, the bound antibody was collected by elution with glycine buffer (pH = 3.0), which was collected directly into fractions containing neutralizing Tris buffer (pH = 9.0). The unwanted serum albumin eluted during the initial washing as evident by bands at 67 kDa in the SDS PAGE

of the washing (W1, W2, W3) fractions (Figure 4-11B). The desired antibody was present in the first two fractions (1, 2) after elution using glycine buffer; distinct bands at 50 kDA and 23 kDA were observed. An undenatured sample from fraction 1 (N1) also showed a band at 140 kDA, which corresponds to the intact antibody. The fractions were combined and then a buffer exchange was performed to finally suspend the antibody in 100  $\mu$ L of PBS buffer. The final antibody concentration using bicinchoninic acid assay (BCA assay) was 0.38 mg/mL.

With the purified antibody sample in hand, I performed another series of BLI experiments with the glycans. Similar experiment cycles were performed but using a different set of antibody concentrations during the analysis (9.6  $\mu$ g/mL, 19.3  $\mu$ g/mL and 29.0  $\mu$ g/mL). The sensograms corresponding to the measurements for biotinylated glycan **4.4** are shown below (Figure 4-12). In comparison, the signals collected from these set of experiments are noticeably weaker. These results showed that the purification of the antibody helped to eliminate the unwanted non-specific binding of the biosensors and the antibody components. These also supported the fact that the antibody did not significantly bind or interact with the immobilized glycan. The subtracted and stacked sensograms at different concentrations also did not show any concentration-dependent binding between **4.4** and WIC29.26 mAb (Figure 4-13). As I saw with the unpurified protein, unfortunately, all the other glycans gave similar results.

**A. Sensogram for Binding Analysis, Ligand (Glycan 4.4) sensors, with purified WIC 29.26 mAb**



**B. Sensogram for Binding Analysis, Reference sensors, with purified WIC 29.26 mAb**

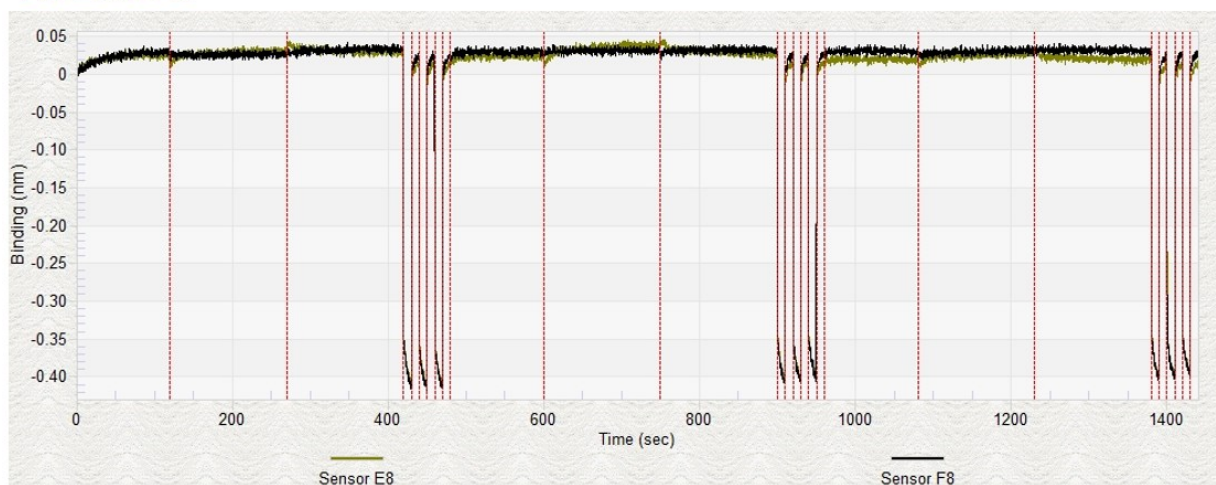
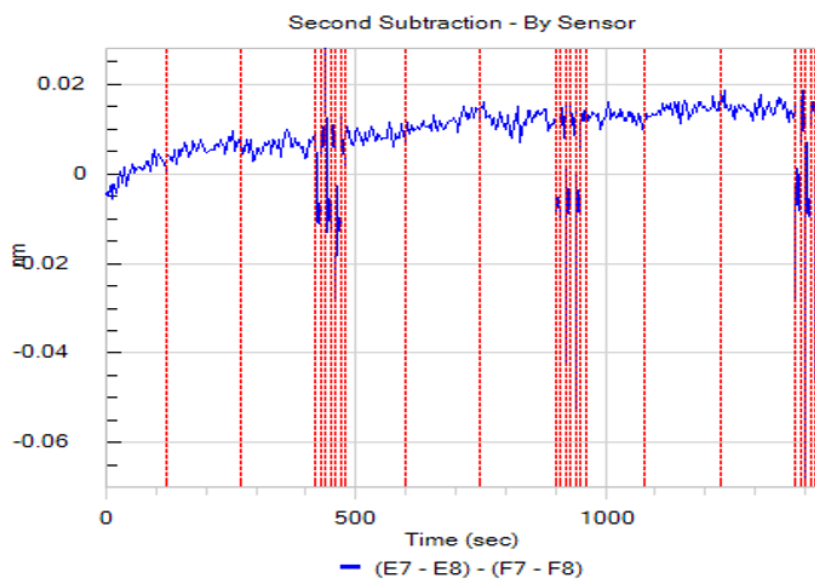


**Figure 4-12:** **A)** Sensogram for the binding analysis of sensors with glycan 4.4 immobilized using purified WIC29.26 mAb. **B)** Sensogram for the binding analysis using reference sensors with purified WIC29.26 mAb.

**A. Subtracted sensogram for binding analysis of glycan 4.4 and purified WIC 29.26 mAb**



**B. Stacked subtracted sensograms for binding analysis of glycan 4.4 and purified WIC 29.26 mAb**

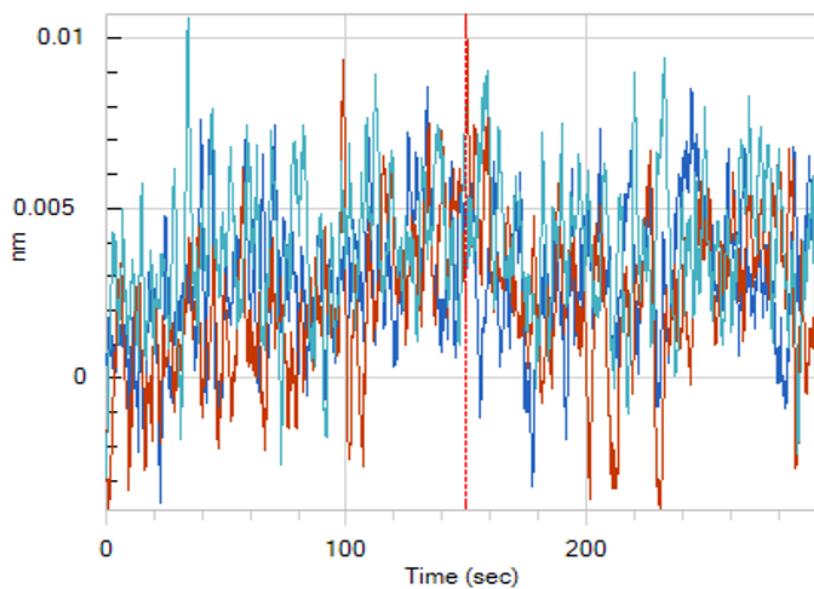


**Figure 4-13.** **A)** Subtracted sensogram for the binding analysis using sensors with glycan 4.4 immobilized with purified WIC29.26 mAb. **B)** Stacked sensogram for the binding analysis using reference sensors with purified WIC29.26 mAb at multiple concentrations. Blue = 9.6  $\mu\text{g/mL}$ , Red = 19.3  $\mu\text{g/mL}$ , Teal = 29.0  $\mu\text{g/mL}$ .

### 4.2.3 Binding analysis with WIC29.26 mAb using a dot blot assay

With failed results from the binding analysis using BLI, I decided to perform a qualitative binding analysis of the glycans with WIC29.26 mAb using a dot blot assay. In this assay, I used a nitrocellulose membrane to immobilize the mAb. The membrane with immobilized mAb was then subjected to different biotinylated glycans. After this, the membranes were exposed to a solution containing a fluorescent-labeled neutravidin (Figure 4-14). If there is binding between the biotinylated glycan and the mAb, the fluorescent-labeled neutravidin will bind to the biotin and the fluorescence detected after washings will qualitatively determine the binding.

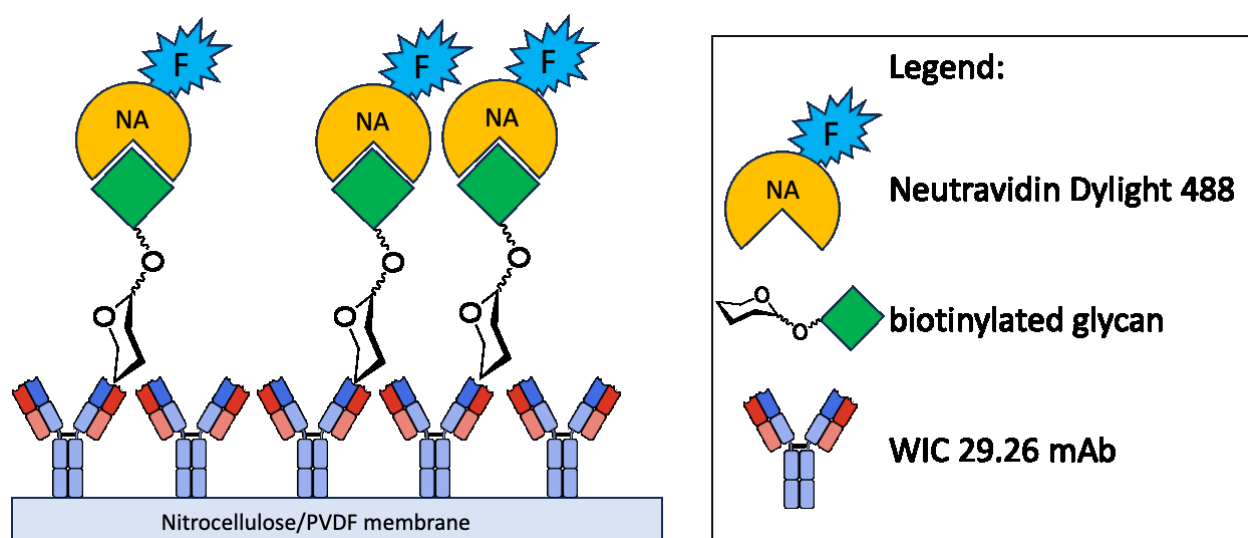


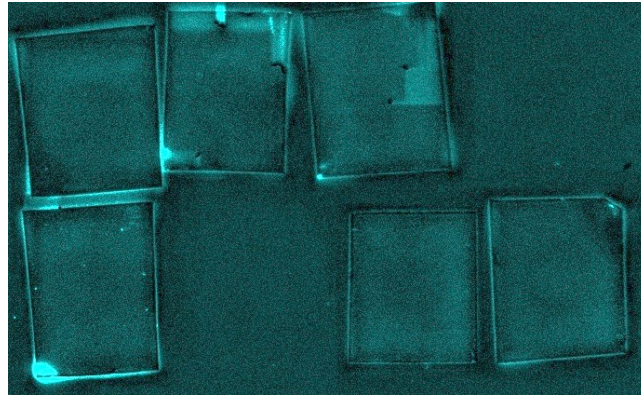
**Figure 4-14:** Schematic diagram for dot blot assay to analyze WIC29.26 mAb–glycan interaction.

The experiment started with immobilization of the monoclonal antibody on the nitrocellulose membrane by spotting 3  $\mu\text{L}$  of a 0.5  $\mu\text{g}/\text{mL}$  solution of WIC29.26 mAb. After allowing it to be immobilized on the membrane, the rest of the membrane's surface was blocked with 0.25% BSA in TBST (Tris-buffered saline solution with Tween 20) to reduce non-specific binding with the membrane. The membranes were then incubated with different biotinylated

glycans (100  $\mu\text{g}/\text{mL}$ ) overnight. After removal of the glycan solution, the membranes were incubated with neutravidin Dylight 488. After washing the membranes with TBST buffer, they were scanned for fluorescence.

The membranes incubated with the glycans did not show significant fluorescence around where the spots of the antibody were blotted (Figure 4-15A). This indicates that there is no significant binding between the glycans and the mAb. In addition, the membranes show a spread of weak fluorescence on the surface, even where the spots were not blotted. This observation can be attributed to non-specific binding of the neutravidin Dylight 488 to the nitrocellulose membrane. The absence of expected significant fluorescence around the mAb spots can also be the result of being masked by the weak fluorescence caused by non-specific binding. To improve this, I performed one more set of experiments where the concentration of the immobilized mAb was increased from 0.5  $\mu\text{g}/\text{mL}$  to 20  $\mu\text{g}/\text{mL}$ . I hypothesized that a higher amount of fluorescence could be detected if a higher concentration of the mAb were used. To resolve issues with non-specific binding, the concentration of BSA was also increased in the blocking buffer, from 0.25% to 3.0% BSA in TBST buffer. However, even with these adjustments, the same results were observed (Figure 4-15B).

A.



B.

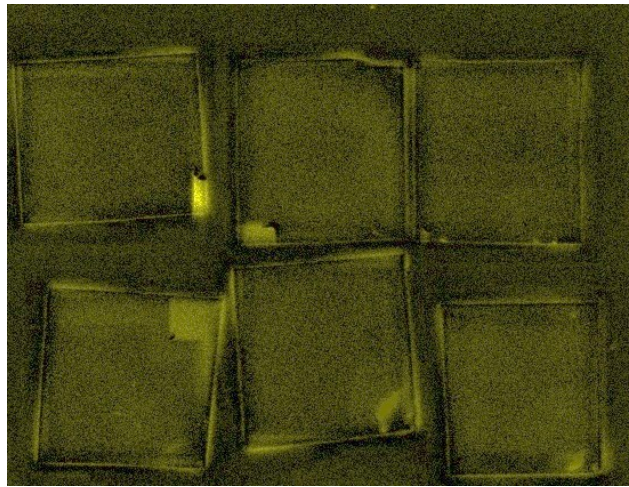


**Figure 4-15.** Fluorescence imaging of nitrocellulose membrane blotted with WIC29.26 mAb after incubation with biotinylated glycans then with Neutravidin Dylight488. A) An antibody concentration of 0.5  $\mu\text{g}/\text{mL}$  and 0.25% BSA in TTBS buffer was used. B) The same experiment as in A, but an antibody concentration of 20.0  $\mu\text{g}/\text{mL}$  and 3.0% BSA in TTBS buffer was used. From top-right, then clockwise: blank, glycan 4.2, glycan 4.3, glycan 4.5, glycan 4.4, linker 4.1.

### 4.3 Summary, conclusions and recommendations

In this chapter, I have discussed different attempts to determine the binding interaction between the synthetic fragments of the glycan epitope of the GP72 glycoprotein and WIC29.26 mAb. The initial binding analysis was performed using bio-layer interferometry (BLI) on a ForteBio's OctaRED96 instrument. BLI detects real time interactions between analytes and ligands without the need to label either species. This method was chosen due to the convenience of the 'dip and read' format of the analysis and the low amount of required antibody solution during the analysis. The method requires the immobilization of one of the binding partners onto a biosensor, which is then dipped in a solution containing a possible binding partner. The interactions are measured by the wavelength shift resulting to the formation of a secondary surface during binding. The analysis started with the immobilization of the glycans onto the biosensors. A biotin containing tag was attached to the glycans using the aminooctyl linker via formation of an amide bond. The resulting biotinylated glycans were then successfully immobilized onto Streptavidin coated biosensors (SAX). Binding analysis using these biosensors showed non-specific binding interactions between the biosensors and the WIC29.26 mAb. Changing the buffer components did not improve the antibody binding, nor eliminate the unwanted non-specific interactions. The antibody sample was successfully purified using affinity chromatography to eliminate other sample components including serum albumin. The purified antibody sample was used in another series of BLI experiments but, unfortunately, no meaningful antibody interaction was detected to all the sample glycans aside from the ubiquitous non-specific binding.

With the unsuccessful attempt of the BLI experiments, a dot blot assay was developed to qualitatively determine if any of the glycans bind to the WIC29.26 mAb sample. In this method, the antibody was immobilized by blotting a small amount on a nitrocellulose membrane, which

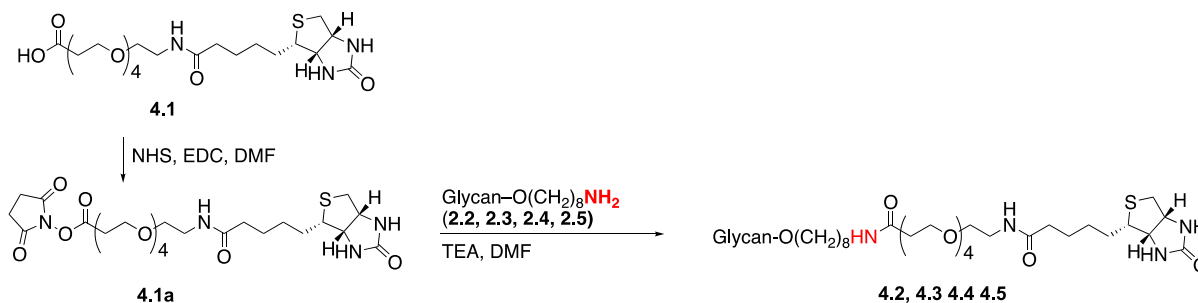
was then incubated with a solution containing the biotinylated glycan followed by incubation with a fluorescent-labeled neutravidin Dylight 488. Any interaction can be detected by fluorescence. Unfortunately, this method also did not clearly show any significant binding between the WIC29.26 mAb and the glycans. Non-specific binding between the membrane and the protein dye masks any detectable fluorescence. Increasing the antibody concentration and BSA concentration in the buffer solution to eliminate non-specific binding did not improve the results.

These results showed that these synthetic glycan fragments of the GP72 antigenic glycan have little to no measurable interaction with WIC29.26 mAb. There could be some explanations for these results. First, these fragments possibly adopt conformations that are not the same as in the whole glycan epitope found in the glycoprotein, which could lead to the antibody not being able to recognize these smaller fragments.<sup>34</sup> In Chapter 2, the NMR data of hexasaccharide **2.2** and heptasaccharide **2.3** deviate for some sugar residues when compared to that of the native glycan. These deviations could suggest such conformational differences. Synthesizing the entire glycan fragment could probably lead to better binding with the antibody. Another possibility is that the proposed structure of the native glycan probably is incorrect and requires some revision. The deviations in the NMR data described in Chapter 2 could also suggest structural, as well as conformational, differences between the actual and published structures. Another reason for the binding results could be the absence of the phosphate moieties in the synthetic glycans tested. Previous affinity chromatographic purifications of GP72 or GP72 derived glycopeptides had mostly eluted structures containing anionic phosphates.<sup>19,20</sup> Combining this observation, and the results presented in this chapter, suggests that the presence of the phosphate groups, moieties that can participate in ionic interactions with proteins,<sup>35,36</sup> is essential for antibody recognition. This hypothesis can be supported if the synthesis of phosphorylated glycan fragments can be achieved.

The synthesis of phosphate-containing glycans poses great challenges and combining that with the already complex ‘hyper-branched’ structure of the target glycan, the synthesis would require great effort and time. In addition, the exact position of the phosphorylation in the glycan is still unknown.<sup>20</sup> Last but not the least, it is also possible that the WIC29.26 mAb sample that I was using denatured at some point and lost its binding capabilities. I could have tested if the mAb is still working, but I did not have any access to a positive control, which is a protein lysate from *T. cruzi* containing glycoprotein GP72. The preparation of this protein lysate is tedious, and storage and transportation of a sample is challenging due to the instability of the lysate. To continue this project, we are planning to send our glycans to our collaborators in University of Dundee where they can further investigate and perform binding analysis between the glycans and the mAb.

## 4.4 Experimental methods

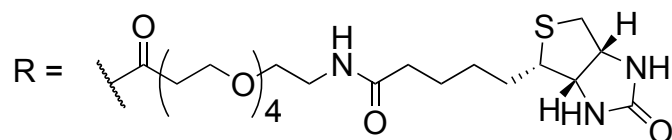
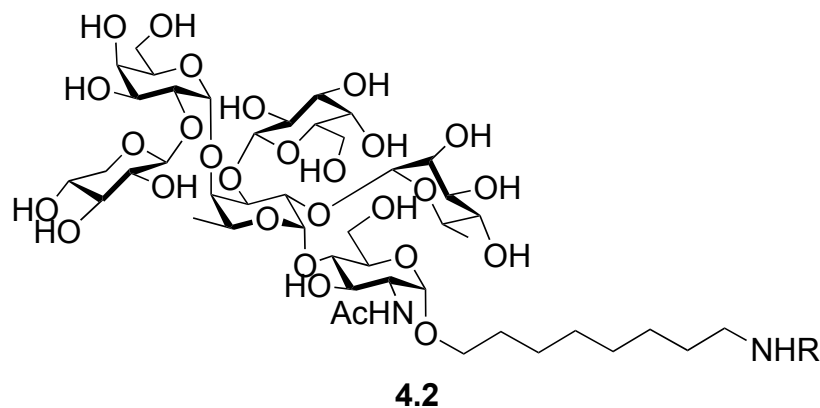
### 4.4.1 Synthesis of biotinylated glycans 4.2–4.5



#### General Procedure 1: Synthesis of biotin-PEG<sub>4</sub>-linker tagged glycans

To a solution of biotin-PEG<sub>4</sub>-COOH linker (**4.1**) in DMF (1.0 mL) was added *N*-hydroxysuccinimide (2.0 eq) and EDC·HCl (2.0 eq) at 0 °C. The mixture was stirred overnight at before a solution of 8-amino-1-octyl glycoside (1.0 eq) (**2.2–2.5**) and triethylamine (3.0 eq) in DMF (0.5 mL) were added at 0 °C. After stirring for 3 h, the mixture was concentrated to dryness. The resulting crude residue was purified by C<sub>18</sub> reversed-phase chromatography (H<sub>2</sub>O to 9:1 H<sub>2</sub>O–MeOH) to give a product

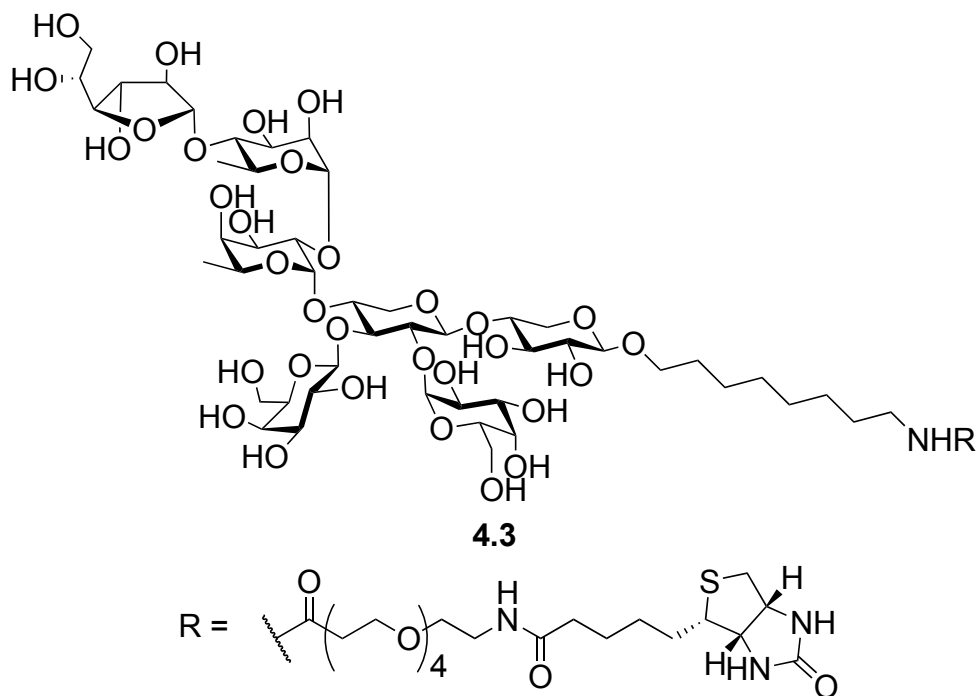
that was redissolved in distilled water. The resulting solution was frozen and then lyophilized to afford the biotin-PEG<sub>4</sub>-linker tagged glycans (**4.2–4.5**).



**N-(N-biotinyl-15-amino-4,7,10,13-tetraoxa-pentadecanoyl)-8-amino-octyl [β-D-galactopyranosyl-(1→3)-[α-L-rhamnopyranosyl-(1→2)]-[[β-D-xylopyranosyl-(1→2)]-α-D-galactopyranosyl-(1→4)]-α-L-fucopyranosyl-(1→4)]-N-acetyl-2-amino-2-deoxy-α-D-glucopyranoside (**4.2**).**

Synthesized according to General Procedure 1 using 8-amino-1-octyl glycoside **3.2** (0.90 mg, 0.82 μmol) to afford **4.2** (1.00 mg, 76%) as a white solid: <sup>1</sup>H NMR (500 MHz, D<sub>2</sub>O) δ 5.98 (d, *J* = 3.9 Hz, 1H), 5.23 (d, *J* = 3.8 Hz, 1H), 5.00 (s, 1H), 4.90 (d, *J* = 3.6 Hz, 1H), 4.82 (d, *J* = 7.9 Hz, 1H), 4.66–4.59 (m, 1H), 4.62 (d, *J* = 8.4 Hz, 1H), 4.52–4.42 (m, 3H), 4.32 (dd, *J* = 10.1, 3.9 Hz, 1H), 4.29–4.24 (m, 2H), 4.19 (dd, *J* = 10.4, 3.3 Hz, 1H), 4.07–4.00 (m, 4H), 3.98 (dd, *J* = 10.6, 3.8 Hz, 1H), 3.96–3.91 (m, 4H), 3.91–3.85 (m, 5H), 3.83–3.74 (m, 6H), 3.73–3.68 (m, 15H), 3.67–3.62 (m, 4H), 3.56–3.40 (m, 9H), 3.40–3.32 (m, 2H), 3.29–3.23 (m, 1H), 3.21 (app t, *J* = 7.0 Hz, 2H), 3.03 (dd, *J* = 13.1, 5.1 Hz, 1H), 2.81 (d, *J* = 13.0 Hz, 1H), 2.53 (app t, *J* = 6.0 Hz, 2H), 2.31 (app

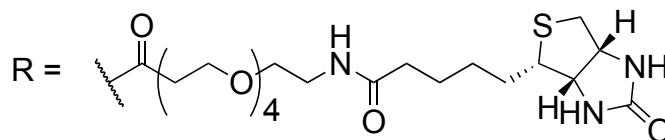
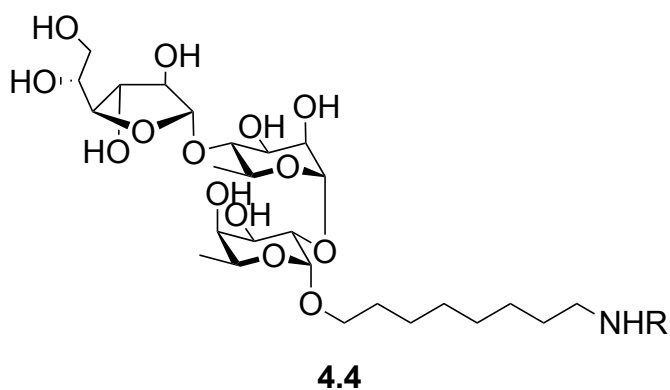
t,  $J = 7.2$  Hz, 2H), 2.07 (s, 3H), 1.80–1.71 (m, 1H), 1.70–1.58 (m, 5H), 1.56–1.50 (m, 2H), 1.48–1.42 (m, 2H), 1.40–1.31 (m, 8H), 1.35 (d,  $J = 6.4$  Hz, 3H), 1.28 (d,  $J = 6.6$  Hz, 3H); HRMS (ESI-TOF)  $m/z$ :  $[M + Na]^+$  Calcd for  $C_{66}H_{115}N_5NaO_{35}S$  1592.6991; Found 1592.6990.



**N-(N-biotinyl-15-amino-4,7,10,13-tetraoxa-pentadecanoyl)-8-amino-octyl [ $\beta$ -D-galactopyranosyl-(1 $\rightarrow$ 3)-[ $\alpha$ -D-galactopyranosyl-(1 $\rightarrow$ 2)]-[[[ $\beta$ -D-galactofuranosyl-(1 $\rightarrow$ 4)]- $\alpha$ -L-rhamnopyranosyl]-(1 $\rightarrow$ 2)- $\alpha$ -L-fucopyranosyl-(1 $\rightarrow$ 4)]- $\beta$ -D-xylopyranosyl-(1 $\rightarrow$ 4)]- $\beta$ -D-xylopyranoside (4.3)**

Synthesized according to General Procedure 1 using 8-amino-1-octyl glycoside **3.3** (0.60 mg, 0.51  $\mu$ mol) to afford **4.3** (0.50 mg, 57%) as a white solid:  $^1H$  NMR (600 MHz,  $D_2O$ )  $\delta$  5.48 (d,  $J = 3.7$  Hz, 1H), 5.33 (d,  $J = 1.9$  Hz, 1H), 5.23 (d,  $J = 3.5$  Hz, 1H), 4.94 (d,  $J = 1.9$  Hz, 1H), 4.85 (d,  $J = 6.6$  Hz, 1H), 4.65–4.60 (m, 2H), 4.62 (d,  $J = 7.8$  Hz, 1H), 4.46 (d,  $J = 7.8$  Hz, 1H), 4.48–4.42 (m, 1H), 4.23 (dd,  $J = 8.2, 4.3$  Hz, 1H), 4.20 (dd,  $J = 12.2, 4.4$  Hz, 1H), 4.18–4.15 (m, 2H), 4.14 (dd,  $J = 3.9, 1.8$  Hz, 1H), 4.09 (dd,  $J = 6.6, 3.8$  Hz, 1H), 4.02 (dd,  $J = 6.5, 3.9$  Hz, 1H), 4.00 (dd,  $J =$

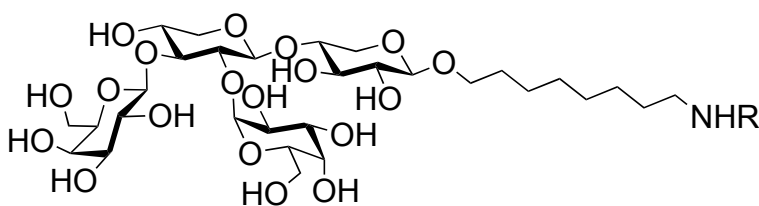
9.6, 3.4 Hz, 1H), 3.99–3.95 (m, 2H), 3.95–3.90 (m, 3H), 3.90–3.78 (m, 9H), 3.78–3.69 (m, 7H), 3.70–3.57 (m, 20H), 3.53 (dd,  $J = 9.9, 7.7$  Hz, 1H), 3.51–3.42 (m, 4H), 3.28 (dd,  $J = 9.3, 7.8$  Hz, 1H), 3.04–2.95 (m, 2H), 3.02 (dd,  $J = 13.1, 4.9$  Hz, 1H), 2.81 (d,  $J = 13.0$  Hz, 1H), 2.56 (app t,  $J = 6.0$  Hz, 2H), 2.30 (t,  $J = 7.2$  Hz, 2H), 1.80–1.71 (m, 1H), 1.70–1.58 (m, 5H), 1.56–1.50 (m, 2H), 1.48–1.42 (m, 2H), 1.40–1.31 (m, 8H), 1.33 (d,  $J = 6.4$  Hz, 3H), 1.24 (d,  $J = 6.6$  Hz, 3H); HRMS (ESI-TOF)  $m/z$ :  $[M + Na]^+$  Calcd for  $C_{69}H_{120}N_4NaO_{39}S$  1683.7148; Found 1683.7123.



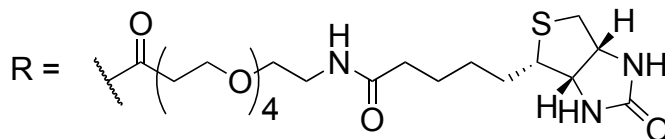
**N-(N-biotinyl-15-amino-4,7,10,13-tetraoxa-pentadecanoyl)-8-aminoctyl  $\beta$ -D-galactofuranosyl-(1 $\rightarrow$ 4)- $\alpha$ -L-rhamnopyranosyl-(1 $\rightarrow$ 2)- $\alpha$ -L-fucopyranoside (4.4)**

Synthesized according to General Procedure 1 using 8-amino-1-octyl glycoside **3.4** (4.4 mg, 7.3  $\mu$ mol) to afford **4.4** (6.6 mg, 82%) as a white solid:  $^1H$  NMR (500 MHz,  $D_2O$ )  $\delta$  5.32 (d,  $J = 1.9$  Hz, 1H), 5.12 (d,  $J = 3.4$  Hz, 1H), 4.94 (d,  $J = 1.8$  Hz, 1H), 4.63 (dd,  $J = 8.0, 5.0$  Hz, 1H), 4.45 (dd,  $J = 8.0, 4.5$  Hz, 1H), 4.15 (dd,  $J = 4.0, 1.9$  Hz, 1H), 4.12–4.05 (m, 2H), 4.04 (dd,  $J = 6.5, 4.0$  Hz, 1H), 4.00 (dd,  $J = 9.7, 3.4$  Hz, 1H), 3.98–3.92 (m, 2H), 3.90 (d,  $J = 3.1$  Hz, 1H), 3.89 (d,  $J = 3.4$  Hz, 1H), 3.87–3.83 (m, 2H), 3.82–3.76 (m, 3H), 3.78–3.67 (m, 15H), 3.67–3.63 (m, 3H), 3.61

(d,  $J = 10.0$  Hz, 1H), 3.57 (app dt,  $J = 11.0, 5.7$  Hz, 1H), 3.42 (app t,  $J = 5.4$  Hz, 2H), 3.36 (app dt,  $J = 9.9, 5.2$  Hz, 1H), 3.21 (app t,  $J = 6.9$  Hz, 2H), 3.02 (dd,  $J = 13.1, 5.0$  Hz, 1H), 2.81 (d,  $J = 13.1$  Hz, 1H), 2.53 (app t,  $J = 6.0$  Hz, 2H), 2.30 (app t,  $J = 7.3$  Hz, 2H), 1.81–1.71 (m, 1H), 1.70–1.57 (m, 5H), 1.53–1.46 (m, 2H), 1.45–1.38 (m, 2H), 1.39–1.32 (m, 8H), 1.33 (d,  $J = 6.4$  Hz, 3H), 1.24 (d,  $J = 6.6$  Hz, 3H); HRMS (ESI-TOF)  $m/z$ :  $[M + Na]^+$  Calcd for  $C_{47}H_{84}N_4NaO_{21}S$  1095.5241; Found 1095.5242.



**4.5**



**N-(N-biotinyl-15-amino-4,7,10,13-tetraoxa-pentadecanoyl)-8-amino-octyl  $\beta$ -D-galactopyranosyl-(1 $\rightarrow$ 3)-[ $\alpha$ -D-galactopyranosyl-(1 $\rightarrow$ 2)]- $\beta$ -D-xylopyranosyl-(1 $\rightarrow$ 4)- $\beta$ -D-xylopyranoside (4.5)**

Synthesized according to General Procedure 1 using 8-amino-1-octyl glycoside **4.5** (2.3 mg, 3.1  $\mu$ mol) to afford **4.5** (3.1 mg, 79%) as a white solid:  $^1H$  NMR (500 MHz,  $D_2O$ )  $\delta$  5.41 (d,  $J = 3.9$  Hz, 1H), 4.71 (d,  $J = 6.6$  Hz, 1H), 4.58 (d,  $J = 7.7$  Hz, 1H), 4.64–4.59 (m, 1H), 4.37 (d,  $J = 7.9$  Hz, 1H), 4.46–4.35 (m, 2H), 4.10 (dd,  $J = 11.8, 5.2$  Hz, 1H), 4.06 (dd,  $J = 12.0, 5.0$  Hz, 1H), 3.93 (d,  $J = 3.1$  Hz, 1H), 3.90–3.87 (m, 2H), 3.86–3.84 (m, 1H), 3.82 (dd,  $J = 9.4, 2.6$  Hz, 1H), 3.77–3.68 (m, 12H), 3.67–3.62 (m, 14H), 3.63–3.55 (m, 4H), 3.57–3.51 (m, 2H), 3.45–3.37 (m, 3H), 3.36 (app t,  $J = 5.4$  Hz, 2H), 3.30 (app dt,  $J = 9.7, 5.1$  Hz, 1H), 3.23 (dd,  $J = 9.4, 8.0$  Hz, 1H), 3.18–

3.09 (m, 2H), 2.96 (dd,  $J = 13.1, 5.0$  Hz, 1H), 2.75 (d,  $J = 13.1$  Hz, 1H), 2.47 (app t,  $J = 6.0$  Hz, 2H), 2.24 (app t,  $J = 7.3$  Hz, 2H), 1.74–1.66 (m, 1H), 1.64–1.51 (m, 5H), 1.49–1.42 (m, 2H), 1.42–1.35 (m, 2H), 1.34–1.24 (m, 8H); HRMS (ESI–TOF)  $m/z$ :  $[M + Na]^+$  Calcd for  $C_{51}H_{90}N_4NaO_{26}S$  1229.5456; Found 1229.5450.

#### **4.4.2 Bio-layer interferometry experiments**

##### **4.4.2.1 Immobilization of biotinylated glycans on SAX biosensors**

BLI immobilization experiments were done using measured in 96-well microplates at 25 °C using an OctetRed96 system (FortéBio). The biotinylated glycans were prepared using General procedure 1 and diluted to a final concentration of 200 nM. The synthetic biotinylated glycans were chosen to be immobilized on Octet SAX (high-precision streptavidin) biosensors. The binding buffer used in this experiment is 1x PBS (pH = 7.4) containing 0.1% BSA and 0.05% Tween 20. Two Octet SAX (high-precision streptavidin) biosensors per biotinylated glycan were rehydrated in a biosensor rack with a 96-well black plate containing 200  $\mu$ L of binding buffer for 10 mins. The immobilization assay was done with an initial 60 sec baseline step, 300 sec loading step, and a final 600 sec baseline step. Baseline steps were carried out in binding buffer only. The process was monitored by measuring the changes in the layer thickness (in nanometers) of biosensors in time. The free streptavidin sites on the biosensors were then blocked by biocytin (10 mg/ml) to avoid non-specific interactions. The blocking protocol was done with an initial 60 sec baseline step, 120 sec blocking step and a final 600 sec baseline step. Two additional SAX biosensors, which were used as reference sensors, were coated with biocytin following the same blocking protocol. The loaded and reference biosensors were stored by dipping the tips on 200  $\mu$ L

of binding buffer until binding assay. BLI sensograms for these binding analyses are shown in Appendix, Figure 6.1–6.3.

#### **4.4.2.2 Binding assay with WIC29.26 mAb**

BLI binding assay experiments were done using measured in 96-well microplates at 25 °C by Octet Red system (FortéBio). A freeze-dried sample of WIC29.26 mAb (from Dr. Michael Ferguson, University of Dundee, UK) was rehydrated in 20.0  $\mu$ L of water and was kept on ice for 30 minutes, with occasional shaking. The sample was spun for about 10 sec and was ready to use. The total protein concentration, determined by the bicinchoninic acid assay (BCA assay), was 10.0 mg/mL. Two solutions of the mAb were prepared to final concentrations of 100  $\mu$ g/mL and 200  $\mu$ g/mL in the assay buffer (1x PBS containing 0.1% BSA and 0.05% Tween 20). The kinetic assay was carried out by placing a glycan-immobilized biosensor into the wells containing WIC29.26 mAb solutions (200  $\mu$ L in each well) and measuring changes in layer thickness (in nanometers) of biosensors over time. One additional parallel SAX biosensor loaded with biotinylated glycan was only incubated with assay buffer to serve as control. The assay was done with an initial 120 sec baseline step, 300 sec association step, and 300 sec dissociation step. Baseline and dissociation steps were carried out in assay buffer only. Two additional parallel SAX biosensors loaded with biocytin (reference biosensors for double reference method) only were incubated with WIC 29.26 mAb solutions and assay buffer following the same kinetic assay protocol above. Biosensors were regenerated using three cycles of 10 sec in glycine solution (pH = 2.5) followed by 10 sec in neutralizing buffer (1x PBS, pH = 7.4). All the data were processed and calculated using Fortebio software assuming a 1:1 binding model. BLI sensograms of the binding analysis are shown in the Appendix, Figure 6.4–6.6. Similar kinetic assays as above were used in this binding experiment

but using 50 mM Tris buffer (pH = 7.4, 0.15 M NaCl, 0.25% BSA and 0.05% Tween 20, 0.05% NaN<sub>3</sub>). BLI sensograms for these binding analyses are shown in Appendix, Figure 6.7–6.9.

#### **4.4.2.3 Binding assay with purified WIC29.26 mAb**

The purification of WIC29.26 mAb sample was performed using affinity chromatography with an agarose gel column functionalized with Protein A. A freeze-dried sample of WIC29.26 mAb (from Dr. Michael Ferguson, University of Dundee, UK) was rehydrated in 20.0 µL of water and was kept on ice for 30 min, with occasional shaking. The sample was spun for about 10 sec and was ready to use. The antibody solution was loaded onto a Protein A agarose gel column prepared with 1x PBS buffer. The unbound proteins were eluted using 3 mL of 1x PBS buffer, collecting 1 mL fractions at a time. The bound mAb was collected by elution with 0.1 M glycine buffer (pH = 3.0), which was collected directly into fractions (1 mL per fraction) containing 0.5 M Tris buffer (pH = 9.0, 1 mL per fraction). The contents of all the fractions were checked using SDS PAGE to determine fractions containing the mAb (bands at 50kDa and 23 kDa). The fractions were combined and then a buffer exchange was performed to finally suspend the antibody in 100 µL of 1x PBS buffer. The final antibody concentration using the bicinchoninic acid assay (BCA assay) was 0.38 mg/mL. Three solutions of the mAb were prepared to final concentrations of 9.6 µg/mL, 19 and 39 µg/mL in the assay buffer (1x PBS containing 0.1% BSA and 0.05% Tween 20). Similar kinetic assays as above were used in this binding experiment but using the purified mAb solutions instead. BLI sensograms for these binding analyses are shown in Appendix, Figure 6.10–6.12.

#### **4.4.3 Sodium dodecyl sulfate polyacrylamide gel electrophoresis**

All samples analyzed by tris glycine sodium dodecyl sulfate polyacrylamide gel electrophoresis (SDS-PAGE) followed this protocol. Protein samples were checked using a 12% acrylamide resolving gel (3.3 mL ddH<sub>2</sub>O, 4.0 mL 30% acrylamide mix, 2.5 mL 1.5 M tris (pH 8.8), 0.1 mL 10% SDS, 0.1 mL 10% APS, and 4.0 µL tetramethylethylenediamine), and 5% acrylamide stacking gel (2.1 mL ddH<sub>2</sub>O, 0.5 mL 30% acrylamide mix, 0.38 mL 1.5 M tris (pH 8.8), 0.03 mL 10% SDS, 0.03 mL 10% APS, and 2.0 µL tetramethylethylenediamine). Tris-Glycine-SDS was used as the running buffer. All samples were pre-stained with 0.1% bromophenol blue and pre-heated for 5 minutes at 95 °C. A volume of 10 µL of the samples was loaded onto the gels. Bio-Rad Precision Plus Protein Dual Color Standard (4 µL) was used as reference protein ladder. The electrophoresis was conducted at 90 volts for 30 minutes, and the voltage was increased to 120 volts for 90 min. Gels were stained using InstantBlue® Coomassie Protein Stain for 20 minutes with shaking. Gels were destained twice using ddH<sub>2</sub>O for 20 minutes with shaking.

#### **4.4.4 Dot Blot Assay Protocol**

The immobilization of the monoclonal antibody was performed by spotting 3 µL (0.5 µg/mL or 20.0 µg/mL) solution of WIC 29.26 mAb on six nitrocellulose membranes (Control, biotin-PEG4-COOH, glycan **4.2**, **4.3**, **4.4**, and **4.5**) and then was incubated for 1 h at room temperature. The membrane was then incubated with the blocking buffer (50mM Tris-HCl pH = 7.4, 0.15M NaCl, 0.25% BSA, 0.05%(w/v) Tween-20, 0.05% NaN<sub>3</sub> and 2% (w/v) fish skin gelatin) for 1 h at room temperature. The blocking solution was removed and replaced with solutions of linker and different biotinylated glycans (100 µg/mL in TBST) and was incubated overnight at 4 °C. The control, linker and glycan solutions were removed, the membranes were

washed two times (10 minutes each time) with TBST buffer at room temperature. The membranes were then incubated with neutravidin–Dylight 488 (1  $\mu\text{g}/\text{mL}$ ) for 1 h at room temperature in TTBS. Afterwards, the fluorescent containing solution was removed and the membranes were washed two times (10 minutes each time) with TBST buffer. Finally, the membranes were scanned for fluorescence using iBright FL1000 Imaging Systems (Thermo Scientific).

## 4.5 References

- (1) Clark, D. P.; Pazdernik, N. J.; McGehee, M. R. Protein Structure and Function. In *Molecular Biology*; Elsevier, 2019; pp 445–483.
- (2) Van Kooyk, Y.; Rabinovich, G. A. Protein-Glycan Interactions in the Control of Innate and Adaptive Immune Responses. *Nat Immunol* **2008**, *9* (6), 593–601.
- (3) Gao, Y.; Luan, X.; Melamed, J.; Brockhausen, I. Role of Glycans on Key Cell Surface Receptors That Regulate Cell Proliferation and Cell Death. *Cells* **2021**, *10* (5), 1252.
- (4) Seyrek, K.; Richter, M.; Lavrik, I. N. Decoding the Sweet Regulation of Apoptosis: The Role of Glycosylation and Galectins in Apoptotic Signaling Pathways. *Cell Death Differ.* **2019**, *26* (6), 981–993.
- (5) Fuster, M. M.; Esko, J. D. The Sweet and Sour of Cancer: Glycans as Novel Therapeutic Targets. *Nat. Rev. Cancer* **2005**, *5* (7), 526–542.
- (6) Johnson, J. L.; Jones, M. B.; Ryan, S. O.; Cobb, B. A. The Regulatory Power of Glycans and Their Binding Partners in Immunity. *Trends Immunol.* **2013**, *34* (6), 290–298.
- (7) Comstock, L. E.; Kasper, D. L. Bacterial Glycans: Key Mediators of Diverse Host Immune Responses. *Cell* **2006**, *126* (5), 847–850.
- (8) Tra, V. N.; Dube, D. H. Glycans in Pathogenic Bacteria – Potential for Targeted Covalent Therapeutics and Imaging Agents. *Chem. Commun.* **2014**, *50* (36), 4659–4673.
- (9) Krumm, S. A.; Doores, K. J. Targeting Glycans on Human Pathogens for Vaccine Design. In *Vaccination Strategies Against Highly Variable Pathogens*; Hangartner, L., Burton, D. R., Eds.; Current Topics in Microbiology and Immunology; Springer International Publishing: Cham, 2018; Vol. 428, pp 129–163.

- (10) Zimmermann, S.; Lepenies, B. Glycans as Vaccine Antigens and Adjuvants: Immunological Considerations. In *Carbohydrate-Based Vaccines*; Lepenies, B., Ed.; Methods in Molecular Biology; Springer New York: New York, NY, 2015; Vol. 1331, pp 11–26.
- (11) Kay, E.; Cuccui, J.; Wren, B. W. Recent Advances in the Production of Recombinant Glycoconjugate Vaccines. *npj Vaccines* **2019**, *4* (1), 16.
- (12) Sher, A.; Snary, D. Specific Inhibition of the Morphogenesis of *Trypanosoma cruzi* by a Monoclonal Antibody. *Nature* **1982**, *300* (5893), 639–640.
- (13) Cooper, R.; De Jesus, A.; Cross, G. Deletion of an Immunodominant *Trypanosoma cruzi* Surface Glycoprotein Disrupts Flagellum-Cell Adhesion. *J. Cell Biol.* **1993**, *122* (1), 149–156.
- (14) Nozaki, T. Characterization of the *Trypanosoma brucei* Homologue of a *Trypanosoma cruzi* Flagellum-Adhesion Glycoprotein. *Mol. Biochem. Parasitol.* **1996**, *82* (2), 245–255.
- (15) Rocha, G. M.; Brandão, B. A.; Mortara, R. A.; Attias, M.; De Souza, W.; Carvalho, T. M. U. The Flagellar Attachment Zone of *Trypanosoma cruzi* Epimastigote Forms. *J. Struct. Biol.* **2006**, *154* (1), 89–99.
- (16) Rocha, G. M.; Seabra, S. H.; De Miranda, K. R.; Cunha-e-Silva, N.; De Carvalho, T. M. U.; De Souza, W. Attachment of Flagellum to the Cell Body Is Important to the Kinetics of Transferrin Uptake by *Trypanosoma cruzi*. *Parasitol. Int.* **2010**, *59* (4), 629–633.
- (17) Sunter, J. D.; Gull, K. The Flagellum Attachment Zone: ‘The Cellular Ruler’ of Trypanosome Morphology. *Trends Parasitol.* **2016**, *32* (4), 309–324.

- (18) Basombrío, M. A.; Gómez, L.; Padilla, A. M.; Ciaccio, M.; Nozaki, T.; Cross, G. A. M. Targeted Deletion of the Gp72 Gene Decreases the Infectivity of *Trypanosoma cruzi* for Mice And Insect Vectors. *para* **2002**, *88* (3), 489–493.
- (19) Haynes, P. A.; Ferguson, A. J.; Cross, G. A. M. Structural Characterization of Novel Oligosaccharides of Cell-Surface Glycoproteins of *Trypanosoma cruzi*. *Glycobiology* **1996**, *6* (8), 869–878.
- (20) Allen, S.; Richardson, J. M.; Mehlert, A.; Ferguson, M. A. J. Structure of a Complex Phosphoglycan Epitope from Gp72 of *Trypanosoma cruzi*. *J. Biol. Chem.* **2013**, *288* (16), 11093–11105.
- (21) Dam, T. K.; Talaga, M. L.; Fan, N.; Brewer, C. F. Measuring Multivalent Binding Interactions by Isothermal Titration Calorimetry. In *Methods in Enzymology*; Elsevier, 2016; Vol. 567, pp 71–95.
- (22) Lee, Y. C. Fluorescence Spectrometry in Studies of Carbohydrate-Protein Interactions. *J. Biochem.* **1997**, *121* (5), 818–825.
- (23) Geuijen, K. P. M.; Halim, L. A.; Schellekens, H.; Schasfoort, R. B.; Wijffels, R. H.; Eppink, M. H. Label-Free Glycoprofiling with Multiplex Surface Plasmon Resonance: A Tool to Quantify Sialylation of Erythropoietin. *Anal. Chem.* **2015**, *87* (16), 8115–8122.
- (24) Ji, Y.; Woods, R. J. Quantifying Weak Glycan-Protein Interactions Using a Biolayer Interferometry Competition Assay: Applications to ECL Lectin and X-31 Influenza Hemagglutinin. In *Glycobiophysics*; Yamaguchi, Y., Kato, K., Eds.; Advances in Experimental Medicine and Biology; Springer Singapore: Singapore, 2018; Vol. 1104, pp 259–273.

- (25) Kitova, E. N.; El-Hawiet, A.; Schnier, P. D.; Klassen, J. S. Reliable Determinations of Protein–Ligand Interactions by Direct ESI-MS Measurements. Are We There Yet? *J. Am. Soc. Mass Spectrom.* **2012**, *23* (3), 431–441.
- (26) Murali, S.; Rustandi, R.; Zheng, X.; Payne, A.; Shang, L. Applications of Surface Plasmon Resonance and Biolayer Interferometry for Virus–Ligand Binding. *Viruses* **2022**, *14* (4), 717.
- (27) Rich, R. L.; Myszka, D. G. Higher-Throughput, Label-Free, Real-Time Molecular Interaction Analysis. *Anal. Biochem.* **2007**, *361* (1), 1–6.
- (28) Petersen, R. Strategies Using Bio-Layer Interferometry Biosensor Technology for Vaccine Research and Development. *Biosensors* **2017**, *7* (4), 49.
- (29) Shah, N. B.; Duncan, T. M. Bio-Layer Interferometry for Measuring Kinetics of Protein-Protein Interactions and Allosteric Ligand Effects. *JoVE* **2014**, No. 84, 51383.
- (30) Ezzati Nazhad Dolatabadi, J.; De La Guardia, M. Tips on Ligand Immobilization and Kinetic Study Using Surface Plasmon resonance. *Bioimpacts* **2016**, *6* (3), 117–118.
- (31) Stayton, P. S.; Freitag, S.; Klumb, L. A.; Chilkoti, A.; Chu, V.; Penzotti, J. E.; To, R.; Hyre, D.; Le Trong, I.; Lybrand, T. P.; Stenkamp, R. E. Streptavidin–Biotin Binding Energetics. *Biomol. Eng.* **1999**, *16* (1–4), 39–44.
- (32) Apiyo, D. O. Biolayer Interferometry (Octet) for Label-Free Biomolecular Interaction Sensing. In *Handbook of Surface Plasmon Resonance*; Schasfoort, R. B. M., Ed.; The Royal Society of Chemistry, 2017; pp 356–397.
- (33) Dubrow, A.; Zuniga, B.; Topo, E.; Cho, J.-H. Suppressing Nonspecific Binding in Biolayer Interferometry Experiments for Weak Ligand–Analyte Interactions. *ACS Omega* **2022**, *7* (11), 9206–9211.

- (34) Zhang, S.; Chen, K. Y.; Zou, X. Carbohydrate-Protein Interactions: Advances and Challenges. *Commun. Inf. Syst.* **2021**, *21* (1), 147–163.
- (35) Wassef, N. M.; Roerdink, F.; Swartz, G. M.; Lyon, J. A.; Berson, B. J.; Alving, C. R. Phosphate-Binding Specificities of Monoclonal Antibodies against Phosphoinositides in Liposomes. *Mol. Immunol.* **1984**, *21* (10), 863–868.
- (36) Haji-Ghassemi, O.; Müller-Loennies, S.; Rodriguez, T.; Brade, L.; Kosma, P.; Brade, H.; Evans, S. V. Structural Basis for Antibody Recognition of Lipid A. *J. Biol. Chem.* **2015**, *290* (32), 19629–19640.

## **Chapter 5**

### **Summary and Future Work**

## 5.1 Summary and future work

In this thesis, I have investigated the synthesis of a highly immunogenic oligosaccharide epitope from glycoprotein GP72 of *Trypanosoma cruzi*.<sup>1</sup> This includes the synthesis of smaller glycan fragments (Chapter 2), and efforts to synthesis the whole tridecasaccharide glycan epitope (Chapter 3). Binding analyses using BLI and a dot blot assay were performed between the smaller fragments synthesized in Chapter 2 and the monoclonal antibody WIC29.26 (Chapter 4).

### 5.1.1 Synthesis of glycan epitope of GP72

The glycan epitope of GP72 has a unique and complex structure containing two ‘hyper-branched’ residues, a fucose and a xylose. The synthesis of ‘hyper-branched’ oligosaccharides is challenging due to the increasing steric hindrance on the growing molecule that could affect both the yields and stereoselectivities of the reactions. The correct glycosylation sequence must be employed to obtain these highly congested oligosaccharide targets.

In Chapter 2, I described my work on the syntheses of four fragments (**2.2–2.5**) of the antigenic glycan epitope of the *T.cruzi* glycoprotein GP72 (Figure 5-1). Glycan fragments hexasaccharide **2.2** and heptasaccharide **2.3**, each containing a ‘hyper-branched’ residue. A versatile approach of installing three orthogonal groups around the building block corresponding to the ‘hyper-branched’ residues was employed to access all possible glycosylation sequence during the synthesis.

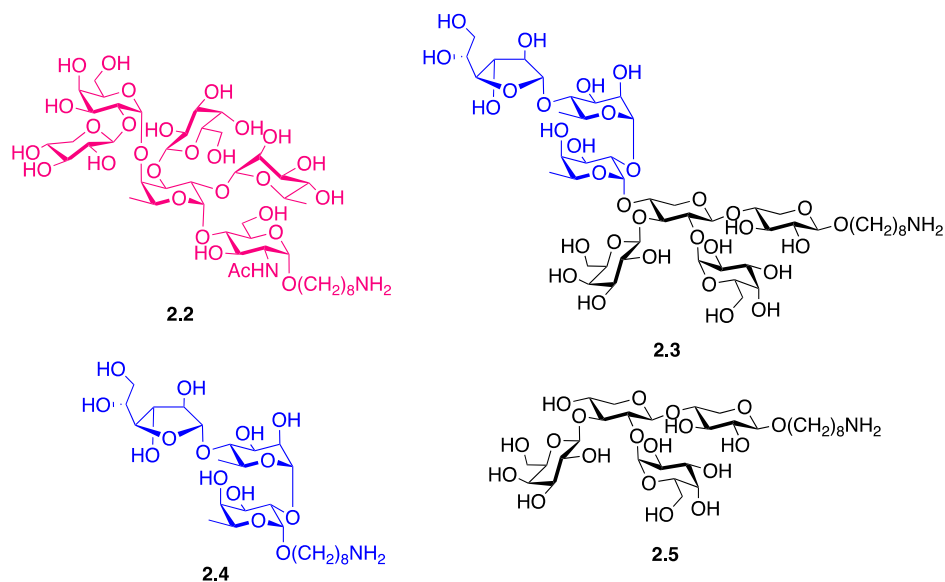
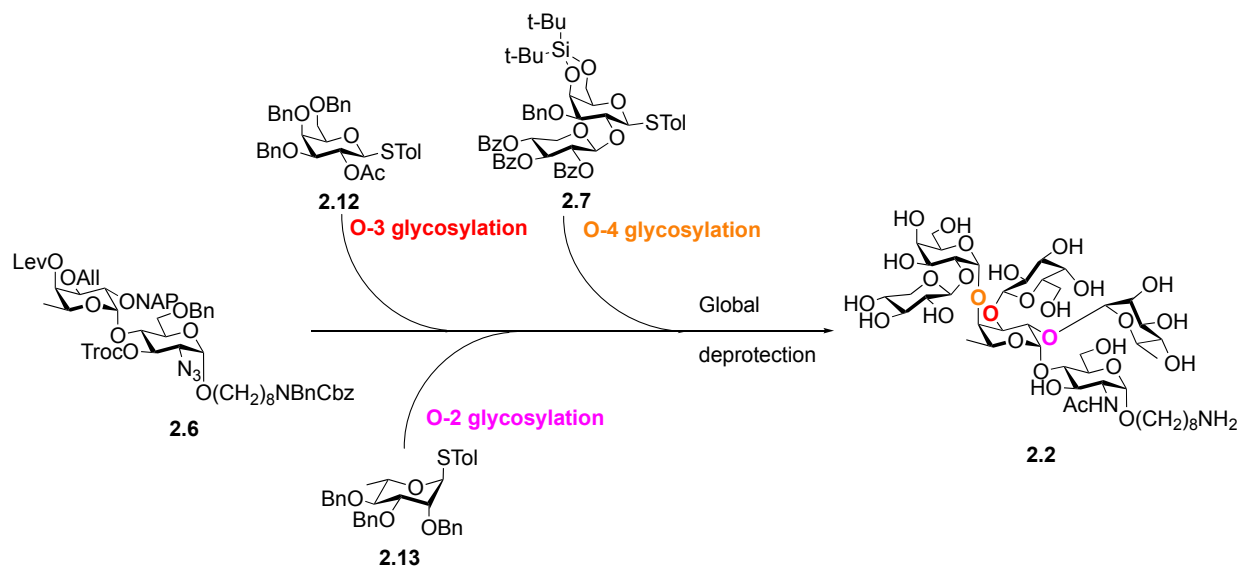


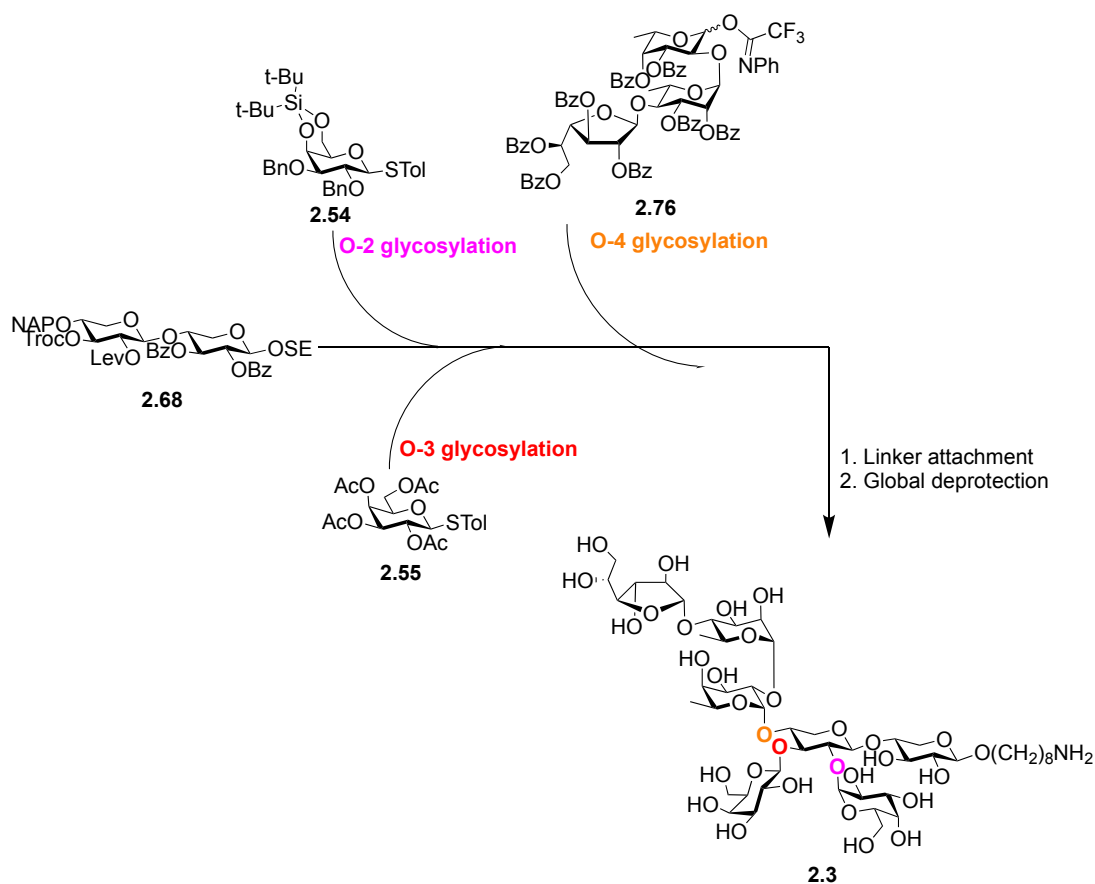
**Figure 5-1:** Structures of synthesized fragments derived from the immunogenic glycan epitope from GP72.

The first attempt to synthesize hexasaccharide **2.2** using a ‘counterclockwise’ approach based on the previous report of the synthesis of ‘hyper-branched’ fucose residues in chlorovirus *N*-glycans.<sup>2,3</sup> Unfortunately, it was found to be futile, as multiple attempts on glycosylation at O-3 failed when O-4 was glycosylated. It was concluded that the ‘counterclockwise’ strategy is not applicable to the synthesis of this ‘hyper-branched’ fucose from GP72. This is perhaps not surprising considering that the sugar compositions and linkages of the ‘hyper-branched’ fucoses in each of the glycan structures are different. A ‘clockwise’ approach was then attempted where glycosylation starts at O-2 followed by O-3 and finally, at O-4. While this sequence afforded the desired tetrasaccharide intermediate, glycosylation at O-3 required large amounts of donor due to weak reactivity of the acceptor. Finally, another sequence – a ‘pendulum’ approach – where glycosylation is performed at O-3 followed by O-2 and O-4 was explored. This approach succeeded in providing the desired hexasaccharide in high yield and stereoselectivity.



**Scheme 5-1:** Successful synthesis of hexasaccharide **2.2** by ‘pendulum’ addition of sugar building blocks.

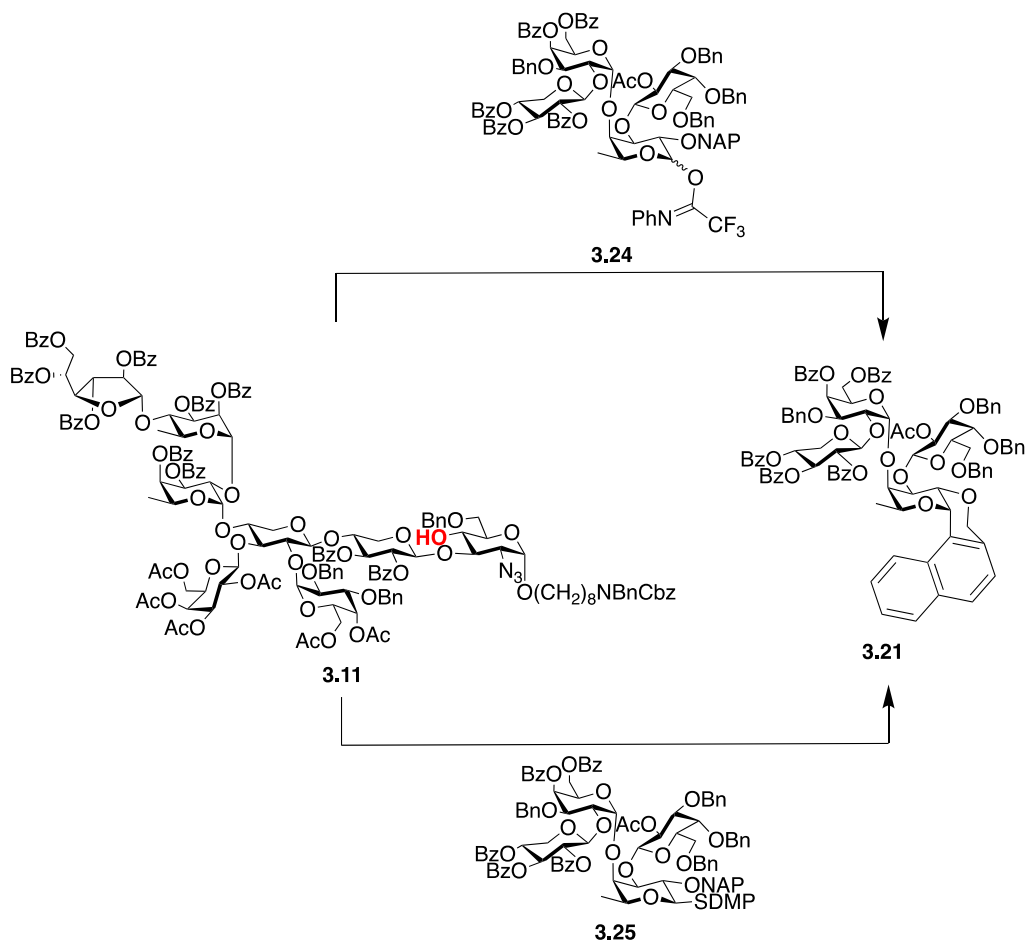
The synthesis of the heptasaccharide **2.3**, which contains a ‘hyper-branched’ xylose residue, was done using a ‘clockwise’ approach, requiring initial glycosylation at O-2, followed by O-3 and a final [4+3] glycosylation at O-4. The rationale behind this sequence was based on the following reasonings: 1) Previous protecting group installation shows O-3 is more reactive than O-2. I hoped to glycosylate at the least reactive site first; 2) in the eventual synthesis of the heptasaccharide, I decided to do an end-stage [4+3] glycosylation at O-4 of the xylose using a trisaccharide donor and thus the same intermediate could be used; 3) It makes more sense to glycosylate at O-3 before O-4 as the reversed sequence would require reaction at an extremely hindered O-3 position flanked by two sugar substituents. This was the only sequence attempted and fortunately, gave the product in good yield and stereoselectivity.



**Scheme 5-2:** Successful synthesis of heptasaccharide **2.3** by ‘clockwise’ addition of sugar building blocks.

In Chapter 3, I reported my efforts on the attempted synthesis of the full trisaccharide glycan epitope. This work highlighted strategies I could use to make the larger compound, specifically the appropriate glycosylation sequences to access these highly congested sugar residues. The intermediates and strategies, specifically the glycosylation sequences described in the previous chapter was used to investigate the synthesis of the whole glycan fragment. Multiple attempts to synthesize the whole glycan fragment starting with a glycosylation using heptasaccharide donor **2.78** and different acceptors. However, it was found that O-3 glycosylation of the 2-azido-2-deoxyglucose residue is not feasible if an existing glycosylation is at O-4.

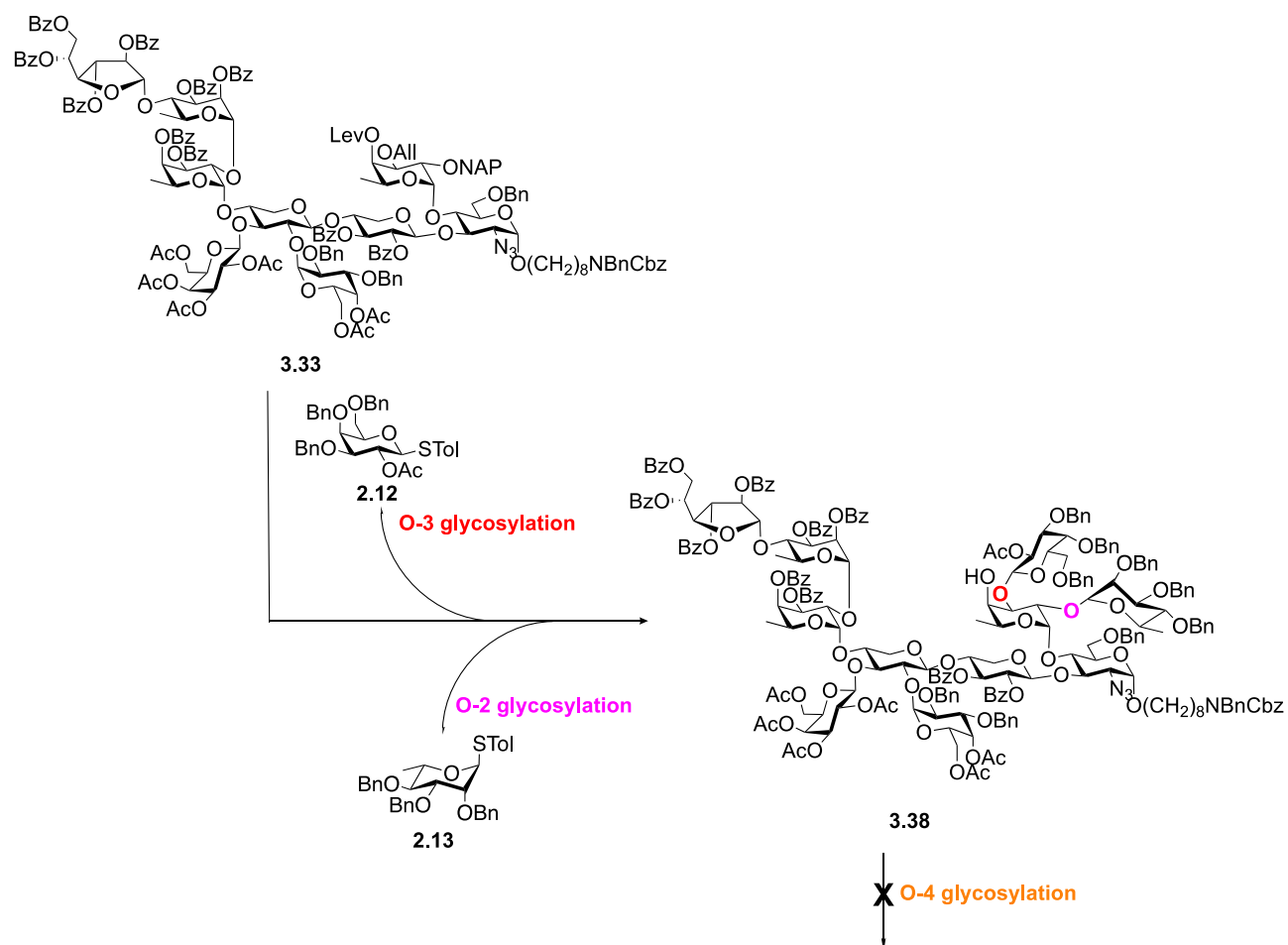
Glycosylation of monosaccharide acceptor **3.9** with donor **2.78** successfully provided octasaccharide **3.10**, which was transformed to **3.11** in a single step. Efforts to perform [8+5] and [8+4] glycosylation with acceptor **3.11** was unsuccessful either due to unsuccessful synthesis of the required donor or the formation of unwanted bicyclic side product **3.21**. Compound **3.21** was proposed to form as a result of an intramolecular Friedel-Crafts reaction of the oxocarbenium ion intermediate derived from the donor and the adjacent NAP ether.



**Scheme 5-3:** Attempted [8+4] glycosylations resulted to intramolecular reaction of the donor.

As a result, I investigated the linear addition of the rest of the sugar residues using the same ‘pendulum’ glycosylation sequence as previously applied to build the ‘hyper-branched’ fucose in

hexasaccharide **2.2**. Glycosylations on O-3 followed by on O-2 were successful to give eventually undecasaccharide **3.38**. The proposed final [11+2] glycosylation reaction was attempted using various donors and reaction conditions, but all the attempts were unsuccessful. Glycosylation attempts just resulted in cleavage of some sugar residues in acceptor **3.38** due to the acidic conditions of the glycosylation. The failure of some of the attempts is due to the weak reactivity of the acceptor causing the donor to either undergo hydrolysis or form the donor dimer. Due to the limited and depleted amount of undecasaccharide **3.38** and the number of steps required to synthesize it, I have decided to finish my work at this point.



**Scheme 5-4:** Synthesis of **3.38** through linear addition but failed final [11+2] O-4 glycosylation.

To continue this research in the future, I propose other synthetic routes deemed worthy to be investigated. The addition of the last two residues onto **3.38** in a stepwise manner might give the desired product. Another possible approach is to investigate another glycosylation sequence wherein glycosylation on O-4 of the fucose precedes glycosylation of O-2. This glycosylation sequence, the ‘reversed pendulum’ was also found successful to build a ‘hyper-branched’ fucose residue in pentasaccharide **3.19**.

### **5.1.2 Binding analysis between synthetic glycan fragments and WIC29.26 mAb**

In Chapter 4, I have described binding analyses I performed between the synthetic fragments of the glycan epitope of the GP72 glycoprotein and WIC 29.26 mAb. The initial binding analysis was performed using bio-layer interferometry (BLI) on a ForteBio’s OctaRED96 instrument. A biotin containing linker was attached to the glycans using the aminooctyl linker and the resulting biotinylated glycans were then successfully immobilized onto Streptavidin coated biosensors (SAX). Binding analysis using these biosensors showed non-specific binding interactions between the biosensors and the WIC 29.26 mAb. Changing the buffer components nor purification of the antibody sample did not improve the antibody binding, nor eliminate the unwanted non-specific interactions.

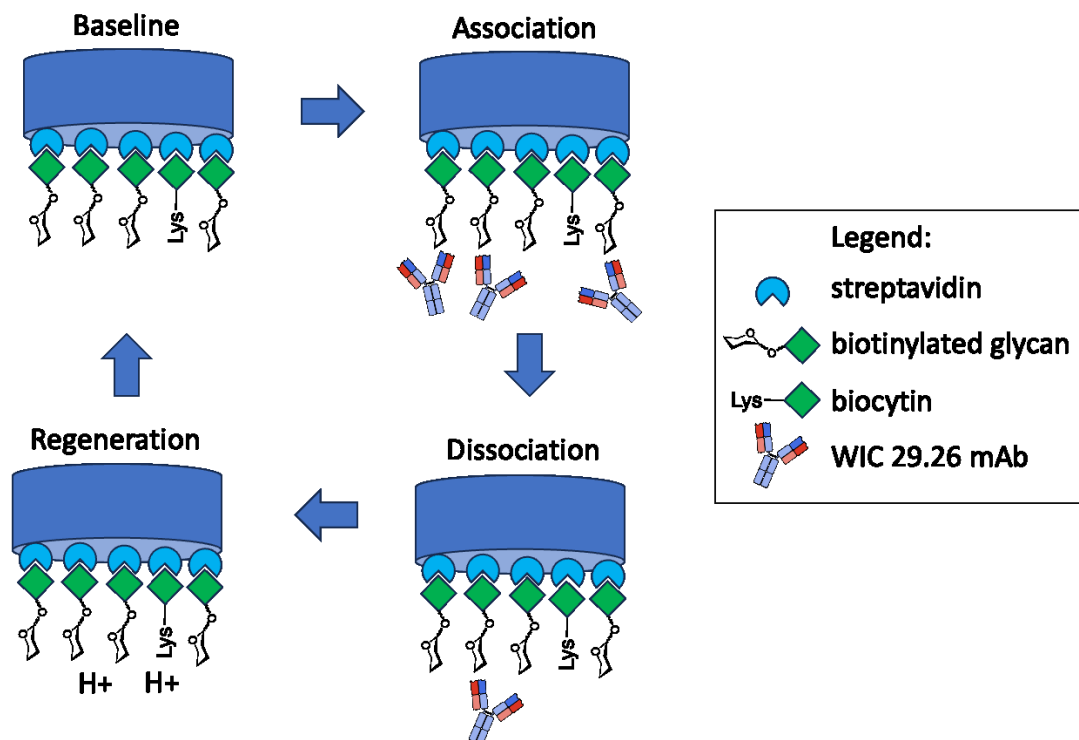


**Figure 5-2:** Schematic diagram of the BLI binding analysis between immobilized glycans and WIC 29.26 mAb.

A dot blot assay was developed to qualitatively determine if any of the glycans bind to the WIC29.26 mAb sample. In this method, the antibody was immobilized by blotting on a nitrocellulose membrane, which was then incubated with a solution containing the biotinylated glycan followed by incubation with a fluorescent-labeled neutravidin Dylight 488. Any interaction can be detected by fluorescence. Unfortunately, this method also did not clearly show any significant binding between the WIC 29.26 mAb and the glycans only showing non-specific binding between the membrane and the protein dye.

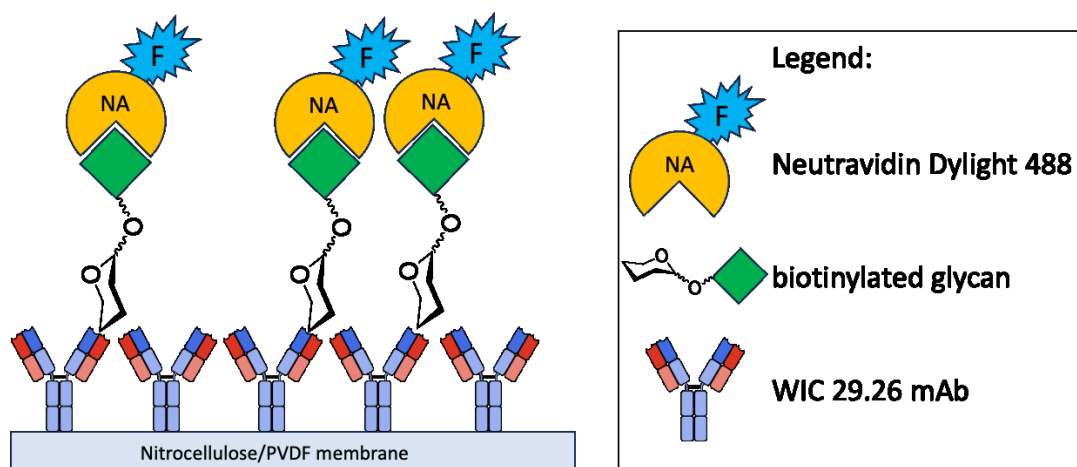


**Figure 5-3:** Schematic diagram for dot blot assay to analyze WIC29.26 mAb–glycan interaction.

These results showed that these synthetic glycan fragments of the GP72 antigenic glycan have little to no measurable interaction with WIC 29.26 mAb. There is a possibility that these fragments adopt conformations that are not the same as in the whole glycan epitope found in the glycoprotein. The deviations in the NMR data described in Chapter 2 between the glycan fragments and the native glycan could also suggest structural, as well as conformational, differences between the two structures. Another reason for the binding results could be the absence of the phosphate moieties in the synthetic glycans tested. Previous affinity chromatographic purifications of GP72 or GP72 derived glycopeptides had mostly eluted structures containing anionic phosphates.<sup>4,5</sup> Combining this observation, and the results presented in this chapter, suggests that the presence of the phosphate groups, moieties that can participate in ionic interactions with proteins,<sup>6,7</sup> is essential for antibody recognition.

To continue this project, we are planning to send our glycans to our collaborators in University of Dundee where they can further investigate and perform binding analysis between the glycans and the mAb. It is also possible to explore the synthesis of glycan fragments that contains the phosphate moiety and use these fragments for future binding analysis.

## 5.2 References

- (1) Sher, A.; Snary, D. Specific Inhibition of the Morphogenesis of *Trypanosoma cruzi* by a Monoclonal Antibody. *Nature* **1982**, *300* (5893), 639–640.
- (2) Lin, S.; Lowary, T. L. Synthesis of the Highly Branched Hexasaccharide Core of Chlorella Virus N-Linked Glycans. *Chem. Eur. J.* **2018**, *24* (64), 16992–16996.
- (3) Lin, S.; Lowary, T. L. Synthesis of a Highly Branched Nonasaccharide Chlorella Virus N-Glycan Using a “Counterclockwise” Assembly Approach. *Org. Lett.* **2020**, *22* (19), 7645–7649.
- (4) Haynes, P. A.; Ferguson, A. J.; Cross, G. A. M. Structural Characterization of Novel Oligosaccharides of Cell-Surface Glycoproteins of *Trypanosoma cruzi*. *Glycobiology* **1996**, *6* (8), 869–878.
- (5) Allen, S.; Richardson, J. M.; Mehlert, A.; Ferguson, M. A. J. Structure of a Complex Phosphoglycan Epitope from Gp72 of *Trypanosoma cruzi*. *J. Biol. Chem.* **2013**, *288* (16), 11093–11105.
- (6) Wassef, N. M.; Roerdink, F.; Swartz, G. M.; Lyon, J. A.; Berson, B. J.; Alving, C. R. Phosphate-Binding Specificities of Monoclonal Antibodies against Phosphoinositides in Liposomes. *Mol. Immunol.* **1984**, *21* (10), 863–868.
- (7) Haji-Ghassemi, O.; Müller-Loennies, S.; Rodriguez, T.; Brade, L.; Kosma, P.; Brade, H.; Evans, S. V. Structural Basis for Antibody Recognition of Lipid A. *J. Biol. Chem.* **2015**, *290* (32), 19629–19640.

## **Bibliography**

## Bibliography

- Ágoston, K.; Streicher, H.; Fügedi, P. Orthogonal Protecting Group Strategies in Carbohydrate Chemistry. *Tetrahedron: Asymmetry* **2016**, *27* (16), 707–728.
- Allen, S.; Richardson, J. M.; Mehlert, A.; Ferguson, M. A. J. Structure of a Complex Phosphoglycan Epitope from GP72 of *Trypanosoma cruzi*. *J. Biol. Chem.* **2013**, *288* (16), 11093–11105.
- Álvarez-Hernández, D.-A.; Franyuti-Kelly, G.-A.; Díaz-López-Silva, R.; González-Chávez, A.-M.; González-Hermosillo-Cornejo, D.; Vázquez-López, R. Chagas Disease: Current Perspectives on a Forgotten Disease. *Rev. Med. Hosp. Gen. (Mex)* **2018**, *81* (3), 154–164.
- American Trypanosomiasis Chagas Disease: One Hundred Years of Research*, Second edition.; Telleria, J., Tibayrenc, M., Eds.; Elsevier: Amsterdam, Netherlands, 2017.
- Apiyo, D. O. Biolayer Interferometry (Octet) for Label-Free Biomolecular Interaction Sensing. In *Handbook of Surface Plasmon Resonance*; Schasfoort, R. B. M., Ed.; The Royal Society of Chemistry, **2017**; pp 356–397.
- Arafuka, S.; Koshiba, N.; Takahashi, D.; Toshima, K. Systematic Synthesis of Sulfated Oligofucosides and Their Effect on Breast Cancer MCF-7 Cells. *Chem. Commun.* **2014**, *50* (69), 9831–9834.
- Bai, S.; Wu, Z.; Huang, Q.; Zhang, L.; Chen, P.; Wang, C.; Zhang, X.; Wang, P.; Li, M. Efforts to Total Synthesis of Philinopside E: Convergent Synthesis of the Sulfated Lanostane-Type Tetraglycoside. *RSC Adv.* **2016**, *6* (7), 5442–5455.
- Ballesteros-Rodea, G.; Santillán, M.; Martínez-Calvillo, S.; Manning-Cela, R. Flagellar Motility of *Trypanosoma cruzi* Epimastigotes. *J. Biomed. Biotechnol.* **2012**, *2012*, 1–9.

- Basombrío, M. A.; Gómez, L.; Padilla, A. M.; Ciaccio, M.; Nozaki, T.; Cross, G. A. M.  
Targeted deletion of the gp72 gene decreases the infectivity of *Trypanosoma cruzi* for mice and insect vectors. *J. Parasitol.* **2002**, *88* (3), 489–493.
- Bérces, A.; Whitfield, D. M.; Nukada, T.; Do Santos Z., I.; Obuchowska, A.; Krepinsky, J. J.  
Is Acyl Migration to the Aglycon Avoidable in 2-Acyl Assisted Glycosylation Reactions? *Can. J. Chem.* **2004**, *82* (7), 1157–1171.
- Bern, C. Chagas Disease. *N Engl J Med* **2015**, *373* (5), 456–466.
- Campetella, O.; Buscaglia, C. A.; Mucci, J.; Leguizamón, M. S. Parasite-Host Glycan Interactions during *Trypanosoma cruzi* Infection: Trans-Sialidase Rides the Show. *BBA. Molecular basis of disease* **2020**, *1866* (5), 165692.
- Chagas disease (American trypanosomiasis). <https://www.who.int/health-topics/chagas-disease> (accessed 2023-09-01).
- Chagas, C. Nova Tripanozomiaze Humana: Estudos Sobre a Morfologia e o Ciclo Evolutivo Do *Schizotrypanum cruzi* n. Gen., n. Sp., Ajente Etiolojico de Nova Entidade Morbida Do Homem. *Mem. Inst. Oswaldo Cruz* **1909**, *1* (2), 159–218.
- Chauvin, A.-L.; Nepogodiev, S. A.; Field, R. A. Synthesis of a 2,3,4-Triglycosylated Rhamnoside Fragment of Rhamnogalacturonan-II Side Chain A Using a Late Stage Oxidation Approach. *J. Org. Chem.* **2005**, *70* (3), 960–966.
- Christensen, H. M.; Oscarson, S.; Jensen, H. H. Common Side Reactions of the Glycosyl Donor in Chemical Glycosylation. *Carbohydr. Res.* **2015**, *408*, 51–95.
- Clark, D. P.; Pazdernik, N. J.; McGehee, M. R. Protein Structure and Function. In *Molecular Biology*; Elsevier, **2019**; pp 445–483.

- Clark, E. H.; Bern, C. Chagas Disease in People with HIV: A Narrative Review. *TropicalMed* **2021**, *6* (4), 198.
- Comstock, L. E.; Kasper, D. L. Bacterial Glycans: Key Mediators of Diverse Host Immune Responses. *Cell* **2006**, *126* (5), 847–850.
- Cooper, R.; De Jesus, A.; Cross, G. Deletion of an Immunodominant *Trypanosoma cruzi* Surface Glycoprotein Disrupts Flagellum-Cell Adhesion. *J. Cell Biol.* **1993**, *122* (1), 149–156.
- Cooper, R.; Inverso, J. A.; Espinosa, M.; Nogueira, N.; Cross, G. A. M. Characterization of a Candidate Gene for GP72, an Insect Stage-Specific Antigen of *Trypanosoma cruzi*. *Mol. Biochem. Parasitol.* **1991**, *49* (1), 45–59.
- Cortez, C.; Sobreira, T. J. P.; Maeda, F. Y.; Yoshida, N. The Gp82 Surface Molecule of *Trypanosoma cruzi* Metacyclic Forms. In *Proteins and Proteomics of Leishmania and Trypanosoma*; Santos, A. L. S., Branquinha, M. H., d'Avila-Levy, C. M., Kneipp, L. F., Sodr , C. L., Eds.; Subcellular Biochemistry; Springer Netherlands: Dordrecht, **2014**; Vol. 74, pp 137–150.
- Cruz, M. C.; Souza-Melo, N.; Da Silva, C. V.; DaRocha, W. D.; Bahia, D.; Ara jo, P. R.; Teixeira, S. R.; Mortara, R. A. *Trypanosoma cruzi*: Role of  $\delta$ -Amastin on Extracellular Amastigote Cell Invasion and Differentiation. *PLoS ONE* **2012**, *7* (12), e51804.
- Cucunub , Z. M.; Nouvellet, P.; Peterson, J. K.; Bartsch, S. M.; Lee, B. Y.; Dobson, A. P.; Bas n ez, M.-G. Complementary Paths to Chagas Disease Elimination: The Impact of Combining Vector Control with Etiological Treatment. *Clin. Infect. Dis.* **2018**, *66* (4), S293–S300.

- Cumpstey, I. On a So-Called “Kinetic Anomeric Effect” in Chemical Glycosylation. *Org. Biomol. Chem.* **2012**, *10* (13), 2503.
- Cyr, N.; Perlin, A. S. The Conformations of Furanosides. A  $^{13}\text{C}$  Nuclear Magnetic Resonance Study. *Can. J. Chem.* **1979**, *57* (18), 2504–2511.
- Dam, T. K.; Talaga, M. L.; Fan, N.; Brewer, C. F. Measuring Multivalent Binding Interactions by Isothermal Titration Calorimetry. *Methods Enzymol.* **2016**, *567*, pp 71–95.
- Das, R.; Mukhopadhyay, B. Chemical O-Glycosylations: An Overview. *ChemistryOpen* **2016**, *5* (5), 401–433.
- De Castro, C.; Molinaro, A.; Piacente, F.; Gurnon, J. R.; Sturiale, L.; Palmigiano, A.; Lanzetta, R.; Parrilli, M.; Garozzo, D.; Tonetti, M. G.; Van Etten, J. L. Structure of *N*-Linked Oligosaccharides Attached to Chlorovirus PBCV-1 Major Capsid Protein Reveals Unusual Class of Complex *N*-Glycans. *Proc. Natl. Acad. Sci. U.S.A.* **2013**, *110* (34), 13956–13960.
- De Castro, C.; Speciale, I.; Duncan, G.; Dunigan, D. D.; Agarkova, I.; Lanzetta, R.; Sturiale, L.; Palmigiano, A.; Garozzo, D.; Molinaro, A.; Tonetti, M.; Van Etten, J. L. *N*-Linked Glycans of Chloroviruses Sharing a Core Architecture without Precedent. *Angew. Chem. Int. Ed.* **2016**, *55* (2), 654–658.
- De Oliveira, A. B. B.; Alevi, K. C. C.; Imperador, C. H. L.; Madeira, F. F.; Azeredo-Oliveira, M. T. V. D. Parasite–Vector Interaction of Chagas Disease: A Mini-Review. *The Am. J. Trop. Med. Hyg.* **2018**, *98* (3), 653–655.
- Demizu, Y.; Kubo, Y.; Miyoshi, H.; Maki, T.; Matsumura, Y.; Moriyama, N.; Onomura, O. Highly Regioselective Protection of Sugars Catalyzed by Dimethyltin Dichloride. *Org. Lett.* **2008**, *10*, 21, 5075–5077.

- Ding, N.; Li, C.; Liu, Y.; Zhang, Z.; Li, Y. Concise Synthesis of Clarhamnoside, a Novel Glycosphingolipid Isolated from the Marine Sponge *Agela clathrodes*. *Carbohydr. Res.* **2007**, *342* (14), 2003–2013.
- Dobson, D. E.; Kamhawi, S.; Lawyer, P.; Turco, S. J.; Beverley, S. M.; Sacks, D. L. Leishmania Major Survival in Selective *Phlebotomus papatasi* Sand Fly Vector Requires a Specific SCG-Encoded Lipophosphoglycan Galactosylation Pattern. *PLoS Pathog* **2010**, *6* (11), e1001185.
- Dubrow, A.; Zuniga, B.; Topo, E.; Cho, J.-H. Suppressing Nonspecific Binding in Biolayer Interferometry Experiments for Weak Ligand–Analyte Interactions. *ACS Omega* **2022**, *7* (11), 9206–9211.
- Eugenia Giorgi, M.; De Lederkremer, R. M. Trans-Sialidase and Mucins of *Trypanosoma cruzi*: An Important Interplay for the Parasite. *Carbohydr. Res.* **2011**, *346* (12), 1389–1393.
- Ezzati Nazhad Dolatabadi, J.; De La Guardia, M. Tips on Ligand Immobilization and Kinetic Study Using Surface Plasmonresonance. *BioImpacts* **2016**, *6* (3), 117–118.
- Ferguson, M. A. J.; Allen, A. K.; Snary, D. Studies on the Structure of a Phosphoglycoprotein from the Parasitic Protozoan *Trypanosoma cruzi*. *Biochem. J.* **1983**, *213* (2), 313–319.
- Ferguson, M. A. J.; Snary, D.; Allen, A. K. Comparative Compositions of Cell Surface Glycoconjugates Isolated from *Trypanosoma Cruzi* Epimastigotes. *BBA - General Subjects* **1985**, *842* (1), 39–44.
- Forsyth, C. J.; Hernandez, S.; Olmedo, W.; Abuhamidah, A.; Traina, M. I.; Sanchez, D. R.; Soverow, J.; Meymandi, S. K. Safety Profile of Nifurtimox for Treatment of Chagas Disease in the United States. *Clin Infect Dis.* **2016**, *63* (8), 1056–1062.

- Fu, J.; Laval, S.; Yu, B. Total Synthesis of Nucleoside Antibiotics Plicacetin and Streptocytosine A. *J. Org. Chem.* **2018**, *83* (13), 7076–7084.
- Furukawa, J.; Kobayashi, S.; Nomizu, M.; Nishi, N.; Sakairi, N. Total Synthesis of Calonyctin A2, a Macrolidic Glycolipid with Plant Growth-Promoting Activity. *Tetrahedron Lett.* **2000**, *41* (18), 3453–3457.
- Fuster, M. M.; Esko, J. D. The Sweet and Sour of Cancer: Glycans as Novel Therapeutic Targets. *Nat Rev Cancer* **2005**, *5* (7), 526–542. <https://doi.org/10.1038/nrc1649>.
- Gallo-Rodriguez, C.; Gandolfi, L.; De Lederkremer, R. M. Synthesis of  $\beta$ -D-Galf-(1 $\rightarrow$ 3)-D-GlcNAc by the Trichloroacetimidate Method and of  $\beta$ -D-Galf-(1 $\rightarrow$ 6)-D-GlcNAc by SnCl<sub>4</sub>-Promoted Glycosylation. *Org. Lett.* **1999**, *1* (2), 245–248.
- Gao, Y.; Luan, X.; Melamed, J.; Brockhausen, I. Role of Glycans on Key Cell Surface Receptors That Regulate Cell Proliferation and Cell Death. *Cells* **2021**, *10* (5), 1252.
- Gerbst, A. G.; Ustuzhanina, N. E.; Grachev, A. A.; Khatuntseva, E. A.; Tsvetkov, D. E.; Whitfield, D. M.; Berces, A.; Nifantiev, N. E. Synthesis, NMR, And Conformational Studies of Fucoidan Fragments. III. Effect of Benzoyl Group At O-3 On Stereoselectivity of Glycosylation By 3-O-And 3,4-Di-O-Benzoylated 2-O-Benzylfucosyl Bromides. *J. Carbohydr. Chem.* **2001**, *20* (9), 821–831.
- Geuijen, K. P. M.; Halim, L. A.; Schellekens, H.; Schasfoort, R. B.; Wijffels, R. H.; Eppink, M. H. Label-Free Glycoprofiling with Multiplex Surface Plasmon Resonance: A Tool To Quantify Sialylation of Erythropoietin. *Anal. Chem.* **2015**, *87* (16), 8115–8122.
- Glibstrup, E.; Pedersen, C. M. Scalable Synthesis of Anomerically Pure Orthogonal-Protected GlcN<sub>3</sub> and GalN<sub>3</sub> from D-Glucosamine. *Org. Lett.* **2016**, *18* (17), 4424–4427.

- Gürtler, R. E.; Kitron, U.; Cecere, M. C.; Segura, E. L.; Cohen, J. E. Sustainable Vector Control and Management of Chagas Disease in the Gran Chaco, Argentina. *Proc. Natl. Acad. Sci. U.S.A.* **2007**, *104* (41), 16194–16199.
- Gustafson, G. L.; Milner, L. A. Occurrence of N-Acetylglucosamine-1-Phosphate in Proteinase I from *Dictyostelium discoideum*. *Journal of Biological Chemistry* **1980**, *255* (15), 7208–7210.
- Haji-Ghassemi, O.; Müller-Loennies, S.; Rodriguez, T.; Brade, L.; Kosma, P.; Brade, H.; Evans, S. V. Structural Basis for Antibody Recognition of Lipid A. *J. Biol. Chem* **2015**, *290* (32), 19629–19640.
- Hasegawa, A.; Ando, T.; Kato, M.; Ishida, H.; Kiso, M. Synthesis of the Methyl Thioglycosides of 2-,3-, and 4-Deoxy-L-Fucose. *Carbohydr. Res.* **1994**, *257* (1), 55–65.
- Haynes, P. A.; Ferguson, A. J.; Cross, G. A. M. Structural Characterization of Novel Oligosaccharides of Cell-Surface Glycoproteins of *Trypanosoma Cruzi*. *Glycobiology* **1996**, *6* (8), 869–878.
- Haynes, P. A.; Russell, D. G.; Cross, G. A. M. Subcellular Localization of *Trypanosoma Cruzi* Glycoprotein Gp72. *J. Cell Sci.* **1996**, *109* (13), 2979–2988.
- Holland, C. V.; Horton, D.; Jewell, J. S. Favored Conformation of Tri-O-Acetyl-Beta-D-Xylopyranosyl Chloride. An All-Axial Tetrasubstituted Six-Membered Ring. *J. Org. Chem.* **1967**, *32* (6), 1818–1821.
- Huang, C.; Wang, N.; Fujiki, K.; Otsuka, Y.; Akamatsu, M.; Fujimoto, Y.; Fukase, K. Widely Applicable Deprotection Method of 2,2,2-Trichloroethoxycarbonyl (Troc) Group Using Tetrabutylammonium Fluoride. *J. Carbohydr. Chem.* **2010**, *29* (6), 289–298.

- Imamura, A.; Matsuzawa, N.; Sakai, S.; Udagawa, T.; Nakashima, S.; Ando, H.; Ishida, H.; Kiso, M. The Origin of High Stereoselectivity in Di-*Tert*-Butylsilylene-Directed  $\alpha$ -Galactosylation. *J. Org. Chem.* **2016**, *81* (19), 9086–9104.
- Jaeschke, S. O.; Lindhorst, T. K.; Auer, A. Between Two Chairs: Combination of Theory and Experiment for the Determination of the Conformational Dynamics of Xylosides. *Chem. Eur. J.* **2022**, *28* (56), e202201544.
- Jansen, A. M.; Xavier, S. C. D. C.; Roque, A. L. R. *Trypanosoma cruzi* Transmission in the Wild and its Most Important Reservoir Hosts in Brazil. *Parasite Vector* **2018**, *11* (1), 502.
- Jansson, K.; Frejd, T.; Kihlberg, J.; Magnusson, G. 2-Trimethylsilylethyl Glycosides. Anomeric Deblocking of Mono- and Disaccharides. *Tetrahedron Lett.* **1988**, *29* (3), 361–362.
- Ji, Y.; Woods, R. J. Quantifying Weak Glycan-Protein Interactions Using a Biolayer Interferometry Competition Assay: Applications to ECL Lectin and X-31 Influenza Hemagglutinin. In *Glycobiophysics*; Yamaguchi, Y., Kato, K., Eds.; Advances in Experimental Medicine and Biology; Springer Singapore: Singapore, 2018; Vol. 1104, pp 259–273.
- Johnson, J. L.; Jones, M. B.; Ryan, S. O.; Cobb, B. A. The Regulatory Power of Glycans and their Binding Partners in Immunity. *Trends Immunol.* **2013**, *34* (6), 290–298.
- Kamhawi, S.; Modi, G. B.; Pimenta, P. F. P.; Rowton, E.; Sacks, D. L. The Vectorial Competence of *Phlebotomus sergenti* is Specific for *Leishmania tropica* and is Controlled by Species-specific, Lipophosphoglycan-mediated Midgut Attachment. *Parasitology* **2000**, *121* (1), 25–33.

- Kay, E.; Cuccui, J.; Wren, B. W. Recent Advances in the Production of Recombinant Glycoconjugate Vaccines. *npj Vaccines* **2019**, *4* (1), 16.
- Kitova, E. N.; El-Hawiet, A.; Schnier, P. D.; Klassen, J. S. Reliable Determinations of Protein–Ligand Interactions by Direct ESI-MS Measurements. Are We There Yet? *J. Am. Soc. Mass Spectrom.* **2012**, *23* (3), 431–441.
- Kropf, S. P.; Sá, M. R. The Discovery of *Trypanosoma Cruzi* and Chagas Disease (1908-1909): Tropical Medicine in Brazil. *Hist. cienc. saude-Manguinhos* **2009**, *16* (suppl 1), 13–34.
- Krumm, S. A.; Doores, K. J. Targeting Glycans on Human Pathogens for Vaccine Design. In Vaccination Strategies Against Highly Variable Pathogens; Hangartner, L., Burton, D. R., Eds.; Current Topics in Microbiology and Immunology; Springer International Publishing: Cham, 2018; Vol. 428, pp 129–163.
- Lay, L.; Nicotra, F.; Panza, L.; Russo, G.; Adobati, E. Oligosaccharides Related to Tumor-Associated Antigens. Part I. Synthesis of the Propyl Glycoside of the Trisaccharide A-L-Fucp-(1→2)-B-D-Galp-(1→3)-B-D-Galpnac, Component of a Tumor Antigen Recognized by the Antibody Mbr1. *Helv. Chim. Acta* **1994**, *77* (2), 509–514.
- Lee, Y. C. Fluorescence Spectrometry in Studies of Carbohydrate-Protein Interactions. *J. Biochem.* **1997**, *121* (5), 818–825.
- Lemieux, R. U.; Hendriks, K. B.; Stick, R. V.; James, K. Halide Ion Catalyzed Glycosidation Reactions. Syntheses of Alpha-Linked Disaccharides. *J. Am. Chem. Soc.* **1975**, *97* (14), 4056–4062.
- Li, Z.; Gildersleeve, J. C. Mechanistic Studies and Methods to Prevent Aglycon Transfer of Thioglycosides. *J. Am. Chem. Soc.* **2006**, *128* (35), 11612–11619.

- Lian, G.; Zhang, X.; Yu, B. Thioglycosides in Carbohydrate Research. *Carbohydr. Res.* **2015**, *403*, 13–22.
- Lin, S.; Lowary, T. L. Synthesis of a Highly Branched Nonasaccharide Chlorella Virus *N*-Glycan Using a “Counterclockwise” Assembly Approach. *Org. Lett.* **2020**, *22* (19), 7645–7649.
- Lin, S.; Lowary, T. L. Synthesis of the Highly Branched Hexasaccharide Core of Chlorella Virus *N*-Linked Glycans. *Chem. Eur. J.* **2018**, *24* (64), 16992–16996.
- Lin, W.; Zhang, X.; He, Z.; Jin, Y.; Gong, L.; Mi, A. Reduction of Azides to Amines or Amides with Zinc and Ammonium Chloride as Reducing Agent. *Synth. Commun.* **2002**, *32* (21), 3279–3284.
- Long, D. E.; Karmakar, P.; Wall, K. A.; Sucheck, S. J. Synthesis Of Alpha-L-Rhamnosyl Ceramide and Evaluation of its Binding with Anti-Rhamnose Antibodies. *Bioorg. Med. Chem.* **2014**, *22* (19), 5279–5289.
- Malik, L. H.; Singh, G. D.; Amsterdam, E. A. The Epidemiology, Clinical Manifestations, and Management of Chagas Heart Disease: Chagas Heart Disease. *Clin. Cardiol.* **2015**, *38* (9), 565–569.
- Manne-Goehler, J.; Umeh, C. A.; Montgomery, S. P.; Wirtz, V. J. Estimating the Burden of Chagas Disease in the United States. *PLoS Negl Trop Dis* **2016**, *10* (11), e0005033.
- Martín-Escolano, J.; Marín, C.; Rosales, M. J.; Tsaousis, A. D.; Medina-Carmona, E.; Martín-Escolano, R. An Updated View of the *Trypanosoma cruzi* Life Cycle: Intervention Points for an Effective Treatment. *ACS Infect. Dis.* **2022**, *8* (6), 1107–1115.

- Mathers, C. D.; Ezzati, M.; Lopez, A. D. Measuring the Burden of Neglected Tropical Diseases: The Global Burden of Disease Framework. *PLoS Negl Trop Dis* **2007**, *1* (2), e114.
- Mattos, E. C.; Tonelli, R. R.; Colli, W.; Alves, M. J. M. The Gp85 Surface Glycoproteins from *Trypanosoma cruzi*. In *Proteins and Proteomics of Leishmania and Trypanosoma*; Santos, A. L. S., Branquinha, M. H., d'Avila-Levy, C. M., Kneipp, L. F., Sodr e, C. L., Eds.; Subcellular Biochemistry; Springer Netherlands: Dordrecht, 2014; Vol. 74, pp 151–180.
- McConville, M. J.; Turco, S. J.; Ferguson, M. A.; Sacks, D. L. Developmental Modification of Lipophosphoglycan During the Differentiation of *Leishmania Major* Promastigotes to an Infectious Stage. *EMBO J.* **1992**, *11* (10), 3593–3600.
- Miller, D. A.; Hernandez, S.; Rodriguez De Armas, L.; Eells, S. J.; Traina, M. M.; Miller, L. G.; Meymandi, S. K. Tolerance of Benznidazole in a United States Chagas Disease Clinic. *Clin. Infect. Dis.* **2015**, *60* (8), 1237–1240.
- Miranda-Arboleda, A. F.; Zaidel, E. J.; Marcus, R.; Pinazo, M. J.; Echeverr a, L. E.; Saldarriaga, C.; Sosa Liprandi,  .; Baranchuk, A.; On Behalf of the Neglected Tropical Diseases and other Infectious Diseases Affecting the Heart (NET-Heart) Project. Roadblocks in Chagas Disease Care in Endemic and Nonendemic Countries: Argentina, Colombia, Spain, and the United States. The NET-Heart Project. *PLoS Negl Trop Dis* **2021**, *15* (12), e0009954.
- Moncayo,  .; Silveira, A. C. Current Epidemiological Trends of Chagas Disease in Latin America and Future Challenges. In *American Trypanosomiasis Chagas Disease*; Elsevier, 2017; pp 59–88.

- Mong, K. T.; Nokami, T.; Tran, N. T. T.; Nhi, P. B. Solvent Effect on Glycosylation. In *Selective Glycosylations: Synthetic Methods and Catalysts*; Bennett, C. S., Ed.; Wiley, 2017; pp 59–77.
- Mori, M.; Ito, Y.; Ogawa, T. Total Synthesis of the Mollu-Series Glycosyl Ceramides  $\alpha$ -D-Manp-(1→3)- $\beta$ -D-Manp-(1→4)- $\beta$ -D-Glcp-(1→1)-Cer and  $\alpha$ -D-Manp-(1→3)-[ $\beta$ -D-Xylp-(1→2)]- $\beta$ -D-Manp-(1→4)- $\beta$ -D-Glcp-(1→1)-Cer. *Carbohydr. Res.* **1990**, *195* (2), 199–224.
- Moura E Castro, F. A.; Soares, R. P.; Almeida, I. C.; Freitas, G. F.; Torrecilhas, A. C.; Romanha, A. J.; Murta, S. M.; Assis, R. R.; Rocha, M. N.; Santos, S. L.; Marques, A. F. Intraspecies Variation in *Trypanosoma cruzi* GPI-Mucins: Biological Activities and Differential Expression of Alpha-Galactosyl Residues. *Am. J. Trop. Med. Hyg.* **2012**, *87* (1), 87–96.
- Murali, S.; Rustandi, R.; Zheng, X.; Payne, A.; Shang, L. Applications of Surface Plasmon Resonance and Biolayer Interferometry for Virus–Ligand Binding. *Viruses* **2022**, *14* (4), 717.
- Namchuk, M. N.; McCarter, J. D.; Becalski, A.; Andrews, T.; Withers, S. G. The Role of Sugar Substituents in Glycoside Hydrolysis. *J. Am. Chem. Soc.* **2000**, *122* (7), 1270–1277.
- Neglected tropical diseases -- GLOBAL*. <https://www.who.int/health-topics/neglected-tropical-diseases>.
- Nozaki, T. Characterization of the *Trypanosoma brucei* Homologue of a *Trypanosoma cruzi* Flagellum-Adhesion Glycoprotein. *Mol. Biochem. Parasitol.* **1996**, *82* (2), 245–255.

- Nozaki, T.; Cross, G. A. M. Functional Complementation of Glycoprotein 72 in a *Trypanosoma cruzi* Glycoprotein 72 Null Mutant. *Mol. Biochem. Parasitol.* **1994**, *67* (1), 91–102.
- Nunes, M. C. P.; Dones, W.; Morillo, C. A.; Encina, J. J.; Ribeiro, A. L. Chagas Disease. *J. Am. Coll. Cardiol.* **2013**, *62* (9), 767–776.
- Page, S. W. Antiparasitic Drugs. In *Small Animal Clinical Pharmacology*; Elsevier, 2008; pp 198–260.
- Pech-Canul, Á. D. L. C.; Monteón, V.; Solís-Oviedo, R.-L. A Brief View of the Surface Membrane Proteins from *Trypanosoma cruzi*. *J. Parasitol. Res.* **2017**, *2017*, 1–13.
- Petersen, R. Strategies Using Bio-Layer Interferometry Biosensor Technology for Vaccine Research and Development. *Biosensors* **2017**, *7* (4), 49.
- Quijano-Hernandez, I.; Dumonteil, E. Advances and Challenges Towards a Vaccine Against Chagas Disease. *Hum. Vaccines* **2011**, *7* (11), 1184–1191.
- Rajão, M. A.; Furtado, C.; Alves, C. L.; Passos-Silva, D. G.; De Moura, M. B.; Schamber-Reis, B. L.; Kunrath-Lima, M.; Zuma, A. A.; Vieira-da-Rocha, J. P.; Garcia, J. B. F.; Mendes, I. C.; Pena, S. D. J.; Macedo, A. M.; Franco, G. R.; De Souza-Pinto, N. C.; De Medeiros, M. H. G.; Cruz, A. K.; Motta, M. C. M.; Teixeira, S. M. R.; Machado, C. R. Unveiling Benznidazole's Mechanism of Action Through Overexpression of DNA Repair Proteins in *Trypanosoma Cruzi*: Unveiling Benznidazole's Mechanism. *Environ. Mol. Mutagen.* **2014**, *55* (4), 309–321.
- Rajput, V. K.; Mukhopadhyay, B. Concise Synthesis of a Pentasaccharide Related to the Anti-Leishmanial Triterpenoid Saponin Isolated from *Maesa balansae*. *J. Org. Chem.* **2008**, *73* (17), 6924–6927.

- Rao, Y.; Boons, G.-J. A Highly Convergent Chemical Synthesis of Conformational Epitopes of Rhamnogalacturonan II. *Angew. Chem. Int. Ed.* **2007**, *46* (32), 6148–6151.
- Rassi, A.; Rassi, A.; Marin-Neto, J. A. Chagas Disease. *Lancet* **2010**, *375* (9723), 1388–1402.
- Rich, R. L.; Myszka, D. G. Higher-Throughput, Label-Free, Real-Time Molecular Interaction Analysis. *Anal. Biochem.* **2007**, *361* (1), 1–6.
- Rocha, G. M.; Brandão, B. A.; Mortara, R. A.; Attias, M.; De Souza, W.; Carvalho, T. M. U. The Flagellar Attachment Zone of *Trypanosoma cruzi* Epimastigote Forms. *J. Struct. Biol.* **2006**, *154* (1), 89–99.
- Rocha, G. M.; Seabra, S. H.; De Miranda, K. R.; Cunha-e-Silva, N.; De Carvalho, T. M. U.; De Souza, W. Attachment of Flagellum to the Cell Body is Important to the Kinetics of Transferrin Uptake by *Trypanosoma cruzi*. *Parasitol. Int.* **2010**, *59* (4), 629–633.
- Sánchez-Valdéz, F. J.; Pérez Brandán, C.; Ferreira, A.; Basombrío, M. Á. Gene-Deleted Live-Attenuated *Trypanosoma cruzi* Parasites as Vaccines to Protect Against Chagas Disease. *Expert Rev. Vaccines* **2015**, *14* (5), 681–697.
- Seyrek, K.; Richter, M.; Lavrik, I. N. Decoding the Sweet Regulation of Apoptosis: The Role of Glycosylation and Galectins in Apoptotic Signaling Pathways. *Cell Death Differ* **2019**, *26* (6), 981–993.
- Shah, N. B.; Duncan, T. M. Bio-Layer Interferometry for Measuring Kinetics of Protein-Protein Interactions and Allosteric Ligand Effects. *JoVE* **2014**, *84*, 51383.
- Shen, K.; Bai, B.; Liu, Y.; Lowary, T. L. Synthesis of a Tridecasaccharide Lipooligosaccharide Antigen from the Opportunistic Pathogen *Mycobacterium kansasii*. *Angew. Chem.* **2021**, *133* (47), 25063–25067.

- Sher, A.; Snary, D. Specific Inhibition of the Morphogenesis of *Trypanosoma cruzi* by a Monoclonal Antibody. *Nature* **1982**, *300* (5893), 639–640.
- Shiozaki, M.; Tashiro, T.; Koshino, H.; Shigeura, T.; Watarai, H.; Taniguchi, M.; Mori, K. Synthesis and Biological Activity of Hydroxylated Analogues of KRN7000 ( $\alpha$ -Galactosylceramide). *Carbohydr. Res.* **2013**, *370*, 46–66.
- Snary, D. Cell Surface Glycoproteins of *Trypanosoma cruzi*: Protective Immunity in Mice and Antibody Levels in Human Chagasic Sera. *Trans. R. Soc. Trop. Med. Hyg.* **1983**, *77* (1), 126–129.
- Sommer, R.; Neres, J.; Piton, J.; Dhar, N.; Van Der Sar, A.; Mukherjee, R.; Laroche, T.; Dyson, P. J.; McKinney, J. D.; Bitter, W.; Makarov, V.; Cole, S. T. Fluorescent Benzothiazinone Analogues Efficiently and Selectively Label DPRE1 In Mycobacteria and Actinobacteria. *ACS Chem. Biol.* **2018**, *13* (11), 3184–3192.
- Sosa-Estani, S.; Segura, E. L. Integrated Control of Chagas Disease for its Elimination as Public Health Problem - A Review. *Mem. Inst. Oswaldo Cruz* **2015**, *110* (3), 289–298.
- Stayton, P. S.; Freitag, S.; Klumb, L. A.; Chilkoti, A.; Chu, V.; Penzotti, J. E.; To, R.; Hyre, D.; Le Trong, I.; Lybrand, T. P.; Stenkamp, R. E. Streptavidin–Biotin Binding Energetics. *Biomol. Eng.* **1999**, *16* (1–4), 39–44.
- Suárez, C.; Nolder, D.; García-Mingo, A.; Moore, D. A.; Chiodini, P. L. Diagnosis and Clinical Management of Chagas Disease: An Increasing Challenge in Non-Endemic Areas. *RRTM* **2022**, *13*, 25–40.
- Sunter, J. D.; Gull, K. The Flagellum Attachment Zone: ‘The Cellular Ruler’ of Trypanosome Morphology. *Trends Parasitol.* **2016**, *32* (4), 309–324.

- Tra, V. N.; Dube, D. H. Glycans in Pathogenic Bacteria – Potential for Targeted Covalent Therapeutics and Imaging Agents. *Chem. Commun.* **2014**, 50 (36), 4659–4673.
- Trost, B. M.; Kalnmals, C. A.; Tracy, J. S.; Bai, W.-J. Highly Chemoselective Deprotection of the 2,2,2-Trichloroethoxycarbonyl (Troc) Protecting Group. *Org. Lett.* **2018**, 20 (24), 8043–8046.
- Tyler, K. M.; Engman, D. M. The Life Cycle of *Trypanosoma cruzi* Revisited. *Int. J. Parasitol.* **2001**, 31 (5–6), 472–481.
- Van Kooyk, Y.; Rabinovich, G. A. Protein-Glycan Interactions in the Control of Innate and Adaptive Immune Responses. *Nat Immunol* **2008**, 9 (6), 593–601.
- Verma, P. R.; Mukhopadhyay, B. Concise Synthesis of a Tetra- And a Trisaccharide Related to the Repeating Unit of the O-Antigen from *Providencia rustigianii* O34 in the form of their *p*-Methoxyphenyl Glycosides. *RSC Adv.* **2013**, 3 (1), 201–207.
- Walvoort, M. T. C.; Moggré, G.-J.; Lodder, G.; Overkleeft, H. S.; Codée, J. D. C.; Van Der Marel, G. A. Stereoselective synthesis of 2,3-Diamino-2,3-dideoxy- $\beta$ -D-mannopyranosyl Uronates. *J. Org. Chem.* **2011**, 76 (18), 7301–7315.
- Wang, Y.; Wu, Y.; Xiong, D.; Ye, X. Total Synthesis of a Hyperbranched *N*-Linked Hexasaccharide Attached to ATCV- 1 Major Capsid Protein Without Precedent. *Chin. J. Chem.* **2019**, 37 (1), 42–48.
- Wang, Z.; Zhou, L.; El-Boubbou, K.; Ye, X.; Huang, X. Multi-Component One-Pot Synthesis of the Tumor-Associated Carbohydrate Antigen Globo-H based on Preactivation of Thioglycosyl Donors. *J. Org. Chem.* **2007**, 72 (17), 6409–6420.

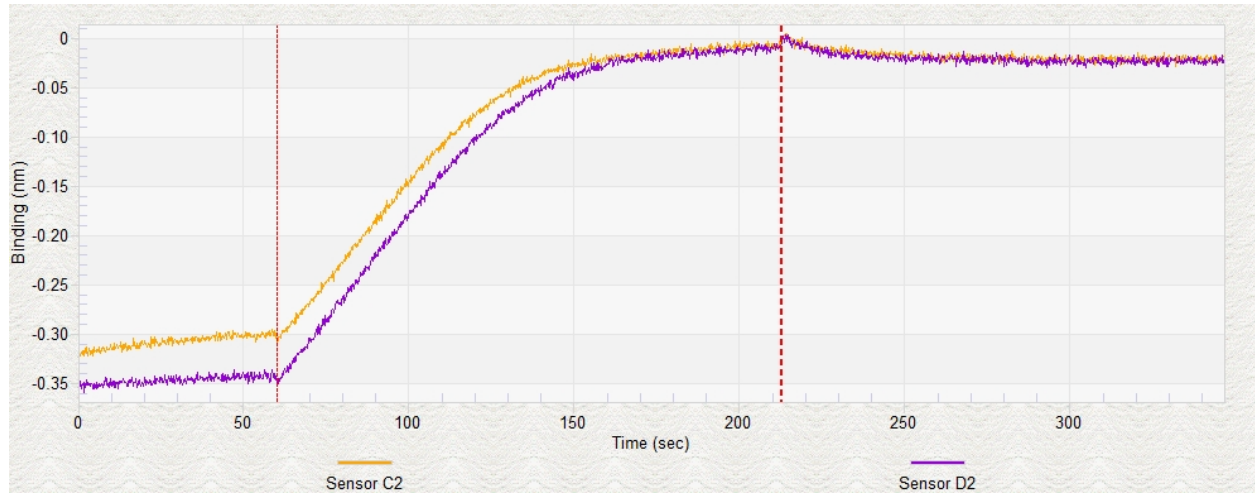
- Wassef, N. M.; Roerdink, F.; Swartz, G. M.; Lyon, J. A.; Berson, B. J.; Alving, C. R. Phosphate-Binding Specificities of Monoclonal Antibodies Against Phosphoinositides in Liposomes. *Mol. Immunol.* **1984**, *21* (10), 863–868.
- Wilstermann, M.; Magnusson, G. Synthesis of Xyl $\beta$ Cer, Gal $\beta$ 1–4Xyl $\beta$ Cer, NeuA $\alpha$ 2–3Gal $\beta$ 1–4Xyl $\beta$ Cer and the Corresponding Lactone and Lactam Trisaccharides. *J. Org. Chem.* **1997**, *62* (23), 7961–7971.
- Yuasa, H.; Hashimoto, H. Bending Trisaccharides by a Chelation-Induced Ring Flip of a Hinge-Like Monosaccharide Unit. *J. Am. Chem. Soc.* **1999**, *121* (21), 5089–5090.
- Zhang, J.; Li, C.; Sun, L.; Yu, G.; Guan, H. Total Synthesis of Myrmekioside A, A Mono- *O*-Alkyl- Diglycosylglycerol from Marine Sponge *Myrmekioderma Sp.* *Eur J Org Chem* **2015**, *2015* (19), 4246–4253.
- Zhang, S.; Chen, K. Y.; Zou, X. Carbohydrate-Protein Interactions: Advances and Challenges. *Commun. Inf. Syst.* **2021**, *21* (1), 147–163.
- Zhao, W.; Kong, F. Facile Synthesis of the Heptasaccharide Repeating Unit of *O*-Deacetylated GXM of *C. neoformans* Serotype B. *Bioorg. Med. Chem.* **2005**, *13* (1), 121–130.
- Zhao, W.; Kong, F. Synthesis of a Heptasaccharide Fragment of the *O*-Deacetylated GXM of *C. neoformans* Serotype C. *Carbohydr. Res.* **2005**, *340* (10), 1673–1681.
- Zimmermann, S.; Lepenies, B. Glycans as Vaccine Antigens and Adjuvants: Immunological Considerations. In *Carbohydrate-Based Vaccines*; Lepenies, B., Ed.; *Methods in Molecular Biology*; Springer New York: New York, NY, 2015; Vol. 1331, pp 11–26.
- Zingales, B.; Andrade, S.; Briones, M.; Campbell, D.; Chiari, E.; Fernandes, O.; Guhl, F.; Lages-Silva, E.; Macedo, A.; Machado, C.; Miles, M.; Romanha, A.; Sturm, N.; Tibayrenc, M.; Schijman, A. A New Consensus for *Trypanosoma cruzi* Intraspecific

Nomenclature: Second Revision Meeting Recommends TcI to TcVI. *Mem. Inst. Oswaldo Cruz* **2009**, *104* (7), 1051–1054.

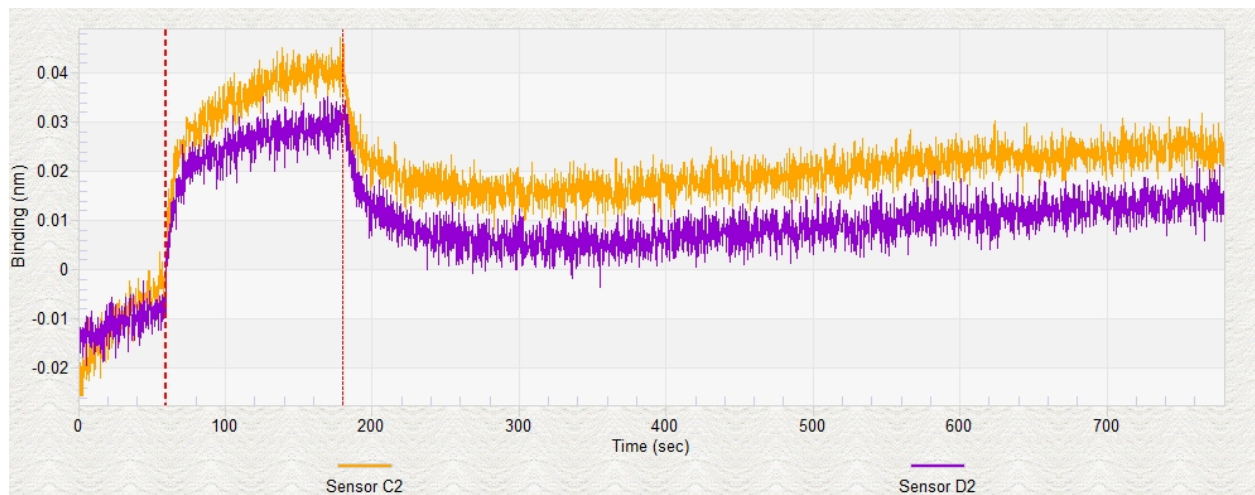
## **Appendix**

## BLI sensograms for immobilization of biotinylated glycans on SAX sensors

**A**

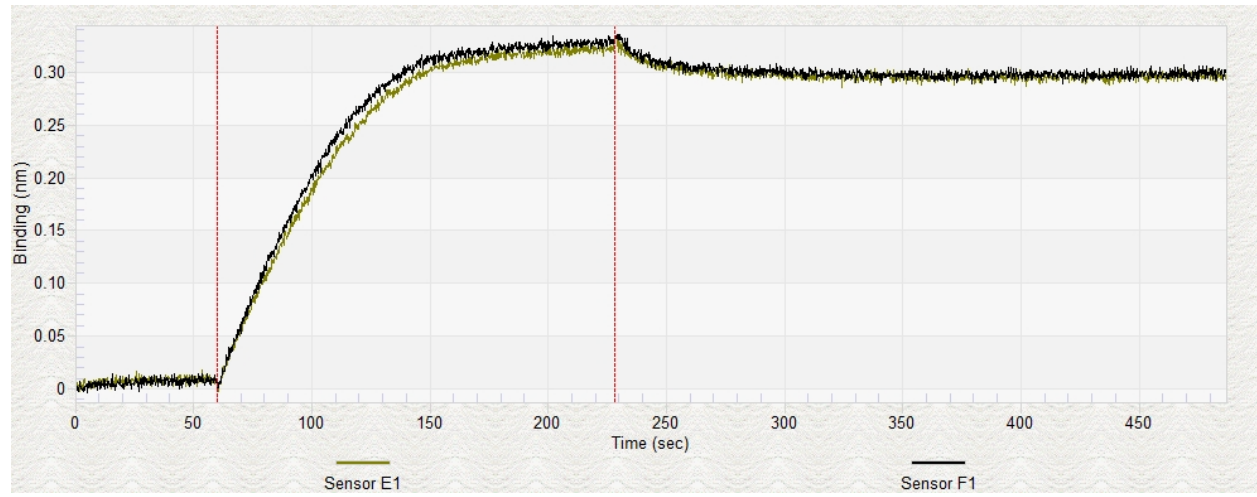


**B**

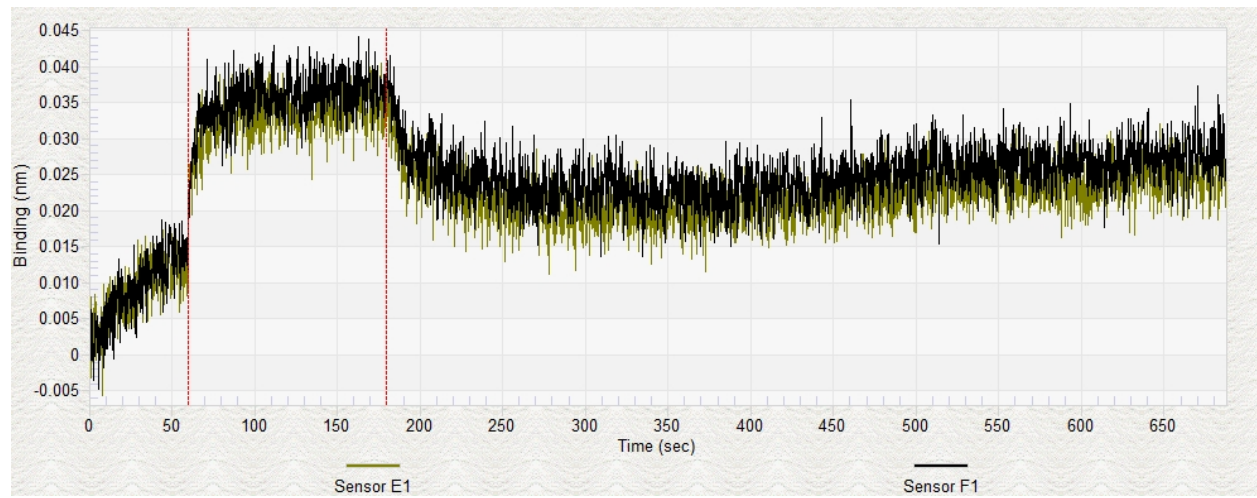


**Appendix 1.1:** Sensograms during the **A**) immobilization and **B**) blocking steps of glycan 4.2.

**A**

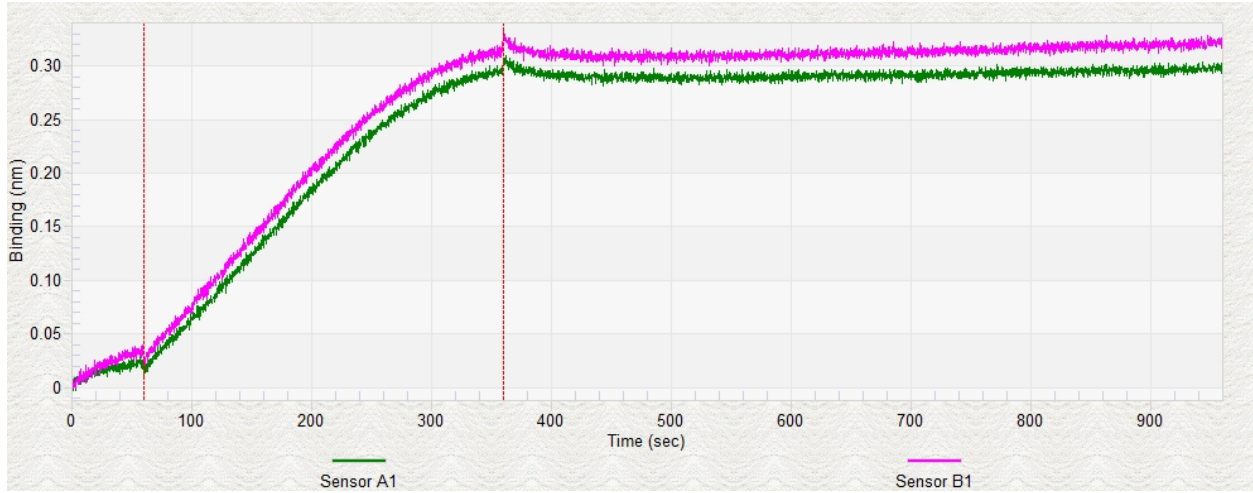


**B**

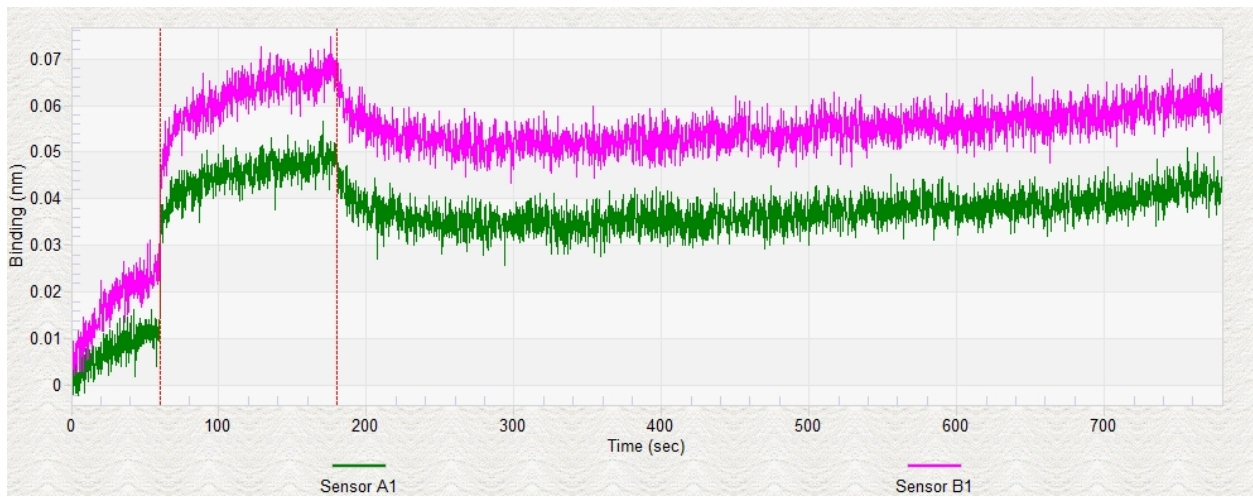


**Appendix 1.2:** Sensograms during the **A)** immobilization and **B)** blocking steps of glycan 4.3.

**A**



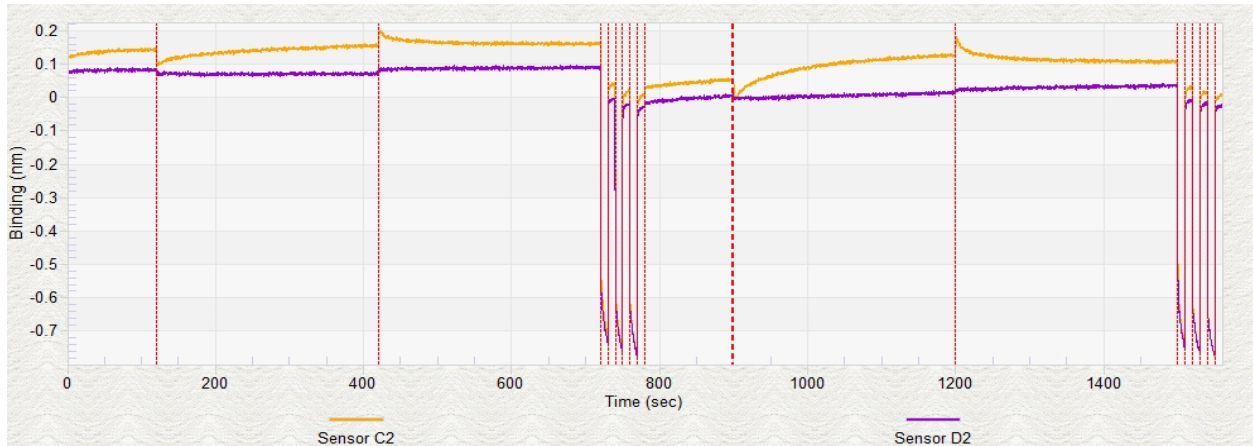
**B**



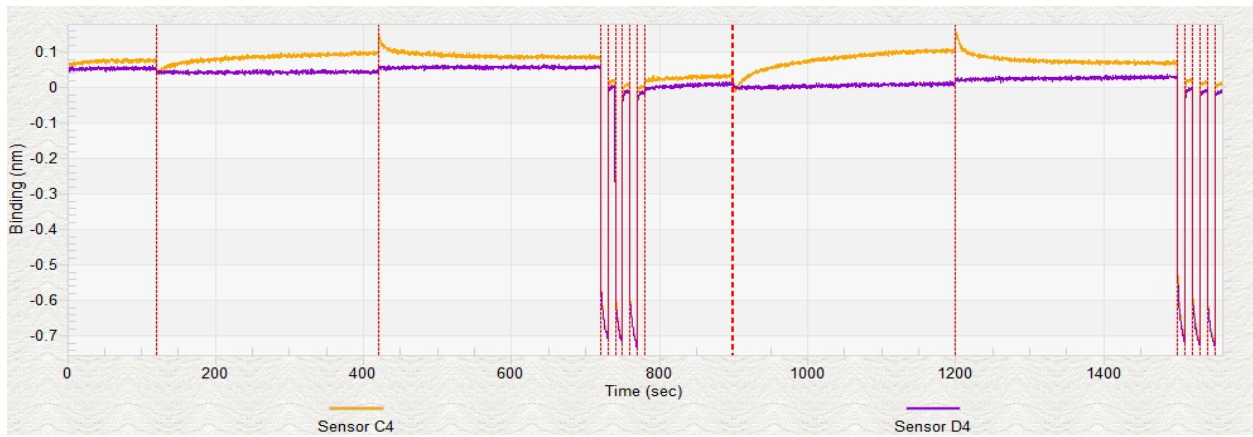
**Appendix 1.3:** Sensograms during the **A)** immobilization and **B)** blocking steps of glycan 4.4.

**BLI sensograms for binding analysis of glycan fragments with WIC29.26 mAb using 1x PBS containing 0.1% BSA and 0.05% Tween 20 as the buffer assay**

**A**

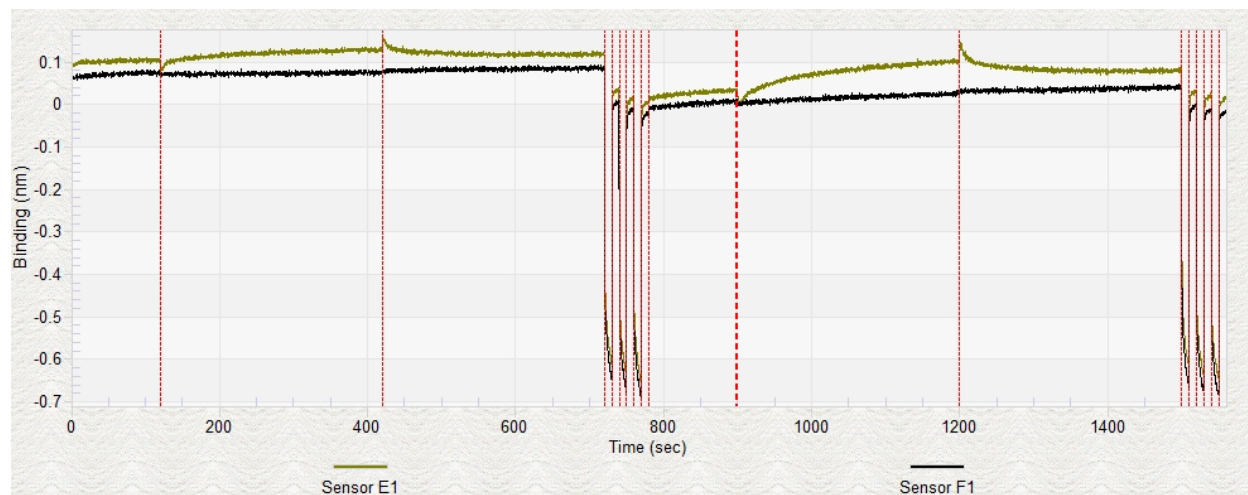


**B**

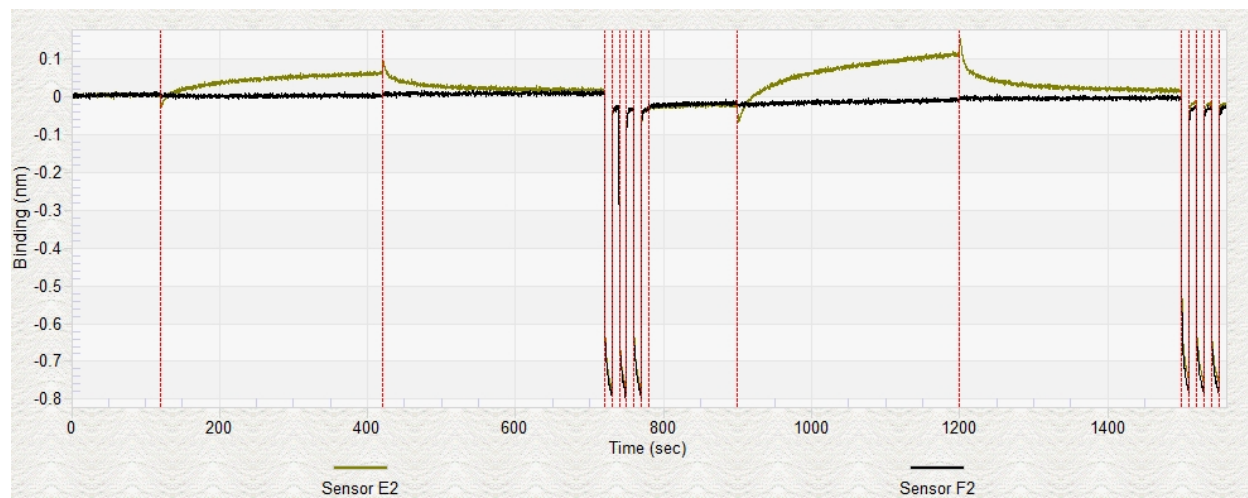


**Appendix 1.4: A)** Sensogram for the binding analysis using ligand sensors immobilized with glycan **4.2**. Sensor C2 sensogram corresponds to experiment with mAb; Sensor D2 sensogram corresponds to the experiment with blank. **B)** Sensogram for the binding analysis using reference sensors. Sensor C4 sensogram corresponds to experiment with mAb; Sensor D4 sensogram corresponds to the experiment with blank.

**A**

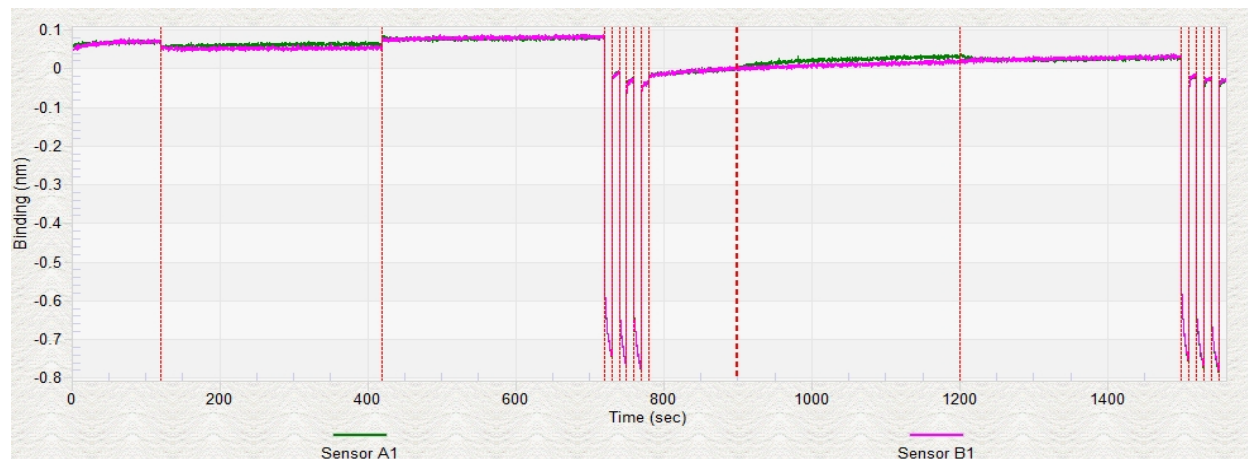


**B**

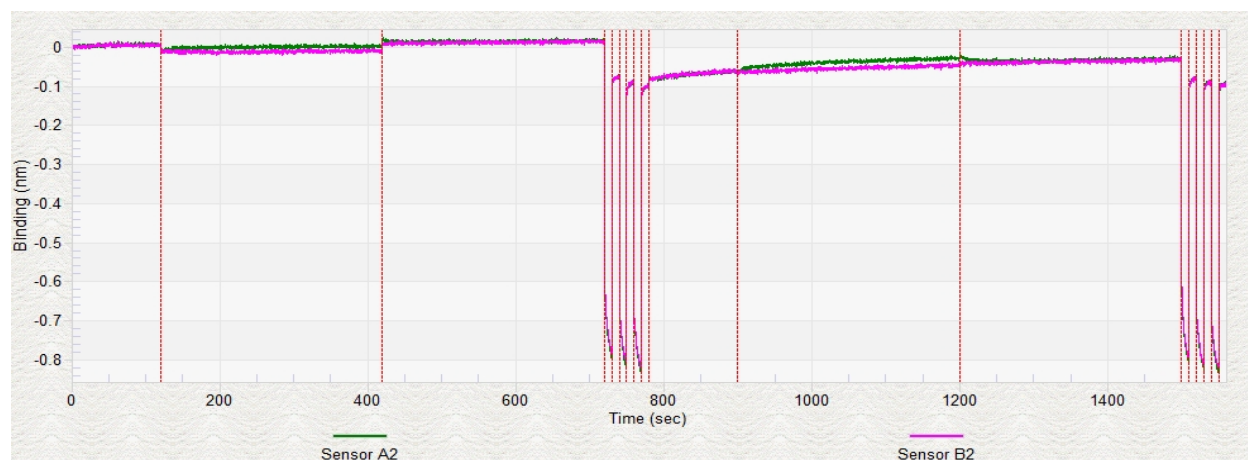


**Appendix 1.5: A)** Sensogram for the binding analysis using ligand sensors immobilized with glycan **4.3**. Sensor E1 sensogram corresponds to experiment with mAb; Sensor F1 sensogram corresponds to the experiment with blank. **B)** Sensogram for the binding analysis using reference sensors. Sensor E2 sensogram corresponds to experiment with mAb; Sensor F2 sensogram corresponds to the experiment with blank.

**A**



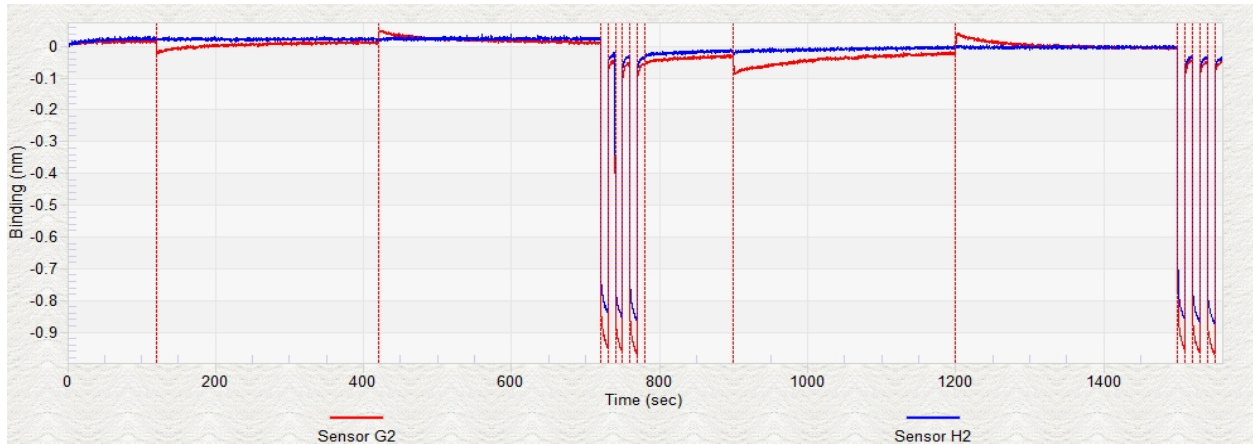
**B**



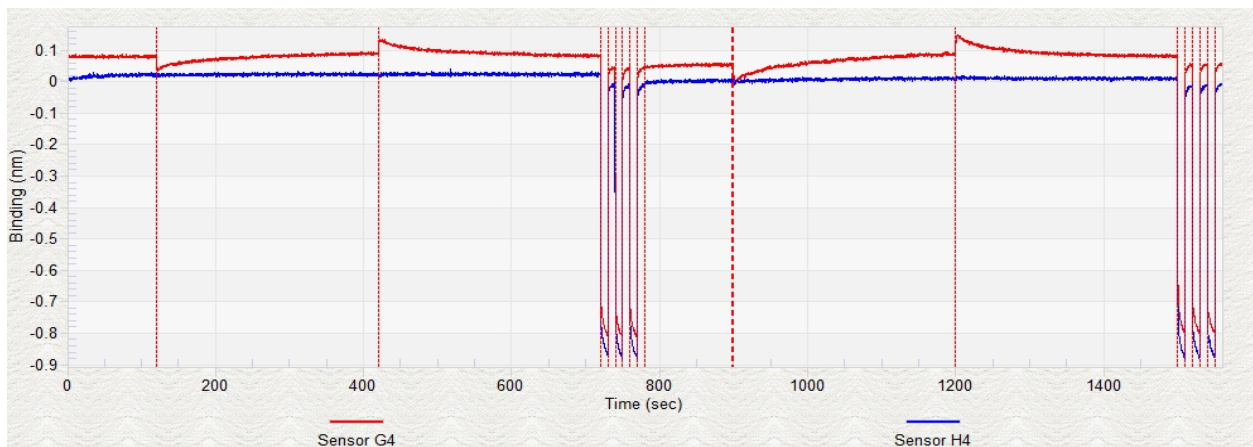
**Appendix 1.6: A)** Sensogram for the binding analysis using ligand sensors immobilized with glycan **4.4**. Sensor A1 sensogram corresponds to experiment with mAb; Sensor B1 sensogram corresponds to the experiment with blank. **B)** Sensogram for the binding analysis using reference sensors. Sensor A2 sensogram corresponds to experiment with mAb; Sensor B2 sensogram corresponds to the experiment with blank.

**BLI sensograms for binding analysis of glycan fragments with WIC29.26 mAb using 50 mM Tris buffer (pH = 7.4, 0.15 M NaCl, 0.25% BSA and 0.05% Tween 20, 0.05% NaN<sub>3</sub>)**

**A**

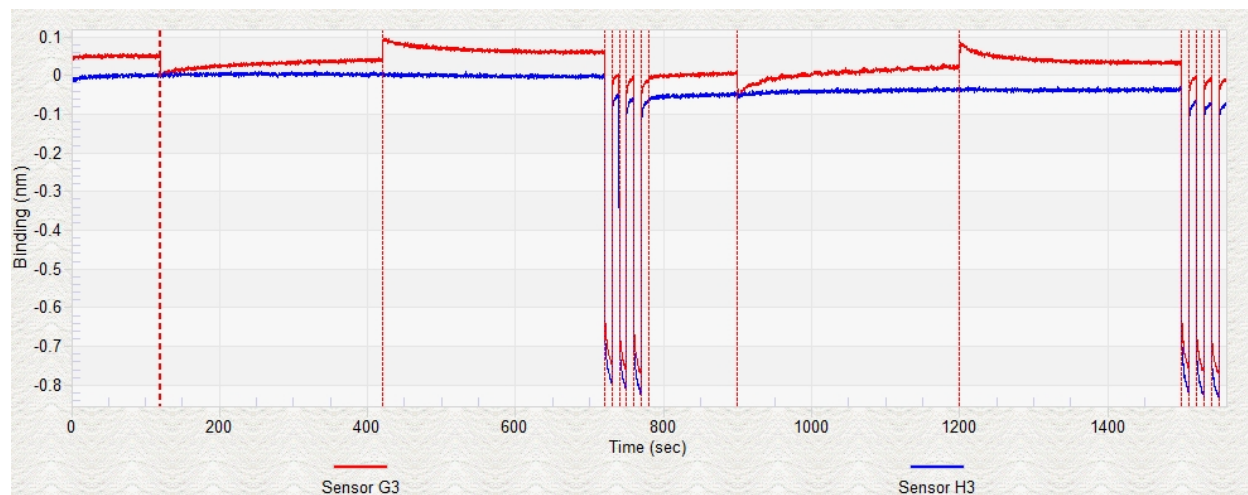


**B**

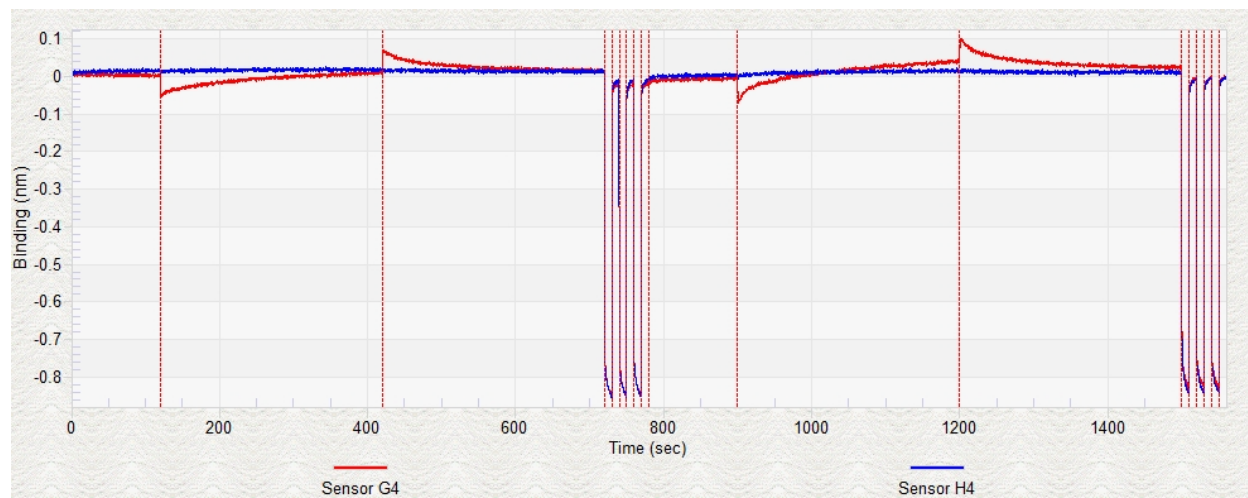


**Appendix 1.7: A)** Sensogram for the binding analysis using ligand sensors immobilized with glycan **4.2**. Sensor G2 sensogram corresponds to experiment with mAb; Sensor H2 sensogram corresponds to the experiment with blank. **B)** Sensogram for the binding analysis using reference sensors. Sensor G4 sensogram corresponds to experiment with mAb; Sensor H4 sensogram corresponds to the experiment with blank.

**A**

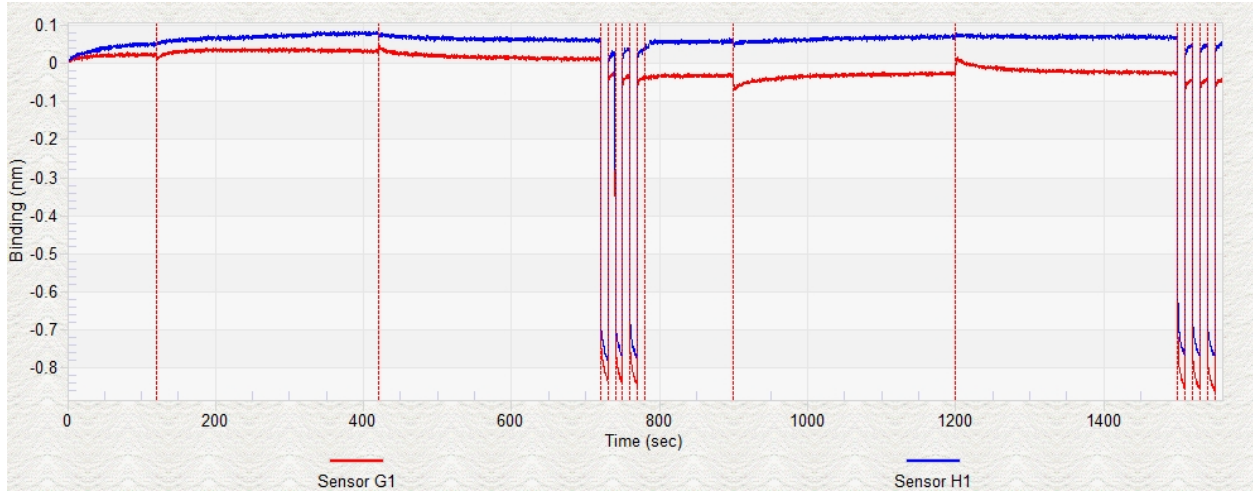


**B**

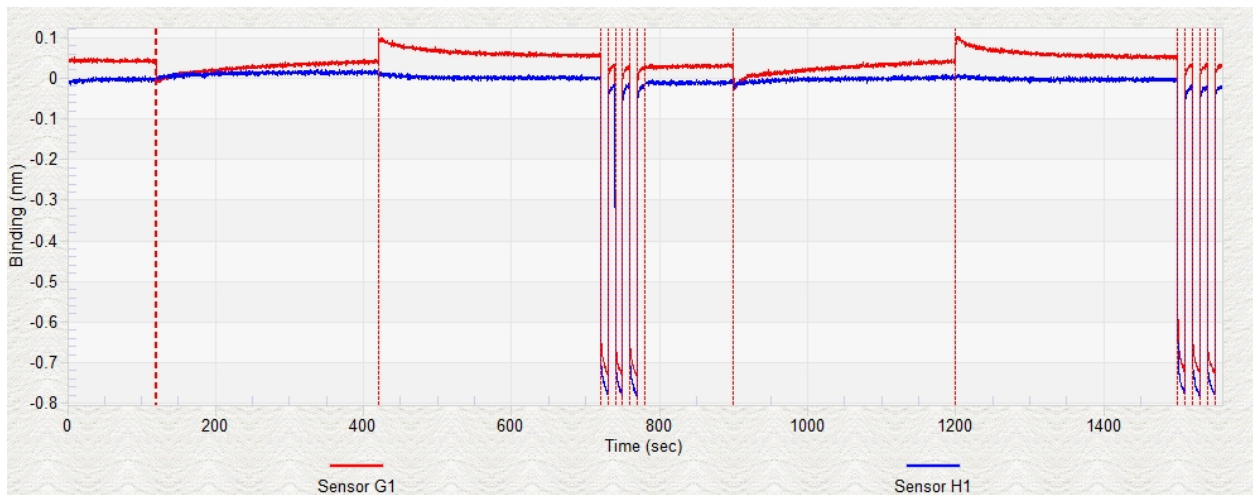


**Appendix 1.8:** **A)** Sensogram for the binding analysis using ligand sensors immobilized with glycan **4.2**. Sensor G3 sensogram corresponds to experiment with mAb; Sensor H3 sensogram corresponds to the experiment with blank. **B)** Sensogram for the binding analysis using reference sensors. Sensor G4 sensogram corresponds to experiment with mAb; Sensor H4 sensogram corresponds to the experiment with blank.

**A**



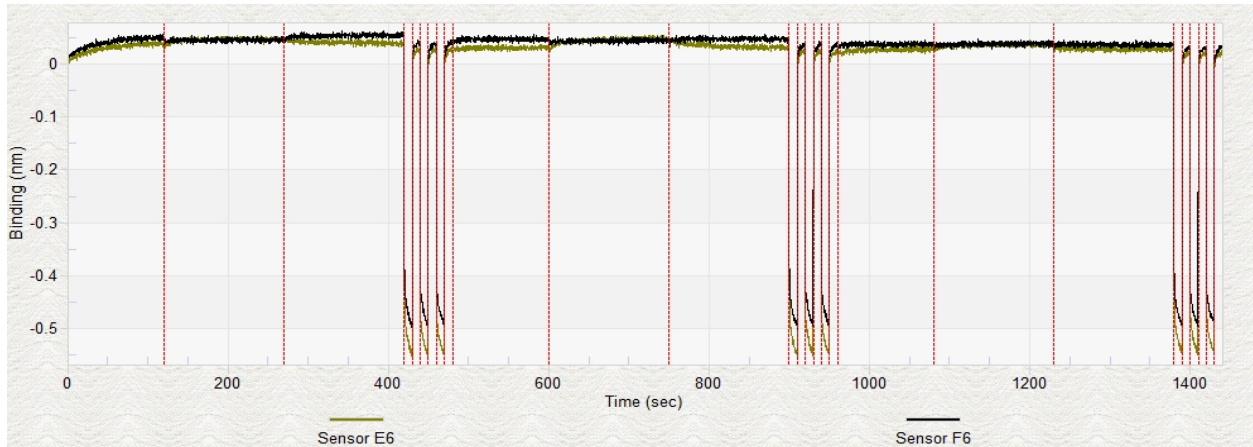
**B**



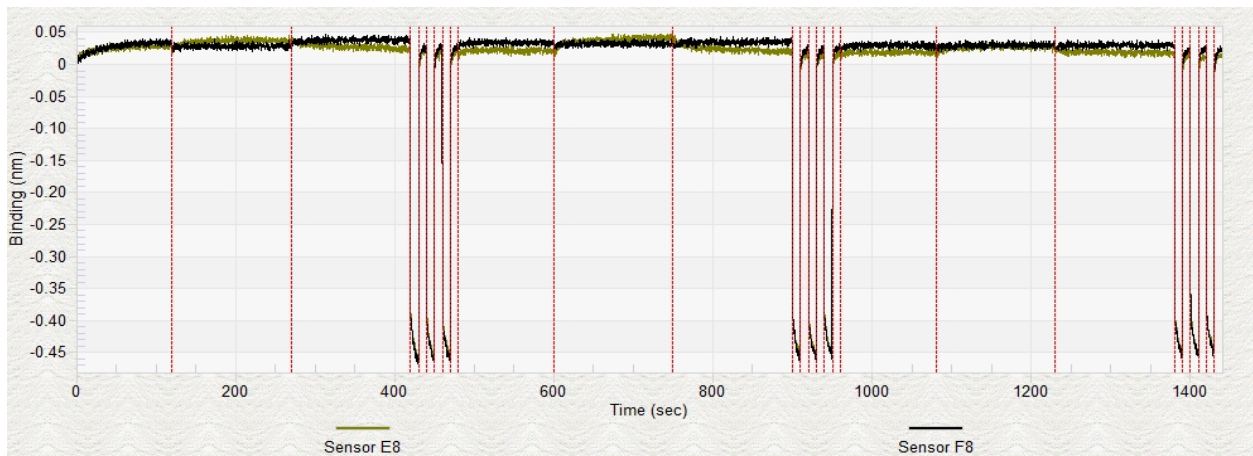
**Appendix 1.9: A)** Sensogram for the binding analysis using ligand sensors immobilized with glycan 4.2. Sensor G1 sensogram corresponds to experiment with mAb; Sensor H1 sensogram corresponds to the experiment with blank. **B)** Sensogram for the binding analysis using reference sensors. Sensor G1 sensogram corresponds to experiment with mAb; Sensor H1 sensogram corresponds to the experiment with blank.

**BLI sensograms for binding analysis of glycan fragments with purified WIC29.26 mAb using 1x PBS containing 0.1% BSA and 0.05% Tween 20 as the buffer assay**

**A**

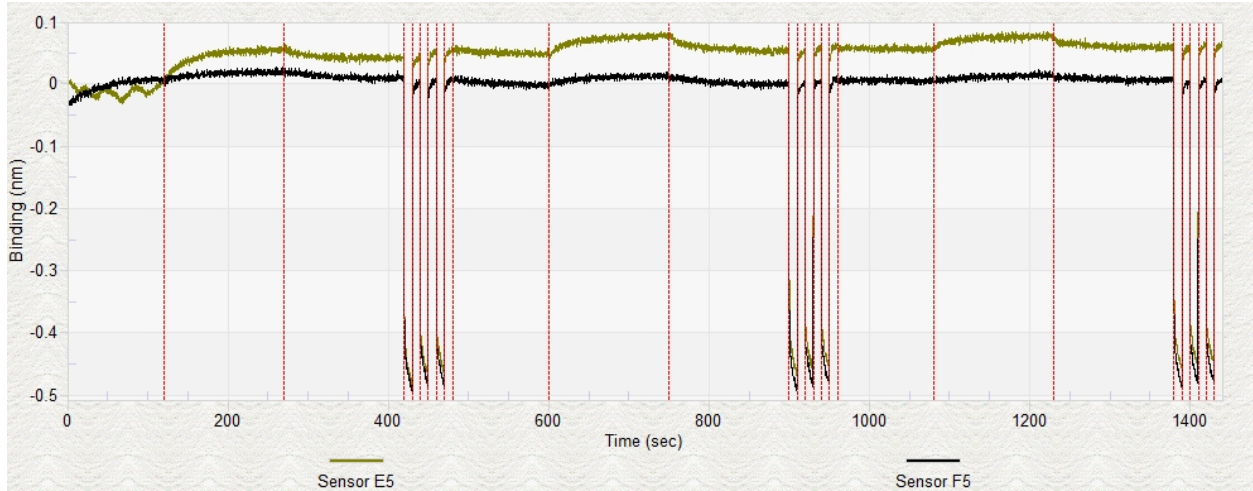


**B**

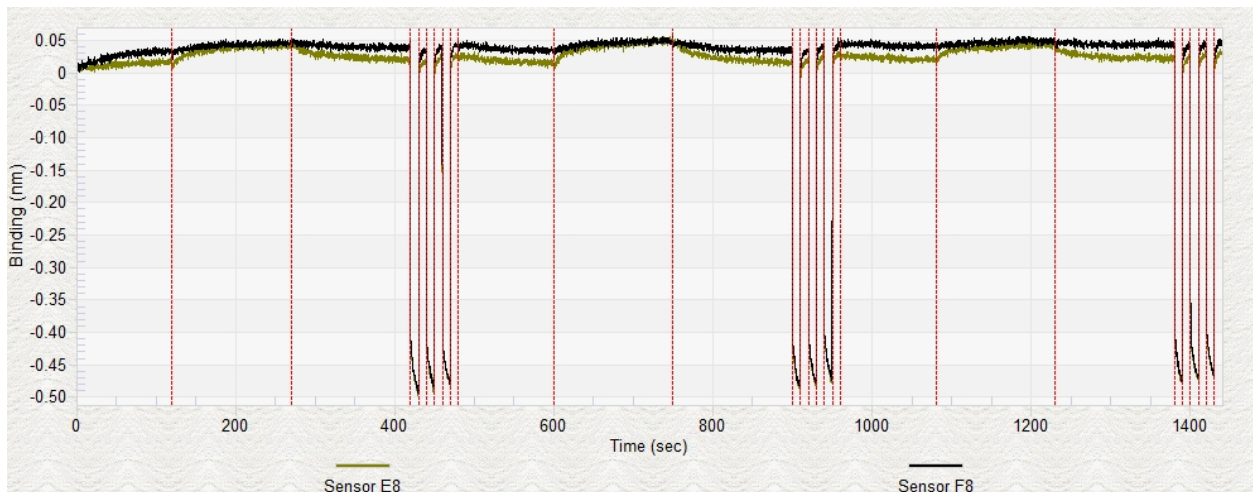


**Appendix 1.10: A)** Sensogram for the binding analysis using ligand sensors immobilized with glycan **4.2**. Sensor E6 sensogram corresponds to experiment with mAb; Sensor F6 sensogram corresponds to the experiment with blank. **B)** Sensogram for the binding analysis using reference sensors. Sensor E8 sensogram corresponds to experiment with mAb; Sensor F8 sensogram corresponds to the experiment with blank.

**A**

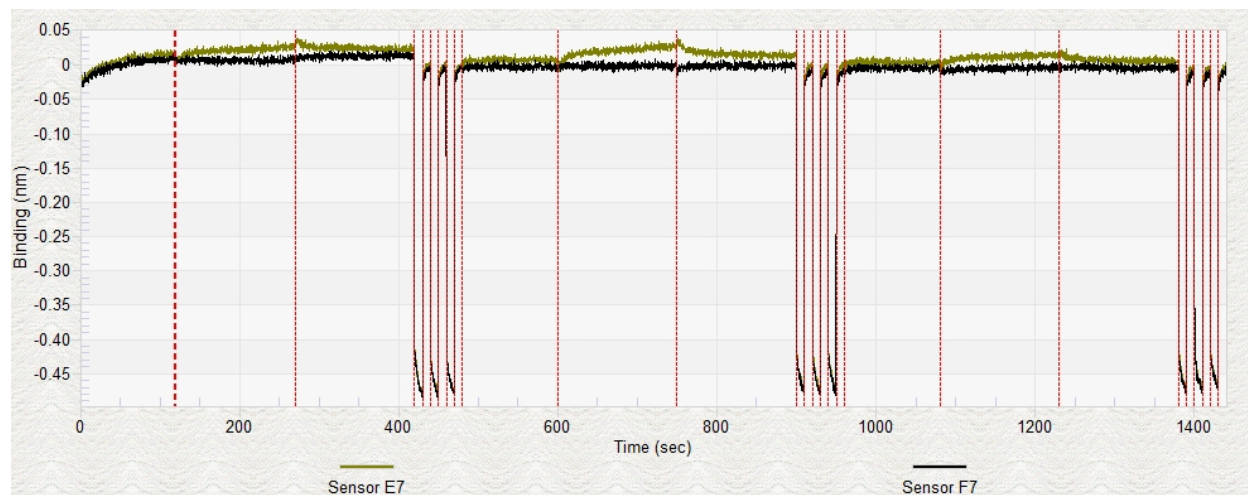


**B**

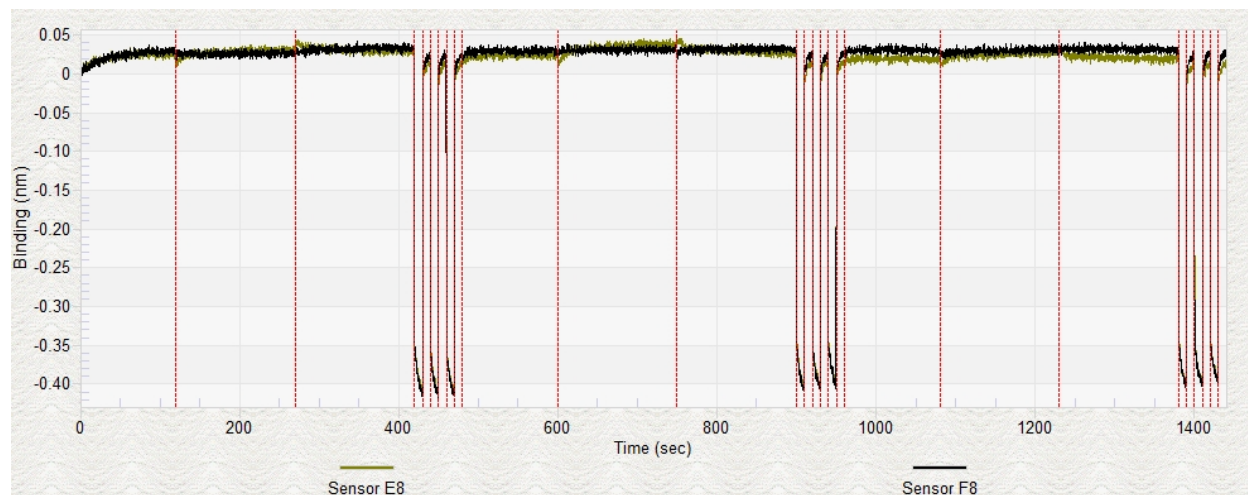


**Appendix 1.11: A)** Sensogram for the binding analysis using ligand sensors immobilized with glycan **4.3**. Sensor E5 sensogram corresponds to experiment with mAb; Sensor F5 sensogram corresponds to the experiment with blank. **B)** Sensogram for the binding analysis using reference sensors. Sensor E8 sensogram corresponds to experiment with mAb; Sensor F8 sensogram corresponds to the experiment with blank.

**A**



**B**



**Appendix 1.12: A)** Sensogram for the binding analysis using ligand sensors immobilized with glycan 4.4. Sensor E7 sensogram corresponds to experiment with mAb; Sensor F7 sensogram corresponds to the experiment with blank. **B)** Sensogram for the binding analysis using reference sensors. Sensor E8 sensogram corresponds to experiment with mAb; Sensor F8 sensogram corresponds to the experiment with blank.